Jessica A. Cano
Senior Attorney
Florida Power & Light Company
700 Universe Boulevard
Juno Beach, FL 33408-0420
(561) 304-5226
(561) 691-7135 (Facsimile)

June 24, 2016

VIA ELECTRONIC DELIVERY

Ms. Carlotta Stauffer
Commission Clerk
Florida Public Service Commission
2540 Shumard Oak Boulevard
Tallahassee, FL 32399-0850

Re: Docket No. 160000; Staff's First Data Request -- 2016 FEECA Report Data Collection

Dear Ms. Stauffer:

Please find enclosed FPL's responses to Staff's First Data Request, Nos. 1-12. Please contact me if there are any questions regarding this filing.

Sincerely,

s/ Jessica A. Cano

Jessica A. Cano
Fla. Bar No. 0037372

Enclosure

QUESTION:
For each DSM program offered during 2015, please provide the implementation date for each of the new / modified program approved by the Commission for the recent goal period and the termination date for each retired program approved under the prior goal period.

RESPONSE:
The implementation date for all FPL's new/modified DSM programs was November 9, 2015. The retired energy efficiency programs were terminated by October 1, 2015. The Solar Pilot programs were terminated by December 31, 2015.

QUESTION:
Please provide a detailed description of the company's research and development programs related to customer-owned solar technologies and how these programs may impact the company's conservation efforts. Please provide any final reports or data to support your findings.

RESPONSE:
Please see the provided final reports for the five solar-related research projects' descriptions and findings. These projects were conducted as part of FPL's Renewable Research and Demonstration (RRD) pilot program.

- Solar Heat Pump Seasonal and Peak Demand Energy Analysis
- Solar Assisted Air-Conditioning Unit
- Solar Tracker
- Hybrid Photovoltaic Solar-Thermal
- Solar Hybrid Thin Film

FPL does not have plans at this time to modify its DSM efforts based on these technologies. Please note that customer and company names have been redacted from the reports so that they may be filed publicly.

QUESTION:
Please provide a detailed description of the company's research and development programs related to emergent DSM technology and how these efforts may impact the company's conservation efforts.

RESPONSE:
FPL's program for tracking and evaluating emerging DSM technologies is the Conservation Research and Development (CRD) program. CRD is an umbrella program under which FPL researches a wide variety of new technologies to evaluate their potential for reductions in peak load and energy as well as customer bill savings. Florida's climatic conditions are unique so the studies must incorporate the effects of our hot humid environment. Favorable evaluation results can lead to incorporation in FPL's DSM programs. Since 1995, FPL's CRD program has completed 36 technology evaluations and a number of these have resulted in new DSM programs or the addition of measures to existing programs, such as: Energy Recovery Ventilators; Demand Control Ventilation; and Residential Air Conditioning Duct Plenum Seal. Examples of other potentially viable candidates currently being considered are: variable speed pool pumps; hotel occupancy sensors; and residential heat pump water heaters.

FPL partners with the Florida Solar Energy Center and engineering departments of several Florida universities in its research projects. In addition, FPL participates in relevant co-funded projects through the U.S. Department of Energy ("DOE"). This co-funding enables FPL to participate in larger research projects at a fraction of the total cost.

From 2011 through 2015, FPL also managed the Renewable Research and Demonstration (RRD) pilot. The objectives and processes of the research activities within this program were the same as CRD, but the focus was solely on renewable technologies (see FPL's response to Data Request No. 2).

QUESTION:

On page x of the 1 2015 DSM Annual Report, FPL states that it did not achieve its Commercial winter peak demand goal.

a. Please describe the company's assessment for not achieving its Commercial - winter peak demand goal.

b. Is the company evaluating changes or modifications to any DSM programs to address this result? If so, please describe the company's considerations.

RESPONSE:

a. A significant portion of the Business Winter Peak Demand Goal was planned to be achieved with the Energy Recovery Ventilation (ERV) and Demand Control Ventilation (DCV) measures included in the Business HVAC program. FPL's 2015 DSM Plan significantly increased the rebates for these two measures. However, because program modifications, including these higher rebates, were implemented in November (as discussed in FPL's response to Data Request No. 1), it was too late in the year to influence the previously-projected customers' participation. FPL did achieve 2015 DSM savings within 15% of all the goals for the business and residential sectors and on a combined basis as well. The value of demand and energy savings for FPL's general body of customers is unrelated to whether the savings occur in the residential or business sector.
b. No. As discussed in subpart a, the variance from projections stemmed from the late-2015 implementation of program modifications which will not be a factor going forward. Additionally, FPL did achieve 2015 DSM savings within 15% threshold of all the Business sector goals, including that for Winter Peak Demand.

QUESTION:
For following programs, please describe the company's assessment on why it did not achieve the projected participation levels for 2015. Also, please describe any efforts the company is implementing to increase future participation levels.
a. Residential Load Management, page 3 of the 3/1/2016 DSM filing for 2015
b. Residential Low Income Program, page 7 of the 3/1/2016 DSM filing for 2015
c. Business HVAC Program, page 11 of the 3/1/2016 DSM filing for 2015
d. Business Lighting Program, page 12 of the 3/1/2016 DSM filing for 2015

RESPONSE:
For planning purposes in the 2015 DSM Plan, FPL developed participation projections on a program-level basis designed in the aggregate to achieve the Commission-approved overall Residential and Business sector-level MW and GWh goals. While these program-level projections represent an initial set of targets, which in the aggregate would meet the sector-level goals, normal market conditions can be expected to cause deviations from the originally-projected participation amounts. Therefore, FPL uses a portfolio management approach to balance these natural deviations (whether over or under) in order to ensure we meet the Commission-approved sector goals.

a. Residential Load Management – In an effort to most cost-efficiently manage to the residential sector goals, FPL temporarily reduced promotion of this program due to the very strong participation in the Residential Air Conditioning program.
b. Residential Low Income – Because program modifications were implemented in November, participation in FPL's new Energy Retrofit channel was not possible in 2015.
c. Business HVAC – Please see FPL's response to Data Request No. 4.
d. Business Lighting – Though lower than originally forecasted, 2015 achievements were approximately 20 percent above 2014. This represents natural fluctuations due to market conditions.

No further actions are planned. FPL achieved 2015 DSM savings within 15% of all the goals for the business and residential sectors, as well as on a combined basis, and expects to do so in 2016.

QUESTION:
Staff notes the participation levels in the Business Customer Incentive program increased considerably over previous years. Please describe the efforts taken by the company to increase the participation level in this program. (page 13 of the 3/1/2016 DSM filing for 2015)

RESPONSE:
Due to the customer-driven nature of the Business Custom Incentive (BCI) program, it is expected that there will be year-to-year variation in participation. Given that, 2015 participation was roughly in line with typical participation levels since 2010. However, 2015 participation was higher than the unusually low 2014 participation due to customer-related delays in finishing several of the 2014 projects which were then carried over into 2015.

<u>QUESTION</u>:
Please describe the company's process for monitoring any new energy efficiency standards or Florida Building Code requirements and modifying programs to reflect these changes if necessary.

<u>RESPONSE</u>:
FPL monitors the progress of new energy efficiency standards through participation in industry organizations, collaboration with peer utilities and by monitoring websites dedicated to appliance standards (e.g., Office of Energy Efficiency and Renewable Energy, Appliance Standards Awareness Project). The company monitors proposed Florida Building Code changes by regularly attending Florida Building Commission and the Energy Technical Advisory Committee meetings. Any changes in codes and standards are incorporated as modifications to FPL's DSM Program Standards based on when the changes take effect and submitted to Staff for approval.

QUESTION:
Please refer to page 22 of the company's March 1, 2016 filing. What did FPL learn from the three projects completed in 2015 in the Conservation Research and Development Program? Please provide any final reports from these projects.

RESPONSE:
Please see the provided final reports for the three research projects' findings.

- Smart and Learning Thermostats (2 individual reports for this project)
- Field Monitoring and Comparison of Rooftop HVAC Units Retrofitted with Variable Speed Drives at Retail Store
- AMI-Enabled Load Control Switch Lab Test Results

Please note that customer and company names have been redacted from the reports so that they can be filed publicly.

QUESTION:
Please refer to page 22 of the company's March 1, 2016 filing. What did FPL learn from the 12 projects completed in 2015 in the Renewable Research and Demonstration Program? Please provide any final reports from these projects.

RESPONSE:
The Renewable Research and Demonstration (RRD) Pilot Program's overall objectives were two-fold: (a) to increase awareness of mainstream solar technologies; and (b) to evaluate emerging renewable technologies and their applications. The 12 projects in question were "demonstration" photovoltaic (PV) systems installed in public venues from 2012 through 2015 to meet RRD's first objective of educating the public about PV. Examples included: Kennedy Space Center Visitor Center; Miami Museum of Science; Museum of Discovery and Science; Imaginarium Science Center; and Brevard, Palm Beach and Central Florida Zoos. Because these were not research projects, no reports were prepared.

QUESTION:

Please describe the process for ensuring low-income customers are aware of and have access to conservation programs offered by the company.

RESPONSE:

FPL uses a multi-prong approach to assist low income customers. The first prong is energy efficiency education. FPL's Residential Energy Survey, offered through field visits, by phone or online channels, provides education on actions customers can take to reduce their electric cost by participating in FPL's DSM programs and also by taking actions and implementing measures, many at low or no cost, which are not offered as part of FPL's DSM programs. The second prong is offering participation in FPL's Residential programs, such as Residential Load Management, etc. Over the years, participation rates for low income customers in FPL's DSM programs have been in approximately the same proportion as FPL's customer base as a whole. The third prong is participation in FPL's Low Income program which is targeted specifically at low income customers. Delivery of the Low Income program is through two channels. The first is through state Weatherization Assistance Provider ("WAP") agencies to which FPL provides rebates for certain energy saving measures as part of the total assistance they provide to their selected low income customers. The second is via FPL conducting Energy Retrofits in selected neighborhoods. FPL Energy Retrofits include promotional events followed by concentrated installations of DSM measures. FPL conducts an Energy Survey for each customer and installs, as appropriate, measures which address the main areas of energy use: weatherization (caulking, weather stripping and door sweeps); air conditioning (duct testing and repair, air conditioning unit maintenance and outdoor unit coil cleaning); and water heating (low flow showerheads, faucet aerators and pipe wrap).

QUESTION:
Please describe the overall advertising approach taken by the company to promote the current DSM programs to its customers.

RESPONSE:
FPL's advertising approach for DSM programs is key to driving customer awareness of its DSM programs, with a specific focus on getting customers to go to www.FPL.com for more information and to sign up for an energy survey. While FPL advertises throughout the year, DSM subjects are mostly communicated between May and November. This timing aligns with customers' interest in controlling consumption due to the impact of the warmer weather on their bills. FPL extends the benefit of advertising through public relations, communications issued through our corporate channels (print and digital) and special events/home shows. Another important aspect of FPL's advertising approach is that two campaigns are conducted, one directed at residential customers and a second focused on business customers.

QUESTION:
Please describe the company's approach to educate customers on potential self-initiated conservation opportunities

RESPONSE:
FPL uses its Residential Energy Survey and Business Energy Evaluation to educate customers on actions they can take to increase their energy efficiency and thereby reduce their electric cost. The surveys encourage customers to participate in FPL's DSM programs and also provide information on actions and measures they can implement themselves, many at low or no cost, which are not offered as part of FPL's DSM programs. Residential surveys are delivered through three channels: (1) Home Energy Survey ("HES"), which is a walk-through performed by an FPL representative at the customer's home; (2) Online Home Energy Survey ("OHES"), which is performed by the customer using FPL's online application; and (3) Phone Energy Survey ("PES"), which is performed by an FPL representative with information provided by the customer over the phone. Business surveys are delivered through two channels: (1) as a walk-through performed by an FPL representative at the customer's business; and (2) online.

FLORIDA SOLAR ENERGY CENTER®

FINAL REPORT

Solar Heat Pump Seasonal and Peak Demand Energy Analysis

FSEC-CR-1957-13

November 19, 2013

Submitted to:

Craig V. Muccio
General Office, GO
Florida Power & Light
9250 W. Flagler Street, DMO-GO
Miami, Florida 33174

Submitted by:

James B. Cummings
Charles R. Withers, Jr.
Houtan Moaveni
David Hoak

1679 Clearlake Road, Cocoa, FL 32922-5703 • Phone: 321-638-1000 • Fax: 321-638-1010
www.fsec.ucf.edu

A Research Institute of the University of Central Florida

FINAL REPORT

Solar Heat Pump Seasonal and Peak Demand Energy Analysis

FSEC-CR-1957-13
November 19, 2013

FPL PO# 2000052433; C# 4600002848
FSEC Project # 20128241

Submitted to: Craig V.
Muccio General
Office, GO Florida
Power & Light
9250 W. Flagler Street, DMO-GO
Miami, Florida 33174

Prepared by: James B.
Cummings Charles R.
Withers, Jr. Houtan
Moaveni
David Hoak

Florida Solar Energy Center
1679 Clearlake Road
Cocoa, Florida 32922

TABLE OF CONTENTS

List of Figures

List of Figures (cont.)

List of Figures (cont.)

List of Tables

List of Tables (cont.)

ACKNOWLEDGEMENTS

The authors would like to acknowledge assistance and guidance provided by Dave Click, Principal Research Scientist at the Florida Solar Energy Center, support and encouragement from Craig Muccio – project monitor from Florida Power and Light, and for financial support for this research from Florida Power and Light.

EXECUTIVE SUMMARY

A research project was conducted to evaluate the potential annual and peak electrical energy reduction resulting from the addition of a solar powered mini-split heat pump system to an existing home with central heat and cooling in the Florida Power and Light service territory. Experiments were performed to characterize the performance of a solar powered mini-split heat pump over a 12-month period and to determine seasonal and peak demand savings for both heating and cooling periods. The 1.5-ton mini-split heat pump, along with 2 kW of photovoltaic (PV) panels, 8 deep discharge batteries, a charge controller, and an inverter were installed in a 2000 ft^2 facility called the Building Science Lab building on the Florida Solar Energy Center (FSEC) campus. Instrumentation was installed to record solar and outdoor temperature, indoor temperature and relative humidity (RH), and electrical energy flows from PV, batteries, inverter, and utility grid to heat pump.

The mini-split heat pump was a 1.5-ton Fujitsu model with 19.2 SEER and 10.0 HSPF energy efficiency ratings. Cooling capacity of the system is variable and ranges from 7000 to 23,000 Btu/h. Heating capacity is variable and ranges from 7000 to 29,000 Btu/h. The mini-split has two modes of operation; 1) Standard and 2) Economy. In Standard cooling mode, the supply air temperature is about 46^{o}F when the return air is about 75^{o}F. This 29^{o}F temperature drop is unusually large for an A/C system. The cold coil (and cold supply air) yields excellent indoor RH control, with typical RH levels being 39-42% in the lab building (it is an unoccupied building without mechanical ventilation but had water vapor added to the space at a rate of about 8 pounds/day). In Economy mode, the compressor cooling capacity is reduced much of the time and the supply air was delivered typically at a temperature of about 52^{o}F. This supply air temperature is still sufficiently cold to provide good RH control, typically about 46% indoor RH on hot and humid summer days. It was found that Economy mode allows the system to operate considerably more efficiently and utilize the available solar energy considerably more effectively.

Experiments were operated variously with Standard and Economy modes, with 8 batteries and 4 batteries acting as storage, and with the mini-split operated from solar alone or from the utility grid. A 5-ton central ducted heat pump, with a SEER rating of approximately 11, operated as back-up to the mini-split heat pump when the space conditioning load could not be otherwise met.

Energy analysis. Electrical energy flows were monitored for the PV system, the charge controller, the batteries, the inverter to the mini-split heat pump, and the utility grid to either the mini-split or the central system.

Regression analysis was performed to characterize cooling and heating energy delivered to the Building Science Lab by the solar powered mini-split heat pump, by the mini-split heat pump when operating from the utility grid, and by the central ducted heat pump. While the experiments were carried out in the Building Science Lab, seasonal energy savings and peak demand reduction were determined for the MH Lab. The MH Lab is a highly instrumented 1600 ft^2 lab wood frame house, space conditioned by a split direct-expansion 3-ton SEER 13 heat pump having central air distribution through essentially leak free ducts in the attic space. MH Lab cooling and heating loads and heat pump performance characteristics had been characterized in previous experiments. Seasonal and peak energy consumption and savings from operation of the solar mini-split heat pump (and also from operation of the mini-split from the grid when the solar resource was depleted) were characterized for the MH Lab based on regression analysis equations and Typical Meteorological Year (TMY3) data from four Florida cities (weighted to characterize the FPL service territory).

Seasonal cooling savings. Cooling savings were characterized for a variety of experimental configurations versus the 3-ton SEER 13 central heat pump which serves the MH Lab. Annual cooling energy consumption for the SEER 13 system with attic ductwork (in all cases weighted for the FPL service territory) was 6204 kWh when operating by itself. When the solar-powered mini-split was operated, between 34% and 54% of the annual cooling load was satisfied by the solar heat pump depending upon the number of batteries used and whether Standard or Economy mode was employed (Table ES-1). Economy mode yielded about 24% greater annual cooling energy savings compared to Standard mode. The larger battery bank (8-batteries) yielded about 32% greater annual cooling energy savings compared to 4 batteries. The title of last row in Table ES-1 uses the term "100% mini-split" meant to indicate that this system is free to operate at all times even if solar generated power is not available. The central system was also still able to operate if the mini-split could not keep up with the load. Additional savings resulted when the mini-split operated on grid power after the solar resource was depleted. In total, when operated from solar and the grid, savings of 4442 kWh/y or 72% of space cooling energy that would have otherwise been consumed in the MH Lab house by the central system, are achieved.

Table ES-1

Annual cooling energy required by the [redacted] Lab SEER 13 central system and annual energy savings provided by the solar heat pump system using 5 different system configurations.

	Annual Cooling kWh	Annual Savings %
[redacted] SEER 13 Average Annual kWh	6204	0%
8 Battery Economy kWh Savings	3322	53.5%
8 Battery Standard kWh Savings	2683	43.3%
4 Battery Economy kWh Savings	2516	40.6%
4 Battery Standard kWh Savings	2101	33.9%
100% Mini-Split Economy kWh Savings[1]	4442	71.6%

[1] These savings assume that the mini-split also operates on the grid when the solar resources has been depleted, is limited, by assumption, to meeting no more than 80% of the space cooling load during hours when it operates on the utility grid, and the PV system uses 8 batteries.

Peak demand cooling savings. Cooling peak demand savings were characterized for a variety of experimental configurations versus the MH Lab central heat pump. Peak cooling demand for the hottest hours of the hottest TMY3 day for each of the four FPL cities was determined based on regression analysis. Generally, the solar heat pump is very effective at meeting cooling demand during the 3-5 PM peak period. Depending upon which of the solar heat pump configurations was active, peak demand savings ranged from 69% to 100% (Table ES-2). Peak demand savings were about 20% higher with Standard mode than with Economy mode. Likewise, peak demand savings were about 20% higher with 8 batteries than with 4 batteries. Maximum peak demand savings were 2.25 kW for the solar heat pump.

Table ES-2
Peak cooling energy required by the MH Lab SEER 13 central system and peak demand reduction provided by the solar heat pump system for 4 different system configurations.

	Cooling Peak kW	Peak Reduction %
[redacted] SEER13 Cooling Peak Demand	2.25	0%
8 Battery Standard Peak Reduction	2.25	100.0%
8 Battery Economy Peak Reduction	1.91	85.1%
4 Battery Standard Peak Reduction	1.91	84.9%
4 Battery Economy Peak Reduction	1.55	69.1%

Seasonal heating savings. Early in the heating evaluation period, it was determined that the solar heat pump system would not meet a substantial portion of the heating load with 4 batteries or under Standard control mode. Therefore, the heating experiments focused on operation with 8 batteries with Economy control mode. (Clarification: Economy mode yielded greater solar heating savings because the mini-split operated at about 34% higher efficiency in Economy mode versus Standard mode.) Heating savings were characterized for one experimental configuration (Economy with 8 batteries) versus the [redacted] Lab central heat pump. Annual heating energy consumption for the SEER 13 system with attic ductwork (in all cases weighted for the FPL service territory) was 260 kWh when operating by itself, based on the regression equations and TMY3 data. When the solar-powered mini-split was operated, 213 kWh (or 82%) of the annual heating load was satisfied by the solar heat pump (Table ES-3). In total, when operated from solar and the grid, 232 kWh/y or 89% of space heating energy that would have occurred by the central system, are saved.

Table ES-3
Annual heating energy required by the [redacted] Lab SEER 13 central system and annual energy savings provided by the solar heat pump system based on two operating modes.

	Annual Heating kWh	Annual Savings %
[redacted] SEER 13Aveage Annual	260	0%
8 Battery Economy Savings	213	81.9%
100% Mini-Split Economy Savings[2]	232	89.2%

[2] These savings are based on the assumption that the mini-split operating on the grid meets no more than 80% of the space heating load that would otherwise be met by the SEER 13 central system.

Peak demand heating savings. There was insufficient peak heating data to perform regression analysis. The research team examined a representative sample experimental peak demand periods on cold winter mornings and found that in no case did the solar heat pump operate at all during the 6-8 AM (EST) period. It is concluded, therefore, that the solar heat pump system was unable to achieve any peak demand savings on winter mornings, because the batteries could not carry sufficient electrical energy forward through a cold night to keep the system operating.

Lessons learned.

1. The tested solar heat pump system can meet over 70% of the annual space conditioning energy usage, but does not yield attractive economic returns, with typical payback on the order of 20 years when taking into account maintenance and periodic equipment replacement (for batteries, inverters, and mini-split) .
    a. On the other hand, the solar heat pump system does produce substantial cooling peak demand reduction which can be attractive to the utility.
    b. It also provides some space conditioning and potentially 120V alternating current service to the customer during periods when the grid goes down
2. Batteries are the weak link in the solar heat pump system. When subjected to nearly daily cycling from 45% to 90% state-of-charge (SOC), the batteries exhibited evidence of significantly diminished storage capacity by the end of 12 months.
    a. It is noteworthy that the battery manufacturer recommends that only about 50% of total battery storage capacity be used on a regular basis. However, even limiting battery discharge to about 50% of full capacity, the 8 AGM batteries used in this work had essentially failed by the end of 12 months of service.
3. The inverter proved to be more inefficient than originally anticipated (84% monitored efficiency). It will be important, for future stand-alone applications, to find higher efficiency inverters.
4. A bimodal inverter (able to both receive from and deliver to the central grid) is needed in order to use excess solar energy that is available on sunny days with limited space conditioning loads.
    a. Based on the findings of this research effort, it is recommended that an inverter for this type of stand-alone system be bimodal, that is having the capability to also send power to the electric utility grid. Converting this system to bimodal would make the overall yearly solar heat pump system operation more energy efficient because excess PV power that is not needed by the mini-split heat pump on mild autumn, winter, and spring days could then be put to good use (that is, the excess power could be sent back to the grid). As it was, there were a significant number of days when a significant portion of the available solar could not be used, because of limited cooling or heating load on the building.
5. An optimized stand-alone bimodal system design is proposed in this report that will make the system more cost-effective by delivering all of the available solar energy either to the mini-split or to the utility grid and by greatly extending the life of the batteries.

a. This bimodal system can operate in grid-integrated mode or as a stand-alone system. Compared to the "as-tested" system, there are two main differences.
b. The first difference is that the inverter can also deliver excess solar to the utility grid, allowing essentially all potential solar power to be put to effective use, either going to the solar heat pump or directed to the grid.
c. The second difference is that in normal everyday operation this bimodal system will limit the battery SOC range to only about 5% of full capacity. With this small cycling range, it is expected that battery life will increase by an order of magnitude. However, the system can still be effective as a stand-alone back-up system because when the utility grid goes down the batteries can be exercised across a larger range of SOC (to 50% or more of full capacity) in order to allow the system to deliver significant back-up solar power to the home.

Economic analysis summary and conclusions. Economic analysis was performed for a total of four solar heat pump configurations. Additionally, three other variations of the "as-tested" solar heat pump system were examined.

All seven of the designs had battery back-up with the exception of 1) a grid-tied solar system with a separate mini-split heat pump system (operating in parallel but not integrated); this was the baseline against which the other system designs were compared. Other examined designs included 2) the "as-tested" solar heat pump system, 3) the dc-powered solar heat pump system which was originally proposed but was unavailable for testing, and 4) an optimized bimodal ac-powered solar heat pump system. Three additional variations of the "as-tested" system also examined were; 5) operation of the system with 4 batteries versus 8 batteries, 6) operation of the system with a lower or a higher efficiency mini-split heat pump, and 7) operation of the system with expanded PV/battery capacity.

- Table ES-4 presents a summary of economic analysis results for the four primary solar heat pump system design variations (economic analysis of the three additional variations on the "as-tested" system are presented later in the report). While energy savings analysis derived from the year-long monitoring and regression analysis is available for the "as-tested" system, that analysis is not available for the other configurations. Therefore, the economic performance of the other configurations has been examined using a solar simulation tool called [redacted]. In order to provide internally consistent results, the analysis has also been performed for the "as-tested" system using the same [redacted] software. Therefore, analysis results from [redacted] for all four of the primary system configurations are presented in the table. The following information is presented in Table ES-4:Solar generated electricity
- Electrical energy savings that result from the operation of the mini-split using solar generated electricity as a result of avoided electrical energy use that the central ducted SEER 13 system would have used
- Electrical energy savings that result when the mini-split heat pump operates on the grid when the solar resource has been depleted. The savings occur because the mini-split is essentially two times as efficient as the central ducted system

- Gross and net system cost
- Payback period taking into account maintenance and replacement costs for batteries, inverters, and mini-split.

Table ES-4

Seasonal Savings and Payback Period for Four Solar Heat Pump System Designs Taking into Account Maintenance and Component Replacement Costs over a 20-year Period

	PV produced kWh/y	PV+M-S avoided kWh/y	Mini-split on grid savings kWh/y	Seasonal savings kWh/y	Gross system cost	Net system cost [1]	Payback period years
Grid-integrated	2968	3877	1274	6151	$11,200	$7840	12
"As-tested" [2]	2734	5386	539	5925	$15,200	$10,640	20
DC	2441	4247	-	4247	$12,860	$9002	22
Bimodal	2968	3877	1274	6151	$13,600	$9520	17

[1] after 30% Federal tax credits
[2] Economy mode with 8 batteries

All of the systems employed a mini-split heat pump. In all cases a substantial portion of the seasonal energy savings occurred as a result of the high efficiency of the mini-split heat pump. The ac-powered mini-split had a net efficiency that was 1.97 times that of the central SEER 13 ducted heat pump (which has an effective SEER of 9.75 after including 25% attic duct system losses). The dc-powered mini-split's net efficiency was 1.74 times that of the central system. The fact that in most cases all of the solar power was being delivered through the mini-split means that the mini-split can be thought of as an amplifier, in effect doubling (or nearly doubling) the delivered savings that the solar system would otherwise have provided. In the case of the baseline system (grid-tied system with the mini-split heat pump operating in parallel), the solar power is not actually delivered through the mini-split but can in effect be thought to be substantially delivered through the mini-split.

There is another source of seasonal energy savings apart from solar powering of the mini-split, and that is operation of the mini-split from the grid when the solar resource has been depleted. While the solar heat pump system meets about 54% of the heating and cooling load of the house ([redacted] Lab, in this case; see Table ES-1), the remaining space conditioning load can be substantially met by operation of the high efficiency mini-split operating from the utility grid. The "as-tested" solar heat pump system in our lab building had a relay installed that allowed the mini-split to switch seamlessly from solar to grid power when the solar resource was depleted. For this analysis, the research team assumed that 80% of the remaining heating and cooling load that had not been met by the solar heat pump would, in fact, be met by the mini-split operating off of the grid. The fact that the mini-split could provide the required space conditioning at approximately twice the efficiency of the central ducted heat pump meant that the energy represented by the remaining 46% of the yearly load not met by solar would then be effectively cut in half. As a result, about 72% of the energy use that would have occurred with the central ducted system was saved by the mini-split heat pump system when operating from solar <u>and</u> the grid.

This is a key point. While the 2 kW of solar panels can typically deliver about 2400 to 3000 kWh annually to end uses in a typical year (depending upon which system is being examined), the delivered energy savings (from avoided space conditioning energy consumption by the SEER 13 central, ducted system) increases to the 4200 to 6200 kWh per year range when tied in with a high efficiency mini-split.

In spite of the energy savings enhancement provided by the mini-split, the economic benefits are not particularly attractive strictly from yearly energy savings. For most of the examined systems, the payback period is on the order of 17-22 years. The grid-tied (baseline) system (2 kW of PV with a SEER 19.2 mini-split heat pump, but no batteries) has a payback of about 12 years.

The reader may have noticed that the predicted annual kWh savings of the “as-tested” system based on monitored data, regression analysis, and TMY3 data is about 25% lower than that predicted by the simulation tool [redacted]. Inevitably, measured data (with simplified modeling based on regression analysis) and complex modeling using [redacted] do not provide the same answers. There are too many variables to account correctly for all effects. Furthermore, models are only as good as the software developer and the data upon which the model was constructed and verified. The [redacted] modeled results tend to yield greater annual savings.

It would be difficult for the research team to point to any one item or group of items that explains the difference between these modeling approaches. However, based on the research team’s observations, it is likely that battery charging issues and load scheduling may contribute significantly to the modeled differences.

- In our 12-month experiments, the research team observed that the batteries go through three stages – BULK, ABSORB, and FLOAT. In BULK, the batteries are able to accept energy at a high rate and can accept all of the solar available from the PV panels. As State of Charge (SOC) approaches 90%, charging goes into ABSORB mode, and the rate of energy acceptance by the batteries is cut substantially, so that about 50% of the available solar may be thrown away while in this charging mode. When charging goes into FLOAT, perhaps 90-95% of the available solar is thrown away. It is uncertain whether the [redacted] model can fully account for the energy acceptance rate of the batteries that occurs in actual system operation, since these charging rates change from minute to minute as solar input and load output fluctuate in real time.
- Regarding load, the [redacted] model assumes a single, typical daily load profile for each day of a given month. This simplification may well miss important outcomes from the variability which occurs in real weather patterns. For example, in the month of March, real weather may include 6 days of cold weather, followed by other days when neither heating nor cooling is required, and then mixed with days of significant space cooling. While the solar heat pump system will provide certain savings results when exposed to the variability of real weather and building loads, the predicted system performance based on average daily load may yield different annual savings. It is

difficult to predict how load profile simplifications like this can affect the annual predicted space conditioning savings.

- Nevertheless, the authors feel that the modeling results across the four primary system configurations, and three variations on the "as-tested" system, are sufficiently representative of actual seasonal performance that the relative economic performance of the systems can be meaningfully compared.

In order to observe differences in annual energy savings, the [redacted] model was run for the various configurations based on a single TMY3 weather station (Melbourne). Melbourne was chosen to make comparison to the 12-months of our measured lab results (in Cocoa) most comparable. The objective of this exercise was not to provide service territory-weighted annual savings for the FPL service territory but rather to allow internally consistent comparison of each system to all of the others and to identify the relative economic performance of the systems. Following is a partial list of economic results and conclusions.

- All of the solar heat pump systems with battery back-up have a payback period on the order of 17-22 years. On the other hand, the grid-tied system with mini-split heat pump operating in parallel (but no battery storage) showed a payback period of about 12 years.
- A direct current-powered solar heat pump system is projected to have a similar level of cost-effectiveness compared to the "as-tested" system. On one hand, it would deliver slightly more solar space conditioning (because there are no inverter losses) and is estimated to be less costly. On the other hand, the ac-powered mini-split can provide additional annual cooling and heating energy savings by operating on grid power during periods when the solar resource has been depleted.
- A bimodal, optimized stand-alone solar heat pump system (as described earlier) would provide greatly expanded battery life and therefore greatly expanded functionality. On the other hand, as the system was modeled, it yields a longer payback period because the system expends more of its solar energy providing uninterruptable power to other end uses (i.e., computers, communications, refrigeration, and lighting) besides the mini-split, which unlike the high-efficiency mini-split, do not have the capability of amplifying the energy output of the solar system.

While cooling and heating savings do not make a compelling economic case for the solar heat pump systems (though the grid-tied solar heat pump system without batteries has a much shorter payback), cooling season peak demand savings is an attractive feature from an electric utility perspective, with fairly reliable 2.2 kW peak savings. If incentives are made available to the customer, the payback periods would be even more attractive. On the other hand, the systems with battery backup provide additional functionality which can offer significant value to the customer. The ability of the systems operating on alternating current to provide uninterruptable power to the house and power for both short-term and more extended grid power disruption can be seen as a major bonus. The ability of the optimized bimodal system to provide those functions and optimize battery life (which has been identified as major issue in this research project) will make it an attractive option for many consumers.

Strategies for Achieving Maximum Seasonal Energy Savings

During the 12-months of experiments, the research team made observations regarding how the solar heat pump system can be operated for maximum savings. Most of these observations relate to how operation in Economy mode yields substantial energy efficiency benefit.

Greater cooling energy savings can be achieved by operating the solar heat pump in Economy mode versus Standard mode, for three reasons.

1. In Economy mode, the supply air is significantly warmer, about 54^{o}F compared to 46^{o}F. Heat pumps operate more efficiently when they are pushing energy flows against a smaller temperature differential. In Economy mode, monitored cooling EER (Energy Efficiency Ratio) is 34% higher compared to Standard control mode when outdoor temperature is 82^{o}F (Figure ES-1). From the regression analysis equations, it can be calculated that the mini-split operates with 17.6 EER in Economy mode compared to 13.1 EER in Standard mode.
2. The fact that the supply air is about 8^{o}F warmer means that the heat pump in Economy mode is providing proportionately less latent cooling (less water vapor removal from the room air) and is expending more of its space cooling energy on lowering room air temperature (sensible cooling). It therefore meets the thermostat setpoint sooner.
    a. Instead of producing typical 40% indoor RH (which it does while operating in Standard control mode), it produces about 46% indoor RH while operating in Economy control mode.
        i. 40% indoor RH is significantly lower than is necessary for most applications (46% RH is sufficiently low for essentially all circumstances), and the energy used to draw the humidity down to the lower level is largely wasted. Humidity in the 38 - 40% range can lead to drying of skin and eyes, and can contribute to static electricity discharges.
        ii. One could however argue that a lower indoor RH can produce similar occupant comfort at a higher temperature, which means that the thermostat could be raised by say 1^{o}F with the lower RH. This would, however, require some thermostat adjustment on the part of the occupants, and it is uncertain that this sort of adjustment actually occurs in real homes.
        iii. Another way to say this is that in Economy mode the system is spending less of its energy on latent cooling (moisture removal) and more of its energy on lowering the space (drybulb) temperature. Since thermostats control based on room air temperature, higher equipment operating SHR leads to reduced space cooling energy use.
3. When the mini-split is in Economy mode, it draws about 600 W compared to about 1000W in Standard mode. The relevance of the lower power draw in Economy mode to system efficiency relates to how this power draw interacts with the batteries. The smaller power draw of Economy mode tends to keep the system operating for an extended period. By contrast, the larger power draw of Standard mode tends to trigger premature cut-out of the inverter. As a result, more of its operation time (when in Economy mode) occurs at night when outdoor temperatures are cooler and the system operates more efficiently.

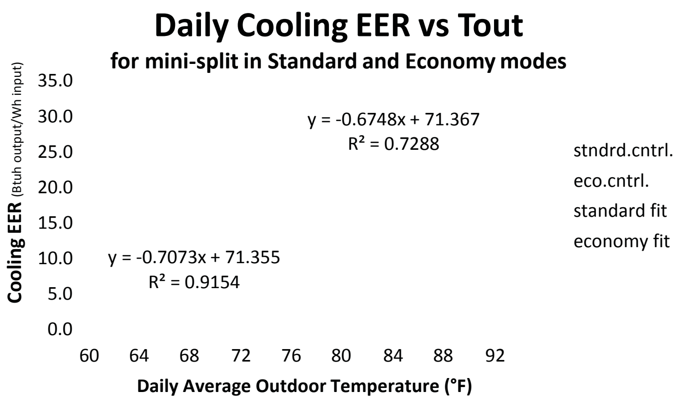

Figure ES-1. Monitored mini-split heat pump EER for Standard and Economy modes as a function of daily outdoor temperature with indoor temperature held constant at about 76°F.

Top Findings

This research project was primarily designed to measure the performance of a solar-powered mini-split heat pump with battery backup. Analysis was also performed for three additional system variations that were not tested in the lab based on simulations using the [redacted] software. The simulations evaluated the economic merit of other system variations, including grid tied, dc-powered mini-split, and bimodal inverter options. Based on the economic analysis, the top two options with the best return on investment were:

1. Grid integrated PV no battery backup (12 years)

This is the only option evaluated that did not have battery backup. Because there are no expensive batteries, this system requires much less investment, but provides no benefit during storm events where grid power may not be available.

2. Bimodal inverter with 4 battery (17 years)

This system utilizes a bimodal inverter, permitting PV power to go to the mini-split, to the batteries, or to the grid when excess PV power is available. This system also employs electrical energy exchange between the grid and batteries to keep batteries within a narrow range of higher SOC which would extend battery life. While this system has a considerably longer payback period compared to the grid-tied system with no batteries, it has the significant advantage of providing uninterruptable power supply during periods of short power outages and providing power back-up during more extended periods of power outage.

Other major findings were:

- Money spent on upgrading the efficiency of the mini-split is more cost-effective than adding additional PV capacity, with payback periods of 8 years and 20 years, respectively.
- Operating with 4 batteries instead of 8 is more cost effective, but yields less effective back-up power during grid outages, reduced summer peak reduction, and about 4 hours less solar cooling on an average summer day.
- Better charge controllers are needed to more effectively manage battery SOC for optimum battery life. Drawing charges down to about half capacity requires careful monitoring on the part of the customer.
- Repeated cycling of the batteries (of about 45% typically on a daily basis) brings about shortened battery life and reveals significant performance and economic weakness of the batteries in this type of solar heat pump system. A bimodal system which reduces the daily range of SOC cycling from a 45% limit to about a 95% limit is projected to greatly extend battery life.
- Table ES-5 presents peak demand and annual energy savings developed from monitored data and modeling based on regression analysis and TMY3 weather input. Summer peak demand savings from solar ranged from 69% to 100%. Winter peak demand savings from solar was 0% in all cases. On the other hand, when the mini-split was also enabled to operate off of the grid, peak demand reduction was 45%. Seasonal space conditioning savings ranged from 33% to 72%.

Table ES-5

TMY3 Projected Demand and Annual Energy Savings for the FPL Territory.

	Summer Peak Demand (kW)	Summer Peak Demand Reduction	Winter Peak Demand (kW)	Winter Peak Demand Reduction	Annual Cool+Heat kWh	Annual Savings
MHL SEER 13	**2.25**	**-**	**2.16**	**-**	**6464**	**-**
8 Battery Economy Savings	**1.91**	**85.1%**	**2.16**	**0%**	**3535**	**55%**
8 Battery Standard Savings	**2.25**	**100.0%**	**2.16**	**0%**	**2768 [2]**	**43%**
4 Battery Economy Savings	**1.55**	**69.1%**	**2.16**	**0%**	**2569 [2]**	**40%**
4 Battery Standard Savings	**1.91**	**84.9%**	**2.16**	**0%**	**2133 [2]**	**33%**
100% Mini-Split Economy Savings	**1.91**	**85.1%**	**0.98 [1]**	**45.4%**	**4674**	**72%**
Grid Tied No Batteries Savings	**2.25**	**100.0%**	**0.98 [1]**	**45.4%**	**5674[3]**	**88%**

[1] Due to limited heating season data, winter peak demand and demand savings are estimated based on the assumption that during the peak hour (34°F ambient temperature) the mini-split meets 70% of the heating requirement while the SEER 13 central ducted system meets 30% of the heating requirement.

[2] Due to limited heating season data, annual heating energy savings have been estimated for three of the tested configurations. Because space heating represents such a small portion of the total space conditioning energy in the heavily south-Florida weighted region (about 4%), even significant errors in these heating estimates would yield very small errors in annual space conditioning.

[3] Based on 4674 kWh/y saved through PV and MS economy + 1000 kWh/y from PV power to other household use or utility grid per [redacted].

1. INTRODUCTION

Renewable sources of energy, such as wind power and solar electricity, are being more widely implemented within homes. The power generated by these sources is in the form of direct current (dc). If this energy is to be used to power appliances within the home (or delivered to the electric grid), the dc current must, in nearly all cases, be converted to alternating current (ac), because nearly all household appliances use ac power. This conversion process requires a relatively expensive inverter and involves some loss in overall system efficiency. The research team was lead to believe that the inverter that was installed in this system would have a conversion efficiency of about 90 to 95%. Based on our monitored results, however, it was found that the actual operating inverter efficiency was 84% (see Appendix A for details on measured solar heat pump system component efficiency). To avoid the extra first cost and system inefficiency associated with dc to ac conversion, it may make sense to operate dc appliances within the home.

One home end-use that can be provided in the form of dc power is space heating and cooling. Dc-powered mini-split heat pumps have, in recent years, been introduced to the marketplace. One specific product ([redacted]) was available in the marketplace at the time that the original proposal was written in 2011 but not when the project was scheduled to start. More on why FSEC was unable to test [redacted] product and why an ac-powered solar heat pump was actually tested is presented in Section 2.

The company marketing the [redacted] product stated verbally that this heat pump would have energy efficiency equivalent to a SEER 17 rating (though no actual rating was available and no literature to that effect existed). The dc-powered unit would have a system efficiency equivalency of SEER 20.2 if compared to an ac-powered system with an 84% efficient inverter. The ac-powered mini-split actually tested in this project had a SEER rating of 19.2. Consequently, based on the SEER ratings of the dc- and ac-powered units, and the 84% inverter efficiency, the dc heat pump system would then have had an efficiency advantage of 5% compared to the ac heat pump.

2. PROJECT DESCRIPTION

This project originated when Florida Power and Light (FPL) requested that a solar powered heat pump be examined to determine seasonal and peak demand savings in a typical residential application. The Florida Solar Energy Center (FSEC) proposed that a dc-powered mini-split heat pump, along with photovoltaic (PV) panels and batteries, be installed in the 2000 ft^2 Building Science Lab located on the FSEC campus. A dc-powered 1.5-ton [redacted] mini-split had been identified for use in the experiments. When it was time to purchase the proposed [redacted] dc heat pump, it was learned that this product was between production cycles and it was not clear when it would be available. It was then decided, with approval from FPL, to test an ac-powered heat pump, using an inverter to convert the dc power to ac power. Since it was an objective of the project to examine the efficiency benefits of avoiding an inverter (use dc power from PV source to heat pump load), FSEC proposed to install energy meters that would monitor energy flows and allow characterization of inverter operating efficiency (as well as the efficiency of all other elements of the Solar Heat Pump system). An assessment of solar heat pump system component efficiency (and associated derate factors) is presented in Appendix A.

When discussing this change in scope of work, it was pointed out to FPL that a significant advantage of the ac system would be the capability of powering other household appliances (e.g., refrigerator, computer, lighting, etc.) in times of grid power outage. It was also pointed out that there would be other significant benefits of examining the ac-powered version of the solar-powered heat pump; 1) ac-powered mini-split heat pumps would likely have lower price and greater reliability (because of their high-volume production and opportunity to work out the bugs), 2) some mini-split heat pumps have SEER ratings as high as 27.2 (or 42% higher than that of unit tested in this project), 3) finding service personnel to make repairs would be easier, and 4) finding replacement parts would be more practicable. Furthermore, having a dc-to-ac inverter would allow transfer of electrical energy from the PV/battery system to the utility grid during periods when the PV system produces more power than is required by the heat pump. It should be noted that the type of inverter used in this project does not allow transfer of electrical energy to the grid, though this type of inverter is now available on the market.

2.1 Building Science Lab

The solar heat pump experiments were carried out in the Building Science Lab located on the FSEC campus (Figure 1). This 2000 ft^2 building has a slab foundation, concrete block walls with R-5 rigid board insulation, and 153 ft^2 of single-pane window glazing area. R-19 insulation batts are located on top of a suspended T-bar ceiling (2' x 4' panels), which is located 9.5 feet above the floor. The approximately 6-foot high space between the ceiling and the roof deck can be either vented or unvented (by opening up to 21 8"x16" vent openings, or not), and during these experiments was unvented. The nearly flat roof assembly has a dark roof membrane, about 2.5 inches of lightweight concrete, a low-emissivity (0.28 emissivity typical) reflective galvanized metal deck underneath the concrete, and no insulation (as stated before, insulation batts are located on the ceiling).

Figure 1. The Building Science Lab is a 2000 ft^2, highly instrumented lab building located on the FSEC campus.

The floor plan of the Building Science Lab has one large room in the central zone surrounded on the east by four spaces (offices, entry foyer, bathroom, and storage room) and on the west by two rooms (office and mechanical room). The central zone is fully open to unrestricted air flow and represents 50% of the total floor area. A single floor fan was located on the north side of the central zone and operated continuously to move air in a circular motion in the central zone. Doors to all of the rooms (except the mechanical room, bathroom, and storage room) remained open throughout the experiments.

A 5-ton central, ducted heat pump serves the building. The AHU is located in the mechanical room and the supply ductwork is positioned in the ceiling space. This central system has a SEER rating of approximately 11 based on performance testing.

Some internal loads were introduced into the space. One bank of lights remained operating at all times, drawing 720 W. The floor fan (55 W) and a computer combined with miscellaneous smaller electricity consumption (134 W) operated continuously. The batteries, charge controller, and inverter were all located in the southwest office; they give off a significant but unspecified amount of heat to the space. During the cooling season (but not the heating season), latent load (water vapor) was introduced to the space by means of a positive displacement pump and a mist-generating humidifier. This humidifier, which has a fan that moves about 400 cfm, throws small water droplets into the air which then evaporate, adding water vapor to the air. A positive displacement pump delivers water to the humidifier continuously at a rate of 8.4 pound/day. The evaporation of this amount of water represents 368 Btu/h of sensible space (evaporative) cooling. By comparison, the 63 W of humidifier fan power represents 215 Btu/h of space heating. So on a net basis, the humidifier provides 153 Btu/h of sensible space cooling, equal to 1.3% of a ton of continuous cooling.

The Building Science Lab has a measured airtightness of 4.6 ACH50, meaning that it is of approximately average airtightness compared to typical new Florida homes. Tracer gas decay tests were performed, and it was found that typical natural air infiltration rate (natural means air infiltration driven by wind and temperature differential) was 0.28 ach (air changes per hour), which converts to about 80 cfm of air exchange with outdoors. No intentional ventilation was provided to the space.

2.2 The Stand-Alone Solar Heat Pump System Design

It is common practice when designing a PV system to first review the total electricity usage of the building. This provides insight into what size of PV system will be compatible with the application. This electricity usage and cost data for the building is then typically reviewed to ensure that the system would not produce more than the expected load would consume on a month-to-month basis. Most stand-alone systems are inherently more complex, with more complicated interactions between components, than regular grid-interactive PV systems. The stand-alone PV system sizing is directly proportional to the heat pump load as it requires a balance between energy generation and energy demand. The system design is an iterative process until the system output matches the load requirement. In common practice, a stand-alone PV system is designed to meet the average daily load, which in this case is for space cooling and heating from a mini-split heat pump. Installing a larger system will result in considerable excess solar power generation on days with little or no space conditioning load, which would result in considerable PV-generated electricity being thrown away. If the stand-alone system has the capability of selling excess electricity to the grid, then there is little downside to a larger system size. An optimized, bimodal solar heat pump system is proposed in Section 8 which incorporates bimodal electrical energy flow (from the grid and to the grid) and avoids stranded solar electricity.

As stated earlier, the solar heat pump experiments were carried out in the Building Science Lab. This 2000 ft^2 facility has a peak cooling load of about 2 tons. [redacted] mini-split heat pump has a nominal capacity of 1.5-tons but maximum capacity of 1.92 tons (23,000 Btu/h). The nominal capacity of the mini-split heat pump, namely 1.5 tons, was selected due to the fact that the original solar powered dc heat pump (brand [redacted]) had a nominal capacity rating of 1.5 tons. As it turns out, this was a fairly appropriately size for the Building Science Lab. At its maximum capacity, it is very nearly able to meet the cooling load of the building on the hottest days.

Selecting an appropriate PV system size is a multiple step iterative process. First, a simplified hourly load profile for a typical day for each month was developed for the mini-split heat pump. Required battery capacity, which is defined as the product of the current in amps (A) multiplied by the number of hours the current is flowing, is calculated by dividing average daily electrical load by the nominal inverter efficiency, nominal direct current system voltage (24 V), allowable depth of discharge, and battery discharge-rate derating factor. For many stand-alone solar systems, an autonomy factor is taken into account. However, since additional power could be imported from the grid during periods of below average sunshine, this step was neglected in the design of the “as-tested” system.

Deep-discharge lead acid batteries were selected for the system as they are the most appropriate for the amount of required storage and the frequency of cycling that would be occurring in this system.

- The number of battery strings was determined by dividing the required battery capacity by the nominal battery capacity (305 Ah) supplied by the manufacture. In order to size the PV array, the array peak current was calculated from the simplified average daily load divided by the nominal battery efficiency, nominal system voltage (24 V), a derating factor (0.95), and monthly peak sun hours for Cocoa.
- The number of PV module strings was determined by dividing the array peak current by the nominal PV module maximum power current (provided by the manufacturer).
- Finally, the number of PV modules to be installed in series was calculated based on the maximum array voltage, which needs to be higher than the battery bank voltage (in order to charge the batteries). It should be noted that the system was designed to optimize energy yield and maximize the levelized cost of energy produced throughout the system’s lifetime. A widely used software tool, [redacted], was used to simulate annual system performance, using TMY3 hourly weather data for Cocoa. A description of the selected components for the PV system is included here as follows.

2.2.1 Photovoltaic Array

Several PV module types were available for selection. Monocrystalline PV modules have the highest efficiency. Amorphous PV modules are also available. However, since their efficiency is about 3 times lower than that of the polycrystalline, a good deal of roof surface area, mounting hardware, and installation labor is required. Polycrystalline PV modules represent a reasonable compromise between efficiency and cost. Eight (8) [redacted] modules [redacted]) were selected for this system. Each module is rated to produce 250 W under standard test conditions (STC) of 1000 W/m^2 and 25^{o}C (77^{o}F). Figure 2 shows the I-V (current-voltage) curves for the selected [redacted] modules at 25^{o}C cell temperature.

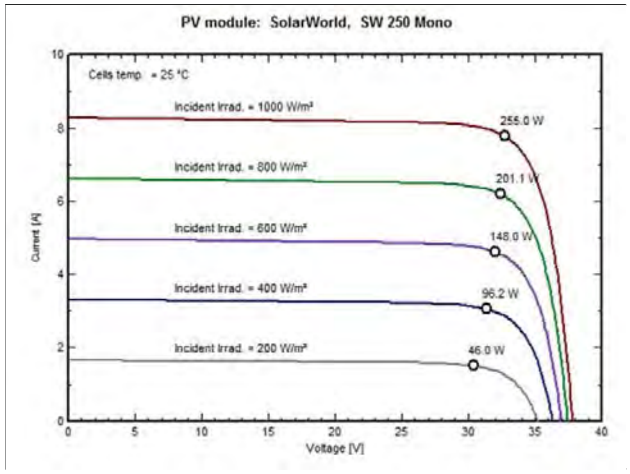

Figure 2. [redacted] I_V Curves at 25°C cell temperature.

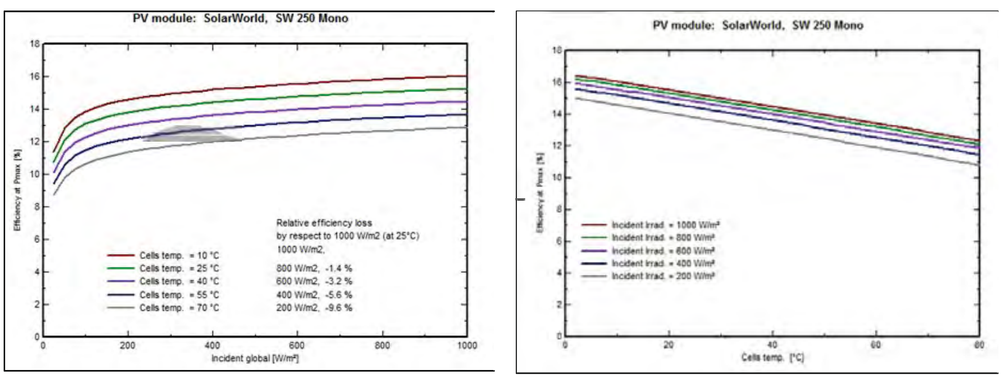

Figure 3. [redacted] module efficiency versus irradiance and cell temperature.

Each PV module has a surface area of 1.593 m^2 (17.14 ft^2) and combined, the 8 modules have a total surface area of 12.74 m^2 (137.1 ft^2). The PV array nameplate capacity at Standard Test Conditions (STC) is 2 kWdc and was installed in four strings of two modules in series. Each module is rated to produce 250 W under STC of 1000 W/m^2 and 25°C (77°F). They are also rated at 183.3 W under 800 W/m^2 and 25°C (77°F). Under STC, they have a rated efficiency of 14.91%, which means that 14.91% of the solar energy striking the top surface of the module is converted to electrical energy. However, typical PV panel temperature conditions are considerably warmer than 77°F, even as high as 150°F. At warmer temperatures, PV system efficiency declines. A formula can be used to adjust typical PV panel electrical output as a function of panel temperature and the module temperature coefficient of power (MTCOP). Percent change in PV module output = (MTCOP) x (T_{module} – 25°C), with the value of MTCOP = -0.5% for typical mono- or poly crystalline cell modules. During the peak sun hours of September 3, 2012, for example, the panel reached a temperature of 145°F, as can be seen in Figure 4. Based on this temperature and the MTCOP of -0.5%, the calculated panel efficiency at this peak temperature would be 12.09% (0.811 x 14.91% = 12.09%). While the rated capacity is 250 W, the actual operating capacity at this peak summer hour would be 203 W under full sun and 145°F panel temperature.

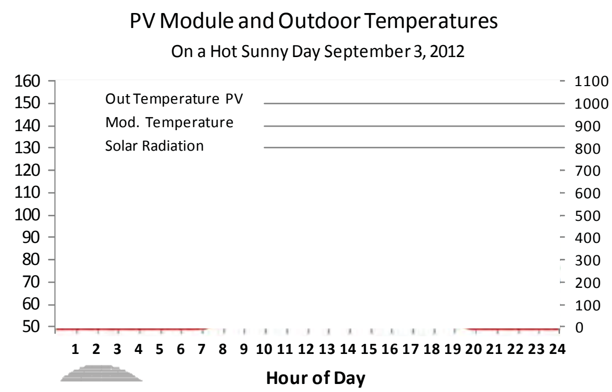

Figure 4. Ambient air temperature, PV module temperature, and solar radiation on a typical summer day (September 3, 2012) with near full sun.

However, panel efficiency is considerably higher than 12.09% for average summer conditions. Table 1 provides an average daily profile of ambient temperature, PV module temperature, and solar radiation for the 32-day period of August 3 through September 3, 2012. The solar radiation-weighted average PV module temperature turns out to be 114.4°F for this period. PV module efficiency reduction is calculated, then, to be 13.36% during typical summer weather or 10.4% lower than the nominal rating.

For this project, all PV source and output circuit wiring was secured to module frames and mounting rails. Each circuit of the PV modules was protected by an inline overcurrent protective device of proper voltage and current rating (15 A). The PV array was grounded using appropriate grounding clips. The PV modules were installed on pre-fabricated tilted roof units, sloped at an angle of 20 degrees, and oriented to the south (Figure 5). This tilt is fairly typical of many older homes in Florida. Newer homes often have a steeper roof which would tend to decrease solar electricity production in the summer and increase production in the winter.

Table 1

A composite of average measured daily outdoor temperature, PV module temperature, and solar radiation for the period August 3 – September 3, 2012. The average panel temperature during this hot summer period is about 126°F at peak temperature and 114.4°F for the solar radiation-weighted average PV module temperature for this period.

	Hour	T ambient	T pv-module	SOLAR
		°F	°F	W/m^2
	1.00	77.21	74.16	0
	2.00	76.74	73.74	0
	3.00	76.31	73.32	0
	4.00	75.90	73.08	0
	5.00	75.51	72.79	0
	6.00	75.06	72.35	0
	7.00	74.95	72.25	0
	8.00	75.76	73.67	32.93
	9.00	78.97	79.60	119.88
	10.00	82.83	98.24	372.00
	11.00	85.71	115.38	565.70
	12.00	87.27	122.85	646.16
	13.00	88.18	126.84	705.24
	14.00	88.49	125.63	689.10
	15.00	87.92	119.64	618.29
	16.00	86.26	111.65	512.32
	17.00	85.11	104.33	387.27
	18.00	83.48	94.83	234.51
	19.00	81.75	86.21	108.44
	20.00	80.15	79.81	27.91
	21.00	79.07	76.68	9.80
	22.00	78.55	75.81	0
	23.00	77.98	74.92	0
	24.00	77.55	74.34	0
AVG		80.70	89.67	209.56
SUM				5029.55

Figure 5. Building Science Lab building with 8 PV panels in the foreground. The outdoor unit of the 1.5-ton mini-split heat pump can be seen along the south wall of the building. Batteries, charge controller, inverter, and 8 batteries are located in a lab building room closest to the PV panels.

2.2.2 Inverter and Charge Controller

The inverter needs to converts dc power to ac power in sufficient quantity up to the mini-split's maximum power draw. In cooling mode, the mini-split's maximum draw is rated at 1350 W. In heating mode, the maximum draw is rated at 1800 W. "Maximum Power Input" for the mini-split, however, was listed on the product specification sheet as 3.01 kW in both cooling and heating modes. Because of uncertainty regarding the actual full power draw, the research team selected a 4.0 kW inverter. The inverter was capable of providing a high percentage of its full rated output into one phase for extended periods of time, without allowing the voltage on the unloaded leg to spike. The inverter, which was purchased and installed as part of the solar heat pump system, was a Midnight Solar, Inc. Magnum MNEMS4024PAECL150 ($3528.57 from Midnight Solar, Inc., Arlington, VA, phone 360 403-7207). It is a pre-wired combination system that includes a 4.0 kW inverter and the PV/battery system charge controller. It has the capability of delivering 240V AC power to a load (in this case, a mini-split heat pump) from a 24-V bank of batteries and also directly from the PV system. It does not have the capability to deliver power from the solar system to the grid. The charge controller size and model was determined based on array configuration and specifications.

2.2.3 Batteries

Lead-acid batteries are the most commonly used type for small-scale stand-alone PV systems. The battery bank designed and installed for this system contained 8 deep-discharge lead acid batteries ([redacted], Solar Battery Manufactured [redacted] of the absorbed glass mat (AGM) type. Sizing of the battery bank was determined by the inverter input voltage (24 V) and PV-output storage requirements. The characteristics of [redacted] batteries are per manufacturer literature:

- They are not vented and are maintenance free.
- They produce relatively little hydrogen, but still must have some ventilation.
- They use much less electrolyte (battery acid), are considered "Non-spillable", and can be shipped "[redacted] by any means".

There are three typical deep-discharge lead acid battery types; flooded, gel, and AGM. There are advantages and disadvantages to each type (Table 2).

Table 2
Advantages and disadvantages of three types of deep discharge batteries.

	Flooded	**Gel**	**AGM**
ADVANTAGES	Lowest cost	Longer life	[redacted] transport requirements Resistant to overcharging problems
DISADVANTAGES	Spillage danger Vapor discharge	Overcharging can "fry" the battery	More costly Fewer cycles

According to Trojan Battery Company (the largest manufacturer of deep-cycle batteries and which manufactures all three battery types), deep-cycle flooded batteries have the lowest cost, provide the most cost-effective storage solution, and "are very versatile and should be the first choice for renewable energy systems where maintenance can be carried out and ventilation is available." Proper maintenance is critical, especially keeping the hydrogen production well ventilated and adding distilled water to keep the plates submerged on a regular basis.
[redacted]

Gel-type batteries have a higher cost but offer longer life. They are, however, more vulnerable to damage from overcharging.

The AGM battery type, while the most expensive, is considered by many to be the most compatible with residential applications because of greater safety and fewer maintenance requirements. Furthermore, there is less risk of damaging [redacted] batteries compared to flooded or gel types from overcharging. Nevertheless, the homeowner must still take a number of battery maintenance steps to achieve good battery life, even with the [redacted] batteries.

The battery bank nominal capacity was 14.64 kWh. The price paid for these 8 batteries was $2638. The batteries were placed in an enclosure separate from other PV system components and vented to the room using a muffin fan.

2.3 Solar Heat Pump

The solar heat pump system consists of a Fujitsu 18RLXFW 1.5-ton mini-split heat pump, 8 solar panels (250 W x 8 = 2000 W nominal capacity), 8 batteries, a charge controller, and an inverter. The batteries have total storage capacity of 14.64 kWh. However, only about 6.5 kWh of storage was available in the typical daily operational range of 45% to 90% SOC (state of charge represents the amount of energy stored in the batteries at a given time compared to the maximum amount that can be stored in the batteries). In order to enhance control of the heat pump, a timer with relay was installed to activate or deactivate the inverter power (to the mini-split) to prevent short-cycling of the mini-split heat pump and provide extended periods for solar charging of the batteries. The timer was typically set to shut off inverter power to the mini-split for the period from 7 AM to 1 PM during the cooling season, allowing the battery bank the opportunity to reach substantially full charge by the time the mini-split would start operation at 1 PM. Later in the experiments, when the size of the battery bank was cut in half (from 8 to 4 batteries) to examine an alternative system configurations, power to the mini-split was initiated earlier so that the system was typically starting at about 9 AM. During the heating season, several different timer schedules were used.

A relay was also installed which would allow transfer of the mini-split from the inverter (solar power) to utility grid power. This configuration, when selected, would permit the mini-split to continue to operate for the remainder of the day on the utility grid after the solar resource had been exhausted. This has the advantage that the homeowner could then use the high efficiency mini-split to displace much of the space conditioning that would normally be done by the central system. This option would be available to the homeowner only if the installed solar heat pump system used an ac mini-split. If a dc-powered mini-split were installed, there would be no option to run the mini-split off of the utility grid.

2.4 Three Experimental Configurations

Three experimental configurations were examined.

1. BASELINE OPERATION
    a. Cooling season; the mini-split was operated (enabled) with power from the inverter for up to 18 hours per day from 1 PM till 7 AM, depending upon whether there was enough PV power available for the entire period. The 5-ton central heat pump was operated for the hours of 7 AM till 1 PM, plus any additional hours during which the solar power was no longer available. This 7 AM to 1 PM period was also a period in which the batteries could be charged from approximately 45% SOC to approximately 90% SOC (assuming bright sun but less if the day had more cloud cover).
    b. Heating season; the mini-split was operated (enabled) with power from the inverter for up to 19 hours per day from 5:30 AM till 12:30 AM (with some variations prior to settling on this schedule). Actual solar powered operation time, as was also true for cooling, depended upon whether there was enough PV power available for the entire

period. The 5-ton central heat pump was operated for the hours of 12:30 AM till 5:30 AM, plus any additional hours during which the solar power was depleted. The period of actual operation varied depending upon the amount of solar radiation and outdoor temperature (colder days created more heating load and earlier heat pump shut-down). Charging of the batteries from approximately 45% SOC to approximately 90% SOC (assuming bright sun and less if more cloudy) would occur during the period of sun-up to sun-down since there would typically be limited heating load during the sunny hours of the day, especially after 10 AM.

2. 100% MINI-SPLIT OPERATION
   a. Cooling season; in this configuration, the operation was identical to that of the BASELINE cooling experiments except that the mini-split system would switch over to the FPL grid and continue to operate in place of the central 5-ton system.
   b. Heating season; in this configuration, the operation was identical to that of the BASELINE heating experiments except that the mini-split system would switch over to the FPL grid and continue to operate in place of the central 5-ton system.
3. 100% 5-TON OPERATION
   a. Cooling season; generally once every 5 to 10 days, the batteries were allowed to go through their full charging cycle (BULK, ABSORB, and FLOAT). To enable this full charging cycle, the mini-split was disconnected from the solar/batteries/inverter. In most cases, the 5-ton heat pump was operated (more specifically, enabled) 24 hours per day during those battery full-charge periods.
   b. Heating season; generally it was not necessary to force the mini-split off in order to allow the batteries to go through their full charging cycle (BULK, ABSORB, and FLOAT), so therefore it was unnecessary to go into 100% 5-ton mode. The reason this was different from the cooling season is that during normal operation heating would typically only last for 3 to 5 days at a time, after which the batteries could then naturally go to full charge.

The experiments described above were carried out over a 12-month period. Data was collected for both the cooling and heating seasons in 15-minute time increments and stored on the FSEC central computer system.

3. SOLAR HEAT PUMP SYSTEM DISCRIPTION AND OBSERVATIONS

A number of general observations can be made regarding the solar heat pump system which consists of the mini-split heat pump plus photovoltaic panels, charge controller, batteries, and inverter.

3.1 The Mini-split Heat Pump

The [redacted] mini-split heat pump has a nominal capacity of 1.5-tons. It consists of an outdoor unit (compressor and condenser coils) and an indoor fan coil unit (FCU). The FCU was located outdoors along the south wall of the large central room. It has oscillating vanes to throw air side to side. Horizontal vanes adjust themselves to throw air upward during cooling operation and downward during heating operation.

This heat pump has a SEER rating of 19.2 and HSPF (Heating Season Performance Factor) of 10.0. It is a variable capacity system. While it is nominally rated at 18,000 Btu/h for cooling and 21,600 Btu/h for heating, its capacity can vary from 7000 to 23,000 Btu/h in cooling and 7000 to 29,000 Btu/h in heating. Therefore, maximum cooling and heating capacities are 28% and 34% greater than the nominal rating. During much of the year, the mini-split does not cycle off but rather modulates its cooling or heating capacity in response to a temperature differential between room temperature (as detected by the return air sensor) and the space temperature thermostat set- point. So, unlike a fixed-capacity system which will cycle on and off throughout the day, the mini- split may remain on continuously for 24 hours per day on typical warm to hot summer days. During cooler spring and fall days, however, the mini-split (in cooling mode) is likely to cycle on and off during portions of the day, especially during the cooler overnight hours.

The standard mini-split thermostat is a hand-held unit that looks a lot like a TV remote and can be located anywhere in the room. It operates in tandem with a temperature sensor located inside the return air plenum of the FCU. The thermostat location, therefore, does not impact space temperature control since the sensor detecting room temperature is located in the return plenum. The system can also be installed with a more standard, wall-mounted thermostat (connected by wire to the mini-split) which we purchased and installed. Contrary to our expectations, however, it provided little additional functionality and actually used the same temperature sensor located in the return plenum of the FCU. Because the thermostat sensor is not (under normal circumstance) directly exposed to the room air, the FCU cycles the fan on (if the mini-split has cycled off) on a regular basis (15-20 times per hour) in order to sample room conditions at a low fan speed (at about 50% of normal low-speed operation).

During periods of low cooling load (such as on mild spring or autumn days), when the cooling load falls below 7000 Btu/h, the mini-split will cycle on and off. In order to better control the system, the research team pulled the temperature sensor out (about 15 inches out) of the FCU return so it would more readily detect room space temperature. With the sensor now located outside of the FCU, it would no longer in theory be necessary for the FCU fan to cycle on to detect room temperature. However, even though the temperature sensor was relocated outside of the FCU, the research team was unable to disable the cycling of the FCU fan, so this fan cycling continued to operate during all periods when the FCU was off.

This fan cycling has an important implication for indoor relative humidity (RH) control, for periods of low cooling load, such as during warm/humid days in autumn. With the system off, the fan cycles on for about 25-30% of the time (at a low fan speed) sampling room air temperature, but in doing this it evaporates moisture from the coil and drain pan whenever the fan moves air through the FCU. The evaporated moisture returns to the room increasing indoor RH. In actual practice, however, this fan cycling does not represent a large problem. Because the mini-split can operate continuously down to as little as 7000 Btu/h, there are few daytime hours during the cooling season when this fan cycling (with no compressor operation; so the coil is warm) occurs. This most commonly occurs during nighttime periods during the autumn and spring seasons. It can, however, reduce the ability of the mini-split to control indoor RH during those periods, because of this moisture evaporation.

The [redacted] mini-split has two modes of operation; 1) Standard and 2) Economy. In Standard cooling mode, the supply air temperature is about 46°F when the return air is about 75°F. This 29°F temperature drop is unusually large for an A/C system. The cold coil (and cold supply air) yields excellent indoor RH control, with typical RH levels being 39-42% in the lab building (it is an unoccupied building but had water vapor added to the space at a rate of about 8 pounds/day). In Economy mode, the compressor cooling capacity is reduced much of the time and the supply air was delivered at a temperature of about 52°F. This supply air temperature is still sufficiently cold to provide good RH control, typically about 46% indoor RH on hot and humid summer days. It was found that Economy mode was a much better choice for operation with the solar system (in terms of efficiency), allowing the system to operate considerably more efficiently and allowing it to operate up to 70% more hours on the available solar energy.

3.2. Inverter and Charge Controller

Based on the findings of this research effort, it is recommended that an inverter for this type of stand-alone system be bimodal, that is having the capability to also send power to the electric utility grid. Converting this system to bimodal would make the overall yearly solar heat pump system operation more energy efficient because excess PV power that is not needed by the mini-split heat pump on mild autumn, winter, and spring days could then be put to good use (that is, the excess power could be sent back to the grid). As it was, there were a significant number of days when a significant portion of the available solar could not be used, because of limited cooling or heating load on the building.

3.3 Batteries

Batteries are a key element of a stand-alone system or even of a grid-integrated system that can operate in a stand-alone fashion when the utility grid goes down.

3.3.1 Battery State of Charge and System Cycling

As indicated earlier, SOC represents the amount of energy stored in the batteries at a given time compared to the maximum amount that can be stored in the batteries. SOC then varies from 0% to 100%. It is the nature of batteries in general and these batteries in specific that the full range of stored energy is not available for use on each cycle. To be more accurate, it is not so much that the full stored energy is not available, but rather that draining the batteries below a specific level on a repeated basis will shorten the life of the batteries. The manufacturer recommends that it "is always good to have twice the battery capacity that an application requires. This will promote long battery life and also reduce the amount of recharge time" (source: [redacted] product brochure document No. [redacted]

Therefore, during the cooling season, the typical daily cycle would take the batteries from about 90-95% SOC down to about 45% SOC. Thus only 45-50% of the full battery capacity was being regularly used.

It might seem surprising that 90-95% was the typical upper level SOC instead of 100%. This occurs for a practical reason related to the way that (the rate at which) the batteries are charged. There are three modes of charging; BULK, ABSORB, and FLOAT. Most of the time, charging occurs in BULK mode. During our experiments, it was found that in BULK mode, all of the available PV energy could be delivered into the batteries. This is a rate issue. The amount of PV power being generated under full sun could be delivered into the batteries while in BULK mode. (It is also relevant to note that during the cooling season, a significant portion of the PV power is shunted directly to the inverter and on to the mini-split, bypassing the batteries. During the heating season, by contrast, most of the PV power delivered to the mini-split had to be stored in the batteries during sunny hours and then delivered to the mini-split during the overnight and early morning hours.)

However, as SOC approaches 85-90%, the batteries go into ABSORB and then FLOAT modes, where anywhere from 50% to 95% of the available solar is discarded as the batteries go through their final stages of charging. The reason that 50% to 95% of the available solar is thrown away during ABSORB and FLOAT modes, respectively, is because the rate at which energy is delivered into the batteries is substantially slowed (for ABSORB mode) and greatly slowed (for FLOAT mode). This is one of several ways in which batteries are the weak link in the solar heat pump system, namely that it is necessary to fully charge the batteries on a regular basis and when doing so, a significant portion of the solar is thrown away.

Periodic full charging is important to the health of the batteries. The manufacturer states that it "is recommended that batteries be recharged to 100% at least every 5-10 cycles", which for this application means once every 5 to 10 days. While we might have achieved 90-95% SOC on most sunny days, the research team also took steps to push SOC to 100% every 10 days or so.

- During the period from late-October through early May, getting the batteries to 100% SOC on a regular basis is typically not a problem for two reasons. First, periods of substantial heating are intermittent, and the milder days in-between require less heating power and therefore commonly allow the batteries to reach 100% charge. Second, during the warmer periods of November through April, when some cooling is needed, there are intermittent days with smaller cooling loads which allow for full battery charge even while the mini-split system operates a portion of the time.

- During the period of May through late-October (the primary cooling season), more attention needs to be paid to intermittently achieving 100% SOC. Throughout most of this period, all of the available PV power can be (will be) consumed by space cooling (in a properly sized solar heat pump system), and so without intervention, the battery would rarely reach 100% SOC. It becomes necessary, therefore, to interrupt the normal system operation and force the charging process to go into ABSORB and then FLOAT modes, thus achieving 100% SOC. This forced intervention results in periods of discarded solar energy, since the ABSORB and FLOAT modes necessitate throwing away significant amounts of solar energy during those portions of the charging cycle. Therefore, good battery maintenance practice requires some scheduling of battery full-charge periods and by necessity some waste of solar energy.
    - In our experiments, the research team dealt with this during the primary cooling season by shutting down the mini-split for a day once every 7 to 10 days and allowing the batteries to be charged to 100% SOC while the central 5-ton A/C system was used to condition the space.
    - In our typical daily operation schedule, we shut down the mini-split from 7 AM till 1 PM (by means of a relay controlled by a timer), during which time the battery would often go from about 45% SOC to about 90% SOC.
    - An alternative approach to achieving 100% SOC could also be implemented, which would use power from the electric utility grid to charge the batteries overnight. This approach might provide some advantages to the electric utility since it would allow it to sell electricity to the customer during night hours (perhaps controlled by the "On-Call" system) when excess capacity is often available, thus shifting system demand from daytime hours to nighttime hours. The FSEC research team did not explore this option and some experimentation would likely be needed to optimize the scheduling of these charging patterns.
- Once the batteries reach about 85-90% SOC, they go into the ABSORB cycle which typically operates for 2 hours (this length of time is user selectable), then goes into FLOAT for a period of about 2 hours.
- It was not clear whether the batteries need to get to the full 100% SOC to maintain good battery health, or whether getting to say 98% SOC achieves essentially the same outcome.

It should be noted that the inverter/charge controller used in these experiments has a SOC indicator, but its accuracy is sufficiently poor that the user knows very little about the actual SOC. Therefore, throughout the entire project, the research team did not know actual SOC.

There is an exception to this statement. SOC can be accurately known when the battery is in "resting" state that is when no energy is being delivered into the batteries or being drawn from the batteries. During the hotter days of the year (high of say 84°F or above), battery energy (for the 8-battery bank) is typically depleted sometime during the night, often between 12 AM and 4 AM, at which time the mini-split turns off. During the period between mini-split turn off and sunrise, no power flows into or out of the battery bank, and the batteries are therefore resting. A battery voltage reading taken when the batteries are resting provides an accurate reading of SOC. Data provided by the battery manufacturer (Figure 6) allows an accurate determination of SOC based on battery voltage.

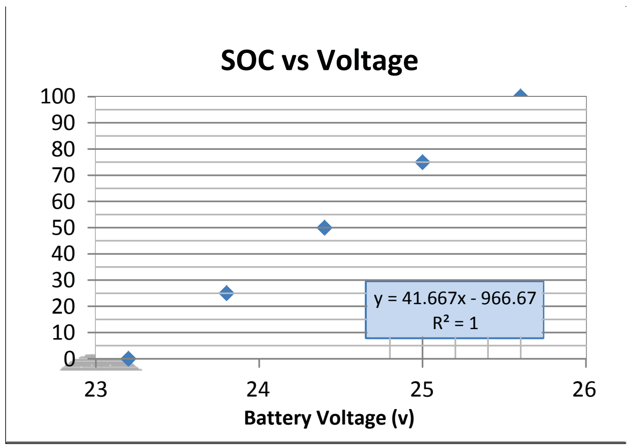

Figure 6. Battery SOC versus Battery Resting Voltage (data from battery manufacturer).

3.3.2 Cooling and Heating Season Battery Requirements

The eight 6-volt deep-discharge batteries used in these experiments were configured in two parallel banks of four batteries in series, creating a nominal 24V DC power system. Each battery is rated at 305 amp-hours of energy storage, which converts to 1.83 kWh. The 8-battery bank then has a total rated storage capacity of 14.64 kWh. Since the batteries were exercised on a daily basis typically across a 45% to 90% SOC range, the effective battery storage capacity was about 6.6 kWh. Total power produced by the nominal 2 kW PV array on a typical summer day is on the order of 8 kWh, or about 20% more than what the batteries can hold across the 45% to 90% SOC range. On the other hand, since the mini-split typically consumes about 4 kWh during the period from 1 PM to sunset (summer weather), the eight batteries therefore have more than sufficient capacity for the portion that needs to be carried forward into the evening and night hours.

During the cooling season, the time periods when cooling is required and the PV system produces power are closely matched, with a typical 3 hour lag. Peak power from the PV system typically occurs about 1:30 PM (DST) while the peak cooling load occurs about 4:30 PM (DST). As a result, much of the mini-split power consumption occurs during the hours of PV energy production.

Consequently, it is not necessary to carry a large portion of the PV energy into the night. Therefore, the amount of PV energy that must be carried forward (by means of battery storage) during the cooling season is smaller compared to the storage need for heating. This has important design implications for whether this stand-alone system is optimized for the space-cooling season or designed for both cooling and heating. If designed for space cooling only (or for cooling as the primary task), the battery bank could be somewhat smaller.

During the heating season, by contrast, relatively little of the PV power is typically used by the mini-split during hours when the sun is shining. On a typical cold Florida winter day (low 40°F and high 60°F), most of the heating load occurs during the hours of 10 PM and 10 AM. During the other 12 hours of the day, the heating system would generally be off or operating only intermittently till after sundown. As a consequence, perhaps 80% or more of the PV energy to be used for space heating must be stored in the batteries and used 8 to 12 hours later. Therefore, the battery bank must be on the order of 2 or 3 times as large for optimal heating season performance.

3.3.3 Maintenance Issues and Battery Degradation

One important characteristic of stand-alone systems is that they employ batteries for energy storage, and batteries require maintenance. Therefore, when trying to optimize energy savings, battery life and health must be taken into account. While the [redacted]-type batteries do not require water-adding maintenance, they do require following of a regular charging schedule (e.g., taking SOC to 100% once every 10 days or less). There is a tension, then, between using as much of the available solar energy (produced by the PV panels) as possible while still protecting the life of the batteries. This means letting cooling and heating operate as many hours as possible while avoiding draining the batteries below 45% SOC on a frequent basis but still achieving 100% SOC on a regular basis (once every 7-10 days).

The [redacted] owner's manual states that "For maximum life, batteries must be periodically recharged to 100% capacity. Continually recharging to less than 100% may result in premature capacity loss. It is recommended that batteries be recharged to 100% at least every 5-10 cycles." For this application, this means that the batteries must be charged to 100% once every 5 to 10 days. During the approximately 6 months of substantial cooling loads, this means that the mini-split heat pump must be disabled for a full day (or a large fraction of a day) at least once every 10 days so that the batteries can go through their full charging cycle, which includes BULK, ABSORB, and FLOAT. During other portions of the year, cooling and heating loads are sufficiently small or intermittent so that the batteries are typically charged to 100% every few days or week as a result of normal weather patterns.

Alternatively, the batteries could be brought to 100% SOC during the overnight hours using the utility grid, once a week, or so. On the days when overnight charging occurs, it would be preferable to disable the timer which locks out operation of the mini-split till 1 PM. On the overnight charging days, the mini-split could be operated from the grid for the period that the batteries are being charged.

Additionally, once every 6 to 12 months the bank of batteries should be "equalized", which is another form of required maintenance. This involves applying a steady charge to the batteries through the inverter for a period of 8 hours. To achieve this, a 240V source must be provided to the inverter while solar production is curtailed.

With regular use, battery capacity diminishes over time, sometimes at different rates per cell within the battery, resulting in a shortened battery life. In a bank of batteries, when these voltages differ too much from battery to battery, each battery can take on a unique charge/discharge profile. As a result, some of the batteries in the bank become overcharged while others are undercharged. To bring these battery voltages back to balance, an equalization charge may be required once every 6 to 12 months. Equalization is a process during which the entire bank of batteries is overcharged for a period of time to bring the voltage of each battery in the bank and each cell within each battery to the same value. The desired outcome from an equalization charge would be nearly identical battery charge/discharge characteristics for all batteries and battery cells.

It is important to note that equalization is somewhat damaging to the batteries in that some electrolyte is lost in the charge process. In a sealed [redacted], the lost electrolyte cannot be replaced so equalization is only used when substantially lower battery capacity is detected.

By March 2013 (after about 8 months of system operation), battery performance for the as-tested system showed signs of deterioration. The primary indicator of this battery degradation was a sharp downward spike in battery voltage after battery voltage had declined to about 23.8V, with this occurring on a daily basis. After an 8-hour equalization was implemented, no improvement in battery performance could be detected.

By early June 2013, some of the batteries had deteriorated to the point where they were causing sudden dips in voltage of the 8-battery bank on a nightly basis. In this new battery-failure-induced pattern, battery voltage would decline slowly into the nighttime hours, and then suddenly a plunge in battery voltage would occur, cutting out the inverter which then causes a potentially premature shutdown of the mini-split heat pump for the night.

Tracking of voltage of individual batteries over a several day period identified that 3 of the 8 batteries were experiencing more rapid voltage drop. At that point, the 4 best-performing batteries were identified, and these were assembled into a four-battery bank. From June 6 through July 15, 2013, the system was operated with only 4 batteries instead of the original 8 batteries. This allowed us to evaluate the performance of the solar heat pump system with the smaller bank of batteries.

The reduction in battery capacity caused a significant but not critical reduction in the ability of the system to deliver PV power to the task of space cooling, because (as discussed earlier) the batteries did not have to carry as much PV-power forward. If we had attempted to operate the system with 4 batteries during heating weather on a regular basis, the outcome would have been less satisfactory. In fact, operation of the solar heat pump system with 4 batteries had been implemented early in the winter season, and it was quickly identified that a larger battery bank (8 batteries) was crucial for the heating season.

By July 15, 2013, even the 4 batteries which had performed the best began to deteriorate badly. This bank of 4 batteries started to cycle the inverter off on the order of every 15 minutes (due to collapsing battery voltage). As a result, the mini-split was, by the second week of July, short-cycling in a manner that would diminish the operational efficiency of the system and perhaps endanger the mini-split compressor.

In order to better understand normal battery operation and the problems occurring with the batteries, the research team requested answers to a number of questions from the manufacturer.

Q: What is the typical battery SOC at the point when it goes into ABSORB mode and then again the SOC at the point when it goes into FLOAT mode.

> *A*: The SOC at which charging goes from BULK to ABSORB depends upon V_{abs} (voltage at which the batteries go into Absorption mode) which in turn depends upon the net charging rate (net charging rate = rate of charging [ROC] minus rate of discharge [ROD]). SOC at V_{abs} can range from 80% up to about 95% depending upon net charging current. Higher net charging current gives lower SOC at V_{abs}. Because our charging rate was continuously variable (because of varying energy input from solar and varying discharge to the variable capacity heat pump), SOC at V_{abs} was in continuous flux.

Q: "How often does the battery need to be fully charged to 100% SOC, in order to maintain the batteries health? Can it be charged to less than 100% - say 95% - and achieve the same health?"

> *A*: It should be charged to 100% (not 95% or even 98%) every 7-10 days, otherwise the plates will become sulfated.

Q: Can you explain why our batteries died at the end of 12 months of service.

> *A*: Based on their understanding of how we used the batteries, they concluded that the research team "chronically undercharged the batteries, leading to premature sulfation of the cells".

Q: Is there any way of conditioning the batteries in their current state that might help restore the batteries?

> *A*: Periodic "conditioning charge" per Section 5.5 of the Manufacturer's Technical Manual is recommended. You can implement a conditioning charge to equalize the batteries in each string? You might consider a voltage balancer, such as:
> [redacted]

Note that the research team has continued to perform some remediation work on the batteries with preliminary indications of some success in restoring a portion of the battery functionality. No conclusive outcome can be reported at this time.

3.3.4 Conclusions Regarding the Battery Bank

Batteries are expensive. The 8 [redacted] batteries with total capacity of 14.64 kWh cost nearly the same as the 8 PV panels, which had nominal 2 kW electrical energy production rating. Since the original purchase of the heat pump system components in May 2012, the price for PV panels has declined by about 30% while the cost of batteries has remained fairly stable.

Not only are the batteries expensive, they appear to represent a weak link in the solar heat pump system. By the end of 12 months, the 8 batteries had reached a point where they were not functioning effectively. Members of the research team believe that reasonable steps were taken to follow the manufacturer's instructions regarding fully charging the batteries every 7-10 days and taking the 8-battery bank through an equalization process once every 6 to 12 months (as recommended). Nevertheless, the batteries appear to have reached, or nearly reached, the end of their life by July 2013. It seems unlikely that most homeowners will work as hard as the research team did to comply with battery maintenance recommendations.

Since battery cost and life-expectancy have been identified as a major weak link in this solar heat pump system, an alternative (optimized with bimodal inverter) solar heat pump system design is presented later in this report that may go a long way toward extending the life of the batteries and improving the overall functionality and cost-effectiveness of the system. Battery life would be greatly extended by reducing the range of SOC operation to perhaps 80-85% under most day-to-day operation. Power from the grid would prevent the SOC from falling below 80%, while excess energy would be sold to the grid once SOC reached 85%. Periodic charging of the batteries to 100% SOC would occur from the grid. See Section 8.4 for more details about the proposed optimized bimodal solar heat pump system.

3.4 Typical Operation of the Solar Heat Pump System

Tables 3 and 4 illustrate environmental conditions and solar heat pump operation for a mild cooling day and a hot cooling day, respectively. Throughout much of the cooling season, the project research team employed a timer to cut-out mini-split operation for the period 7 AM to 1 PM (DST).

- In Table 4 it can be seen that the PV/battery system provides sufficient power to operate the mini-split for all hours of the day (18 hours) except for the 6-hour period from 7 AM to 1 PM (DST). From this table, the following operating characteristics can be observed. During the hours of 9 AM to 1 PM, the PV system is charging the batteries at a rate of about 1265 W, taking them from about 45% to about 75% SOC during this period (this period has essentially full sun). Battery voltage rises during this six hour period from 23.4 V to 28.1 V.
- For the remainder of the bright sunlight hours (from 1 PM to 6 PM), the PV mini-split draws about 580 W (in Economy mode) while the PV system delivers an average of about 880 W

over a five-hour period, leaving 300 W net power to go to the batteries. The net charging rate of about 300 W to the batteries for this six-hour period would then bring the SOC up to perhaps 85-90%.

Table 3

Data for a warm and sunny spring day (April 11, 2013) showing outdoor and indoor temperatures, solar radiation, PV system energy output (PVw), mini-split and central system energy consumption, and mini-split sensible cooling for the solar heat pump with 8-batteries and Economy mode. Time is DST.

Day	Hour	Toutdoors °F	Tindoors °F	Solar W/m^2	PVw Wh/h	PVw/ solar (ratio)	Battery voltage V	Mini-split heat pump Wh/15-min	Mini-split heat pump Wh/h	Mini-split runtime (%)	Mini-split sensible cooling Btu/h	Central heat pump Wh/h
2013101	1:00	74.2	74.9	0	0	0	24.6	93	373	95%	6807	0
2013101	2:00	74.2	74.8	0	0	0	24.6	86	342	94%	6610	0
2013101	3:00	73.9	74.8	0	0	0	24.5	82	328	85%	5943	0
2013101	4:00	73.2	74.7	0	0	0	24.5	72	288	83%	5678	0
2013101	5:00	73.1	74.7	0	0	0	24.4	66	264	76%	5115	0
2013101	6:00	73.0	74.8	0	0	0	24.3	67	268	76%	4902	0
2013101	7:00	72.8	74.5	0	0	0	24.3	45	180	63%	3581	0
2013101	8:00	73.1	74.6	41	54	1.67	24.7	0	0	0%	0	810
2013101	9:00	75.1	75.2	172	364	2.24	25.3	0	0	0%	0	740
2013101	10:00	77.5	75.7	517	969	1.88	25.9	0	0	0%	0	1010
2013101	11:00	78.5	74.8	673	1217	1.81	26.3	0	0	0%	0	1430
2013101	12:00	80.0	75.7	887	1524	1.72	27.1	0	0	0%	0	1130
2013101	13:00	79.8	74.8	991	1350	1.37	28.1	0	0	0%	0	1510
2013101	14:00	80.9	76.3	1027	1320	1.29	28.1	129	517	94%	6504	0
2013101	15:00	80.2	76.2	974	808	0.83	26.4	145	580	100%	7285	0
2013101	16:00	79.9	76.4	817	784	0.96	26.2	147	588	100%	7301	0
2013101	17:00	79.2	76.8	632	772	1.25	26.2	145	579	100%	7359	0
2013101	18:00	78.3	76.8	409	705	1.73	26.0	150	598	100%	7503	0
2013101	19:00	76.8	76.6	171	269	1.56	25.4	141	565	100%	7419	0
2013101	20:00	75.4	76.1	34	24	1.40	25.2	132	529	100%	7469	0
2013101	21:00	75.3	75.8	0	0	0.0	25.0	129	514	100%	7638	0
2013101	22:00	75.3	75.5	0	0	0.0	25.0	124	496	100%	7739	0
2013101	23:00	75.1	75.3	0	0	0.0	24.8	120	478	100%	7865	0
2013102	0:00	75.1	75.1	0	0	0.0	24.7	108	431	100%	7701	0
AVG		**76.2**	**75.4**	**306.0**	**423.3**	**0.8**	**25.5**	**82.5**	**329.9**			**276.3**

As can be seen in Table 3, indoor temperature tends to be cooler during nighttime hours and then goes to a slightly warmer temperature for 7 AM to 1 PM when the 5-ton central system is operating. Subsequently, indoor temperature rises substantially for the time period of 1 PM to 7 PM with mini-split operation, and then declines overnight. What explains this pattern of indoor temperature variation?

First, during the six-hour period from 7 AM to 1 PM, the 5-ton central system provides all of the space conditioning and its thermostat is set to about 0.5 to 1°F warmer than the mini-split. So the 7 AM to 1 PM period averages about 0.5°F warmer than that produced by the mini-split during the nighttime hours. Second, the mini-split allows indoor temperature to drift upward during periods when the cooling load increases. This can be seen in Table 3 during the hours from 1 PM to 7 PM where the mini-split operation allows average temperature to rise to 76.6°F, or about 1.9°F warmer than during night hours.

The explanation for this mini-split induced temperature variation is illustrated in Figure 7. This figure presents indoor temperature in the central zone (where the mini-split thermostat is located) and in the building as a whole (4-room average) during a 7-day period when only the mini-split was operating. To understand why the mini-split produces this indoor temperature pattern, it is necessary to understand how the mini-split varies its capacity (recall that it is a variable capacity system, with capacity ranging from 7000 to 23,000 Btu/h). The mini-split increases its cooling capacity based on deviation of space temperature from the set point. A large temperature deviation is required before the mini-split will push its capacity to higher levels.

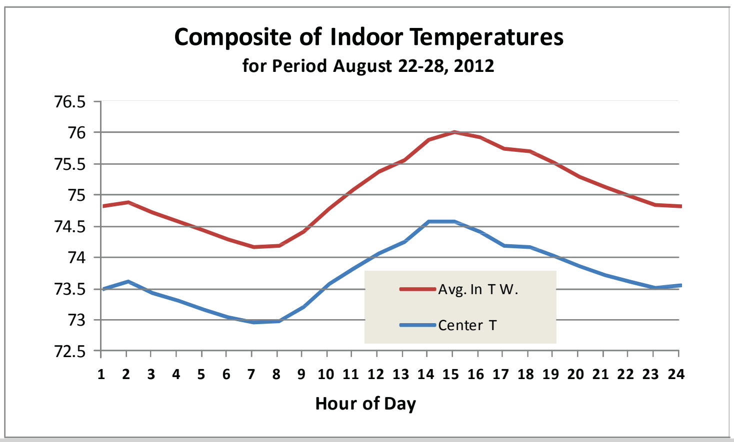

Figure 7. Twenty-four hour space temperature profiles in the Building Science Lab with only the mini-split conditioning the space. Temperature is shown for the central zone (blue line) and 4-room average (red line). The mini-split is powered on these particular days by PV solar for about half the day and from the utility grid for the remainder of the day, while the central ducted system does not operate during the entire 7-day period. It can be seen that room temperature rises in direct proportion to the cooling load.

The 5-ton central system has a SEER rating of approximately 11 while the Fujitsu mini-split has a SEER rating of 19.2. Referring back to Table 3, the relative performance of the mini-split and the central ducted 5-ton system can be seen for the three hours of 10 AM to 1 PM (79.4°F outdoors and 75.1°F indoors) versus the five hours of 1 PM to 6 PM (79.7°F outdoors and 76.3°F indoors). The central, ducted system consumes an average of 1357 W compared to 572 W for the mini-split for cooling loads that are approximately comparable, indicating savings of about 58% by using the mini-split. This suggests that the central system in the Building Science Lab has an effective SEER value of 8.1 after figuring in approximately 26% losses due to the attic duct system (note: the attic temperature ranges, on average, from 80°F to 92°F for all days with average outdoor temperature of 77°F and higher.) Typical cooling season operating patterns can be seen in Tables 3 and 4, for a mild cooling day and a hot and humid day, respectively.

Table 3 has data from a warm (but not hot) and very sunny spring day. The PV system combined with 8 batteries and operating in Economy mode provides sufficient energy to operate the solar heat pump (in cooling mode) for the entire 24-hour period, except for the 7 AM to 1 PM period when a timer is used to intentionally disable inverter power to the mini-split (the batteries are allowed to charge substantially during that 7 AM to 1 PM period). Some additional solar heat pump characteristics can also be observed.

1. Room temperature rises from about 74.5^{o}F just before sunrise and rises to a high of 76.8^{o}F in the late afternoon, a rise of 2.3^{o}F from low to high.
2. The mini-split heat pump draws a daily average of 330 W, or 119% of the power being drawn by the central heat pump for the average hour.
3. Starting about noon, the PV system charging starts to decline as the system moves into the ABSORB mode, where some of the solar must be discarded as the permitted charging rate is lowered (by the charge controller) below the rate of the entering solar resource.
   a. This can be observed in the column titled PVw/solar (ratio).
   b. A ratio of 1.8 or higher indicates that charging is in BULK mode.
   c. During the hours of 12 (noon) to 5 PM, this ratio declines from about 1.8 to as low as 0.83, indicating that the batteries have dropped into ABSORB mode and as much as 55% of the available solar is discarded during specific hours.
4. Battery voltage declines overnight to a low of 24.3 V, and then rises throughout the sunlight hours largely in proportion to the intensity of the solar radiation.
5. It can be seen that the mini-split operates continuously from 1 PM through midnight (see mini-split runtime column) and then cycles off a number of times during the overnight hours.
6. While the mini-split has a nominal cooling capacity of 18,000 Btu/h which would correspond to about 13,000 Btu/h of sensible cooling (this cooling is associated with lowering the air temperature), throughout much of the day. It can be seen that the sensible capacity runs no higher than about 7800 Btu/h, or 60% of full nominal sensible capacity. If the system were operated in Standard rather than Economy mode, sensible capacity would increase significantly.
7. It is interesting that while the central system operates for only 25% of the day (6 hours), it consumes 45% of the day's total space cooling energy use. There are two primary reasons for the relative energy consumption discrepancy.
   a. The mini-split heat pump consumes about 58% less energy per unit of cooling compared to the 5-ton central system in the BS Lab, including distribution system losses.
   b. The thermostat controlling the 5-ton system maintains a space temperature of about 75.2^{o}F while the mini-split allows room temperature to rise to about 76.8^{o}F during the hotter hours of the day. Therefore, the 5-ton unit is actually meeting a larger space cooling load during the hours that it is operating.

In a second example, Table 4 shows data from a hot and very sunny summer day (July 8, 2013). The mini-split was also operating in Economy mode, but it was operating with a reduced battery bank (4 batteries) and the timer (controlling the inverter) disabled power to the mini-split for only one hour from 7 AM to 8 AM. A number of differences can be observed in the system operating characteristics as a result of the hotter temperatures, changed timer schedule, and 4-battery storage. Solar power is sufficient to operate the solar heat pump (in cooling mode) for just over 11 hours on this day. Some additional solar heat pump characteristics can also be observed.

1. Room temperature rises from about 75.0°F just before sunrise to a high of 77.3°F in the late afternoon, a similar pattern to that seen in Table 4.
2. The mini-split heat pump draws an average of 290 W, or 23% of the power being drawn by the central heat pump for the average hour.

Table 4

Data for a hot and sunny summer day (July 8, 2013) showing outdoor and indoor temperatures, solar radiation, PV system energy output (PVw), mini-split and central system energy consumption, and mini-split sensible cooling for the solar heat pump with 4-batteries and Economy mode. Time is DST.

Day	Hour	Toutdoors °F	Tindoors °F	Solar W/m²	Battery voltage V	PVw Wh/h	PVw/solar (ratio)	Mini-split heat pump Wh/15-min	Mini-split heat pump Wh/h	Mini-split runtime (%)	Mini-split sensible cooling Btu/h	Central heat pump Wh/h
2013189	1:00	79.4	75.0	0	24.7	0	0	0	0	0%	0	1850
2013189	2:00	79.3	75.0	0	24.7	0	0	0	0	0%	0	1810
2013189	3:00	78.9	75.5	0	24.7	0	0	0	0	0%	0	1540
2013189	4:00	78.5	75.1	0	24.6	0	0	0	0	0%	0	1090
2013189	5:00	78.2	74.9	0	24.6	0	0	0	0	0%	0	1670
2013189	6:00	77.9	75.5	0	24.6	0	0	0	0	0%	0	840
2013189	7:00	77.5	75.0	12	24.6	4	1.24	0	0	0%	0	1580
2013189	8:00	79.1	75.7	38	25.1	64	1.66	0	0	0%	0	820
2013189	9:00	81.7	75.5	155	25.5	199	1.40	0	0	1%	22	1780
2013189	10:00	84.7	75.8	471	25.8	854	1.80	110	442	93%	6503	800
2013189	11:00	86.4	75.7	660	26.4	1207	1.83	114	454	96%	6586	1240
2013189	12:00	87.6	75.5	795	27.5	1313	1.66	110	441	92%	6270	1060
2013189	13:00	88.6	76.0	944	28.3	1029	1.09	125	501	95%	6494	810
2013189	14:00	88.4	77.1	962	27.8	946	0.98	160	642	100%	7647	0
2013189	15:00	88.2	77.0	927	26.2	820	0.88	158	631	100%	7648	780
2013189	16:00	87.5	77.3	773	26.1	704	0.92	137	546	100%	7404	720
2013189	17:00	87.1	76.8	663	26.1	823	1.27	165	660	100%	7951	1690
2013189	18:00	86.4	76.9	456	25.6	789	1.74	197	788	100%	9086	800
2013189	19:00	85.1	77.0	229	24.9	379	1.65	207	828	100%	9619	810
2013189	20:00	82.8	76.9	36	24.4	71	1.80	201	803	100%	9754	730
2013189	21:00	81.0	77.0	0	24.4	0	0	54	216	27%	2654	1120
2013189	22:00	80.2	76.4	0	24.8	0	0	0	0	0%	0	1820
2013189	23:00	79.9	76.1	0	24.8	0	0	0	0	0%	0	2080
2013190	0:00	79.7	74.9	0	24.8	0	0	0	0	0%	0	2250
AVG		**82.7**	**76.0**	**546.7**	**25.5**	**707.62**	**1.44**	**129.6**	**289.7**			**1237.1**

3. Starting about 9:15 AM, battery voltage rises to about 26 V which is the level at which inverter power is restored to the mini-split. The battery charging rate starts to decline as the system moves into the ABSORB mode around 11:30 AM, where some of the solar must be discarded as the permitted charging rate is lowered below the rate of the entering solar resource. This can be observed in the column titled PVw/solar (ratio). A ratio of 1.8 or higher indicates that charging is in BULK mode and that all of the available solar is being successfully delivered into

the batteries. During the hours of 11:30 AM to 5 PM, this ratio declines from about 1.8 to as low as 0.88, indicating that as much as 50% of the available solar is being discarded during specific hours.

4. Because of the limited battery capacity (4 batteries) and the relatively large power draw (over 800 W) of the mini-split (a large power draws pulls battery voltage down more precipitously), battery voltage declines to 24.4 by 8:15 PM at which time the mini-split turns off. The mini-split remains off until battery voltage reaches 26 V around 9:15 AM the next day.
5. In spite of the much earlier mini-split shut-down, the solar heat pump operates at relatively high capacity throughout the peak cooling hours. The central heat pump meets about 30% of the space cooling load, on average, from 9 AM to 8 PM, while the solar heat pump meets about 70% of the load. However, because the central ducted system is about 58% less energy efficient than the mini-split, it uses more energy during that period than the mini-split.
6. It can be seen that the mini-split operates nearly continuously from about 9 AM through 8 PM and remains off till about 9 AM the following morning.
7. While the mini-split has a nominal cooling capacity of 18,000 Btu/h which would correspond to about 13,000 Btu/h of sensible cooling (sensible cooling is associated with lowering the air temperature), throughout much of the day, sensible capacity runs no higher than about 9750 Btu/h, or 75% of full nominal sensible capacity. The mini-split cooling output would likely increase to a higher level if the system was operated in Standard mode.

3.5 Strategies for Achieving Maximum Seasonal Energy Savings

The customer can achieve maximum cooling energy savings by operating the mini-split in Economy mode versus Standard mode, for three reasons.

1. In Economy mode, the supply air is significantly warmer, about 54^{o}F compared to 46^{o}F. Heat pumps operate more efficiently when they are pushing energy flows against a smaller temperature differential. In Economy mode, cooling EER (Energy Efficiency Ratio) is 34% higher compared to Standard control mode when outdoor temperature is 82^{o}F (Figure 8). From the regression analysis equations, it can be calculated that the mini-split operates with 17.6 EER in Economy mode compared to 13.1 EER in Standard mode.

2. The fact that the supply air is about 8^{o}F warmer means that the heat pump in Economy mode is providing proportionately less latent cooling (less water vapor removal from the room air) and is expending more of its space cooling energy on lowering room air temperature (sensible cooling). It therefore meets the thermostat setpoint sooner.

a. Instead of producing typical 40% indoor RH while operating in Standard control mode, it produces about 46% indoor RH while operating in Economy control mode. 40% indoor RH is significantly lower than is necessary for most applications (46% RH is sufficiently low for essentially all circumstances), and the energy used to draw the humidity down to that level is largely wasted. Humidity in the 38 - 40% range can lead to drying of skin and eyes, and can contribute to static electricity discharges.

b. One could argue that a lower indoor RH can produce similar occupant comfort at a higher temperature, which means that the thermostat could be raised by say 1°F with the lower RH. This would, however, require some thermostat adjustment on the part of the occupants, and it is uncertain that this sort of adjustment actually occurs in real homes. Another way to say this is that in Economy mode the system is spending less of its energy on latent cooling (moisture removal) and more of its energy on lowering the space (drybulb) temperature. Since thermostats control based on room air temperature, higher equipment operating SHR leads to reduced space cooling energy use.

4. When the mini-split is in Economy mode, it draws about 600 W compared to about 1000 W in Standard mode. The relevance to system efficiency relates to how this power draw interacts with the batteries. The smaller power draw of Economy mode tends to keep the system operating for an extended period. By contrast, the larger power draw of Standard mode tends to trigger premature cut-out of the inverter. As a result, more of its operation time (when in Economy mode) will occur at night when outdoor temperatures are cooler and the system will operate more efficiently.

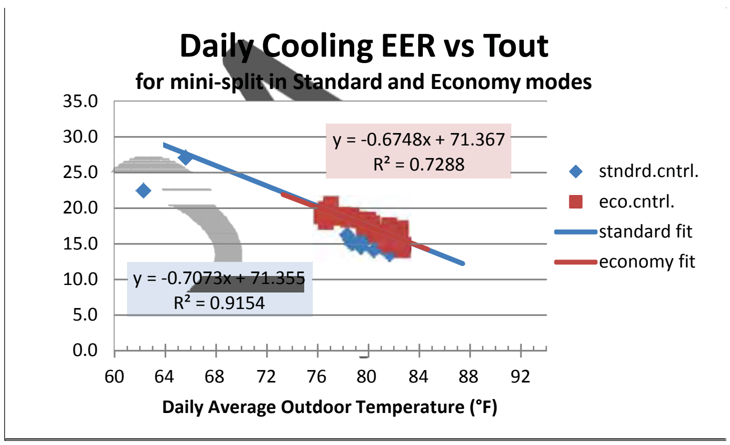

Figure 8. Monitored mini-split EER for Standard and Economy modes as a function of daily outdoor temperature with indoor temperature held constant at about 76°F.

4. COOLING SEASON ENERGY SAVINGS FROM THE SOLAR POWERED HEAT PUMP

The solar heat pump system produces electrical power when the sun shines onto 2 kW of PV panels and delivers it to the house. However, the energy savings experienced by the homeowner is amplified because all of the solar power is delivered to the building by means of a 1.5-ton mini-split heat pump, which has cooling (and heating) efficiency which is essentially twice that of the central SEER 13 ducted system in the [redacted] Lab. Space conditioning energy savings have also been assessed when operating in both Economy and Standard control modes and with the number of batteries at 8 and 4.

Additional savings occur when the high efficiency mini-split heat pump is operated using utility grid power after the solar resource has been depleted. Operation of the mini-split on the utility grid offsets a portion of the electrical energy which would otherwise be used by the less efficient central ducted system.

While the experiments were carried out in the Building Science Lab, the energy savings have been calculated as if the cooling and heating provided by the mini-split had been delivered into the MH Lab, a three bedroom two bath 1600 ft^2 home. Measured data had been collected in the MH Lab over a couple-year period to determine the cooling and heating loads over a wide range of outdoor temperatures. Regression analysis was completed so that the space cooling and heating loads could be predicted from TMY3 data. From experiments carried out in the Building Science Lab over the past 12 months, regression analysis has also been performed to characterize the cooling and heating energy that can be delivered to the MH Lab using the solar powered heat pump.

4.1 Cooling Season Energy Savings Calculation Methodology

Typically the difference between outdoor and indoor temperature (delta-T) accounts for 85%-95% of the variability in delivered cooling energy. However, the solar heat pump is designed to meet only a portion of the house space conditioning load (it turned out to be about 55% for the entire year), the solar powered mini-split heat pump delivered cooling energy predominantly as a function of the amount of solar radiation striking the PV panels. On the other hand, it was also a function of outdoor temperature. To account for the driving forces of both solar and delta-T, multivariate regression analysis was performed. This yielded equations which predict daily cooling energy delivered by the solar mini split system as a function of daily solar radiation and average outdoor temperature. Delivered cooling (DC) is calculated by the following equation:

$$DC = M1 \times \text{solar radiation at tilt } (W/m^2) + M2 \times \text{Outdoor Temperature } (^oF) + C$$

where M1 = solar coefficient, M2= temperature coefficient, and C = constant

Table 5 presents the results of the multivariate analysis for 5 different experimental variations.

Table 5

Regression analysis results for cooling derived from monitored data of 100% mini-split (M-S) operation and 8 batteries. Calculated cooling energy savings (last column) are based on typical summer values with daily average temperature of 76°F indoors and 80°F outdoors, with solar radiation of 5500 Wh/m^2-day.

	# days	M1	M2	C	r^2	kBtu/d
100% M-S economy	27	0.00469	13.039	-806.664	0.855	262.2
8 battery economy	68	0.01185	5.8794	-372.914	0.545	162.6
8 battery standard	38	0.01436	-3.654	322.678	0.618	109.3
4 battery economy	35	0.00990	-3.045	290.215	0.684	101.0
4 battery standard	13	0.00866	2.498	-148.399	0.774	99.1

While regression analysis has been completed using solar radiation and outdoor temperature, cooling energy versus both cannot be shown in a two-dimensional plot. Instead cooling energy delivered to the Building Science Lab has been plotted vs daily total solar radiation for Standard control mode using the eight battery storage bank (Figure 9). The plot shows measured delivered cooling versus solar radiation only as blue data points. However, the red data points show the predicted cooling energy based on both variables (solar and temperature). Figure 10 shows delivered cooling versus solar radiation for the mini-split using the Economy thermostat control mode with 8 battery bank. By examining the best-fit lines and equations of Figures 9 and 10, it can be seen that Economy mode yields considerably greater delivered cooling for a given amount of solar radiation.

In both Figure 9 and Figure 10, it can be seen that a significant amount of scatter is eliminated when outdoor temperature is also taken into account. The fact that r^2 values improve from 0.559 to 0.859 and from 0.243 to 0.446 in Figures 9 and 10, respectively, confirms what can be seen visually, that including the effect of outdoor temperature significantly improves uncertainty in the predicted delivered cooling.

For each day of the year, the amount of cooling electrical energy savings (based on cooling energy provided to the MH Lab by the solar heat pump) is determined (calculated) in a 4-step process.

- STEP 1: Determine the maximum amount of solar-powered cooling that could be delivered to the [redacted] Lab based on daily solar radiation for each TMY3 day using the best-fit ("predicted") equations from Table 5.
- STEP 2: Determine the cooling load of the [redacted] Lab for each individual day in the following manner. For each day of the TMY3 data, daily average outdoor temperature is used to determine delta-T (Tout – 77°F). Total cooling load for that day is then calculated based on delta-T for that day and the best-fit equation in Figure 11.
- STEP 3: The lesser of Step 1 or Step 2 is then the actual cooling delivered to the MH Lab for that day of the (TMY3) year.
  - The reason for this step: the solar heat pump system cannot deliver space cooling to the [redacted] Lab that exceeds the cooling load of the [redacted] Lab for each specific TMY3 day.

- So, in Step 1, the maximum solar-powered cooling that the system could deliver if the [redacted] Lab cooling load were infinite. In Step 2, the amount of delivered cooling which the Lab can accept was calculated.
- In Step 3, then, the amount of cooling that is delivered to the [redacted] Lab is determined by selecting the smaller cooling load of Steps 1 and 2.

- STEP 4: Actual cooling delivered to the [redacted] Lab by the solar powered heat pump is converted to daily electrical energy savings by dividing the delivered cooling for each specific TMY3 day by the average operating EER of the SEER 13 [redacted] central system heat pump based on the average outdoor temperature for that TMY3 day (Figure 12).

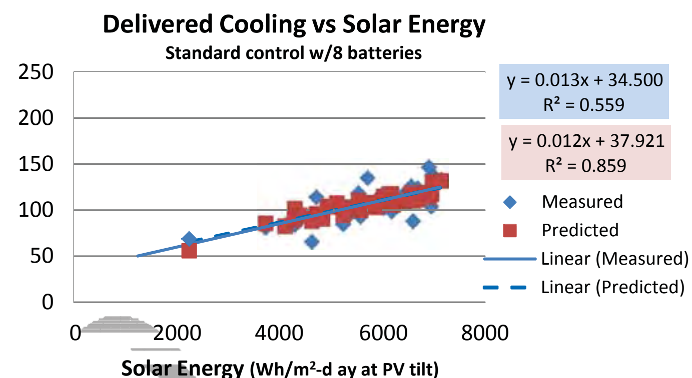

Figure 9. Cooling energy delivered by the solar heat pump system as a function of daily solar radiation for Standard thermostat control mode when using the eight battery storage bank.

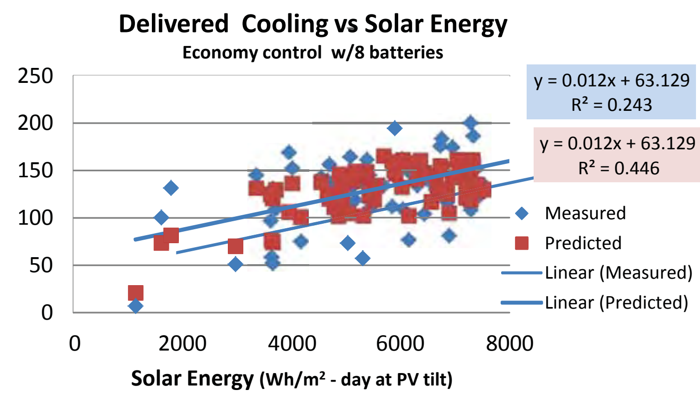

Figure 10. Delivered mini split cooling versus solar radiation using Economy control mode when using the eight battery storage bank.

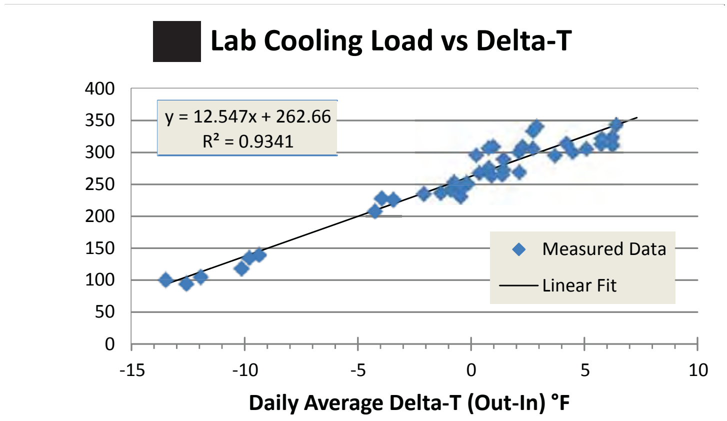

Figure 11. Daily [redacted] Lab cooling load versus delta-T (out – in) when using attic ducts.

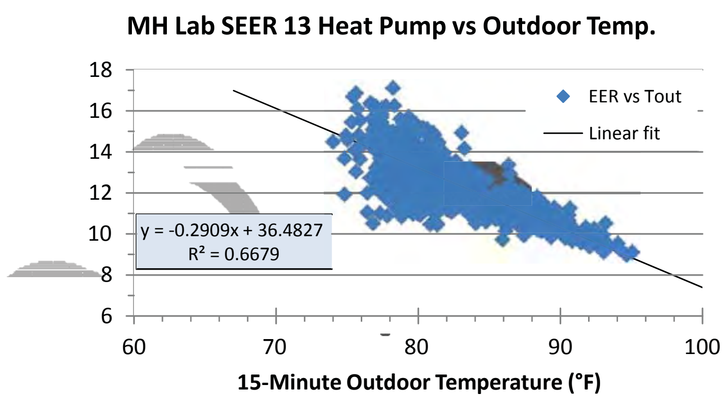

Figure 12. Measured cooling EER for the central ducted 3-ton SEER 13 [redacted] Lab heat pump as a function outdoor temperature. Duct losses are not considered when calculating EER.

These calculations are performed for each day of the year for which cooling is required (based on TMY3 data) for each of the four FPL service territory cities. Weighting for the four cities are as follows; Daytona Beach (15.17%), Miami (43.19%), West Palm Beach (22.43%), and Fort Meyers (19.21%). Similar calculations with identical weighting will also be performed for the heating season.

4.1.1 Example Calculation of Cooling Energy Savings from the Solar Heat Pump System

Following is an example of delivered cooling calculation for a particular TMY3 day (in this case, January 29, 1995) in Miami, which has average daily average conditions of 73.5°F drybulb temperature and 2472 Wh/m^2 solar radiation on the horizontal.

Over the past year, solar radiation was measured at the Building Science Lab at the PV panel tilt. However, since TMY3 solar radiation represents solar on the horizontal, it has to be converted to solar radiation incident at the tilt angle of the PV panels. Conversion is done based upon a regression of the solar ratio (horizontal solar versus PV tilt solar) versus the day of year from solstice. Days from December 21 to June 21 increase from 1 to 183 and days from June 21 to December 21 decrease from 183 to 1. The solar ratio was developed based on measurements from two pyranometers, one horizontal and one at PV tilt. The solar ratio and best-fit line are represented in Figure 13. Each TMY3 day is assigned a "day from solstice", which is then used to calculate the solar ratio multiplier. For the case of January 29, this day is given the solstice day number of 40. Applying the regression equation, the solar ratio is calculated to be 0.8586. The TMY3 solar on the horizontal is then converted to solar at PV tilt by dividing TMY3 horizontal solar by the solar ratio, yielding 2879 Wh/day on the PV tilt (2472/0.8586 = 2879).

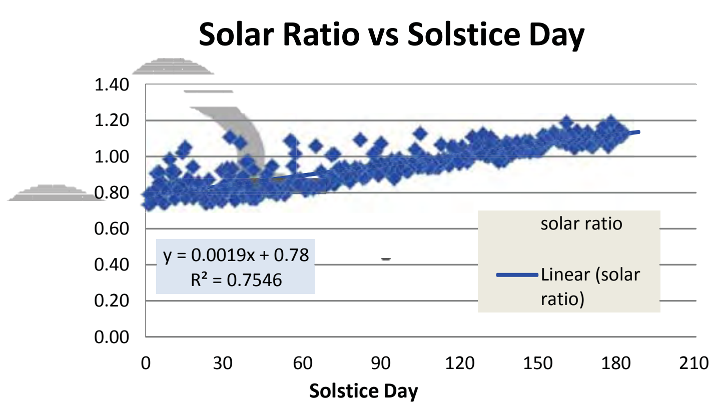

Figure 13. Solar ratio, which is used to convert solar radiation on the horizontal to solar radiation at PV array tilt, varies as a function of day of the year. Solstice day increases from 1 to 183 from December 21 to June 21, and then decreases from 183 to 1 from June 21 to December 21.

Following the calculation steps laid out in Section 4.1, electrical energy savings for January 29, 1995 is calculated as follows.

STEP 1 -- POTENTIAL SOLAR HEAT PUMP COOLING DELIVERY: Based on the solar radiation of 2879 Wh/m^2-day of TMY3 solar on the PV tilt and the regression equations (from Table 5; not from

Figures 9 and 10), the potential space cooling that could be provided by the solar heat pump is 93,457 Btu/d when using Economy mode and 95,380 Btu/d when in Standard mode.

STEP 2 -- REQUIRED COOLING LOAD: Based on an average daily ambient temperature of 73.5^{o}F, a delta-T of -3.5^{o}F (73.5^{o}F – 77^{o}F = -3.5^{o}F), and the best-fit equation for MH Lab cooling load (Figure 11), the MH Lab space cooling load is calculated to be 216,500 Btu/d (when the MH Lab is located in Miami on January 29, 1995).

Step 3 – DETERMINE ACTUAL SPACE COOLING DELIVERED: The smaller of Steps 1 and 2 is 93,457 Btu/d when operating in Economy mode and 95,380 Btu/d in Standard mode.

Step 4 – DETERMINE COOLING ENERGY SAVINGS: Cooling electrical energy savings provided by the solar heat pump to the MH Lab house is determined by dividing delivered cooling (Step 3) by the EER of the MH Lab central system which is obtained from the best-fit regression equation from Figure 12. In this case, EER for that day is calculated to be 15.09 Btu/Wh (Y = -0.2909 (73.5^{o}F) + 36.483 = 15.09). The energy savings of 93,457 Btu/d (in Economy mode) yields electrical energy savings of 6.19 kWh/d (93,457 /15.09= 6193) and the energy savings of 95,380 Btu/d (in Standard control mode) yields electrical energy savings of 6.32 kWh/d (95,380 /15.09 = 6321).

4.2 Seasonal Cooling Energy Savings from the Solar Heat Pump

Annual cooling energy consumption and cooling energy savings are shown in Table 6 based on TMY3 weather data for four Florida cities and calculations outlined in Section 4.1.

When the mini-split heat pump is operated only when solar power (from PV and batteries) is available (in other words, the mini-split is not operated on grid power and the central system picks up where the solar heat pumps drops out), annual cooling savings from 33.9% to 53.5% are achieved depending upon the system operational configuration.

- When the mini-split is operated with 8 batteries and Economy mode (with warmer supply air), this configuration yields 3322 kWh (or 53.5%) annual cooling savings.
- When the mini-split is operated with 8 batteries and Standard mode (with colder supply air), this configuration yields 2683 kWh (or 43.3%) annual cooling savings.
- When the mini-split is operated with 4 batteries and Economy mode (with warmer supply air), this configuration yields 2516 kWh (or 40.6%) annual cooling savings.
- When the mini-split is operated with 4 batteries and Standard mode (with colder supply air), this configuration yields 2101 kWh (or 33.9%) annual cooling savings.

Table 6

Annual cooling energy required by the [redacted] Lab SEER 13 central system (first data row) and annual energy savings provided by the solar heat pump system for 5 different system configurations (data rows 2–6).

	Daytona kWh	Miami kWh	West Palm Beach kWh	Ft. Myers kWh	4 city weight-avg kWh	Annual savings %
S13 MHL annual kWh	4749	6745	6109	6246	6204	
8 Bat. Economy kWh savings	2584	3594	3275	3346	3322	53.5%
8 Bat. Standard kWh savings	2430	2738	2704	2736	2683	43.3%
4 Bat. Economy kWh savings	2269	2575	2527	2569	2516	40.6%
4 Bat. Standard kWh savings	1700	2246	2078	2122	2101	33.9%
100% MS Economy kWh savings[1]	3400	4830	4374	4472	4442	71.6%

[1] These savings assume that the mini-split cooling output is limited, by assumption, to meeting no more than 80% of the space cooling load during hours when it operates on the utility grid.

We can conclude that there are large seasonal cooling energy savings benefits of operating the mini-split in Economy mode versus Standard mode.

- With 8 batteries, annual savings increase by 24% going from 2683 to 3322 kWh when going from Standard to Economy modes.
- With 4 batteries, annual savings increase by 20% going from 2101 to 2516 kWh when going from Standard to Economy modes.

There are also large seasonal cooling energy savings resulting from operating the mini-split using 8 batteries compared to 4 batteries.

- When operating in Economy mode, annual savings increase by 32% going from 2516 to 3322 kWh when going from 4 batteries to 8 batteries.
- When operating in Standard mode, annual savings increase by 28% going from 2101 to 2683 kWh when going from 4 batteries to 8 batteries.

4.3 Additional Cooling Season Savings from Operating the Mini-split from the Utility Grid

Because of the considerable efficiency advantage of the mini-split system compared to the central ducted heat pump system, an additional system design feature was also examined in this project that would allow the mini-split to run 100% of the time. A relay was installed in the Building Science Lab that would automatically switch the mini-split power from inverter (PV power) to the utility's grid when the batteries had run out of energy (more specifically the battery SOC had declined to a specified level). With this relay and control setup (which we would recommend to customers who purchase this "stand-alone" solar powered heat pump system), the mini-split can operate 24 hours per day (on the PV/battery power for as long as that is available and then on grid power when the solar power has been depleted), and thus displace a large proportion of the home's yearly heating and cooling energy requirements. This switch-over relay worked flawlessly through the year of data collection and automatically switched over to the grid when the batteries had drained to a specified (user-selectable) level.

Considerable savings can occur in this mode. Consider, for example, if the central system has a SEER 13 rating and delivers its energy to the space through attic ductwork with 25% average overall energy losses, then the central system net efficiency equates to SEER 9.75 (SEER 13 * (1 – 0.25) = 9.75 SEER). Since the mini-split has no ductwork and therefore no duct-related losses, its efficiency will not be reduced below its SEER rating of 19.2. (Note that other mini-split systems that could be used in this type of application have SEER ratings as high as 27.2, and could therefore yield even greater savings in this mode of operation.) Therefore, the mini-split operation by itself, apart from the solar energy delivered to the house, could save 30-70% on seasonal cooling energy savings compared to the central system, depending upon the SEER ratings of the mini-split and central systems, the SEER rating of the central system, and the energy losses of the ductwork serving the central system. Operating the mini-split during all hours when the solar resource has been depleted increases annual cooling energy savings by 34% from 3322 to 4442 kWh (Table 6). When the mini-split is operated from solar power and then also powered from the utility grid when the solar resource has been depleted, annual cooling energy savings from the solar heat pump system is then 72%.

5. COOLING SEASON PEAK DEMAND SAVINGS PRODUCED BY THE SOLAR HEAT PUMP SYSTEM

The peak cooling demand period of most interest to FPL occurs during the hour of 4 to 5 PM. The combination of solar radiation and battery storage on hot summer afternoons ensures that the mini-split will be operating continuously during those peak hours in all circumstances, and using solar power alone. The only question that remains to be determined is – "What proportion of the space cooling is met by the mini-split during that hour."

There are several factors which determine whether the mini-split will meet the entire cooling load during those peak hours (recall that the mini-split is a variable capacity system). Figure 14 illustrates a typical pattern of cooling energy use when the mini-split is in Standard control using the 8 battery bank for a hot 8-day summer period. Based on timer control, solar power is delivered from the inverter to the mini-split starting at 1 PM EDT (blue line). By 2 PM the central ducted system (dotted red line) has cycled off because the mini-split setpoint is below that of the central system. From 2 PM to 6 PM, then, the central ducted system cycles off completely, and the solar heat pump system meets 100% of the cooling demand for the peak hour(s). The solid red line shows the predicted SEER 13 cooling electrical energy consumption for the MH lab house, based on regression analysis, when no other supplemental cooling occurs.

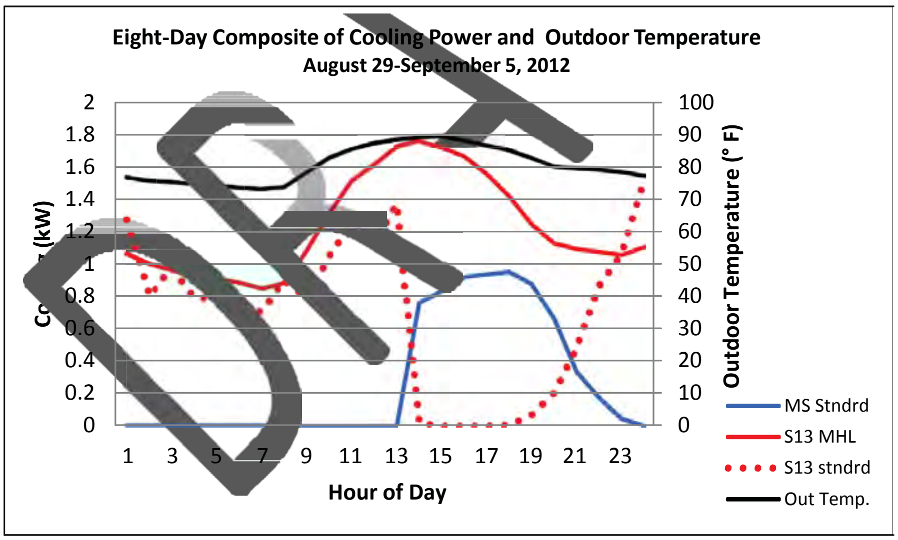

Figure 14. During the 8-day period August 29-September 5, 2012, the central ducted system does not cycle ON during the hours of 4 to 6 PM (EDT) because the mini-split, which is in Standard mode, meets the entire building cooling load during those peak hours. Therefore, the solar heat pump system meets 100% of the cooling demand on the peak hours of those 8 hot summer days.

Based on regression analysis, it was found that operation of the solar heat pump with 8 batteries and Standard control yields 100% peak demand reduction. For all days of the year, the combination of solar energy from the PV modules and energy stored in the 8-battery bank allows the mini-split to operate on solar power alone and meet the entire space cooling load peak demand (Figure 14 and Table 7).

Figure 15 illustrates hourly space cooling operation for another data set. Cooling power is shown for a total of 17 days, allowing for comparison of Economy and Standard control modes. The red line represents the electrical demand produced by the [redacted] Lab central system when the solar heat pump system is taken off line. When the solar heat pump system is activated, it can be seen that the central ducted system does not operate at all for the 4-5 PM period (blue dots) since the mini-split (in Standard control mode) meets 100% of the space cooling load at that time. When the system is switched to Economy mode, the solar heat pump does not meet all of the peak cooling demand because the central SEER 13 system cycles on occasionally during those peak hours (green dashed line in Figure 15).

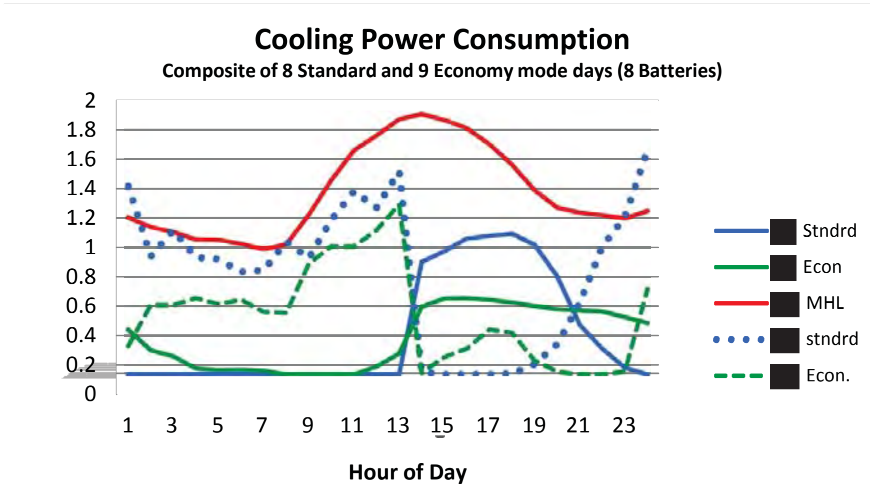

Figure 15. Twenty-four hour cooling power consumption profile for Standard and Economy mini-split operation when using 8 batteries, plus cooling power consumption for the [redacted] Lab SEER 13 central system. Figure 15 has added economy profile to Figure 14.

When in Standard mode and the battery bank is reduced to 4 batteries, the solar heat pump does not meet all of the peak cooling demand. It can be seen that the central system cycles on occasionally during those peak hours (Figure 16). When in Economy mode and the battery bank is reduced to 4 batteries, the solar heat pump does not meet nearly the entire peak cooling demand and the central system cycles on more frequently during those peak hours.

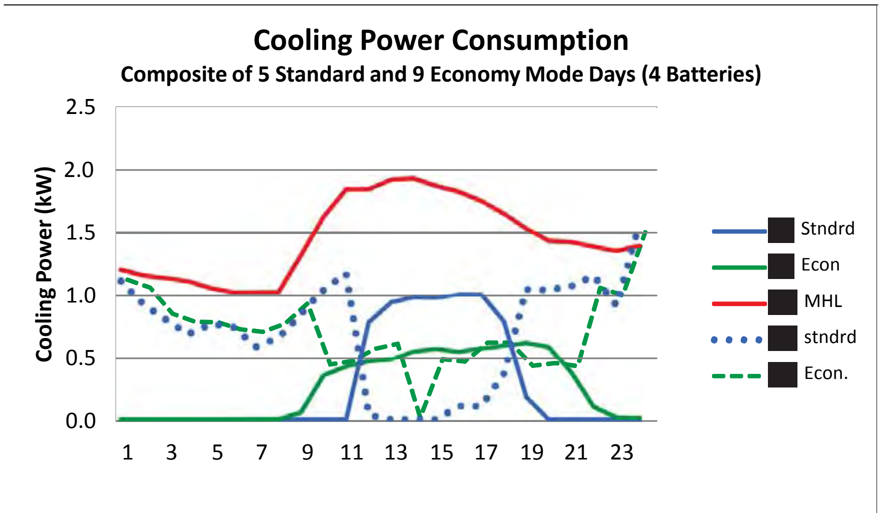

Figure 16. Twenty-four hour cooling power consumption profile for Standard and Economy mini-split operation when using 4 batteries, plus cooling power consumption for the [redacted] Lab SEER 13 central system.

Figures 15 and 16 are complicated and this section will therefore benefit from further explanation.

- The cooling energy consumption patterns shown in Figure 15 are a combination of monitored data and simulated energy consumption, all based on a composite derived from a number of days and representative of typical summer temperature and solar. Table 7 also shows relative peak demand for the hottest summer hours based on TMY3 data for the four chosen FPL market cities.
- The solid blue line in Figure 15 is measured energy consumption of the solar heat pump (provided by the PV/battery system) when operating in Standard mode.
- The solid green line is the measured energy consumption of the solar heat pump (provided by the PV/battery system) when operating in Economy mode.
- The blue dotted line is the simulated energy consumption of the [redacted] Lab central system if the solar heat pump (mini-split) were operating in the [redacted] Lab in Standard mode.
- The green dashed line is the simulated energy consumption of the [redacted] Lab central system if the solar heat pump (mini-split) were operating in the [redacted] Lab in Economy mode.
- The red solid line (labeled S13 [redacted] is the regression analysis-based simulated energy that the SEER 13 [redacted] Lab central system would have consumed if the solar heat pump (mini-split) were not operating.
- The peak demand reduction produced by the solar heat pump with Standard control and 8 batteries would then be the gap between the red line and the dotted blue line in Figure 15.

- The peak demand reduction produced by the solar heat pump with Economy control and 8 batteries would then be the gap between the red line and the dashed green line in Figure 15.
- The peak demand reduction produced by the solar heat pump with Standard control and 4 batteries would then be the gap between the red line and the dotted blue line in Figure 16.
- The peak demand reduction produced by the solar heat pump with Economy control and 4 batteries would then be the gap between the red line and the dashed green line in Figure 16.

The following can be learned from Figures 15 and 16 regarding the 31 days represented in those composite plots.

- When the solar heat pump operates in Standard mode with 8 batteries, 100% of the peak demand which would have occurred during the 4-5 PM period by operation of the central ducted system is met by the solar heat pump.
- When the solar heat pump operates in Economy mode with 8 batteries, approximately 80% of the peak demand which would have occurred during the 4-5 PM period by operation of the central ducted system is met by the solar heat pump.
- When the solar heat pump operates in Standard mode with 4 batteries, approximately 95% of the peak demand which would have occurred during the 4-5 PM period by operation of the central ducted system is met by the solar heat pump.
- When the solar heat pump operates in Economy mode with 4 batteries, approximately 65% of the peak demand which would have occurred during the 4-5 PM period by operation of the central ducted system is met by the solar heat pump.
- While the solar heat pump operated continuously throughout the peak demand hours for both Standard and Economy modes, only the Standard control mode allows the mini-split to operate at a sufficiently high capacity to meet the entire cooling load.
- An interesting control option would be conceivable, namely that advanced algorithms could be implemented that would result in Economy mode operation most of the time (thus achieving maximum seasonal operation efficiency) but Standard mode operation during periods when peak demand reduction is advantageous. This control approach could result in operational outcomes that are maximized for both the customer and the electric utility.

Table 7 summarizes TMY3 modeled peak demand for the [redacted] Lab central system (as if the solar heat pump were not available) and also the peak demand reduction yielded by operation of the solar heat pump with various battery and control mode configurations for peak cooling load periods for the 4 representative cities of the FPL service territory. These results are obtained from simulation of peak demand based on calculation using the hottest 4-5 PM (EDT) hours of the hottest TMY3 day for each city.

Table 7
Peak cooling energy required by the [redacted] Lab SEER 13 central system and peak demand reduction provided by the solar heat pump system for 4 different system configurations.

	MHL SEER13 Cooling Peak Demand					Peak Demand Reduction			
HOUR ending	Daytona kW	Miami kW	WPB kW	Ft. Myers kW	weight-avg kW	8 batt-standard kW	8 batt-economy kW	4 batt-standard kW	4 batt-economy kW
4:00 PM	2.51	2.01	2.51	2.51	2.29	2.29	1.95	1.95	1.58
5:00 PM	2.35	1.93	2.35	2.51	2.20	2.20	1.87	1.87	1.52
AVG	2.43	1.97	2.43	2.51	2.25	2.25	1.91	1.91	1.55
			Peak Demand reduction %			100.0%	85.1%	84.9%	69.1%

The following can be learned from Table 7.

- When operated with 8 batteries in Standard mode, the solar heat pump produces 100% demand reduction which is equal to a 4-city weighted average 2.25 kW reduction.
- When operated with 8 batteries in Economy mode, the solar heat pump produces 85% demand reduction which is equal to a 4-city weighted average 1.91 kW reduction.
- When operated with 4 batteries in Standard mode, the solar heat pump produces 85% demand reduction which is equal to a 4-city weighted average 1.91 kW reduction.
- When operated with 4 batteries in Economy mode, the solar heat pump produces 69% demand reduction which is equal to a 4-city weighted average 1.55 kW reduction.

There are three factors which determine the extent of demand reduction produced by the solar heat pump for the 4 to 5 PM period on the hottest days.

- The first factor is the capacity of the mini-split. While this 1.5-ton unit has nominal cooling capacity of 18,000 Btu/h, the unit actually has capacity up to 23,000 Btu/h. It appears to be true of nearly all variable-capacity systems, including mini-split heat pumps, that maximum capacity is considerably greater than the nominal capacity. When one considers that mini-split heat pumps experience no duct losses, it then has capacity approximately equivalent to a central ducted system of about 3-ton capacity when duct conduction and duct air leakage losses are included. In many cases, then, the 1.5-ton mini-split will be able to meet or nearly meet the peak cooling load of many mid-sized homes. In the case of the Building Science Lab, the peak cooling load is about 2 tons. (The MH Lab also has a peak cooling load of about 2 tons, when operating with the attic duct system.) Therefore, this 1.5-ton mini-split can meet the cooling load of either of these buildings even on the hottest days.
- The second factor is whether the system is operated in Standard or Economy modes. For a given amount of daily solar radiation, the solar powered mini-split provides almost 50% more daily cooling when operating in Economy mode. On the other hand, when operating in Standard mode, the mini-split draws nearly 60% more power. Therefore, it makes the most sense for the homeowner to operate in Economy mode under most circumstances. In Economy mode, and with the central ducted system operating at about 1^{o}F higher

temperature than the mini-split setting, the mini-split will meet most of the cooling load but the 5-ton will also cycle "on" intermittently during these peak hours, with the solar powered mini-split meeting, on average, about 85% of the peak demand.

- The third factor is how close the thermostat setpoints of the mini-split and central ducted system are to each other. Because of the way that variable capacity systems (such as the mini-split heat pumps) operate, space temperature tends to drift upward during peak hours (as can be seen in Figure 7). This is an inherent function of how variable capacity systems (including this mini-split model) modulate their output. They increase their cooling (or heating) output based on the deviation between setpoint and measured room temperature. In Economy mode, this deviation is allowed to expand slightly more than in Standard mode, in order to keep the system in lower capacity, where it operates at higher efficiency a greater proportion of the time. So, the fraction of the peak demand that is met by the solar heat pump depends in substantial part upon how close the thermostat setpoints are to each other. While a 1^{o}F difference in setpoint might be a good selection in order to maintain continuity of space temperature as space cooling transitions from mini-split to central system, and higher mini-split operating efficiency, a 2^{o}F difference on the other hand would allow the solar mini-split to meet all or nearly all of the peak demand on the hottest days even while operating in Economy mode.

Conclusion: While the Economy mode yields the greater yearly cooling energy savings to the customer, Standard mode yields the greatest peak demand savings to the electric utility. If the central ducted system setpoint were to be set a couple degrees higher than that of the solar heat pump, then the solar mini-split could be operated in Economy mode while still meeting 100% of the peak hour electrical demand.

5.1 Peak Demand Savings as a Function of Temperature Setpoints of the Mini-split and Central Systems

The home cooling load reaches its maximum during the hottest hours of the day. As cooling load increases throughout the day, the mini-split allows space temperature to drift upward because increasing delta-T (Troom – Tstat) is what pushes the mini-split to increase its capacity. The amount of space temperature increase is typically on the order of 1 to 2^{o}F, depending upon the range of cooling load and outdoor temperature swings. Figure 17 has the same room temperature data from Figure 7 but with the mini-split thermostat setpoint shown as a blue line and the central heat pump setpoint shown as a green line. As the building cooling load increases, the upward drift in space temperature produced by the mini-split allows the central ducted system to cycle on. As the central system cycles on and caps or actually pushes indoor temperature down, it will tend to limit the mini-split's compressor capacity. In this manner, the central system displaces some of the electrical energy savings which could have been produced by the mini-split. In what might be considered the most common configuration of the mini-split and the central system, the mini-split thermostat might use a 0.5 to 1.0^{o}F lower setpoint. In this arrangement, the mini-split will run continuously, but not at full capacity, because the central system will intermittently cycle on as room temperature is allowed (by the mini-split) to drift upward.

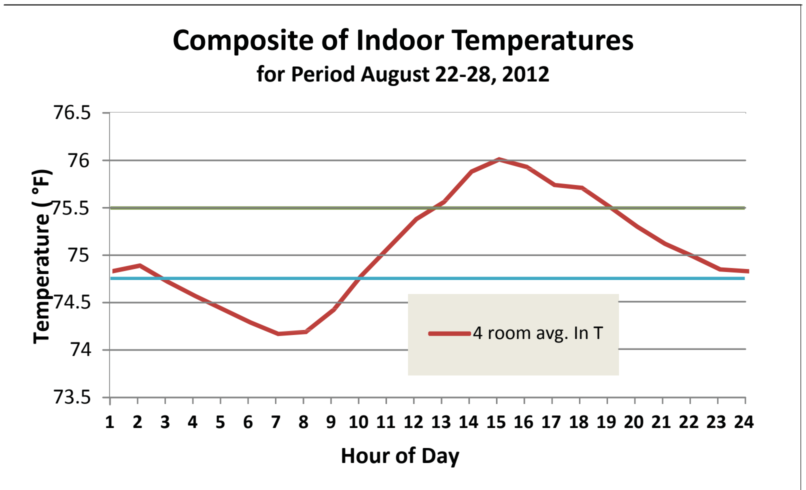

Figure 17. The red line is a measured 24-hour space temperature profile in the Building Science Lab for a 7-day period with only the mini-split conditioning the space, with space temperature setpoints used by the mini-split (blue line) and central system (orange line) illustrated.

Selecting close setpoints causes the mini-split to operate at a lower capacity factor, which in turn allows it to operate at higher efficiency. Selecting Economy mode results in additional operational efficiency. However, both of these factors -- close setpoints and use of Economy mode -- result in the mini-split being considerably less effective at displacing peak demand.

In fact, during the 12 months of solar heat pump experiments, the setpoints of the mini-split heat pump and the Building Science Lab central heat pump were about 0.5°F different. Because the setpoints were so close, the central system was more likely to activate during peak load periods of the day as the mini-split allowed the space temperature to drift upward (for more details, see Section 2.4 and Figure 7), especially when economy mode was employed. Economy mode allows the room temperature to drift upward to a greater degree before the unit goes into higher cooling capacity. Conversely, Standard mode tends to make the deadband between mini-split setpoint and room temperature tighter, thus minimizing the likelihood that the central system will cycle on. If the homeowner is willing to set the central system thermostat setpoint to perhaps 1.5 to 2°F warmer than that of the mini-split, then the central system is unlikely to cycle on even when it operates in Economy mode.

In the real world, there will be tension between what would be most convenient and comfortable for the customer, namely setting the central ducted system thermostat to a level just slightly higher than that of the mini-split (thus causing the mini-split to operate in lower capacity and higher efficiency) versus a higher temperature setting which would, for the most part, prevent or resist the central system from activating. A smaller difference between setpoints will yield a more seamless transition from mini-split to central system operation and greater occupant comfort, since indoor space temperature will remain stable. By contrast, what would be best for the electric utility would be to have the solar-powered mini-split meet the entire cooling load during the peak periods. Of course, incentives could be put in place to encourage the customer to control the mini-split so that a larger portion of the peak demand is met by the mini-split. An “on-demand” system could also operate to disable the central system (or adjust the thermostat upward) on days (and hours) of high peak demand, thus forcing the mini-split to meet the entire space cooling load.

A discussion regarding optimizing peak demand reduction is presented in Appendix B.

6. HEATING SEASON ENERGY SAVINGS PRODUCED BY THE SOLAR HEAT PUMP SYSTEM

Because of limited heating season data, and because the mini-split provides solar-powered space heating much more efficiently in Economy mode, only a limited amount of Standard-mode space heating was available.

6.1 Heating Energy Savings Calculation Methodology

As was done for cooling season analysis, multivariate regression analysis was performed to account for the driving forces of both solar and delta-T (outdoor minus indoor temperature). This yielded equations which predict daily heating energy delivered by the solar mini-split system as a function of daily solar radiation and average outdoor temperature. The regression results are shown in the form of an equation which allows calculation of delivered heating (DH), as follows:

$$DH = M1 \times \text{Solar at tilt} + M2 \times \text{Outdoor Temperature (F)} + C$$

where M1 = solar coefficient, M2= temperature coefficient, and C = constant

Table 8 presents the results of the multivariate analysis for 2 different experimental variations, 100% mini-split operation (part of the day powered by solar and the remainder of the day by the grid) and Baseline (both mini-split and central system operating) with 8 batteries and Economy control mode.

Table 8

Regression analysis results for heating derived from monitored data of 100% mini-split (M-S) operation and 8 battery Economy control mode. Calculated heating energy savings (last column) are based on daily average temperature of 72°F indoors and 50°F outdoors, with solar radiation of 5500 Wh/m²-day.

	# days	M1	M2	C	r^2	kBtu/d
100% M-S economy [1]	50	-0.00065	-9.1681	668.357	0.876	206.4
8 batt economy	60	0.001073	-3.70685	279.619	0.528	100.2

[1] Note: 100% M-S economy means that these 50 days of monitored data were with the mini-split (M-S) operating 100% of the time, on solar power when that is available and on the grid when the solar resource has been depleted.

For each day of the year, the amount of heating electrical energy savings (heating energy provided to the MH Lab by the solar heat pump) is determined (calculated) in a 4-step process, similar to that which was employed for space cooling.

- STEP 1: The maximum amount of solar-powered heating that could be delivered to the [redacted] Lab (based on daily solar radiation) is determined by the solar radiation level for each TMY3 day in conjunction with the regression equation in Table 8.
- STEP 2: The heating load of the MH Lab is determined in the following manner. For each day of the TMY3 data, the daily average outdoor temperature is used to determine delta-T (Tamb – 72°F). Then based on the delta-T for that day and the equation in Figure 18, the total heating load for that day is then calculated.

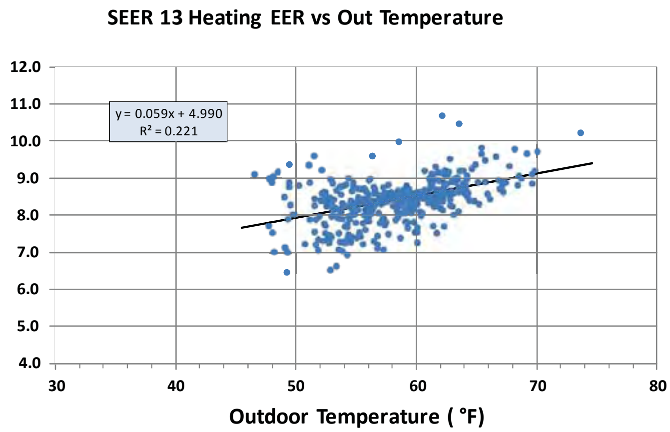

Figure 18. Daily heating load (Btu/day) versus delta-T (out – in) for the [redacted] Lab excluding duct losses.

- STEP 3: The lesser of Step 1 or Step 2 is then the actual delivered heating.

[redacted] converted to daily heating electrical energy savings by dividing the delivered heating by the heating EER of the MH Lab central system for that day. Figure 19 provides heating EER for the MH Lab central heat pump as a function of daily average ambient temperature.

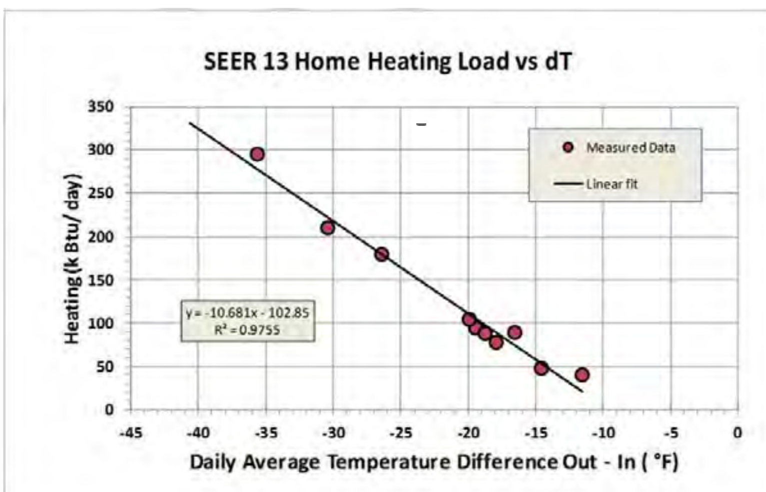

Figure 19. Measured system 15-minute heating EER for the 3-ton SEER 13 [redacted] Lab heat pump as a function outdoor temperature.

These calculations are then performed for each day of the year for which heating is required (based on TMY3 data) for each of the four FPL service territory cities.

6.2 Seasonal Heating Energy Savings from the Solar Heat Pump

Annual heating energy consumption and heating energy savings shown in Table 9 are calculated based on TMY3 weather data for four Florida cities and the calculation methodology outlined in Section 6.1.

When the mini-split is operated with 8 batteries and Economy mode, the solar heat pump yields 213 kWh annual heating savings with 72°F setpoint. This represents heating season energy savings of 82% compared to operating only the central ducted SEER 13 heat pump. The predicted annual percentage savings are quite high for the 8 battery Economy configuration, in part due to relatively mild TMY3 winter data in the heavily weighted south Florida cities. While high percent annual heating savings are indicated, the savings are only $21.30 per year. So while the heating savings are valuable, they only represent about 3% of total annual heating and cooling energy use to the customer. If the space temperature setpoints were increased to say 75°F, heating energy consumption and heating energy savings would be very substantially higher.

It should also be understood that occupant controlled factors could result in very different realized savings. If the Solar Heat Pump were operated in Standard mode, the mini-split heat pump would typically operate at a higher heating capacity which would result in reduced system efficiency and diminished savings.

If the mini-split were allowed to operate on the utility grid when the solar resource has been depleted, then additional savings could be achieved. Annual savings, in this case, would increase to 232 kWh/y, an 89.2% reduction compared to there being no solar heat pump system.

Table 9

Annual heating energy required by the [redacted] Lab SEER 13 central system and annual energy savings provided by the solar heat pump system using 2 different system configurations.

	Daytona kWh	Miami kWh	West Palm Beach kWh	Ft. Myers kWh	4 city weight-avg kWh	Annual savings %
SEER 13 [redacted]	**777**	**99**	**288**	**179**	**260**	
8 Bat. Econ. savings	**603**	**96**	**237**	**138**	**213**	**81.9%**
100% MS Economy savings[2]	**673**	**97**	**257**	**154**	**232**	**89.2%**

[2] These savings are based on the assumption that the mini-split operating on the grid meets no more than 80% of the space cooling load that would otherwise be met by the SEER 13 central system.

7. HEATING SEASON PEAK DEMAND SAVINGS PRODUCED BY THE SOLAR HEAT PUMP SYSTEM

Heating peak demand has been examined for the hours of 6 AM to 8 AM on cold winter mornings during the 2012-2013 winter seasons. While the solar heat pump provided 69%-100% of peak cooling demand (depending upon whether Economy or Standard control is used and the number of batteries employed), no peak demand reduction was observed for heating, for any 6 AM to 8 AM period throughout the 12-month monitoring period. It was found that it would be very difficult for the solar heat pump to meet peak heating loads on cold winter mornings.

Why is this? First, there is no solar radiation during this peak period so all of the solar heating during this 2-hour window must be powered solely from battery storage. Second, all of the power to run the solar heat pump during the peak hours must come from the batteries. Third, the power draw of the solar heat pump is typically quite large on the coldest hours of the coldest days, so this tends to draw down the battery voltage quickly which in turn leads to a premature shut down of the inverter.

Peak demand performance is typically assessed by means of regression analysis of a sample the coldest hours of the coldest days. However, the sample size was insufficient to do that analysis for peak heating. As an alternative, a number of individual cold mornings were examined, and the resulting peak demand reduction (or lack of peak reduction) was characterized. In all cases, the solar heat pump did not operate during the critical 6 AM to 8 AM period. Plots are provided to illustrate typical peak period solar heat pump operation.

Figure 20 shows a 24-hour composite of outdoor temperature and solar heat pump operation for two very sunny but cold days. It can be seen that the solar heat pump becomes active at about noon (when battery voltages rises to a level sufficient to activate the inverter), operates throughout the afternoon and evening hours, shutting off for the night at about 11 PM (all times EDT).

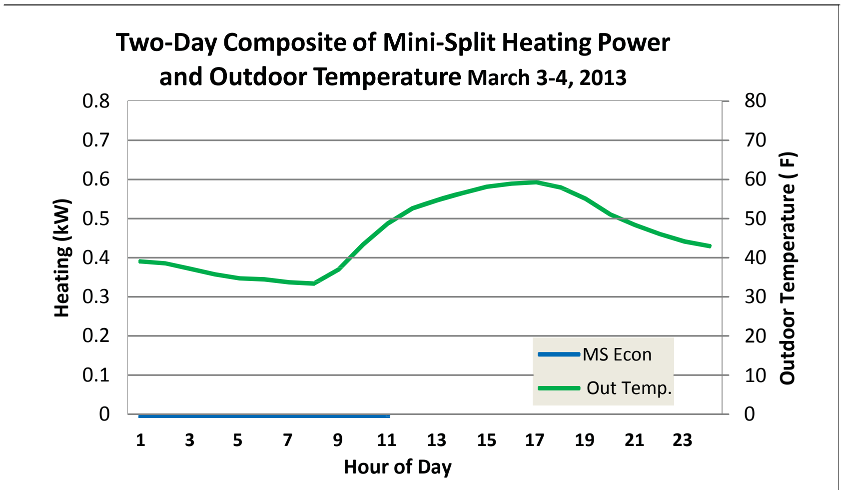

Figure 20. Twenty-four hour composite of solar heat pump operation on a cold two-day period, with average morning low of 33°F and nearly cloudless skies.

Figure 21 shows the same two-day composite period, but with more information about space heating activities. As in Figure 20, outdoor temperature and solar heat pump operation are shown. In addition, however, the mini-split power from the grid (for hours when the solar resource was no longer available) and the central heat pump power are shown. It can be noted that the central 5-ton heat pump also operated during the hours from about 1 AM to 1 PM (purple line).

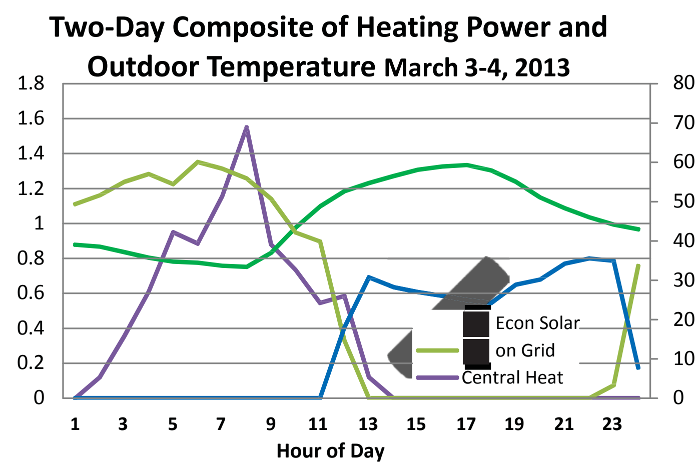

Figure 21. Twenty-four hour composite of solar heat pump operation on a cold two-day period, showing heating power for the mini-split operating on solar (blue line) and on the grid (olive green line), and heating power for the central 5-ton system (purple line).

One might guess that the central system was operating during the 1 AM to 1 PM period because the mini-split could not meet the total heating load. This might be a correct guess, but not entirely. It should be noted that thermostat of the 5-ton system was set at about 1°F lower temperature than that of the mini-split, so that it could act as back-up. As the reader will recall (see Figures 7 or 17), the mini-split (at this time operating on grid power) allows room temperature to deviate increasingly from setpoint as the need for more compressor capacity increases. As the space heating load increased, the mini-split allowed room temperature to drift lower, thus drooping into the deadband of the 5-ton system thermostat and therefore allowing the central 5-ton system to come on. The interaction between the two systems is even more complicated than this. Because the 5-ton system caps the downward space temperature droop, it prevents the mini-split from moving to higher capacity (note that the maximum power draw of the mini-split is 1800 W, per manufacturer specifications) and therefore meeting a higher proportion of the heating load.

Having said all that, it is also possible that the mini-split would not have had sufficient capacity to meet the total heating load during the cold overnight hours, even if the central system setpoint had not been so close to that of the mini-split setpoint. Since the central system uses 2.4 times as much energy per unit of heating output compared to the mini-split heat pump, the spike in central system energy consumption occurring at about 8 AM exceeds the energy consumption of the mini-split by about 20%, but its heating energy output is only about 50% of the heating output being produced by the mini-split.

If the solar heat pump system had more PV panels and a larger battery bank, sufficiently large so that it could have operated continuously through the entire peak demand period, it is likely that it could have met 80-85% of the peak demand for the 6-8 AM period for the March 3-4, 2013 period, just based on its maximum heating capacity. However, the size and cost of that greatly oversized solar heat pump system would yield a system much less cost-effective than the as-tested system.

Figure 22 presents a composite of mini-split power and outdoor temperature for a period of milder heating weather in late March 2013. While the days March 3-4 were quite cold, with average daily temperatures of 44.3°F and 47.5°F, respectively, the period of March 27-29 had average daily temperatures of 53.7°F, 50.6°F, and 53.9°F. Again, these three days had essentially cloudless skies. Even with these milder temperature conditions and full sun, the solar mini-split only operated until about 4 AM, at which time it would shut down until about 9 AM. At this point solar radiation raised battery voltage to the level required to activate the inverter. The research team concludes, therefore, that under normal operation patterns, the solar heat pump (while operating on solar) cannot meet any of the heating 6-8 AM peak demand on peak heating days or even for moderately cold days.

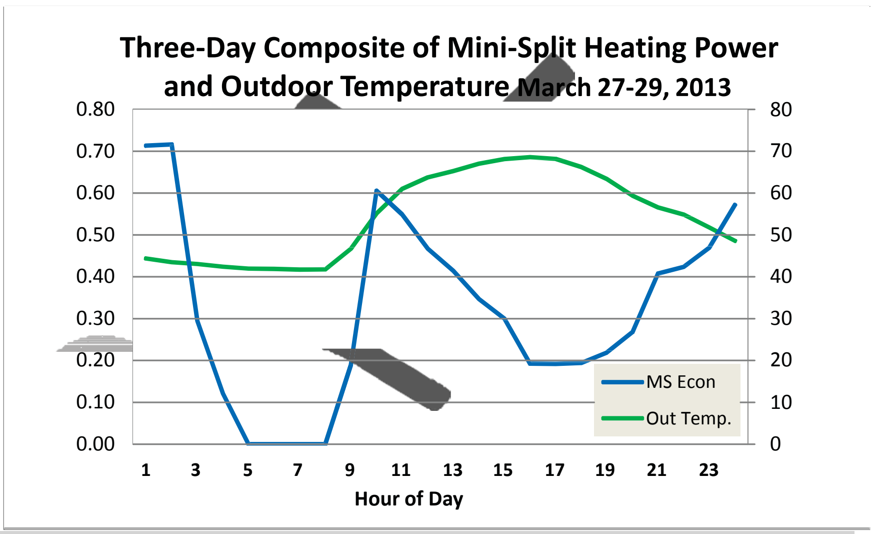

Figure 22. Composite of three moderately cold days in late March shows that there is insufficient stored battery energy to allow the solar heat pump to operate during the 6 to 8 AM peak period.

On the other hand, a management system could be implemented which would control both the solar heat pump and the central ducted system to allow solar-powered peak demand reduction. As the authors envision this control, a system such as "On Call" could (on days when a peak demand event was anticipated the following morning) be used to deactivate the solar heat pump system in the early evening perhaps around 6 PM, when the batteries would be nearly fully charged. The central ducted system would remain active and meet space heating requirements through the night. Then at 6 AM, the solar heat pump would be activated and the central system would be deactivated. With this arrangement, it is anticipated that the solar heat pump would be able to meet 2 or 3 hours of space heating peak demand.

Conclusion: Insufficient data was available to produce peak heating regression analysis. Alternatively, the research team has examined data for a number of cold winter mornings and concluded that the solar heat pump cannot meet any of the 6 - 8 AM heating peak demand. On the other hand, a large fraction of the peak demand (perhaps 85% or more) could be met by the solar heat pump if the central and mini-split heat pumps were controlled by the "On Call" system.

8. ECONOMIC ANALYSIS OF VARIOUS SYSTEM CONFIGURATIONS

An economic analysis has been carried out to determine the relative economic competitiveness of seven solar heat pump system configurations. It should be clarified that the energy performance results presented in Sections 4 through 7 of this report are based on 12 months of monitored data and regression analysis for the "as-tested" stand-alone solar heat pump system. In this section (Section 8), supplemental modeling of several system configurations is performed using a solar simulation tool called [redacted]

All of the system designs evaluated in this section had battery back-up with the exception of 1) a grid-tied solar system with a separate (not integrated) heat pump system; this was the baseline against which the other system designs were compared. Other examined designs included 2) the "as-tested" solar heat pump system, 3) the dc-powered solar heat pump system which was originally proposed but was unavailable for testing, and 4) an optimized bimodal ac- powered solar heat pump system. Three additional variations of the "as-tested" system are also evaluated in this section; 5) the "as-tested" system comparing operation with 8 batteries and 4 batteries, 6) the "as-tested" system with a lower and a higher efficiency mini-split heat pump, and 7) the "as-tested" system with expanded PV/battery capacity. All of the systems used a 1.5 ton mini-split heat pump with SEER 19.2 (SEER rating of 17 for the dc-powered mini-split), though in the case of the system 1, the mini-split operated completely independently of the solar system.

System number 1, which serves as a basis of economic comparison, is a standard grid-integrated solar system with a mini-split heat pump installed in the house but obtaining its power completely from the grid. Just to clarify, the base system consists of a standard grid-integrated PV system (PV panels, charge controller, and inverter) sending solar electricity to the house or the utility grid, with a non-integrated mini-split. The mini-split (1.5 ton, 19.2 SEER unit) heat pump is installed to serve the house but does not operate directly from the PV system. It can be considered, however, to be operating indirectly from the solar system. Because there are no batteries, this base system has no stand-alone operation nor can it serve as a back-up system in case of grid power outage.

In all cases, a substantial portion of the seasonal energy savings occurred as a result of the high efficiency of the mini-split heat pump. The ac-powered mini-split had a net efficiency that was 1.97 times that of the [redacted] Lab central SEER 13 ducted heat pump (which has an effective SEER of 9.75 after including 25% attic duct system losses). The dc-powered mini-split's net efficiency was 1.74 times that of the central system. The fact that in most cases all of the solar power was being delivered through the mini-split means that the mini-split can be thought of as an amplifier, in effect doubling (or nearly doubling) the delivered savings that the solar system would otherwise have provided.

There is another source of seasonal energy savings apart from solar powering of the mini-split, and that is operation of the mini-split from the grid when the solar resource has been depleted. This applies to all of the systems except the dc-powered system, which can operate only while the sun is shining or the batteries have stored energy. While the "as-tested" solar heat pump system meets about 53% of the heating and cooling load of the house ([redacted] Lab, in this case) from solar alone, the remaining space conditioning load can be substantially met by operation of the high efficiency mini-split operating from the utility grid. The "as-tested" solar heat pump system had a relay installed that allowed the mini-split to switch seamlessly from solar to grid when the solar resource was depleted. For this analysis, the research team assumed that 80% of the remaining heating and cooling load that had not been met by the solar heat pump would, in fact, be met by the mini-split operating off of the grid. The fact that the mini-split could provide the required space conditioning at approximately twice the efficiency of the central system, meant that the energy represented by the remaining 47% of the yearly load not met by solar would then be effectively cut in half. As a result, about 72% of the energy use that would have occurred with the central ducted system was saved by the mini-split heat pump system when operating from solar and the grid.

Economic analysis has been carried out for four solar heat pump system configurations, plus three additional variations on the "as-tested" system, to identify which systems provide the best economic performance. There are a variety of economic evaluation methods for Life Cycle Cost (LCC) analysis, each with advantages and disadvantages. This section uses payback period as the metric of economic comparison, taking into account fuel cost escalation, the time value of money, and the replacement cost for batteries every 7 years, the inverter every 10 years, and the mini-split every 15 years.

Since the objective of this economic analysis is to compare each of the systems on an even playing field rather than predicting energy outcomes for the full FPL service territory, all of the modeling is performed using the TMY3 data from Melbourne, Florida. The electricity utility rate is assumed to be $0.10/kWh for on-peak/off-peak electricity. Following are economic assessments for seven system configurations. National Renewable Energy Laboratory's [redacted] software has been used to perform the economic analysis. The cash flow analysis captures installation and operating costs, taxes, incentives, and the cost of debt. [redacted] uses the system's hourly output for a single year generated by the performance model (and TMY data), and then calculates a series of annual cash flows for revenues from electricity sales and incentive payments, tax liabilities (accounting for any tax credits for which the project is eligible), loan principal, and interest payments. [redacted] reports a set of economic metrics, such as the levelized cost of energy (LCOE), which it calculates from the cash flow. Currently, residential systems cost about $3.5/W or less. Of course, this cost will vary from contractor to contractor due to their differing degrees of buying power, overhead, installation practices, and profit margin. Each of the solar heat pump systems has 2.0 kW of PV. For this analysis, a cost of $3.5/W was assumed for the solar portion of the grid-tied system, including the inverter and charge controller. The full cost of the solar portion of the system is $7000. The 1.5-ton mini-split heat pump is assigned an installed cost of $4200. The net cost of the system after a 30% Federal Tax Credit is $7840 for systems without batteries. Analysis is also based on annual rise in retail electricity rates of 5%, a 5% inflation rate, a 5% real discount rate, and a PV panel performance degradation rate of 0.5% per year. It should be noted that the values for these assumptions, including the installed cost of PV systems, will vary by geographic region and utility.

Table 10 presents results from economic analysis results for four solar heat pump design variations. Shown are simulated seasonal electrical energy savings and payback period taking into account net system initial cost (after 30% Federal tax credit), replacement costs for batteries, inverter, and mini-split heat pump with an assumed electricity cost of $0.10/kWh in the first year and escalating by 5% per year. Following Table 10 are descriptions and discussions in Sections 8.1-8.4 of the four solar heat pump system variations. Three additional system design variations of the "as-tested" system are presented in Sections 8.5-8.6, with economic assessments of using four batteries instead of eight batteries and the relative cost-effectiveness of installing a higher efficiency mini-split heat pump versus adding more PV/battery capacity.

Table 10. Seasonal Savings and Payback Period for Four Solar Heat Pump System Designs Taking into Account Maintenance and Component Replacement Costs over a 20-year Period

	PV produced kWh/y	PV+M-S avoided kWh/y	Mini-split on grid savings kWh/y	Seasonal savings kWh/y	Gross system cost	Net system cost [1]	Payback period years
Grid-integrated	2968	3877	1274	6151	$11,200	$7,840	12
"As-tested"	2734	5386	539	5925	$15,200	$10,640	20
DC	2441	4247	-	4247	$12,860	$9,002	22
Bimodal	2968	3877	1274	6151	$13,600	$9,520	17

[1] after 30% Federal tax credits

8.1 Analysis for a Grid-tied Photovoltaic System with Heat Pump but No Batteries

This is a traditional grid-tied PV system, consisting of PV modules, charge controller, and inverter, but which also incorporates a mini-split heat pump that operates independently of the solar system (Figure 23). The system has no batteries. Each module, when exposed to sunlight, generates dc electrical energy. An inverter converts the dc electricity to ac electricity, which can be consumed immediately by electronics in the building or exported to the grid. When the central utility's electric grid goes down, the homeowner has no electrical service or space conditioning service, as would be the case with the systems evaluated in Sections 8.2 and 8.4, since the system has no battery back-up and the PV power must disconnect from the grid when there is a power outage.

The grid-tied PV system without battery back-up has an efficiency advantage because the batteries decrease system performance by about 6%.

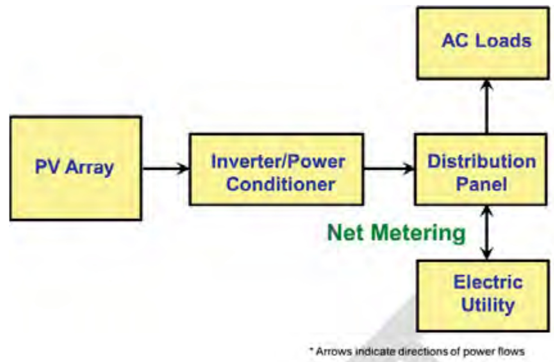

Figure 23. Utility Grid-Interactive PV System

8.1.1. System Description

For this analysis, a 2 kW grid-interactive system using the same PV modules as that of the Stand-alone System as tested this past year and a grid-tied inverter. The system cost is $7000 for the PV system and $4200 for the 1.5-ton mini-split, for a combined gross cost of $11,200. Net cost is $7840 after 30% Federal Tax credits. Life-cycle cost analysis assumes a 20-year evaluation period, modeled energy output for the system ([redacted]), a 0.85 dc-to-ac derate factor (accounting for various types of losses that occur in the PV system), estimated annual PV system O&M costs of $25, periodic replacement costs for the inverter and mini-split heat pump, and an effective SEER for the central ducted system of 9.75 (a SEER 13 system taking into account duct losses).

8.1.2. Economic performance

Figure 24 shows simulated hourly electricity from the PV system in red, electricity from the grid to the mini-split and central heat pumps in purple, electricity to house ac loads in blue, and electricity to grid in green. Peak electricity consumption and production occur during the summer months when the demand for cooling is high.

The PV system delivers a simulated 5144 kWh/y into the utility grid. In addition, the mini-split heat pump produces 306 kWh/y energy savings when the mini-split displaces heating and cooling that would otherwise occur with the central ducted system operating (more discussion on mini-split energy savings is found in Section 8.2). Together, first year net savings from this system is 5450 kWh, yielding a payback period of approximately 12 years.

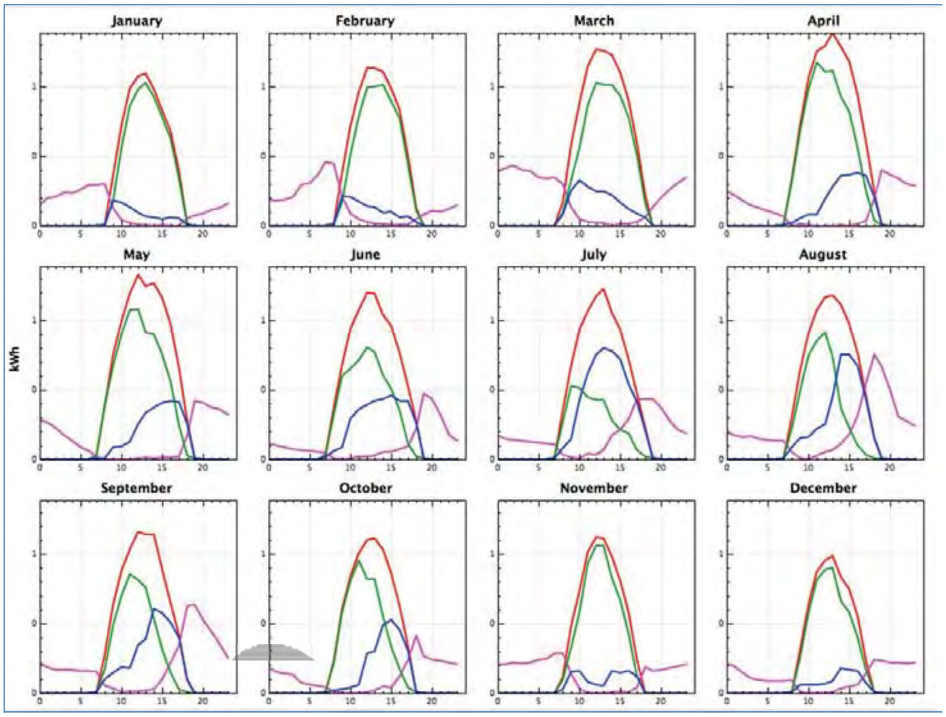

Figure 24. Grid Interactive monthly 24-hour profile PV system supply/demand energy flows.

8.1.3. Discussion

The grid tied solar system (with mini-split which operates in parallel to the solar) is found to be considerably more cost-effective than the other systems because there are no battery costs. However, this system does not provide a critical back-up service function for periods when the grid goes offline.

8.2 Analysis for the Stand-alone System as Tested This Past Year

The stand-alone solar heat pump system, as tested over the past 12 months in the Building Science Lab and described in earlier sections of this report, consists of PV modules, a charge controller, a bank of batteries, an inverter, and an ac-powered mini-split heat pump (Figure 25). The solar system provides power exclusively to the heat pump (although the inverter could be configured to provide power to other end uses within the home). Because the mini-split has a high SEER rating and has no distribution system losses, it delivers space conditioning to the building at 1.97 times the efficiency of the central ducted system.

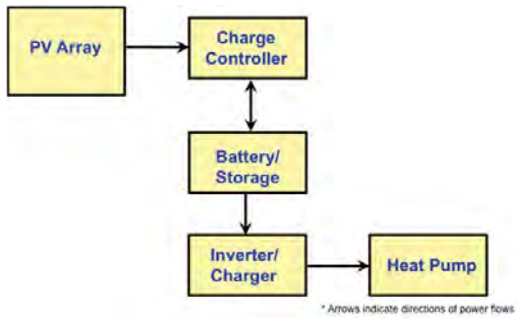

Figure 25. "As-tested" Stand-Alone Solar Heat Pump System

8.2.1. System Description

The inverter has the capability of receiving power from the grid but it cannot deliver electrical energy to the grid. The fact that the inverter can obtain power from the grid allows the mini-split to operate through all hours of the day (if so selected), thus providing significant additional energy savings compared to operating the central ducted heat pump during hours when the solar resource has been depleted.

The cost of this stand-alone solar heat pump system has been estimated to be $15,200 based on current (September 2013) costs of system components, right-sizing the inverter (a 4 kW inverter was purchased but only 2 kW was required), and estimating contractor mark-ups, plus the $4200 installed cost of a 1.5-ton Fujitsu 19.2 SEER mini-split heat pump. After 30% tax credits, the net system cost to the customer is estimated to be $10,640.

8.2.2. Economic performance and discussion

The solar heat pump system saves energy in two ways. In the first place, the PV system delivers energy to the mini-split which then provides space conditioning to the residence that displaces electrical energy that would otherwise be consumed by the central ducted system (a SEER 13 heat pump with attic ducts that have delivery efficiency of 75%). These savings can be considered savings from solar energy. However, the solar generated electricity is enhanced by being delivered to the house by means of a high efficiency (SEER 19.2) mini-split (with zero cooling and heating distribution losses). Because its effective efficiency is essentially twice that of the central heat pump system, total solar savings are greatly enhance. In the second place, the mini-split heat pump can, on a regular basis, be powered by the grid after the solar resource has been depleted (based on operation of a simple relay), thus displacing additional space conditioning energy that would otherwise be consumed by the central ducted system.

On the other hand, since excess solar electricity (that which cannot be used when the space conditioning load has been satisfied) is in effect thrown away, savings are reduced.

Based on the simulation performed in [redacted], the PV system delivers 2734 kWh/y to the heat pump operating in Economy mode and using 8 batteries. Because the mini-split operates at 1.97 times the efficiency of the central ducted system, the combination of solar and mini-split saves 5386 kWh/y in electrical energy use that the central system would otherwise have consumed. An additional 539 kWh of annual energy savings result when the mini-split is powered by the grid during hours when the solar resource has been depleted. Combined, these result in first year energy savings of 5925 kWh. With these savings, the payback period is approximately 21 years.

8.3 Analysis for a dc-powered Solar Heat Pump System

This system is comprised of an array of PV modules, a charge controller, a bank of batteries, and a dc-powered mini-split heat pump (Figure 26). No inverter is required since the electrical load is a dc-powered heat pump.

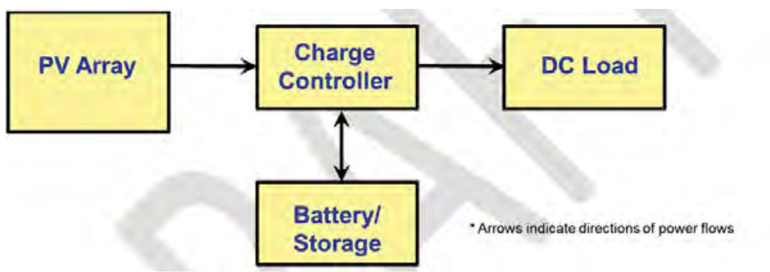

Figure 26. Solar Powered Heat Pump System

8.3.1. System Description

This dc-powered system (this is [redacted] system which was originally proposed for this project) is similar to the preceding "as-tested" ac system (including PV modules, charge controller, and batteries). However, there are several important differences. This system would have no inverter, the mini-split heat pump would operate on dc power, there would be no critical-service ac-circuit within the house (to provide power to the homeowner during grid outages), and the mini-split could operate only when the solar resource is available (i.e., there is no way to operate the heat pump on the grid). [redacted] software was used to simulate annual solar energy production and consumption. The full cost of the system is estimated to be $12,860 and the net system cost is estimated to be $9,002 (after tax credits). These first costs are lower than for the ac-powered system because no inverter is required. PV system efficiency is higher because the 10-15% inefficiency losses from the inverter are avoided. On the other hand, the SEER 19.2 ac mini-split has an approximate 13% efficiency advantage over the SEER 17 dc-powered mini-split.

8.3.2. Economic performance

Based on the simulation, the dc-powered system delivers 2441 kWh/y to the dc-heat pump [redacted] from the PV/battery system. Because the dc-powered mini-split has 1.74 times the efficiency of the central ducted system, this yields savings of 4247 kWh/y of avoided energy consumption of the central system. There are no additional savings from operating the mini-split using grid power, since the dc unit cannot operate on ac current. With these savings, the payback period is approximately 22 years.

8.3.3. Discussion

The payback period of the dc-powered solar heat pump is a little longer compared to the "as-tested" ac-powered solar heat pump. It could also be argued that there are additional factors that might make the ac-powered mini-split more attractive. First, ac-powered mini-splits are being widely used around the world and have a reputation for excellent reliability. It is less certain that dc-powered mini-splits are reliable. Second, when service and repair are required, it will be more difficult to get service and parts for the dc system. Third, the ac-powered system offers more versatility, by potentially providing critical service to a variety of ac end uses such as communication, lighting, and refrigeration during periods of grid power disruption. Fourth, the dc-powered system can only supply power to dc appliances, so excess solar power (not consumed by the heat pump) will go to waste, whereas excess power in the ac-powered system could be delivered to other ac appliances.

8.4 Analysis for an Optimized Solar Heat Pump System with Bimodal Inverter

An optimized bimodal, grid-interactive solar heat pump system with battery backup is proposed as a significant improvement compared to the "as-tested" system that can help with reliability of the battery bank. This system consists of an array of PV modules, charge controller, bank of four batteries, bimodal inverter, and 1.5-ton SEER 19.2 ac-powered mini-split heat pump (Figure 27). The system can operate as a grid-interactive system and as an Uninterrupted Power Supply. The inverter would have two-way energy flow capability (intermittently purchasing electrical energy from the grid and selling electrical energy to the grid). Because of battery storage and the dc-to-ac inverter, a critical-service ac-circuit could also be provided to the house to meet ancillary service to communication, lighting, refrigeration, and other uses during grid power interruption. When solar is unavailable, power from the grid would maintain the standby load circuits through the batteries/inverter.

It should be noted that a four-battery storage system was selected for this system to optimize cost-effectiveness. An eight-battery system could also be examined, but it would have the disadvantage of costing about $1500 more at first cost and at each of the 7-year battery replacement cycles. On the other hand, a bank of eight batteries would allow the system to provide improved power back-up to the home during periods when the grid goes down. For the homeowner, then, the choice is whether to pay more to have greater back-up when the grid goes down or whether to have a more cost-effective system that provides reduced back-up capability during power outages. Since the larger battery bank also helps the utility with meeting peak demand, incentives from the utility could be provided to the customer to incentivize purchase of the larger battery storage.

In normal operation, the inverter would use utility power, as needed, to charge the battery bank to maintain a minimum SOC. When utility grid goes down, the batteries can serve as a power source for the ac critical loads. When the batteries are fully charged, excess power generated by the PV array can be exported to the grid.

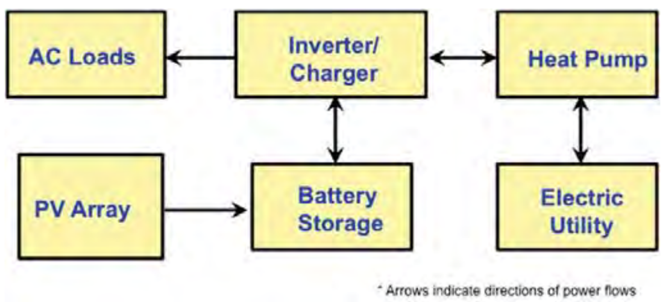

Figure 27. Bimodal PV System

8.4.1. System Description:

The proposed optimized solar-powered heat pump system would have essentially the same components as the "as-tested" stand-alone system except that the battery bank would use four batteries instead of eight and the inverter would have bimodal capability. To improve battery life, the utility grid is designed to charge the batteries when SOC falls to 80% and discontinue charging at 85% SOC. Electrical energy would flow rather freely back and forth between the solar/battery system and the grid. In this design, power would be provided to the mini-split and also to a separate 120V critical loads circuit from the inverter/batteries. This would serve the function of providing an uninterruptable power supply to critical end uses on a relatively continuous basis. Additionally, battery/inverter power would also be available to this circuit during grid power outages, for shorter periods (for minutes to hours) and for more extended periods (multiple days resulting from storm or other causes). While the SOC range would be limited to 5 percentage points during normal operation, during grid outages, the SOC range could be increased by a factor of about 10 to allow expanded storage and delivery of available solar electricity.

8.4.2 Economic performance

The system cost is estimated to be $13,600 ($1600 less than the "as-tested" system because it uses 4 fewer batteries) including the $4200 mini-split heat pump. After 30% federal tax credits, the net system cost is projected to be $9520.

The bimodal system generates 2968 kWh/y in PV electricity. Of this 2968 kWh/y, 1968 kWh/y of solar power goes to the heat pump operating in Economy mode, which then generates 3877 kWh/y in avoided energy consumption by the central ducted heat pump system. Another 1000 kWh/y is projected to be consumed by other household ac end uses or be sold to the utility. Additionally, an additional 1274 kWh/y of avoided space conditioning energy consumption occurs when the mini-split operates on the grid. With these savings, the payback period is approximately 17 years.

8.4.3 Discussion

Compared to the “as-tested” stand-alone system, this optimized system is about 10% less expensive and yields about 4% greater energy savings. Additionally, this bimodal system will be much more reliable because of greatly enhanced battery life. While the batteries in the “as-tested” system failed after about 12 months of service, it is anticipated that the batteries in this proposed bimodal system should have a life-expectancy of seven years.

Since batteries are expensive and represent a weak link in the “stand-alone” system and dc-powered system concepts, it is anticipated that the small range of SOC cycling will greatly extend the life of the batteries. This would, in some ways, be comparable to the success of some brands of hybrid auto electrical storage system, which have had very low rates of battery failure over a 10-year operation period, achieved in large part by having a very narrow range of SOC operation. Using this configuration, the inverter would be available to serve both the mini-split and other critical loads. The only time that the critical loads circuit would be unavailable would be if the grid has been down for an extended period and the solar resource is insufficient to maintain the battery bank charge. When the utility grid goes down for longer periods (days), the battery SOC operation can be expanded to allow greater operational performance from the system. With the battery SOC widened for only a few days per year, the life of the batteries would still be greatly extended while the robust back-up function is preserved for periods of grid outage.

8.5 A Cooling Season Optimized System (4 batteries versus 8 batteries)

Economic performance has also been examined for a smaller battery bank (4 batteries versus 8 batteries) for the “as-tested” system. As was discussed in Section 2.3.2, the amount of battery storage required for good system performance varies substantially between the cooling season and the heating season. In our monitoring results, the 4-battery system performed reasonably well during cooling weather. However, the 4-battery system performed very poorly during heating weather. Even the 8-battery system performed only marginally during the heating season, especially at peak hours. Since the FPL service territory is heavily weighted toward cooling (with cooling degree days on the order of 5 to 10 times that of heating degree days across most of the service territory), it might make sense to optimize the system for the cooling season.

When modeling (based on regression analysis of monitored data) is done with 8 batteries and 4 batteries, the predicted annual savings for the "as tested" stand-alone system is found to be 2683 kWh/y and 2101 kWh/y, respectively, with Standard control. When operated in Economy mode, the 8-battery and 4-battery options yielded 3322 kWh/y and 2516 kWh/y savings, respectively. Since the extra four batteries represent about $1600 of extra cost to the customer, and the savings from having 4 additional batteries is only $58 per year (assume $0.10/kWh) for Standard control and $81 per year for Economy control, it appears that sizing the system for cooling optimization (4 batteries) is the more cost-effective approach.

On the other hand, having 8 batteries yields a more favorable outcome for peak demand and is likely to make the system more functional to the customer as a back-up system during grid outages.

8.6 Evaluation of Two Additional System Design Alternatives

The economic benefits of two options 1) installing a higher efficiency mini-split and 2) installing greater PV and battery capacity are examined.

1 *Purchasing a higher efficiency mini-split.* Analysis has been done to identify the incremental cost of higher efficiency mini-split heat pumps. The cost of purchasing mini-split equipment only (installation additional) is shown in Figure 28 for ¾-ton, 1-ton, 1.5-ton, and 2-ton systems. It can be seen that while there is no strong correlation between SEER and cost, there is a general upward price increase trend with increase in SEER rating. For this cost analysis, we have chosen to focus on 1-ton systems, because there is a fairly good sample size and the data trend is reasonably well behaved. For this size of system, there is an increase in cost of about $600 (from about $1200 to about $1800) as SEER goes from 16 to 25. The 1-ton systems, therefore, show equipment an efficiency cost increment of approximately $67 per SEER rating point. Extrapolating the price increment to 1.5-ton units, this would be $100 per SEER point.

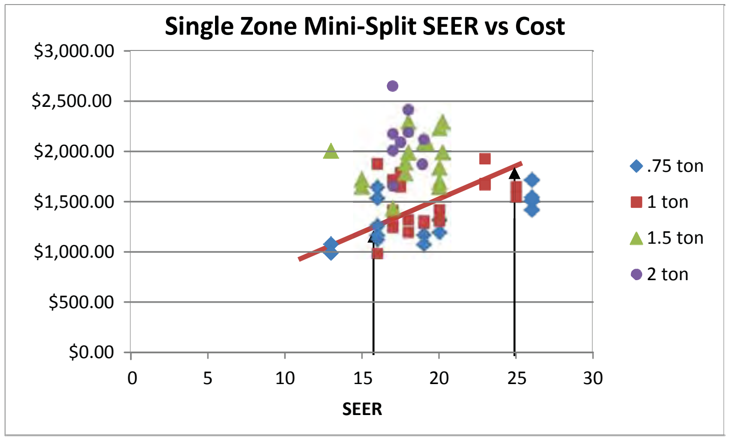

Figure 28. Equipment cost versus SEER rating for four sizes of mini-split heat pumps based on an on-line survey, including a best-fit line for the 1-ton units. (Source: survey performed by [redacted] in 2011.)

To examine the cooling energy savings related to mini-split SEER rating, we will begin at the low end of the efficiency spectrum, with a SEER 16 rating. We will also assume that the solar heat pump system has been configured so that the mini-split can be operated from the grid as well as from solar. Simulations found that the SEER 19.2 mini-split saves 4442 kWh/y in cooling energy savings when operated from both solar and the grid (Table 6). These savings are derived under the assumption that this mini-split delivers all of the solar-source cooling, that it operates off of the grid to meet 80% of the remaining yearly cooling that would otherwise be met by the MH Lab SEER 13 central ducted system, and that the SEER 13 central system operates at an effective SEER of 9.75 because of duct losses.

- Given that the 19.2 SEER mini-split saves 4442 kWh/y, we calculate that the annual cooling savings would be 3842 kWh if using a SEER 16 mini-split.
- Given that the 19.2 SEER mini-split saves 4442 kWh/y, we calculate that the annual cooling savings would be 5242 kWh if using a SEER 25 mini-split.
- Yearly cooling savings from going from SEER 16 to SEER 25 is then 1400 kWh.
- If we assume that heating energy savings are equal to 15% of the cooling savings (this is based on HDD being about 15% of CDD in the FPL service territory), then yearly heating savings from going from SEER 16 to SEER 25 is then 210 kWh.

Annual cooling and heating electricity savings to the customer from installing a SEER 25 heat pump versus a SEER 16 unit would be 1610 kWh/y ($161/year). Given that the installed cost of the SEER 25 system is estimated to be $900 more than that of the SEER 16 system, the payback period for purchasing a higher efficiency mini-split is less than 8 years.

2 *Adding greater PV/battery capacity.* For this analysis, 500 W of additional PV capacity with proportional additional battery capacity is added to the "as-tested" system. Incremental net

cost will be $963 ($700 for the 500 W of PV and $675 for the battery each with 30% tax credit). Energy savings produced by the incremental PV/battery system is found to be 474 kWh/y ($47/y). Therefore, the incremental cost of $963 for the added PV and battery capacity yields a payback of about 20 years. Because the payback period for purchasing a high efficiency mini-split is less than 8 years, it is clear that purchasing increased mini-split efficiency is a much better investment.

9. Summary and Conclusions

Lab research was conducted to evaluate annual and peak energy savings from operation of a solar powered mini-split heat pump system in a home also served by a central ducted heat pump system. The mini-split can also operate on grid power when the solar resource has been depleted. Energy and peak demand savings are based on TMY3 simulation and weighted for four cities (Daytona Beach, West Palm Beach, Miami and Ft. Myers). The five configurations evaluated over a 12-month period were:

- PV power, 8 battery back-up, mini-split with Economy control
- PV power, 8 battery back-up, mini-split with Standard control
- PV power, 4 battery back-up, mini-split with Economy control
- PV power, 4 battery back-up, mini-split with Standard control
- PV power, 8 battery back-up, with mini-split also operated on the grid (100% MS) when the daily solar resource had been depleted.

Regression analysis and simplified simulation using TMY3 data provided savings results for these five configurations.

A more complex hourly model was used to simulate several variations on the as-tested system and a base-line system (grid-integrated solar system with no batteries).

FPL also requested answers to the following:

- Which system type (PV-grid integrated solar system with no batteries and separate mini-split heat pump versus the as-tested solar heat pump system with batteries) is more cost-effective and what level of peak demand reduction is achievable by each?
- Which upgrade is more cost-effective; 1) money to upgrade heat pump efficiency or 2) money to expand the PV/battery system?

The results of this analysis are presented in Section 8 and briefly summarized in the following list.

1. The "as-tested" solar heat pump system (with battery back-up) meets up to 72% of annual space conditioning energy consumption, but the economic returns are not attractive with payback on the order of 20 years. Furthermore, there are significant maintenance requirements and on-going costs associated with the batteries that further cut into possible savings. On the other hand,
   a. The solar heat pump system produces substantial cooling peak demand reduction (2.20 kW) which can be attractive to the utility. It was, on the other hand, ineffective in meeting heating peak demand.
   b. As configured and operated in the MH Lab, the mini-split can meet up to 54% of the annual space conditioning requirement from solar alone. Another 18 percentage points of space conditioning savings can be achieved by operating the high efficiency mini-split from utility grid power thus displacing energy that would otherwise be consumed by the lower efficiency central ducted heat pump system, bringing savings to 72% (4442 kWh/y).

   c. The system can also potentially provide 120V ac service for other appliances during periods when the grid goes down.

2. Batteries are the weak link in the stand-alone solar heat pump system. When subjected to nearly daily cycling from 45% to 90% state-of-charge (SOC), the batteries experienced dramatically diminished storage capacity by the end of 12 months.
3. The inverter proved to be more inefficient (84% monitored efficiency) than originally anticipated compared to expected 90-95% efficiency. It will be important, for future stand-alone applications, to find a higher efficiency inverter.
4. A bimodal inverter (able to both receive from and deliver to the central grid) is needed in order to use excess solar energy that is available on sunny days with limited space conditioning loads.
5. An optimized bimodal stand-alone system design is proposed in this report that will make the system more cost-effective by delivering all of the available solar energy either to the mini-split, the house, or to the utility grid, and by greatly extending the life of the batteries.
6. A grid-tied PV system, with a mini-split heat pump operating independently of the PV but without batteries, was modeled and found to have a payback period of about 12 years. It cannot, however, provide back-up for when the grid goes down. It meets 100% of the cooling peak demand of the HVAC system when operated in tandem with the high efficiency SEER 19.2 mini-split heat pump but 0% of the heating peak demand.
7. The solar heat pump system with battery back-up provides considerably more yearly cooling and heating electricity savings while operating in Economy mode.
   a. Indoor RH control was very good for both control modes typically 39% for Standard mode and 46% for Economy mode.
8. The “as-tested” solar heat pump system (using Standard control) achieved 100% peak demand savings on the hottest hours of the hottest days – on the order of 2.2 kW reduction. By contrast, Economy mode produces peak savings of about 85% during those same hours. If the “as-tested” system is operated with only 4 batteries, 85% of the peak cooling demand is met in Standard mode and 69% is met in Economy mode.
9. A direct current-powered solar heat pump system would be slightly less cost-effective compared to the “as-tested” system. It would deliver lower energy savings but is expected to have a lower first cost. On the other hand, the dc mini-split would be unable to provide high-efficiency space conditioning using power from the grid during periods when the solar resource has been depleted and would not be able to provide space conditioning or 120V ac back-up service when the grid goes down.
10. An optimized bimodal stand-alone solar heat pump system is proposed in this report as a means to yield longer battery life and lowered battery maintenance/replacement costs while also reducing or even eliminating the solar power that must be discarded by the “as-tested” system during periods of low space conditioning loads.

11. A 4-battery (instead of 8-battery) version of the “as-tested” system might be slightly more cost-effective to the homeowner but less effective in summer peak demand reduction and at providing critical service during grid outages.
12. Installing a higher efficiency mini-split system is cost-effective, with a payback of less than 8 years for the added cost for higher efficiency.
13. Installing more PV/battery capacity is less cost-effective, with a payback on the order of 20 years.

APPENDIX A

Performance Analysis of Components of the Stand Alone System

When this research project began, the dc-[redacted] heat pump was not available from the manufacturer. FSEC then offered to monitor the energy delivery efficiency of the inverter (which would not have been required for the dc heat pump) in order to account for this inefficiency when simulating the dc-heat pump system performance. Power meters were installed at various junctions of the solar heat pump system, thus providing data that can be used to determine the efficiency of each component of the system. Figure A-1 illustrates system components and energy flow patterns.

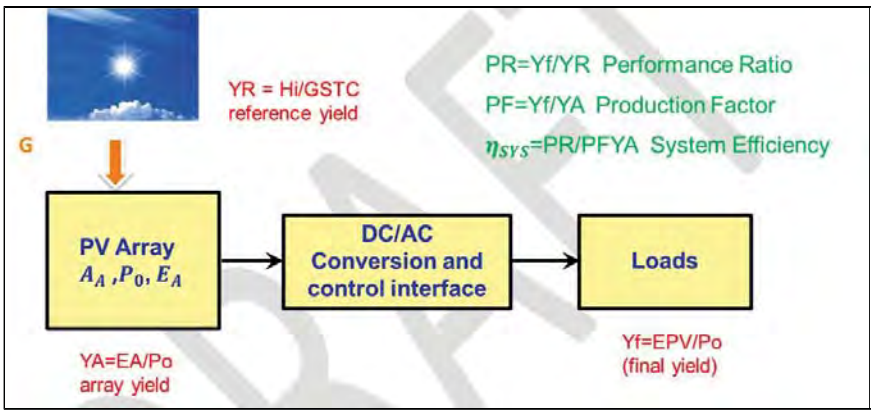

Figure A-1. System Operation Energy Flow Patterns and Definitions.

The method of analysis presented here provides a means of evaluating the performance of the monitored solar heat pump system and each component separately. An understanding of some PV terminology is helpful in understanding this analysis. PV system power rating refers to the nameplate dc power rating of the PV array provided by the module manufacturer. This is the sum of the ratings for all of the PV modules connected, and refers to their electrical power output under Standard Test Conditions (STC). STC for a PV array are an irradiance of 1000 W/m^2 incident on the modules, spectral distribution of 1.5 atmospheres, and cell temperature of 25°C (77^{o}F). PV system yield, YA, is defined as the array dc energy output divided by the PV system power rating. Moreover, final PV system yield, Yf, is defined as the net ac output energy divided by the dc nameplate power of the array under STC. The higher this number, the more energy the array has generated relative to its potential. Reference yield, YR, is defined by the total plane-of-array (POA) solar irradiation incident on the array, [redacted] divided by the reference irradiance at STC, which is 1000 W/m^2. The performance ratio (PR) is simply the final PV system yield divided by the reference yield (YR). This parameter allows for a more appropriate comparison of one PV system to another by normalizing the difference in irradiance incident on the individual arrays. The higher PR is, the better the system is using its potential. A low PR value means production losses due to technical or design problems are high. The production factor (PF) is defined as final PV system yield divided by reference yield (YR) (Figure A-2). Finally, system efficiency is simply the performance ratio (PR) divided by the production factor (PF). The empirical relationship between PF and PR is shown in Figure A-3.

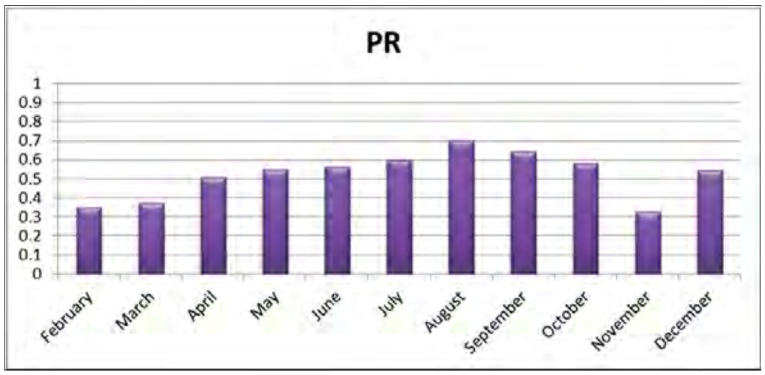

Figure A-2. Calculated Performance Ratio (PR) values are determined based on monitored data from the “as-tested” solar heat pump system for each month of the year.

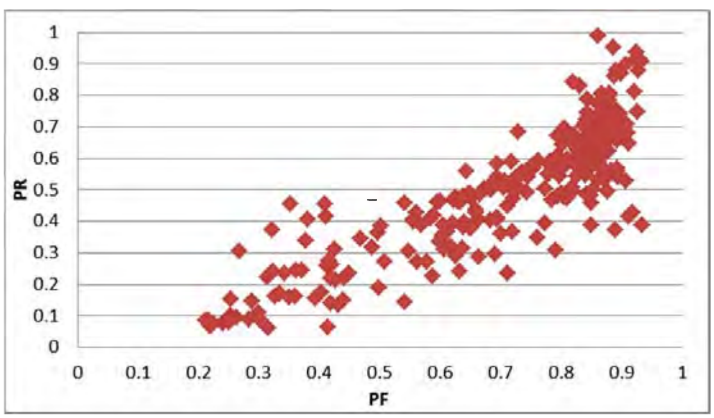

Figure A-3. Performance Ratio plotted versus Production Factor based on monitored data.

Lower monthly PF values indicate that system production is limited by low consumption (low space conditioning loads) during that month.

Between the sun and the electrical end use, various inefficiencies emerge. PV system losses (or PV system derate factor) is determined for the system through each system component. It is the product of all of the system efficiencies and miscellaneous sub-factors including: module mismatch and nameplate tolerance, inverter, wiring losses, charge controller, and battery bank charging and discharging.

The first is panel mismatch. To determine the module mismatch and nameplate tolerance, the four PV module strings' operating voltages and currents were measured using an IV curve tracer (PV600). Measurements were taken at the combiner box for the array. Plane-of-array irradiance values and modules temperatures were measured using a reference PV cell and thermocouple. Due to the dynamic nature of PV module performance and constantly changing operating conditions, the performance specifications of a module or array have meaning only when the rating conditions are given. Measured operation data were translated to the Standard Test Condition (STC) using translation formulas for temperature and irradiance, the two principal factors affecting PV performance. String measurements were taken. The instantaneous efficiency for each array was developed. As can be seen, the four PV panel strings have an average derate factor of 6.5% (Table A-1). The efficiency loss of the PV strings is caused by differences in maximum power point voltage. The panel with the lowest voltage pulls voltage down for the other panel in the string.

Table A-1

Analysis of the solar heat pump system PV strings (1 modules per string) over the period July 15, 2012 – July 15, 2013 finds that PV module mismatch produces losses of 6 to 7% for each of the four strings of panels.

	Vmp Volts	Imp Amps	Pmax Watts	Voc Volts	Isc Amps	FF	PF %	Irradiance (W/m^2)	Temp. deg C	Vmp(trans) Volts	Imp(trans) Amps	Pmax(trans) Watts	Voc(trans) Volts	Isc(trans) Amps	ΔP Watts
String #1	55.3	4.94	273	69.0	5.28	0.750	95.4	634	42.8	60.16	7.78	468.28	72.87	8.32	-6%
String #2	54.9	4.98	273	68.9	5.39	0.736	94.9	638	42.8	59.63	7.81	465.64	72.81	8.44	-7%
String #3	55.1	5.05	278	69.0	5.44	0.741	95.7	640	41.7	59.58	7.89	470.01	72.62	8.50	-6%
String #4	55.6	5.03	280	69.0	5.45	0.744	95.3	647	41.1	59.98	7.78	466.41	72.49	8.42	-7%

The average module mismatch and nameplate tolerance value is 0.94, which means that the strings are only delivering 94% of the potential energy that could be produced under ideal mismatch and nameplate tolerance circumstances. This is a typical value for an average efficiency crystalline module. Based on a comprehensive data analysis, the average efficiency for all the other components has been calculated as follows:

Inverter = 0.84
Charge Controller = 0.96
Battery Bank = 0.94
Wiring = 0.98

When all of these losses are considered together, the resulting system derating factor is 0.70. This is calculated as the product of all system derating sub- factors (0.94 x 0.84 x 0.96 x 0.94 x 0.98 = 0.70).

The largest surprise from this analysis was the low efficiency of the inverter. The research team had been expecting overall dc to ac conversion efficiency through the inverter to be closer to 90-95%.

APPENDIX B

Improving Solar Heat Pump System Control to Achieve Maximum Peak Demand Savings

For the cooling season, peak demand savings are likely to be achieved on all peak days, especially when the mini-split is operated in Standard mode, which tends to produce maximum cooling output. The reason for this is that the hottest hours generally have substantial solar radiation, and if not, the battery is nearly always near full charge at this peak time. Furthermore, the solar heat pump is always producing cooling during the hours of 4 PM to 6 PM on these hotter than average days, either by solar directly from the PV or from stored energy in the batteries.

For the heating season, peak demand savings can in most cases be achieved during the utility's peak demand period but only by careful scheduling of heat pump operation using a timer. Another way to express this is that the homeowner would need to be significantly motivated to get the solar powered heating to occur during the winter peak period. The project research team implemented several timer schedules with the objective of having the mini-split operate fully during the 6-8 AM peak demand period. We were generally not successful, because the batteries can carry forward only a limited amount of energy.

There is tension between several operational factors. On one hand, we want to allow the system to operate for as many hours as possible on solar power, so that little or no collected solar power is thrown away. However, since we would also like to shift the heat pump operation to the coldest hours of the cold winter morning, this means shutting down the solar powered space heating fairly early in the evening on a cold winter night. On our first try, we scheduled the heat pump to operate on solar till 12:30 AM (EDT) and then turn back on at 5:30 AM (EDT). This worked well on moderately cold nights with low temperature of 45^{o}F to 50^{o}F. For colder nights, too much of the stored battery power was expended by 11:30 PM, so that the battery SOC was too low at 6 AM.

March 3, 2013 was the coldest day of the 2012-2013 heating season, with a low of 34^{o}F and a high of 55^{o}F. Space heating was needed for every hour of the day in part because of the relatively high space heating setpoint of 76^{o}F (this elevated temperature was chosen in order to increase the potential for the heating system to operate on a maximum number of days; for our modeling we use 72^{o}F as the house heating setpoint). Solar powered heating occurred from about 11:55 (EDT) till 2250 (EDT), but then remained off till 1130 (EDT) the next day when the batteries reached their cut-in battery voltage (27.0V for a five minute period; this is user selectable).

If the batteries are "resting" (no power being drawn out of the battery and none being pushed into the battery), then battery voltage is a good indicator of SOC. Figure B-1 shows the relationship between battery voltage (BV) and state of charge (SOC) based on manufacturer data for a resting battery. Battery voltage is not, however, a good indicator of battery SOC under most operational circumstances, because power flows into and out of the batteries.

- If power is being delivered into the batteries from the PV panels, then BV is pushed upward by the force of the current being pushed into the batteries.

- If power is being drawn from the batteries from the mini-split heat pump, then BV is drawn downward by the force of the current being drawn from the batteries.
- If the PV panels are delivering power to the batteries and the heat pump is drawing power from the batteries, the net effect will be higher or lower BV (compared to resting BV) based on whether the PV power delivery is greater than the heat pump power draw. Under bright sun, the PV system was typically delivering power that was on the order of twice that of the power draw of the heat pump.

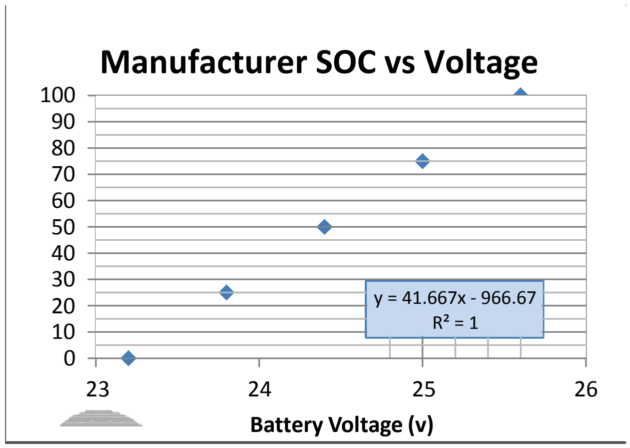

Figure B-1. Battery SOC versus Battery Resting Voltage (data from battery manufacturer).

The greater the (net) draw of power, the greater will be the downdraft on BV compared to its resting voltage. Also, the greater the (net) input of power to the batteries, the greater will be the updraft of BV compared to its resting voltage. These power fluxes create system control problems because the BV cutout (shut off) will be prematurely reached if the mini-split is drawing at a maximum rate (such as on a cold winter morning). The manufacturer of the inverter/charge controller equipment has assured us that better controllers are now being introduced which can provide accurate SOC measurement. Once this SOC control option is readily available, customers will be more able to manage the scheduling of the heat pump system. If a utility cost structure or other incentive was available to the customer to provide incentive to operate the mini-split heat pump from solar, battery power, or both during peak periods, then the customer could schedule solar-powered heating operation (delivered by means of battery storage) for the winter morning peak demand period with greater effectiveness (compared to our none-too-successful attempts to schedule operation based on BV).

A couple of other options might also be available to help meet winter peak demand (recall that the solar heat pump meets 100% or near 100% of cooling peak in nearly all circumstance) by means of utility intervention (such as “on call” control). One possibility, for a cold winter night, is that the utility could use their remote activation technology to deactivate the heat pump during the preceding evening and overnight and then activate the heat pump on solar power (through the batteries) for the period starting at 6 AM. Another complementary option could include automatically charging the bank of batteries using power from the electric grid on cold nights, during a nighttime period such as 10 PM till AM, thus ensuring that the bank of batteries would have sufficient power to operate the mini-split heat pump through the entire peak demand period.

PERFORMANCE EVALUATION OF THE ENERGY SAVING POTENTIAL OF [redacted] SOLAR ASSISTED AIR-CONDITIONING UNIT

Project Team

D. Yogi Goswami, Ph.D., P. E. (PI)
Distinguished University Professor

Elias K. Stefanakos, Ph.D. (Co-PI)
Professor

Chand K. Jotshi, Ph.D. (Co-PI)
Research Scientist

Mehdi Zeyghami
Graduate Research Assistant

December 5, 2015

Clean Energy Research Center
University of South Florida
4202 E. Fowler Ave.,
Tampa, FL 33620

Executive Summary

This report presents a performance assessment of a solar assisted air-conditioning unit manufactured by [redacted], tested under the ASHRAE Standard 37-2009 and ARI Standard 210/240 conditions. This system is claimed to improve the performance of conventional air conditioning system by adding a solar collector to a vapor compression cycle. Since the [redacted] air-conditioning unit is a split system, containing an indoor and outdoor unit, the ASHRAE standard conditions require two separate climate controlled areas for testing (simulating ambient indoor and outdoor conditions). The USF Clean Energy Research Center (CERC) has set up a test facility where air conditioning units can be tested according to ASHRAE/ARI standards. The air conditioning system test facility can be used to measure the cooling capacity, Coefficient of Performance (COP) and Energy Efficiency Ratio (EER) of air conditioning equipment for cooling and heating. A full description of the test facility is given in the detailed full report.

The [redacted] unit consists of a 2 ton [redacted] Air conditioning unit with a 60”x65” evacuated tube solar collector. The solar collector is inserted between the compressor and the condenser unit. A schematic of the test facility and the [redacted] Aire unit is shown below.

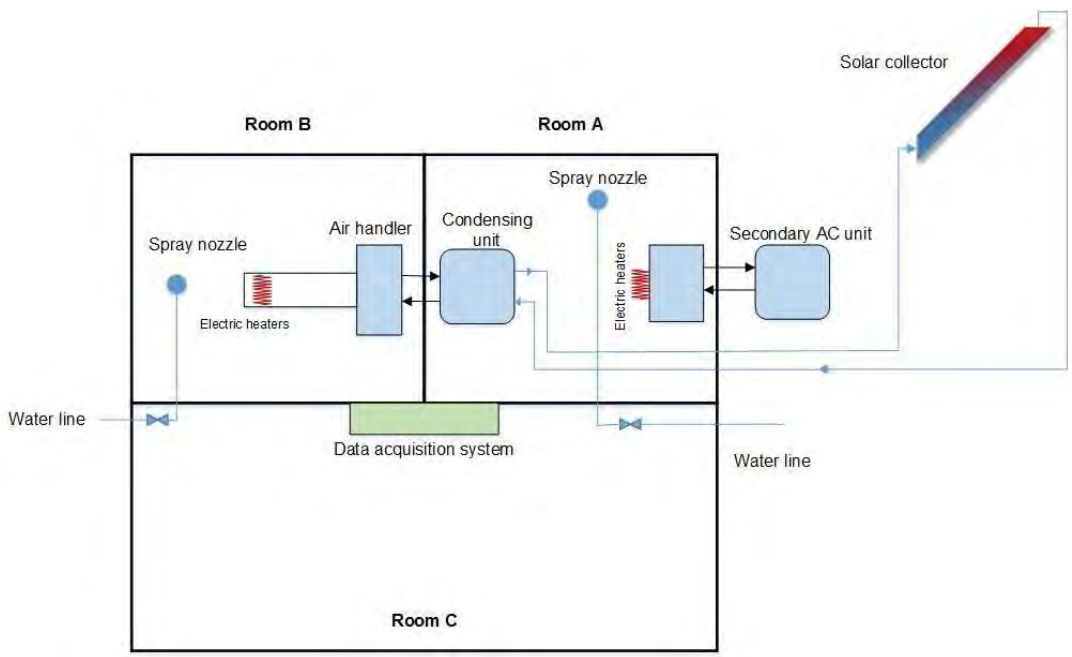

Schematic diagram of the test facility and the installed equipment

As configured at the test facility, the total pipe length between the condenser unit and the solar collector was 92 feet (47 feet from the compressor to the solar collector and 47 feet from the collector to the condenser). Therefore, during non-sunshine hours, the additional piping and the solar collector would work as an extension of the condenser, because of the heat loss from them. Even during sunny periods, when the solar radiation is low, the heat loss from the pipes could be more than the heat gained in the solar collector. Therefore the tests were conducted under three conditions:

1. Without solar collector;
2. With solar collector, when the solar heat gain is less than the heat loss from the associated pipes; and
3. With solar collector, when the solar heat gain is more than the heat loss from the associated pipes.

The results showed that heating the refrigerant in a solar collector, after the compressor and before entering the condenser has a small adverse effect on the COP of the cycle when the solar radiation is enough to overcome the heat loss in the associated piping. When the solar radiation is not enough, the associated piping acts as an extension of the condenser. However, the COP in such cases is about the same as that without the solar collector. The reason for the small differences in the COP for all the cases is that the additional superheat provided by the solar collector, if any, is a very small fraction of the total heat rejected in the condenser, latent heat of the refrigerant being a much larger part of the heat rejected in the condenser. A theoretical simulation of the system confirms these results.

Adding heat to the vapor compression cycle of an air conditioning system by a solar thermal collector or by any other means will reduce the efficiency of the system not increase it. Therefore, adding a solar collector between the compressor and condenser of an air conditioning unit reduces the efficiency and performance of the air conditioning unit.

Table of Contents

List of Figures

List of Tables

1. Introduction

The objective of this report is to present the performance assessment of a solar assisted air-conditioning unit manufactured by [redacted], tested under standard ASHRAE conditions. This system is claimed to improve the performance of conventional air conditioning system by adding a solar collector to a vapor compression cycle. Since the [redacted] air-conditioning unit is a split system, containing an indoor and outdoor unit, the ASHRAE standard conditions require two separate climate controlled areas for testing (simulating ambient indoor and outdoor conditions). Both of those areas must have humidity and temperature controls that can offset and stabilize any changes the air-conditioning unit makes to the ambient conditions. In other words, those areas will need adequate HVAC to keep the rooms at steady state. The USF Clean Energy Research Center (CERC) has set up such a test facility where air conditioning units can be tested according to ASHRAE/ARI standards.

The air conditioning system test facility can be used to measure the cooling capacity, Coefficient of Performance (COP) and Energy Efficiency Ratio (EER) of air conditioning equipment for cooling and heating. The test conditions can be modified to represent different environmental conditions, from standard ASHRAE conditions to different locations. Therefore for an AC unit, performance indicators can be tested at standard conditions along with real life conditions.

2. Description of the Test Facility

An environmental controlled air conditioning system test facility has been established at CERC as per ASHRAE standard 37-2009. Figure 1 shows the layout of the module which has been partitioned into three separate sections, Labeled A, B and C. Sections A and B are instrumented environmental controlled chambers simulating the inside and the outside conditions respectively. Section C is the space for operators and the data acquisition system. Figure 2 shows a schematic diagram of the test facility and installed equipment in each room. The dimensions of room A and B are 3.26 (m) × 3.26 (m) × 2.34 (m high). Both rooms have access doors that are insulated and have viewing windows of 0.3 (m^2). The adjacent space C is used for controls and the computer data acquisition system. Room A, which simulates the indoor conditions, is equipped with 10.25 kW resistance heaters to put the required heat load on the cooling system. Room B, which simulates the outside environmental condition, is cooled by a secondary refrigeration system with a capacity of 5 tons. The room is equipped 11.25 kW resistance heaters, to stabilize the temperature at test conditions. There are water spray nozzles in both rooms to provide the required humidity control in each room according to the standard test conditions.

To minimize the heat transfer between test rooms and uncontrolled environment, both rooms A and B are insulated from inside with an aluminum sheet (1/8 inch), a layer of R30 insulation

(3,3/4 inch), a plastic sheet (1/16 inch), a plywood board (1/2 inch) and the fiber glass wall insulation between studs (3,1/2 inch).

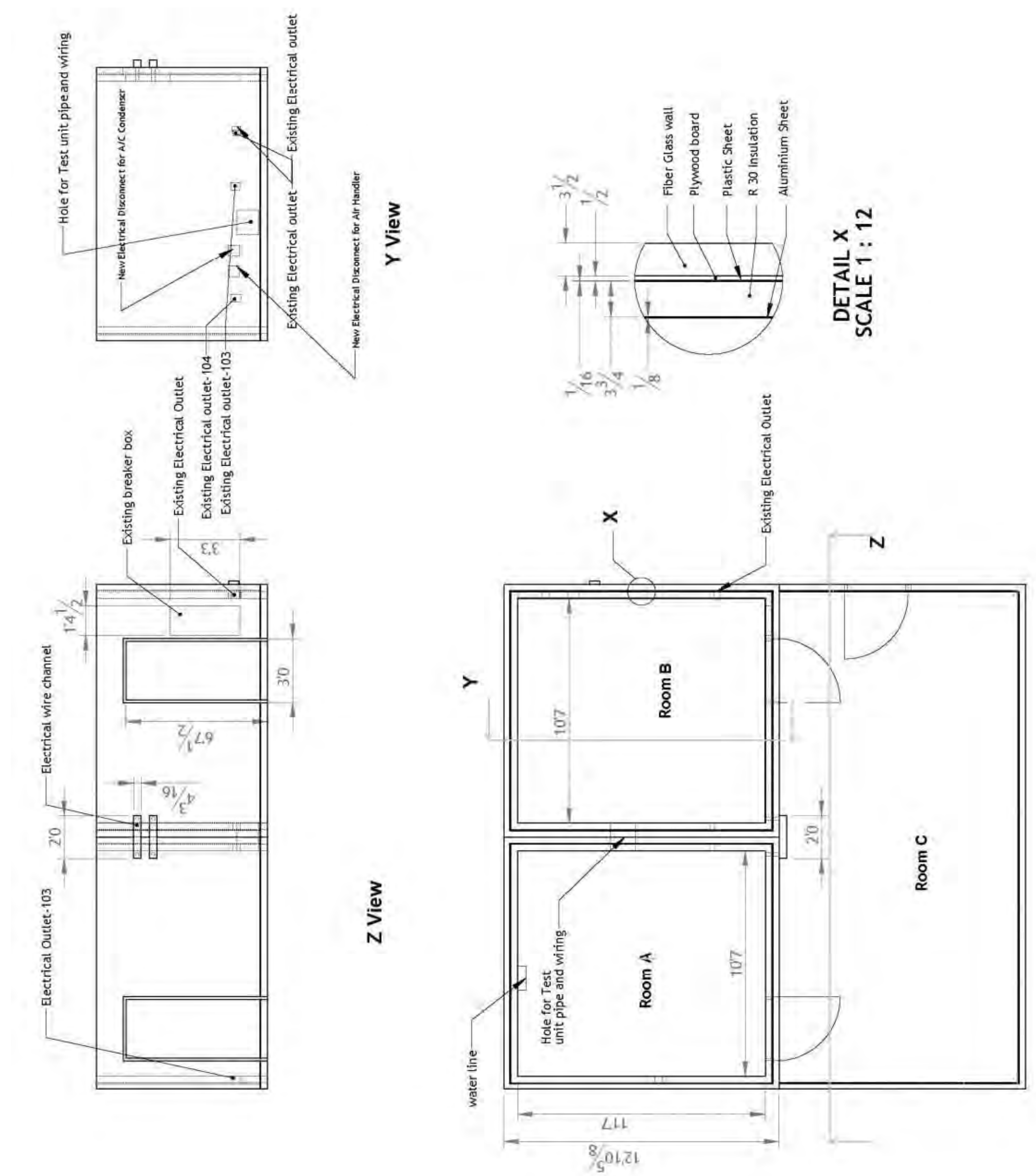

Figure 1: HVAC facility Layout

The [redacted] solar assisted air-conditioning unit is tested according to the ASHRAE Standard 37-2009 [1] and ANSI/ARI Standard 210/240 [2]. These standards provide test methods for determining the cooling capacity of unitary air conditioning equipment and the cooling and/or heating capacities of unitary heat pump equipment. According to these standards the tests must be performed at the indoor room conditions of 80 F dry bulb temperature and 67 F wet bulb temperature and the outdoor room conditions of 95 F dry bulb temperature and 75 F wet bulb temperature.

3. Description of the [redacted] System

The system consists of a [redacted] air conditioning unit with an associated [redacted] air-handling unit (AHU) and an evacuated tube solar thermal collector. Table 1 shows the specification of the [redacted] Solar Assisted Air Conditioning system with 2 tons cooling capacity. The refrigerant from the compressor flows into the solar collector from where it goes into the condenser. At the test facility, the collector is installed on a high rack (for unobstructed view of the sun, at a tilt angle of 28 degrees, which is equal to the latitude of Tampa. The complete [redacted] system was installed by a trained [redacted] dealer in Tampa. Figure 2 shows a schematic of the test configuration. It is worth noting that the total pipe length between the condenser unit and the solar collector is 92 feet (47 feet from the compressor to the solar collector and 47 feet from the collector to the condenser). It is also worth noting that during non-sunshine hours, the additional piping and the solar collector would work as an extension of the condenser, because of the heat loss from them. Even during sunny periods, when the solar radiation is low, the heat loss from the pipes could be more than the heat gained in the solar collector. Therefore the tests were conducted under three conditions:

1. Without solar collector,
2. with solar collector when the solar heat gain is less than the heat loss from the associated pipes, and
3. With solar collector when the solar heat gain is more than the heat loss from the associated pipes

4. Instrumentation and Control

In this section details of the instrumentation and controls installed in the test facility (rooms A, B, C and solar collector) are presented. The evaporator of the AC unit is installed in room A and the condenser unit is installed in room B. these two parts are connected through the wall between the two rooms.

Table 1: Specifications of the AC unit

	Model	Manufacturer	Additional Comments
AHU unit	[redacted]	[redacted]	2 ton cooling capacity
Condenser unit	[redacted]	[redacted]	Two stage compressor – R410A refrigerant
Solar collector	Evacuated tube	N.A.	60”×65” – Tilted 28 degrees facing south

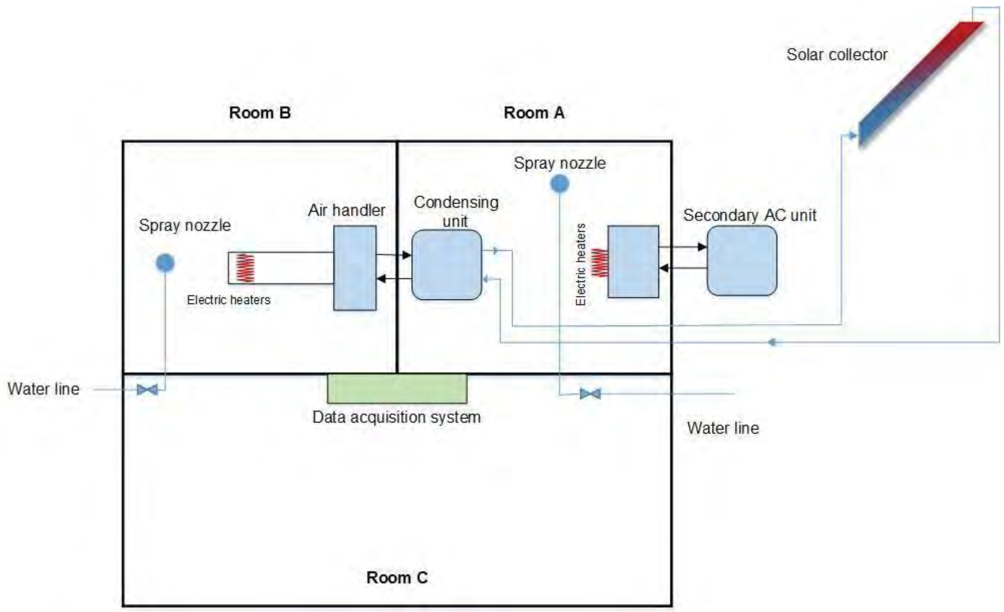

Figure 2: Schematic diagram of the test facility and installed equipment

4.1 Room A (indoor)

This room is used to simulate the indoor condition for the unit to be tested. The temperature and humidity in this room are controlled by electric resistance heating elements and a water spray nozzle. The Air Handling Unit (AHU) or evaporator of the AC unit is installed in this room. The room is instrumented for measuring the inlet and outlet temperature and relative humidity of the air flow in the AHU. A complete description of the components and instruments in this room is given below:

AHU: The evaporator and AHU of the test unit are located in this room. A drain pipe is used to remove the water condensate from the evaporator and dispose it to the outside of the room. An air duct is installed on the AHU outlet to direct the air into the room and for proper mixing and provide the required pressure drop according to the test standards. The AHU inlet and outlet temperature and relative humidity are monitored by using [redacted] probes. The external pressure drop on the exiting air flow is measured by a water manometer.

Heaters: To impose the cooling load on the test unit, heaters with a total capacity of 10.5 kW are installed at the end of the air duct. Individual heaters of capacities 2.5, 3.0 and 4.75kW can be switched on and off by individual switches. The heater with 2.5 kW capacity has a [redacted] for controlling the power input. Once the AHU inlet air temperature reaches close to the desired set point, the [redacted] is adjusted to keep the temperature constant during the test.

Humidifier: As the indoor room air passes over the evaporator coil the moisture is condensed and is removed from the test room. The air moisture is reduced continuously and hence a humidifier is needed to maintain the desired wet bulb temperature according to the standard. Moisture is added to the room at the same rate of moisture condensing over the evaporator coil by utilizing water spray. The mass flow rate of the water sprayed into the room is adjusted by a control valve installed in the room C.

Instrumentation: Three [redacted] humidity and temperature probes are installed at inlet of the AHU to monitor the air flow conditions into the unit. Another set of three sensors of the same type are installed to monitor the outlet conditions of the flow. The power input to the AHU is monitored by using a power transducer (see Figure 3).

4.2 Room B (outdoor)

This room is used to simulate the ambient conditions for the unit to be tested. The temperature and humidity of this room are controlled by a secondary AC unit and electric resistance heaters and a water spray nozzle. The condenser unit (condenser and compressor) of the AC is installed in this room. The room is instrumented for measuring the inlet and outlet temperature and relative humidity of the air flow in the condenser unit. A complete description of the components and instruments in this room is given below:

Secondary AC unit: An AC unit with cooling capacity of 5 tons is installed in room B to remove the heat from the condenser unit and reject it to the outside. The AHU of this unit is installed in room B and equipped with a drain pan to collect the condensate and remove it from the evaporator coil. The condensing unit of this AC is located outside the test facility (see Figure 2).

Humidifier: as the air circulates in the room it passes over the evaporator coil of the secondary AC unit and the moisture is condensed. The moisture is reduced on a continuous basis and hence a humidifier is required to maintain the relative humidity in the room at desired value. For this purpose a water spray nozzle is installed in room B to add makeup water to the air.

Heaters: The secondary AC unit is not adjustable and whenever it is on, it works with the maximum cooling capacity. Therefore to adjust room B temperature electrical heaters totaling 12.0 kW are installed in the room. Individual heaters of capacities 4.0 kW each can be switched on and off by individual switches. One of the heaters has a [redacted] for controlling the power input. Once the temperature of room B reaches close to the desired set point, the [redacted] is adjusted to keep the temperature constant during the test.

Instrumentation: the ambient air is drawn into the condenser from the sides and the hot air is exhausted from the top of the unit. Three [redacted] humidity and temperature probes are installed at inlet of the condensing unit to monitor the air flow conditions into the unit. Another set of three sensors of the same type are installed to monitor the outlet conditions of the flow. The power input to the condensing unit is monitored by using a power transducer (see Figure 3).

4.3 Room C

This space is used for the operators, controls and the data acquisition system. This room has the following components:

- Computer data acquisition system: A PC is used to run the [redacted] code and store the data. Figure 5 shows the details of this system. Figure 3 shows the location of the sensors in the test facility and the unit under test. Table 2 gives a summary of the sensors used in the test.
- Main disconnects: the electrical disconnects are located near the computer system that may be used to shut down the systems in case of emergency. Figure 4 shows a schematic of the circuit breakers and disconnects.
- Water valves: Two control valves for rooms A and B are installed in this room to control the water flow into the spray nozzles.
- [redacted]: Two [redacted] for adjusting the temperatures in rooms A and B are installed in this room.

4.4 Solar Collector

The super-heated refrigerant vapor after the compressor flows into an evacuated tube solar collector. After heating up, the fluid is returned to the condenser and by heat transfer with the air in room B transforms into liquid. Thermocouples are installed at the compressor outlet and condenser inlet to monitor the temperature change of refrigerant, leaving the condensing unit and returning from the solar collector, (see Figure 3). Also to monitor the temperature rise across the solar collector thermocouples are installed at the inlet and outlet of the collector. A pyranometer is installed on the solar collector plate to record the global horizontal solar. Figure 6 (a)-(c), shows the solar collector, condensing unit and air handling unit.

Table 2 Details of the instrumentation

Variable	Location	Sensor/Instruments for measurement	Make/Model and specification	Comments
Temperature	Inlet and outlet of AHU and condenser unit	Humidity and Temperature Probe	[redacted], Range (-40)-80 °C, Accuracy ±0.2 °C	Used to keep the test conditions according the standard and calculate air enthalpies
Humidity			[redacted], Range 0-100 % RH, Accuracy ±1.7 % RH	
Temperature	Condensing unit outlet to the solar collector and inlet from the solar collector	Thermocouple	[redacted] Aluminum-Nickle, Range –200 to 1250°C, Accuracy 0.75%	Monitor the temperature of refrigerant leaving the Condensing unit and returning from solar collector
Power	Control room C	Power transducer for AHU	[redacted], 0-2.0 kW, ± 10W	Monitor the input power to the cycle
		Power transducer for condensing unit	[redacted] 110C, 0-4.0 kW, ± 20W	
Air velocity	Inlet and outlet of AHU and condensing unit	Rotating Vane Anemometer	[redacted] 0.25-30 m/s, ±1.0%	Used to calculate the air flow rates – not continuous monitoring
Solar radiation	Solar collector	Pyranometer	[redacted], 0-1200 W/m2, ±5.0 %	Monitor the solar radiation effects

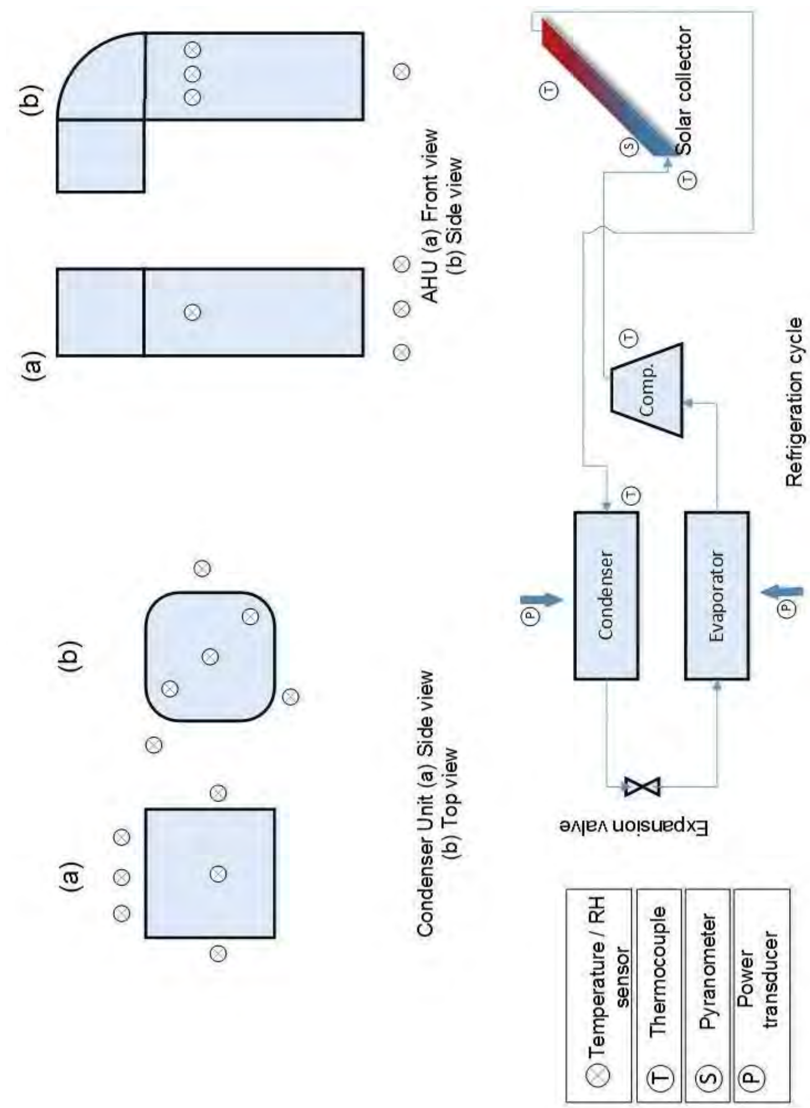

Figure 3: Locations of the sensors for monitoring the unit under test

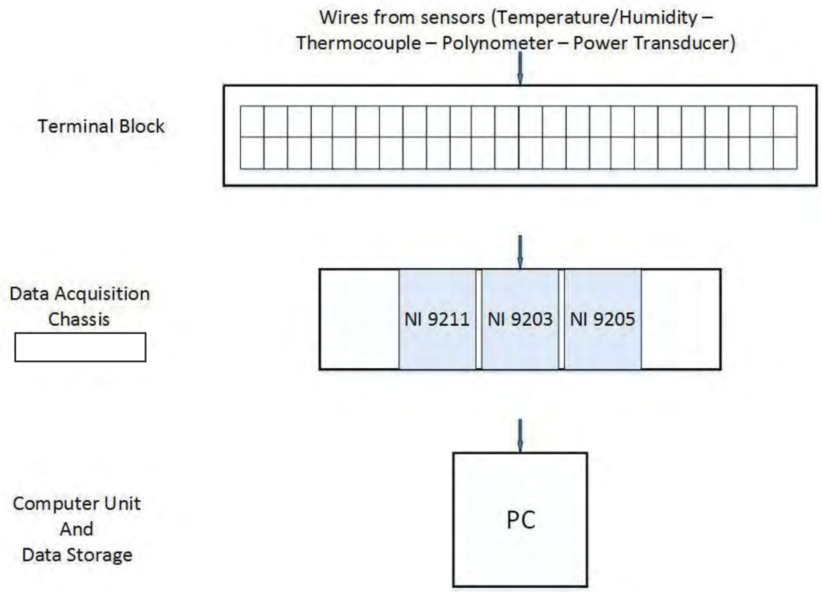

Figure 4: Data Acquisition System

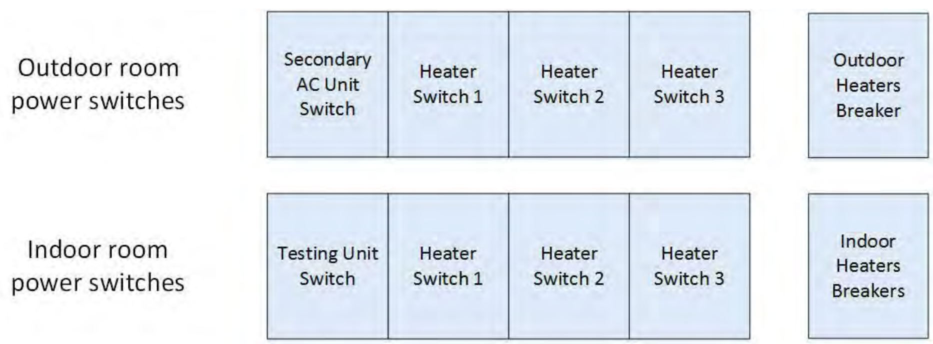

Figure 5: Circuit breakers and electric disconnects

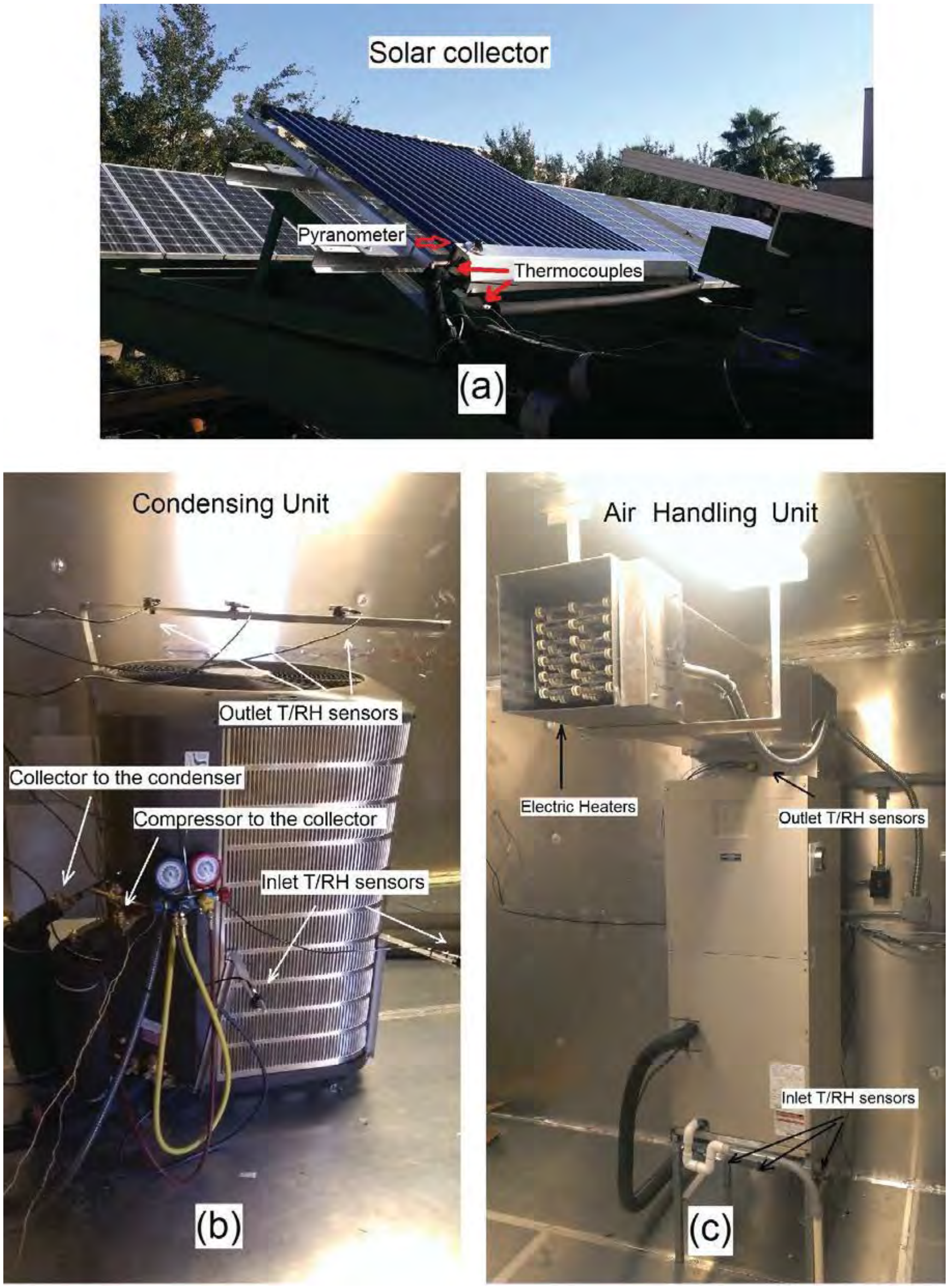

Figure 6: (a) solar collector, (b) condensing unit and (c) air handling unit

5. Test Procedure

The test is conducted in accordance with the ARI Standard 210/240-89 and ANSI/ASHRAE Standard 37-2009 for testing unitary equipment. ASHRAE's "Air Enthalpy Method" has been used to determine the performance of the AC unit. The following procedure has been used for testing the solar assisted AC unit for cooling capacity and performance:

ASHRAE conditions are maintained during the test for room A and B. Test conditions for room A (indoor conditions) dry bulb temperature 26.7 °C and wet bulb temperature 19.4 °C (≈ 50.7 % RH). Test conditions for room B (outdoor conditions) dry bulb temperature 35 °C and wet bulb temperature 23.9 °C (≈ 39.9 % RH). According to ARI Standard 210/240-89 "the wet bulb temperature condition is not required when testing air cooled condensers which do not evaporate condensate". Hence in room B only the dry bulb temperature is used as the control factor. Table 3 presents the observed data tolerances for test according to ANSI/ASHRAE Standard 37-2009. The maximum permissible variation of any observation during the capacity test is listed under Test Operating Tolerance. This represents the greatest permissible difference between maximum and minimum instrument observations during the test. The maximum permissible variations of the average of the test observations from the standard or desired test conditions are shown under Test Condition Tolerance.

Table 3: Test tolerances

	Test Operating Tolerance (Total Observed Range)	Test Condition Tolerance (Variation of Average from Specified Test Conditions)
Outdoor dry bulb temperature Entering	1.0	0.3
Outdoor dry bulb temperature Leaving	1.0	-
Outdoor wet bulb temperature Entering	0.5*	0.2*
Outdoor wet bulb temperature Leaving	0.5*	-
Indoor dry bulb temperature Entering	1.0	0.3
Indoor dry bulb temperature Leaving	1.0	-
Indoor wet bulb temperature Entering	0.5	-
Indoor wet bulb temperature Leaving	0.5	-

* Not considered because testing air cooled condensers which do not evaporate condensate

Start up and shut down steps of the test unit and auxiliary systems is presented in Table 4. From the beginning the computer data acquisition system is turned on to show the conditions in each room. It is essential to run the AC unit under test and secondary AC unit on continues basis to avoid temperature swings of the air inside Rooms A and B due to cycling of the units. Therefore thermostats for both AC units have been set to a lower temperature (i.e. 15 °C).

At first step the unit under test will be turned on. The AHU blower starts right away and it will take a few minutes for the compressor to start. When the compressor starts and cooling effect is provided to the indoor room, it is time to turn on the electric heaters in the room A. By adjusting the indoor [redacted], in a few minutes the indoor room temperature reaches to the test set point. Once the desired dry bulb temperature has been achieved for room A, the relative humidity should be set equal to the test conditions. Since moisture condenses over the evaporator coil, moisture must be added into the room. This is achieved with the help of water spray nozzle. The water flow can be varied to the nozzle by control valve installed in room C.

During the time needed for room A to reach the test set points, heat is rejected to room B by the condensing unit and its temperature rises close to the set point for outdoor room. At this point the secondary AC unit is turned on and at the same time the electric heaters are switched on too. By use of the outdoor room heater [redacted] the temperature is kept constant in room B according to the standard set point.

The only unsteady factor of the test is the solar radiation on the collector. The change in solar radiation on the collector would change the amount of heat added to the system that must be rejected by the condenser to room B. Hence the operator would need to modify the heat added to the room by electrical heaters by the [redacted] continuously.

It will take around 60 minutes for steady state conditions to be achieved. At this time the data logger starts to store the data from the sensors at the rate of 1 sample per second. The system performance was monitored under in different solar radiation conditions. For each test one hour of data was recorded and analyzed.

Table 4: Sequence of operation for test unit

Sequence of operations	
Start up	1- Turn on the under test AC unit 2- Turn on the heaters in Room A 3- Adjust the water flow to the spray nozzle in room A 4- Turn on the secondary AC unit in room B 5- Turn on the heaters in room B 6- Start the data storage
Shut down	1- Stop data logging 2- Turn off the water flow to the room A 3- Turn off the heaters in room A 4- Turn off the heaters in room B 5- Turn off the under test AC unit 6- Turn off the secondary AC unit

6. Data Analysis

This section describes the methods and equations needed to calculate the system performance based on the air side enthalpies.

The air flow rates over the evaporator and the condenser coils were measured using a Rotating Vane Anemometer. For the evaporator coil, the flow was measured at the outlet of the duct. The duct has a cross section of 10 inches by 10 inches which was subdivided into 9 equal elements. The air velocity was measured at the center of each individual element. The average flow velocity for the evaporator is calculated by averaging the velocity measured for each element. For the condenser coil, the flow was measured at the top of the condenser unit. The velocity of the air flow is measured at 11 equally spaced points from the center to the edge of the surface. The total air flow rate for the condenser is measured by numerical summation of the air flows in each area section by assuming average air velocity on each section. Figure 7 shows the details of the measurements.

1. Evaporator energy balance: Based on the evaporator air flow inlet and outlet states $(t_{e1}, RH_{e1}, t_{e2}, RH_{e2})$, the enthalpies of both states may be calculated from the equations presented in appendix A:

$$\dot{m} = \frac{\dot{V}}{v} \qquad \text{(Eq. 1)}$$

$$\dot{Q}_e = \dot{m}_e(h_{e1} - h_{e2}) \qquad \text{(Eq. 2)}$$

2. Condenser energy balance: Based on condenser inlet and outlet airflow states $(t_{c1}, RH_{c1}, t_{c2}, RH_{c2})$ the amount of heat rejected from the condensing unit can be calculated by the following equation:

$$\dot{Q}_c = \dot{m}_c(h_{c2} - h_{c1}) \quad \text{(Eq. 3)}$$

3. Performance Indicators: Coefficient of Performance (COP) and Energy Efficiency Ratio (EER) of the unit under test is calculated from the following equations:

$$COP = \frac{\dot{Q}_e}{\dot{W}} \quad \text{(Eq. 4)}$$

$$EER = 3.412\ COP \quad \text{(Eq. 5)}$$

Here h is the moist air specific enthalpy [kJ/kg_{da}], $\dot{m}$ is the mass flow rate of the air [kg/s], $\dot{Q}$ is the heat transfer rate [kW], $\dot{W}$ is the total electric power consumption of the AC unit [kW], subscripts e and c represent the evaporator and the condenser respectively. State 1 is the inlet and state 2 is the outlet of the heat exchanger.

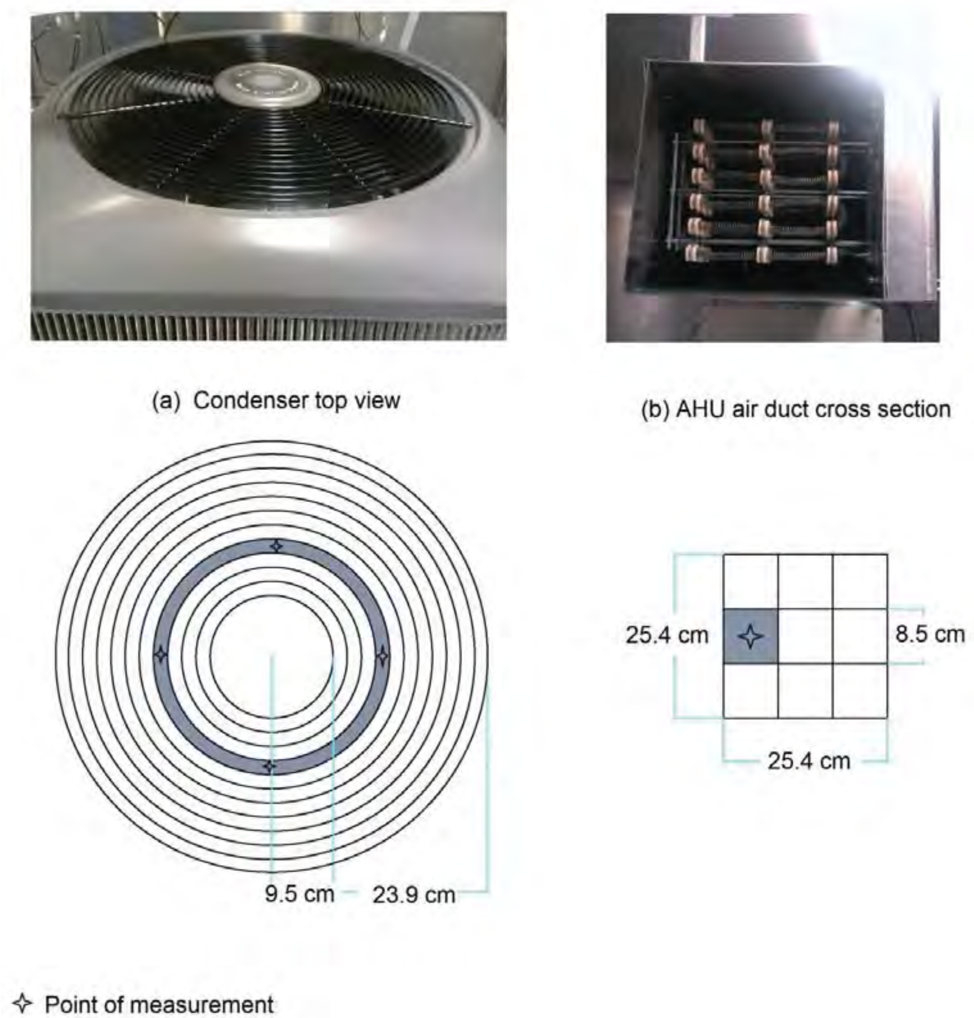

Figure 7: Air flow measurement points

6.1 Uncertainty Analysis

Uncertainty analysis in test results was done using the method of [redacted] Suppose a set of measurements is made and the uncertainty in each measurement may be expressed with the same odds. These measurements are then used to calculate some desired results of the experiments. We wish to estimate the uncertainty in the calculated result on the basis of the uncertainties in the primary measurements. The result R is a given function of the independent variables $x_1, x_2, x_3, \ldots, x_n$. Thus:

$$R = R(x_1, x_2, x_3, \ldots, x_n) \qquad \text{(Eq. 7)}$$

Let w_R be the uncertainty in the result and $w_1, w_2, \ldots, w_n$ be the uncertainties in the independent variables. If the uncertainties in the independent variables are all given with the same odds, then the uncertainty in the result having these odds is given as

$$w_R = \left[\left(\frac{\partial R}{\partial x_1} w_1\right)^2 + \left(\frac{\partial R}{\partial x_2} w_2\right)^2 + \ldots + \left(\frac{\partial R}{\partial x_n} w_n\right)^2\right]^{1/2} \qquad \text{(Eq. 8)}$$

7. Results and Discussion

In the following section the test performance data for a 2 ton [redacted] solar assisted AC unit are presented. First the unit was tested without the solar collector, using the bypass path at the condensing unit. The valves on the refrigerant lines connecting the condensing unit to the solar collector are closed and the valve on the bypass line is opened in this setup (see Fig. 5). The results of this setup show the performance of the AC unit without the solar part. The second test is with the solar collector as configured by [redacted]. This was done by closing the bypass valve and opening the valves in the refrigerant lines to and from the solar collector. To make the test conditions as similar as possible, the amount of refrigerant in the system was adjusted for each setup according to the installation manual of the unit.

7.1 Bypass test

Figure 8 shows room A and B temperature and relative humidity (for room A) during a sample bypass test (Test 10-22- Bypass 2). The test conditions are kept within the tolerances presented in Table 3. Figure 9 presents the AHU and Condensing Unit electric energy consumption during the test. Figure 10 shows the COP of the AC unit for 5 different bypass tests. And Table 5 presents the test data and calculated performance indicators.

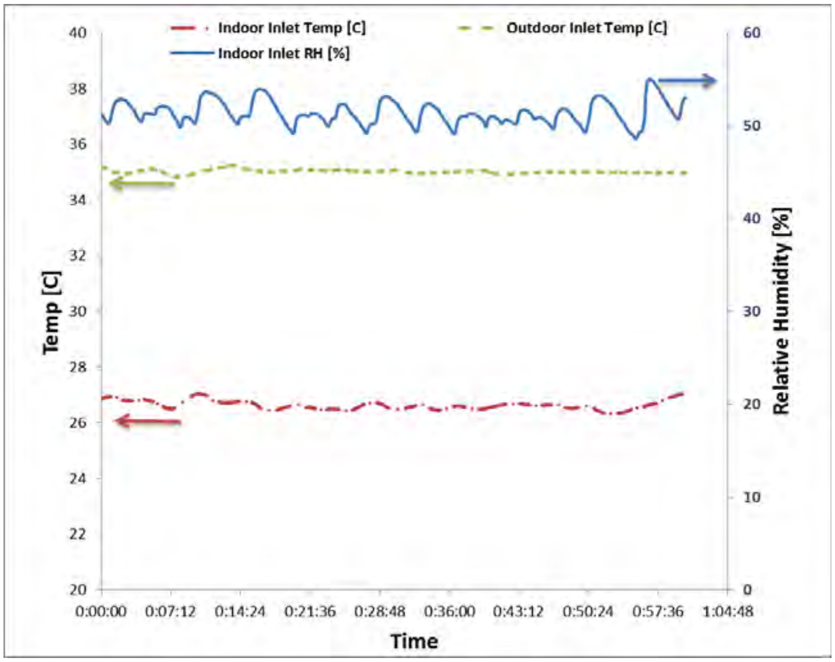

Figure 8: Bypass test conditions for rooms A and B

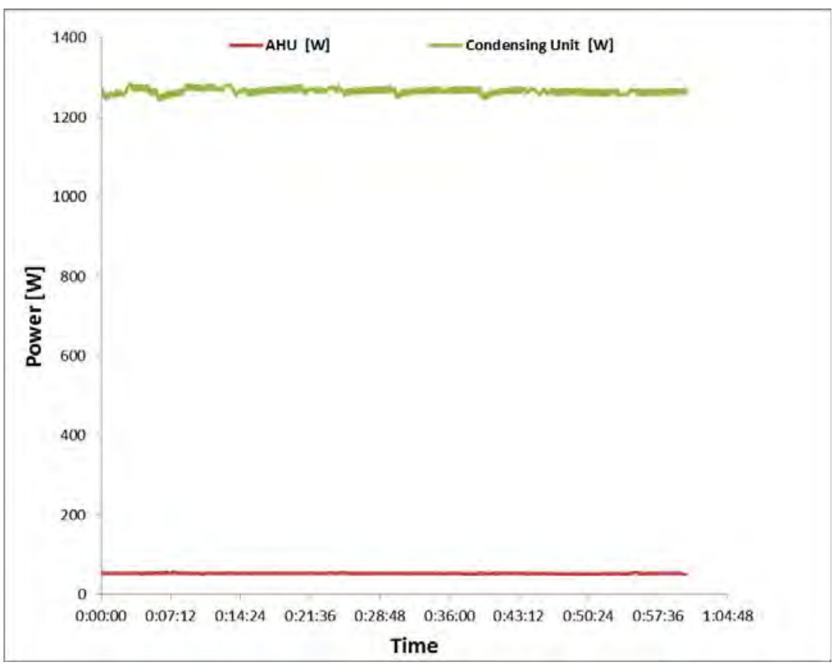

Figure 9: Bypass test AHU and condensing unit electric power consumption

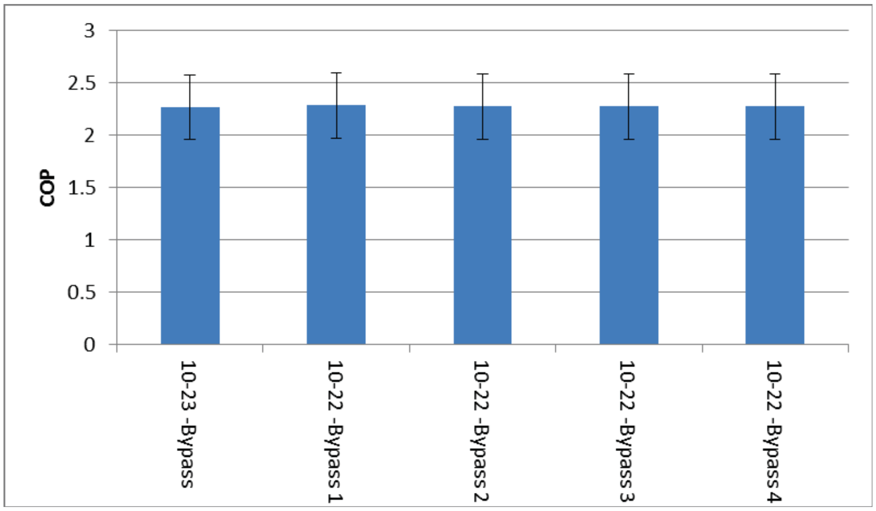

Figure 10: Bypass test performance of the AC unit

Table 5: Summary of test data and results for bypass tests

Test	10-23 - Bypass	10-22 -Bypass 1	10-22 -Bypass 2	10-22 -Bypass 3	10-22 -Bypass 4
t_{e1} [C]	26.7	26.6	26.6	26.6	26.7
RH $_{e1}$ [%]	51.5	51.4	51.4	51.4	51.6
t_{e2} [C]	20.4	20.3	20.4	20.4	20.5
RH $_{e2}$ [%]	65.4	65.9	65.4	65.4	65.3
m_{air_e} [kg/s]	0.29	0.29	0.29	0.29	0.29
t_{c1} [C]	35.0	34.9	35.0	35.0	35.0
RH $_{c1}$ [%]	16.5	17.9	17.6	17.6	17.2
t_{c2} [C]	37.1	37.1	37.1	37.1	37.1
RH $_{c2}$ [%]	14.9	16.2	15.8	15.8	15.6
m_{air_c} [kg/s]	1.8	1.8	1.8	1.8	1.8
Q_e [kW_{th}]	2.98	3.00	2.99	2.99	2.97
Q_c [kW_{th}]	3.99	4.08	4.05	4.05	4.05
W_{tot} [kW_e]	1.32	1.32	1.32	1.32	1.31
COP	2.26	2.28	2.27	2.27	2.27

Based on the uncertainties in the parameters used for calculating the COP, uncertainty in the COP was calculated using the procedure described in section 5.1 was found to be 13.6%. The uncertainty is in the calculated values in Fig. 10.

7.2 Solar test

When the bypass valve is closed and refrigerant flows through the solar collector, two situations were observed, depending to the amount of solar radiation.

a. CASE I is when the refrigerant inflow from the solar collector (at the condenser inlet) is cooler than the refrigerant flow leaving the compressor (To the solar collector). Due to high temperature of the fluid in the pipe connecting the compressor and the collector and the condenser there is a heat loss in the piping system. The total length of the pipe in the set up is 92 feet. If the solar radiation is not high enough to overcome this heat loss the solar collector and the connecting pipes act as a part of the condenser. In this case, some of the load is removed from the condenser heat exchanger but at the same time there is some pressure loss in the piping system. Under these conditions, the cycle COP was found to be in the same range as the bypassed system (COP = 2.23-2.35).

b. CASE II is when the refrigerant inflow from the solar collector (at the condenser inlet) is hotter than the refrigerant flow leaving the compressor (To the solar collector). In this case the calculated COP from the test data is slightly lower than the bypass test. Depending on the conditions the COP was found to be between 2.23 and 2.32.

Figure 11 shows the temperatures for rooms A and B and the relative humidity for room A during a sample solar test (Test 10-31-1). The test conditions were kept within the tolerances presented in Table 3. Figure 12 presents the AHU and condensing unit electric energy consumption during the test. Figure 13 presents the refrigerant temperatures at compressor outlet, and condenser inlet respectively. The global horizontal solar radiation on during the test is presented in Figure 14. Figure 15 shows the COP of the AC unit for 3 sample solar tests when refrigerant inflow from the solar collector (at the condenser inlet) is cooler than the refrigerant flow leaving the compressor (To the solar collector). And Table 6 presents the test data and calculated performance indicators.

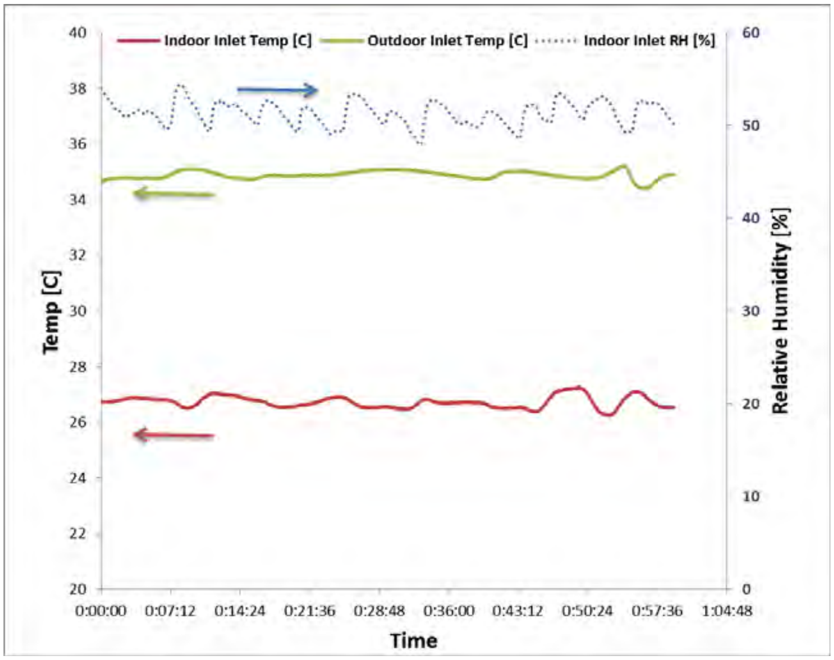

Figure 11: Solar test conditions for rooms A and B (CASE I)

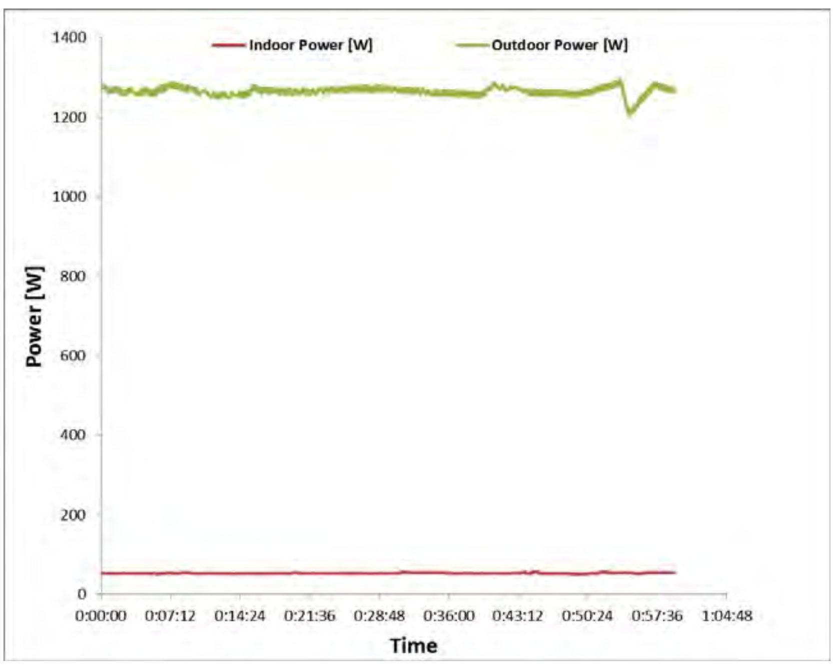

Figure 12: Solar test AHU and condensing unit electric power consumption (CASE I)

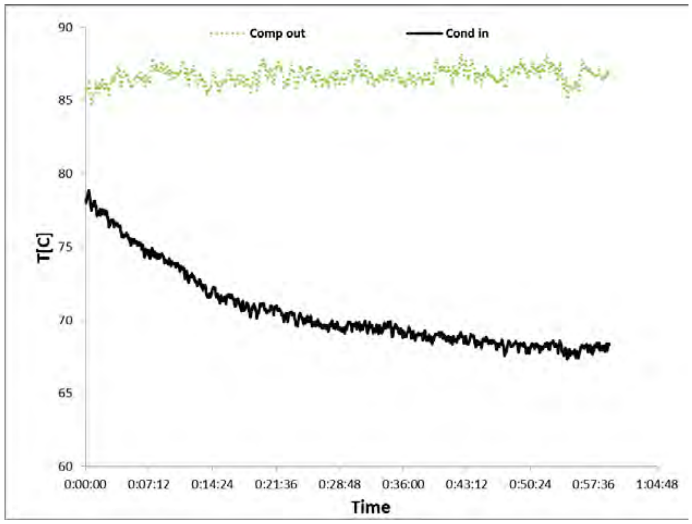

Figure 13: Solar test, refrigerant temperature profile between compressor outlet and condenser inlet (CASE I)

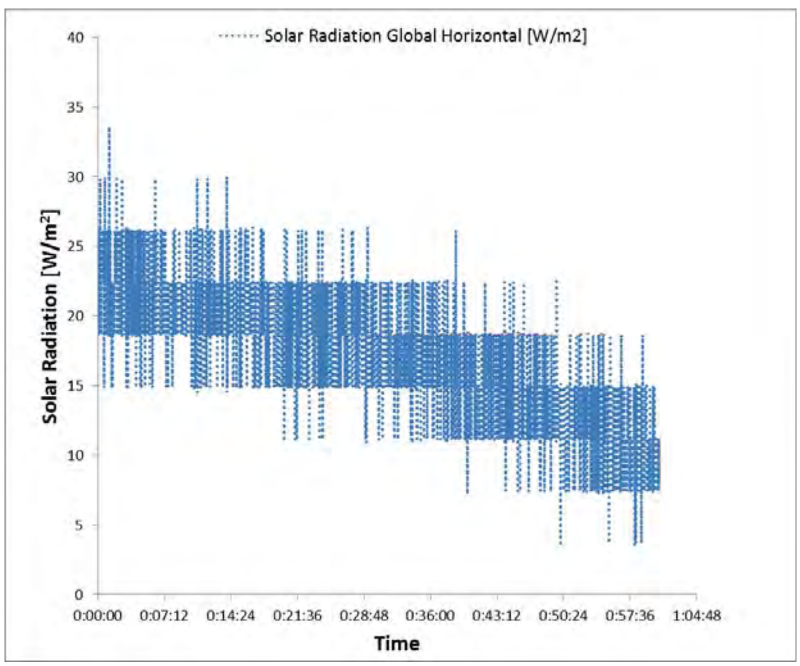

Figure 14: Solar test, solar radiation (CASE I)

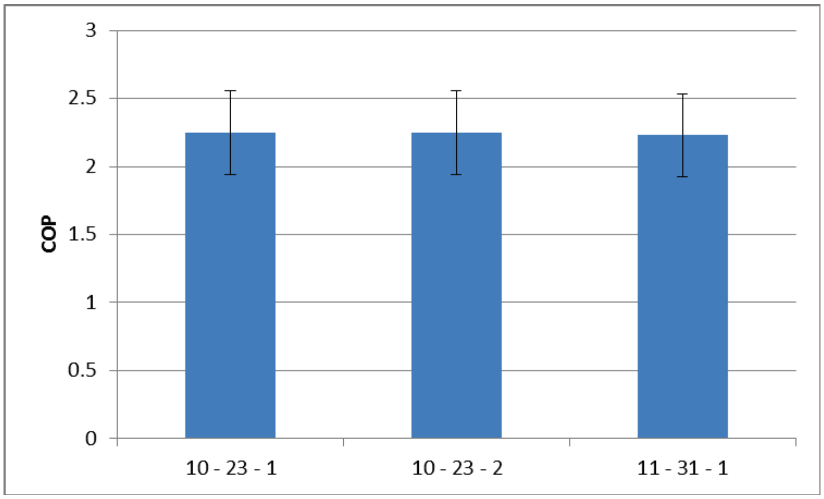

Figure 15: Solar test performance of the AC unit (CASE I)

Table 6: Summary of test data and results for solar test (CASE I)

Test	10 - 31 - 1	10 - 23 - 1	10 - 23 - 2
t_{e1} [C]	26.8	26.7	26.7
RH $_{e1}$ [%]	51.3	51.9	20.5
t_{e2} [C]	20.7	20.4	52.1
RH $_{e2}$ [%]	64.5	65.8	65.9
$m_{air\ e}$ [kg/s]	0.29	0.29	0.29
t_{c1} [C]	34.9	34.9	35.1
RH $_{c1}$ [%]	17.3	18.5	18.3
t_{c2} [C]	36.7	36.9	36.9
RH $_{c2}$ [%]	15.8	17.4	16.7
$m_{air\ c}$ [kg/s]	1.7	1.7	1.7
Temperature difference between average refrigerant temperature at compressor outlet and condenser inlet [C]	-15.9	-9	-18.0
Q_e [kW_{th}]	2.93	2.99	3
Q_c [kW_{th}]	3.52	3.81	3.42
W_{tot} [kW_e]	1.32	1.33	1.33
COP	2.23	2.25	2.25

When the absorbed solar energy is not high enough to overcome the heat loss in connecting pipelines from the condensing unit and the collector, there is a drop in refrigerant temperature between the compressor outlet and condenser inlet (see Fig. 13). In this case the solar collector and transmission pipelines act as a part of the condenser. Although there is lower heat load on the condenser (depending on amount of temperature drop) but, it does not have much positive effect on the performance of the system at standard test conditions. COP of an AC unit is the ratio of cooling provided to electrical energy consumed.

Figure 16 shows room A and B temperature and relative humidity profiles (for room A) during a sample solar test (Test 10-23-5), when the solar radiation is high enough to overcome the heat losses in the transmission piping (Case II). The test conditions are kept within the tolerances presented in Table 3. Figure 17 presents the AHU and condensing unit electric energy consumption during the test. Figure 18 presents the refrigerant temperatures at compressor outlet, solar collector inlet, solar collector outlet and condenser inlet respectively. The global horizontal solar radiation during the test is presented in Figure 19. Figure 20 shows the COP of the AC unit for 5 sample tests when refrigerant inflow from the solar collector (at the condenser inlet) is hotter than the refrigerant flow leaving the compressor. Table 7 presents the test data and calculated performance indicators.

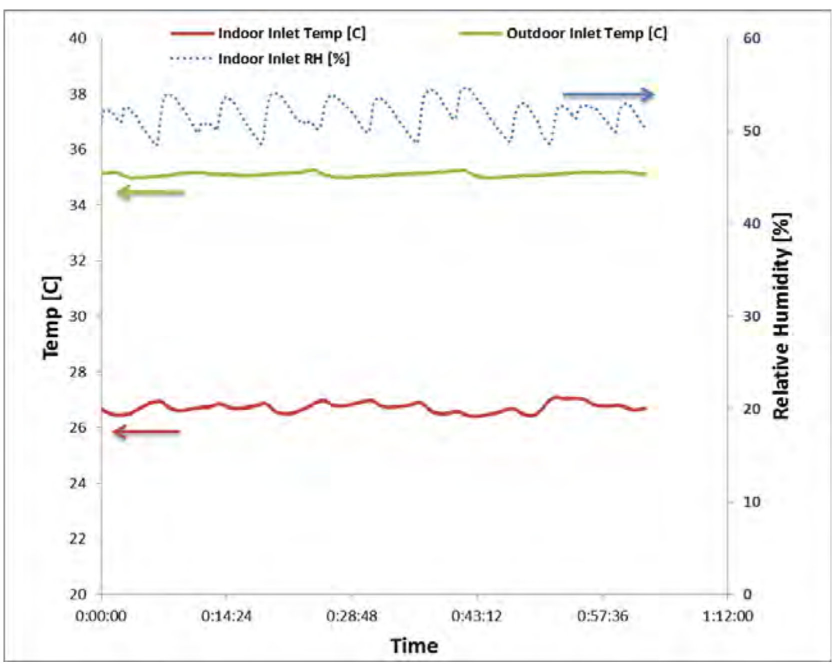

Figure 16: Solar test conditions for rooms A and B (CASE II)

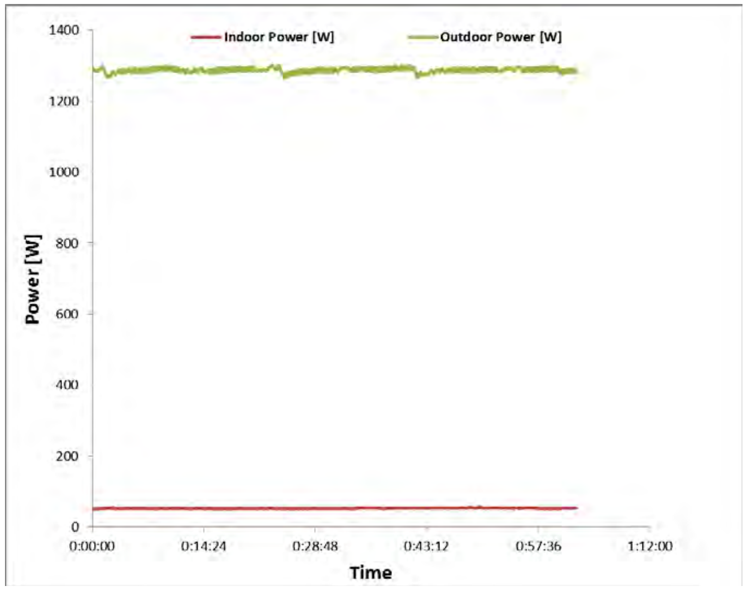

Figure 17: Solar test AHU and Condensing Unit electric power consumption (CASE II)

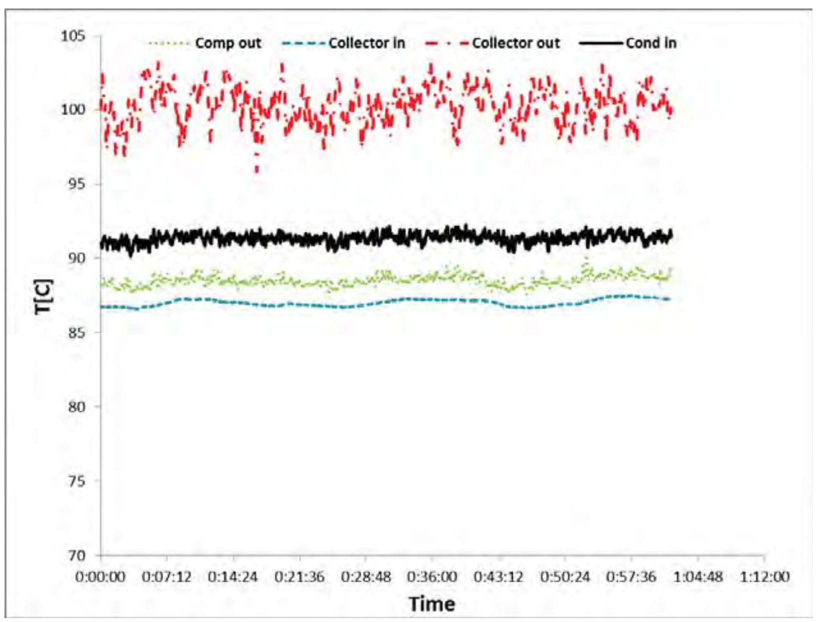

Figure 18: Solar test, refrigerant temperature profile between compressor outlet, solar collector inlet, solar collector outlet, and condenser inlet (CASE II)

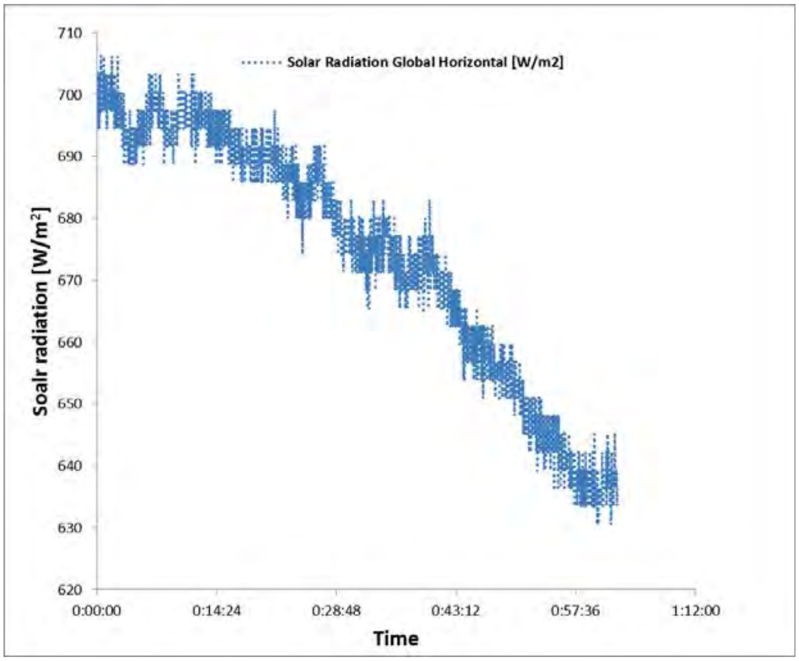

Figure 19: Solar test, solar radiation – at 10-23-5 13:00-14:00 (CASE II)

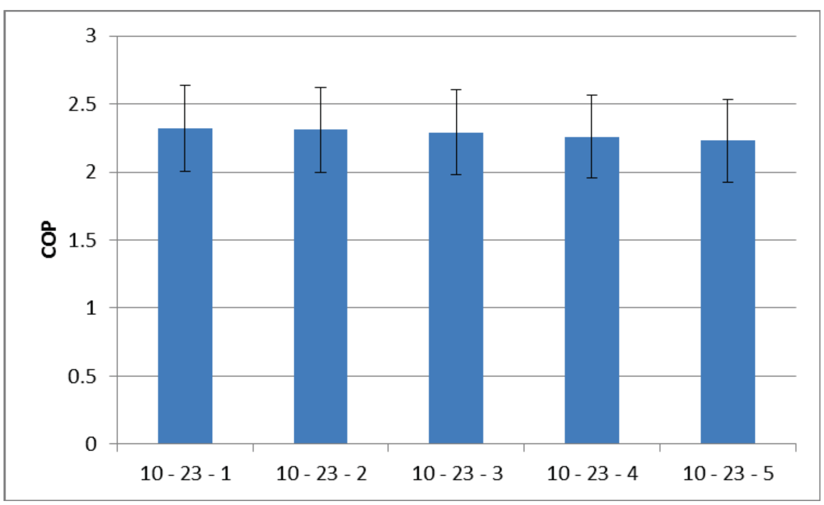

Figure 20: Solar test performance of the AC unit (CASE II)

Table 7: Summary of test data and results for solar test (CASE II)

Test	10 - 23 - 1	10 - 23 - 2	10 - 23 - 3	10 - 23 - 4	10 - 23 - 5
t_{e1} [C]	26.7	26.7	26.7	26.7	26.7
RH_{e1} [%]	51.5	51.9	51.4	51.8	52.0
t_{e2} [C]	20.3	20.3	2.3	20.3	20.5
RH_{e2} [%]	66.1	66.4	65.8	65.9	65.9
m_{air_e} [kg/s]	0.29	0.29	0.29	0.29	0.29
t_{c1} [C]	35.1	35.1	35.1	35.1	35.1
RH_{c1} [%]	17.8	18.0	18.2	18.3	18.4
t_{c2} [C]	37.2	37.2	37.2	37.2	37.2
RH_{c2} [%]	15.9	16.1	16.3	16.4	16.5
m_{air_c} [kg/s]	1.7	1.7	1.7	1.7	1.7
Temperature difference between average refrigerant temperature at compressor outlet and condenser inlet [C]	1.1	1.9	2.4	2.9	2.2
Q_e [kW_{th}]	3.1	3.09	3.06	3.03	2.99
Q_c [kW_{th}]	4.00	4.03	4.06	4.05	4.04
W_{tot} [kW_e]	1.34	1.34	1.34	1.34	1.34
COP	2.32	2.31	2.29	2.26	2.23

When the absorbed solar energy is high enough to overcome the heat loss in the connecting pipelines from the condensing unit and the collector, there is an increase in the refrigerant temperature between the compressor outlet and condenser inlet (see Fig. 18). Due to refrigerant's high temperatures in the pipes between the condensing unit and solar collector and the large length of the pipe there is high amount of heat loss in transmission lines. As it is shown in Fig. 18, although the refrigerant temperature at solar collector outlet is 12-13^{0}C higher than its temperature at the condenser outlet, it is only 2-3^{0}C hotter by the time it reaches the condenser. It is worth mentioning that, the tests have been performed with insulation provided by the installation company (i.e. 0.75 inch wall thickness [redacted] on refrigerant vapor line from the compressor to the solar collector and from the collector to the condenser) the overall effect was always cooling of the refrigerant. To reduce the heat loss from the hot refrigerant vapor to the environment, another layer of insulation with 1inch thickness has been added to the refrigerant lines.

Presented results in table 7 show that temperature increase of the refrigerant between compressor and condenser reduces the cooling COP of the cycle slightly, although it is within the uncertainty limits. The refrigerant sub-cooling would be slightly lower due to higher refrigerant temperature at condenser inlet, which would result in slightly lower cooling COP.

7. Modelling

In this part the effect of cooling and heating the refrigerant flow after the compressor and before entering the condenser is studied. A simulation code has been developed to evaluate the performance of a Vapor Compression Cycle (VCC) at different working conditions, in terms of COP. First the performance of a traditional VCC was evaluated trough simulation using the By-pass test conditions (test 10-23 By-pass). After that, the working conditions of the cycle have been altered in order to predict the performance of the system at different situations.

In order to simulate the VCC, mass and energy balances for each component of the cycle as well as the whole cycle have been performed.

$$\sum \dot{m}_{in} = \sum \dot{m}_{out} \qquad \text{(Eq. 9)}$$

$$\dot{Q} + \dot{W} = \sum \dot{m}_{out} h_{out} - \sum \dot{m}_{in} h_{in} \qquad \text{(Eq. 10)}$$

$$Q^{\cdot}_{e} + \dot{W} + Q^{\cdot}_{solar} = Q^{\cdot}_{c} \qquad \text{(Eq. 11)}$$

Where $\dot{m}$ is the mass flow rate, $\dot{Q}$ and $\dot{W}$ are the net heat and work inputs respectively and h is the enthalpy. Subscripts in and out depict the input and exit states. Figure 21 presents the schematic of the VCC and in Figure 22 the T-s Diagram of the cycle is depicted. A computer code has been developed to determine the working fluid state at the main locations in the cycle: compressor inlet, compressor outlet, condenser inlet, condenser outlet and evaporator inlet. The measured values of evaporator and condenser pressures in the test AC unit were used in the model. Also the temperatures at compressor inlet and outlet and condenser inlet and outlet were taken as the mean hourly data collected (test 10-23 Bypass). To find the thermodynamic properties of the refrigerant (R-410a) [redacted] was used.

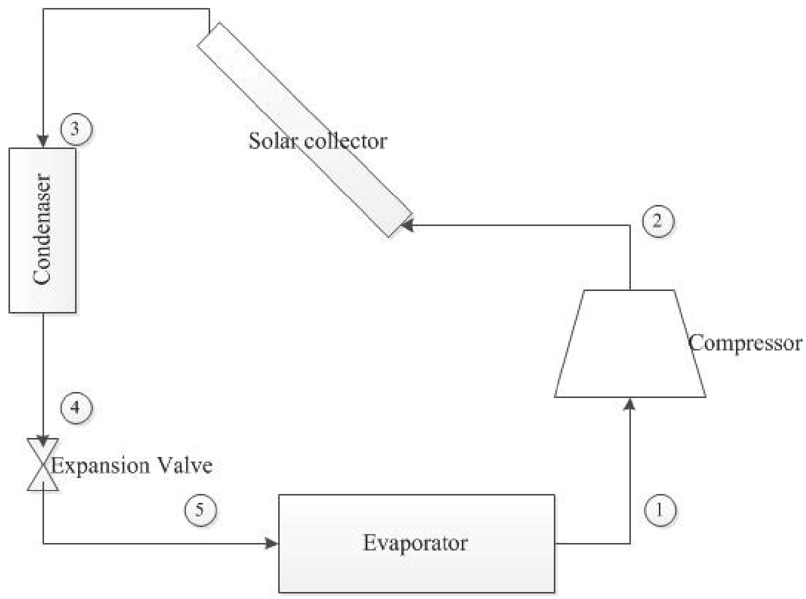

Figure 21: Schematic of the [redacted] solar assisted AC unit

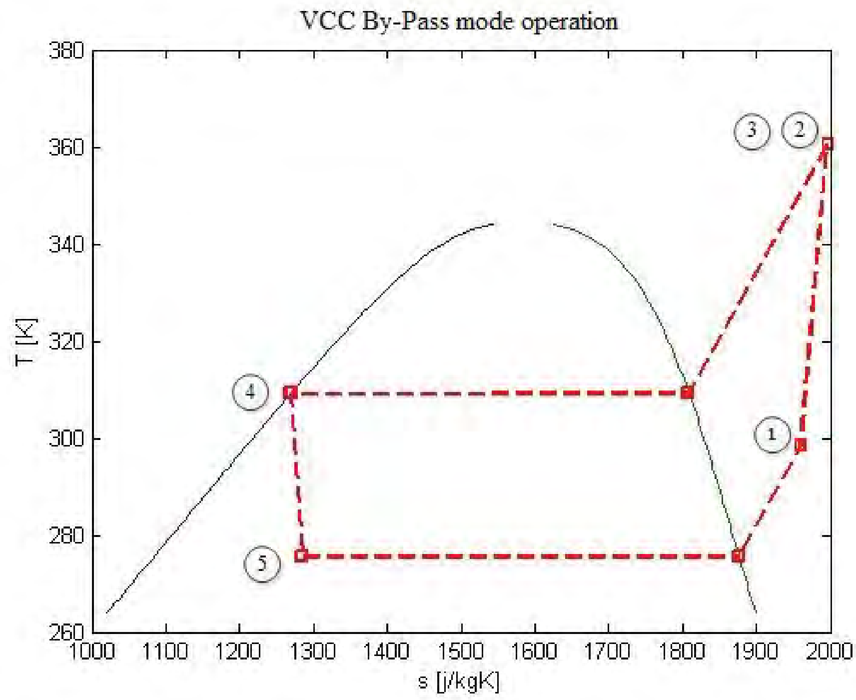

Figure 22: VCC by-pass T-s diagram

The fluid conditions at different points of the cycle for the base case have been presented in Table 8. And cycle cooling performance calculations have been summarized in Table 11.

Table 8 Refrigerant conditions and thermodynamic properties - by-passed cycle

Point	State	T [K]	P [kPa]	h [kJ/kg]	s [kJ/kg C]	$\dot{m}$ [kg/s]
1	Superheated vapor	299.3	827.37	4488.3	1.97	0.016
2	Superheated vapor	359.8	2309.7	4900.1	1.99	0.016
3	Superheated vapor	359.8	2309.7	4900.1	1.99	0.016
4	Sub-cooled liquid	309.9	2309.7	2614.1	1.27	0.016
5	mixture	274.2	827.37	2614.1	1.29	0.016

It is worth mentioning, there is no pressure and heat loss were considered in the simulated cycle. In order to investigate the effect of the refrigerant temperature increase/decrease between the compressor and condenser, two cases have been considered. The heating case is when the refrigerant absorbs enough heat inside the solar collector to overcome the heat losses inside the connecting pipelines. And cooling case is when the amount of heat absorbed inside the solar collector is not enough to provide higher refrigerant temperature at condenser inlet with respect to compressor outlet. For both cases, extreme conditions have been investigated. In heating case it is assumed that the refrigerant temperature at the condenser inlet is 15^0C higher than its temperature at compressor outlet. And for the cooling case the temperature at condenser inlet is 15^0C lower than compressor outlet.

In order to calculate the refrigerant conditions and air temperature leaving the condenser the following calculation procedure is performed. A large portion of the heat transfer inside the condenser takes place along the refrigerant constant temperature and the temperature changes of the air flow is not very large. Therefore, it is a valid assumption to take the overall heat transfer coefficient (U) constant across the condenser for different cases. The overall heat transfer coefficient is calculated using the By-pass test conditions (test 10-23 By-pass), and is used to calculate the air and refrigerant outlet temperatures at condenser outlet. When evaluating the condensing heat transfer rate, the logarithmic mean temperature difference approach was used. Because of existence of de-superheating and sub-cooling parts in refrigerant condensing pr*ocess, the temperature of the condensing stream usually varies substantially from inlet to outlet. Therefore, the temperature of the condensing stream usually varies substantially from inlet to outlet. Furthermore, the stream enthalpy varies nonlinearly with temperature in this situation, so mean temperature difference is no calculated as same as pure condensation case (constant temperature). In order to evaluate the heat transfer inside the condenser the zone analysis presented by Gully [7] is executed.

$$Q^{\cdot}_{c} = UA\Delta T_{wm} \quad \text{(Eq. 12)}$$

$$\Delta T_{wm} = \frac{Q^{\cdot}_{total}}{\frac{\dot{Q}_{sup.heat}}{LMTD}_{Sup.heat} + \frac{\dot{Q}_{2phase}}{LMTD}_{2phase} + \frac{\dot{Q}_{sub.cool}}{LMTD}_{sub.cool}} \quad \text{(Eq. 13)}$$

$$LMTD = \frac{\Delta T_{in} - \Delta T_{out}}{\ln(\frac{\Delta T_{in}}{\Delta T_{out}})} \quad \text{(Eq. 14)}$$

Here, A is the heat transfer arear, U is the overall heat transfer coefficient, $\dot{Q}$ is the heat transfer rate and LMTD stands for logarithmic mean temperature difference. Subscripts $sup.heat$, $2phase$ and $sub.cool$ represent the superheated, two phase and sub-cooled sections of the heat exchanger respectively.

Using equation (4) along with the energy balance across the condenser heat exchanger it is possible to calculate the refrigerant and air temperatures at condenser outlet. Knowing the temperature values at the condenser inlet and solving the equations iteratively the temperatures at the outlet of the condenser are calculated. The fluid conditions at different points of the cycle for the heating and cooling cases have been presented in Table 9 and Table 10 respectively. For the sake of easier interpretation some more points are presented in these tables. Also the T-s diagrams are presented for each case in Figure 23 and Figure 24.

Table 9: Refrigerant conditions and thermodynamic properties - (CASE II)

Point	State	T [C]	P [kPa]	h [kJ/kg]	s [kJ/kg C]	$\dot{m}$ [kg/s]
Evaporator saturates vapor	vapor	274.3	827.37	422.86	1.88	0.016
1	Superheated vapor	299.3	827.37	448.83	1.97	0.016
2	Superheated vapor	359.8	2309.74	490.01	1.99	0.016
3	Superheated vapor	374.8	2309.74	506.74	2.04	0.016
Condenser saturated vapor state	Vapor	311.3	2309.74	426.83	1.80	0.016
Condenser saturated liquid state	liquid	311.1	2309.74	263.85	1.28	0.016
4	Sub-cooled liquid	309.9	2309.74	261.61	1.27	0.016
5	mixture	274.2	827.37	261.61	1.29	0.016

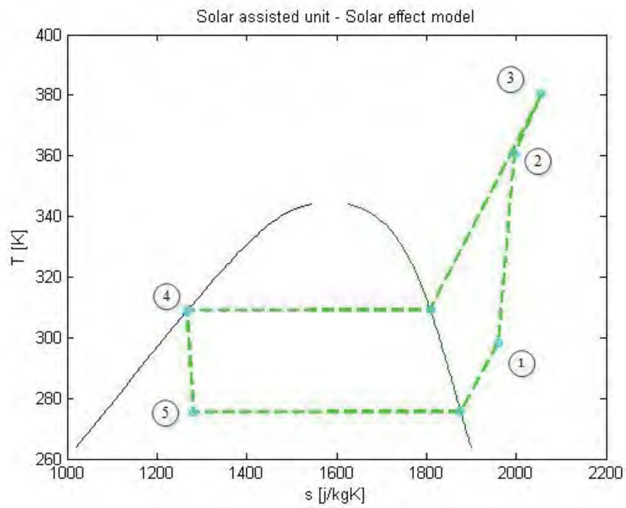

Figure 23: VCC T-s diagram - (CASE II)

Table 10: Refrigerant conditions and thermodynamic properties - (CASE I)

Point	State	T [C]	P [kPa]	h [kJ/kg]	s [kJ/kg C]	$\dot{m}$ [kg/s]
Evaporator saturates vapor	vapor	274.3	274.29	827.37	422.86	1.88
1	Superheated vapor	299.3	299.25	827.37	448.83	1.97
2	Superheated vapor	359.8	359.77	2309.74	490.01	1.99
3	Superheated vapor	344.8	344.77	2309.74	472.68	1.94
Condenser saturated vapor state	Vapor	311.3	311.26	2309.74	426.83	1.80
Condenser saturated liquid state	liquid	311.1	311.14	2309.74	263.85	1.28
4	mixture	311.1	309.71	2309.74	261.14	1.27
5	mixture	274.2	274.21	827.37	261.14	1.29

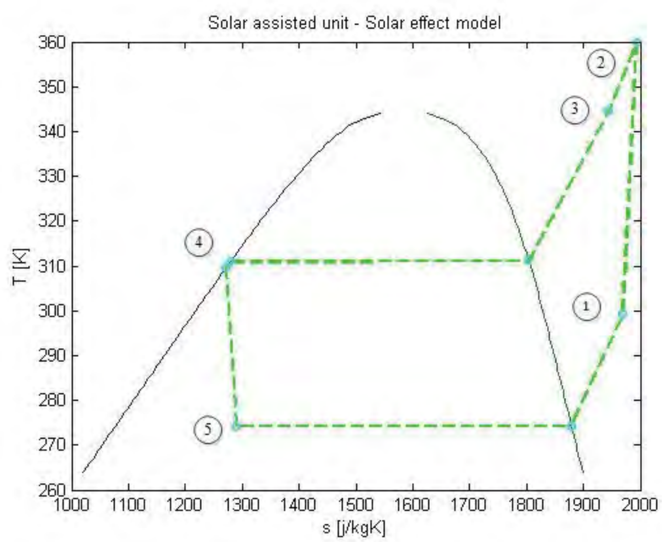

Figure 24: VCC T-s diagram - (CASE I)

Table 11: VCC performance comparison

Case	By-pass	(CASE II)	(CASE I)
Q_e [kW]	3.022	3.019	3.022
Q_c [kW]	3.864	3.9531	3.494
W_{tot} [kW]	1.32	1.32	1.32
Q_{soalr} [kW]	0	0.270	-0.279
ΔT_{solar}[C]	0	+15	-15
T_{c1} [C]	35.0	35.0	35.0
T_{c2} [C]	37.1	37.3	36.9
COP	2.292	2.290	2.296

Superheating the vapor refrigerant furthermore at the compressor outlet puts more heat load on the condenser heat exchanger. Refrigerant leaves the condenser at a higher temperature (sub-cooling value 1.2 ^{0}C) compared with the by-pass test (sub-cooling value 1.3^{0}C). COP of the VCC is defined as the ratio between thermal energy absorbed inside the evaporator to the work input to the cycle. Therefore the heating case result to slightly lower COP when compared to the by-pass cycle, due to lower amount of sub-cooling inside the condenser. On the other hand when the refrigerant is cooled before entering the condenser, the heat load on the heat exchanger is reduced. Also, lower heat load will result lower air temperature at condenser outlet. Therefore, the refrigerant leaves the condenser at lower temperature (sub-cooling value 1.4^{0}C), with less enthalpy compared to by-pass test. Because other working conditions (i.e. Evaporator temperature and pressure) are kept constant, the COP of the cycle in cooling case would be higher than by-pass conditions.

7.1 Cooling Performance at Different Locations

In order to compare the performance of the unit under different conditions, three locations including Tampa, Miami and Daytona have been selected. The outdoor conditions for cooling season from the AHRAE handbook fundamentals [6] have been used to analyze the performance of the unit (Table 12). For each location three cases have been studied; 1- no solar effect, 2- heating the flow case and 3- cooling the flow case. COPs of the unit for constant cooling load at each location (annual percentile 0.4%) and three different cases are presented in Table 13.

Table 12: Cooling design conditions for selected locations [6]

	Latitute	Longitute	Elvation	Cooling DB/MCWB					
				0.4 %		1.0 %		2.0 %	
Tampa	27.96	82.54	10	33.55	25.22	32.94	25.17	32.39	25.11
Miami	25.82	80.30	30	32.22	25.33	32.61	25.28	32.09	25.36
Daytona	29.18	81.06	43	33.72	24.94	32.67	24.95	31.78	24.83

Table 13: COP of the unit at different working conditions

	By-pass case (ΔT_{solar} = 0 C)	(CASE I) (ΔT_{solar} = -15 C)	(CASE II) (ΔT_{solar} = 15 C)
Tampa	2.59	2.60	2.59
Miami	2.73	2.74	2.72
Daytona	2.57	2.58	2.57

8. Conclusions

A two ton [redacted] solar assisted AC unit has been tested according to the ASHRAE Standard 37-2009 and its performance has been evaluated at different outdoor conditions. The additional pipe length between the condenser unit and the solar collector, which is 94 feet in the test installation acts as an extension of the condenser. The results showed that heating the refrigerant in a solar collector, after the compressor and before entering the condenser has a small adverse effect on the COP of the cycle when the solar radiation is enough to overcome the heat loss in the associated piping. When the solar radiation is not enough, the associated piping acts as an extension of the condenser. However, the COP in such cases is about the same as that without the solar collector. The reason for the small differences in the COP for all the cases is that the additional superheat provided by the solar collector is a very small fraction of the total heat rejected in the condenser, latent heat of the refrigerant being a much larger part of the heat rejected in the condenser. A theoretical simulation of the system confirms these results.

Adding heat to the vapor compression cycle of an air conditioning system by a solar thermal collector or by any other means will reduce the efficiency of the system not increase it. Therefore, adding a solar collector between the compressor and condenser of an air conditioning unit reduces the efficiency and performance of the air conditioning unit.

Nomenclature

t	[C]
A	[m^2]
COP	Coefficient of Performance
EER	Energy Efficiency Ratio
h	[kJ/kg]
m	[kg/s]
P	[kPa]
Q	[kJ]
s	[kJ/kgK]
T	[K]
U	[W/m2 K]
V	[m^3/s]
v	[m^3/kg]
W	[kW]
RH	[%]
subscripts	
1	Inlet
2	Outlet
2phase	2phase flow
c	Condenser
e	Evaporator
in	Inlet
out	Outlet
sub.cool	Subcooled flow
sup.heat	Superheat flow
tot	Total
wm	Weighted medium

References

[1] ASHRAE Standard 37-2009, Methods of Testing for Rating Electrically Driven Unitary Air-Conditioning and Heat Pump Equipment. www.ashrae.org

[2] ANSI/ARI Standard 210/240-89, Unitary Air-Conditioning and Air-Source Heat Pump Equipment. Air-Conditioning and Refrigeration Institute 1989.

[3] 2013 ASHRAE Handbook - Fundamentals (SI Edition). American Society of Heating, Refrigerating and Air-Conditioning Engineers, Inc.. Online version available at: http://app.knovel.com/hotlink/toc/id:kpASHRAEC1/ashrae-handbook-fundamentals/ashrae-handbook-fundamentals

[4] http://www.handsdownsoftware.com/ PSYCHOMETRIC ANALYSIS CD.

[5] [redacted]

[6] 2009 ASHRAE Handbook - Fundamentals (SI) January 15, 2009. American Society of Heating Refrigerating and Air-Conditioning Engineers.

[7] [redacted].

Appendix A

To calculate the thermodynamic properties of moist air, the procedure presented in ASHRAE Handbook – Fundamentals has been used [3].

Moist air is a mixture of dry air and water vapor. The amount of water vapor varies from zero to a maximum that depends on temperature and pressure. To determine the thermodynamic properties of moist air two parameters is required e.g. (T_{db}, RH), (T_{db}, W),(T_{db}, T_{wb}), or (T_{db}, T_{dp}). Of these, T and RH are currently the easiest to measure. Dry bulb temperature and relative humidity (correspondent to wet bulb temperature) are the measured parameters in this study. The required thermodynamic properties are calculated from equations below;

The water vapor saturation pressure is required to determine a number of moist air properties, principally the saturation humidity ratio. The saturation pressure over liquid water for the temperature range of 0 to 200 C is given by:

$$\ln p_{ws} = C_8/\mathrm{T} + C_9 + C_{10}\mathrm{T} + C_{11}T^2 + C_{12}T^3 + C_{13}\ln \mathrm{T}$$

$$C_8 = -5.8002206E + 3$$

$$C_9 = 1.3914993E + 0$$

$$C_{10} = -4.8640239E - 3$$

$$C_{11} = 4.1764768E - 5$$

$$C_{12} = -1.4452093E - 8$$

$$C_{13} = 6.5459673E + 0$$

$$T = 273.15 + t$$

Here t [C] is the dry bulb temperature, T [K] is the absolute temperature and p_{ws} [Pa] is the saturation pressure.

Relative Humidity (or RH) is the ratio of the mole fraction of water vapor in a given moisture air sample to the mole fraction in an air sample saturated at the same pressure and temperature:

$$RH = \frac{p_w}{p_{ws}}$$

Here p_w and p_{ws} are partial pressure of water vapor in the mixture and saturated mixture respectively.

Humidity ratio W, is defined as the ratio of the mass of water vapor to the mass of the moist air in the sample:

$$W = 0.621945 \frac{p_w}{p - p_w}$$

Here p [Pa] is the barometric pressure of the sample.

The specific enthalpy [kJ/kg] and specific volume [m^3/kg] of the moist air can be calculated from the next equations:

$$h = 1.006t + W(2501 + 1.86t)$$

$$v = \frac{RT}{28.966(p - p_w)}$$

$$\dot{m} = \frac{\dot{V}A}{v}$$

Here R is the universal gas constant, 9314.472 [J/kmolK], $\dot{m}$ is the air mass flow rate [kg/s], $\dot{V}$ is the air velocity [m/s] and A is the cross section area [m^2].

A computer code in [redacted] has been developed to calculate the required moist air properties at different conditions. To evaluate the results, calculated values are compared with values extracted from commercial software [redacted] and presented in Table A1, for some selected points.

Table 14: Thermodynamic values for selected points

	T_{db} [C]	RH [%]	h [kJ/kg] Calculated	h [kJ/kg] HDP software
AHU inlet	26.74	50.4	55.1	55.13
AHU outlet	22.07	58.51	55.8	54.83
Condenser inlet	35.06	20.19	53.4	53.4
Condenser outlet	37.25	18.08	55.9	55.85

[redacted] ASSESMENT STUDY

FINAL REPORT

August 2014 to Agues 2015 Data Analysis

November 25, 2015

Submitted by:

Professor Amir Abtahi, PhD, PE
And
Hadis Moradi, PhD Candidate
College of Engineering and Computer Science
FAU
Boca Raton, Florida

1. Introduction

The [redacted] research team is assessing the performance of a solar tracker on FAU campus. The purpose of the study is to compare the annual performance of a solar tracking array with a non-tracking solar array. The contractor designed and installed 2 equivalent solar arrays each featuring 24 [redacted] modules. The tracking array has a generally North-South axis and the non-tracking array has an East-West axis with panels set at 26^{o} inclination angle. The arrays were originally designed for a rating of 7.4 kW each, but there has been some deviation from the original design that will be discussed in more detail in this report. The FAU team started the monitoring of the system in August 2014 when the system was officially commissioned and has continued to monitor and evaluate the system so that missing seasonal performance data can be filled into for a full calendar year assessment.

2. System Architecture Design

The [redacted] system was initially designed as two equivalent arrays of 7.4 kW each with 24 [redacted] watt modules each. The non-tracking array is designed on an East-West axis with a 26o inclination angle for "near-optimum" annual generation. This angle setting is generally considered as good year-around inclination to generate the best year-around energy production. The tracking array is designed to be installed on a North-South axis and tracking from East to West throughout the day. It appears that the system was also designed to revert to a horizontal setting at light time and also in the event of winds exceeding 30 MPH. The design of the tracking algorithm have not been made available to the FAU team for assessment. The output of each array is fed to two [redacted] 7-kW inverters. The local programming for grid-feed profile or limits were not made available to the FAU team. The net output from the inverters to the grid are monitored by [redacted] and this output data is currently the only information available to the FAU team.

The following is a snap-shot of the system information as originally uploaded to the [redacted] website:

PV System Profile | [redacted] - FAU Solar 1

Location:	Boca Raton, United States
Commissioning:	8/6/2014
PV system power:	14.800 kWp
Annual Production:	approx. 22,200 kWh (1,500 kWh/kWp)
CO2 avoided:	Approx. 23.4 tons per annum
Modules:	[redacted]
Communication:	
Inverter:	

The array was originally designed with 24 [redacted]-watt modules, thus the 7.4 kW on each array, and while the [redacted] site shows the revised design of using 285-watt panels instead, the overall corrected output of 6.2 kW each for a total of 12.4 kW is not reflected for the "PV Power System."

3. System As-Installed

a. Array Orientations

The non-tracking array has been installed on an East-West orientation. The inclination angle appears to be closer to 24 to 25 degrees, however this observation was made from a distance as the FAU team has not had access to the arrays and has not been able to measure the actual angle of the arrays. The tracking array appears to have been installed on a North-West to South-East orientation with approximately 15 degrees of deviation. This orientation favors early morning generation and the FAU team has not been able to ascertain the cause or the basis for this specific orientation. The generation data will show the results of this orientation in the following sections.

b. Array Configuration

Both arrays are configured with the same solar panels and with the following architecture:

Strings in parallel: 4
Modules per string: 6
Total number of modules per array: 24
Max power rating for each [redacted] module@1000W/m2: 285 W
Max capacity of each array: 24 × 285 W = 6.84 kW

- Solar Panels: [redacted]

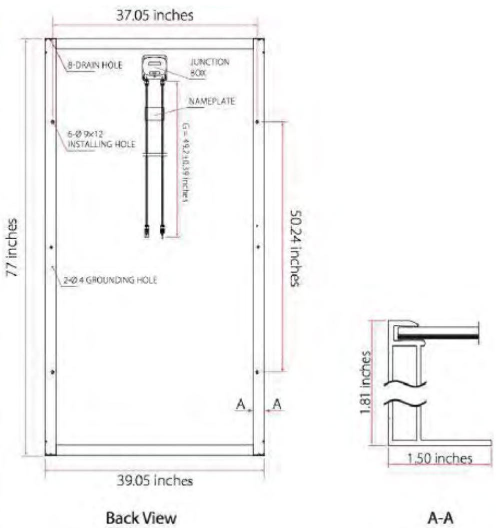

Electrical Data @ STC	[redacted]
Peak Power Watts-P_{MAX} (WP)	
Power Output Tolerance-P_{MAX} (%)	0/+3
Maximum Power Voltage-VMAX (V)	36.3
Maximum Power Current-I_{MPP} (A)	7.86
Open Circuit Voltage-VOC (V)	44.5
Short Circuit Current-ISC (A)	8.49
Module Efficiency η_m (%)	14.7

Mechanical Data	[redacted]
Solar cells	Multicrystalline 6 inches (156 x 156mm)
Cells orientation	72 cells (6x12)
Module dimension	77 x 39.05 x 1.81inches (1956 x 992 x 46mm)
Weight	61.7lb (28kg)

[redacted] Webconnect:

"[redacted] Webconnect provides an option for simplified system monitoring, which is a critical component of any PV system. "With free online connectivity to Sunny Portal, system owners can access PV system data anytime and anywhere via the Internet or Sunny Portal application for [redacted] touch and [redacted], further adding to its convenience."

Webconnect provides direct data transmission from the inverter to [redacted] via an [redacted] cable. Data is streamed "live" similar to the way that live video is transmitted. When these inverters are equipped with Webconnect, this data is gathered and sent directly to [redacted]. Data retrieval can also be done locally using [redacted], a [redacted] software for PC. Connection to [redacted] is not required for data retrieval, but Webconnect must be installed with the correct time and date stamping. This local connection between [redacted] and the Webconnect is referred to as [redacted]-specific protocol based on [redacted]

[redacted] cable is connected directly to Webconnect within the inverter and can be accessed via [redacted]

[redacted]:

[redacted] is the name given to [redacted] automation systems. The name comes from the combination of the words [redacted]. Products under this range allow the automation of industrial machines and therefore a full system will often comprise of [redacted] components linking with drives from the [redacted] range. This device controls and monitoring with widescreen displays and integrated multi-touch functions.

Highlights
• Ideal entry-level range for simple [redacted] applications
• Installation compatibility with [redacted] and existing [redacted] Basic Panels 4" and 6"
• Flexible scalability within the [redacted] range
• High-resolution, dimmable wide-screen displays with 64.000 colors
• Innovative user interface and improved usability thanks to new controls and graphics
• Touch / key functionality for intuitive operation
• Interface for connection with various PLCs
• Versions for [redacted]
• Archiving via [redacted]
• Engineered in the [redacted]

Basic panels are ideal for simple visualization tasks, even in harsh environments. There are options for 3", 4", 6" and 10" devices with keypads or a 15" touch screen device. There are both color and mono versions available to suit the requirements and budget.

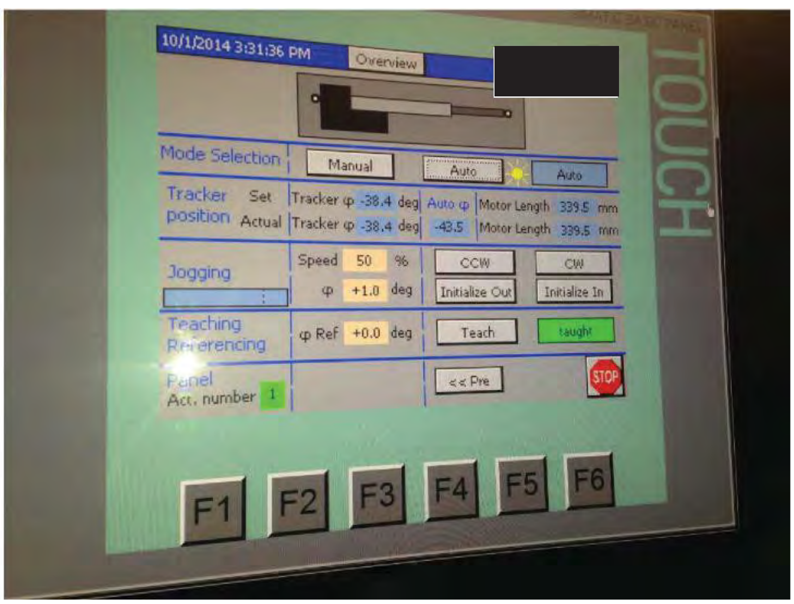

Picture of monitoring screen captured on site

- Inverter: [redacted]

PV Array Connection

Maximum MPP voltage	250 V ... 480 V
Nominal operating voltage	310 V
Range of input operating voltage	250 V ... 600 V
Maximum generator input power	8 750 W
Maximum DC power	7 500 W
PV start voltage	300 V
Maximum DC input current	30 A
Maximum input short-circuit current	36 A
Maximum utility back-feed current to PV array	50 A AC
DC voltage ripple	< 10 %

Grid Connection

AC operating voltage range at 208 V nominal	183 V ... 229 V
AC operating voltage range at 240 V nominal	211 V ... 264 V
AC operating voltage range at 277 V nominal	244 V ... 305 V
AC operating frequency range	59.3 Hz ... 60.5 Hz
AC frequency, nominal value	60 Hz
Maximum continuous AC output power	7 000 W
Current THD	< 4 %
Maximum continuous AC output current at 208 V	34 A
Maximum continuous AC output current at 240 V	29 A
Maximum continuous AC output current at 277 V	25.3 A
Maximum output failure current	57.6 A
Maximum output overcurrent protection	50 A
Synchronization of inrush current	9.23 A
Trip limit accuracy	±2 %
Trip time accuracy	±0.1 %
Power consumption at night	0.1 W

Range of output power factor	0.95 ... 1.0
Output power factor, nominal value	0.99%
Peak inverter efficiency	97.1%
CEC weighted efficiency at 208 V AC	95.5%
CEC weighted efficiency at 240 V AC	96.0%
CEC weighted efficiency at 277 V AC	96.0%

Device Characteristics

Max capacity of both units: 48 × 285 W = 13.68 kW
While on the [redacted] website, this number is 14.8 kW. As shown in the following figure:

Device Characteristics

Data Collection:	●
Device Class:	Photovoltaic inverter
Product Group:	[redacted]
Serial Number:	
PIC:	
Manufacturer:	
Device Name:	Fixed
Automatic updates:	● Automatically update device
Description:	---
Phase:	● L1 ● L2 ● L3
Generator capacity:	7.400 kWp
Meter reading Data logger object energy:	3,443.45 kWh (10/28/2014 5:50 PM)

Device Characteristics

Data Collection:	●
Device Class:	Photovoltaic inverter
Product Group:	[redacted]
Serial Number:	
PIC:	
Manufacturer:	
Device Name:	Tracker
Automatic updates:	● Automatically update device
Description:	---
Phase:	● L1 ● L2 ● L3
Generator capacity:	7.400 kWp
Meter reading Data logger object energy:	3,812.99 kWh (10/28/2014 5:50 PM)

Tracker solar system:

Different Positions of Tracker Solar Unit on Sunday October 19

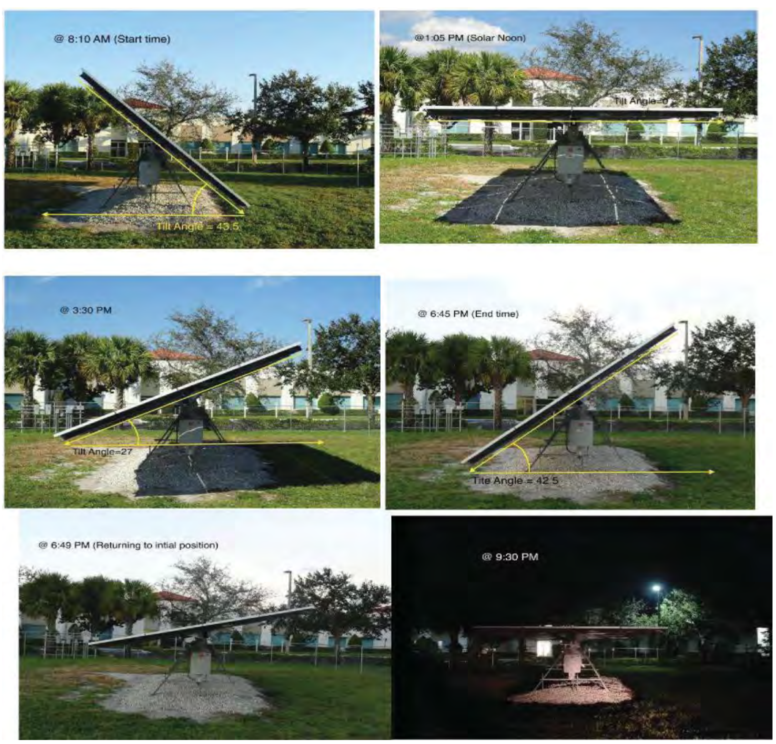

The single-axis tracker starts in the morning with a tilt angle of about 45° facing 15 degrees South of East and completes its daily path with atilt angle of about 45° facing 15 degrees North of West. It has a broad turn range (0 to 90°) and remains flat with tilt angle of zero degree during night.

We have been given no information on the exact tracking algorithm or whether the program uses time, light sensing or a combination of the two to accomplish its tasks. If data on sensors is available at the local computer or through [redacted] is not clear as we have not been given access to this information. The following picture shows the sensor on the tracker. It also appears that the sensor may be under the anemometer, but this could not be ascertained from a distance. The picture below shows the sensor on the tracker one. As it's shown in the picture, the sensor is located under the anemometer.

Fixed solar system:

South face fixed solar unit

Self-Shading:

Two systems have been installed a sufficient distance from each other to prevent inter-array shading.

Tracker solar system vs. fixed solar system:

The [redacted] diagrams for Boca Raton, for the monitoring period (August through November) are shown below.

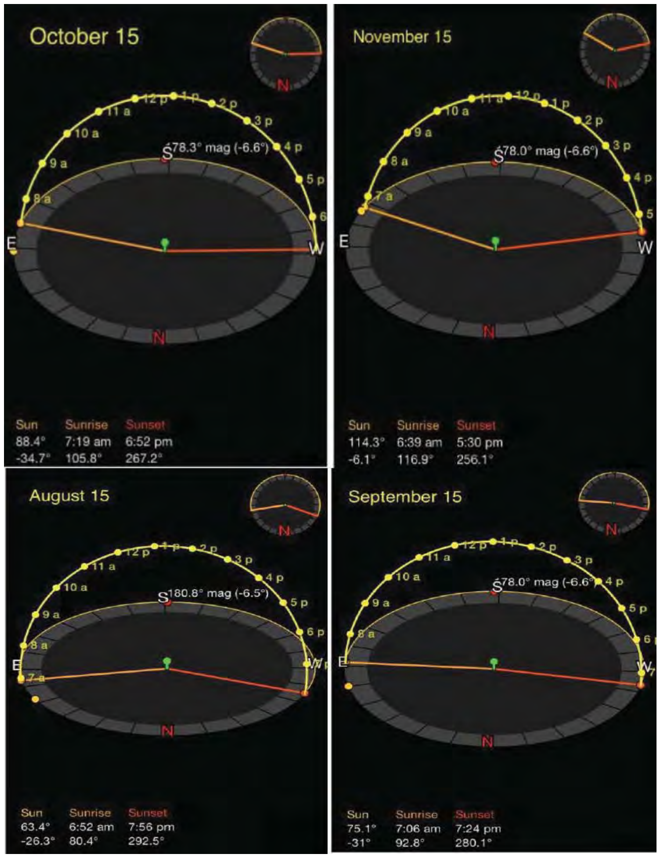

The apparent path of the sun in midwinter and midsummer in Florida are also shown in the following figure:

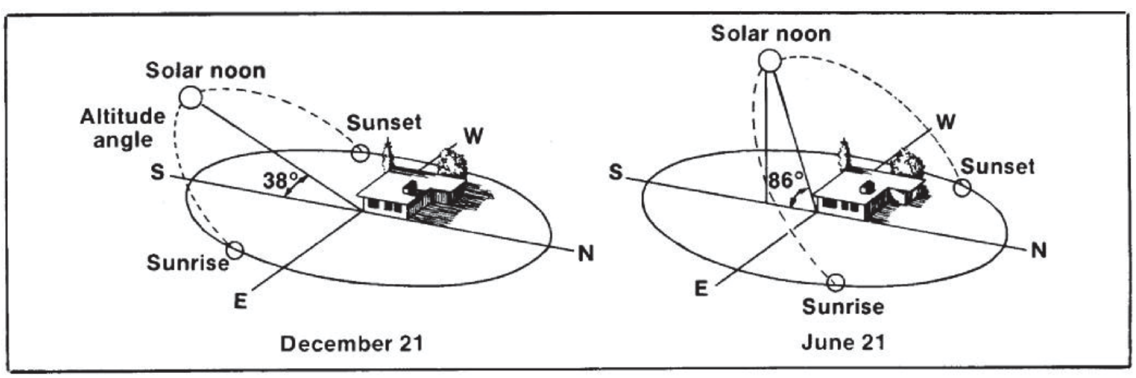

Sun path diagrams for 28° north.

Since the tracker axis is horizontal with the tilt angle of zero at solar noon, its production is biased to the summer months when the sun is overhead at noon, and at a disadvantage in the winter months when the non-tracking array receives more solar radiation in the mid-day period.

Preliminary Assessment

The following diagrams show typical generation patterns that are available through the SMA monitoring website. The red curves represent the tracker output, and the blue lines represent the non-tracker output.

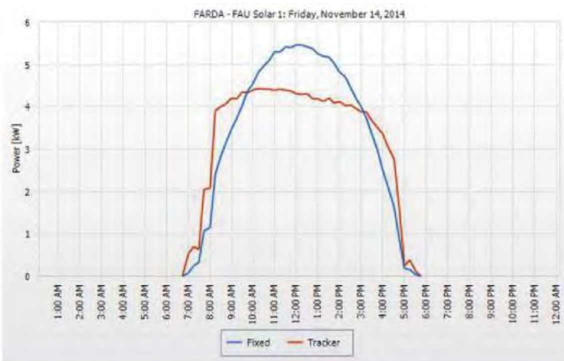

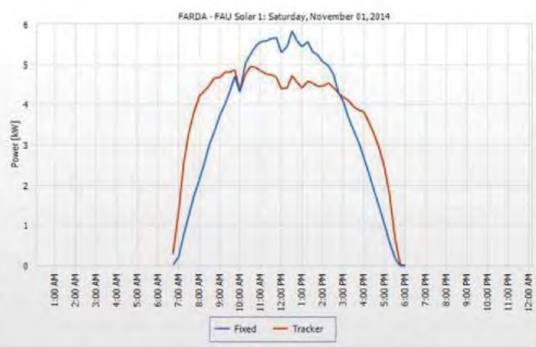

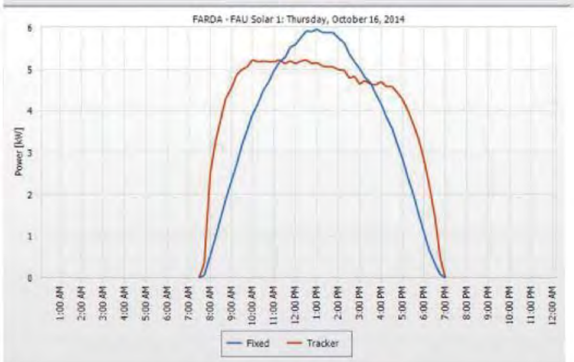

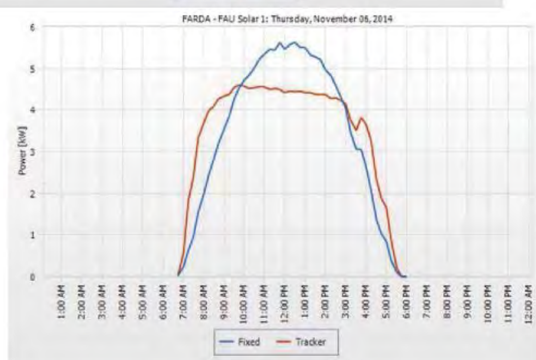

The diagrams show the non-symmetric nature of the tracker output as caused by the 15 degree deviation from the North-South axis. The following graphs show the total daily generation shown as the blue colored area in the first graph, versus the individual outputs for tracker versus non-tracker outputs shown in the second graph.

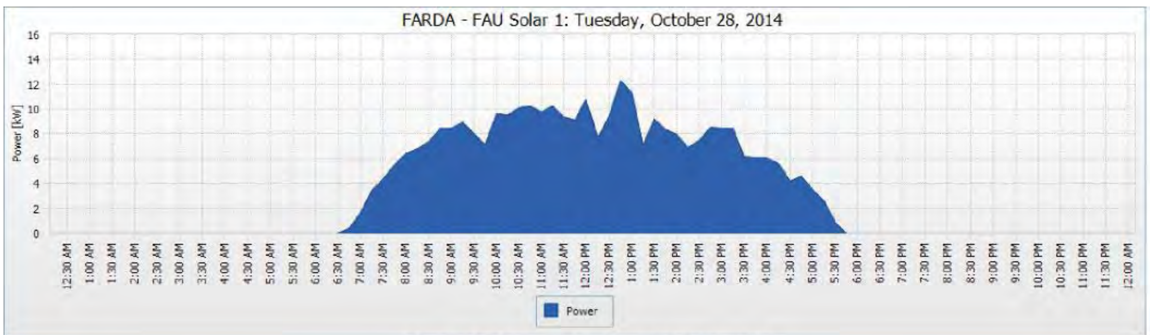

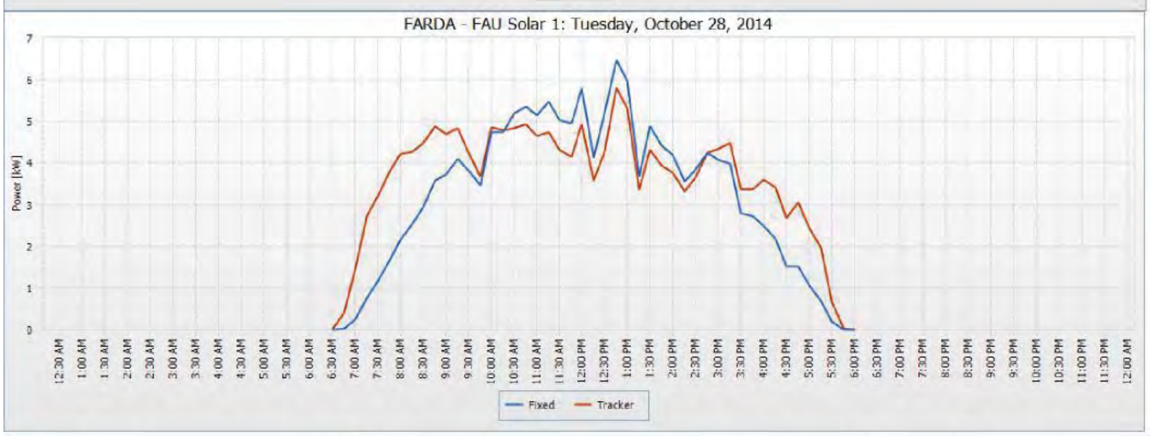

2014	Sunrise/set		Daylength		Astro. Twilight		Naut. Twilight		Civil Twilight		Solar noon	
Oct	Sunrise	Sunset	Length	Diff.	Start	End	Start	End	Start	End	Time	Mil. mi
28	7:27 AM (104°)	6:41 PM (256°)	11:14:01	−1:23	6:09 AM	7:59 PM	6:36 AM	7:32 PM	7:03 AM	7:05 PM	1:04 PM (50.4°)	92.359

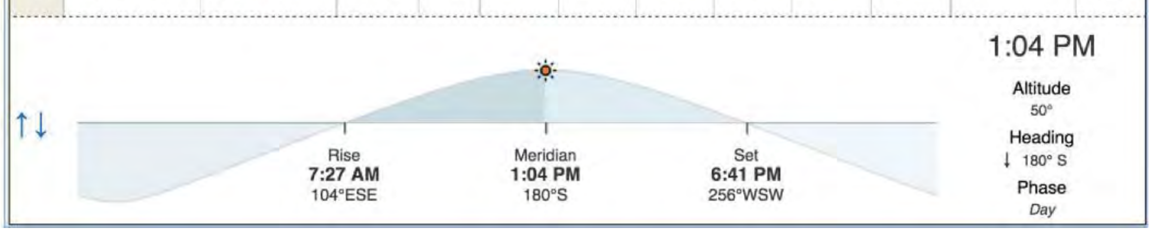

A summary comparison of monthly energy production for the arrays is illustrated in the chart below.

Energy Produced by Tracker and Fixed systems during August18th to August 31th, 2014

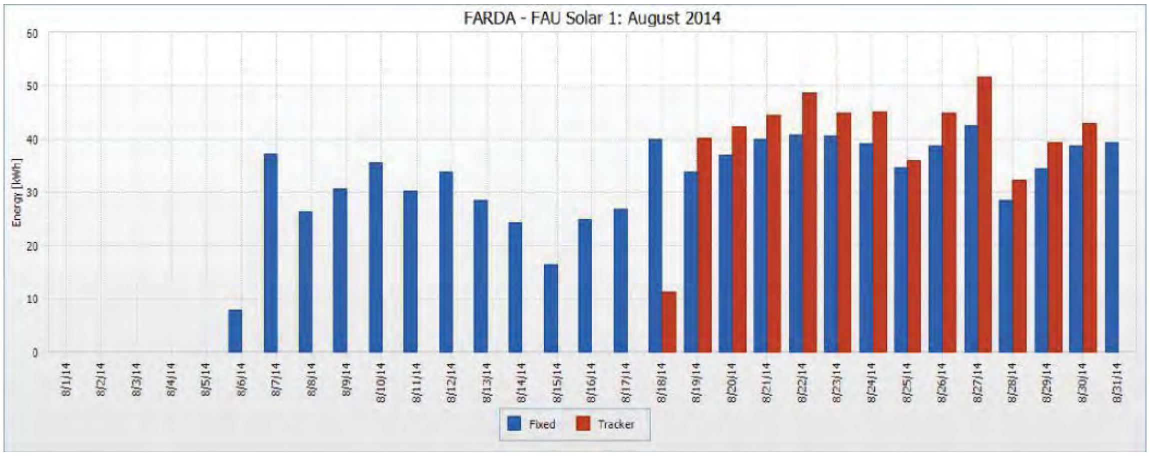

	Augest		
	Fixed	Tracker	%
8/18/14	39.925	11.338	-71.60
8/19/14	33.912	40.261	18.72
8/20/14	37.095	42.365	14.21
8/21/14	40.069	44.644	11.42
8/22/14	40.829	48.632	19.11
8/23/14	40.583	45.041	10.98
8/24/14	39.205	45.232	15.37
8/25/14	34.661	36.062	4.04
8/26/14	38.814	44.884	15.64
8/27/14	42.563	51.726	21.53
8/28/14	28.462	32.245	13.29
8/29/14	34.482	39.474	14.48
8/30/14	38.774	42.899	10.64
8/31/14	39.371		-100.00
TOTAL	449.449	513.465	14.24

There have been some discrepancies in the data which may have been caused by reprogramming or other adjustments or errors on the [redacted] website. For example there was no data available for August 31, 2014. In this case the sum of tracker production is higher (566.343 kWh) than the day-by-day production, which is 524.803 kWh.

	Fixed Data logger object energy Meter change [kWh]	Tracker Data logger object energy Meter change [kWh]
Jan 14		
Feb 14		
Mar 14		
Apr 14		
May 14		
Jun 14		
Jul 14		
Aug 14	851.785	566.343
Sep 14	891.884	978.488
Oct 14	991.086	1112.413
Nov 14	372.839	383.742
Dec 14		

Energy Produced by Tracker and Fixed systems in September 2014

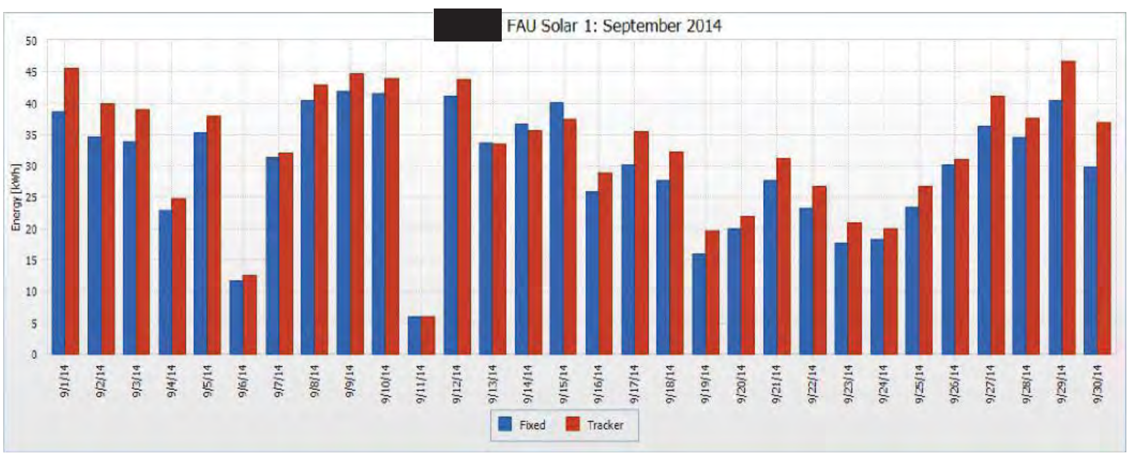

	September		
	Fixed	Tracker	%
9/1/14	38.629	45.467	17.70
9/2/14	34.735	39.996	15.15
9/3/14	33.905	38.924	14.80
9/4/14	22.984	24.704	7.48
9/5/14	35.327	38.015	7.61
9/6/14	11.73	12.491	6.49
9/7/14	31.29	32.052	2.44
9/8/14	40.498	42.982	6.13
9/9/14	41.842	44.652	6.72
9/10/14	41.57	43.958	5.74
9/11/14	5.985	5.994	0.15
9/12/14	41.116	43.666	6.20
9/13/14	33.665	33.509	-0.46
9/14/14	36.643	35.599	-2.85
9/15/14	40.093	37.418	-6.67
9/16/14	25.947	28.868	11.26
9/17/14	30.245	35.411	17.08
9/18/14	27.756	32.223	16.09
9/19/14	16.078	19.64	22.15
9/20/14	20.014	21.913	9.49
9/21/14	27.766	31.237	12.50
9/22/14	23.305	26.676	14.46
9/23/14	17.687	20.895	18.14
9/24/14	18.28	20.042	9.64
9/25/14	23.487	26.655	13.49
9/26/14	30.221	31.011	2.61
9/27/14	36.335	41.045	12.96
9/28/14	34.474	37.661	9.24
9/29/14	40.427	46.709	15.54
9/30/14	29.85	36.935	23.74
TOTAL	891.884	976.348	9.47

Energy Produced by Tracker and Fixed systems in October 2014

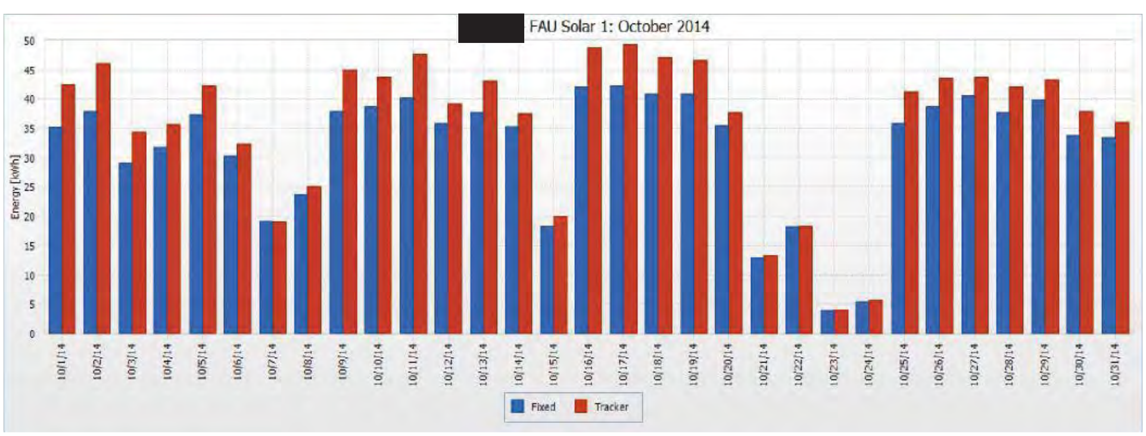

	October		
	Fixed	Tracker	%
10/1/14	35.178	42.349	20.38
10/2/14	37.809	46.099	21.93
10/3/14	29.203	34.334	17.57
10/4/14	31.866	35.737	12.15
10/5/14	37.437	42.264	12.89
10/6/14	30.338	32.361	6.67
10/7/14	19.128	19.039	-0.47
10/8/14	23.67	25.083	5.97
10/9/14	37.927	44.929	18.46
10/10/14	38.784	43.757	12.82
10/11/14	40.298	47.669	18.29
10/12/14	35.864	39.214	9.34
10/13/14	37.676	43.026	14.20
10/14/14	18.326	20.1	9.68
10/15/14	35.432	37.539	5.95
10/16/14	42.046	48.753	15.95
10/17/14	42.211	49.248	16.67
10/18/14	40.911	47.118	15.17
10/19/14	40.919	46.678	14.07
10/20/14	35.506	37.79	6.43
10/21/14	12.928	13.231	2.34
10/22/14	18.235	18.33	0.52
10/23/14	3.95	4.028	1.97
10/24/14	5.434	5.659	4.14
10/25/14	35.926	41.279	14.90
10/26/14	38.675	43.582	12.69
10/27/14	40.535	43.851	8.18
10/28/14	37.632	42.048	11.73
10/29/14	39.915	43.295	8.47
10/30/14	33.827	37.961	12.22
10/31/14	33.5	36.062	7.65
TOTAL	991.086	1112.413	12.24

Energy Produced by Tracker and Fixed systems in November 2014

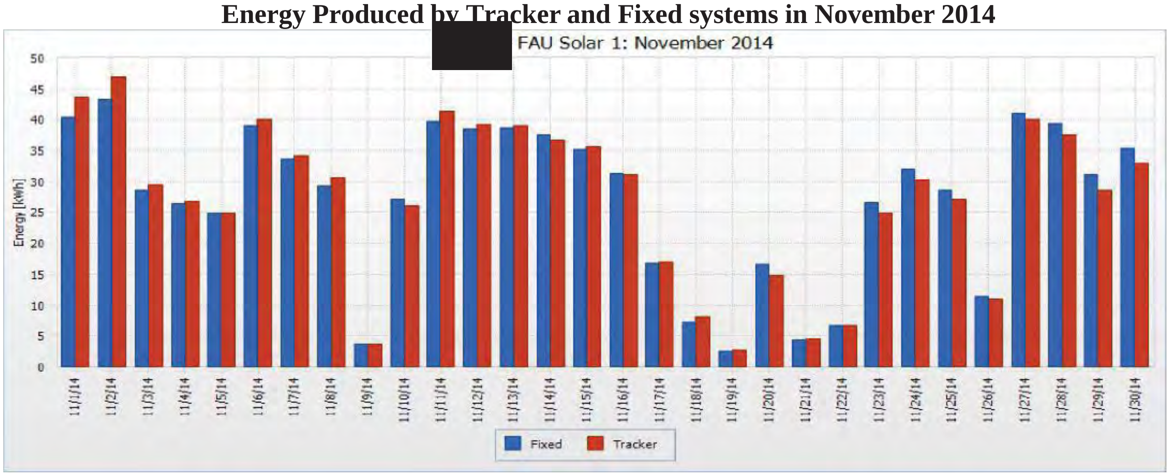

	November		
	Fixed	Tracker	%
11/1/14	40.359	43.631	8.11
11/2/14	43.274	46.93	8.45
11/3/14	28.64	29.413	2.70
11/4/14	26.401	26.765	1.38
11/5/14	24.914	24.902	-0.05
11/6/14	39.001	39.995	2.55
11/7/14	33.727	34.159	1.28
11/8/14	29.338	30.7	4.64
11/9/14	3.677	3.724	1.28
11/10/14	27.069	26.14	-3.43
11/11/14	39.764	41.382	4.07
11/12/14	38.565	39.148	1.51
11/13/14	38.674	39.037	0.94
11/14/14	37.484	36.689	-2.12
11/15/14	35.258	35.674	1.18
11/16/14	31.386	31.222	-0.52
11/17/14	16.831	16.987	0.93
11/18/14	7.295	8.078	10.73
11/19/14	2.573	2.687	4.43
11/20/14	16.664	14.847	-10.90
11/21/14	4.38	4.515	3.08
11/22/14	6.778	6.757	-0.31
11/23/14	26.523	24.835	-6.36
11/24/14	31.982	30.274	-5.34
11/25/14	28.687	27.105	-5.51
11/26/14	11.488	10.916	-4.98
11/27/14	41.084	40.015	-2.60
11/28/14	39.39	37.62	-4.49
11/29/14	31.118	28.623	-8.02
11/30/14	35.435	33.059	-6.71
TOTAL	817.759	815.829	-0.24

As the monitoring enters the winter months, it is expected that the non-tracker array with an inclination angle favored for lower sun angles would outperform the tracker. The data confirms this trend. The data from the first few days in December also confirm this trend. The FAU team will be closely monitoring the output of the two arrays as we approach the winter solstice on December 21/22.

Energy Produced by Tracker and Fixed systems during in December 2014

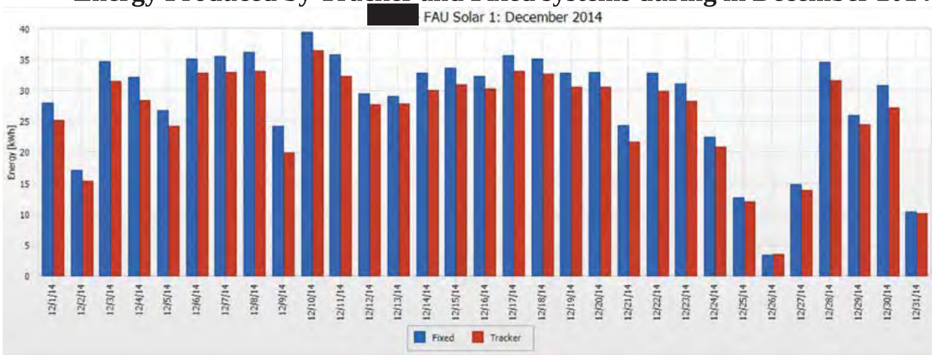

	Dec		
	Fixed	Tracker	%
12/1/14	28.021	25.212	-10.02
12/2/14	17.06	15.397	-9.75
12/3/14	34.801	31.57	-9.28
12/4/14	32.14	28.374	-11.72
12/5/14	26.751	24.177	-9.62
12/6/14	35.131	32.887	-6.39
12/7/14	35.543	33.031	-7.07
12/8/14	36.196	33.114	-8.51
12/9/14	24.272	19.968	-17.73
12/10/14	39.494	36.538	-7.48
12/11/14	35.88	32.387	-9.74
12/12/14	29.459	27.766	-5.75
12/13/14	29.119	27.85	-4.36
12/14/14	32.828	30.043	-8.48
12/15/14	33.616	31.017	-7.73
12/16/14	32.352	30.264	-6.45
12/17/14	35.699	33.092	-7.30
12/18/14	35.155	32.703	-6.97
12/19/14	32.891	30.611	-6.93
12/20/14	33.011	30.634	-7.20
12/21/14	24.324	21.643	-11.02
12/22/14	32.826	29.861	-9.03
12/23/14	31.064	28.219	-9.16
12/24/14	22.546	20.904	-7.28
12/25/14	12.632	12.035	-4.73
12/26/14	3.318	3.524	6.21
12/27/14	14.806	13.929	-5.92
12/28/14	34.662	31.628	-8.75
12/29/14	25.94	24.504	-5.54
12/30/14	30.81	27.149	-11.88
12/31/14	10.427	10.157	-2.59
TOTAL	882.774	810.188	-8.22

Energy Produced by Tracker and Fixed systems during in January 2015

	Jan		
	Fixed	Tracker	%
1/1/15	8.751	8.832	0.93
1/2/15	26.397	23.889	-9.50
1/3/15	25.174	22.815	-9.37
1/4/15	33.347	31.289	-6.17
1/5/15	28.771	27.356	-4.92
1/6/15	31.433	29.977	-4.63
1/7/15	30.74	28.61	-6.93
1/8/15	21.913	21.83	-0.38
1/9/15	25.229	23.761	-5.82
1/10/15	36.33	33.983	-6.46
1/11/15	9.514	9.649	1.42
1/12/15	23.850	23.511	-1.42
1/13/15	22.262	22.374	0.50
1/14/15	18.467	18.64	0.93
1/15/15	17.001	16.756	-1.44
1/16/15	25.277	23.887	-5.82
1/17/15	36.759	34.448	-6.71
1/18/15	35.013	33.188	-5.5
1/19/15	35.476	33.787	-5
1/20/15	7.100	7.172	1.01
1/21/15	35.362	35.821	1.28
1/22/15	32.256	32.881	1.9
1/23/15	27.713	28.482	2.7
1/24/15	9.500	10.011	5.1
1/25/15	33.924	37.37	9.22
1/26/15	29.650	30.473	2.7
1/27/15	39.860	43.378	8.11
1/28/15	40.050	43.585	8.11
1/29/15	25.988	26.352	1.38
1/30/15	37.536	38.518	2.55
1/31/15	28.924	31.96	9.5
TOTAL	839.569	834.585	-0.59

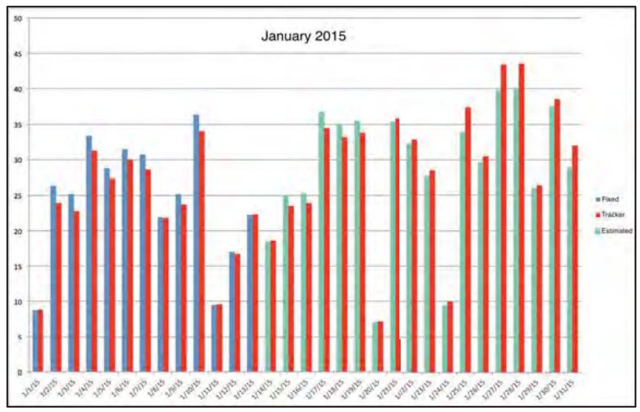

Energy Produced by Tracker and Fixed systems during in February 2015

	Feb		
	Fixed	Tracker	%
2/1/15	22.323	25.804	13.49
2/2/15	21.388	23.117	7.48
2/3/15	31.366	35.704	12.15
2/4/15	29.072	30.487	4.64
2/5/15	7.028	7.672	8.4
2/6/15	24.481	26.035	5.97
2/7/15	35.545	37.794	5.95
2/8/15	36.204	41.595	12.96
2/9/15	19.453	21.493	9.49
2/10/15	35.438	39.089	9.34
2/11/15	34.203	40.003	14.5
2/12/15	37.717	45.829	17.7
2/13/15	37.730	45.132	16.4
2/14/15	38.987	47.714	18.29
2/15/15	39.043	47.555	17.9
2/16/15	37.951	42.994	11.73
2/17/15	33.687	39.391	14.48
2/18/15	24.013	25.538	5.97
2/19/15	44.231	54.384	18.67
2/20/15	41.105	48.906	15.95
2/21/15	26.431	29.664	10.9
2/22/15	33.765	39.794	15.15
2/23/15	23.086	26.989	14.46
2/24/15	35.670	40.981	12.96
2/25/15	33.816	42.472	20.38
2/26/15	19.742	22.038	10.42
2/27/15	9.7	10.044	3.42
2/28/15	10.47	10.801	3.06
TOTAL	823.646	949.019	15.22

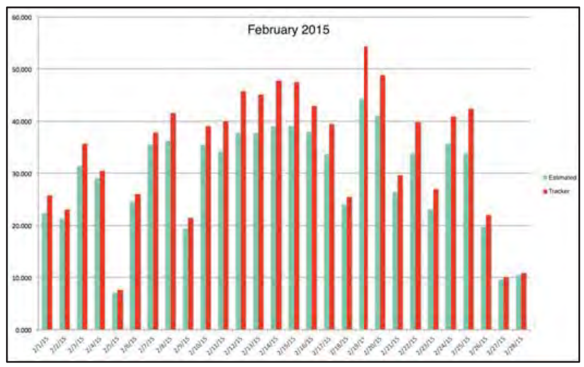

Energy Produced by Tracker and Fixed systems during in March 2015

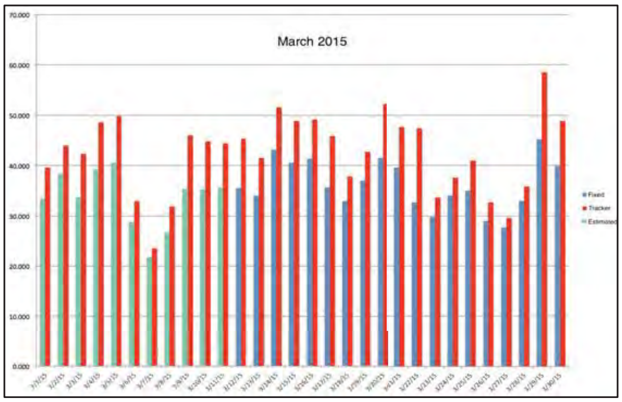

	March		
	Fixed	Tracker	%
3/1/15	33.470	39.61	15.5
3/2/15	38.296	43.928	12.82
3/3/15	33.722	42.354	20.38
3/4/15	39.282	48.562	19.11
3/5/15	40.539	49.888	18.74
3/6/15	28.796	32.913	12.51
3/7/15	21.802	23.565	7.48
3/8/15	26.691	31.809	16.09
3/9/15	35.340	45.998	23.17
3/10/15	35.260	44.86	21.4
3/11/15	35.618	44.412	19.8
3/12/15	35.512	45.31	27.59
3/13/15	34	41.531	22.15
3/14/15	43.19	51.674	19.64
3/15/15	40.613	48.943	20.51
3/16/15	41.444	49.212	18.74
3/17/15	35.692	45.833	28.41
3/18/15	32.892	37.843	15.05
3/19/15	37.028	42.774	15.52
3/20/15	41.565	52.307	25.84
3/21/15	39.558	47.682	20.54
3/22/15	32.641	47.352	45.07
3/23/15	29.85	33.639	12.69
3/24/15	34.017	37.621	10.59
3/25/15	35.046	41.009	17.01
3/26/15	29.016	32.645	12.51
3/27/15	27.692	29.477	6.45
3/28/15	32.951	35.844	8.78
3/29/15	45.243	58.532	29.37
3/30/15	39.954	48.919	22.44
TOTAL	1056.721	1276.046	20.76

- The rest of data for other mouths can be found in excel file.

Total energy production comparison by Tracker and Fixed systems from August 18th, 2014 till August 18th, 2015

Total Fixed Data energy Meter [kWh]	Total Tracker Data energy Meter [kWh]	Percentage of more power that tracker produced in comparison with the fixed
11218.488	13001.088	15.89%

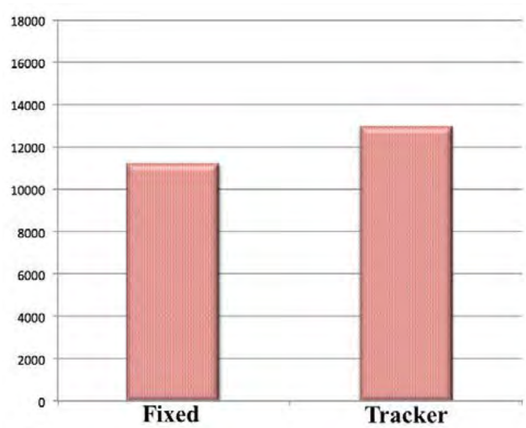

5. Analysis of Results

The table above shows the energy generated the fixed and by the tracker arrays between August 18th, 2014 and August 18th, 2015. Calculations show that tracker array has generated 15.89% more annual energy than the fixed array and tracker unit has better performance during summertime.

There are also a number of unknowns in the overall assessment:

1. What were the reasons for the deviation from North-South axis orientation for the tracker array?
2. What are the details of the inverter programming and the local interface modules? Specifically are there any limits on production from the inverters separately or in combination.
3. What is the control strategy of sun tracking?
4. What are the maintenance issues with the tracker system that caused the lock-up of the tracker system for extended periods?

The lack of communication from the tracking system designer, Mr. [redacted] both in regards to the control algorithm and access to the site, affected the FAU team's ability to be involved with some of the critical issues that should be considered in comparing tracking versus non-tracking options. Specifically, since the O&M (Operation and Maintenance) costs of tracking systems need to be carefully considered for PV installations, the details of "how" and "why" the trackers failed and the programming details that may have limited inverter outputs were critical for this study. Our team was not privy to this information.

Building a Test Bed for Hybrid Photovoltaic Solar-Thermal (PVT) Systems

FINAL REPORT

12/15/2014

Nezih Pala, PhD
Assistant Professor
Electrical & Computer Engineering
Florida International University

Lead Organization:	Florida International University
Funding Organization:	Florida Power & Light Company
Project Period:	8/1/2013 – 12/31/2014

Technical POC	
Salutation:	Dr.
Last Name:	Pala
First Name:	Nezih
Address:	EC 3914 10555 W Flagler Street
City:	Miami
Sate:	FL
Zip:	33174
Phone:	(305) 348 3016
Fax:	(305) 348 3707
E-mail:	npala@fiu.edu

Administrative POC	
Salutation:	Mr.
Last Name:	Gutierrez
First Name:	Robert
Address:	MARC 430 11200 SW 8th Street
City:	Miami
Sate:	FL
Zip:	33199
Phone:	(305) 348 2494
Fax:	(305) 348 4117
E-mail:	gutierrr@fiu.edu

Table of Content

1. Executive Summary

1.1 Goal

Photovoltaic solar cells absorb the solar radiation into semiconductor materials (e.g. Si) and converts photon energy into electrical energy. However, their efficiency decreases with increasing temperature. Typically efficiency of a solar cell decreases with 0.5% for every 1 °C (1.8 °F) above 25 °C (77 °F). That makes heat transfer and temperature control important design considerations in PV technology. Two approaches could be taken to reduce the operation temperature of the PV panels: (1) Passive cooling by natural air flow; (2) Active cooling by hybrid PV-thermal (PVT) methods.

The overarching goal of this project was to build an integrated research and knowledge transfer scheme on assessing the efficiency and feasibility of current technologies for hybrid photovoltaic thermal (PVT) systems. More particularly, it was aimed to set up a test bed to assess the efficiency of representative PVT systems available in the market using FIU solar house which was built for 2005 solar decathlon and is currently placed at FIU Engineering Center. For the completed phase of the project, the specific aim was to test the performance of cooled and uncooled panels of the [redacted] Hybrid PVT modules from [redacted] It was expected that by regulating panel temperature using a fluid cooling system, a balance can be produced, trading off between PV efficiency and thermal output. Using this principle, it is possible to obtain a higher electrical yield, coupled with enough free heat to offset a low energy building's annual water heating requirements.

1.2 Method

A test bed comprising of an 8 feet high rack which could hold 6 PVT panels, a hot water tank connected to the PVT panels, a weather station to monitor the ambient weather conditions, thermal end electrical measurement equipment and a data logger with UPS capability has been completed. The PV panels were mounted facing south at a slope angle of 26 degrees to gain the most sunlight possible. For a comparative analysis, 3 of the 6 PVT panels are connected to the hot water tank through copper pipes to remove the heat from their backpanels while the other 3 are not connected. Temperature of the water flowing in and out of the PVT panels and of the water in the tank, open circuit voltage and short circuit current of the PV panels are logged with 15 minute intervals throughout the days along with the measured solar irradiance.

1.3 Summary of the Results

The Figure 1.1 shows a sample data for the electrical power generated by the cooled and un-cooled PVTs for a period of 5 days in 9/21/2014 – 9/26/2014. From the plots we can see the water cooled panels generate more power when compared to non-water cooled ones. Sharp drops in the data represent the nature of PV's and are due to the lack of inertia associated with this type of power generation. The gaps within the data is the transitional period between days. The difference between the power generated by the cooled and uncooled PVTs is shown in Figure 1.2 for the same time period. It is clearly observed that the cooled PVTs generate on average 20% more electrical power than the un-cooled ones do. This difference reaches as high as 60% for the times when the ambient temperature is substantially high. Similar plots for other time periods are provided in the Appendices of this report.

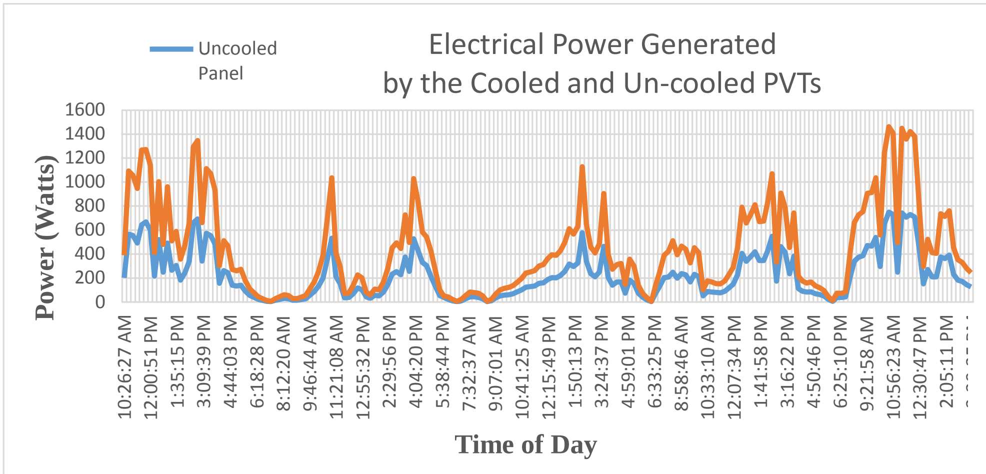

Figure 1.1: Electrical power generated by the cooled and un-cooled PVTs for a period of 5 days in 9/21/2014 – 9/26/2014.

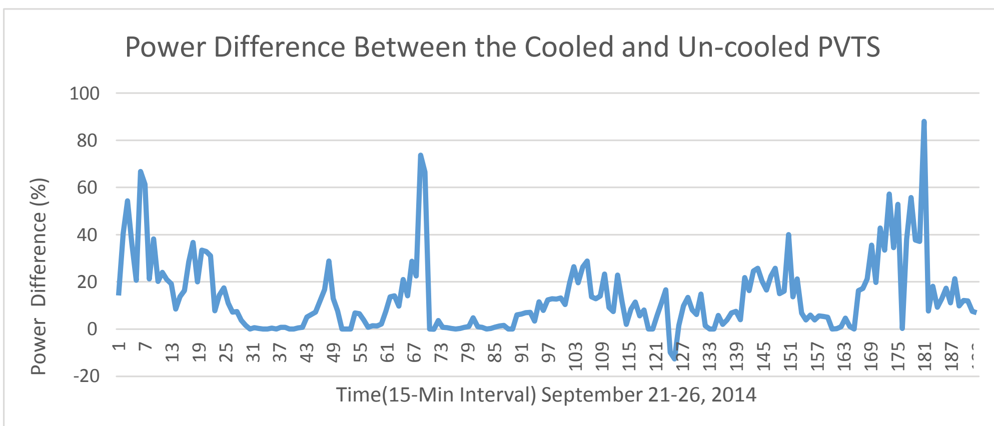

Figure 1.2: The difference between the power generated by the cooled and uncooled PVTs in the same time period for Figure 1.1.

Total energy generation of both types of panels are calculated by using the aggregate data a sample of which is shown in Figure 1.1 and the results are summarized in Table 1.1. The cooled PVTs generate about 20% more energy on average more than the uncooled PVTs. It should be noted the reported values are based on measured real data affected by actual weather conditions such as overcast and rain. And therefore lower than the maximum efficiency reported in the spec sheets of the panels.

Table 1.1: Comparison of measured electrical energy generation by single PVT panels.

	Cooled Single PVT Panel	Uncooled Single PVT Panel
Average Daily Total Energy (kWh)	0.833	0.691
Average Annual Total Energy (kWh)	304.0	252.2

1.4 Conclusions

Despite a significant delay due to the bureaucratic processes for installation permits, the project successfully achieved the main objective of building a test bed to assess the efficiency of representative PVT systems available in the market. The delays restricted the data collection only to about 4 months (September-December, 2014) rather than the initially planned 1 full year.

The test bed allowed the measurement of the electrical power generation of the [redacted] Hybrid PVT modules from [redacted]. The data observed does show great potential of the cooled PVT hybrid units with an average 20% more power generation over the uncooled ones.

The measured date indicates a sub-optimal heat removal from the cooled PVTs in the present test bed. Therefore, the thermal energy generation performance is not included in his report since we believe that any number would not reflect the true potential of the PVTs and be misleading.

We already planned an improvement in the set by replacing the water with a coolant which has higher thermal conductivity, replacing the hot water in the tank by a cold one periodically and using a lower pressure pump. Water may not be the ideal fluid for the heat absorption element as while it conduct it also does not lose the heat fast enough by the time it returns to the panels, with the same heat or minimal heat loss the entire heat removal process has minimal effect. This can be seen in the data logged where temp-out and temp in seems to have little difference. Moving forward a new system design is proposed which includes a heat exchanger within the water tank with a coolant such as propylene glycol solution with specific heat and thermal conductivity of [redacted] at the temperatures of (40-90 ^{o}C) is about 3.6 – 3.8 kJ/kg.K and 0.37 - 0.38 W/mK, respectively. This fluid will be circulated using a specialized pump that is able to handle high temperature. The solution conducts the heat from the panels at a faster rate than water does and once a certain temperature is reached the system will pump this solution to the heat exchanger in the tank which will be transferred to the water in the tank. This system will be a more efficient energy/thermal unit.

In the possible extension of this project, we plan to acquire PVT panels with a better specs form a different manufacturer and assess their performance with the improved test bed.

2. Project Description

2.1 Objective:

Photovoltaic solar cells absorb the solar radiation into semiconductor materials (e.g. Si) and converts photon energy into electrical energy. However, their efficiency decreases with increasing temperature. Typically efficiency of a solar cell decreases with 0.5% for every 1 °C (1.8 °F) above 25 °C (77 °F). That makes heat transfer and temperature control important design considerations in PV technology. Two approaches could be taken to reduce the operation temperature of the PV panels: (1) Passive cooling by natural air flow; (2) Active cooling by hybrid PV-thermal (PVT) methods.

PVT technology combines the PV cells/modules and heat extraction components into a single module and allows cooling of the PV cells leading to increased electrical efficiency and in the meantime, simultaneously utilizing the extracted heat for heating or other energy applications. The dual functions of the PVT systems result in a higher overall solar conversion rate than that of solely PV or solar collector and thus enable a more effective use of solar energy. To increase electrical efficiency of the PVs and make good use of the incident solar radiation that is not absorbed in the semiconductor materials of the cells, it is most desired to remove the accumulated heat from the PV surface and use this part of heat appropriately.

A recently renewed interest in solar technologies has spurred a spate of development of photovoltaic (PV) and solar thermal panels. Increasingly, home and business owners, encouraged by government rebate programs, are utilizing valuable roof space to generate electricity and hot water. Combining PV panels with solar thermal collectors results in a hybrid system that presents compelling advantages over standard PV panels. Homeowners no longer have to worry about attempting to accommodate two different types of collectors as the hybrid panels produce both electricity and hot water. The idea of hybridizing a solar electric panel with a solar thermal panel in not new but it has not been explored to its full possibilities. Specifically, there is no data available for their efficiency under environmental and climate conditions of Miami. Currently Florida Solar Energy Center (FSEC) tests and certifies photovoltaic and solar thermal collectors (STC) equipment, but not hybrid PVT systems. FSEC tests alone do not provide utility companies the inputs that they need for cost effectiveness testing. Establishment of a dedicated test bed specialized in PVT performance assessment at an independent research institution would further serve as a vehicle to develop new technologies by providing rapid feedback. Moreover, collaboration with FIU and FPL in renewable energy technologies would lead a strategic partnership for future joint research endeavors, grant proposal development for state and federal agencies. And last but not least, the proposed research effort will help developing solar energy work force that our nation needs and south Florida economy which has a strong potential for solar energy related technologies.

The overarching goal of this project was to build an integrated research and knowledge transfer scheme on assessing the efficiency and feasibility of current technologies for hybrid photovoltaic thermal (PVT) systems. More particularly, it was aimed to set up a test bed to assess the efficiency of representative PVT systems available in the market using FIU solar house which was built for 2005 solar decathlon and is currently placed at FIU Engineering Center. For the completed phase of the project, the specific aim was to test the performance of cooled and uncooled panels of the [redacted] Hybrid PVT modules from [redacted] It was expected that by regulating panel temperature using a fluid cooling system, a balance can be produced, trading off between PV efficiency and thermal output. Using this principle, it is possible to obtain a higher electrical yield, coupled with enough free heat to offset a low energy building's annual water heating requirements.

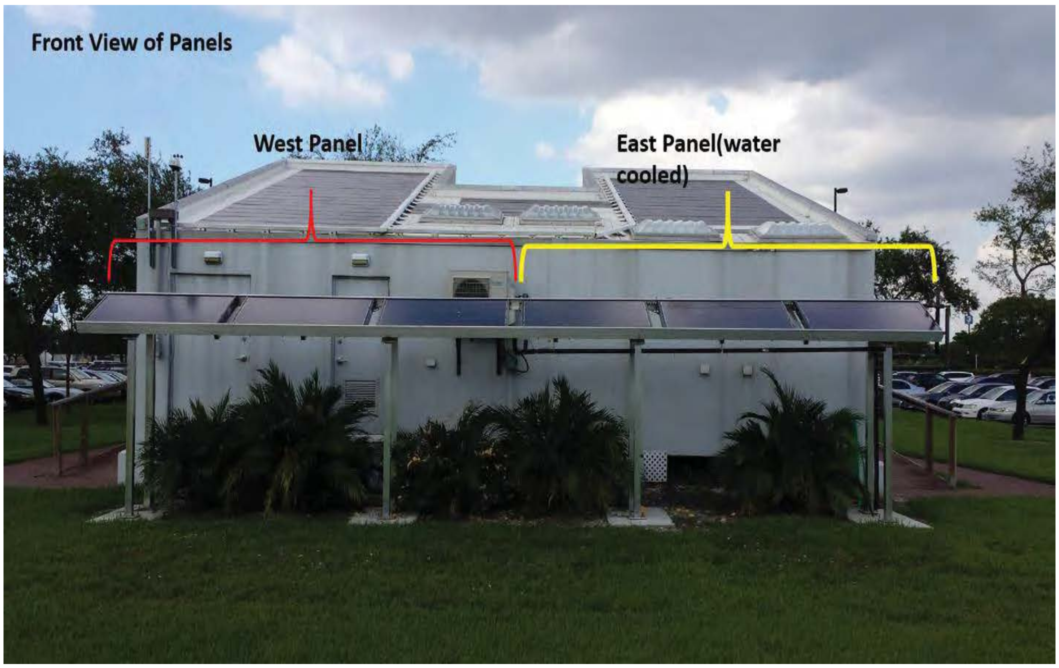

Figure 2-1: The PVT test bed installed at the south end of the FIU Solar House.

2.2 Description of PVT Test Bed

The system consist of several component that were bought with the objective in mind to collect the most accurate data possible

- Data logger
- Power Meter
- Weather Station
- Microcontroller
- Water Tank
- Water Pump
- [redacted] Laptop
- [redacted]

The Test system consists of two separate sets of panels that are connected in parallel. The panels are named East and west panels respectively, with west being the non-water cooled and East being the water cooled. Each identified set consist of three [redacted] Panels each making a total of six panels for the experiment. The PV panels were mounted facing south at a slope angle of 26 degrees to gain the most sunlight possible. Both set of panels are mounted beside each other with the exact configuration the only difference being east panels are water cooled, west panels non-cooled.

The system was designed and implemented considering the dual functionality nature of the PVT panels:

- (up to 25%) more energy generation
- Heating of domestic hot water.

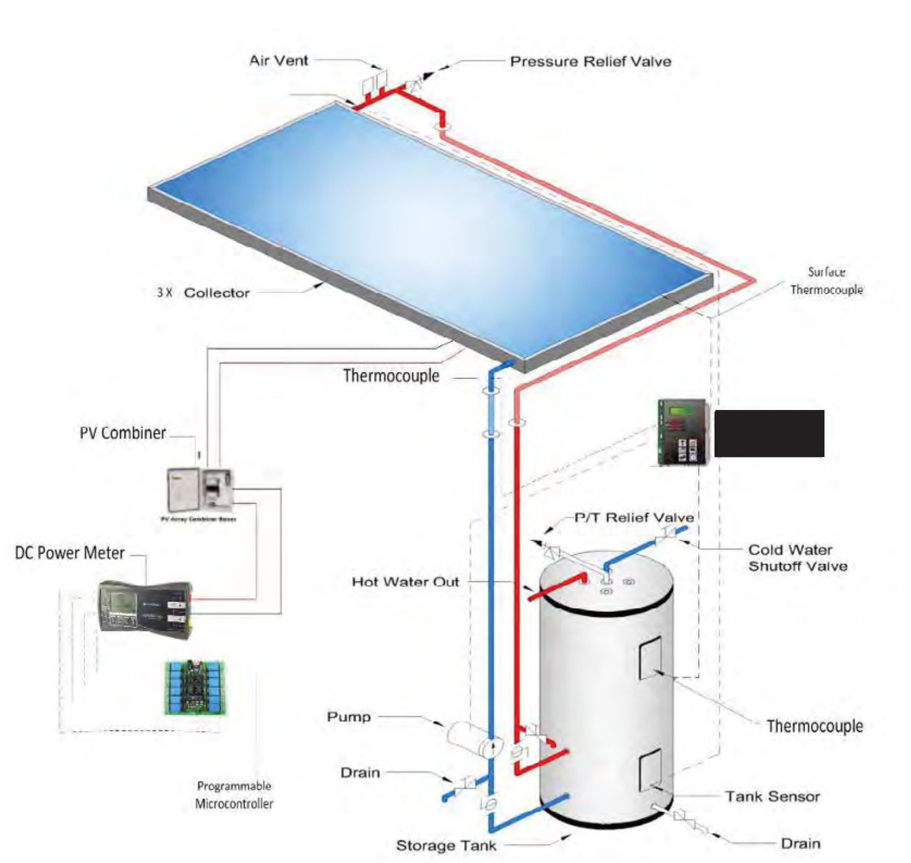

Figure 2-2: Schematic description of the PVT test bed.

2.2.1 Data logger

The data logger chosen for this project is the [redacted] includes the following features and functions.

- 8 channel high-accuracy [redacted] for a total of 15 inputs:
  - 7 inputs: 3 low resolution analog, 4 hi-speed digital,
  - 8 bi-polar differential inputs,
- 5 outputs:
  - [redacted]

There are five thermocouple inputs, 2-Surface thermocouple to acquire the temperature difference between the cooled and non-cooled panel. Three thermocouple used for the temperature of the water, 1-Water in Temp, 2-Water out temp and Tank temperature. The other input to the data logger is used for the pump Flow rate.

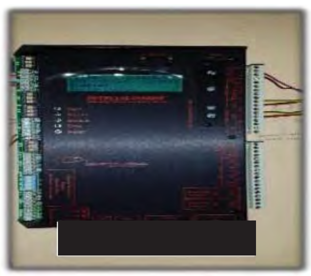

Figure 2-3: Actual data logger used int his project

2.2.2 Power Meter

[redacted] power meters are used to record the data in preset intervals of 15min to acquire data points to be analyzed. The increment in recording is controlled by a microprocessor which can be programmed at different recording intervals as required.

The meters are used to record the open circuit voltage V_{oc} and the short circuit current I_{sc}; The test instruments are for testing PV modules and strings with up to 1,000V/20A.In addition to insulation measurement, polarity testing and ground fault testing, protective conductor continuity can also be tested.

The device comes with an additional accessory [redacted] and is capable of measuring solar irradiation intensity (W/m^2) of the photovoltaic systems and Measurement of the inclination angle at photovoltaic modules. [redacted] is capable of measuring up 10,000 measurements. The PV system and the associated string are selected for measurement. The measurement is stored after successful testing every 15min interval. After having successfully completed all tests and measurements, the entire data is read and downloaded in a simple and reliable manner via the USB interface and the associated software.

Figure 2-4: DC Power Meter

2.2.3 Weather Station

The [redacted] station was chosen for its ease of installation as well as the wireless connectivity of the receiver module. The console displays and records the station's weather data, provides graph and alarm functions, and interfaces to a computer using the optional [redacted]. The wireless [redacted] station transmits outside sensor data from the [redacted] to the console via a low-power radio. Variables that are recorded include, rain fall, wind direction, out-door temp and out-door Humidity. The station is also capable of recording and storing data at set interval in our case every 15 minutes.

Figure 2-5: [redacted] Weather Station

2.2.4 Water Pump

The water pump is used to circulate the water through the east panels to reduce the PV's cell temperature. There are three different flow rates, low, medium and high. For our application it is observed that the minimum flow rate produced the best results.

2.2.5 Water Tank

The 80-gallon water tank was also chosen to produce insulation and storage of the water collected from the panels. Modifications include the addition of a thermocouple for in-tank water temperature.

2.2.6 Dell Laptop

The dell laptop is used for data acquisition for all the different modules.

2.2.7 [redacted]

The [redacted] Provides back up power for the [redacted] Power meter that requires power 24hrs to maintain recording functionalities. The UPS also ensures that the system does not have to be monitored at all times, without this, the meters would require manual power on every morning when the Solar House batteries are drained overnight. The [redacted] id capable of providing 9hrs of run time to the system without the battery backup which extends the system to 18 hrs of runtime, which enables the system to run throughout the night from 6pm to 9am.

2.2.8 Microcontroller

This is USB controlled relay module with 4 relays [redacted] and each can handle 7A at 250VAC or 10A at 125VAC. This is used for its simple ON/OFF switching for automation. The board uses the PIC chip [redacted] which is programmed via [redacted] The chip is programmed in a while loop to activate each relay in a particular sequence. The power meter did not have automation so it was necessary to add automation for successful data collection, thus the device was modified to give theses functionalities.

2.2.9 Outdoor Plumbing

The water pipes are insulated with [redacted] to ensure minimal interference from ambient temperatures as well as heat loss.

2.2.10 Electrical Connections

Figure 2.7 shows the microcontroller used to take the measurements at the set intervals along with the DC-disconnect and combiner within the test area, also the surface thermocouple mounted on the panel, one per test set.

Figure 2-6 Outdoor Plumbing

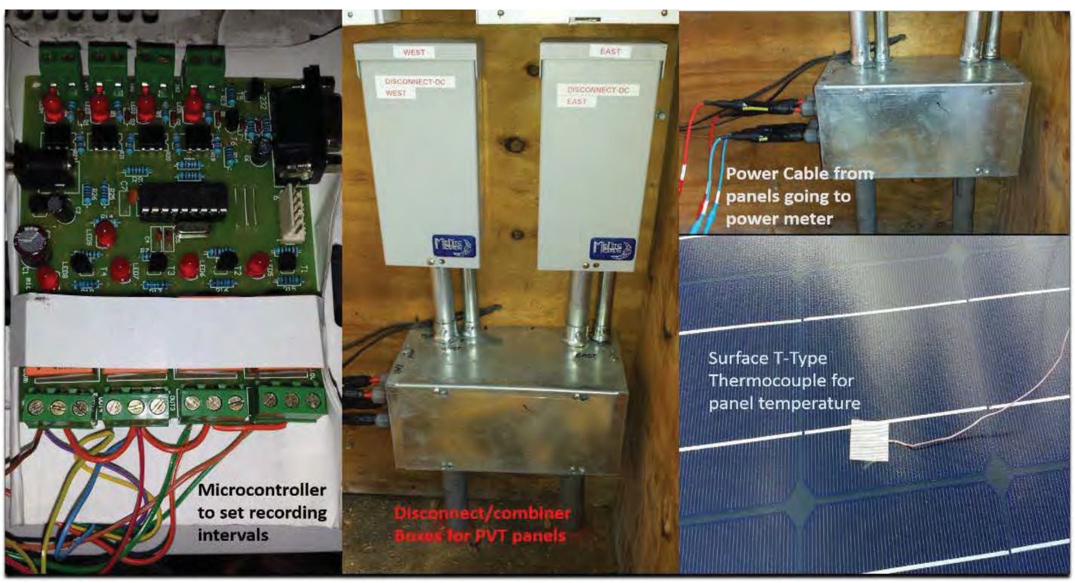

Figure 2-7 Microcontroller, DC-disconnect/Combiner, Surface thermocouple.

2.3 System Operation

The system is synchronized to take measurement every 15 minutes. Each device will record at the same time interval to ensure consistency in data when analyzed. Normal operational hours are from ~8:00am sunrise to ~7:00pm seven days a week. Data is collected once a week on Fridays via [redacted] Laptop and sorted for analysis. Thermocouple wires are routed from outside via water proof duct to the solar house. The solar house provides power during the day for all equipment.

Due to the nature of the Power meter which does not have the capability of returning to an on state when power is restored, it is necessary to have this unit powered by the UPS. The water is pumped through the system via a 1hp pump at minimum flow rate.

T-type thermocouples are placed at the inlet to the panels to measure water temperature going into the panels as well as at the outlet to measure water temperature going out the panels. Thermocouple is placed in the tank to record tank water temperature; additionally two thermocouple is placed on the surface of the panels to acquire the temperature difference of both set of panels. [redacted] weather station collects, ambient temperature, rain fall, wind speed and wind direction, this information will correlate with the power and thermal data collected to give an overall analysis of all variables affecting the system performance when analyzed.

3. Analysis

The east (water cooled) set of panels convert heat into thermal energy via heat exchangers for our application moving fluid (water). Theoretically it is expected to increase the panels energy by >25%. Moreover, the efficiency decreases with increasing temperature. A general rule of thumb is that the efficiency of a solar cell decreases with 0.5% for every 1 °C (1.8 °F) above 25 °C (77 °F). This means that on a hot summer day, in which, temperature of a solar cell could reach up to 70 °C (158 °F) the efficiency could drop as much as 25%. Thus heat transfer and temperature control was achieved by the system design of the hybrid PVT panels. The approach taken reduces the operational temperature of the PV panels by passing a cooling fluid, water, through the hybrid PV-thermal (PVT) panels.

The system implemented collected weather data as well as solar PVT energy data, where thermal energy in the form of hot water stored via a water tank. Factors taken into consideration for the test bed explored the effects of different conditions such as cloudy vs. sunny weather, wind speed, ambient conditions to both electrical conversion efficiency and heat conversion efficiency. PV conversion efficiency is estimated by the ratio of the output power of the PV panel to the available solar energy. Solar irradiance collected is also compared with the output energy generated by the panels. The non-cooled panels are evaluated based on the same operating conditions as the water cooled panels without thermal unit taken in consideration.

After the system was installed and data logging begun, we had to recalibrate the data logger as the measurements we observed to be off. Early data collected may show similarities that in theory are supposed be different or higher compare to the other. Data collected later shows better results as the system was constantly being modified to produce more reliable data. I this section we present and analyze only sample data for a limited period of time. The complete set of the collected data is included in the Appendix.

The Figure 3.1 shows a sample data for the electrical power generated by the cooled and un-cooled PVTs for a period of 5 days in 9/21/2014 – 9/26/2014. From the plots we can see the water cooled panels generate more power when compared to non-water cooled ones. Sharp drops in the data represent the nature of PV's and are due to the lack of inertia associated with this type of power generation. The gaps within the data are the transitional period between days. The difference between the power generated by the cooled and uncooled PVTs is shown in Figure 3.2 for the same time period. It is clearly observed that the cooled PVTs generate on average 20% more electrical power than the un-cooled ones do. This difference reaches as high as 60% for the times when the ambient temperature is substantially high. Similar plots for other time periods are provided in the Appendices of this report.

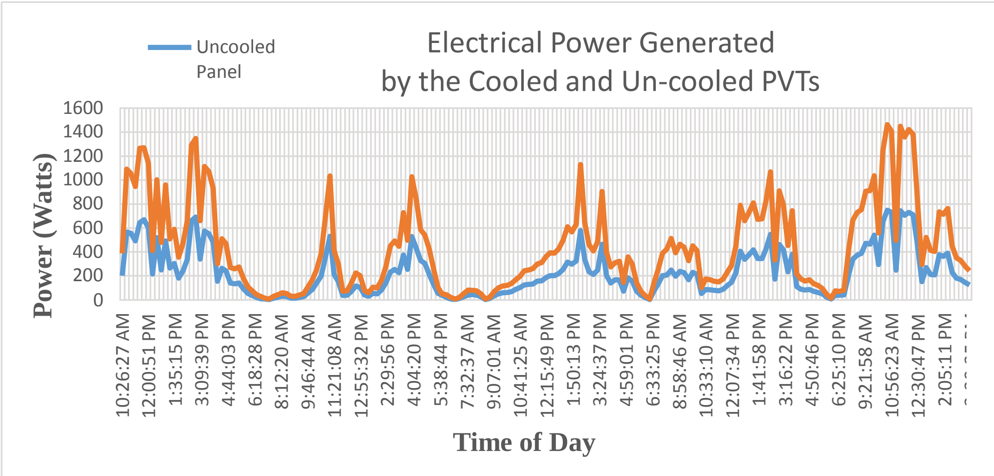

Figure 3-1: Electrical power generated by the cooled and un-cooled PVTs for a period of 5 days in 9/21/2014 – 9/26/2014.

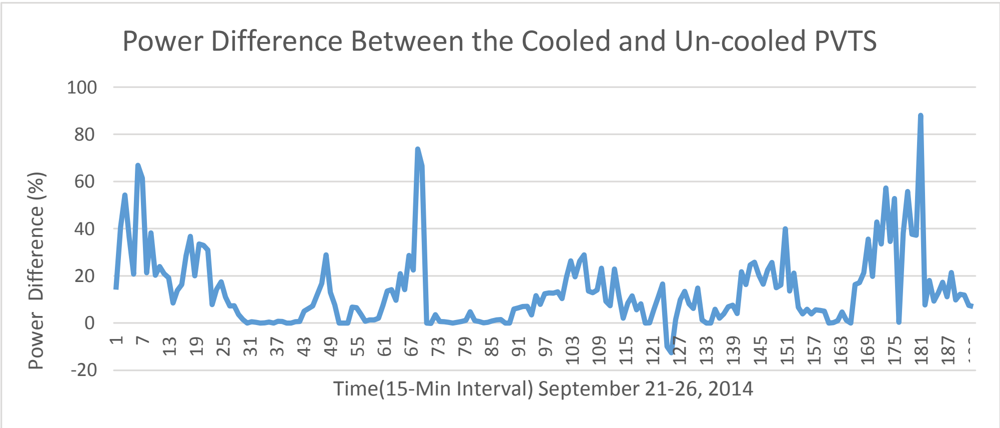

Figure 3-2: The difference between the power generated by the cooled and uncooled PVTs in the same time period for Figure 3-1.

Figure 3.3 gives an overall view of the all the temperature values recorded by the data logger for the cooled PVT panels. From this graph we can deduce that the temperature difference between the water in and out of the PVT panels is not substantial. This indicates a sub-optimal heat removal from the cooled PVTs. We already planned an improvement in the set by replacing the water with a coolant which has higher thermal conductivity and using a lower pressure pump. Temperature of the water in the tank at different levels (Tank high, low and medium) also within the same range as result of this sub-optimal hat collection. Outdoor temperature does fluctuate from day to day as observed.

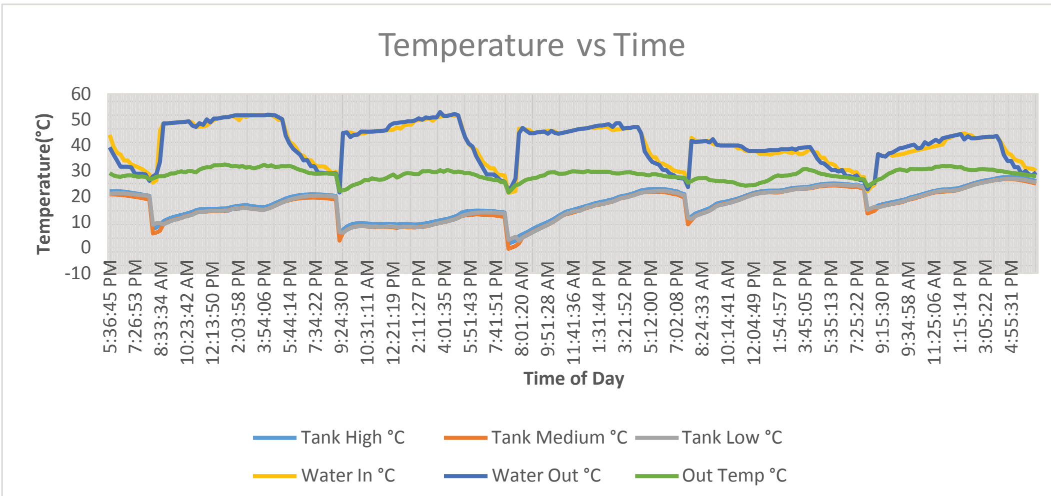

Total energy generation of both types of panels are calculated by using the aggregate data a sample of which is shown in Figure 3.1 and the results are summarized in Table 3.1. The cooled PVTs generate about 20% more energy on average more than the uncooled PVTs. It should be noted the reported values are based on measured real data affected by actual weather conditions such as overcast and rain. And therefore lower than the maximum efficiency reported in the spec sheets of the panels.

Table 3.1: Comparison of measured electrical energy generation by single PVT panels.

	Cooled Single PVT Panel	Uncooled Single PVT Panel
Average Daily Total Energy (kWh)	0.833	0.691
Average Annual Total Energy (kWh)	304.0	252.2

The thermal energy generation performance is not included in his report since we believe that the system needs to be improved in that front and any number would not reflect the true potential of the PVTs and be misleading.

We had a data loss problem due to power interruption for test equipment. The water pump running all day drained the energy from the batteries thus shutting down the data logger. This was resolved by adding a timer to the water pump circuit to operate between sunrise and sunset.

4. Conclusion:

Despite a significant delay due to the bureaucratic processes for installation permits, the project successfully achieved the main objective of building a test bed to assess the efficiency of representative PVT systems available in the market. The delays restricted the data collection only to about 4 months (September-December, 2014) rather than the initially planned 1 full year.

The test bed allowed the measurement of the electrical power generation of the [redacted] modules from [redacted] The data observed does show great potential of the cooled PVT hybrid units with an average 20% more power generation over the uncooled ones.

The measured date indicates a sub-optimal heat removal from the cooled PVTs in the present test bed. Therefore, the thermal energy generation performance is not included in his report since we believe that any number would not reflect the true potential of the PVTs and be misleading.

We already planned an improvement in the set by replacing the water with a coolant which has higher thermal conductivity, replacing the hot water in the tank by a cold one periodically and using a lower pressure pump. Water may not be the ideal fluid for the heat absorption element as while it conducts it also does not lose the heat fast enough by the time it returns to the panels, with the same heat or minimal heat loss the entire heat removal process has minimal effect. This can be seen in the data logged where temp-out and temp in seems to have little difference. Moving forward a new system design is proposed which includes a heat exchanger within the water tank with a coolant such as propylene glycol solution with specific heat and thermal conductivity of [redacted] at the temperatures of (40-90 ^{o}C) is about 3.6 – 3.8 kJ/kg.K and 0.37 - 0.38 W/mK, respectively. This fluid will be circulated using a specialized pump that is able to handle high temperature. The solution conducts the heat from the panels at a faster rate that water and once a certain temperature is reached the system will pump this solution to the heat exchanger in the tank which will be transferred to the water in the tank. This system will be a more efficient energy/thermal unit.

In the possible extension of this project, we plan to acquire PVT panels with a better specs form a different manufacturer and assess their performance with the improved test bed.

5. Appendix

5.1 Appendix 1:The code for the microcontroller

```
//PROGRAMM FOR Board
//PROCESSOR : [redacted]
//CLOCK : 20MHz, EXTERNAL

#include "[redacted]"
#include <pic.h>
#include <stdio.h>
#include "usart.h"
#include <stdlib.h>
#include "htc.h"
// CONFIG
#pragma config FOSC = HS      // Oscillator Selection bits (HS oscillator: High-speed
crystal/resonator on [redacted])
#pragma config WDTE = OFF      // Watchdog Timer Enable bit (WDT disabled)
#pragma config PWRTE = ON      // Power-up Timer Enable bit (PWRT enabled)
#pragma config MCLRE = ON      // RA5/MCLR/VPP Pin Function Select bit (RA5/MCLR/VPP pin
function is MCLR)
#pragma config BOREN = ON      // Brown-out Detect Enable bit (BOD disabled)

#define Relay1 PORTAbits.RA0    //Relay1
#define Relay2 PORTAbits.RA1    //Relay2
#define Relay3 PORTAbits.RA2    //Relay3
#define Relay4 PORTAbits.RA3    //Relay4
#define TRelay1 TRISA0  //TRISRelay1
#define TRelay2 TRISA1  //TRISRelay2
#define TRelay3 TRISA2  //TRISRela3
#define TRelay4 TRISA3  //TRISRelay4
#define _XTAL_FREQ 25000000 //setting the crystal frequency to 25MHz
//Just simple delay
void Delay(unsigned long cntr) {
while (--cntr != 0);
}
// main function
void main( void ) {

  int i=0,j=0;
  INTCON = 0x0; // Disable inerupt
    TRelay1=0; //relay1 as output
    TRelay2=0;
    TRelay3=0;
```

```
    TRelay4=0;
PORTA &= ~0xF; // Clear all relay
TRISB5=0;     // Configure Port H as output port
    PORTBbits.RB5=0;
// Init Uart Interface

    while(1)
    {
      Delay(1000000);//delay_ms(10000)
          Relay1=1;
          Delay(50000);//delay_ms(500);
          Relay1=0;
          Delay(300000);
          Relay2=1;
          Delay(50000);
          Relay2=0;
          Delay(300000);
          Relay3=1;
          Delay(50000);//0.5 sec
          Relay3=0;
          Delay(300000);
          Relay2=1;
          Delay(50000);
          Relay2=0;
          Delay(42857143);
          Relay4=1;
          Delay(50000);
          Relay4=0;
          Delay(1000000);
          Relay4=1;
          Delay(50000);
          Relay4=0;
          Delay(39285714);
```

5.2 Appendix 2: Sample Data

DATE MM/DD/YYYY	TIME HH:MM:SS	East Panel Voc	Est Pnel Isc (A)	East Panel Power	West Panel Voc	West Panel Isc (A)	West Panel Power	West Panel Energy W/m²	West Panel Temperature (°C)	West Panel Tilt Angle	Tank High °C	Tank Medium °C	Tank Low °C	Water In °C	Water Out °C	Pump Flow GPM	Out Temp °F	Wind Speed mph	Wind Dir	Heat Index °F	Rain Fa inch
03.10.2014	5:36:45 PM	36	1	**36**	35	1	**35**	0	42	26	22.0232	20.7549	21.0036	43.9923	39.13		84.2	3	SW	91	
03.10.2014	5:52:29 PM	36	0.7	**25.2**	35	0.7	**24.5**	0	41	26	22.0481	20.7549	21.1777	39.4232	36.3934		82.8	2	SW	89.3	
03.10.2014	6:08:13 PM	37	0.8	**29.6**	36	0.8	**28.8**	0	40	26	22.0232	20.6803	21.2025	37.0043	33.9745		81.9	3	W	87.8	
03.10.2014	6:23:57 PM	38	2	**76**	38	1.9	**72.2**	0	40	26	21.9735	20.6554	21.2274	36.3934	31.5555		81.8	2	W	87.9	
03.10.2014	6:39:41 PM	38	1.8	**68.4**	37	1.8	**66.6**	0	40	26	21.7994	20.4068	21.1279	33.9745	31.5555		82.4	0	S	88.8	
03.10.2014	6:55:25 PM	37	1.1	**40.7**	36	1	**36**	0	41	26	21.6502	20.2327	21.0533	33.9745	31.5555		82.7	0	SW	89.3	
03.10.2014	7:11:09 PM	35	0.4	**14**	34	0.3	**10.2**	0	40	26	21.4263	20.0089	20.9041	32.4596	31.2379		82.8	2	NNE	89.6	
03.10.2014	7:26:53 PM	4	0	**0**	3	0	**0**	0	39	26	21.2025	19.8348	20.8046	31.8487	28.7945		82.1	1	NE	88.3	
03.10.2014	7:42:37 PM	2	0	**0**	2	0	**0**	0	38	26	20.9539	19.5861	20.6803	31.2379	28.7945		81.8	1	NNE	87.6	
03.10.2014	7:58:21 PM	2	0	**0**	2	0	**0**	0	38	26	20.7052	19.3374	20.4814	30.627	28.7945		82	0	NE	88.1	
03.10.2014	8:14:05 PM	3	0	**0**	2	0	**0**	0	38	26	20.4565	19.0141	20.2824	29.6741	28.4524		81.5	1	E	87.7	0.0
03.10.2014	8:29:49 PM	3	0	**0**	2	0	**0**	0	36	26	20.2078	18.7157	20.0089	28.4769	26.027		80	1	E	85.8	0.0
04.10.2014	8:02:06 AM	39	1.9	**74.1**	38	1.8	**68.4**	0	37	26	7.29653	5.44335	8.91762	25.3058	27.7683		80.4	0	---	88	
04.10.2014	8:17:50 AM	39	2.9	**113.1**	38	2.9	**110.2**	0	38	26	7.79855	5.92568	9.46472	26.2508	28.6723		81.8	0	NE	90.9	
04.10.2014	8:33:34 AM	39	2.9	**113.1**	38	4.1	**155.8**	0	38	26	8.99223	6.53495	9.48959	45.6538	33.5347		82.2	1	NE	91.6	
04.10.2014	8:49:18 AM	38	4.1	**155.8**	38	5.2	**197.6**	0	38	26	10.2605	9.19117	9.06683	48.4136	48.4378		82.1	1	ESE	91.7	
04.10.2014	9:05:02 AM	38	6.4	**243.2**	38	6.3	**239.4**	0	39	26	11.0563	9.93722	9.76314	48.4136	48.4378		83	2	E	93.8	
04.10.2014	9:20:46 AM	37	3.6	**133.2**	36	3.5	**126**	0	39	26	11.5288	10.4097	10.3102	48.5826	48.6067		84	2	E	96.1	
04.10.2014	9:36:30 AM	39	9.9	**386.1**	38	9.6	**364.8**	0	40	26	12.0262	10.9319	10.8076	48.7274	48.7515		84.1	3	E	95.3	
04.10.2014	9:52:14 AM	38	12.7	**482.6**	37	12.4	**458.8**	233	41	26	12.3992	11.3298	11.1309	48.7274	48.7515		85.1	3	ESE	96.6	
04.10.2014	10:07:58 AM	35	1.1	**38.5**	34	1.1	**37.4**	0	40	26	12.6479	11.5537	11.5288	49.0411	49.0653		85.6	4	E	97.1	
04.10.2014	10:23:42 AM	38	12	**456**	37	11.7	**432.9**	173	41	26	13.195	12.2748	12.051	49.0411	49.0653		84.8	5	ESE	96	
04.10.2014	10:39:26 AM	36	2.5	**90**	35	2.4	**84**	0	40	26	13.4685	12.424	12.424	49.2825	49.3066		85.9	5	ESE	96.4	
04.10.2014	10:55:10 AM	36	1.4	**50.4**	35	1.3	**45.5**	0	40	26	13.9659	12.9214	12.8468	48.7515	47.5597		85.5	3	ESE	96.2	
04.10.2014	11:10:54 AM	39	14.7	**573.3**	38	14.3	**543.4**	595	41	26	14.6125	13.6177	13.5431	47.0221	47.0465		84.9	4	E	94.8	
04.10.2014	11:26:38 AM	38	15	**570**	36	14	**504**	620	41	26	14.9357	13.941	13.9659	47.2664	48.5102		86.8	3	ESE	97.5	
04.10.2014	11:42:22 AM	38	19.3	**733.4**	37	18.9	**699.3**	1277	43	26	14.9855	13.9659	13.9659	47.2664	47.9017		87.8	5	E	97	
04.10.2014	11:58:06 AM	36	5.5	**198**	34	5.3	**180.2**	0	42	26	15.0849	14.0902	14.2146	47.5841	50.0307		88.5	5	E	98.2	
04.10.2014	12:13:50 PM	38	17.1	**649.8**	36	16.7	**601.2**	1040	42	26	15.1596	14.14	14.2643	48.7998	48.8239		88.5	6	ESE	98.7	
04.10.2014	12:29:34 PM	38	18.1	**687.8**	37	17.7	**654.9**	1212	42	26	15.1347	14.14	14.3886	49.7169	50.3444		89.7	4	ESE	100.2	

04.10.2014	12:45:18 PM	38	17.6	**668.8**	37	17.2	**636.4**	1188	43	26	15.1347	14.2146	14.2394	50.3203	50.3444		89.8	6	E	99.9	
04.10.2014	1:01:02 PM	38	20.1	**763.8**	36	19.6	**705.6**	1583	45	26	15.2342	14.2892	14.2643	50.634	50.6582		89.9	7	ESE	98.1	
04.10.2014	1:16:46 PM	36	4.2	**151.2**	34	4.1	**139.4**	0	42	26	15.2093	14.2643	14.4632	50.8754	50.8995		90.4	7	ESE	100.3	
04.10.2014	1:32:30 PM	37	7.1	**262.7**	36	6.9	**248.4**	0	43	26	15.458	14.4881	14.4384	50.9478	50.9719		89.9	6	ESE	98.6	
04.10.2014	1:48:14 PM	37	13.4	**495.8**	36	13.1	**471.6**	756	41	26	15.9056	15.0601	14.9109	51.2615	51.2857		89	6	ESE	98.7	
04.10.2014	2:03:58 PM	36	4.4	**158.4**	35	4.2	**147**	0	40	26	16.1045	15.1098	15.3336	50.9719	51.5994		89.4	6	ESE	99.3	
04.10.2014	2:19:42 PM	39	10.9	**425.1**	38	10.6	**402.8**	438	42	26	16.3035	15.2839	15.1844	49.7652	51.5994		88.9	6	ESE	98	
04.10.2014	2:35:26 PM	38	16.9	**642.2**	37	16.4	**606.8**	1314	43	26	16.5522	15.5574	15.4082	51.5753	51.5994		89.3	7	ESE	99.1	
04.10.2014	2:51:10 PM	38	14.8	**562.4**	37	14.4	**532.8**	1044	42	26	16.6516	15.6818	15.5823	50.9719	51.5994		88	7	ESE	96.8	
04.10.2014	3:06:54 PM	38	15.2	**577.6**	37	14.8	**547.6**	1179	42	26	16.2786	15.1844	15.2093	51.5753	51.5994		88.7	7	E	97	
04.10.2014	3:22:38 PM	36	7.1	**255.6**	35	7.8	**273**	0	41	26	16.1045	15.0103	14.9855	51.5753	51.5994		87.7	7	ESE	96.4	
04.10.2014	3:38:22 PM	37	9.9	**366.3**	36	9.6	**345.6**	452	43	26	15.9553	15.0103	14.9606	51.5753	51.5994		88.2	8	E	97	
04.10.2014	3:54:06 PM	37	5.1	**188.7**	36	5	**180**	0	42	26	15.831	14.7865	14.7865	51.5753	51.5994		89.1	7	ESE	98	
04.10.2014	4:09:50 PM	37	6.1	**225.7**	36	6	**216**	0	43	26	15.7564	14.7368	14.6871	51.5753	51.5994		90.1	4	SE	100.1	
04.10.2014	4:25:34 PM	39	7.6	**296.4**	38	7.4	**281.2**	120	41	26	16.1543	15.2342	15.1098	51.8166	51.8408		89.1	7	ESE	98.5	
04.10.2014	4:41:18 PM	38	5.6	**212.8**	37	5.5	**203.5**	0	42	26	16.577	15.6569	15.6072	51.889	51.9132		89.8	4	ESE	98.8	
04.10.2014	4:57:02 PM	39	8.4	**327.6**	38	8.1	**307.8**	82	43	26	17.3231	16.3284	16.2786	51.0202	51.6477		88.7	7	ESE	97.9	
04.10.2014	5:12:46 PM	38	7.6	**288.8**	38	6.1	**231.8**	0	43	26	17.9199	17.0247	16.9252	49.8135	51.0443		88.8	6	ESE	98.2	
04.10.2014	5:28:30 PM	38	6.4	**243.2**	37	4.1	**151.7**	97	44	26	18.5416	17.6961	17.6215	50.1272	50.1513		89.2	8	E	99.8	
04.10.2014	5:44:14 PM	37	2.8	**103.6**	37	2.6	**96.2**	0	42	26	19.1882	18.094	18.0691	45.5561	43.748		89.1	7	ESE	98.5	
04.10.2014	5:59:58 PM	37	1.4	**51.8**	36	1.5	**54**	0	41	26	19.6358	18.467	18.5914	41.3779	40.7671		89.5	6	E	98.6	
04.10.2014	6:15:42 PM	36	0.8	**28.8**	35	0.8	**28**	0	41	26	19.984	18.8152	19.039	40.4006	38.5925		88.6	6	ESE	96.3	
04.10.2014	6:31:26 PM	35	0.4	**14**	34	0.4	**13.6**	0	40	26	20.2575	19.0887	19.3623	38.6413	37.4441		87.5	4	SE	97	
04.10.2014	6:47:10 PM	33	0.2	**6.6**	33	0.2	**6.6**	0	40	26	20.4316	19.2877	19.7104	36.2224	36.2224		86.6	3	ESE	95.5	
04.10.2014	7:02:54 PM	26	0	**0**	26	0	**0**	0	39	26	20.6554	19.412	19.9343	35.8559	34.0478		85.9	3	ESE	94.7	
04.10.2014	7:18:38 PM	7	0	**0**	6	0	**0**	0	39	26	20.7549	19.5115	20.1083	34.1211	34.1211		84.9	3	SE	93.7	
04.10.2014	7:34:22 PM	2	0	**0**	2	0	**0**	0	39	26	20.8046	19.5115	20.1829	34.1211	31.7021		84.3	2	SE	93.3	
04.10.2014	7:50:06 PM	2	0	**0**	2	0	**0**	0	39	26	20.8046	19.4618	20.2575	32.313	31.7021		83.9	2	SE	92.1	
04.10.2014	8:05:50 PM	2	0	**0**	2	0	**0**	0	39	26	20.7052	19.4618	20.2824	31.7021	29.2832		83.9	1	ESE	91.7	
04.10.2014	8:21:34 PM	2	0	**0**	2	0	**0**	0	39	26	20.7052	19.3623	20.2575	31.7021	29.2832		84.1	2	SE	92.2	

04.10.2014	8:37:18 PM	2	0	**0**	2	0	**0**	0	39	26	20.5808	19.2628	20.2327	31.5555	29.1366		84.1	1	ESE	92.2	
04.10.2014	8:53:02 PM	3	0	**0**	2	0	**0**	0	39	26	20.4316	19.1633	20.1581	30.1872	28.9655		84	2	ESE	92.3	
04.10.2014	9:08:46 PM	3	0	**0**	2	0	**0**	0	39	26	20.2824	18.9893	19.984	28.9655	28.9655		83.9	3	ESE	92.8	
04.10.2014	9:24:30 PM	3	0	**0**	2	0	**0**	0	38	26	20.1581	18.7406	19.9343	29.5764	28.9655		83.5	2	ESE	92.1	
05.10.2014	8:56:47 AM	39	2.4	**93.6**	39	2.3	**89.7**	0	32	26	5.1641	2.67628	6.02723	22.6946	21.4512		71.9	1	SE	72.7	
05.10.2014	9:12:31 AM	38	2.6	**98.8**	39	2.5	**97.5**	0	32	26	6.94112	5.77337	5.74798	44.7498	44.7742		72.3	1	SE	73.3	
05.10.2014	9:28:15 AM	39	3.9	**152.1**	39	3.8	**148.2**	0	33	26	8.22131	6.91574	6.89035	44.9208	44.9452		72.9	2	SE	73.9	
05.10.2014	9:43:59 AM	40	11	**440**	40	10.7	**428**	5	34	26	8.91762	7.64934	7.5996	44.9941	43.186		74.8	2	SE	76.2	
05.10.2014	9:59:43 AM	40	12.3	**492**	39	11.9	**464.1**	160	34	26	9.31551	8.17157	8.02236	44.5543	43.9679		76.1	3	ESE	76.7	
05.10.2014	10:15:27 AM	39	11.3	**440.7**	38	11	**418**	115	34	26	9.46472	8.32078	8.24618	44.0168	44.0412		76.8	4	SE	77.1	
05.10.2014	10:31:11 AM	39	14.4	**561.6**	37	14.1	**521.7**	517	34	26	9.53933	8.37052	8.29592	44.6276	45.2629		77.7	4	SE	78.1	
05.10.2014	10:46:55 AM	38	13	**494**	36	12.6	**453.6**	412	35	26	9.48959	8.32078	8.32078	44.6276	45.2629		79.4	3	SE	79.8	
05.10.2014	11:02:39 AM	39	15.3	**596.7**	37	15	**555**	693	37	26	9.31551	8.12184	8.27105	45.2384	45.2629		79.2	3	SE	79.5	
05.10.2014	11:18:23 AM	38	16.7	**634.6**	36	16.3	**586.8**	922	36	26	9.24091	8.12184	8.17157	45.2384	45.2629		80.6	3	SE	81.2	
05.10.2014	11:34:07 AM	38	18.2	**691.6**	36	17.7	**637.2**	1142	38	26	9.1663	7.9975	8.19644	45.2384	45.2629		80.1	4	SE	80.5	
05.10.2014	11:49:51 AM	39	16.2	**631.8**	37	15.8	**584.6**	936	36	26	9.11657	7.94776	8.02236	45.5561	45.5805		79.7	3	SE	80.6	
05.10.2014	12:05:35 PM	38	16.1	**611.8**	36	15.6	**561.6**	927	36	26	9.1663	8.0721	8.0721	45.5561	45.5805		79.9	3	SE	80.4	
05.10.2014	12:21:19 PM	38	18.6	**706.8**	36	18.1	**651.6**	1311	37	26	9.26578	8.0721	8.12184	45.8004	45.8249		80.8	3	SE	80.7	
05.10.2014	12:37:03 PM	38	18.2	**691.6**	35	17.8	**623**	1307	40	26	9.24091	8.02236	8.29592	45.8737	47.7063		82.2	3	SE	83.1	
05.10.2014	12:52:47 PM	38	10.9	**414.2**	36	10.6	**381.6**	339	37	26	9.1663	7.94776	8.19644	46.0203	48.4619		83.3	2	SE	84.7	
05.10.2014	1:08:31 PM	38	17.9	**680.2**	36	17.4	**626.4**	1323	39	26	8.96736	7.72395	7.97263	46.8022	48.6309		81.2	3	SE	81.6	
05.10.2014	1:24:15 PM	37	16.2	**599.4**	35	15.8	**553**	1141	40	26	9.1663	8.02236	7.94776	46.4357	48.8722		82.3	2	SE	83.5	
05.10.2014	1:39:59 PM	38	19.8	**752.4**	36	19.3	**694.8**	1647	40	26	9.1663	8.04723	8.14671	47.7063	48.9446		83.8	2	SE	85.1	
05.10.2014	1:55:43 PM	37	13	**481**	34	12.7	**431.8**	751	41	26	9.11657	7.92289	8.12184	48.0239	49.2584		84.3	3	SE	85.7	
05.10.2014	2:11:27 PM	37	11.4	**421.8**	35	11.1	**388.5**	511	41	26	9.11657	7.89802	8.17157	48.0239	49.2584		84	3	ESE	85.5	
05.10.2014	2:27:11 PM	36	5.9	**212.4**	34	5.8	**197.2**	0	38	26	8.99223	7.77368	7.9975	49.548	49.5721		83.6	3	SE	85.6	
05.10.2014	2:42:55 PM	37	14.8	**547.6**	35	14.5	**507.5**	1077	42	26	9.0917	7.97263	7.94776	49.8617	50.4892		83.7	3	SE	85.3	
05.10.2014	2:58:39 PM	37	9.7	**358.9**	35	9.4	**329**	300	39	26	9.26578	8.09697	8.0721	49.8617	49.8859		85.5	2	SE	86.7	

05.10.2014	3:14:23 PM	37	9.9	**366.3**	35	9.6	**336**	354	42	26	9.36525	8.22131	8.44512	50.1755	50.803		85.6	1	SE	86.1	
05.10.2014	3:30:07 PM	37	8.5	**314.5**	35	8.2	**287**	170	40	26	9.71341	8.56947	8.51973	50.4892	50.5134		85.7	1	SE	86.2	
05.10.2014	3:45:51 PM	38	13.1	**497.8**	36	12.8	**460.8**	951	41	26	10.0616	8.94249	8.96736	49.5238	50.7547		85	2	SE	85.6	
05.10.2014	4:01:35 PM	38	13	**494**	36	12.6	**453.6**	1002	44	26	10.36	9.29065	9.26578	50.803	50.8271		85	2	ESE	85.6	
05.10.2014	4:17:19 PM	38	11.3	**429.4**	36	11	**396**	795	41	26	10.6833	9.6388	9.61393	51.1167	52.951		86.3	2	SE	87	
05.10.2014	4:33:03 PM	38	10	**380**	36	9.6	**345.6**	646	45	26	10.9319	9.91235	9.93722	51.4305	51.4546		85.3	2	ESE	86	
05.10.2014	4:48:47 PM	38	8	**304**	36	7.8	**280.8**	355	41	26	11.2304	10.2108	10.161	51.4305	51.4546		86.6	2	SE	87.6	
05.10.2014	5:04:31 PM	38	8.1	**307.8**	37	7.9	**292.3**	0	41	26	11.6283	10.5838	10.5341	51.7442	51.7684		85.7	2	SE	86	
05.10.2014	5:20:15 PM	38	6	**228**	37	3.8	**140.6**	89	41	26	12.0262	11.0563	10.9817	51.4787	52.1062		84.9	2	SE	85.7	
05.10.2014	5:35:59 PM	37	2.8	**103.6**	36	1.9	**68.4**	0	41	26	12.6479	11.6283	11.5288	51.6236	51.6477		85.4	1	SE	85.7	
05.10.2014	5:51:43 PM	37	2	**74**	37	2.1	**77.7**	0	40	26	13.6177	12.2748	12.3992	47.5841	46.9977		85.1	1	SE	85.4	
05.10.2014	6:07:27 PM	38	3.4	**129.2**	38	3.3	**125.4**	0	44	26	14.0653	12.5733	12.7722	43.0638	43.0638		84.3	1	ESE	85.2	
05.10.2014	6:23:11 PM	38	1.8	**68.4**	36	0.9	**32.4**	0	42	26	14.2146	12.6976	13.0955	40.6205	40.6449		84.4	0	ESE	85.5	
05.10.2014	6:38:55 PM	35	0.4	**14**	35	0.4	**14**	0	38	26	14.3389	12.7971	13.3442	38.8124	39.4232		83.6	1	SW	84.6	
05.10.2014	6:54:39 PM	32	0.1	**3.2**	32	0.1	**3.2**	0	37	26	14.5378	12.9711	13.5929	38.2748	35.8559		83	1	SW	83.8	
05.10.2014	7:10:23 PM	19	0	**0**	18	0	**0**	0	37	26	14.4384	12.8717	13.6177	35.7581	33.3392		81.7	2	SW	82	
05.10.2014	7:26:07 PM	3	0	**0**	3	0	**0**	0	36	26	14.4135	12.8219	13.6923	33.3392	30.9202		81.1	2	SW	81.1	
05.10.2014	7:41:51 PM	2	0	**0**	2	0	**0**	0	36	26	14.3638	12.7722	13.7172	32.1175	28.5013		80.5	1	SW	80.9	
05.10.2014	7:57:35 PM	2	0	**0**	2	0	**0**	0	36	26	14.2643	12.6976	13.6923	30.9202	28.5013		80	1	SSW	80.2	
05.10.2014	8:13:19 PM	3	0	**0**	2	0	**0**	0	35	26	14.14	12.5484	13.6426	30.9202	28.5013		79.4	0	SW	79.8	
05.10.2014	8:29:03 PM	3	0	**0**	2	0	**0**	0	35	26	13.9659	12.3992	13.568	28.5013	27.2796		79.5	1	SSW	80	
05.10.2014	8:44:47 PM	3	0	**0**	2	0	**0**	0	35	26	13.8167	12.2002	13.4436	28.4036	25.9772		77.9	0	---	78.5	
05.10.2014	9:00:31 PM	3	0	**0**	2	0	**0**	0	35	26	13.6426	12.0262	13.3442	28.1837	25.7534		78.1	0	SSE	78.8	
06.10.2014	7:45:36 AM	40	1.3	**52**	39	1.2	**46.8**	0	32	26	1.53391	-0.471582	3.05707	21.4015	22.0232		70.6	0	---	72.9	
06.10.2014	8:01:20 AM	40	2	**80**	39	1.9	**74.1**	0	33	26	2.06702	0.0361372	3.59017	21.7248	24.1867		73.2	0	S	75.5	
06.10.2014	8:17:04 AM	40	3.5	**140**	39	3.8	**148.2**	0	35	26	2.62551	0.645401	4.17405	21.9735	26.8887		75.8	0	E	78.8	
06.10.2014	8:32:48 AM	39	2.6	**101.4**	38	2.6	**98.8**	0	35	26	4.50407	1.68623	2.70166	46.3868	44.6032		76.5	0	SSE	79.5	
06.10.2014	8:48:32 AM	38	3.6	**136.8**	38	3.7	**140.6**	0	37	26	5.13872	3.86942	3.84403	46.0936	46.7289		78.1	0	E	81.5	
06.10.2014	9:04:16 AM	38	4.4	**167.2**	38	4.3	**163.4**	0	38	26	5.95107	4.68177	4.631	46.0936	45.5317		79.7	0	SE	83.1	
06.10.2014	9:20:00 AM	38	3.5	**133**	38	3.5	**133**	0	38	26	6.63649	5.49412	5.39258	45.8004	44.6276		80.3	0	SSE	83.8	

06.10.2014	9:35:44 AM	38	3.6	**136.8**	38	3.5	**133**	0	39	26	7.3473	6.20493	6.10339	44.6032	44.6276		80.8	0	SE	84.8	
06.10.2014	9:51:28 AM	38	4.3	**163.4**	37	4.3	**159.1**	0	40	26	8.12184	6.94112	6.89035	44.9208	44.9452		81.2	0	SW	85	
06.10.2014	10:07:12 AM	38	4.2	**159.6**	36	4.1	**147.6**	0	41	26	8.71868	7.54987	7.47423	45.1651	45.1896		82.4	1	SSW	87.4	
06.10.2014	10:22:56 AM	39	16	**624**	38	15.6	**592.8**	711	43	26	9.36525	8.22131	8.14671	45.2384	45.2629		82.8	2	SW	87.4	
06.10.2014	10:38:40 AM	38	8.4	**319.2**	36	8	**288**	0	43	26	9.96209	8.84302	9.01709	45.5561	44.3588		84.6	3	W	90	
06.10.2014	10:54:24 AM	39	15.7	**612.3**	37	15.3	**566.1**	777	45	26	10.6584	9.58906	9.58906	45.5805	45.6049		84.8	4	SW	90.4	
06.10.2014	11:10:08 AM	38	3.9	**148.2**	36	3.8	**136.8**	0	42	26	11.4791	10.4346	10.4843	45.2873	44.7009		84.8	5	SW	90.1	
06.10.2014	11:25:52 AM	39	4.6	**179.4**	38	4.5	**171**	0	41	26	12.3992	11.3796	11.3796	44.3833	44.4077		83.8	5	SW	88.7	
06.10.2014	11:41:36 AM	40	19	**760**	39	18.8	**733.2**	1309	42	26	13.2696	12.3743	12.3494	44.7009	44.7253		83.8	5	W	88.7	
06.10.2014	11:57:20 AM	38	16.4	**623.2**	37	16	**592**	967	45	26	13.9659	13.0209	13.0706	45.0185	45.043		84	6	SW	89.2	
06.10.2014	12:13:04 PM	37	6.7	**247.9**	35	6.1	**213.5**	0	44	26	14.3638	13.369	13.568	45.3362	45.3606		85.1	6	SW	90.3	
06.10.2014	12:28:48 PM	38	16	**608**	36	17.3	**622.8**	1536	47	26	14.7865	13.7918	14.0156	45.6538	45.6783		85.6	6	SW	91.4	
06.10.2014	12:44:32 PM	37	5.4	**199.8**	34	5.3	**180.2**	0	44	26	15.0849	14.0653	14.314	45.9715	45.9959		85.4	6	SW	91.3	
06.10.2014	1:00:16 PM	38	4.6	**174.8**	36	4.5	**162**	0	43	26	15.4331	14.4632	14.4384	46.2891	46.3135		85.2	6	SW	90.9	
06.10.2014	1:16:00 PM	36	7.5	**270**	34	7.3	**248.2**	0	46	26	15.9802	15.0849	15.0352	46.3868	46.4113		84.8	4	SW	90.4	
06.10.2014	1:31:44 PM	37	4.7	**173.9**	35	4.5	**157.5**	0	44	26	16.4278	15.5326	15.7315	46.6067	46.6312		85.8	5	SW	91.8	
06.10.2014	1:47:28 PM	37	5	**185**	35	4.9	**171.5**	0	44	26	16.776	15.8559	15.8807	46.9244	46.9488		85.3	6	SW	91.1	
06.10.2014	2:03:12 PM	39	17.4	**678.6**	37	16.9	**625.3**	1386	45	26	17.2236	16.3532	16.3781	46.6556	47.2909		85.2	5	W	91.6	
06.10.2014	2:18:56 PM	39	15.5	**604.5**	37	15.1	**558.7**	1130	45	26	17.5718	16.6516	16.776	46.9732	47.6085		85.2	6	WSW	91.2	
06.10.2014	2:34:40 PM	38	6	**228**	35	5.9	**206.5**	0	43	26	17.8453	16.9501	16.9501	46.9732	47.6085		85.3	6	WSW	91.4	
06.10.2014	2:50:24 PM	39	17.4	**678.6**	37	16.9	**625.3**	1465	45	26	18.1189	17.2236	17.1987	47.2909	47.9262		85.2	6	SW	90.9	
06.10.2014	3:06:08 PM	40	15.2	**608**	39	14.8	**577.2**	1213	44	26	18.4919	17.6215	17.6464	46.8511	48.0728		85.2	6	SW	90.9	
06.10.2014	3:21:52 PM	40	15.5	**620**	39	15	**585**	1289	44	26	18.8152	17.9448	17.8951	45.8004	47.0465		84.4	6	WSW	90	
06.10.2014	3:37:36 PM	39	15	**585**	38	14.6	**554.8**	1245	45	26	19.412	18.4919	18.467	46.1181	48.5584		84.1	6	WSW	88.8	
06.10.2014	3:53:20 PM	39	12.3	**479.7**	37	12	**444**	909	46	26	19.9094	19.1136	19.039	46.1181	48.5584		84	6	W	89.2	
06.10.2014	4:09:04 PM	39	10.7	**417.3**	37	10.4	**384.8**	650	45	26	20.2078	19.3872	19.4369	46.4357	46.4601		84.7	7	SW	90.2	
06.10.2014	4:24:48 PM	38	5.6	**212.8**	36	5.3	**190.8**	0	44	26	20.4814	19.6856	19.6358	46.68	46.7045		84.9	5	WSW	90.2	
06.10.2014	4:40:32 PM	38	6	**228**	37	5.8	**214.6**	0	44	26	20.9041	20.1083	20.0586	46.7533	46.7778		84.8	6	WSW	90.1	

06.10.2014	4:56:16 PM	38	2.8	**106.4**	37	2.7	**99.9**	0	42	26	21.3269	20.556	20.4814	47.071	47.0954		84.3	5	SW	89.5	
06.10.2014	5:12:00 PM	37	1.7	**62.9**	36	1.7	**61.2**	0	41	26	21.8491	21.0036	20.9787	47.071	47.0954		83.6	6	SW	88.6	
06.10.2014	5:27:44 PM	38	2	**76**	37	2	**74**	0	40	26	22.3216	21.5258	21.4263	44.652	44.652		83.7	4	SW	88.8	
06.10.2014	5:43:28 PM	39	3.6	**140.4**	38	2.7	**102.6**	0	42	26	22.5952	21.6253	21.6004	41.1091	37.4685		83.3	4	SW	88.2	
06.10.2014	5:59:12 PM	38	2.6	**98.8**	38	3.4	**129.2**	0	42	26	22.7692	21.6502	21.7496	37.5907	35.1717		82.8	5	W	87.7	
06.10.2014	6:14:56 PM	38	2.1	**79.8**	37	2	**74**	0	42	26	22.8438	21.7496	21.9237	35.2695	33.4614		83.5	4	WSW	88.7	
06.10.2014	6:30:40 PM	36	0.6	**21.6**	35	0.6	**21**	0	39	26	22.8438	21.7745	21.9983	35.2695	32.8505		83.4	5	WSW	88.1	
06.10.2014	6:46:24 PM	35	0.3	**10.5**	34	0.2	**6.8**	0	39	26	22.8687	21.7745	22.0978	32.8505	32.2641		83.1	5	W	87.4	
06.10.2014	7:02:08 PM	27	0	**0**	26	0	**0**	0	38	26	22.8438	21.6999	22.0978	32.8505	30.4316		82.5	5	W	86.8	
06.10.2014	7:17:52 PM	7	0	**0**	6	0	**0**	0	37	26	22.6946	21.5258	21.9983	32.0198	30.1872		82	4	W	86.1	
06.10.2014	7:33:36 PM	3	0	**0**	2	0	**0**	0	37	26	22.4459	21.2523	21.7994	31.3112	28.8678		81.7	3	W	85.5	
06.10.2014	7:49:20 PM	2	0	**0**	2	0	**0**	0	37	26	22.0978	20.8792	21.4761	30.0895	28.2814		81.5	3	W	85.4	
06.10.2014	8:05:04 PM	3	0	**0**	2	0	**0**	0	37	26	21.9237	20.7052	21.3766	29.7719	27.3529		81.3	3	W	84.8	
06.10.2014	8:20:48 PM	3	0	**0**	2	0	**0**	0	37	26	21.2771	20.0835	20.7798	29.4542	27.0353		81.1	3	WSW	84.8	
06.10.2014	8:36:32 PM	3	0	**0**	2	0	**0**	0	37	26	20.8295	19.5861	20.3819	29.3076	26.8887		81	3	W	84.6	
07.10.2014	8:24:33 AM	38	1.1	**41.8**	38	1.1	**41.8**	0	36	26	10.5838	9.04196	11.4791	23.6645	23.6645		77.5	0	E	81.3	
07.10.2014	8:40:17 AM	38	2.3	**87.4**	38	2.3	**87.4**	0	37	26	12.1754	11.2055	11.1806	42.8195	41.6467		78.7	0	ENE	82.9	
07.10.2014	8:56:01 AM	38	2.7	**102.6**	38	2.6	**98.8**	0	38	26	13.2198	12.2748	12.1256	41.8666	41.2802		80.1	0	SE	84.7	
07.10.2014	9:11:45 AM	38	3.1	**117.8**	38	3	**114**	0	39	26	13.7918	12.9463	12.8219	41.329	41.3535		80.8	0	SW	85.7	
07.10.2014	9:27:29 AM	38	3.9	**148.2**	38	3.7	**140.6**	0	39	26	14.314	13.4436	13.3442	41.4023	41.4268		80.8	1	SW	85.5	
07.10.2014	9:43:13 AM	37	1.8	**66.6**	36	1.8	**64.8**	0	40	26	14.8114	13.8913	13.7669	41.6467	41.6711		81	1	SW	85.6	
07.10.2014	9:58:57 AM	38	1.7	**64.6**	37	1.7	**62.9**	0	38	26	15.3088	14.3886	14.3389	41.6467	41.0603		79.4	3	SW	82.6	
07.10.2014	10:14:41 AM	38	2.2	**83.6**	38	2.2	**83.6**	0	37	26	16.1791	15.3088	15.1596	40.4494	42.3064		79.1	3	SW	82.3	
07.10.2014	10:30:25 AM	38	2.4	**91.2**	38	2.3	**87.4**	0	38	26	17.149	16.3284	16.204	40.1807	40.1807		78.9	4	SW	82.5	
07.10.2014	10:46:09 AM	39	3.2	**124.8**	38	3.2	**121.6**	0	38	26	17.5718	16.7263	16.6019	39.863	39.863		78.7	5	SW	82.2	
07.10.2014	11:01:53 AM	39	3.8	**148.2**	38	3.7	**140.6**	0	38	26	17.7458	16.9998	16.8755	39.863	39.863		78.7	5	SW	82.1	
07.10.2014	11:17:37 AM	39	3.7	**144.3**	38	3.6	**136.8**	0	39	26	18.0691	17.2485	17.1987	39.863	39.863		78.2	5	W	81.5	
07.10.2014	11:33:21 AM	39	3.1	**120.9**	38	3	**114**	0	38	26	18.3676	17.6712	17.5718	39.863	39.863		78.1	3	W	81.4	
07.10.2014	11:49:05 AM	38	1.6	**60.8**	37	1.6	**59.2**	0	38	26	18.7654	18.0691	17.9945	39.863	39.863		77.6	4	W	81	

07.10.2014	12:04:49 PM	38	1.3	**49.4**	38	1.3	**49.4**	0	36	26	19.2131	18.5416	18.4173	38.6413	39.863		76.5	4	W	80	
07.10.2014	12:20:33 PM	39	2.4	**93.6**	39	2.4	**93.6**	0	35	26	19.6856	19.0639	18.9147	38.7879	39.3988		76	3	W	79.4	
07.10.2014	12:36:17 PM	40	4.3	**172**	40	4.3	**172**	0	36	26	20.2078	19.6358	19.5115	37.7373	38.3726		75.4	3	W	78.8	
07.10.2014	12:52:01 PM	39	2.1	**81.9**	39	2.1	**81.9**	0	36	26	20.7052	20.1332	20.0337	37.7373	37.7617		75.7	3	NW	79	0.
07.10.2014	1:07:45 PM	39	3.2	**124.8**	39	3.1	**120.9**	0	36	26	21.2025	20.6306	20.5311	37.7373	37.7617		75.9	2	WNW	79.2	
07.10.2014	1:23:29 PM	39	3.9	**152.1**	39	3.8	**148.2**	0	37	26	21.6253	20.9787	20.9787	37.7373	37.7617		76.2	2	WNW	79.5	
07.10.2014	1:39:13 PM	38	2.3	**87.4**	37	2.3	**85.1**	0	37	26	21.8491	21.2523	21.2025	36.54	37.7617		77.3	1	NE	80.9	
07.10.2014	1:54:57 PM	39	3.6	**140.4**	38	3.5	**133**	0	39	26	21.9983	21.4015	21.3517	36.54	37.7617		77.9	0	ENE	81.7	
07.10.2014	2:10:41 PM	39	6.4	**249.6**	38	6.3	**239.4**	0	41	26	22.1475	21.5258	21.4761	36.6133	37.835		78.8	0	N	82.7	
07.10.2014	2:26:25 PM	39	6.9	**269.1**	38	6.7	**254.6**	0	43	26	22.2221	21.6004	21.6253	36.2468	38.0793		80	1	NW	84.5	
07.10.2014	2:42:09 PM	38	5.3	**201.4**	36	5.2	**187.2**	0	45	26	22.2719	21.5258	21.675	36.8577	38.0793		81.7	1	WNW	87.1	
07.10.2014	2:57:53 PM	39	3.8	**148.2**	37	3.7	**136.9**	0	42	26	22.247	21.501	21.7248	36.8577	38.0793		82.7	3	WSW	87.2	
07.10.2014	3:13:37 PM	39	3.3	**128.7**	37	3.3	**122.1**	0	41	26	22.3216	21.6253	21.675	37.1753	38.397		82.3	2	W	87.5	
07.10.2014	3:29:21 PM	38	3.1	**117.8**	37	3.1	**114.7**	0	41	26	22.5703	21.9735	21.9735	37.7617	38.397		82.6	2	W	87.3	
07.10.2014	3:45:05 PM	39	3.6	**140.4**	38	3.5	**133**	0	41	26	22.8438	22.247	22.2221	37.1753	38.397		82.7	1	W	86.9	
07.10.2014	4:00:49 PM	39	4.3	**167.7**	38	4.2	**159.6**	0	42	26	23.1671	22.5206	22.5206	36.8821	38.7146		83.3	0	SSW	88.2	
07.10.2014	4:16:33 PM	39	8	**312**	38	7.7	**292.6**	130	41	26	23.3412	22.7692	22.7444	37.4929	38.1038		83.6	0	SSW	88.3	
07.10.2014	4:32:17 PM	39	8.8	**343.2**	37	8.5	**314.5**	338	43	26	23.5153	22.9433	22.9433	36.4423	38.8857		85.1	0	W	92.1	
07.10.2014	4:48:01 PM	38	4.9	**186.2**	36	4.8	**172.8**	0	45	26	23.6148	22.9433	23.1174	36.5889	39.0323		86.9	0	SE	95	
07.10.2014	5:03:45 PM	38	3.7	**140.6**	36	3.6	**129.6**	0	43	26	23.6645	22.9433	23.1423	37.2975	39.13		87.3	0	ESE	94.8	
07.10.2014	5:19:29 PM	38	2.6	**98.8**	36	2.5	**90**	0	41	26	23.764	23.0925	23.192	38.7146	39.3499		86.4	1	ESE	93.5	
07.10.2014	5:35:13 PM	37	1.5	**55.5**	36	1.5	**54**	0	41	26	24.137	23.4158	23.565	37.2242	37.2242		86	0	SSE	93	
07.10.2014	5:50:57 PM	37	1.2	**44.4**	36	1.2	**43.2**	0	40	26	24.4354	23.764	23.9629	37.2242	34.8052		84.9	0	SSE	90.9	
07.10.2014	6:06:42 PM	37	1	**37**	36	0.9	**32.4**	0	40	26	24.709	23.9629	24.1867	35.0251	33.217		83.8	0	S	89.4	
07.10.2014	6:22:25 PM	36	0.6	**21.6**	35	0.6	**21**	0	39	26	24.8582	24.0873	24.3857	35.1229	32.7039		83.4	0	SW	89.1	
07.10.2014	6:38:09 PM	34	0.2	**6.8**	34	0.2	**6.8**	0	38	26	24.9576	24.1619	24.4851	32.7039	31.4822		82.8	0	SSW	88	
07.10.2014	6:53:53 PM	30	0	**0**	30	0	**0**	0	38	26	25.0074	24.2116	24.5597	32.7039	30.285		82.5	0	S	87.4	
07.10.2014	7:09:38 PM	12	0	**0**	11	0	**0**	0	38	26	24.9825	24.2116	24.5846	32.0931	30.285		82.1	0	SSE	86.3	
07.10.2014	7:25:22 PM	3	0	**0**	2	0	**0**	0	37	26	24.9576	24.137	24.51	30.285	29.6986		81.8	0	---	86.2	

07.10.2014	7:41:06 PM	3	0	**0**	2	0	**0**	0	37	26	24.8333	24.0873	24.4603	30.285	30.285		81.7	0	SSW	86.2	
07.10.2014	7:56:50 PM	2	0	**0**	2	0	**0**	0	37	26	24.7836	23.9629	24.4105	30.285	27.866		81.3	0	S	85.8	
07.10.2014	8:12:34 PM	2	0	**0**	2	0	**0**	0	36	26	24.6344	23.8386	24.3111	30.285	27.866		81	0	SSW	85.4	
07.10.2014	8:28:18 PM	3	0	**0**	2	0	**0**	0	36	26	24.4851	23.6645	24.137	29.3565	27.524		80.6	0	SSW	84.5	
07.10.2014	8:44:02 PM	3	0	**0**	2	0	**0**	0	36	26	24.6095	23.8634	24.3359	29.4054	28.1837		80.1	0	SSE	84	
07.10.2014	8:59:46 PM	3	0	**0**	2	0	**0**	0	36	26	24.1619	23.3163	23.8137	27.524	26.3005		80.2	0	S	84.3	
07.10.2014	9:15:30 PM	3	0	**0**	2	0	**0**	0	36	26	23.9132	23.0428	23.5899	27.524	26.3005		79.8	0	SSW	83.8	
08.10.2014	8:00:34 AM	39	1.7	**66.3**	38	1.6	**60.8**	0	34	26	14.5627	13.2944	14.7119	22.0481	22.6698		75.2	0	---	79	
08.10.2014	8:16:18 AM	39	1.6	**62.4**	38	1.6	**60.8**	0	35	26	15.0352	13.8415	15.3585	23.6148	24.8333		76.4	0	SE	80.4	
08.10.2014	8:32:02 AM	39	3.2	**124.8**	39	3.3	**128.7**	0	37	26	15.632	14.3886	15.8807	24.5597	25.1566		78.3	0	SE	83.4	
08.10.2014	8:47:46 AM	39	3.3	**128.7**	38	3.4	**129.2**	0	38	26	16.4278	15.632	15.6072	36.4179	36.4423		79.7	0	SSE	85.5	
08.10.2014	9:03:30 AM	39	4.9	**191.1**	39	4.8	**187.2**	0	38	26	16.8257	16.1543	16.0797	35.807	35.8314		80.7	0	ESE	86.9	
08.10.2014	9:19:14 AM	39	5.9	**230.1**	38	5.8	**220.4**	0	39	26	17.1987	16.5024	16.4278	35.5138	35.5382		82.3	0	SE	90.3	
08.10.2014	9:34:58 AM	39	6	**234**	38	5.9	**224.2**	0	40	26	17.4474	16.6765	16.7511	36.7355	36.7599		84	0	SE	94.1	
08.10.2014	9:50:42 AM	39	7.7	**300.3**	37	7.6	**281.2**	0	43	26	17.6712	17.0495	16.9501	35.8314	37.0776		85	0	E	94.6	
08.10.2014	10:06:26 AM	39	8.5	**331.5**	37	7.8	**288.6**	0	44	26	17.9697	17.2982	17.4226	36.1491	37.9816		86.3	0	S	97.1	
08.10.2014	10:22:10 AM	39	8.8	**343.2**	37	8.6	**318.2**	0	45	26	18.3924	17.5966	17.6712	36.3934	38.8368		86.9	1	SW	96.9	
08.10.2014	10:37:54 AM	38	4	**152**	36	4	**144**	0	44	26	18.6411	17.8951	18.1189	36.54	38.9834		86.6	1	SSW	97	
08.10.2014	10:53:38 AM	39	12.2	**475.8**	37	11.9	**440.3**	341	45	26	19.0887	18.3676	18.467	37.0287	39.4721		85.8	1	SW	94.1	
08.10.2014	11:09:22 AM	39	9.8	**382.2**	37	9.5	**351.5**	48	45	26	19.5861	18.8401	19.0141	37.4196	39.863		87.3	1	WSW	97.6	
08.10.2014	11:25:06 AM	38	6.2	**235.6**	36	6.1	**219.6**	0	45	26	19.8596	19.1136	19.3374	37.7373	40.1807		87.4	2	SW	95.3	
08.10.2014	11:40:50 AM	39	8.6	**335.4**	37	8.3	**307.1**	0	45	26	20.357	19.5612	19.7602	38.0549	38.6902		86.9	2	SW	95.4	
08.10.2014	11:56:34 AM	39	8.3	**323.7**	37	8.1	**299.7**	0	46	26	20.7052	20.0586	20.1332	38.3726	39.0078		87.1	2	SW	94.9	
08.10.2014	12:12:18 PM	39	11	**429**	37	10.8	**399.6**	334	47	26	21.1031	20.4814	20.6057	38.6902	41.1336		87.2	3	W	94.3	
08.10.2014	12:28:02 PM	39	8.3	**323.7**	37	8.1	**299.7**	0	46	26	21.501	20.8792	20.9539	39.0078	40.254		87.5	3	SW	94.6	
08.10.2014	12:43:46 PM	38	14.6	**554.8**	36	14.3	**514.8**	839	48	26	21.8988	21.2025	21.3517	39.3255	41.158		87.3	3	W	94	
08.10.2014	12:59:30 PM	38	9.1	**345.8**	36	8.9	**320.4**	118	47	26	22.2719	21.5756	21.7248	39.6431	42.0865		88.9	2	SW	95.9	
08.10.2014	1:15:14 PM	38	11.4	**433.2**	35	11.3	**395.5**	288	48	26	22.4708	21.7496	21.9983	39.9852	41.2313		88.9	2	WSW	95.5	

08.10.2014	1:30:58 PM	37	6.8	**251.6**	34	6.7	**227.8**	0	50	26	22.62	21.8242	22.1475	40.3028	42.7462		89.5	2	SW	97.3	
08.10.2014	1:46:42 PM	38	13.7	**520.6**	36	13.4	**482.4**	818	48	26	22.6946	21.8988	22.247	42.453	43.0638		89	4	SW	96.9	
08.10.2014	2:02:26 PM	38	8.8	**334.4**	35	8.5	**297.5**	123	50	26	22.7692	21.9983	22.1475	42.7706	43.3815		89.4	3	SW	97	
08.10.2014	2:18:10 PM	38	5.2	**197.6**	36	5.1	**183.6**	0	47	26	22.9433	22.1724	22.3713	43.6991	43.6991		88.9	3	SW	95.9	
08.10.2014	2:33:55 PM	38	6.9	**262.2**	36	6.7	**241.2**	0	48	26	23.0925	22.3465	22.4708	44.0168	44.0168		88.4	2	SW	95.9	
08.10.2014	2:49:39 PM	39	6.5	**253.5**	37	6.3	**233.1**	0	45	26	23.5402	22.819	22.819	44.3344	44.3344		88.6	2	SW	96	
08.10.2014	3:05:22 PM	38	3.7	**140.6**	37	3.6	**133.2**	0	44	26	23.938	23.2666	23.3412	44.5787	42.1598		87.4	3	W	95.3	
08.10.2014	3:21:07 PM	39	5.8	**226.2**	38	5.6	**212.8**	0	43	26	24.3608	23.7142	23.6645	44.0412	43.4548		86.7	4	W	95.3	
08.10.2014	3:36:51 PM	39	6.4	**249.6**	37	6.2	**229.4**	0	45	26	24.8333	24.2116	24.1619	43.7724	42.5752		86.5	3	SW	95.6	
08.10.2014	3:52:34 PM	39	7.7	**300.3**	38	7.5	**285**	48	44	26	25.3307	24.709	24.6344	42.5507	42.5752		86.6	4	SW	95.5	
08.10.2014	4:08:19 PM	38	4.9	**186.2**	37	4.7	**173.9**	0	45	26	25.6291	25.0322	24.9825	42.8684	42.8928		86.9	3	SW	95.4	
08.10.2014	4:24:03 PM	39	6.1	**237.9**	37	5.9	**218.3**	0	44	26	25.9524	25.3307	25.3555	42.8684	42.8928		87.2	4	SW	95.4	
08.10.2014	4:39:47 PM	38	3.9	**148.2**	37	3.8	**140.6**	0	45	26	26.2259	25.654	25.5545	43.186	43.2104		87	3	SW	95.2	
08.10.2014	4:55:31 PM	38	3.8	**144.4**	37	3.7	**136.9**	0	43	26	26.4977	25.9524	25.9275	43.186	43.2104		86.8	4	SW	94	
08.10.2014	5:11:15 PM	39	4.2	**163.8**	38	3.9	**148.2**	0	42	26	26.7421	26.1762	26.1513	43.2593	43.2837		86.8	3	SW	94.8	
08.10.2014	5:26:59 PM	39	4.1	**159.9**	37	3.4	**125.8**	0	42	26	26.9864	26.4244	26.4244	43.5036	43.5281		85.9	4	SW	93.2	
08.10.2014	5:42:43 PM	38	2.8	**106.4**	37	2.5	**92.5**	0	42	26	27.2796	26.5955	26.571	41.6955	41.0847		85.9	3	SW	93.5	
08.10.2014	5:58:27 PM	38	2.1	**79.8**	37	2.1	**77.7**	0	41	26	27.4507	26.6688	26.6932	39.2522	36.2224		85.4	4	SW	93.1	
08.10.2014	6:14:11 PM	37	1	**37**	36	1	**36**	0	40	26	27.5484	26.7421	26.8398	36.8332	33.8034		84.8	4	SW	92.1	
08.10.2014	6:29:55 PM	36	0.7	**25.2**	36	0.6	**21.6**	0	39	26	27.524	26.6688	26.8642	36.2224	33.8034		84.5	4	SW	91.6	
08.10.2014	6:45:39 PM	35	0.3	**10.5**	34	0.3	**10.2**	0	39	26	27.4262	26.6199	26.8398	34.4143	31.3845		84.2	3	SW	91.3	
08.10.2014	7:01:23 PM	29	0	**0**	29	0	**0**	0	39	26	27.3774	26.4489	26.7421	33.8034	31.3845		83.8	3	SW	91.5	
08.10.2014	7:17:07 PM	7	0	**0**	6	0	**0**	0	38	26	27.1574	26.2259	26.571	33.4858	28.6479		83.6	3	SW	91.3	
08.10.2014	7:32:51 PM	3	0	**0**	2	0	**0**	0	38	26	26.9375	26.0021	26.3751	31.0669	29.8452		83.1	4	SW	89.7	
08.10.2014	7:48:35 PM	2	0	**0**	2	0	**0**	0	38	26	26.6199	25.654	26.0767	30.8958	28.4769		82.8	4	SW	89.3	
08.10.2014	8:04:19 PM	2	0	**0**	2	0	**0**	0	38	26	26.3254	25.3307	25.7783	30.7492	28.3303		82.5	3	SW	89.1	
08.10.2014	8:20:03 PM	3	0	**0**	2	0	**0**	0	38	26	25.9524	24.9825	25.4799	29.9673	29.3565		82.4	3	SW	88.8	

Figure 5-1 Sample Data collected.

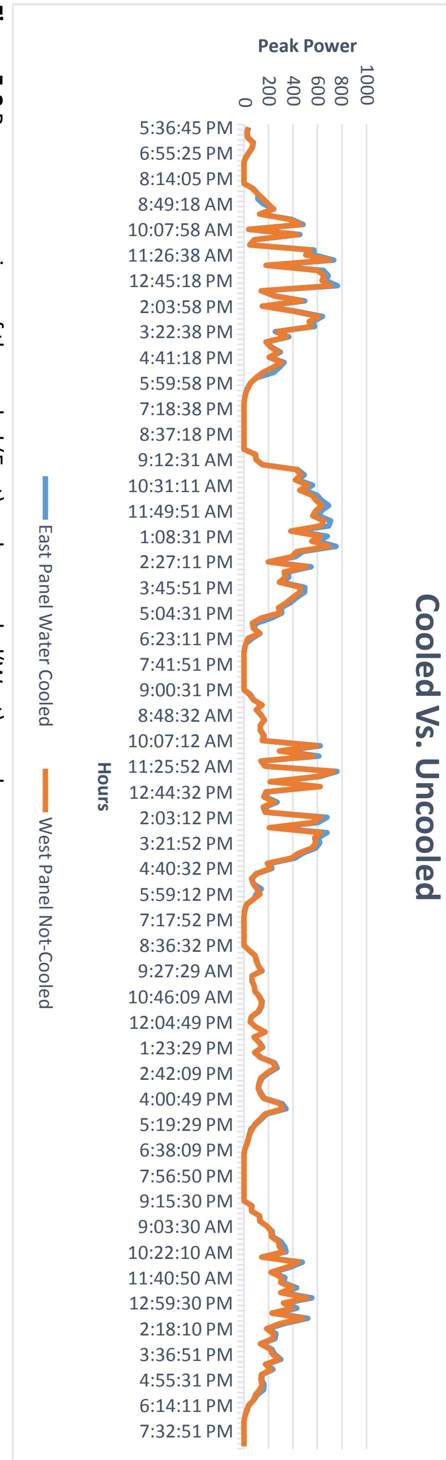

Figure 5-2 Power comparison of the cooled (East) and un-cooled(West) panels.

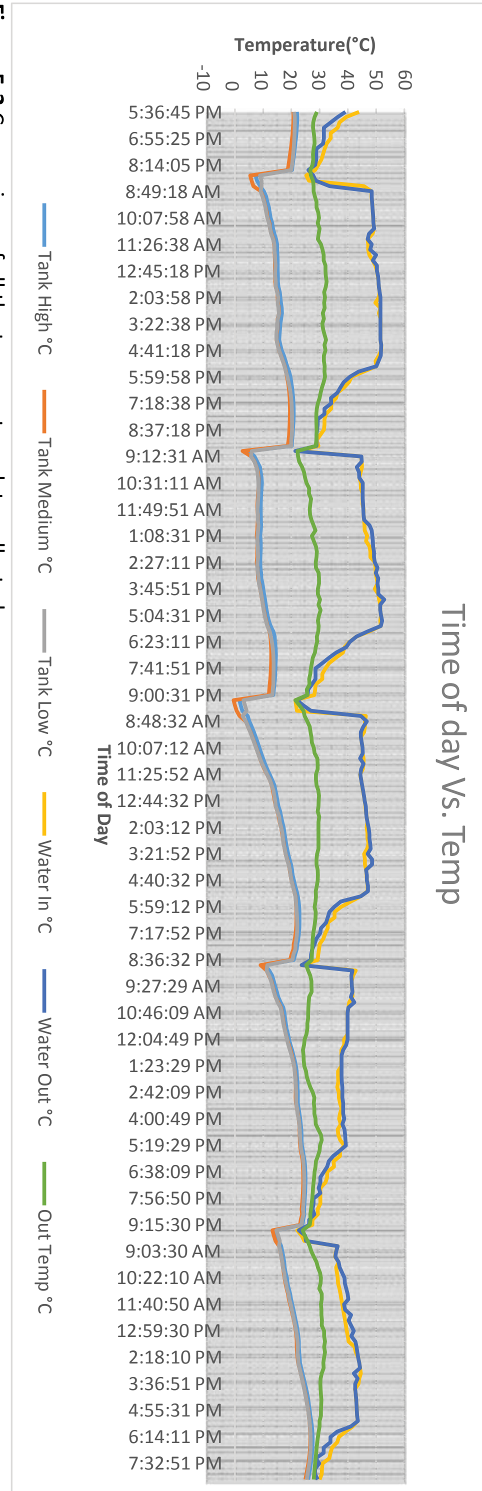

Figure 5-3 Comparison of all the temperature data collected

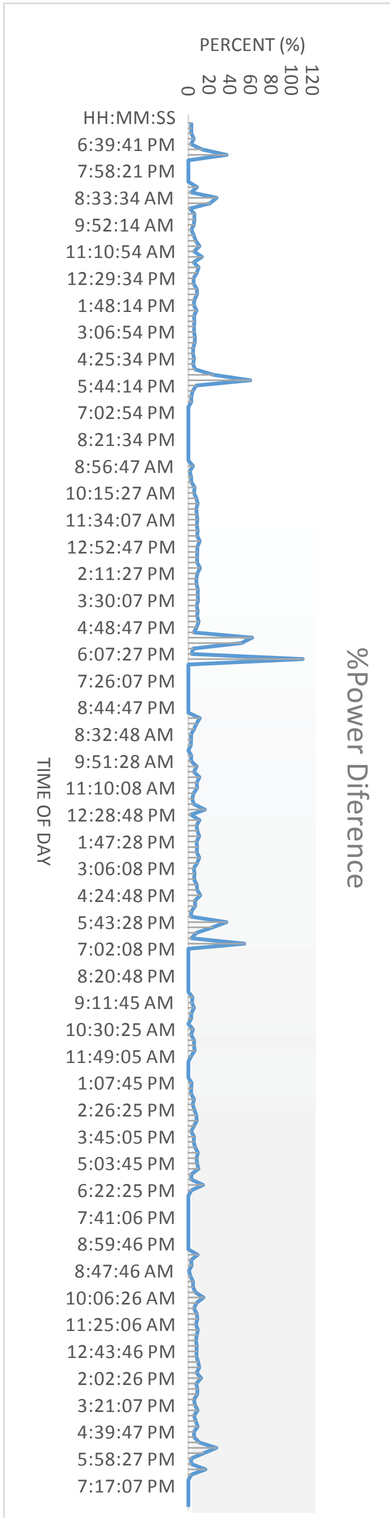

Figure 5-4 Power Difference

5.3 Appendix 3: Data Plots for September 2014

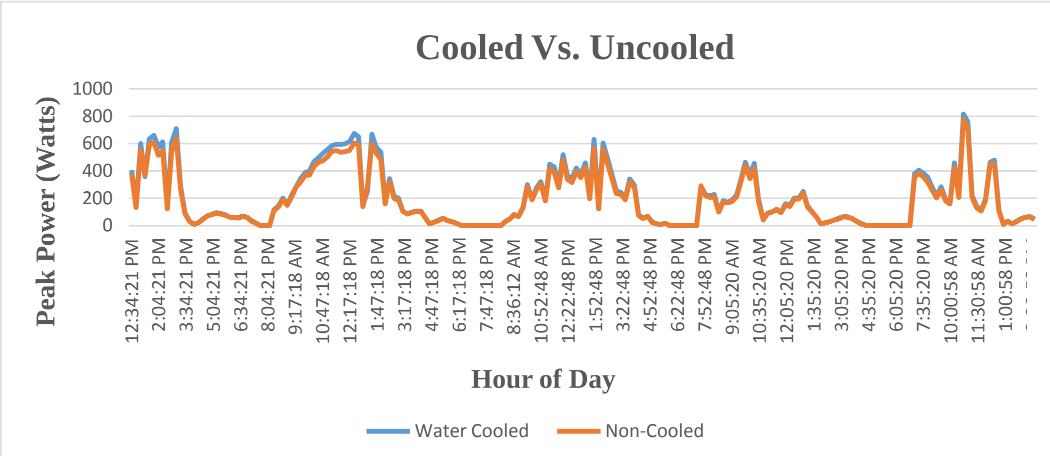

Figure 5-5 Sep-16th-20th

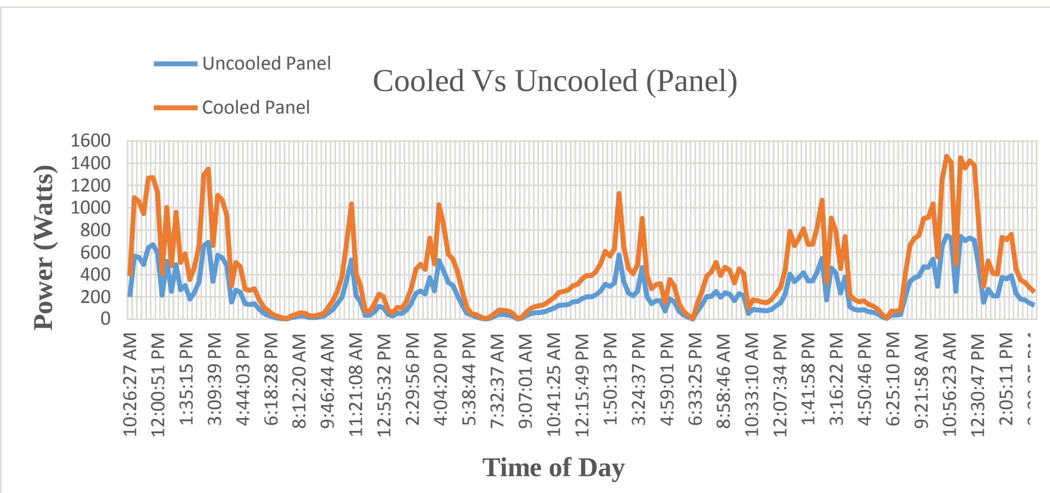

Figure 5-6 Sep-22nd -26th Power

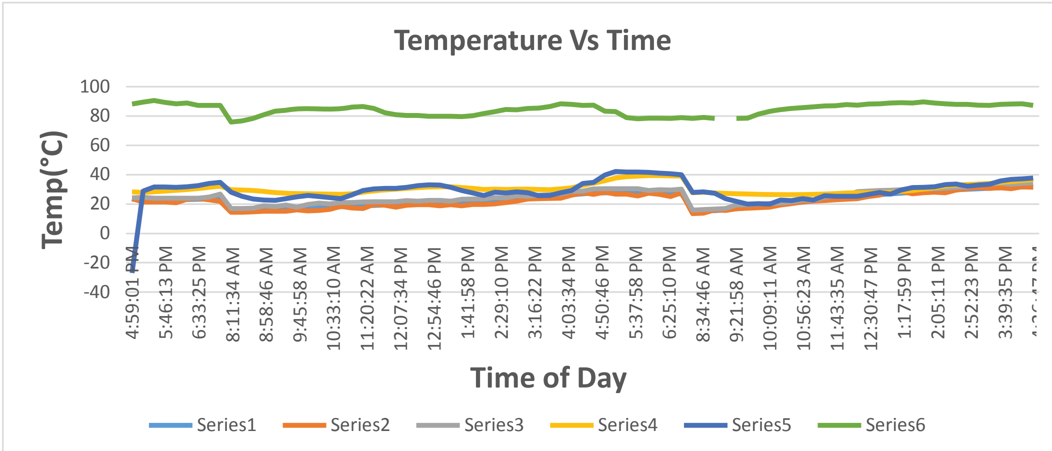

Figure 5-7 Sep-22nd – 26th Temperature

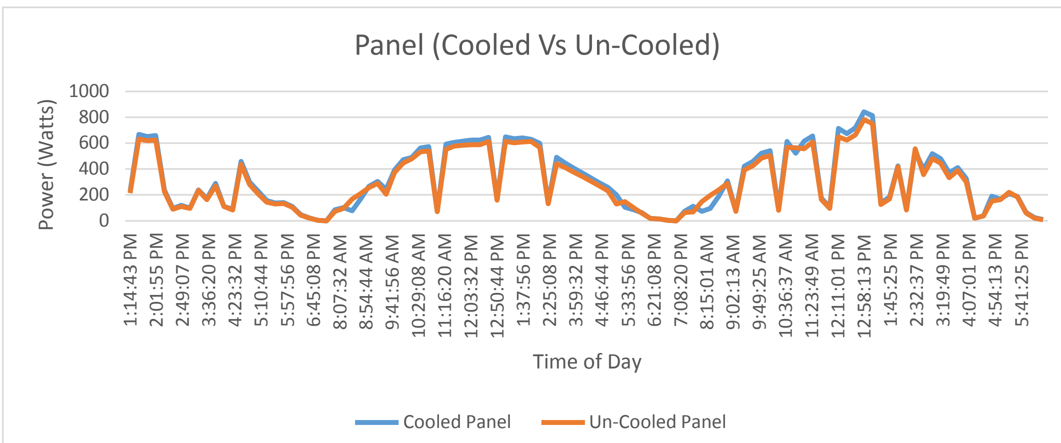

Figure 5-8 Sep-29th -3rd Oct Power

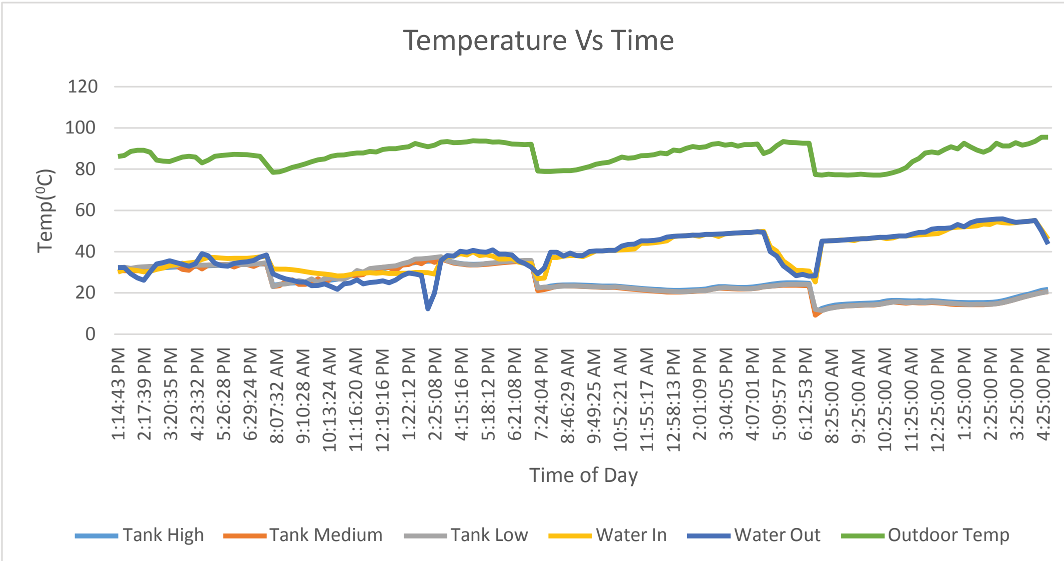

Figure 5-9 Sep-29th -3rd Oct Temperature

5.4 Appendix 4: Data plots for October 2014

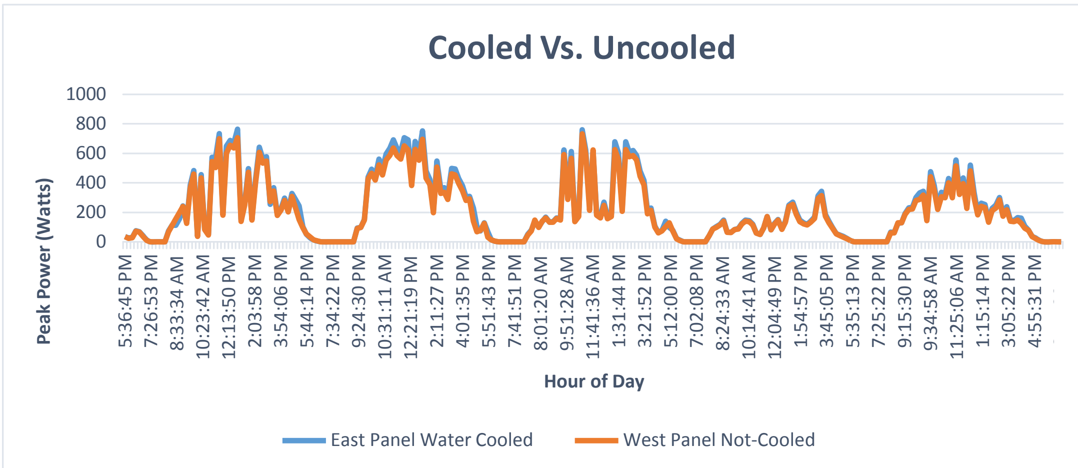

Figure 6-10 Oct-3rd – 9th Power

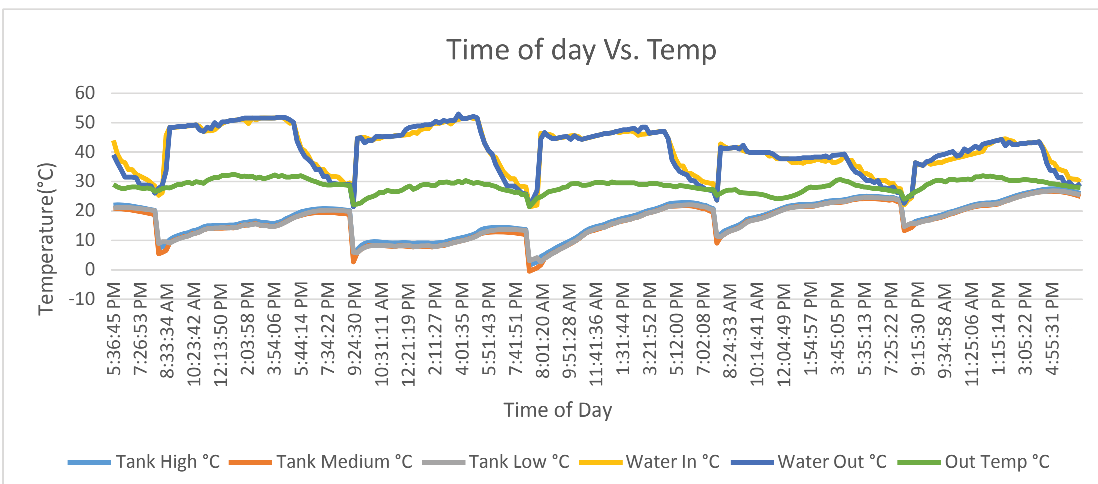

Figure 5-11 Oct-3rd – 9th Temperature

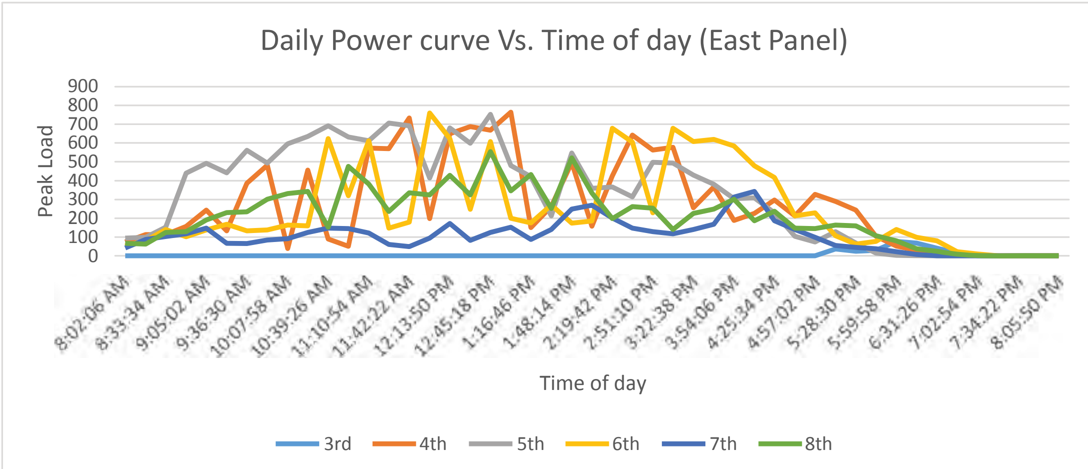

Figure 5-12 Oct-3rd – 9th Power Daily

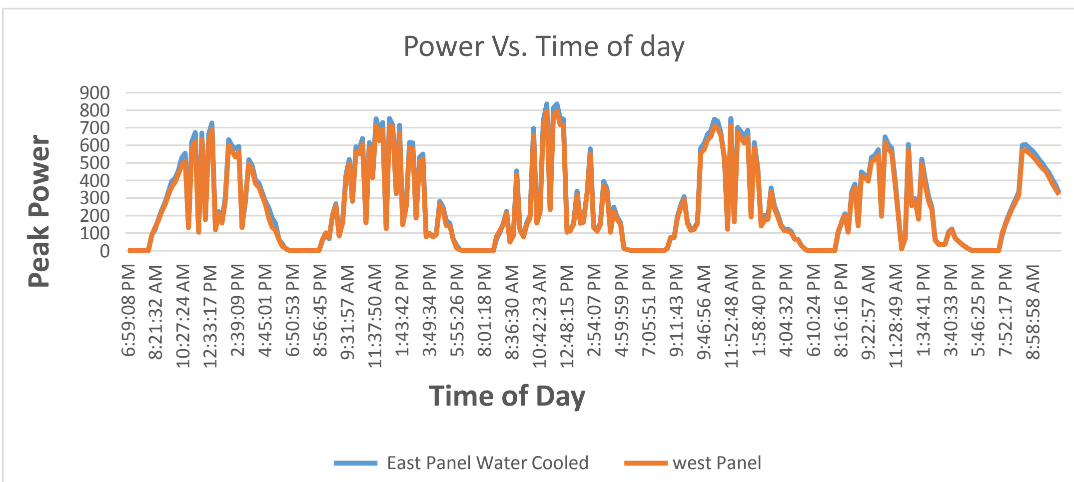

Figure 5-13 Oct-10th – 17th Power

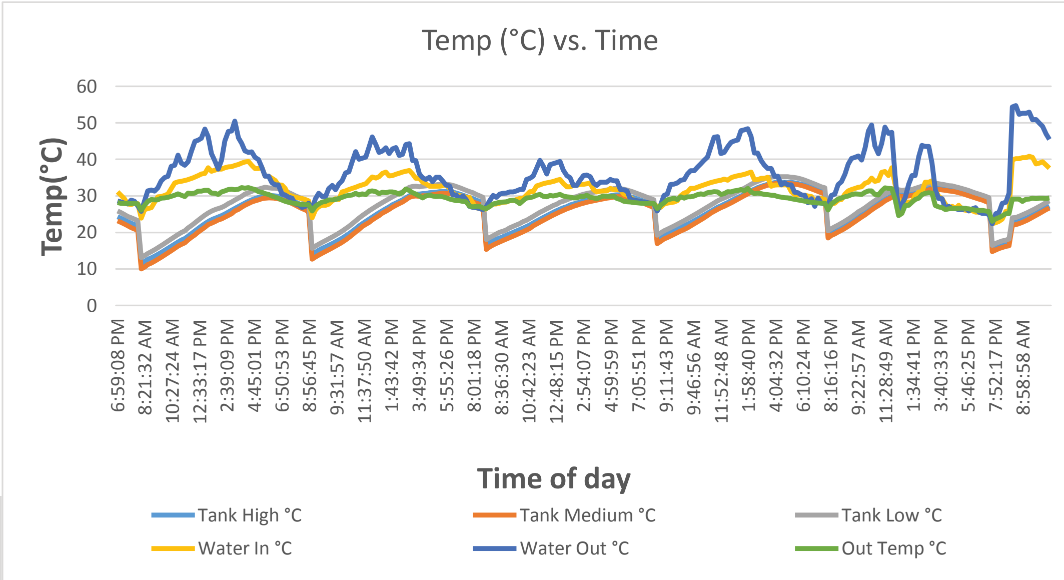

Figure 5-14 Oct-10th – 17th Temperature

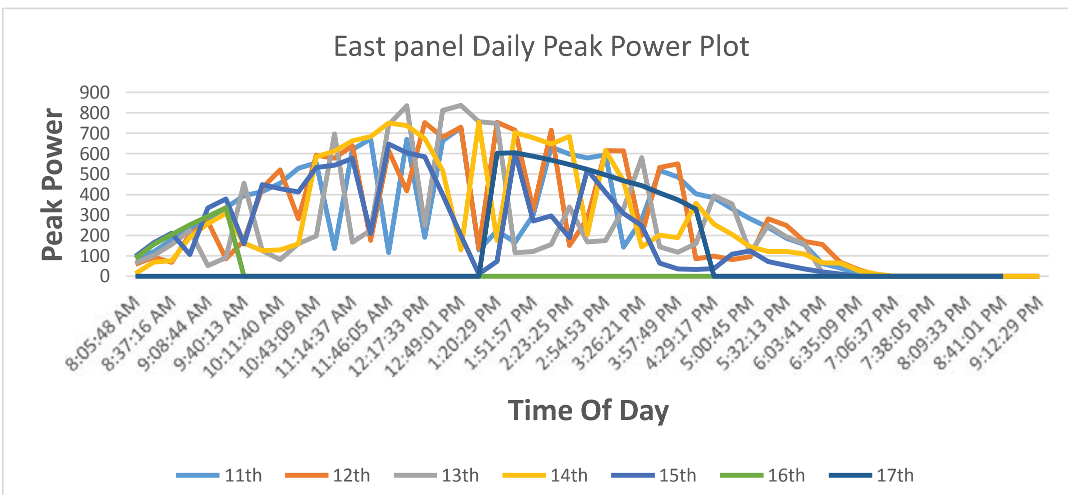

Figure 5-15 Oct-10th – 17th Daily Power

5.5 Appendix 5: Data plots for November 2014:

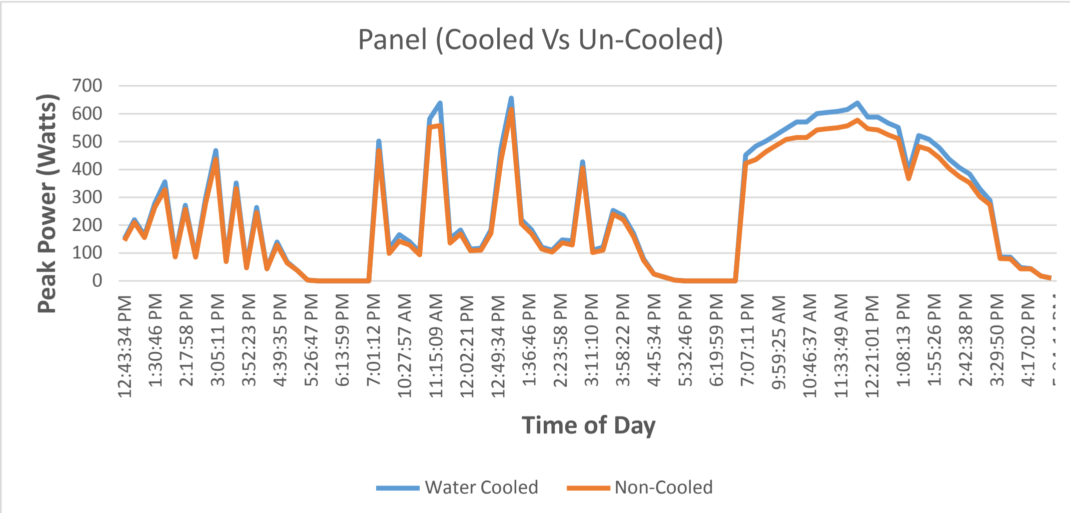

Figure 5-16 November 2nd -8th Power

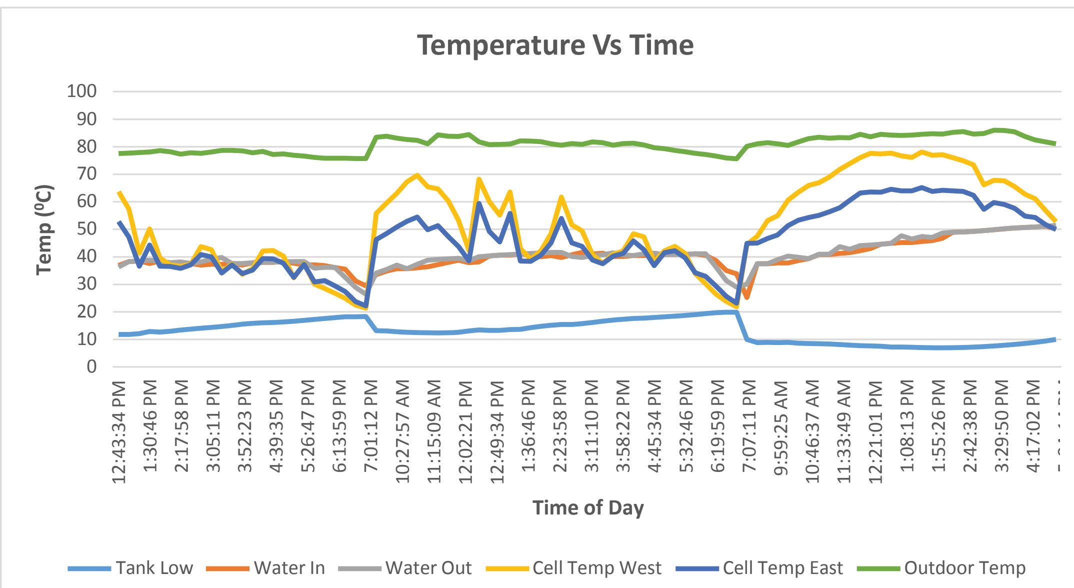

Figure 5-17 November 2nd -8th Temperature

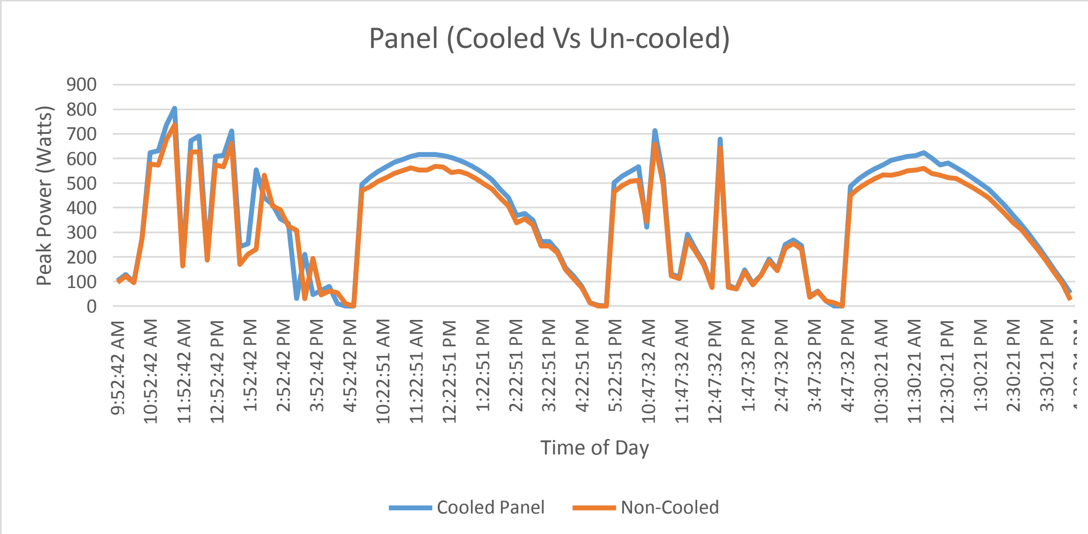

Figure 5-18 November 10nd -14th Power

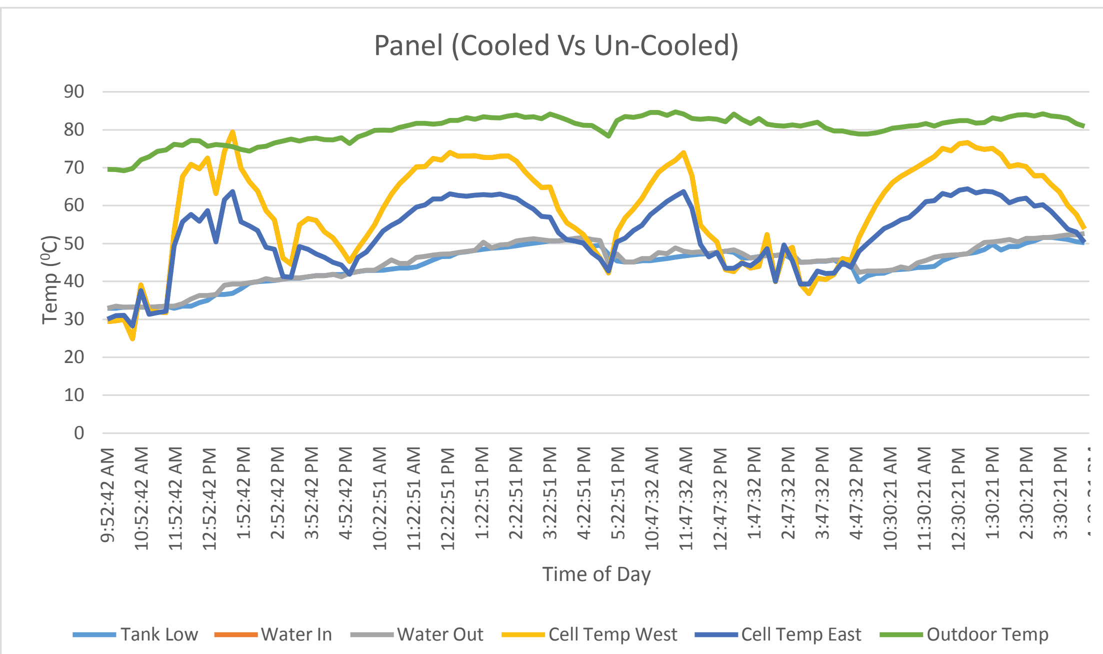

Figure 5-19 November 10nd -14th Temperature

[redacted] Palm City Site
December 2014 to November 2015 Data Analysis

Submitted by:
Professor Amir Abtahi, PhD, PE
And
Hadis Moradi, PhD Candidate College of Engineering and Computer Science FAU Boca Raton, Florida

November 23, 2015

1- Introduction:

The FAU research team is assessing the performance of two solar arrays in Palm City, Florida adjacent to [redacted] The purpose of this study is to compare the annual performance of a solar array with [redacted] panels and a with conventional [redacted] array. The contractor designed and installed two photovoltaic arrays with the same number of panels. Both systems are south-faced with the tilt angle of 30°. Each array comprises 24 solar panels. The monitoring of the system started in December 2014 when the system was officially commissioned. However the only data available was for the "total" generation of both arrays combined since the contractor had not installed sufficient current sensors to distinguish the [redacted] array output and the [redacted] array output. The proper sensors were installed a few months later. There have been issues with the data ports and our study is based on relatively limited data at this point.

2- Project Location:

[redacted], Palm City, FL 34990

Aerial View of the project site:

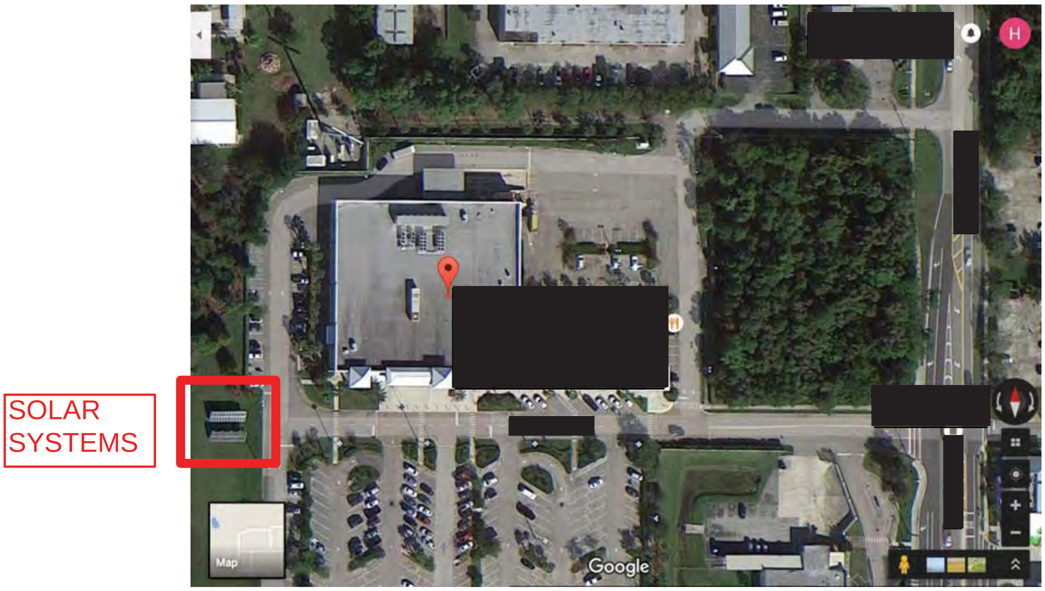

3- [redacted] Solar Panels

This array has been made of 24 [redacted] panels arranged 12 by 2.

Total number of modules per array: 24

Max power rating for each [redacted] module@1000W/m2: 300 W

Max capacity of the array: 24 × 300 W = 7.2 kW

3-1- [redacted] panel specifications:

ELECTRICAL SPECIFICATIONS[1]	290	300	310
STC rated output P_{MPP} (W)	290	300	310
Cell Efficiency	20.7%	21.3%	21.6%
Module Efficiency STC	17.6%	18.2%	18.8%
Standard sorted output	-3%/+5%	-3%/+5%	-3%/+5%
Open Circuit Voltage V_{OC} (V)	43.9	44.9	45.9
Short circuit current I_{SC} (A)	9.2	9.3	9.4
Rated Voltage V_{MPP} (V)	33.7	34.5	35.2
Rated Current I_{MPP} (A)	8.6	8.7	8.8

1: Standard Test Conditions for front-face of panel: 1000 W/m², 25°C

BI-FACIAL OUTPUT*			
With 10% Backside Power Boost			
Power Output (W)	319	330	341
Module Efficiency	19.5%	20.1%	20.7%
With 20% Backside Power Boost			
Power Output (W)	348	360	372
Module Efficiency	21.2%	22.0%	22.6%

*Backside boost for flush mount configuration is ≤5%, resulting in I_{sc} ≤9.56 - 9.77 A

TEST OPERATING CONDITIONS	
Operating Temperature	- 40 to + 85°C
Storage Temperature	- 40 to + 85°C
Maximum Series Fuse	15 A
Maximum System Voltage	1,000VDC (UL & IEC)
Power/Sq.Ft. w/ 20% backside power boost	20.3 W / Sq. Foot
Maximum load capacity	5,400 Pa (snow load) 185 mph wind rating
Fire Class	Class A - Type 3

TEMPERATURE COEFFICIENTS	
Temperature coefficient P_{MPP}	-0.28%/C
Temperature coefficient I_{SC}	+0.015%/C
Temperature coefficient V_{OC}	-0.21%/C
Normal operating cell temperature (NOCT)°C	46C +/- 2

MECHANICAL SPECIFICATIONS	
Dimensions	1,663 x 990 x 6 mm (5.46 x 3.25 x 0.02 ft)
Weight	25.2 kg (55.56 lbs)
Area	1.64 m^2 (17.7 ft^2)
Cell type	[redacted]
Module type	60 Cells, Frameless double glass design with tempered glass, no grounding required
Glass	Tempered 2.9mm anti-reflective coating, low-iron
Junction Box	[redacted]
Cables	$4mm^2$ x 0.9 m cable: MC4 or MC4 compatible Tyco connectors 1.2m needed for landscape mount

4- [redacted] Solar Panels:

This array is comprised of 24 [redacted] solar panels arranged 12 by 2.

Strings in parallel: 2

Modules per string: 12

Total number of modules per array: 24

Max power rating for [redacted] module@1000W/m2: 300 W

Max capacity of the array: 24 × 300 W = 7.2 kW

[redacted]

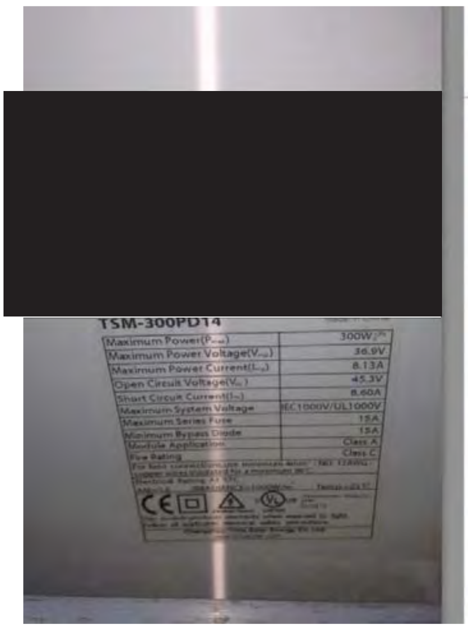
[redacted]
TSM-300PD14
Maximum Power 300W
Maximum Power Voltage 36.9V
Maximum Power Current 8.13A
Open Circuit Voltage 45.3V
Short Circuit Current 8.60A
Maximum System Voltage IEC1000V/UL1000V
Maximum Series Fuse 15A
Minimum Bypass Diode 15A
Module Application Class A
Fire Rating Class C

ELECTRICAL DATA @ STC	[redacted]				
Peak Power Watts-P_{MAX} (Wp)	290	295	300	305	310
Power Output Tolerance-P_{MAX} (%)	0/+3	0/+3	0/+3	0/+3	0/+3
Maximum Power Voltage-V_{MPP} (V)	36.1	36.6	36.9	37.0	37.0
Maximum Power Current-I_{MPP} (A)	8.04	8.07	8.13	8.25	8.38
Open Circuit Voltage-V_{OC} (V)	44.9	45.2	45.3	45.4	45.5
Short Circuit Current-I_{SC} (A)	8.53	8.55	8.60	8.75	8.85
Module Efficiency η_m (%)	14.9	15.2	15.5	15.7	16.0

STC: Irradiance 1000 W/m², Cell Temperature 25°C, Air Mass AM1.5 according to EN 60904-3.
Average efficiency reduction of 4.5% at 200 W/m² according to EN 60904-1.

ELECTRICAL DATA @ NOCT	[redacted]				
Maximum Power-P_{MAX} (Wp)	211	214	218	222	226
Maximum Power Voltage-V_{MPP} (V)	32.6	33.0	33.3	33.7	33.8
Maximum Power Current-I_{MPP} (A)	6.47	6.48	6.55	6.59	6.68
Open Circuit Voltage (V)-V_{OC} (V)	40.9	41.2	41.3	41.4	41.5
Short Circuit Current (A)-I_{SC} (A)	6.97	7.00	7.04	7.06	7.16

NOCT: Irradiance at 800 W/m², Ambient Temperature 20°C, Wind Speed 1 m/s.

MECHANICAL DATA	
Solar cells	[redacted]
Cell orientation	72 cells (6 × 12)
Module dimensions	1956 × 992 × 40 mm (77 × 39.05 × 1.57 inches)
Weight	27.6 kg (60.8 lb)
Glass	High transparency solar glass 4.0 mm (0.16 inches)
Frame	Anodized aluminium alloy
J-Box	IP 65 or IP 67 rated
Cables	Photovoltaic Technology cable 4.0 mm² (0.006 inches²), 1200 mm (47.2 inches)
Connector	[redacted]

TEMPERATURE RATINGS	
Nominal Operating Cell Temperature (NOCT)	45°C (±2°C)
Temperature Coefficient of P_{MAX}	- 0.44%/°C
Temperature Coefficient of V_{OC}	- 0.33%/°C
Temperature Coefficient of I_{SC}	0.046%/°C

MAXIMUM RATINGS	
Operational Temperature	-40~+85°C
Maximum System Voltage	1000V DC(IEC)/ 1000V DC(UL)
Max Series Fuse Rating	15A

5- System Electrical Connections

The arrays are connected to [redacted] for Professional monitoring and controlling for decentralized large-scale PV plants.

First of all, both systems are connected to SMA Connection Unit [redacted] Then it connects to [redacted] inverter with the efficiency of 98.2%.

An HPS three phase dry type transformer has been used in the system as a way to both raise supply voltage caused by line drop or equipment demand on the distribution system; or lower voltage caused by increased system voltages due to supply line adjustments.

6- System Output Energy

The system started working on December 15th, 2014, but the data from Dec 15th till Jan 15th are uncompleted and useless. In fact, the system started working properly since January 15th, 2015. Energy output from the systems is shown in following charts.

[redacted]

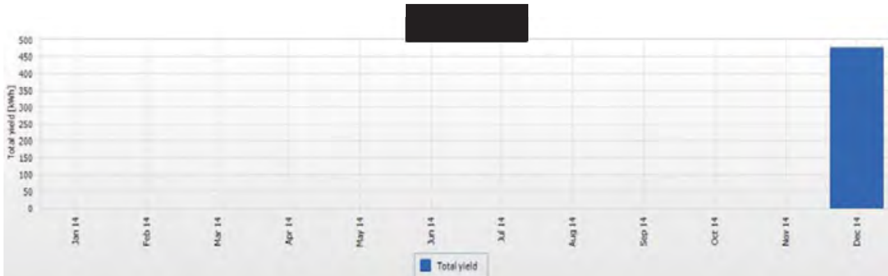

[redacted]

As the figures show, the system faced with many data interruptions and discontinuity. Also, the data is incomplete for several hours in some days. All of these issues affect on the data analysis and getting appropriate results of the system performance.
System annual energy output is presented in figure below for 2014 and 2015.

[redacted]

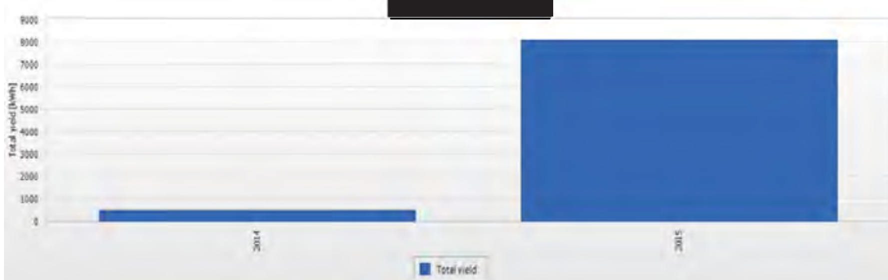

7- Monthly System Energy Output

7.1- Solar System Output Energy [kWh] in December 2014

In table below, the first column is the date, the second column is energy output from the system with [redacted] panels and third column is energy output from the system with Trina panels for that specific date. The fourth column shows the percentage of more power that [redacted] produced in comparison with [redacted]

Dec-14

	[redacted]	[redacted]	%
12/15/14	5265.583	6760.334	-22.11
12/16/14	19709.713	18949.02	4.01
12/17/14	5349.75	7837.817	-31.74
12/18/14	20177.372	19032.55	6.02
12/19/14	15879.767	15962.153	-0.52
12/20/14	14890.133	15526.497	-4.10
12/21/14	10112.608	8921.825	13.35
12/22/14	15839.823	15777.985	0.39
12/23/14	8518.168	9075.821	-6.14
12/24/14	15296.713	14536.001	5.23
12/25/14	7532.758	7809.616	-3.55
12/26/14	2715.31	2676.292	1.46
12/27/14	5915.5	5889.817	0.44
12/28/14	1876	1978.714	-5.19
12/29/14	7683.639	6698.805	14.70
12/30/14	10652.402	10884.861	-2.14
Total	167415.239	168318.108	-0.54

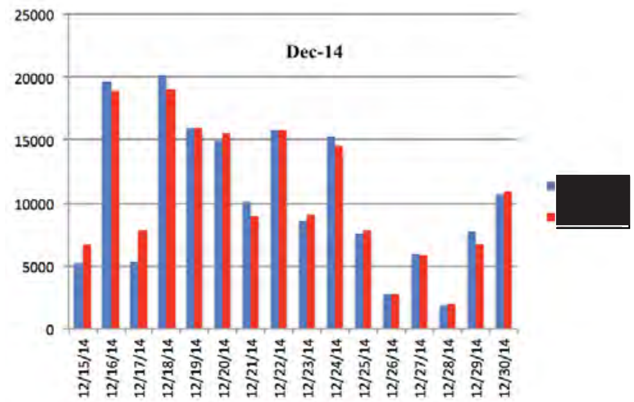

7.2- Solar System Output Energy [kWh] in January 2015

		Jan-15	
	[redacted]	[redacted]	%
1/1/15	4590.667	5359.75	-14.35
1/2/15	7508.884	7979.55	-5.90
1/3/15	0	0	0.00
1/4/15	18763.82	19031.07	-1.40
1/5/15	13818.397	13881.849	-0.46
1/6/15	13760.601	12776.228	7.70
1/7/15	15463.25	15147.651	2.08
1/8/15	2925.838	3081.147	-5.04
1/9/15	10386.618	11138.314	-6.75
1/10/15	17233.596	16694.594	3.23
1/11/15	10326.902	9513.922	8.55
1/12/15	6177.706	6032.602	2.41
1/13/15	7197.936	7176.7	0.30
1/14/15	2462.417	2564.886	-4.00
1/15/15	16584.583	15247.193	8.77
1/16/15	17094.75	17882.958	-4.41
1/17/15	18484.818	17123.749	7.95

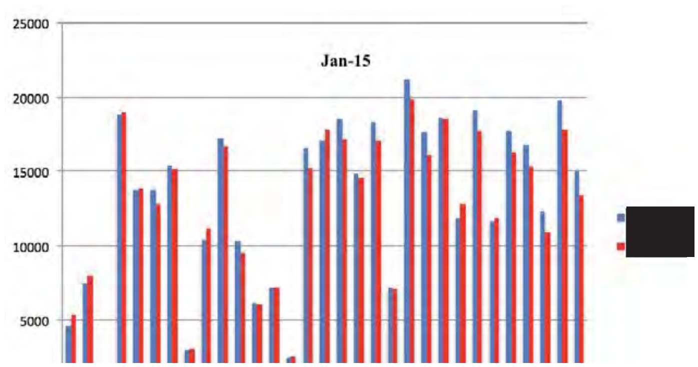

1/18/15	14818.608	14515.166	2.09
1/19/15	18342.333	17043.629	7.62
1/20/15	7178.211	7105.544	1.02
1/21/15	21210.167	19838.167	6.92
1/22/15	17696.385	16120.116	9.78
1/23/15	18608.698	18555.425	0.29
1/24/15	11835.31	12790.143	-7.47
1/25/15	19098.341	17709.356	7.84
1/26/15	11678.977	11872.091	-1.63
1/27/15	17758.378	16332.454	8.73
1/28/15	16758.374	15305.039	9.50
1/29/15	12326.144	10859.803	13.50
1/30/15	19816.909	17875.1	10.86
1/31/15	14988.977	13370.176	12.11
Total	404896.595	389924.372	12.11

7.3- Solar System Output Energy [kWh] in February 2015

		Feb-15	
	[redacted]	[redacted]	%
2/1/15	14371.5	14303.044	0.48
2/2/15	15954.334	14334.706	11.30
2/3/15	19246.752	17531	9.79
2/4/15	14001.75	12723.667	10.04
2/5/15	6175.501	6087.249	1.45
2/6/15	18086.248	16707.5	8.25
2/7/15	15471.749	14175.916	9.14
2/8/15	17484.917	16244.06	7.64
2/9/15	14113.803	13604.681	3.74
2/10/15	17156.857	16710.955	2.67
2/11/15	20147.167	18247.083	10.41
2/12/15	9907.348	7729.159	28.18
Total	182117.926	168399.02	8.15

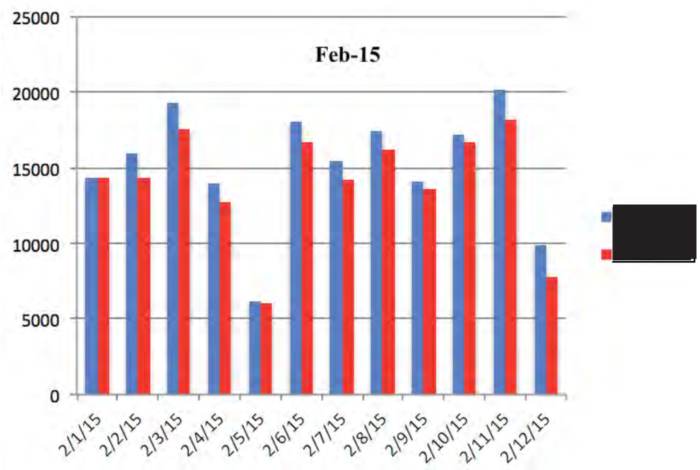

7.4- Solar System Output Energy [kWh] in May 2015

	May-15		
	[redacted]	[redacted]	%
5/7/15	26100.31	25391.631	2.79
5/8/15	39751.166	39237.667	1.31
5/9/15	37529.251	37321.331	0.56
5/10/15	34342.832	34151.332	0.56
5/11/15	41191.166	40133.999	2.63
5/12/15	40572.184	39921.316	1.63
5/13/15	42781.666	43069.135	-0.67
5/14/15	39486.101	39457.551	0.07
5/15/15	34693.034	33893.915	2.36
5/16/15	38830.081	38211.085	1.62
5/17/15	34886.267	33902.566	2.90
5/18/15	36652.115	35251.601	3.97
5/19/15	40464.051	40854.916	-0.96
5/20/15	42287.266	42849.483	-1.31
5/21/15	37231.333	37490.668	-0.69
5/22/15	31251.649	31115.4	0.44
5/23/15	36887.333	36087.083	2.22

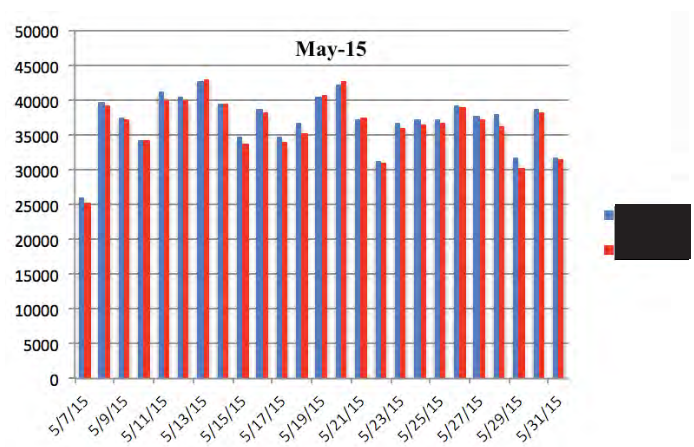

5/24/15	37285.165	36621.832	1.81
5/25/15	37257.415	36835.419	1.15
5/26/15	39342.502	39099.083	0.62
5/27/15	37892.209	37294.585	1.60
5/28/15	37923.25	36326.667	4.40
5/29/15	31719.417	30241.751	4.89
5/30/15	38887.666	38328.001	1.46
5/31/15	31860.475	31510.641	1.11
Total	927105.904	914598.658	1.37

7.5- Solar System Output Energy [kWh] in June 2015

		Jun-15	
	[redacted]	[redacted]	%
6/1/15	31763.965	31821.142	-0.18
6/2/15	21853.252	22031.332	-0.81
6/3/15	40915.167	41011.083	-0.23
6/4/15	30894.749	31079.998	-0.60
6/5/15	38766.503	38800.5	-0.09
6/6/15	28032.016	27953.614	0.78
6/7/15	31140.332	30899.334	0.93
6/8/15	25124.916	24894.334	-0.56
6/9/15	37749.299	37961.183	0.93
6/10/15	25124.916	24894.334	-0.56
6/11/15	37749.299	37961.183	0.39
6/12/15	32693.519	32566.334	-0.78
6/13/15	35235.167	35511.836	-0.83
6/14/15	35364.737	35660.563	-0.09
6/15/15	38766.503	38800.5	0.33
6/16/15	34870.5	34756.084	-0.27

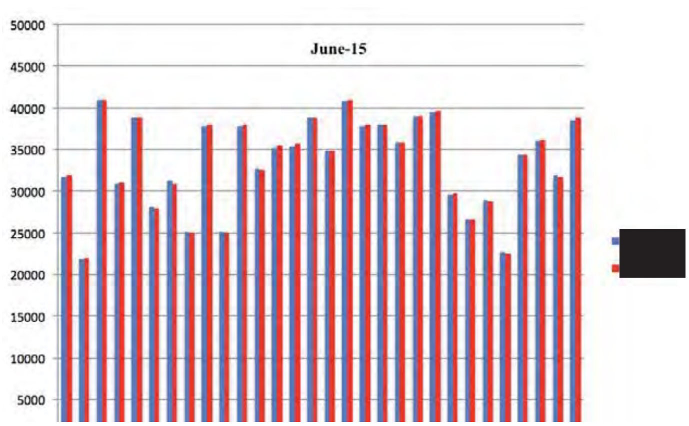

6/17/15	40811.833	40922.334	-0.37
6/18/15	37868.999	38010.998	-0.09
6/19/15	37988.082	38023.917	0.08
6/20/15	35836.251	35805.833	0.21
6/21/15	38988.349	38907.234	-0.46
6/22/15	39491.582	39672.417	-0.39
6/23/15	29527.572	29642.276	0.18
6/24/15	26669.667	26621.416	0.40
6/25/15	28907.165	28793.415	0.91
6/26/15	22662.117	22456.95	-0.08
6/27/15	34390.5	34418.334	-0.35
6/28/15	35976.349	36104.25	0.56
6/29/15	31846.95	31669.583	-0.49
6/30/15	38539.501	38730.666	-0.49

TOTAL	1005549.757	1006382.977	-0.08

7.6- Solar System Output Energy [kWh] in July 2015

		Jul-15	
	[redacted]	[redacted]	%
7/1/15	29504.217	29383.051	0.41
7/2/15	25989.534	26063.834	-0.29
7/3/15	23817.081	23580.001	1.01
7/4/15	24657.249	24808.584	-0.61
7/5/15	18231.683	17999.516	1.29
7/6/15	28814.832	28793.25	0.07
7/7/15	16969.251	16844.168	0.74
7/8/15	39842.294	39956.916	-0.29
7/9/15	39990.982	40105.15	-0.28
7/10/15	38564.017	38775.982	-0.55
7/11/15	38843.85	39107.018	-0.67
7/12/15	37368.583	37419.75	-0.14
7/13/15	33457.834	33533.831	-0.23
7/14/15	34836.417	34835.083	0.00
7/15/15	34459.668	34363.251	0.28
7/16/15	20894.249	20855.166	0.19
7/17/15	34959.918	34864.834	0.27

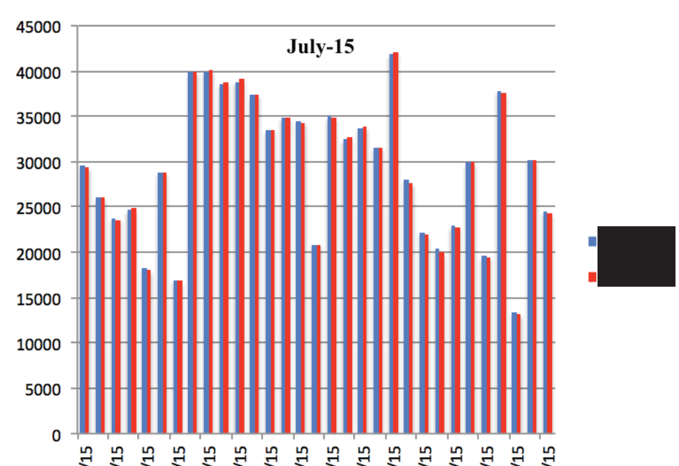

7/18/15	32502.101	32641.533	-0.43
7/19/15	33760.751	33837.666	-0.23
7/20/15	31622.501	31583.25	0.12
7/21/15	41869.251	42159.919	-0.69
7/22/15	27968.165	27580	1.41
7/23/15	22184.126	21879.168	1.39
7/24/15	20489.749	19968.832	2.61
7/25/15	22869.581	22785.917	0.37
7/26/15	29919.001	29975.417	-0.19
7/27/15	19569.916	19516.083	0.28
7/28/15	37854.75	37609.501	0.65
7/29/15	13376.334	13173.335	1.54
7/30/15	30252.332	30131.083	0.40
7/31/15	24479.136	24323.416	0.64
TOTAL	909919.353	908454.505	0.16

7.7- Solar System Output Energy [kWh] in August 2015

		Aug-15	
	[redacted]	[redacted]	%
8/1/15	17447.659	17412.749	0.20
8/2/15	22787.417	22791.667	-0.02
Total	40235.076	40204.416	0.08

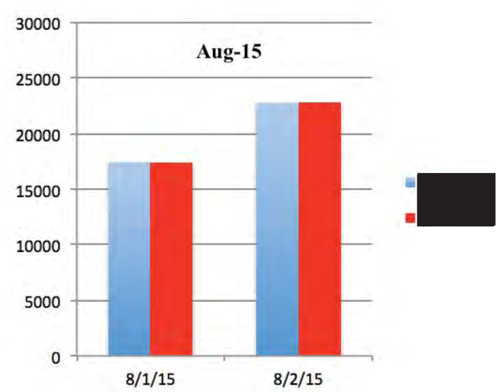

7.8- Solar System Output Energy [kWh] in October 2015

		Oct-15	
	[redacted]	[redacted]	%
10/27/15	17234.36	15908.35	8.34
10/28/15	17628.92	17592.07	0.21
10/29/15	21792.69	21672.33	0.56

Total	131278.37	127673.49	2.82

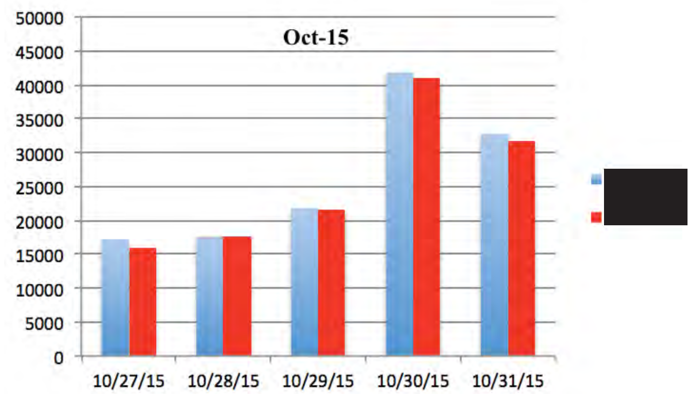

7-8- Solar System Output Energy [kWh] in October 2015

		Nov-15	
	[redacted]	[redacted]	%
11/1/15	34702.12	32686.15	6.17
11/2/15	33252.19	31420.62	5.83
11/3/15	38672.74	37748.02	2.45
11/4/15	35210.72	33799.07	4.18
11/5/15	34706.02	31977.38	8.53
11/6/15	39333.39	37944.1	3.66
11/7/15	28730.8	27445.21	4.68
11/8/15	34509.05	32515.64	6.13
11/9/15	32933.34	31091.64	5.92
11/10/15	31159.32	29599.04	5.27
11/11/15	26783.24	25969.99	3.13
11/12/15	24783.55	24565.69	0.89
11/13/15	22222.91	20745.72	7.12
11/14/15	22120	20764.31	6.53
11/15/15	8790.31	8539.25	2.94
11/16/15	25609.78	25667.53	-0.22
11/17/15	30343.51	29113.41	4.23
11/18/15	24757.75	23471.24	5.48
11/19/15	22141.67	21609.2	2.46

11/22/15	10780.82	10762.75	0.17

Total	598535.2	573627.59	4.34

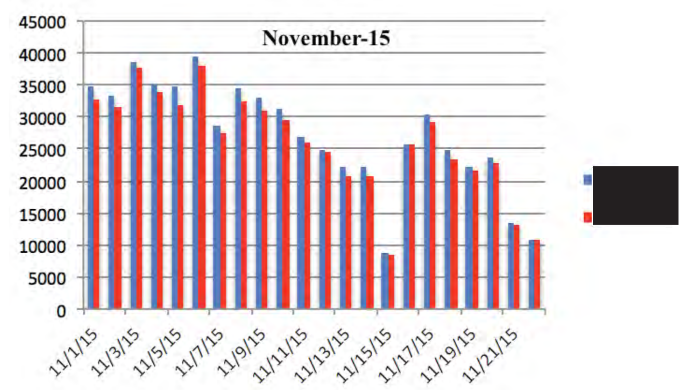

8- Total Energy Generation by two arrays:

		Total Production	
	[redacted]	[redacted]	%
Dec-14	167415.239	168318.108	-0.54
Jan-15	404896.595	389925.372	3.84
Feb-15	182117.926	168399.02	8.15
May-15	927105.904	914598.658	1.37
Jun-15	1005549.76	1006382.98	-0.08
Jul-15	909919.353	908454.505	0.16
Aug-15	40235.076	40204.416	0.08
Oct-15	131278.37	127673.49	2.82
Nov-15	598535.2	573627.59	4.34
Total	4367053.423	4297584.139	1.62

9. Conclusion:

According to the available data, the results show that the first array with [redacted] panels is performing marginally better than the [redacted] array. The less than 2% for the [redacted] array may be the result of the relative position of the 2 arrays, with the [redacted] array receiving less overall diffuse radiation as it is located just North of the [redacted] array with a relatively short clearance. With the limited results that were available, it does appear however that the [redacted] panels have better performance in wintertime and low temperature conditions compared to summertime and high temperature conditions.

The results need to be verified further as the lack of data for significantly long periods, and current sensor issues, our results have a relatively large error component. The research team needs at least 6 to 9 months of continues data to accomplish data analysis and to obtain accurate results.

Itron
Knowledge to Shape Your Future

Electric | Gas | Water
information collection, analysis and application

Final Report

Florida Power & Light Smart Thermostat Trial Impact Evaluation

Prepared for:

Patrick Agnew
Program Manager, In-home Technology and Electric Vehicles

Florida Power & Light

Prepared by:

Dave Hanna
Collin Elliot
Christine Hungeling

Itron, Inc.
12348 High Bluff Drive, Suite 210
San Diego, California 92130

(858) 724-2620

July 7, 2015

Table of Contents

List of Figures

List of Tables

1

FPL Smart Thermostat Trial Final Report

1.1 Executive Summary

Florida Power and Light (FPL) performed a Smart Thermostat Trial (STT) to explore the effects of the installation of smart thermostats in residential homes. In addition to providing trial participants with the ability to control their thermostats through smart phone applications, the smart thermostats allowed FPL to conduct load control events by controlling the cycling of the homes' heating, ventilation, and air conditioning (HVAC) systems. Roughly half of the homes in the STT were randomly given the ability to override the load control while the rest could not. These two segments are referred to henceforth as the Override and No Override groups. To assess the effects of the thermostats on the pilot's participants, Itron completed an impact evaluation to determine the level of energy conservation achieved by the smart thermostats, estimate the impact of the load control on the event days, and characterize participants based on their thermostat set-points and override behavior.

A summary of the key energy impact metrics for the STT developed by the impact evaluation is presented below in Table 1-1. With respect to conservation effects, the analysis found statistically significant energy savings in both the winter and summer months. Savings of 3.3% and 2.3% of daily household consumption in summer and winter, respectively, amounted to annual savings of 451 kWh, or 2.8% of total household consumption and 11.9% of estimated air conditioning kWh.[1] One aspect of the winter savings estimates is that heating degree days were not used in the model, so none of the savings is explicitly associated with heating. Hourly models found summer peak savings of 0.18 kW during the 4 – 5 PM hour, which represented savings of 4.6% of the whole home kW during that hour and 8.4% of estimated cooling kW.

Finally, it is possible that the level of energy savings in the pilot's first year is due to the participants' interest in the novelty of the technology. This is based on analysis that showed daily kWh savings of 2.8% in the first three months of 2014 compared to 1.8% for November and

[1] This metric carries some important caveats. First, whereas the total household consumption comes directly from the interval data, the air conditioning kWh are estimated based on the coefficient for cooling degree days from the same daily consumption regression models used to estimate energy savings. It is possible that some cooling-related consumption is included in the baseline usage – or intercept – from this model. Second, there are likely some savings associated with heating. Because heating degree days were not included in the energy savings analysis – either for determining baseline usage or for estimating impacts – there is no way to estimate what portion of either savings or household consumption are associated with heating,

December. While far from conclusive, this finding does suggest the persistence of savings would be a worthy future research topic.

Table 1-1: Summary of STT Energy and Demand Impacts

Source of Savings	Measure	No Override	Override	Total
Thermostat Conservation	Annual kWh Savings, kWh	n/a	n/a	451
	Annual kWh Savings, % of Whole Home	n/a	n/a	2.8%
	Annual kWh Savings, % of Cooling	n/a	n/a	11.9%
	Summer Peak Hour kW 4 - 5 PM	n/a	n/a	0.18
Load Control	Summer Peak Hour kW 4 - 5 PM	0.63	0.66	n/a
	Winter Peak Hour kW, 7 – 8 AM	0.00	0.00	n/a

The impact of the load control on the event days showed substantial load curtailment during the event hours in the summer months. During FPL's summer peak hour of 4 PM to 5 PM, the Override group reduced load by 0.66 kW versus 0.63 kW for the No Override group. It is important to make clear that the estimated impacts were not statistically significantly different from each other, indicating the two groups are essentially the same.[2] The average reduction over all four event hours was 0.63 kW per hour in the Override group versus 0.61 kW per hour for the No Override group. The small number of homes opting out along with timing of the overrides meant that the number of minutes overridden was only a small percentage of the total, ranging from low of 2.3% to a high of 10.3%. The impacts for all load control hours and overall are presented in Table 1-2, with the summer peak hour in a shaded column.

Table 1-2: Summary of Hourly Summer Load Control Reductions

Group	3 PM – 4 PM	4 PM – 5 PM	5 PM – 6 PM	6 PM – 7 PM	Average
No Override	0.69 kW	0.63 kW	0.59 kW	.051 kW	0.61 kW
Override	0.69 kW	0.66 kW	0.66 kW	.051 kW	0.63 kW

To provide a visual representation of the average event impacts, Figure 1-1 shows for both groups the average observed hourly kW for the summer event days along with the hourly reference kW, which represents an estimate of what would have happened in the absence of an event. The four hours of the control period from 3 PM to 7 PM are shaded in light gray and FPL's peak hour of 4 PM to 5 PM is shaded in dark gray. The annotated values show the kW load reduction or increase for the four control hours and the two hours after, when snapback occurs as homes resume HVAC use. The peak hour impacts are easily discernible in the plots. For example, the 0.63 kW load reduction for the No Override group is represented by the difference between the reference and

[2] The differences in impacts for the load control hours between the Override and No Override groups shown in the tables and graphs were not statistically significant at the 0.05 level.

observed loads for the two points in the dark gray area. The average hourly kW reduction is less clear, as it is based on the difference between the average values for the reference and observed loads during the control period. Overall, the differences between the two groups are small, though the Override group does show a more marked decrease in load reduction in the last hour of the event and a substantially lower snapback effect in the two hours following the event. If anything, a more substantial impact of the ability to override is that it appears to mitigate the snapback effect. The larger snapback effect in the No Override group is likely due to a larger share of the HVAC systems resuming operation at the same time. In general, each summer event showed a similar pattern across all event days. These individual event-specific plots are provided in Appendix 1.

Figure 1-1: Average Load Control Impact in Summer Months

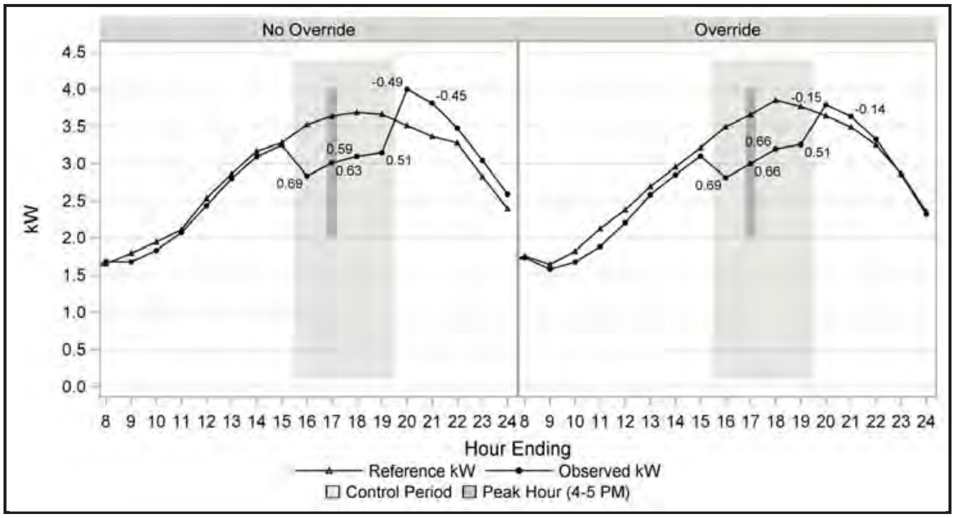

In contrast to the clear influence of the summer curtailment events, the analysis of the winter events did not produce any evidence for savings. This lack of winter impacts appeared to have two related root causes, which were ascertained by analyzing 15-minute interval data on equipment operation from the smart thermostats. First, few of the homes were using any heat whatsoever on the event days. Second, of those that were using heat, most were already cycling their heat at 50% or less so the event had no effect other than to synchronize all the homes' cycling schedule. Itron analyzed the winter events separately because the conditions associated with each of them were substantially different. For example, the first winter event on January 17, 2014 occurred on the second day of a cold spell and approximately 40% of homes were using their heating. In contrast, the second winter event on February 14, 2014 occurred following a relatively warm day and only about 22% of homes where using their heating systems. While the limited heating on both event days was not promising, the intent in modelling the events separately was to see if at least the first event on the colder day would result in statistically significant impacts. Nevertheless, neither event resulted in any evidence for savings for winter load control. In spite of not having any impacts, in the interest of completeness, Figure 1-2 and Figure 1-3 provide visual representations for the January 17 and February 14 events, respectively.

Figure 1-2: Load Control Impact on January 17, 2014

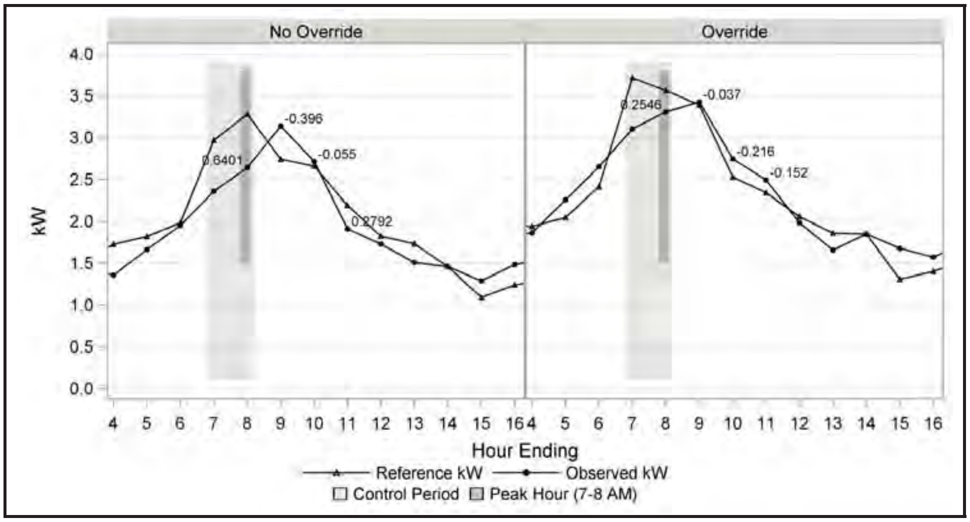

Figure 1-3: Load Control Impact on February 14, 2014

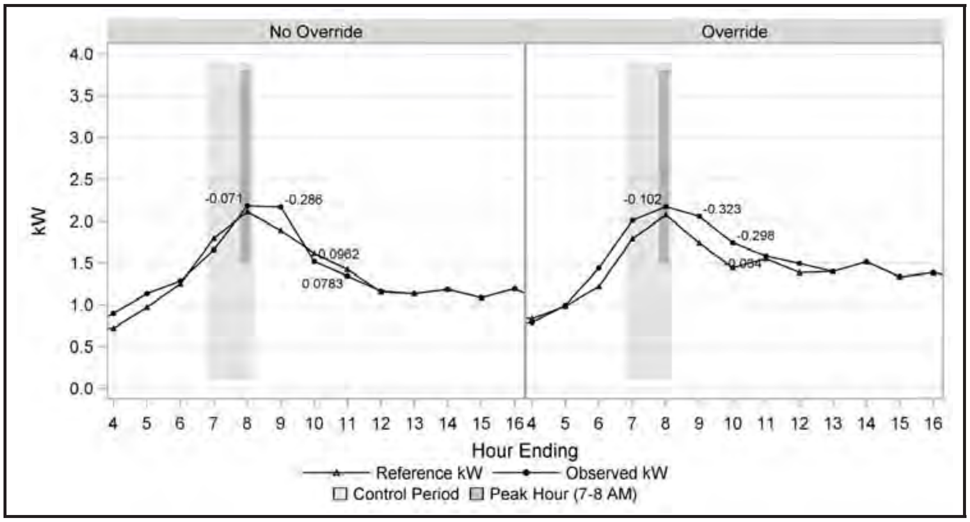

1.2 Introduction

FPL performed the STT to test the performance of smart thermostat technology in residential homes. The smart thermostats employed had the potential for energy savings by offering participants the ability to control their thermostats through smart phone applications. The smart thermostats also allowed FPL to conduct load control events by controlling the cycling of the homes' heating, ventilation, and air conditioning (HVAC) systems, providing opportunities for better management of the power grid. While programmable thermostats (PTs) are not new, FPL believes that the technology associated with the pilot (thermostat and broadband and mobile communications) has evolved significantly since last testing programmable communicating thermostats in 2009. This study investigated the impact of the smart thermostats in a sample of residential homes running through 2014.

The objectives of this study were threefold. First, the study sought to measure the energy conservation savings associated with smart thermostats. Second, the study attempted to measure the demand impacts of HVAC cycling events facilitated by the smart thermostats. Finally, the study looked to assess the customers' response to having smart thermostats installed in terms of programming behavior.

1.3 Pilot Design

FPL designed the STT as an experiment by creating randomized treatment and control sample frames from which to identify final treatment and control groups for the study. The initial sample frame was developed by identifying active residential customers in single family homes within specific ZIP codes of Palm Beach County. Valid customers had to have 12 months of Advanced Metering Infrastructure (AMI) data and an active e-mail address. The sample frame was reduced by eliminating customers already enrolled in FPL's residential load management program, On Call, as well as those with an average monthly consumption lower than 500 kWh for July, August, and September (as a proxy to eliminate seasonal customers). Because the participation solicitation was through FPL's e-mail channels, those who opted out of e-mail correspondence or who indicated they did not wish to be solicited by FPL were also eliminated. Finally, Medically Essential Program customers and accounts not active for at least 12 months were filtered out to reach the final sample frame of 33,135 customers. From this final sample frame, customers were randomly assigned to 12 buckets of 2,500 for participation recruitment purposes. The remaining 3,135 customers were set aside for use as a control group. It should be noted that the customers were not screened based on their type of thermostat installed; therefore, the control group should be representative of the thermostat types in the population.

1.4 Treatment and Control Group Selection

The pilot sought to examine the load impacts of the STT when FPL initiates load control on central air conditioners and electric space heating. As an additional component of this research topic, FPL further divided STT participants into two groups: those who have the option to override (Override) control events and those who cannot (No Override). Therefore, the original 12 buckets for participant recruitment were divided into two groups of six buckets each. Customers were assigned to a group and not given a choice on this feature.

The goal was to recruit from the 12 participant buckets and have the smart thermostats installed and operational for one hundred participants in each of the two groups. The recruitment process resulted in the enrollment of 233 customers in the STT by the beginning of 2014. However, due to a variety of issues, smart thermostats were successfully installed in only 178 homes—80 in the No Override group and 98 in the Override group. Of these, 16 were removed due primarily to unsuitable matches in the effort to identify control group (discussed below). The overall pilot sample design is shown in Figure 1-4.

Figure 1-4: FPL Smart Thermostat Sample Design

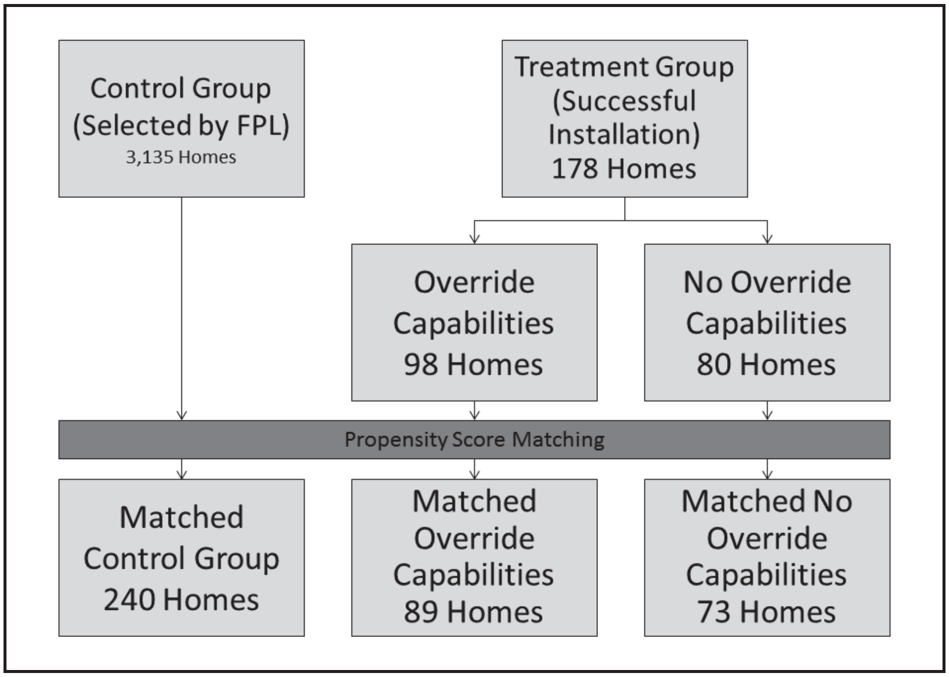

1.5 Control Group

As mentioned above, FPL selected a control group to use in this study. Itron conducted a series of comparisons of the control group to the two smart thermostat treatment groups to validate their comparability using the pre-treatment data that FPL collected for the control and treatment groups. Itron determined that to better match the treatment group, a more refined control group was necessary using a propensity score matching approach to find households in the control sample frame that were most similar to the treatment households in terms of observable energy use characteristics. There was some minor data cleaning to eliminate a few outliers in the interval energy consumption data as well as the removal of all event days from 2014, but otherwise the analysis relied on nearly all available data. Additionally, the analysis used hourly temperature data from Palm Beach International Airport, which was provided by FPL. There were 240 homes chosen to act as the control group for 162 participating homes. Customers in a few homes moved out or dropped out of the program during 2014, so they were dropped from the analysis starting on their move out or drop out date.

1.6 Energy Savings from Thermostat Programming

The energy conservation effects of the PTs were estimated by examining both pre- and post-installation energy consumption for both treatment and control groups. The net energy effect was calculated using a difference-in-differences (DiD) approach. Originally, this analysis was to be conducted separately for homes that did and did not program their thermostats. This was based on a customer survey performed prior to the installation of the smart thermostats that showed there were a substantial number of customers that had PTs but did not use them, as shown in Figure 1-5. In spite of this stated behavior, after the thermostats were installed it was determined that all but six of the treatment groups did program their thermostats. As a result, the treatment group was not divided between programmers and non-programmers.

Figure 1-5: Count of Programmable Thermostats Used (Prior to Treatment)

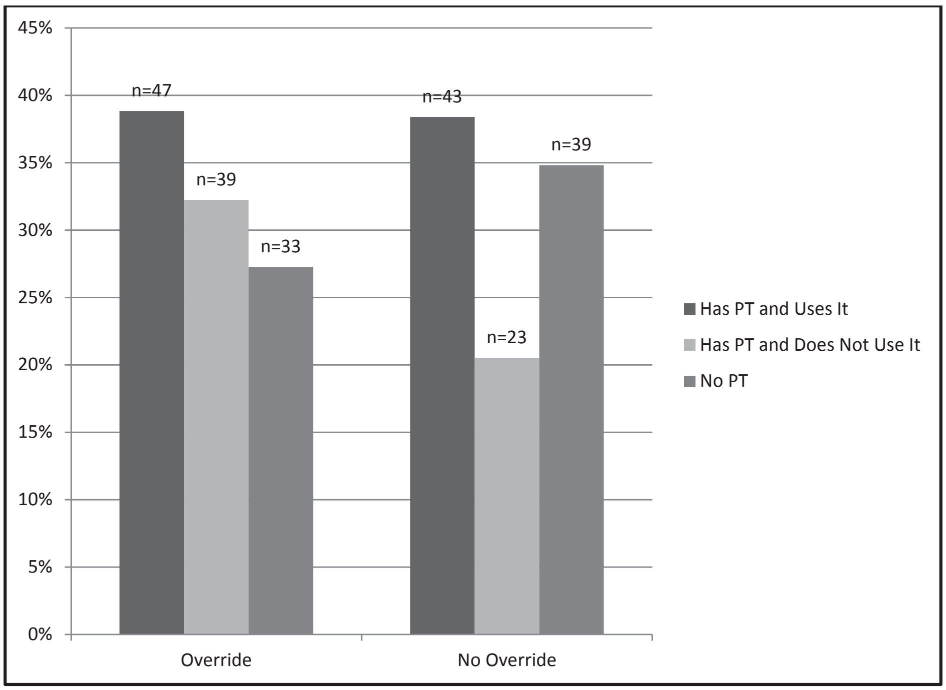

1.6.1 Energy Savings by Season

Differences of Means

The DiD approach for assessing energy savings from conservation was implemented in two approaches, the first of which was a comparison of means in the pre- and post-installation periods for treatment and control groups. This analysis was performed by calculating the aggregate average energy use by season for each of the treatment and control groups for both the pre-treatment period and the treatment period during each season. This approach assumed that even though the treatment and control groups were not likely the same in every respect, at least the differences between them over time were likely to be the same absent any treatment (in this case, the installation of the smart thermostat). As a result, the effect of the treatment can be calculated as the difference in each group's difference from the pre-treatment period to the post-treatment period.

Table 1-3 shows the summary of mean daily kWh for summer along with the associated cooling degree days (CDD[3]) for the two groups in the pre- and post-treatment periods along with the differences for each group. The final DiD is the delta of the daily average kWh from the treatment group minus the delta of the daily average kWh from the control group. These data show that the post-treatment period had very similar average CDD to the pre-treatment period. Although the weather was similar in both periods, the treatment group's daily average kWh decreased by 1.74 kWh in the post period while the control group's daily average kWh decreased by only 0.15 kWh. This resulted in an estimated savings of 1.60 kWh per day in the summer months when applying the DiD approach. The estimated 1.60 kWh per day represented a savings of around 3.2% of what consumption would have been in the absence of participation.

Table 1-3: Summer Average Daily kWh and Cooling Degree Days (Base 72) by Group and Year

Group	Period	Mean Daily kWh	Total CDD72	Mean CDD72/day	Delta Daily kWh	Delta Total CDD	Delta Mean CDD/day	DiD (kWh/day)
Control	Pre	50.71	1,828	8.50				
Control	Post	50.56	1,782	8.47	(0.15)	(45.89)	(0.03)	
Treatment	Pre	51.78	1,828	8.50				
Treatment	Post	50.04	1,831	8.55	(1.74)	3.00	0.05	**1.60**

Similarly, Table 1-4 shows the DiD for the winter months. These data show that the post-treatment period was warmer than the pre-treatment period with a mean CDD of 1.7 versus 1.3 in the pre-

3 For the CDD in this analysis, Itron used a base temperature of 72 based on analysis to determine which threshold best explained the kWh variation. The analysis found no effect from HDD in the winter months yet the CDD of 72 is still significant in the winter months.

treatment period. Even though this analysis was performed on the winter months, there was no apparent effect on kWh as the weather cooled. As a result, heating degree days (HDD) were not included in the analysis. Although the weather was warmer post-treatment, the treatment group's daily average kWh increased by 0.84 kWh less than the control group's daily average kWh during the post-treatment period. The estimated 0.84 kWh per day represented a savings of around 2.3% of what consumption would have been in the absence of participation.

Table 1-4: Winter Average Daily kWh and Cooling Degree Days (Base 72) by Group and Year

Group	Period	Mean Daily kWh	Total CDD72	Mean CDD72/day	Delta Daily kWh	Delta Total CDD	Delta Mean CDD/day	DiD (kWh/day)
Control	Pre	33.45	192	1.28				
Control	Post	35.91	246	1.66	2.45	54.16	0.38	
Treatment	Pre	34.95	192	1.28				
Treatment	Post	36.56	250	1.67	1.61	58.50	0.39	**0.84**

As a means of testing the statistical significance of the estimated savings, Itron estimated a regression model of the average daily kWh as a function of three dummy variables: Group (treatment = 1), Period (Post = 1), and the interaction of the group and period (Group × Period). It is the interaction of treatment group and post period in this model that represents difference in differences. This statistical model was significant overall for summer and winter, showing that these independent variables have explanatory value. However, the parameter estimate for the DiD was only significant in the summer months, which is shown in Table 1-5.

Table 1-5: Parameter Estimates for DiD

Season	Parameter	Estimate	Standard Error	DF	t Value	Pr > |t|
Summer	Treatment=1 × Post=1	-1.5975	0.9179	400	-1.74	0.0825
Winter	Treatment=1 × Post=1	-0.8440	0.7649	400	-1.1	0.2705

The results in Table 1-5 show that the estimated DiD had relatively large standard errors, which makes the results less certain than is desirable.

Panel Time Series Regression

The second DiD approach was a panel time series regression, which was performed to account for more of the variability in consumption due to weather and other behaviors affecting households. This allowed the effect of the program to be estimated with less uncertainty. Of the many models tested, the final model selected based on goodness-of-fit and interpretability of results was as follows:

$$kWh_t = \alpha_i + \beta 1 \times CDD_t + \beta 2 \times Post + \beta 3 \times Post \times CDD_t + \beta 4 \times Treatment \times Post + \beta 5 \times Treatment \times Post \times CDD_t + \epsilon_t$$

Where:

- kWh_t represents the usage for a customer on day *t*,
- α_i is the "customer-specific" intercept (or error) for home *i*, accounting for unexplained difference in use between homes associated with the number of occupants, appliance holdings and lifestyle,
- CDD_t is a cooling degree day variable for day *t*,
- *Post* is a dummy variable indicating that the year is 2014
- *Treatment* is a dummy variable indicating the household is in the treatment group
- *B1* through *B5* is a matrix of coefficients to be estimated that quantify the impacts associated with the various interactions between variables, and
- ϵ_t is the error term.

The effect of the thermostats was estimated by using both a dummy variable (Treatment = 1 × Post = 1) and this same dummy variable interacted with CDD for the winter and summer months separately. Itron included the interaction of participation with weather since the regulation of cooling by the thermostat is assumed to be the source of energy savings.

Summer Energy Savings

The overall summer model was statistically significant. The parameter estimates for key variables are presented in Table 1-6. The variables of interest are in red. The parameter indicating the effects of the treatment had the correct sign to indicate savings was statistically significant. The parameter indicating the effects of the CDD on the treatment group has the correct sign to indicate savings but was not statistically significant. The lack of significance in that variable suggests that the level of CDD during the summer months is not a factor in energy savings, yet simply having the thermostat installed resulted in savings. This is likely due to the thermostat set point of the treatment group compared to the control group which is discussed in more detail later in this report.

Table 1-6: Key Parameter Estimates from Summer Daily kWh Regression Model

Parameter	Estimate	Standard Error	t Value	Pr > |t|
CDD	1.92	0.01	154.28	<.0001
Post	-0.70	0.23	-3.04	0.0023
Post × CDD	0.04	0.02	1.75	0.0807
Treatment × Post	-1.56	0.29	-5.44	<.0001
Treatment × Post × CDD	-0.01	0.03	-.36	0.7221

To calculate the estimated savings, one must multiply the estimate for the interacted variable by the average CDD during the treatment period and then add it to the estimate for the simple dummy for program participation. Following these steps, the model estimates 1.65 kWh per day savings in the summer, which is similar to what the simple DiD approach produced. However, because variables in the model account for so much more of the variability (R^2 = .67) in the dependent variable, the standard errors for these impacts are substantially lower.

Table 1-7: Summer Daily Energy Savings of Smart Thermostats

Season	Treatment	Treatment × CDD	Average Daily CDD	Total Daily Savings	% of Average Daily kWh
Summer	1.55	0.01	8.55	1. 65	3.3%

Hourly Energy Savings

The energy savings models based on daily consumption generate more reliable estimates of energy savings due to less unexplained variability, but for two reasons Itron estimated hourly models of energy savings. First, the effects of the thermostats should vary by the time of the day, so there was value in characterizing the impacts to verify that they conform to expectations. Second, to the extent that there are savings that occur during FPL's summer peak hour, such an analysis helped to quantify those impacts.

The model specification to estimate hourly energy savings was the same as that used for the daily model except that they were done separately for weekends and weekdays. In terms of a general characterization of the hourly energy savings, Figure 1-6 and Figure 1-7 show the hourly impact on the average weekday and weekend, respectively. As expected, the hourly impact on weekdays show substantial savings during the day when people likely have their thermostats set higher while they are at work. Later in the evening, their observed consumption goes higher than the reference line[4] indicating higher consumption, due to either a small snapback effect or the more intentional programming of the thermostat. In contrast, the weekend hourly impact is not as substantial. For example, there is no obvious thermostat set back in the morning as one would see around 8 AM on the weekday.

[4] Reference line is often referred to as the baseline. In this analysis, this is the household load profile in the absence of the treatment effect; i.e., no smart thermostat programming and load control.

Figure 1-6: Summer Hourly Energy Savings on Weekdays

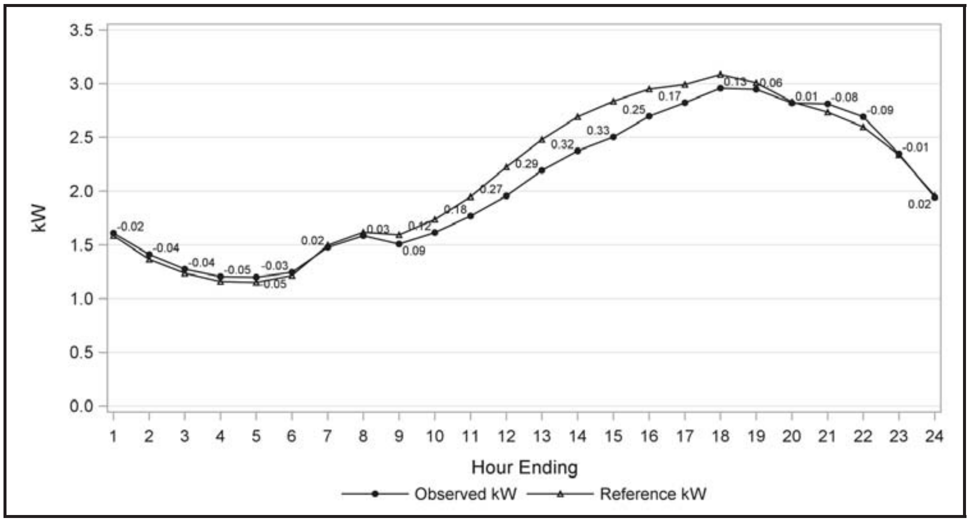

Figure 1-7: Summer Hourly Energy Savings on Weekends

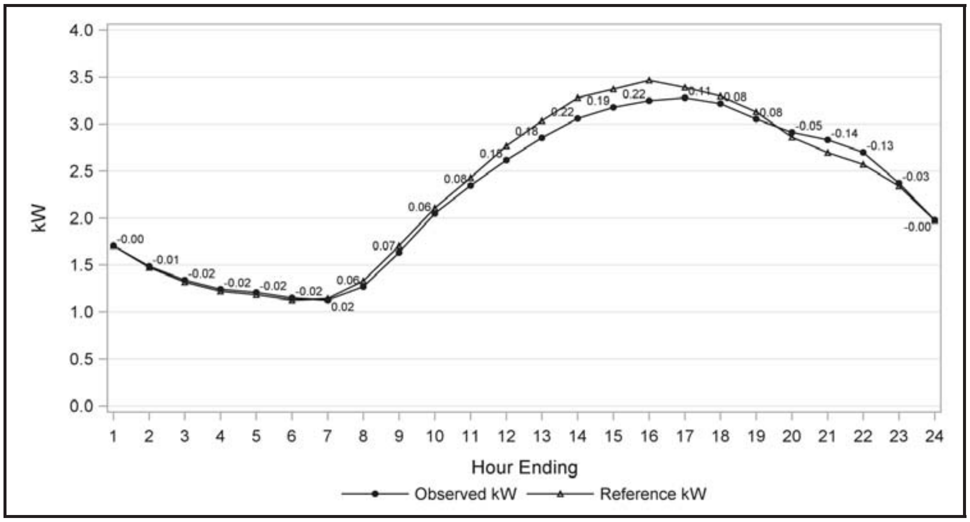

Given the apparent energy savings during the afternoon and early evening on summer weekdays, of greater interest to FPL are the savings during the peak hour from 4 - 5 PM, and particularly on hot days. Table 1-8 shows the hourly reference and observed kW along with the impacts for average summer weather and peak hot days. The average summer day impacts are based on the average cooling season (April through October) weekday temperatures. The peak day impacts were based on averages for the top 20 non-holiday and non-event weekdays in terms of maximum temperature.

Table 1-8: Summer Weekday Energy Savings for Average Day and Peak Hot Day

Hour Ending	Average Day Impacts				Peak Day Impacts			
	kW Reference	kW Observed	kW Impact	Percent Load Reduction	kW Reference	kW Observed	kW Impact	Percent Load Reduction
1:00	1.59	1.61	-0.024	-1.5%	1.98	2.02	-0.042	-2.1%
2:00	1.37	1.41	-0.044	-3.3%	1.76	1.82	-0.061	-3.5%
3:00	1.23	1.27	-0.039	-3.2%	1.60	1.65	-0.049	-3.0%
4:00	1.16	1.20	-0.045	-3.9%	1.50	1.57	-0.071	-4.7%
5:00	1.15	1.20	-0.048	-4.1%	1.46	1.54	-0.073	-5.0%
6:00	1.21	1.24	-0.031	-2.6%	1.50	1.55	-0.048	-3.2%
7:00	1.50	1.48	0.019	1.3%	1.72	1.70	0.019	1.1%
8:00	1.62	1.59	0.031	1.9%	1.83	1.79	0.034	1.8%
9:00	1.59	1.51	0.086	5.4%	1.77	1.66	0.110	6.2%
10:00	1.74	1.62	0.120	6.9%	2.04	1.85	0.189	9.3%
11:00	1.95	1.77	0.181	9.3%	2.42	2.13	0.292	12.1%
12:00	2.22	1.96	0.267	12.0%	2.77	2.42	0.348	12.6%
13:00	2.48	2.19	0.288	11.6%	3.10	2.74	0.360	11.6%
14:00	2.69	2.37	0.317	11.8%	3.43	3.05	0.384	11.2%
15:00	2.84	2.50	0.334	11.8%	3.65	3.26	0.394	10.8%
16:00	2.95	2.70	0.254	8.6%	3.87	3.59	0.278	7.2%
17:00	2.99	2.82	0.170	5.7%	3.97	3.79	0.182	4.6%
18:00	3.09	2.96	0.130	4.2%	4.06	3.95	0.109	2.7%
19:00	3.01	2.95	0.061	2.0%	3.93	3.88	0.047	1.2%
20:00	2.83	2.82	0.012	0.4%	3.60	3.63	-0.028	-0.8%
21:00	2.73	2.81	-0.078	-2.8%	3.44	3.57	-0.140	-4.1%
22:00	2.60	2.69	-0.093	-3.6%	3.28	3.42	-0.141	-4.3%
23:00	2.34	2.35	-0.012	-0.5%	2.96	2.98	-0.025	-0.8%
24:00	1.96	1.94	0.015	0.8%	2.52	2.53	-0.005	-0.2%
Entire Day (kWh)	**50.82**	**48.95**	**1.871**	**3.7%**	**64.17**	**62.10**	**2.067**	**3.2%**

The savings from 4 PM to 5 PM on peak days (in the shaded row in Table 1-8) were 0.18 kW, representing 4.6% of baseline consumption, though as one saw in Figure 1-6, this is an hour where the thermostat savings are starting to diminish relative to the other afternoon hours. Of the two parameters used to estimate savings, only the variable associated with base savings was statistically significant[5]. It is worth noting the savings for peak day weather, while larger in absolute terms, are lower as a percentage of baseline usage than the average summer day, which is due to the higher temperatures resulting in substantially higher baseline consumption.

Finally, one will notice that the over the entire day, the hourly impacts represent a total savings of 1.8 kWh for the average summer day, which is slightly higher than the 1.65 kWh from the daily model. In spite of this, it is important to note that the goodness-of-fit statistics from many of the hourly models are quite low, with very poor precision. For the results of this study, while the hourly profiles are both informative and intuitive – and certianly useful in certain hours – Itron has far more confidence in using the estimates from the daily energy savings models for the reported evaluated impacts.

Winter Energy Savings

Similarly, the overall winter model was statistically significant. The parameter estimates for key variables are presented in Table 1-9. The variables of interest are in red. In the winter months, both parameters of interest indicate savings occurred and both parameters were statistically significant. The significance of the treatment interacted with CDD suggests that temperature had an effect on the savings resulting from the smart thermostat. The hypothesis is that during the summer months, air conditioning is continually running because it is always hot, so the level of heat has less effect. In the winter months, air conditioning is only turned on when it is warm enough to need it, which results in more of an effect due to CDD. As noted early, there did not appear to be an effect on kWh as the temperature decreased in the winter months. Therefore, no HDD was used in the winter model, which means that there are no savings explicitly associated with heating.

Table 1-9: Key Parameter Estimates from Winter Daily kWh Regression Model

Parameter	Estimate	Standard Error	t Value	Pr > |t|
CDD	1.29	0.03	46.97	<.0001
Post	2.20	0.13	17.13	<.0001
Post × CDD	-0.15	0.04	-3.44	0.0006
Treatment × Post	-0.64	0.17	-3.65	0.0003
Treatment × Post × CDD	-0.13	0.05	-2.83	0.0047

As with the summer impacts, to calculate the estimated savings one must multiply the estimate for the interacted variable by the average CDD during the treatment period and then add it to the

5 The impacts are based on two variables in the regression model. The first is a dummy variable intended to capture base impacts, which for the peak hour had a parameter estimate of -0.152 (t = -5.290, p. <.001). The second was a dummy variable interacted with CDH, which had a parameter estimate of -0.002 (t = -0.721, p. = 0.471). The precision of the estimated savings with 90% confidence is +/- 14%.

estimate for the simple dummy for program participation. Following these steps, the model estimates daily energy savings of 0.85 kWh in the winter, which is similar to what the simple DiD approach produced. However, because variables in the model account for so much more of the variability (R^2 = .61) in the dependent variable, the standard errors for these impacts are substantially lower.

Table 1-10: Winter Daily Energy Savings of Smart Thermostats

Season	Treatment Estimate	Treatment × CDD Estimate	Average Daily CDD	Total Daily Savings (kWh/day)	% of Average Daily kWh
Winter	0.64	0.13	1.67	0.85	2.3%

A common concern with a program using a new technology such as smart thermostats is that the effect will decrease over time as the customer's interest in the product wanes. To test the energy savings persistence, Itron estimated the effects of the winter months of January, February, and March when the thermostats were newly installed separately from November and December after the customers had been using the thermostats for almost a year. The results of this comparison are presented in Table 1-11, which shows the model parameters, and Table 1-12, which shows how the results translate into daily energy savings. As expected, the estimated savings from conservation decreased later in the year, although significant savings were still found. This is not conclusive evidence that persistence could be a problem, but does suggest that it is a worthy research question for future studies.

Table 1-11: Key Parameter Estimates from Early vs. Late Winter Daily kWh Regression Model

Winter Period	Parameter	Estimate	Standard Error	t Value	Pr > |t|
Early	Treatment × Post	-0.75	0.22	-3.36	0.0008
Early	Treatment × Post × CDD	-0.17	0.07	-2.60	0.0094
Late	Treatment × Post	-0.46	0.27	-1.68	0.0921
Late	Treatment × Post × CDD	-0.11	0.06	-1.81	0.0696

Table 1-12: Winter Daily Energy Savings of Smart Thermostats by Early vs. Late in the Program Year

Winter Period	Treatment	Treatment × CDD	Average Daily CDD	Total Daily Savings (kWh/day)	% of Average Daily kWh
Early	0.75	0.17	1.51	1.01	2.77%
Late	0.46	0.11	1.90	0.67	1.82%

To further investigate the impact of the smart thermostats on energy savings during the winter, Itron ran the regression for each hour. Figure 1-8 and Figure 1-9 show the hourly impact on the average weekday and weekend, respectively. Similar to the hourly impact on weekdays in the summer months, the winter shows the most savings during the day when people are at work. Around the 8 AM hour, there is a spike in observed consumption followed by the thermostat set back. Unlike the summer months, there is no apparent snapback effect in the evening likely due to the lower temperatures. The weekend hourly impact is not as substantial as the weekday, though it is still clearly visible in the plots. Again, there is no obvious thermostat set back in the morning but there are visible savings at mid-day.

Figure 1-8: Winter Hourly Energy Savings on Weekdays

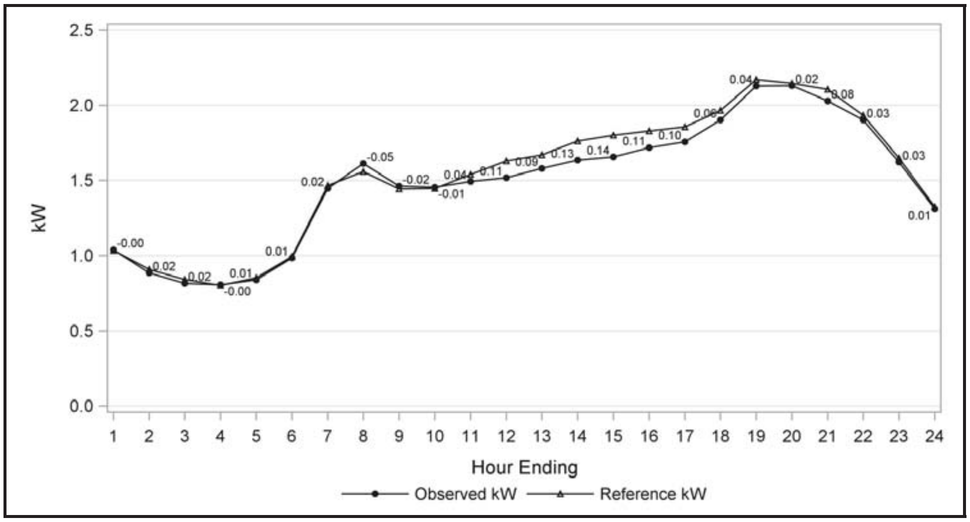

Figure 1-9: Winter Hourly Energy Savings on Weekends

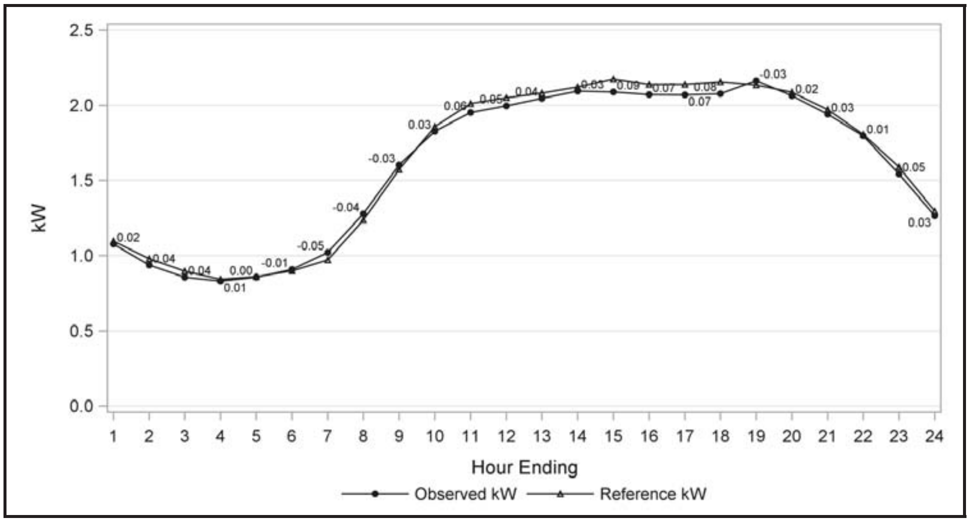

1.7 Demand Impacts from Load Control

On specific days, FPL controlled either air conditioning or electric space heating by sending a signal to the smart thermostats to cycle the HVAC equipment in question. The control took the form of cycling the HVAC equipment off 50% of the time; often referred to as 50% cycling. As long as the actual duty cycle of the HVAC during the controlled hours was greater than 50%, the cycling resulted in a reduction in load. A list of the ten events for 2014 is presented in Table 1-13, along with the event start and end times, the HVAC equipment controlled, and the number of participants included in the analysis.

Table 1-13: FPL SST Control Events for 2014

Event Number	Event Date	Event Start Time	Event End Time	HVAC System Controlled	Modeled Participants - No Override Group	Modeled Participants - Override Group	Total Modeled Participants
1	Jan 17, 2014	6 AM	8 AM	Space Heating	73	89	162
2	Feb 14, 2014	6 AM	8 AM	Space Heating	73	89	162
3	Jun 23, 2014	3 PM	7 PM	AC	73	89	162
4	Jun 24, 2014	3 PM	7 PM	AC	73	89	162
5	Aug 11, 2014	3 PM	7 PM	AC	73	89	162
6	Aug 13, 2014	3 PM	7 PM	AC	73	89	162
7	Aug 20, 2014	3 PM	7 PM	AC	73	89	162
8	Aug 21, 2014	3 PM	7 PM	AC	71	89	160
9	Sep 9, 2014	3 PM	7 PM	AC	69	89	158
10	Sep 15, 2014	3 PM	7 PM	AC	68	89	157

To estimate the effects of the HVAC load control on event days during the treatment period, Itron estimated regression models using both account-level and aggregated load data to model the hourly kW reduction and the snapback effects on the event days. The account-level models were estimated for two reasons. First, they more easily allowed for reflecting the impact of participants that stopped participation in the program after a certain date. Second, they do not require a control group, which means that the models can be estimated on every participant for which there was data available. Nevertheless, account-level data, particularly for residential customers, present major challenges, primarily that the high unexplained variability in individual households can make it difficult for a statistical model to differentiate between an actual program effect and random variation.

As an illustration of this variability, Figure 1-10 shows daily load profiles for a single household for two different event days. In addition to the event day loads, the figure presents the individual load profiles for the ten previous non-holiday weekdays as well as the average for those ten days. If one treats the average of the ten previous days as a reference load, or baseline, one of the event days would have no impact and the other would have a substantial impact.[6] However, on the event day where there is an impact, it is clear that this has nothing to do with air conditioner cycling, but simply reflects a pattern of occupancy where the resident is home on some days and away on others, as is the case for the second event day in the figure. The benefit of aggregating the loads

[6] The use of the ten-day average is a crude approximation of baseline consumption for illustration purposes. It is possible that a regression model might capture temperature effects and show an impact for the event on the left side of the figure.

is that it mitigates this day to day variability to allow the model to more accurately capture program impacts.

Figure 1-10: Illustration of Load Variability in a Single Home for Two Event Days

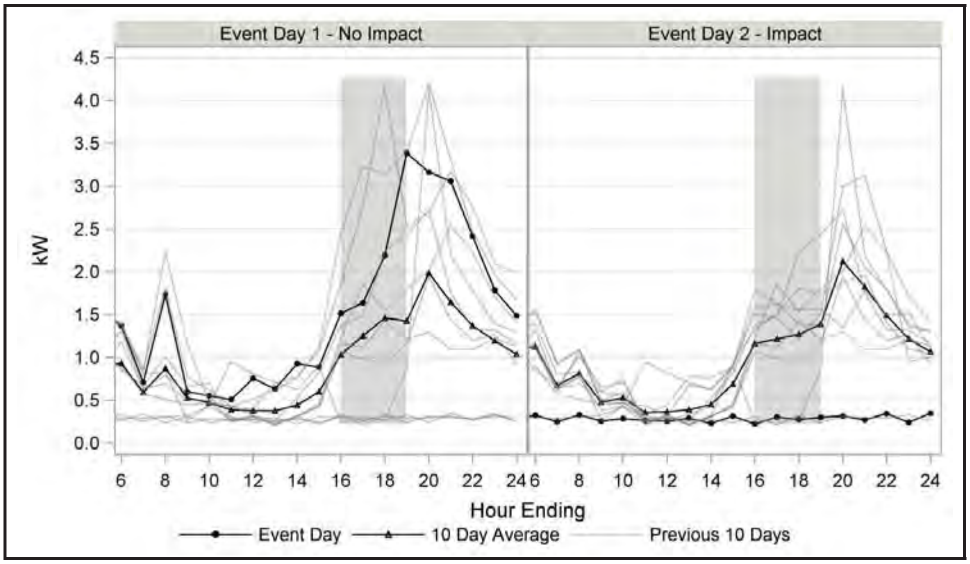

The influence of the type of variability illustrated in Figure 1-10 was apparent in the results from the models for individual households. Consequently, the estimated impacts presented here are based on the models that used aggregated data. The analysis of the aggregate data was further divided in two ways. First, the analysis was conducted separately for the two types of treatment groups (Override and No Override). Second, the analysis was done separately for summer and winter events.

The final regression model used in this analysis for both summer and winter events for the two treatment groups was as follows:

$$kW_t = \alpha_i + \beta 1 \times DH_t + \beta 2 \times DOW + \beta 3 \times Month + \beta 4 \times DOW \times Hour + \beta 5 \times DH_t \times Hour + \beta 6 \times Post + \beta 7 \times Post \times Treatment + \beta 8 \times Post \times Hour + \beta 9 \times Post \times Treatment \times Hour + \beta 10 \times EventDay \times DH_t \times Hour + \beta 11 \times EventDay \times Treatment \times DH_t \times Hour + \epsilon_t$$

Where:

- kW_t represents the kW demand for a customer during hour *t*,
- α_i is the "customer-specific" intercept (or error) for home *i*, accounting for unexplained difference in use between homes associated with the number of occupants, appliance holdings and lifestyle,
- DH_t is a degree hour (cooling degree hours [CDH] for summer, base 72, heating degree hours [HDH] for winter, base 65) variable for hour *t*,
- *DOW* is the day of the week
- *Month* is the month
- *Post* is a dummy variable indicating that the year is 2014
- *Treatment* is a dummy variable indicating the household is in the treatment group
- *EventDay* is a dummy variable indicating the event was called that day
- *B1* through *B11* is a matrix of coefficients to be estimated that quantify the impacts associated with the various interactions between variables, and
- ϵ_t is the error term.

Note that for estimation of winter impacts, due to markedly different weather conditions on the two event days, each event was modeled separately.

1.7.1 Summer Impacts by Override Group

The regression models for the Override and No Override group both resulted in similarly high goodness-of-fit statistics, with adjusted R^2 statistics of .916 and .914, respectively. Summaries of the hourly impact parameters and how they translate into average day impacts are presented in Table 1-14 and Table 1-15 for the two treatment groups. The hours of interest are those of the control period from 3 PM to 7 PM (presented in the darkly shaded rows with FPL's peak hour of 4 PM to 5 PM in bold text) and the two hours following, which help to assess any snapback effects (in lightly shaded rows). For both treatment groups, the regression models resulted in statistically significant negative parameter estimates during the four event hours, which are indicative of load reductions. In the two hours following the event, the models resulted in statistically significant positive parameter estimates, indicating a snapback effect. These parameter estimates represent the kW per CDH, so to convert these into impacts for the average event day they are multiplied by the average hourly CDH across the event days.

At the bottom of the table are summary rows showing the total kWh for the entire day, the event hours, the snapback hours, and the event and snapback hours combined. While the summary of the entire day is presented primarily for thoroughness, the final three summaries provide the total energy savings, the energy consumption associated with snapback, and the net energy savings, respectively.

Table 1-14: Average Summer Hourly Load Impact on Event Days in kW for the No Override Group

Regression Model Statistics					Average Event Day Summary				
Hour Ending	**Parameter Estimate**	**t Value**	**Pr > |t|**	**Standard Error**	**Mean °F**	**Reference kW**	**Observed kW**	**kW Impact**	**Percent Load Reduction**
1:00	0.000	0.000	1.000	0.0138	80.1	1.99	1.99	-0.000	-0.0%
2:00	0.004	0.290	0.772	0.0150	79.4	1.73	1.76	-0.032	-1.9%
3:00	0.004	0.254	0.799	0.0164	78.9	1.53	1.56	-0.029	-1.9%
4:00	0.005	0.289	0.772	0.0181	78.1	1.41	1.45	-0.032	-2.3%
5:00	0.004	0.216	0.829	0.0193	77.8	1.37	1.39	-0.024	-1.7%
6:00	0.010	0.458	0.647	0.0210	77.1	1.34	1.39	-0.049	-3.7%
7:00	0.006	0.286	0.775	0.0213	77.1	1.51	1.54	-0.031	-2.1%
8:00	0.004	0.279	0.780	0.0152	79.5	1.65	1.68	-0.032	-1.9%
9:00	-0.010	-0.983	0.326	0.0105	83.2	1.79	1.68	0.115	6.4%
10:00	-0.008	-0.957	0.338	0.0086	85.8	1.94	1.83	0.113	5.8%
11:00	-0.002	-0.305	0.760	0.0078	87.1	2.11	2.07	0.036	1.7%
12:00	-0.006	-0.817	0.414	0.0071	88.6	2.53	2.43	0.096	3.8%
13:00	-0.004	-0.529	0.597	0.0067	89.6	2.86	2.80	0.062	2.2%
14:00	-0.004	-0.630	0.529	0.0066	89.8	3.17	3.09	0.074	2.3%
15:00	-0.002	-0.255	0.798	0.0069	89.1	3.28	3.25	0.030	0.9%
16:00	-0.040	-5.846	<.001	0.0069	89.1	3.52	2.83	0.690	19.6%
17:00	**-0.039**	**-5.324**	**<.001**	**0.0072**	**88.4**	**3.64**	**3.00**	**0.631**	**17.3%**
18:00	-0.039	-4.972	<.001	0.0078	87.3	3.68	3.10	0.589	16.0%
19:00	-0.036	-4.344	<.001	0.0083	86.3	3.66	3.14	0.515	14.1%
20:00	0.042	4.207	<.001	0.0100	83.6	3.51	4.00	-0.487	-13.9%
21:00	0.043	3.886	<.001	0.0110	82.5	3.36	3.81	-0.449	-13.4%
22:00	0.019	1.711	0.087	0.0109	82.6	3.28	3.47	-0.198	-6.1%
23:00	0.022	1.840	0.066	0.0117	82.0	2.82	3.04	-0.216	-7.6%
24:00	0.020	1.645	0.100	0.0121	81.6	2.40	2.59	-0.191	-8.0%
Entire Day					83.5	60.08	58.90	1.181	2.0%
Event Hours					87.8	14.50	12.08	2.424	16.7%
Snapback Hours					86.2	6.88	7.81	-0.936	-13.6%
Event and Snapback – Net Impacts					86.2	21.38	19.89	1.489	7.0%

Table 1-15: Average Summer Hourly Load Impact on Event Days in kW for the Override Group

Regression Model Statistics					Average Event Day Summary				
Hour Ending	Parameter Estimate	t Value	Pr > |t|	Standard Error	Mean °F	Reference kW	Observed kW	kW Impact	Percent Load Reduction
1:00	-0.008	-0.591	0.554	0.0134	80.1	1.94	1.87	0.064	3.3%
2:00	-0.005	-0.351	0.726	0.0146	79.4	1.71	1.67	0.038	2.2%
3:00	-0.006	-0.394	0.694	0.0160	78.9	1.57	1.53	0.043	2.8%
4:00	-0.010	-0.592	0.554	0.0176	78.1	1.52	1.45	0.064	4.2%
5:00	0.003	0.166	0.868	0.0187	77.8	1.45	1.47	-0.018	-1.2%
6:00	-0.005	-0.256	0.798	0.0204	77.1	1.52	1.49	0.027	1.8%
7:00	-0.007	-0.326	0.744	0.0207	77.1	1.67	1.64	0.035	2.1%
8:00	-0.002	-0.150	0.881	0.0148	79.5	1.75	1.74	0.017	0.9%
9:00	-0.006	-0.596	0.551	0.0102	83.3	1.64	1.57	0.068	4.1%
10:00	-0.011	-1.312	0.189	0.0083	85.8	1.82	1.67	0.150	8.2%
11:00	-0.016	-2.112	0.035	0.0076	87.1	2.12	1.88	0.242	11.4%
12:00	-0.011	-1.534	0.125	0.0069	88.6	2.38	2.20	0.176	7.4%
13:00	-0.006	-0.969	0.333	0.0065	89.6	2.69	2.58	0.111	4.1%
14:00	-0.006	-0.941	0.347	0.0064	89.8	2.95	2.85	0.107	3.6%
15:00	-0.006	-0.967	0.334	0.0067	89.1	3.21	3.10	0.111	3.4%
16:00	-0.040	-5.984	<.001	0.0067	89.1	3.49	2.81	0.686	19.6%
17:00	**-0.040**	**-5.727**	**<.001**	**0.0070**	**88.4**	**3.65**	**2.99**	**0.660**	**18.1%**
18:00	-0.043	-5.703	<.001	0.0076	87.2	3.85	3.20	0.657	17.0%
19:00	-0.036	-4.454	<.001	0.0081	86.2	3.77	3.25	0.513	13.6%
20:00	0.013	1.359	0.174	0.0097	83.6	3.64	3.79	-0.153	-4.2%
21:00	0.013	1.240	0.215	0.0107	82.5	3.49	3.63	-0.139	-4.0%
22:00	0.007	0.661	0.509	0.0106	82.6	3.25	3.32	-0.075	-2.3%
23:00	-0.001	-0.102	0.919	0.0114	82.0	2.86	2.85	0.012	0.4%
24:00	-0.004	-0.325	0.745	0.0117	81.6	2.35	2.32	0.037	1.6%
Entire Day					83.5	60.31	56.88	3.432	5.7%
Event Hours					87.7	14.77	12.25	2.516	17.0%
Snapback Hours					86.2	7.13	7.42	-0.292	-4.1%
Event and Snapback – Net Impacts					86.2	21.90	19.67	2.223	10.2%

The effects of the load control events are presented graphically in Figure 1-11. This shows the average observed load, which is the average of the actual loads on event days, and the average reference load, which represents an estimate of what would have occurred in the absence of the event. It is apparent by the increased slope of the Override group that they begin overriding roughly one hour into the event. Once the event is over, the No Override group shows a larger snapback effect which is likely the result of additional cooling that must occur compared to the group who had the ability to override during the event. In addition to this figure for the average event day, Itron calculated the observed and reference loads for each of the individual event days, which are presented in graphical representations in Appendix 1.

Figure 1-11: Average Summer Event Day Observed Load Compared to Expected Load without the Event

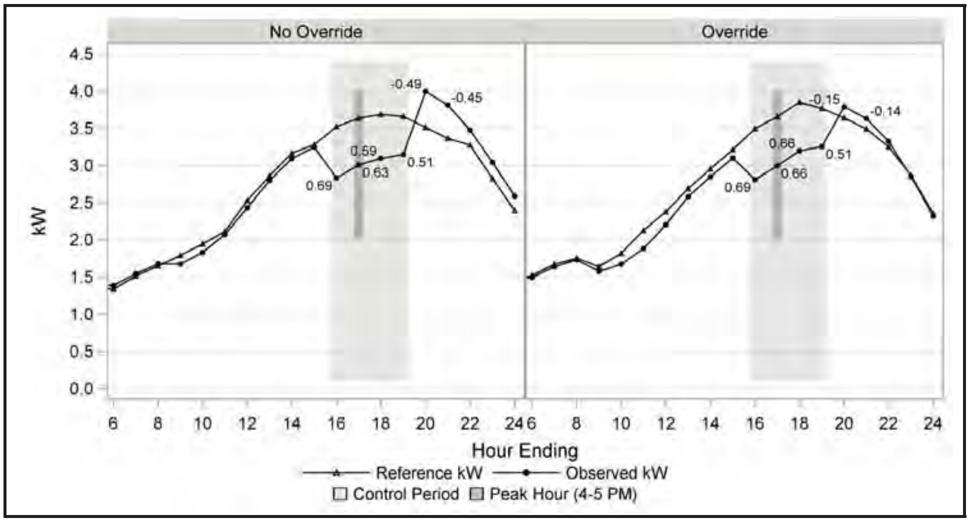

While the control period impacts for both the Override and No Override groups represented in Figure 1-11 are very similar, they do show that the Override group's impacts are larger in the second and third hours of the control period. Given these results, it is important to stress that there was not any statistically significant differences in the impacts during the control period, so one should be hesitant to ascribe any meaning to these counter-intuitive differences. As an illustration of this, Figure 1-12 shows the estimated impacts by group for the control period and the three hours before and after along with the 90% confidence bands. These bands (shaded with dotted outline for the No Override group and no shading with a solid outline for the Override group) indicate the range where the impacts would likely fall 90% of the time given the variability in the data. The third hour of the control period – which is when one would expect overrides to show more influence – is annotated with an arrow and text as to emphasize that the impact for the No Override group falls well within confidence band for the Override group. In contrast, the first hour after the event is also annotated, showing that the estimated snapback effect for the No Override group falls outside of confidence band for the Override group.

Figure 1-12: Illustration of Confidence Bands for Average Hourly Impacts by Treatment Group

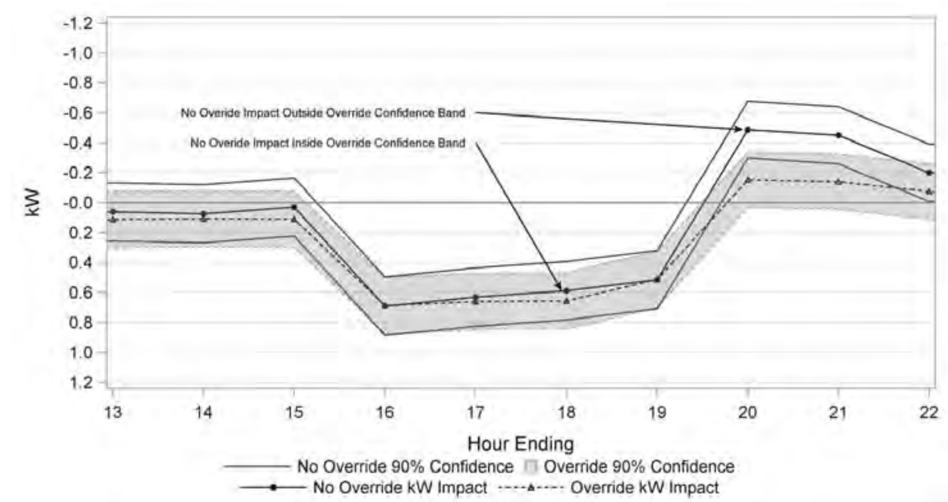

As a final observation on the summer event impacts, the ability of participants to opt out would seem to be a potentially significant factor. In the case of this STT, however, the influence on impacts appears to be marginal at most. For one, relatively few participants used their override capability during the summer event. As shown in Table 1-16, the August 21 event had the most participants opting out, yet just 15 of 95 elected to override the event. Additionally, the overrides were rarely for the full duration of the event. For example, the average time at which participants opted out was always after 4 PM, or at least one hour after the event start time of 3 PM. For several events, the average time to opt out was after 5 PM. The small number of homes opting out along with timing of the overrides meant that the number of minutes overridden was only a small percentage of the total, ranging from low of 2.3% to a high of 10.3%.

Table 1-16: Summary of Households Opting Out for the Override Group

Event Date	Participants Overriding	Average Override Time	% Minutes Override
June 23, 2014	7	17:01	3.7%
June 24, 2014	10	16:52	5.6%
August 11, 2014	6	17:30	2.3%
August 13, 2014	10	16:57	5.4%
August 20, 2014	7	16:55	3.8%
August 21, 2014	15	16:24	10.3%
September 9, 2014	10	17:11	4.7%
September 15, 2014	14	16:48	8.1%

If anything, a more substantial impact of the ability to override is that it appears to mitigate the snapback effect. This was observed in the results from the analysis of the event impacts, where the Override group showed a substantially smaller increase in whole home consumption in the hours following the event. This is echoed in the analysis of thermostat run time data presented in later in this report, though not as markedly.

Concurrent versus Staggered Rollout

The final two events during the summer of 2014 (September 9 and September 15) were implemented by initiating the control in homes gradually over a five-minute period as opposed to a simultaneous start for all participants. The effects of this staggered rollout are best demonstrated in the thermostat data because of its greater detail (15-minute intervals versus hourly for the load data) and the fact that it shows actual HVAC run time (versus whole home load). Figure 1-13 provides a graphical representation of the percent of cooling during an event with concurrent rollout versus an event with a staggered rollout for the Override and No Override groups.[7] The effect of the staggered rollout is best illustrated by examining the duty cycle for the No Override Group, since it does not include the influence of any override behavior. In Figure 1-13, the circled series labeled “A” shows that the duty cycle drops to zero every other 15 minute period on the concurrent event start. Though the difference is subtle, the series labeled “B” shows that the duty cycle does not drop all the way to zero, indicating that a small portion of participants are not cycled to zero for the duration of the 15-minute interval.

Another interesting effect of the five-minute rollout is the snapback effect. As shown in the circled area labeled “C”, on September 15 there appeared to be a secondary snapback after the event period. This is in contrast to the concurrent enrollment event, where the duty cycle peaks immediately after the event and then decreases relatively steadily. This is relevant if the secondary snapback is also associated with lessened initial peak following the event, which might make a

[7] August 20, 2014 and September 15, 2014 were chosen for comparison since they have a similar number of overrides during the event—16 overrides and 18 overrides, respectively.

gradual rollout of the control preferable from a system perspective. Note that this phenomenon appears for the Override group as well, although there is also the influence of event overrides to consider.

Figure 1-13: Comparison of AC Duty Cycles for Concurrent vs. Staggered Rollout

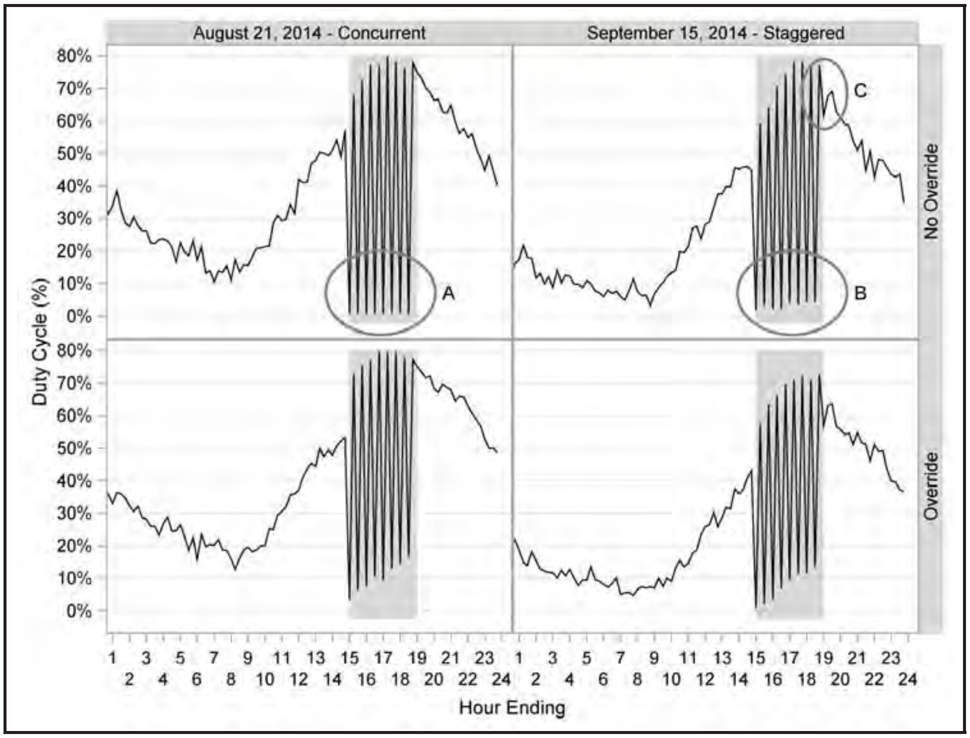

Another value of the thermostat data is that they allow for the allocation of snapback into 15-minute intervals by converting the air conditioning run time into hourly shares and then multiplying these by the estimated snapback effects. Figure 1-14 shows these 15-minute impacts during the three hours following the event. While the snapback is estimated to be in the two hours following the event – and only those hours had statistically significant parameter estimates – a third hour is included to illustrate the level at which any impacts drop off. As with the hourly impacts, it is clear that the Override group has a lower snapback. As the figure illustrates, the snapback is fairly steady across the hour. While the duty cycle itself shows a more defined slope at the scale in Figure 1-13, when the impact is allocated to the 15-minute periods and shown on the kWh scale, the defined slope is not as obvious. These data are presented in tabular format in Table 1-17.

Figure 1-14: Average 15-Minute kW Snapback during the Summer Events

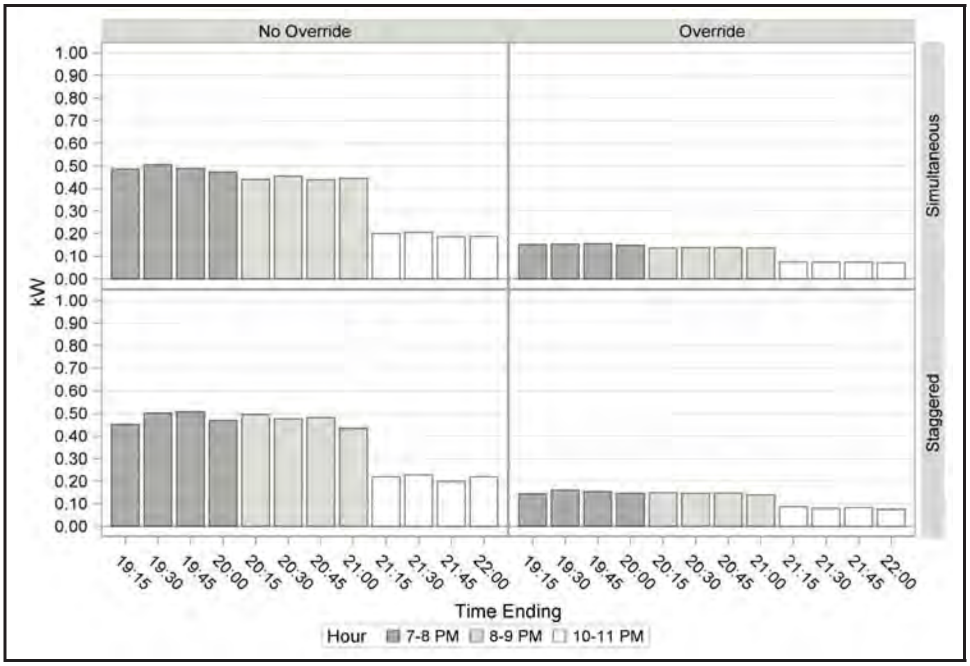

Table 1-17: Average 15-Minute Snapback During Summer Events

Time		No Override		Override	
		Simultaneous	Staggered	Simultaneous	Staggered
7-8 PM	19:15	0.49	0.45	0.15	0.14
	19:30	0.51	0.50	0.15	0.16
	19:45	0.49	0.51	0.16	0.15
	20:00	0.47	0.47	0.15	0.15
8-9 PM	20:15	0.44	0.50	0.14	0.15
	20:30	0.45	0.47	0.14	0.15
	20:45	0.44	0.48	0.14	0.15
	21:00	0.44	0.43	0.14	0.14
10-11 PM	21:15	0.20	0.22	0.07	0.09
	21:30	0.21	0.23	0.07	0.08
	21:45	0.19	0.20	0.07	0.08
	22:00	0.19	0.22	0.07	0.08

1.7.2 Winter Impacts by Override Group

Unlike the summer event days, the winter events did not show any obvious impact on load curtailment. The regression results for the final models, which estimated impacts separately for the treatment groups and the two event dates, are presented in Table 1-18, Table 1-19, Table 1-20, and Table 1-21. For the sake of consistency with the summer impacts, the results are presented for the entire day, but the key results are for hours ending 7 AM and 8 AM, which represent the event period (in dark gray, with FPL's winter peak hour in bold text), and the two hours after, where any potential snapback might occur (in light gray). In the case of the January event day, which was the colder of the two winter events and on the second day of a cold streak, the model did result in negative parameter coefficients for the impact variables, but they were not statistically significant. For the February event, only one of the event hours for the No Override group was negative, but again it was not statistically significant.

Table 1-18: Winter Load Impact on January 17 in kW for the No Override Group

Hour Ending	Regression Model Statistics				Average Event Day Summary				
	Parameter Estimate	t Value	Pr > |t|	Standard Error	Mean °F	Reference kWh	Observed kWh	kWh Impact	Percent Load Reduction
1:00	-0.025	-1.458	0.145	0.0173	44.0	1.93	1.40	0.529	27.4%
2:00	-0.013	-0.752	0.452	0.0173	44.0	1.76	1.48	0.272	15.5%
3:00	-0.002	-0.123	0.902	0.0165	43.0	1.52	1.47	0.045	3.0%
4:00	-0.016	-1.014	0.310	0.0158	42.0	1.72	1.35	0.368	21.4%
5:00	-0.007	-0.426	0.670	0.0158	42.0	1.82	1.66	0.154	8.5%
6:00	-0.001	-0.085	0.932	0.0173	44.0	1.98	1.95	0.031	1.6%
7:00	-0.029	-1.682	0.093	0.0173	44.0	2.97	2.36	0.610	20.5%
8:00	**-0.032**	**-1.765**	**0.078**	**0.0181**	**45.0**	**3.28**	**2.64**	**0.640**	**19.5%**
9:00	0.026	1.092	0.275	0.0242	50.0	2.74	3.14	-0.396	-14.4%
10:00	0.005	0.150	0.880	0.0330	54.0	2.66	2.71	-0.055	-2.1%
11:00	-0.040	-0.770	0.441	0.0518	58.0	2.19	1.91	0.279	12.8%
12:00	-0.023	-0.258	0.796	0.0906	61.0	1.82	1.73	0.094	5.1%
13:00	-0.224	-0.618	0.537	0.3626	64.0	1.73	1.51	0.224	12.9%
14:00	0.000	NA	NA	NA	65.0	1.46	1.46	0.000	0.0%
15:00	0.196	0.541	0.589	0.3626	64.0	1.09	1.28	-0.196	-18.0%
16:00	0.246	0.678	0.498	0.3626	64.0	1.24	1.48	-0.246	-19.9%
17:00	0.085	0.706	0.480	0.1209	62.0	1.30	1.56	-0.256	-19.7%
18:00	-0.010	-0.158	0.875	0.0604	59.0	1.72	1.66	0.057	3.3%
19:00	-0.037	-0.806	0.420	0.0453	57.0	2.16	1.86	0.292	13.5%
20:00	-0.008	-0.207	0.836	0.0363	55.0	2.20	2.12	0.075	3.4%
21:00	0.003	0.069	0.945	0.0363	55.0	1.81	1.83	-0.025	-1.4%
22:00	-0.024	-0.661	0.509	0.0363	55.0	2.00	1.76	0.240	12.0%
23:00	0.014	0.427	0.669	0.0330	54.0	1.74	1.89	-0.155	-8.9%
24:00	-0.011	-0.410	0.682	0.0279	52.0	1.69	1.54	0.149	8.8%
Entire Day					53.2	46.51	43.78	2.730	5.9%
Event Hours					47.5	6.02	5.78	0.244	4.1%
Snapback Hours					51.8	4.85	4.62	0.225	4.6%
Event and Snapback – Net Impacts					51.8	10.87	10.40	0.469	4.3%

Table 1-19: Winter Load Impact on January 17th in kW for the Override Group

Hour Ending	Regression Model Statistics				Average Event Day Summary				
	Parameter Estimate	t Value	Pr > |t|	Standard Error	Mean °F	Reference kWh	Observed kWh	kWh Impact	Percent Load Reduction
1:00	0.005	0.291	0.771	0.0176	44.0	1.98	2.09	-0.108	-5.4%
2:00	-0.004	-0.218	0.827	0.0176	44.0	1.83	1.75	0.081	4.4%
3:00	-0.008	-0.453	0.651	0.0168	43.0	1.96	1.79	0.168	8.6%
4:00	-0.003	-0.201	0.841	0.0161	42.0	1.94	1.86	0.075	3.8%
5:00	0.009	0.568	0.570	0.0161	42.0	2.04	2.26	-0.210	-10.3%
6:00	0.011	0.636	0.525	0.0176	44.0	2.41	2.65	-0.236	-9.8%
7:00	-0.029	-1.649	0.099	0.0176	44.0	3.71	3.10	0.611	16.5%
8:00	**-0.013**	**-0.687**	**0.492**	**0.0185**	**45.0**	**3.56**	**3.31**	**0.255**	**7.1%**
9:00	0.002	0.099	0.921	0.0247	50.0	3.39	3.43	-0.037	-1.1%
10:00	0.020	0.584	0.559	0.0337	54.0	2.53	2.75	-0.216	-8.6%
11:00	0.022	0.410	0.682	0.0529	58.0	2.34	2.49	-0.152	-6.5%
12:00	-0.018	-0.196	0.845	0.0926	61.0	2.05	1.98	0.073	3.5%
13:00	-0.203	-0.548	0.584	0.3705	64.0	1.86	1.65	0.203	10.9%
14:00	0.000	NA	NA	NA	65.0	1.85	1.85	0.000	0.0%
15:00	0.369	0.996	0.319	0.3705	64.0	1.31	1.68	-0.369	-28.2%
16:00	0.173	0.467	0.640	0.3705	64.0	1.40	1.57	-0.173	-12.4%
17:00	0.067	0.543	0.587	0.1235	62.0	1.54	1.75	-0.201	-13.0%
18:00	-0.016	-0.261	0.794	0.0618	59.0	1.89	1.79	0.097	5.1%
19:00	-0.037	-0.803	0.422	0.0463	57.0	2.25	1.95	0.298	13.2%
20:00	-0.014	-0.382	0.702	0.0371	55.0	2.17	2.03	0.142	6.5%
21:00	-0.027	-0.723	0.470	0.0371	55.0	2.23	1.96	0.268	12.0%
22:00	0.001	0.040	0.968	0.0371	55.0	2.05	2.06	-0.015	-0.7%
23:00	0.004	0.109	0.913	0.0337	54.0	1.84	1.88	-0.040	-2.2%
24:00	-0.000	-0.010	0.992	0.0285	52.0	1.62	1.62	0.004	0.2%
Entire Day					53.2	51.78	51.26	0.514	1.0%
Event Hours					47.5	6.95	6.74	0.218	3.1%
Snapback Hours					51.8	4.87	5.24	-0.368	-7.6%
Event and Snapback – Net Impacts					51.8	11.82	11.97	-0.150	-1.3%

Table 1-20: Winter Load Impact on February 14th in kW for the No Override Group

Hour Ending	Regression Model Statistics				Average Event Day Summary				
	Parameter Estimate	t Value	Pr > |t|	Standard Error	Mean °F	Reference kWh	Observed kWh	kWh Impact	Percent Load Reduction
1:00	-0.003	-0.103	0.918	0.0279	52.0	0.87	0.83	0.037	4.3%
2:00	0.003	0.141	0.888	0.0242	50.0	0.79	0.84	-0.051	-6.5%
3:00	-0.002	-0.095	0.924	0.0259	51.0	0.73	0.69	0.035	4.7%
4:00	0.010	0.491	0.624	0.0214	48.0	0.72	0.90	-0.178	-24.7%
5:00	0.009	0.445	0.657	0.0202	47.0	0.97	1.13	-0.161	-16.6%
6:00	0.002	0.098	0.922	0.0182	45.0	1.25	1.29	-0.036	-2.8%
7:00	-0.007	-0.386	0.700	0.0182	45.0	1.80	1.66	0.140	7.8%
8:00	**0.004**	**0.196**	**0.845**	**0.0214**	**48.0**	**2.11**	**2.19**	**-0.071**	**-3.4%**
9:00	0.022	0.787	0.432	0.0279	52.0	1.89	2.17	-0.286	-15.1%
10:00	-0.012	-0.265	0.791	0.0454	57.0	1.62	1.52	0.096	6.0%
11:00	-0.020	-0.216	0.829	0.0908	61.0	1.42	1.34	0.078	5.5%
12:00	0.009	0.024	0.981	0.3631	64.0	1.16	1.16	-0.009	-0.8%
13:00	0.000	NA	NA	NA	66.0	1.13	1.13	0.000	0.0%
14:00	0.000	NA	NA	NA	66.0	1.19	1.19	0.000	0.0%
15:00	0.000	NA	NA	NA	67.0	1.09	1.09	0.000	0.0%
16:00	0.000	NA	NA	NA	68.0	1.20	1.20	0.000	0.0%
17:00	0.000	NA	NA	NA	67.0	1.00	1.00	0.000	0.0%
18:00	0.000	NA	NA	NA	66.0	1.17	1.17	0.000	0.0%
19:00	0.011	0.059	0.953	0.1815	63.0	1.54	1.56	-0.021	-1.4%
20:00	0.062	0.516	0.606	0.1210	62.0	1.59	1.78	-0.187	-11.8%
21:00	0.017	0.282	0.778	0.0605	59.0	1.42	1.52	-0.102	-7.2%
22:00	0.003	0.038	0.969	0.0726	60.0	1.39	1.41	-0.014	-1.0%
23:00	-0.005	-0.151	0.880	0.0363	55.0	1.24	1.18	0.055	4.4%
24:00	0.002	0.043	0.966	0.0363	55.0	1.07	1.08	-0.016	-1.5%
Entire Day					57.3	30.35	31.04	-0.691	-2.3%
Event Hours					50.0	4.00	4.36	-0.357	-8.9%
Snapback Hours					54.5	3.04	2.86	0.175	5.7%
Event and Snapback – Net Impacts					54.5	7.04	7.22	-0.182	-2.6%

Table 1-21: Winter Load Impact on February 14th in kW for the Override Group

	Regression Model Statistics				Average Event Day Summary				
Hour Ending	Parameter Estimate	t Value	Pr > |t|	Standard Error	Mean °F	Reference kWh	Observed kWh	kWh Impact	Percent Load Reduction
1:00	0.009	0.310	0.757	0.0285	52.0	0.70	0.82	-0.115	-16.4%
2:00	-0.002	-0.086	0.932	0.0247	50.0	0.76	0.73	0.032	4.2%
3:00	-0.012	-0.464	0.642	0.0265	51.0	0.89	0.71	0.172	19.5%
4:00	-0.003	-0.125	0.901	0.0218	48.0	0.84	0.79	0.046	5.5%
5:00	0.001	0.029	0.977	0.0206	47.0	0.99	1.00	-0.011	-1.1%
6:00	0.011	0.592	0.554	0.0185	45.0	1.22	1.44	-0.220	-18.0%
7:00	0.011	0.593	0.553	0.0185	45.0	1.79	2.01	-0.220	-12.3%
8:00	**0.006**	**0.274**	**0.784**	**0.0218**	**48.0**	**2.08**	**2.18**	**-0.102**	**-4.9%**
9:00	0.025	0.870	0.385	0.0285	52.0	1.74	2.06	-0.323	-18.6%
10:00	0.037	0.802	0.422	0.0464	57.0	1.44	1.74	-0.298	-20.6%
11:00	0.009	0.092	0.926	0.0927	61.0	1.55	1.59	-0.034	-2.2%
12:00	0.112	0.303	0.762	0.3709	64.0	1.39	1.50	-0.112	-8.1%
13:00	0.000	NA	NA	NA	66.0	1.40	1.40	0.000	0.0%
14:00	0.000	NA	NA	NA	66.0	1.52	1.52	0.000	0.0%
15:00	0.000	NA	NA	NA	67.0	1.33	1.33	0.000	0.0%
16:00	0.000	NA	NA	NA	68.0	1.39	1.39	0.000	0.0%
17:00	0.000	NA	NA	NA	67.0	1.31	1.31	0.000	0.0%
18:00	0.000	NA	NA	NA	66.0	1.39	1.39	0.000	0.0%
19:00	0.030	0.164	0.870	0.1855	63.0	1.55	1.61	-0.061	-3.9%
20:00	-0.066	-0.534	0.594	0.1236	62.0	1.64	1.44	0.198	12.1%
21:00	-0.007	-0.114	0.909	0.0618	59.0	1.64	1.60	0.042	2.6%
22:00	0.031	0.419	0.675	0.0742	60.0	1.44	1.60	-0.155	-10.8%
23:00	-0.001	-0.034	0.973	0.0371	55.0	1.23	1.22	0.012	1.0%
24:00	-0.005	-0.132	0.895	0.0371	55.0	1.22	1.17	0.049	4.0%
Entire Day					57.3	32.44	33.53	-1.098	-3.4%
Event Hours					50.0	3.81	4.24	-0.424	-11.1%
Snapback Hours					54.5	3.00	3.33	-0.332	-11.1%
Event and Snapback – Net Impacts					54.5	6.81	7.57	-0.756	-11.1%

The winter events are presented graphically in Figure 1-15 and Figure 1-16. In contrast to the summer events, the reference and observed series do not present an intuitive portrayal of what one would expect for an event. Throughout the day, the loads are less predictable and the observed loads do not show the same clear drop at the start of the event that was visible in the summer events. Overall, the series suggest that the differences during the event hours are as likely due to noise as they are any event effects.

Figure 1-15: Load Control Impact on January 17, 2014

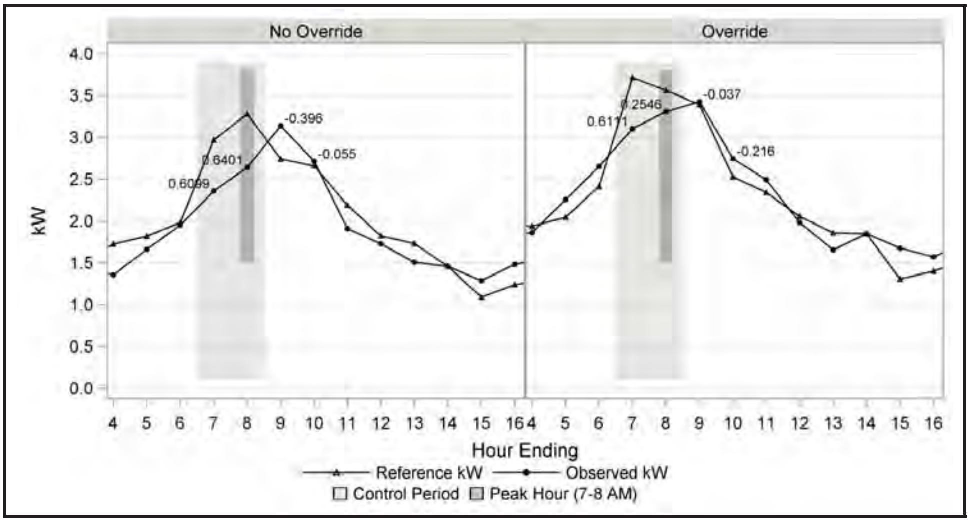

Figure 1-16: Load Control Impact on February 14, 2014

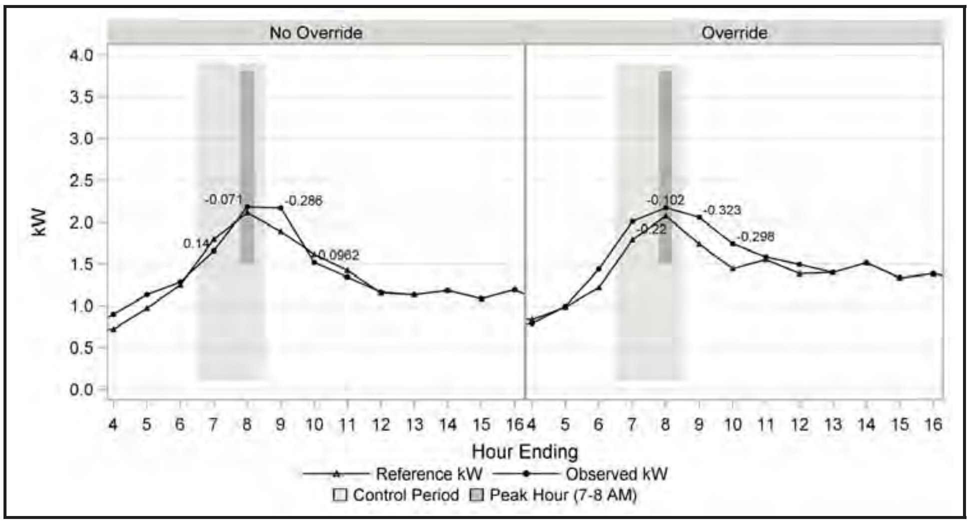

It is important to stress that these results do not mean that there is not any load curtailment in some homes. In fact – though the results have their own caveats – the individual household models did find significant impact parameters in about 8% of the homes. Nevertheless, the cases of curtailment resulting in savings are too few and of too small magnitude to be captured in the aggregate and are not indicative of any substantial savings.

While certainly disappointing from a program perspective, there is ample evidence in the thermostat data to show that the lack of impact in winter is rooted in a limited use of heating in participant homes. First of all, a substantial number of homes were not using any heating during the event hours on either of the event days. For the January event, 57% of the homes had no heating during the event hours. In February, this figure was 72%. Furthermore, for those homes that had any heating, the duty cycle was only marginally higher than 50%, if at all. Figure 1-17 shows the average duty cycles by event date and treatment group for the households that used heating. Although the colder temperatures for the January event are evident, the average duty cycle is still below 50%. Additionally, while the program impact is seen in the synchronization of the duty cycles, there is no evidence to suggest that the event decreased consumption. Therefore, using a cycling strategy during winter events is likely to be less effective in achieving load reductions than a shedding strategy.

Figure 1-17: Heating Duty Cycles by Date and Treatment Group for Homes Using Heating

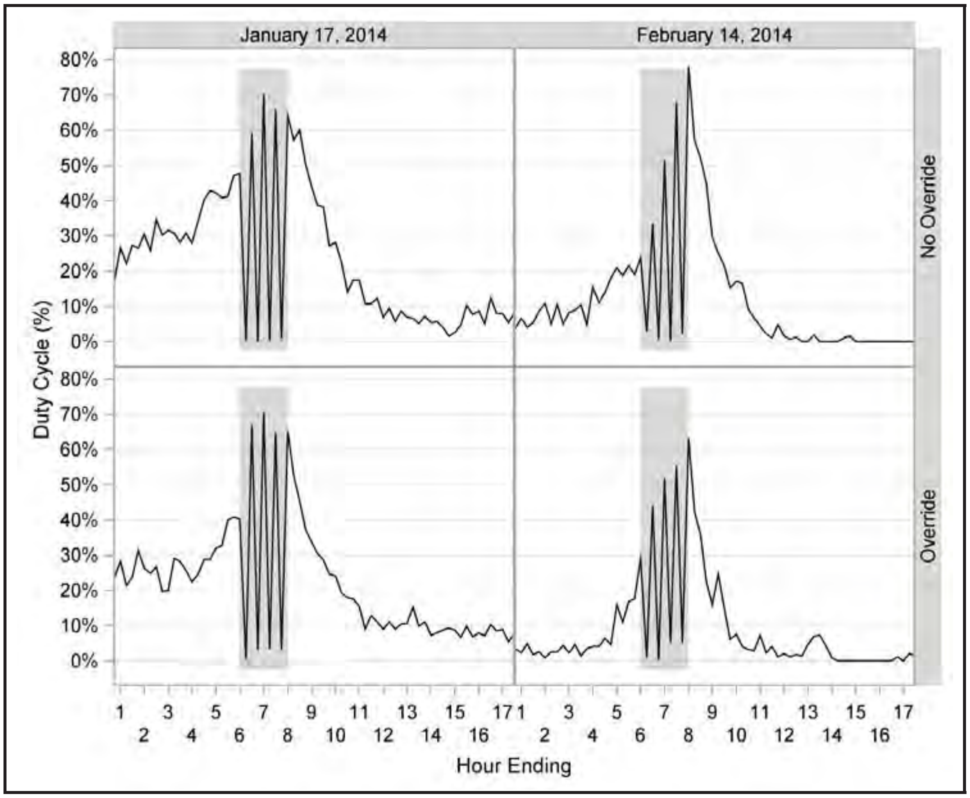

Thermostat Set Point Analysis

For this study's third objective, Itron conducted an analysis of the thermostat set points and indoor temperatures on event days to better understand how customers used the smart thermostats and how indoor temperatures might be related to override behavior.

With respect to scheduling, a report generated by [redacted] indicated that all but six participants had gone through a Scheduling Wizard to set up a schedule of set points. In spite of this, analysis of the actual thermostat data suggests that some of those homes scheduled a single set point that did not vary throughout the day and, therefore, are not truly programming their thermostats. To illustrate this, Figure 1-18 presents the distribution of average daily set point changes by month. The left columns show the percentage of homes that did not change their set point on average throughout the month. The data do not indicate if the set point change was manual or due to a pre-defined schedule. However, it can be noted that more homes altered their set points more frequently during the early summer months.

Figure 1-18: Thermostat Changes per Day as % of Homes Each Month

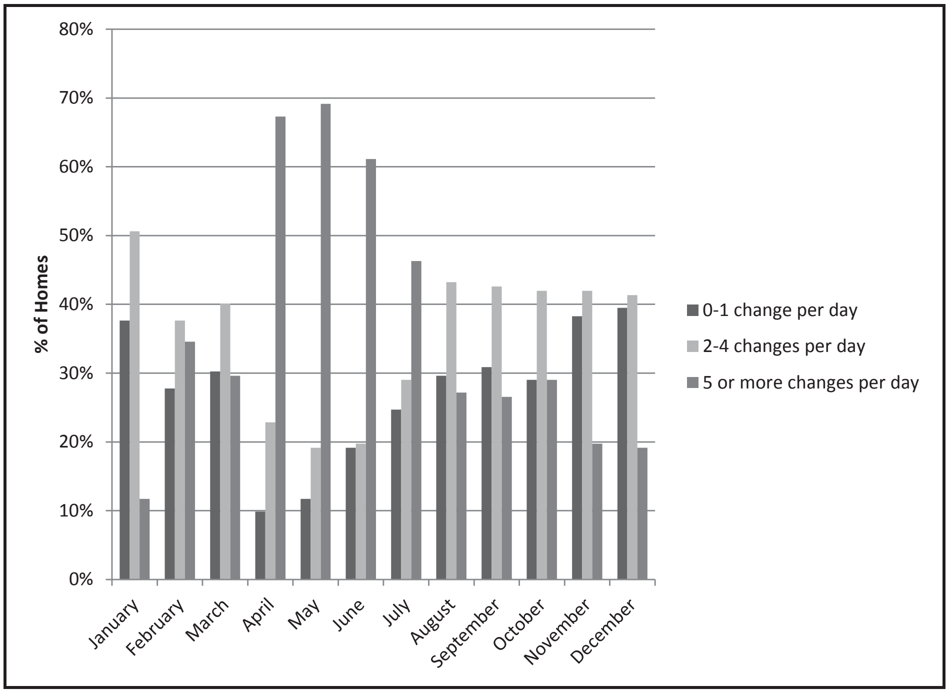

In the analysis of energy savings presented in the previous section, there was an obvious setback around 8:00 AM during the week. The thermostat data concurred with this finding as shown in the percentage of active thermostats (only thermostats in the cooling or heating settings) changed by hour during the week versus weekend in Figure 1-19. This shows that the most set point changes are occurring from 7 AM to 9 AM as people are waking and leaving the home for the day, from 5 PM to 6 PM as people are arriving home, and again from 10 PM to 11 PM when they are going to bed.

Figure 1-19: Hourly Set Point Changes as % of Active Thermostats

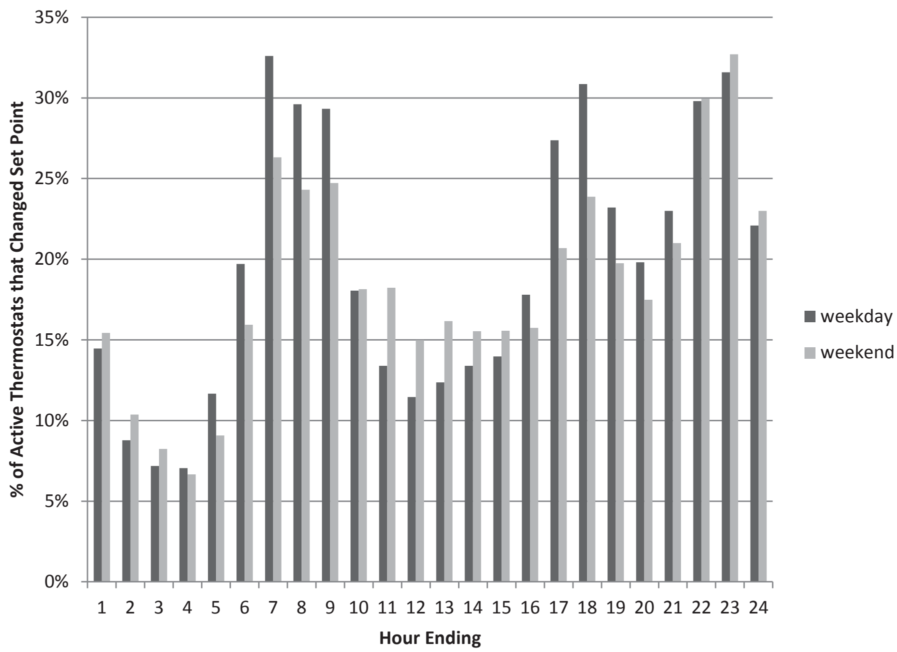

The thermostat data also provided more insight into the temperatures observed within homes during the event periods. Figure 1-1 presents the average indoor temperature of the No Override Group compared to the Override Group. For the Override Group, the dashed line indicates the average indoor temperature on the event days when the overrides took place and the solid line indicates the average on days when the participants did not override. All groups have a similar indoor temperature at the start of events – roughly 78 degrees. However, the No Override group shows an increase in temperature throughout the event, but more noticeably in the first two hours. For the Override group, those who actually overrode show a logical drop in temperature as their air conditioning systems resume operation. For those that did not override, there is an initial increase in temperature in the first half hour and then they exhibit a steady temperature for the remainder the event period.

Figure 1-20: Average Indoor Temperatures on Event Days for the Override Group and No Override Group

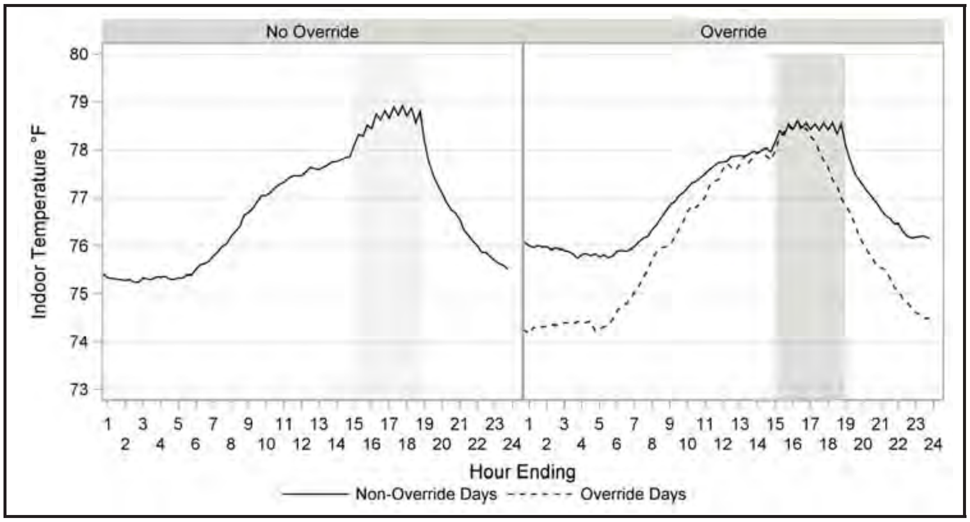

As a final attempt to gain insight into the association between indoor temperatures and override behavior, Figure 1-21 shows the average temperature on event days for Override participants broken out by the number of times they overrode during the summer events. The graph attempts to address the question of whether participants are overriding more often due to higher temperatures in their homes. For those who overrode three times or fewer, the evidence is mixed. For the participants who overrode just once, the indoor temperature was markedly higher on the days they overrode. However, for the group that overrode two or three times, the temperature was actually lower on override days compared to non-override days. For the small number that overrode at least four times, the temperatures were slightly higher on override days, but in general this group appeared to have higher temperatures compared to the other groups.

Figure 1-21: Average Indoor Temperatures on Event Days for the Override Group

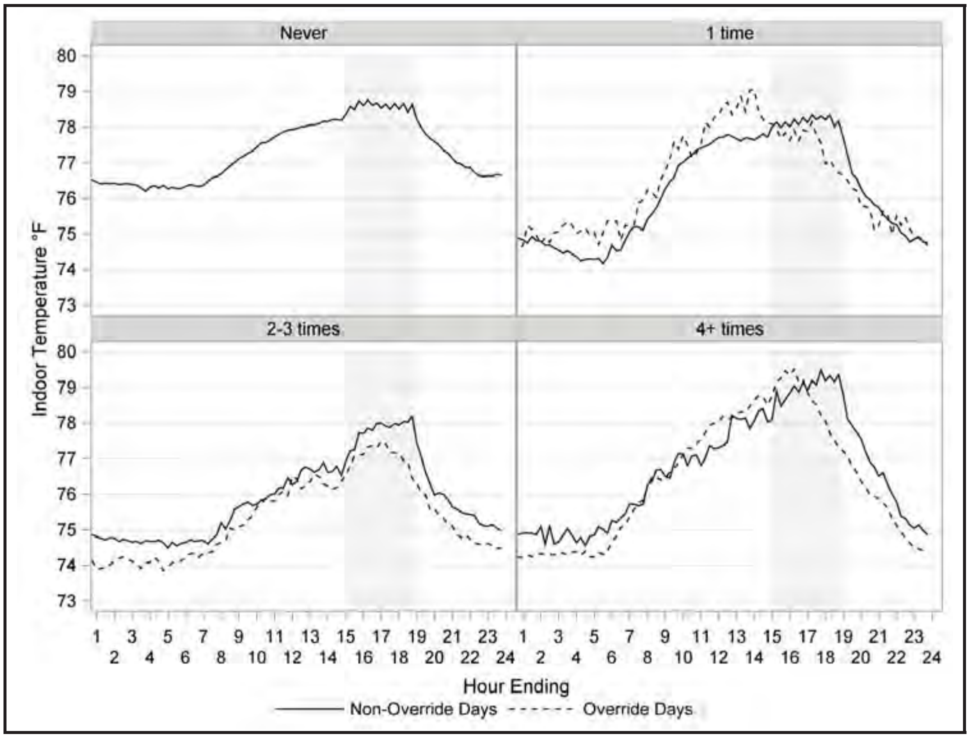

Itron
Knowledge to Shape Your Future

Electric | Gas | Water
information collection, analysis and application

Analysis of Energy Savings for FPL's Customer Trials of the [redacted] Learning Thermostat

Final Report

Submitted to:

Patrick Agnew
Program Manager, In-home Technology and Electric Vehicles

Florida Power & Light

Submitted by:

David Hanna
Collin Elliot

Itron, Inc.
12348 High Bluff Drive, Suite 210
San Diego, California 92130

August 6, 2015

1 ANALYSIS OF ENERGY SAVINGS FOR FPL'S CUSTOMER TRIAL OF THE [redacted] LEARNING THERMOSTAT

1.1 EXECUTIVE SUMMARY

Florida Power and Light (FPL) conducted a customer trial to explore the effects of the installation of [redacted] thermostats in residential homes. The [redacted] thermostat is a new technology that has two main features that are intended to result in energy savings. The first is an algorithm that learns from occupant behavior so that the [redacted] can program itself, helping the thermostat to save energy in cases where the residents would not normally set up a schedule. The second is online connectivity that allows the homeowner to control the [redacted] via a computer, tablet, or smart phone, which can save energy by reducing consumption when the residents are not home at times atypical to the normal routine.

To assess the effects of the [redacted] thermostats on the trial's participants, Itron performed an analysis of customer interval load data to determine the level of energy conservation achieved by the thermostats. The study examined pre- and post-installation consumption data for FPL's cooling season (April through October) for both trial participants and a control group of nonparticipants with similar energy consumption characteristics. Participants in the trial lived in dwellings categorized as either Single Family or Villa/Duplex, and the analysis was conducted for these home types separately and together.

As the key energy and demand impact metrics in Table 1-1 show, the analysis found statistically significant energy savings amounting to average daily savings of 2.5 kWh and 1.3 kWh for the Villa/Duplex and Single Family home types, respectively, which represent savings of 6.7% and 2.4% of the average daily total household consumption. The Villa/Duplex savings represent 21% of the estimated daily air conditioning consumption compared to 7.7% for the Single Family participants.

TABLE 1-1: SUMMARY OF ENERGY AND DEMAND IMPACTS

Measure	Villa/Duplex	Single Family	All Homes
Cooling Season Savings, Average Daily kWh	2.47	1.29	1.81
Cooling Season Savings, Total kWh	527	276	385
Cooling Season Savings, % of Whole Home	6.7%	2.4%	3.9%
Cooling Season Savings, % of Estimated Cooling	21.0%	7.7%	12.4%
Summer Peak Hour Savings, 4 – 5 PM, kW	0.27	0.09	0.17

In addition to average daily energy savings, the study also found statistically significant savings of 0.27 kW for Villa/Duplex and 0.09 kW for Single Family during FPL's summer peak hour of 4 – 5 PM. These peak hour load reductions represented 12% of the whole home load and 26.7% of estimated AC load for the Villa/Duplex homes. For single family, the savings represented 2.3% of the whole home load and 5.4% of estimated AC load.

1.2 INTRODUCTION

FPL conducted a customer trial to explore the effects of the installation of [redacted] thermostats in residential homes. The [redacted] thermostat is a new technology with two main features intended to result in energy savings. The first is an algorithm that learns from occupant behavior so the [redacted] can program itself, helping the thermostat to save energy in cases where the residents would not normally set up a schedule. The second is online connectivity that allows the homeowner to control the [redacted] via a computer, tablet, or smart phone, which can save energy by reducing consumption when the residents are not home at times atypical to the normal routine.

To assess the effects of the [redacted] thermostats on the trial's participants, Itron performed an analysis of customer interval load data to determine the level of energy conservation achieved by the thermostats. The study examined pre- and post-installation consumption data for FPL's cooling season (April through October) for both trial participants and a control group of nonparticipants with similar energy consumption characteristics. Participants in the trial lived in dwellings categorized as either Single Family or Villa/Duplex, and the analysis was conducted for these home types separately and together.

1.3 STUDY DESIGN AND CONTROL GROUP SELECTION

FPL selected participants in the [redacted] trial on a volunteer basis by randomly soliciting customers from a sample frame created for a separate FPL trial of programmable thermostats, thereby leveraging the randomly assigned treatment and control premises. The treatment premises were Palm Beach County homeowners who resided through 2014 in homes with one thermostat (not a [redacted]) and working Wi-Fi. In contrast to the programmable thermostat trial, the [redacted] trial did not disqualify multifamily homes or seasonal residents. Additionally, it did not require that the homeowner have a smart phone (though all but two did) and it allowed participants in FPL's On Call program.

Data Attrition

The initial set of homes with interval load data consisted of 112 treatment homes and 2,958 nonparticipants to serve as control group candidates. These were reduced to sets of 101 and 2,700, respectively, after the removal of homes with data unsuitable for inclusion in the analysis. Table 1-2 shows the causes for this data attrition and the number of homes associated with them. The reasons are generally self-explanatory in terms of why the issue would affect the analysis. The reasons are not mutually exclusive and many homes were removed for more than one reason. The single greatest reason for excluding a home was incomplete data—143 homes in the control group were removed for that reason alone. The next biggest contributor was cases where average usage either increased by 100% or decreased by 50% from 2013 to 2014; this led to the removal of two homes in the treatment group and 52 of the control group candidates. The amount of attrition seen here is typical and does not suggest any systematic issues that could bias the results.

TABLE 1-2: DATA ATTRITION OF CONTROL AND [redacted]

<table>
<tr><th rowspan="2">Final Status</th><th colspan="7">Reason For Removal from Analysis</th><th rowspan="2">Control Accounts</th><th rowspan="2">[redacted] Accounts</th></tr>
<tr><th>Seasonal Occupant</th><th>Large Year/Year Change</th><th>DSM During Analysis Period</th><th>Incomplete Data Issues</th><th>Meter Change</th><th>No PSM Score</th><th>Not Single Family or Duplex</th></tr>
<tr><td>Included</td><td>No</td><td>No</td><td>No</td><td>No</td><td>No</td><td>No</td><td>No</td><td>2,700</td><td>101</td></tr>
<tr><td rowspan="14">Removed</td><td rowspan="12">No</td><td rowspan="7">No</td><td rowspan="5">No</td><td rowspan="3">No</td><td rowspan="2">No</td><td>No</td><td>Yes</td><td>0</td><td>2</td></tr>
<tr><td>Yes</td><td>No</td><td>4</td><td>0</td></tr>
<tr><td>Yes</td><td>No</td><td>No</td><td>39</td><td>0</td></tr>
<tr><td rowspan="2">Yes</td><td>No</td><td>No</td><td>No</td><td>143</td><td>0</td></tr>
<tr><td>Yes</td><td>No</td><td>No</td><td>2</td><td>0</td></tr>
<tr><td rowspan="2">Yes</td><td>No</td><td>No</td><td>No</td><td>No</td><td>17</td><td>5</td></tr>
<tr><td>Yes</td><td>No</td><td>No</td><td>No</td><td>1</td><td>0</td></tr>
<tr><td rowspan="4">Yes</td><td rowspan="4">No</td><td rowspan="2">No</td><td>No</td><td>No</td><td>No</td><td>38</td><td>1</td></tr>
<tr><td>Yes</td><td>No</td><td>No</td><td>7</td><td>0</td></tr>
<tr><td rowspan="2">Yes</td><td>No</td><td>No</td><td>No</td><td>5</td><td>0</td></tr>
<tr><td>Yes</td><td>No</td><td>No</td><td>2</td><td>0</td></tr>
<tr><td rowspan="2">Yes</td><td>No</td><td>No</td><td>No</td><td>No</td><td>No</td><td>No</td><td>0</td><td>2</td></tr>
<tr><td>Yes</td><td>No</td><td>No</td><td>No</td><td>No</td><td>No</td><td>0</td><td>1</td></tr>
<tr><td colspan="8" align="right">Total Removed</td><td>258</td><td>11</td></tr>
</table>

Stratified Propensity Score Matching

Having removed all homes with data issues, the next step used stratified propensity score matching (PSM) to identify homes among the control group candidates who have energy consumption attributes similar to customers in the [redacted] trial. Stratified PSM – in this case the homes were stratified by size, with large and small delineated based on median consumption – is a method that uses observable classification variables (e.g., average weekday consumption by month, correlation between cooling degree days and daily consumption, etc.) in a logit model to estimate the probability of participation within the participants and nonparticipants. The propensity score represents the probability of participation based on pre-program period observable characteristics, in this case for April through October of 2013.

As mentioned previously, the [redacted] trial did not limit participation by home type and the final set of participants consisted of 57 single family homes and 44 duplexes. Ideally the [redacted] trial participants and the nonparticipants would have been stratified by home type in addition to size, but this information was not available for most of the control group candidates. Instead, the approach was to find matches for the single family homes and duplexes separately, allowing each home type to draw from the full set of control households to identify the best matches. The intention is that matching on consumption characteristics will serve as a proxy for home type. Additionally, the customer survey data available for 309 of control group homes showed that single family homes accounted for 59% total. If this share is representative of the entire control group, then the control and treatment groups at least have very similar shares for this home type. Using logistic regression, propensity scores were estimated for the trial participants and nonparticipants. Homes from the group of control candidates with similar scores to the participants were selected as the control group.

Treatment and Control Group Comparison

There are two primary means of assessing how well the homes selected by the PSM will serve as a control group for the treatment households. The first is a statistical comparison where t tests are used to compare the control group with the treatment group before and after the PSM matching. That is, the treatment group is compared with the full set of control homes and then with just the subset identified by the PSM as having similar consumption characteristics. The t tests are done for the independent variables used in the logistic regression model for the PSM and, if the match is good, there should be few or no statistically significant differences between treatment and control after selecting the matching control group. There are dozens of variables used in the logistic regression model to develop propensity score, so for brevity, Table 1-3 shows only the percentage that had statistically significant differences between participants and nonparticipants before and after matching. The results indicate that for the single family homes in the [redacted] trial, the control candidates were not greatly different, with only 24.2% of the variables in the PSM showing a statistically significant difference prior to matching. After the PSM matching, none of the variables showed a statistically significant difference between the participants and the final control group. For the Villa/Duplex participants, the likely prevalence of single family homes among the nonparticipants resulted in 60% of the variables showing a statistically significant difference before matching. After matching, 0.8% of the variables still had a significant difference for all homes, but the PSM still did a good job of identifying a more comparable set of homes for the control group.

TABLE 1-3: PERCENTAGE OF STATISTICALLY SIGNIFICANTLY DIFFERENT VARIABLES PRE- AND POST-PSM

Size	Villa/Duplex		Single Family		All Homes	
	Before Match	After Match	Before Match	After Match	Before Match	After Match
Large	80.0%	0.0%	12.5%	0.0%	46.3%	0.0%
Small	50.0%	2.5%	30.0%	0.0%	40.0%	1.3%
All	60.0%	1.7%	24.2%	0.0%	42.1%	0.8%

The second means of assessing the PSM results is a graphical comparison of the two groups based on average daily kWh by month before and after matching. This comparison is presented in Figure 1-1 for the Villa/Duplex and Figure 1-2 for Single Family. While the objective is to find nonparticipants with similar consumption, the matches are unlikely to be perfect. The main issue is how much closer the matched control group homes are to the treatment homes compared to the full set of nonparticipants.

For the Villa/Duplex home type, there was a very large initial discrepancy between the nonparticipants and [redacted] homes. This makes sense given that the nonparticipants are likely dominated by single family homes, which have much higher consumption. The graphs show that the PSM resulted in a control group that much more closely approximates the average daily usage of the treatment group. Whether or not this match means that the control group consists of other Villa/Duplex homes cannot be known, but at least the match in terms of consumption patterns is greatly improved.

FIGURE 1-1: AVERAGE DAILY KWH BY MONTH PRE AND POST PSM FOR VILLA/DUPLEX

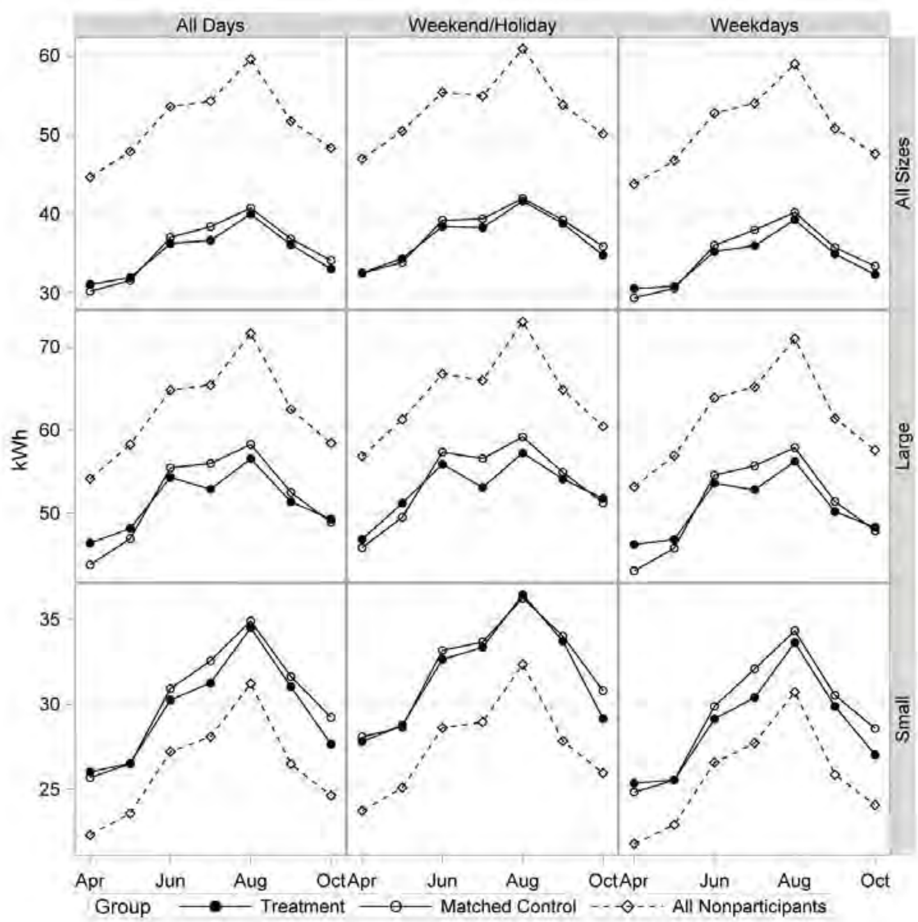

For the Single Family homes, the initial discrepancies are far more evident in small homes, but the PSM routine results in what appears to be a very good match. Overall, based on the t tests and the graphical comparisons, there is little question that the PSM routine resulted in a control group that is much better for conducting the analysis than simply using the full set of nonparticipants.

FIGURE 1-2: AVERAGE DAILY KWH BY MONTH PRE AND POST PSM FOR SINGLE FAMILY

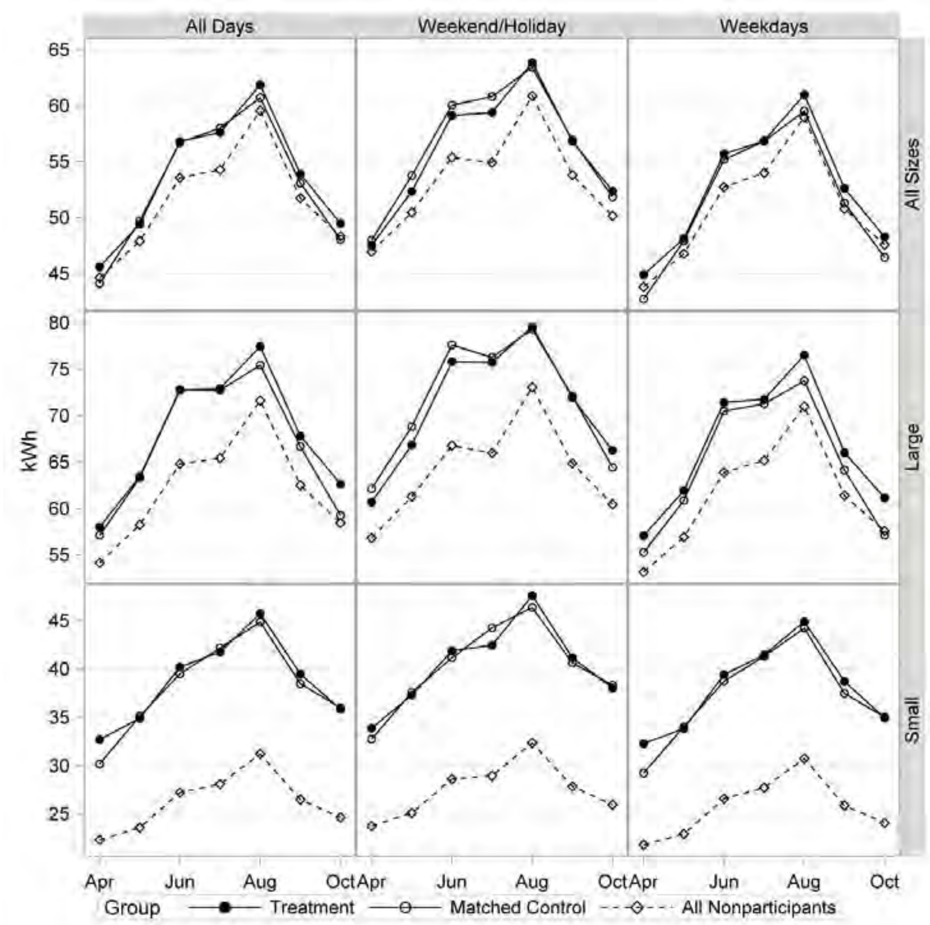

As a final summary to the contol group selection, Table 1-4 shows the average daily kWh by home type for the participants along with the control group homes before (All nonparticipants) and after (Matched

Control) the PSM routine. There are two key takeaways in this table. The first is that the matched control group is much more similar to the participants in terms of average daily usage than the full set of all nonparticipants, though the improvement is far more marked for the Villa/Duplex home type. Average daily kWh for the control group was 96.1% of the participant average daily kWh before matching. This improved to 98.6% after the matching, which is good, but the full set of all participants might have been suitable without the PSM routine for Single Family homes. For the Villa/Duplex, however, the PSM clearly was a critical step on assuring a suitable set of control homes was used in the study.

TABLE 1-4: COMPARISON OF PARTICIPANTS WITH CONTROL HOMES BEFORE AND AFTER MATCHING

Home Type	Unique Homes Participants	Mean Daily kWh Participants	Unique Homes All Nonparticipants	Mean Daily kWh All Nonparticipants	All Nonparticipants kWh as % of Participant kWh	Unique Homes Matched Control	Mean Daily kWh Matched Control	Matched Control kWh as % of Participant kWh
Single Family Detached	57	53.5	2,700	51.5	96.1%	55	52.8	98.6%
Villa/Duplex	44	35.0			146.9%	41	34.7	99.1%

The second takeaway is that the number of unique homes in the matched control group is lower than the number of unique participant homes. This means that some control homes were matched to more than one participant during the PSM routine. This number is small, however (e.g. 55 control homes compared to 57 treatment homes for Single Family), meaning that the matched control group still represented a good variety of homes.

1.4 METHODS AND RESULTS

The study assessed energy savings for the [redacted] trial using two separate analyses based on a Difference-in-Differences (DiD) approach. These two analyses and their results are discussed separately in this section.

Comparison of Means

The first DiD approach for assessing energy savings from conservation was a comparison of means in the pre- and post-installation periods for treatment and control groups. This analysis was performed by comparing the average daily kWh during FPL's cooling season in 2013 (pre) and 2014 (post) for the treatment and control groups. The DiD approach assumed that even though the treatment and control groups were not likely the same in every respect, at least the differences between them over time were likely to be the same absent any treatment (in this case, the installation of the [redacted]). As a result, the effect of the treatment can be calculated as the difference in each group's difference from the pre-treatment period to the post-treatment period.

Table 1-5 shows the summary of mean daily kWh for the cooling season along with the associated cooling degree days (CDD[1]) for the two groups in the pre- and post-treatment periods, along with the differences for each group. The final DiD is the delta of the daily average kWh from the treatment group minus the delta of the daily average kWh from the control group. What these data show is that the post-treatment period had very similar average CDD to the pre-treatment period. The weather was similar in both periods, with only a very small decrease in average daily CDD in the post period. In terms of consumption, the Villa/Duplex control group actually showed a small increase in its average daily kWh. In contrast, the [redacted] group showed a decrease of 2.2 kWh, which resulted in an estimated savings of 2.49 kWh per day based on the DiD approach. For the Single Family homes, the control showed a decrease in average consumption of .08 kWh, whereas consumption in the treatment homes went down 1.41 kWh for a DiD savings of 1.33 kWh. As a percentage of average daily whole home consumption, these DiD savings represented 6.8% for Villa/Duplex, 2.5% for Single Family, and 4% for all homes.

TABLE 1-5: COOLING SEASON AVERAGE DAILY KWH AND COOLING DEGREE DAYS (BASE 72) BY HOME TYPE, GROUP, AND YEAR

Home Type	Group	Period	Mean Daily kWh	Mean Daily CDD	Delta Daily kWh	Delta Daily CDD	DiD (kWh per Day)
Villa/Duplex	Control	Pre	35.5	8.6	-	-	2.49
		Post	35.7	8.5	0.28	-0.01	
	Treatment	Pre	36.1	8.6	-	-	
		Post	33.9	8.5	-2.22	-0.03	
Single Family	Control	Pre	52.7	8.6	-	-	1.33
		Post	52.6	8.5	-0.08	-0.01	
	Treatment	Pre	54.2	8.6	-	-	
		Post	52.8	8.5	-1.41	-0.03	
All Homes	Control	Pre	45.2	8.6	-	-	1.84
		Post	45.2	8.5	0.07	-0.01	
	Treatment	Pre	46.4	8.6	-	-	
		Post	44.6	8.5	-1.76	-0.03	

As a means of testing the statistical significance of the estimated savings, Itron estimated a regression model of the average daily kWh as a function of three dummy variables: Group (treatment = 1), Period (Post = 1), and the interaction of the group and period (Group × Period). It is the interaction of treatment group and post period in this model that represents DiD estimate. The parameter estimate for the DiD, which is shown in Table 1-6, was not statistically significant, however. This result is likely due to two factors. First, the small number of premises included in the model, with 101 participants and their matched control homes, makes it more difficult to find effects that are not particularly large. Second, the aggregation of the data to the average daily kWh per participants means that there is no ability to include other variables – primarily weather – in the model that would account for variability and make it possible to isolate any effects associated with the [redacted] thermostats.

1 For the CDD in this analysis, Itron used a base temperature of 72 based on analysis to determine which threshold best explained the kWh variation.

TABLE 1-6: PARAMETER ESTIMATES FOR DID

Home Type	DiD Estimate	Standard Error	DF	t Value	Pr > |t|	Percent Savings
Villa/Duplex	-2.49	1.524	83	-1.64	0.106	6.8%
Single Family	-1.33	1.489	111	-0.89	0.374	2.5%
All Homes	-1.84	1.067	196	-1.72	0.087	4.0%

Interpretation of DiD results are typically aided by data visualization. Figure 1-3 presents graphical portrayals of all three DiD results, which conveniently have scales that allow them to be shown in the same plot. In this plot, the average daily kWh for the treatment and control groups are shown for the pre- and post-treatment periods, which are annotated with "A" and "B," respectively. The DiD approach assumes that whatever happened to the control group is what also would have happened to the treatment group had they not received the [redacted] thermostats. This counterfactual is also presented in the plots and is annotated with "C," and the DiD estimate is based on the difference between "A" and "C." For example, for the Villa/Duplex participants, the control group shows a slight increase in consumption in the post-treatment period. The DiD approach assumes that the treatment group should have seen the same increase, when in fact the [redacted] homes showed a marked decrease. Consequently, the difference between A and C is the estimated DiD savings of 2.49 kWh per daily, or 6.8% of their daily consumption. This narrative is more or less replicated for the two other DiD models where relatively stable consumption in the control group is contrasted by clear declines for the [redacted] participants.

FIGURE 1-3: AVERAGE DAILY KWH DID ILLUSTRATION

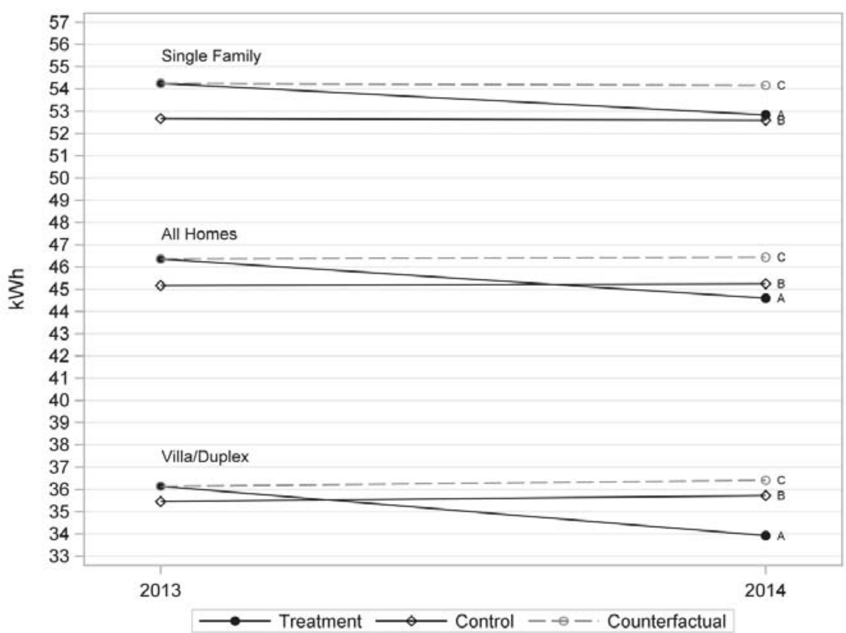

Panel Time Series Regression

The second DiD approach was a panel time series regression, which was performed to account for more of the variability in consumption due to weather and other behaviors affecting households. This allowed the effect of the program to be estimated with less uncertainty. Of the many models tested, the final model selected based on goodness-of-fit and interpretability of results was as follows:

$$kWh_t = \alpha_i + \beta 1 \times CDD_t + \beta 2 \times Post + \beta 3 \times Post \ \times CDD_t + \beta 4 \times Treatment \times Post + \beta 5 \times Treatment \times Post \ \times CDD_t + \epsilon_t$$

Where:

- kWh_t represents the usage for a customer on day t,
- α_i is the "customer-specific" intercept (or error) for home i, accounting for unexplained difference in use between homes associated with the number of occupants, appliance holdings and lifestyle,
- CDD_t is a cooling degree day variable for day t,
- *Post* is a dummy variable indicating that the year is 2014,
- *Treatment* is a dummy variable indicating the household is in the treatment group,
- *B1* through *B5* is a matrix of coefficients to be estimated that quantify the impacts associated with the various interactions between variables, and
- ϵ_t is the error term.

The effect of the thermostats was estimated by using both a dummy variable (Treatment = 1 × Post = 1) and this same dummy variable interacted with CDD. Itron included the interaction of participation with weather since the regulation of cooling by the thermostat is assumed to be the source of energy savings.

The results from the panel regression models are evaluated first in terms of overall model fit and then for the parameter estimates that were used to estimate the savings. With respect to overall model fit, the Villa/Duplex model had an R^2 of 0.607, which indicates that nearly 61% of the variability in the dependent variable was accounted for in the model. The F statistic for this model, which tests for overall statistical significance was 627.22, which had a p value <.0001. The Single Family model had an R^2 of 0.721 (F = 1,060.34, p. <.0001) and the All Homes model had an R^2 of 0.732 (F = 1,141.69, p. <.0001). Overall, these are indicative of good model fit for this type of analysis.

The results for the impact variables are presented in Table 1-7, which shows the parameters and their estimated values for those variables intended to capture the impacts, as well as how those regression outputs translate into average daily kWh Savings. For all three models, the parameter estimates for the impact variables were negative, indicating that the thermostats resulted in a decline in consumption. The parameter estimates that interacted participation with CDD were statistically significant, as shown in the column "Pr > |t|," which shows the probability that the observed t value could have occurred by chance. For the parameter "Treatment × Post," the interpretation of the estimate is simply the average daily kWh associated with the thermostat installation. For the parameter "Treatment × Post × CDD," the estimate means the average daily kWh per CDD, so it needs to be multiplied by the average daily CDD to calculate the total impact. The kWh savings shown is based on the sum of these two impacts (where the CDD-interacted estimate has been multiplied by the average cooling season CDD).

TABLE 1-7: PANEL REGRESSION OUTPUTS AND ESTIMATED AVERAGE DAILY KWH SAVINGS

Home Type	Parameter	Estimate	Standard Error	t Value	Pr > |t|	kWh Savings	Percent of Whole Home Savings	Percent AC Savings
Villa/Duplex	Treatment × Post × CDD	-0.256	0.0436	-5.87	<.0001	2.47	6.7%	21.0%
	Treatment × Post	-0.288	0.4308	-0.67	0.5043			
Single Family	Treatment × Post × CDD	-0.119	0.0476	-2.49	0.0126	1.29	2.4%	7.7%
	Treatment × Post	-0.281	0.4698	-0.60	0.5502			
All Homes	Treatment × Post × CDD	-0.179	0.0332	-5.38	<.0001	1.81	3.9%	12.4%
	Treatment × Post	-0.284	0.3276	-0.87	0.3865			

For the Villa/Duplex model, the panel regression resulted in savings of 2.47 average daily kWh, which represented savings of 6.7% of total household daily kWh. Because the panel model included CDD as an explanatory variable, the parameter estimate for this was used to estimate the consumption associated with air conditioning. The savings for the Villa/Duplex participants represented 21% of this estimated air conditioning kWh. For the Single Family homes, the estimated average daily savings were 1.29 kWh, or 2.4% whole house kWh and 7.7% of air conditioning kWh. The model for all homes resulted average daily savings of 1.81 kWh, which is essentially a weighted average of the other two models.

The results from the panel regression models are very similar to what was produced by the DiD comparison of means; such consistency is generally positive, as it serves to validate the results. The difference is that the panel regression, which explicitly accounted for the variability associated with weather, was able to find statistically significant estimates of savings where the DiD approach could not. It is for this reason that the estimated savings from the panel regression are presented in this report as the official estimates of savings for the [redacted] trial.

Finally, Figure 1-4 shows the daily savings estimates with 90% confidence intervals by home type. In terms of absolute precision, the bands around each estimate are fairly similar. In terms of relative precision, these confidence intervals are plus or minus 14%, 30%, and 15% for Villa/Duplex, Single Family, and all homes, respectively. The high relative precision for the Single Family savings is due to estimated savings being substantially lower.

FIGURE 1-4: DAILY KWH SAVINGS WITH 90% CONFIDENCE INTERVALS

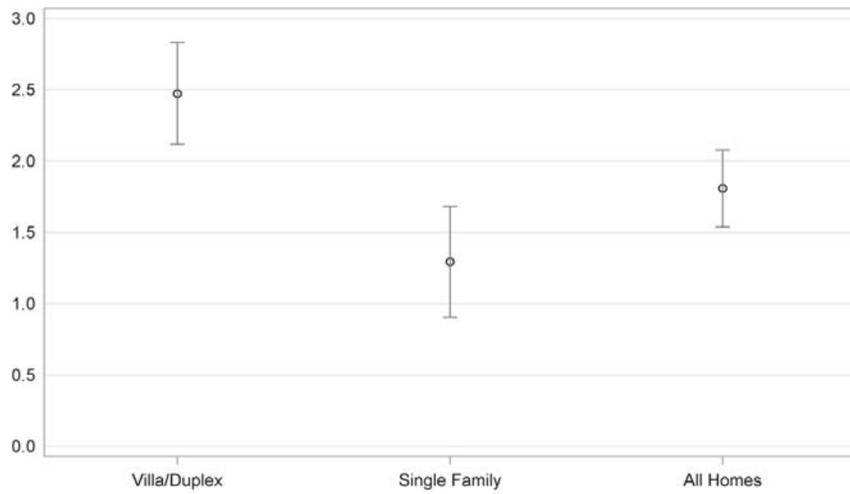

Hourly Savings

The panel regression method was also applied to hourly data separately for weekdays (non-holiday) and weekends. While the hourly data had far greater variability and the overall estimated savings are not as robust as the daily results, these models provided value for estimating [redacted] impacts in FPL's peak summer hour and for exploring how the thermostats influenced the daily load profiles.

As a characterization of the hourly energy savings, Figure 1-5 shows the average observed and reference loads for the Single Family and Villa/Duplex home types for weekdays and weekends. The reference loads – indicated with the triangle marker – represent what the load would have been without the [redacted] impacts in each hour based on the results of the modeling. The observed loads represent that average kW following the installation of the [redacted] thermostats. The differences between the reference and the observed loads in each hour are the impacts, whether positive or negative.

The load profiles presented in Figure 1-5 have a couple of interesting characteristics. First, they show that the [redacted] savings for both home and day types occurred during the middle of the day, generally when one would expect to see the impacts as people leave for work or other activities. Second, the load profiles showed clear differences between the Villa/Duplex and Single Family homes. On weekdays, the observed load for the Villa/Duplex homes showed a drop in consumption after the morning hours compared to a reference load that remained steady. In contrast, the Single Family homes had reduced consumption on weekdays, but still showed a steady increase throughout the day and even had an increase in consumption in the evening hours, suggestive of a possible snapback effect. On weekends, the Villa/Duplex homes still showed substantial savings, but the observed load was generally flatter throughout the day without the dip seen on weekdays. For Single Family homes, compared to the weekdays where the reduced usage during the day was followed by an increase in the evening, on weekends the savings were seen in lower consumption during the middle of the day with nearly identical levels of consumption in all other hours.

FIGURE 1-5: HOURLY LOAD PROFILES BY DAY AND HOME TYPE

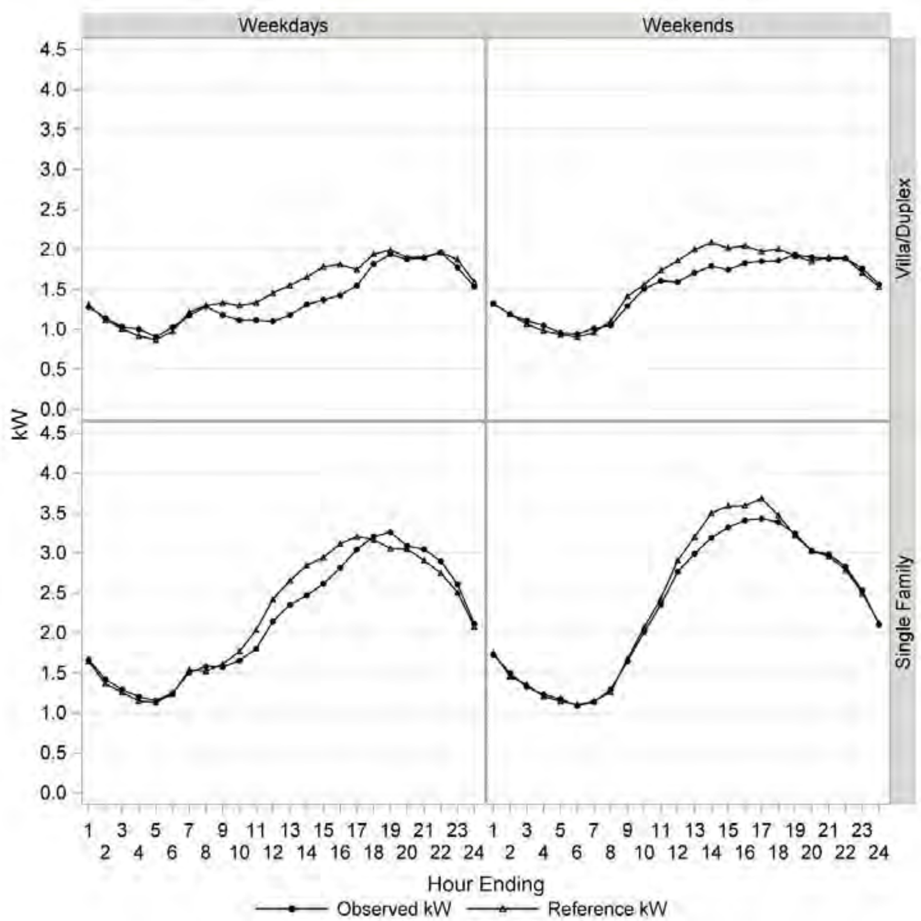

While the comparison of the load profiles is interesting in terms of seeing the differences in impacts among home and day types, the primary results of interest from the hourly models are the actual regression outputs and estimated impacts for the weekdays for the hour ending at 5:00 PM. These results are what indicate what evidence the analysis showed for savings during FPL's summer peak hour, and they are presented in two separate tables for each of the home types. The first table shows the parameter estimates from the regression model used to determine the effects of the [redacted] These impacts were based on a single dummy variable to capture any base impacts and a dummy variable interacted with cooling degree hours to capture any temperature sensitive effects. The parameter estimates for both of these variables are presented along with their t test results and standard errors. The second table shows how these parameter estimates translate into hourly impacts for both an average summer day and for when there are peak day weather conditions. The large amount of information in Table 1-8 through Table 1-13 is presented for thoroughness, but for discussion purposes the emphasis is primarily on the rows for the hour ending at 5:00 PM (17:00 in the tables), which have relevance to FPL's peak hour. As shown in Table 1-8, for the Villa/Duplex homes both base and temperature sensitive impact parameters are negative and statistically significant. These parameters amount to 0.27 kW savings under peak day temperatures, which represent savings of 12% (Table 1-9). For Single Family, Table 1-10 shows that the base impact is negative and statistically significant while the temperature sensitive parameter is positive and statistically significant. As shown in Table 1-11, the combined effect of these parameters indicated savings of 0.09 kWh, or 2.3%. For all homes, the based impact is negative and significant while the temperature sensitive parameter is positive but not significant (Table 1-12). As shown in Table 1-13 , these translate to savings of 0.17 kW, or 5.2%, on peak days.

The interpretation of these parameters is not always an intuitive matter. The models were specified as they were to capture the different ways in which the [redacted] impacts might manifest themselves. It was by no means a given that both base and temperature sensitive impacts will be significant or that both will be negative in sign. It is important to note that this particular hour is around the likely transition where the residents of some homes are likely returning from work and the [redacted] has learned to resume cooling. In general, the other hours during the day have parameter estimates that can be more easily interpreted and also have larger impacts. This makes intuitive sense given how the [redacted] works with the likely occupancy patterns of most homes.

TABLE 1-8: DUPLEX/VILLA WEEKDAY REGRESSION MODEL IMPACT PARAMETERS

Hour Ending	Impact Parameter Type							
	Base Impact				Temperature Sensitive			
	Parameter Estimate	t Value	Pr > |t|	Standard Error	Parameter Estimate	t Value	Pr > |t|	Standard Error
1:00	-0.041	-1.420	0.156	0.0287	0.003	0.794	0.427	0.0039
2:00	0.036	1.499	0.134	0.0238	-0.003	-0.743	0.458	0.0035
3:00	0.067	3.214	0.001	0.0207	-0.009	-2.694	0.007	0.0032
4:00	0.089	4.570	<.001	0.0195	-0.001	-0.404	0.686	0.0032
5:00	0.067	3.442	<.001	0.0194	-0.007	-2.254	0.024	0.0032
6:00	0.067	3.177	0.001	0.0212	-0.005	-1.371	0.170	0.0038
7:00	-0.051	-1.882	0.060	0.0273	0.003	0.575	0.565	0.0049
8:00	0.038	1.194	0.233	0.0316	-0.010	-2.133	0.033	0.0045
9:00	-0.153	-4.006	<.001	0.0382	-0.001	-0.140	0.888	0.0040
10:00	0.022	0.450	0.653	0.0481	-0.020	-4.823	<.001	0.0041
11:00	-0.058	-1.039	0.299	0.0555	-0.013	-3.105	0.002	0.0043
12:00	-0.109	-1.905	0.057	0.0570	-0.020	-4.729	<.001	0.0041
13:00	-0.161	-2.905	0.004	0.0553	-0.016	-4.286	<.001	0.0038
14:00	-0.192	-3.319	<.001	0.0578	-0.012	-2.914	0.004	0.0040
15:00	-0.269	-5.099	<.001	0.0527	-0.012	-3.205	0.001	0.0037
16:00	-0.221	-4.355	<.001	0.0509	-0.014	-3.681	<.001	0.0038
17:00	**-0.063**	**-1.318**	**0.187**	**0.0480**	**-0.012**	**-3.229**	**0.001**	**0.0038**
18:00	0.013	0.239	0.811	0.0534	-0.013	-2.913	0.004	0.0046
19:00	-0.026	-0.464	0.643	0.0558	-0.003	-0.640	0.522	0.0052
20:00	-0.038	-0.724	0.469	0.0519	0.002	0.293	0.770	0.0054
21:00	-0.014	-0.283	0.777	0.0495	0.000	0.047	0.963	0.0056
22:00	-0.008	-0.175	0.861	0.0468	0.001	0.252	0.801	0.0055
23:00	-0.157	-3.702	<.001	0.0424	0.009	1.758	0.079	0.0052
24:00	-0.027	-0.772	0.440	0.0355	-0.005	-1.144	0.253	0.0045

TABLE 1-9: VILLA\DUPLEX WEEKDAY HOURLY IMPACTS FOR AVERAGE AND PEAK DAY

Hour Ending	Average Day Impacts				Peak Day Impacts			
	kWh Reference	kWh Observed	kWh Impact	Percent Load Reduction	kWh Reference	kWh Observed	kWh Impact	Percent Load Reduction
1:00	1.30	1.28	0.02	1.8%	1.57	1.55	0.01	0.8%
2:00	1.12	1.14	-0.02	-2.0%	1.33	1.34	-0.01	-1.0%
3:00	1.01	1.03	-0.03	-2.5%	1.20	1.20	0.00	0.2%
4:00	0.92	1.00	-0.08	-9.1%	1.14	1.22	-0.08	-7.0%
5:00	0.87	0.90	-0.04	-4.1%	1.04	1.06	-0.02	-1.6%
6:00	0.98	1.02	-0.05	-4.8%	1.18	1.22	-0.04	-3.1%
7:00	1.21	1.17	0.04	3.3%	1.33	1.30	0.03	2.6%
8:00	1.30	1.28	0.02	1.2%	1.46	1.43	0.04	2.7%
9:00	1.33	1.17	0.16	11.8%	1.51	1.35	0.16	10.6%
10:00	1.30	1.12	0.18	14.2%	1.55	1.29	0.26	16.8%
11:00	1.33	1.12	0.21	16.2%	1.60	1.32	0.27	17.0%
12:00	1.45	1.10	0.36	24.4%	1.82	1.37	0.44	24.3%
13:00	1.55	1.18	0.37	24.2%	1.90	1.45	0.46	24.0%
14:00	1.65	1.31	0.34	20.8%	2.03	1.63	0.41	20.0%
15:00	1.78	1.37	0.42	23.4%	2.25	1.76	0.49	21.6%
16:00	1.81	1.42	0.38	21.3%	2.29	1.82	0.47	20.5%
17:00	**1.75**	**1.55**	**0.20**	**11.3%**	**2.29**	**2.01**	**0.27**	**12.0%**
18:00	1.94	1.82	0.12	6.3%	2.44	2.24	0.20	8.2%
19:00	1.99	1.93	0.06	2.8%	2.49	2.42	0.08	3.0%
20:00	1.90	1.87	0.02	1.3%	2.28	2.26	0.02	0.8%
21:00	1.91	1.89	0.01	0.6%	2.33	2.32	0.01	0.5%
22:00	1.96	1.96	-0.00	-0.1%	2.30	2.31	-0.01	-0.3%
23:00	1.87	1.78	0.10	5.2%	2.17	2.11	0.06	2.6%
24:00	1.59	1.53	0.06	3.7%	1.93	1.85	0.08	4.3%
Entire Day	35.82	32.96	2.87	8.0%	43.41	39.81	3.60	8.3%

TABLE 1-10: SINGLE FAMILY WEEKDAY REGRESSION MODEL IMPACT PARAMETERS

<table>
<tr><th rowspan="3">Hour Ending</th><th colspan="8">Impact Parameter Type</th></tr>
<tr><th colspan="4">Base Impact</th><th colspan="4">Temperature Sensitive</th></tr>
<tr><th>Parameter Estimate</th><th>t Value</th><th>Pr > |t|</th><th>Standard Error</th><th>Parameter Estimate</th><th>t Value</th><th>Pr > |t|</th><th>Standard Error</th></tr>
<tr><td>1:00</td><td>-0.082</td><td>-2.792</td><td>0.005</td><td>0.0295</td><td>0.018</td><td>4.392</td><td><.001</td><td>0.0041</td></tr>
<tr><td>2:00</td><td>0.023</td><td>0.954</td><td>0.340</td><td>0.0242</td><td>0.005</td><td>1.475</td><td>0.140</td><td>0.0035</td></tr>
<tr><td>3:00</td><td>0.017</td><td>0.813</td><td>0.416</td><td>0.0211</td><td>0.005</td><td>1.424</td><td>0.154</td><td>0.0033</td></tr>
<tr><td>4:00</td><td>0.030</td><td>1.532</td><td>0.126</td><td>0.0195</td><td>0.006</td><td>1.844</td><td>0.065</td><td>0.0032</td></tr>
<tr><td>5:00</td><td>0.029</td><td>1.511</td><td>0.131</td><td>0.0193</td><td>-0.002</td><td>-0.654</td><td>0.513</td><td>0.0032</td></tr>
<tr><td>6:00</td><td>0.033</td><td>1.526</td><td>0.127</td><td>0.0218</td><td>-0.005</td><td>-1.300</td><td>0.194</td><td>0.0040</td></tr>
<tr><td>7:00</td><td>0.027</td><td>0.984</td><td>0.325</td><td>0.0276</td><td>-0.015</td><td>-2.942</td><td>0.003</td><td>0.0050</td></tr>
<tr><td>8:00</td><td>0.136</td><td>4.171</td><td><.001</td><td>0.0325</td><td>-0.014</td><td>-2.984</td><td>0.003</td><td>0.0046</td></tr>
<tr><td>9:00</td><td>0.133</td><td>3.257</td><td>0.001</td><td>0.0409</td><td>-0.021</td><td>-4.825</td><td><.001</td><td>0.0043</td></tr>
<tr><td>10:00</td><td>-0.030</td><td>-0.555</td><td>0.579</td><td>0.0533</td><td>-0.008</td><td>-1.739</td><td>0.082</td><td>0.0046</td></tr>
<tr><td>11:00</td><td>-0.129</td><td>-2.068</td><td>0.039</td><td>0.0623</td><td>-0.009</td><td>-1.863</td><td>0.062</td><td>0.0049</td></tr>
<tr><td>12:00</td><td>-0.123</td><td>-1.823</td><td>0.068</td><td>0.0675</td><td>-0.012</td><td>-2.428</td><td>0.015</td><td>0.0049</td></tr>
<tr><td>13:00</td><td>-0.149</td><td>-2.347</td><td>0.019</td><td>0.0634</td><td>-0.012</td><td>-2.735</td><td>0.006</td><td>0.0044</td></tr>
<tr><td>14:00</td><td>-0.317</td><td>-5.026</td><td><.001</td><td>0.0632</td><td>-0.004</td><td>-1.023</td><td>0.306</td><td>0.0044</td></tr>
<tr><td>15:00</td><td>-0.351</td><td>-6.265</td><td><.001</td><td>0.0560</td><td>0.002</td><td>0.413</td><td>0.680</td><td>0.0040</td></tr>
<tr><td>16:00</td><td>-0.335</td><td>-6.248</td><td><.001</td><td>0.0536</td><td>0.003</td><td>0.725</td><td>0.469</td><td>0.0040</td></tr>
<tr><td>17:00</td><td>-0.288</td><td>-5.554</td><td><.001</td><td>0.0519</td><td>0.011</td><td>2.776</td><td>0.006</td><td>0.0040</td></tr>
<tr><td>18:00</td><td>-0.070</td><td>-1.251</td><td>0.211</td><td>0.0557</td><td>0.011</td><td>2.251</td><td>0.024</td><td>0.0047</td></tr>
<tr><td>19:00</td><td>0.066</td><td>1.187</td><td>0.235</td><td>0.0555</td><td>0.015</td><td>2.908</td><td>0.004</td><td>0.0051</td></tr>
<tr><td>20:00</td><td>-0.024</td><td>-0.452</td><td>0.652</td><td>0.0533</td><td>0.008</td><td>1.410</td><td>0.159</td><td>0.0055</td></tr>
<tr><td>21:00</td><td>0.058</td><td>1.138</td><td>0.255</td><td>0.0513</td><td>0.011</td><td>1.925</td><td>0.054</td><td>0.0058</td></tr>
<tr><td>22:00</td><td>0.077</td><td>1.570</td><td>0.116</td><td>0.0488</td><td>0.010</td><td>1.759</td><td>0.079</td><td>0.0057</td></tr>
<tr><td>23:00</td><td>-0.005</td><td>-0.120</td><td>0.905</td><td>0.0435</td><td>0.016</td><td>2.980</td><td>0.003</td><td>0.0053</td></tr>
<tr><td>24:00</td><td>-0.073</td><td>-2.000</td><td>0.045</td><td>0.0365</td><td>0.017</td><td>3.683</td><td><.001</td><td>0.0047</td></tr>
</table>

TABLE 1-11: SINGLE FAMILY WEEKDAY HOURLY IMPACTS FOR AVERAGE AND PEAK DAY

Hour Ending	Average Day Impacts				Peak Day Impacts			
	kWh Reference	kWh Observed	kWh Impact	Percent Load Reduction	kWh Reference	kWh Observed	kWh Impact	Percent Load Reduction
1:00	1.65	1.66	-0.02	-1.1%	2.02	2.10	-0.08	-4.0%
2:00	1.37	1.42	-0.05	-3.7%	1.68	1.74	-0.07	-4.0%
3:00	1.25	1.29	-0.04	-3.1%	1.60	1.65	-0.05	-3.4%
4:00	1.15	1.20	-0.06	-4.9%	1.44	1.51	-0.07	-5.0%
5:00	1.13	1.15	-0.02	-1.8%	1.40	1.41	-0.01	-1.0%
6:00	1.24	1.25	-0.01	-1.1%	1.51	1.51	-0.00	-0.2%
7:00	1.53	1.50	0.03	2.1%	1.75	1.69	0.06	3.5%
8:00	1.52	1.58	-0.06	-3.9%	1.71	1.74	-0.02	-1.4%
9:00	1.61	1.57	0.03	2.1%	1.89	1.79	0.10	5.5%
10:00	1.77	1.65	0.11	6.4%	2.09	1.95	0.14	6.8%
11:00	2.04	1.80	0.23	11.5%	2.45	2.17	0.27	11.1%
12:00	2.42	2.14	0.27	11.3%	2.91	2.58	0.33	11.2%
13:00	2.66	2.35	0.31	11.5%	3.24	2.88	0.36	11.3%
14:00	2.85	2.47	0.38	13.2%	3.55	3.15	0.40	11.3%
15:00	2.94	2.61	0.33	11.2%	3.73	3.40	0.32	8.6%
16:00	3.11	2.81	0.30	9.7%	3.96	3.67	0.28	7.2%
17:00	**3.21**	**3.04**	**0.16**	**5.1%**	**4.06**	**3.97**	**0.09**	**2.3%**
18:00	3.17	3.21	-0.04	-1.2%	3.99	4.09	-0.10	-2.5%
19:00	3.06	3.26	-0.20	-6.7%	3.82	4.11	-0.29	-7.5%
20:00	3.05	3.09	-0.04	-1.3%	3.82	3.90	-0.08	-2.0%
21:00	2.91	3.05	-0.14	-4.8%	3.62	3.82	-0.19	-5.3%
22:00	2.75	2.89	-0.15	-5.3%	3.37	3.57	-0.19	-5.7%
23:00	2.51	2.61	-0.10	-4.0%	3.07	3.24	-0.17	-5.6%
24:00	2.08	2.11	-0.03	-1.6%	2.60	2.71	-0.11	-4.2%
Entire Day	52.93	51.72	1.20	2.3%	65.28	64.36	0.92	1.4%

TABLE 1-12: ALL HOMES WEEKDAY REGRESSION MODEL IMPACT PARAMETERS

Hour Ending	Impact Parameter Type							
	Base Impact				Temperature Sensitive			
	Parameter Estimate	t Value	Pr > |t|	Standard Error	Parameter Estimate	t Value	Pr > |t|	Standard Error
1:00	-0.064	-3.075	0.002	0.0209	0.011	3.976	<.001	0.0029
2:00	0.029	1.660	0.097	0.0172	0.002	0.723	0.469	0.0025
3:00	0.039	2.579	0.010	0.0150	-0.001	-0.489	0.625	0.0023
4:00	0.056	3.990	<.001	0.0139	0.003	1.211	0.226	0.0023
5:00	0.045	3.289	0.001	0.0138	-0.004	-1.890	0.059	0.0023
6:00	0.048	3.121	0.002	0.0154	-0.005	-1.859	0.063	0.0028
7:00	-0.007	-0.359	0.720	0.0196	-0.007	-1.986	0.047	0.0035
8:00	0.093	4.045	<.001	0.0230	-0.012	-3.660	<.001	0.0033
9:00	0.009	0.301	0.764	0.0285	-0.012	-3.987	<.001	0.0030
10:00	-0.007	-0.198	0.843	0.0367	-0.013	-4.173	<.001	0.0032
11:00	-0.098	-2.285	0.022	0.0428	-0.011	-3.286	0.001	0.0033
12:00	-0.117	-2.558	0.011	0.0456	-0.015	-4.601	<.001	0.0033
13:00	-0.154	-3.552	<.001	0.0433	-0.014	-4.640	<.001	0.0030
14:00	-0.263	-5.979	<.001	0.0439	-0.008	-2.503	0.012	0.0030
15:00	-0.315	-8.008	<.001	0.0393	-0.004	-1.544	0.123	0.0028
16:00	-0.285	-7.565	<.001	0.0377	-0.004	-1.580	0.114	0.0028
17:00	**-0.190**	**-5.256**	**<.001**	**0.0362**	**0.001**	**0.379**	**0.705**	**0.0028**
18:00	-0.034	-0.862	0.389	0.0393	0.000	0.078	0.938	0.0034
19:00	0.026	0.648	0.517	0.0399	0.007	1.896	0.058	0.0037
20:00	-0.030	-0.792	0.429	0.0378	0.005	1.297	0.195	0.0039
21:00	0.027	0.743	0.457	0.0362	0.006	1.568	0.117	0.0041
22:00	0.040	1.154	0.249	0.0343	0.006	1.561	0.119	0.0040
23:00	-0.071	-2.314	0.021	0.0308	0.013	3.428	<.001	0.0038
24:00	-0.053	-2.058	0.040	0.0258	0.007	2.255	0.024	0.0033

TABLE 1-13: ALL HOMES WEEKDAY HOURLY IMPACTS FOR AVERAGE AND PEAK DAY

Hour Ending	Average Day Impacts				Peak Day Impacts			
	kWh Reference	kWh Observed	kWh Impact	Percent Load Reduction	kWh Reference	kWh Observed	kWh Impact	Percent Load Reduction
1:00	1.50	1.50	-0.00	-0.0%	1.82	1.86	-0.04	-2.2%
2:00	1.26	1.30	-0.04	-3.0%	1.53	1.57	-0.04	-2.9%
3:00	1.15	1.18	-0.03	-2.9%	1.43	1.46	-0.03	-2.1%
4:00	1.05	1.11	-0.07	-6.5%	1.31	1.38	-0.08	-5.8%
5:00	1.02	1.04	-0.03	-2.6%	1.24	1.26	-0.02	-1.2%
6:00	1.12	1.15	-0.03	-2.5%	1.37	1.38	-0.02	-1.3%
7:00	1.39	1.36	0.04	2.6%	1.57	1.52	0.05	3.1%
8:00	1.42	1.45	-0.03	-1.9%	1.60	1.60	0.00	0.2%
9:00	1.49	1.40	0.09	5.9%	1.73	1.60	0.13	7.4%
10:00	1.56	1.42	0.14	9.2%	1.85	1.66	0.19	10.4%
11:00	1.73	1.50	0.23	13.1%	2.08	1.80	0.27	13.1%
12:00	2.00	1.69	0.31	15.5%	2.43	2.06	0.38	15.5%
13:00	2.17	1.84	0.34	15.4%	2.66	2.25	0.40	15.2%
14:00	2.33	1.96	0.36	15.6%	2.89	2.48	0.40	13.9%
15:00	2.44	2.07	0.37	15.1%	3.08	2.69	0.39	12.7%
16:00	2.55	2.21	0.34	13.3%	3.23	2.86	0.36	11.3%
17:00	**2.57**	**2.39**	**0.18**	**6.9%**	**3.29**	**3.12**	**0.17**	**5.2%**
18:00	2.63	2.60	0.03	1.2%	3.31	3.28	0.03	0.9%
19:00	2.59	2.68	-0.09	-3.5%	3.24	3.37	-0.13	-4.0%
20:00	2.55	2.56	-0.01	-0.4%	3.15	3.19	-0.04	-1.1%
21:00	2.47	2.54	-0.07	-3.0%	3.06	3.17	-0.10	-3.4%
22:00	2.40	2.49	-0.08	-3.5%	2.91	3.02	-0.11	-3.9%
23:00	2.23	2.24	-0.01	-0.6%	2.67	2.75	-0.07	-2.7%
24:00	1.87	1.86	0.01	0.4%	2.31	2.33	-0.03	-1.1%
Entire Day	45.48	43.55	1.93	4.2%	55.75	53.67	2.09	3.7%

1.5 SUMMARY AND CONCLUSIONS

In spite of the challenge of unidentified home types for the nonparticipants, the PSM routine generated a control group that represented a very good match for the trial participants, which was confirmed by both statistical and graphical comparisons. Energy consumption data for the treatment and control group were analyzed using two separate DiD approaches that resulted in similar estimates for savings. The more robust panel regression models showed statistically significant evidence for energy reduction in homes with the [redacted] thermostats.

Savings were higher for the Villa/Duplex homes in both absolute terms and as a percentage of consumption. With few preconceived notions about how the [redacted] thermostats might work in different home types, these results are likely to raise questions about why the two home types had such different results. Nevertheless, they are the product of rigorous methodological approaches that minimized bias wherever possible and the preponderance of evidence is that the [redacted] thermostats are responsible for energy savings in the participant homes.

CONFIDENTIAL

UNIVERSITY OF MIAMI **Department of Industrial Engineering**

Field Monitoring and Comparison of Rooftop HVAC Units Retrofitted with Variable Speed Drives at Retail Stores in Miami-Dade County, Florida
(Final Report)

Prepared by

Dr. Shihab Asfour, Professor and Chairman

and

Sayan Maity, Graduate Research Assistant
Joel Zahlan, Graduate Research Assistant

Submitted to

Ms. Zoila Morales

Florida Power & Light Company

5th February 2016

CONFIDENTIAL

Table of Contents

Executive Summary

This is a field test to compare energy consumptions between the use of the existing (baseline) Danfoss controller and the new [redacted] controller for the existing air conditioning unit at [redacted] supermarket site conducted by the University of Miami's Department of Industrial Engineering (UMIE). [redacted] controller modulate the Supply Fan speed, resulting in fewer compressors running and significantly lowering the Supply Fan speed, thus saving a considerable amount of energy when compared to the Standard (baseline) Mode. The vendor has installed both controllers in parallel and is switching the control of the air conditioning unit from the [redacted] controller to the [redacted] controller every two weeks.

The goal of the research is to evaluate energy savings accomplished by upgrading the existing [redacted] Controller with a new [redacted] Controller for the existing air conditioning unit at [redacted] supermarket site. Florida Power & Light Company (FPL) has retained UMIE to evaluate the energy savings. To measure the impact of the Enerfit technology, the University of Miami, Department of Industrial Engineering team installed, 23 dedicated data loggers and current transformers (CT), 9 loggers at the main A/C disconnect, 2 loggers on each of the four compressors, and 6 loggers on the supply fan at the [redacted] in Miami, Florida. These loggers were installed to acquire the power consumption at the main A/C unit for a full one year. 10 temperature and humidity loggers were also installed to monitor both the indoor and outdoor temperature and humidity of the space. Three Fluke 1735 Power Loggers were installed (One on the Main Unit, One on the Supply Fan, and One on the Compressors) to monitor actual power (kWh) and the power factor on the unit. The [redacted] controller was switched ON/OFF every two weeks to minimize the effect of the weather variation.

We adopted the practices used by FPL to divide the entire year in Winter (November-March) & Summer (April-October) seasons. Results in three data sets representing three periods of data monitored corresponding to Winter, Summer and Combined.

This report explains the methodology followed by the University of Miami team, presents the main results obtained, and explains the analysis techniques followed to investigate the

performance of the [redacted] Controller to determine whether or not the installation of the [redacted] Controller on the A/C unit will result in a reduction in the power consumption (kWh).

The multiple regression technique is the statistical tool used to analyze the data obtained. Power consumption of the A/C unit (Main kWh), Power consumption of the four compressors (Compressor kWh), and Power consumption of the supply fan (Supply Fan kWh), used as the response in three separate Regression equations, to describe the relationship between the outside temperature and the status of the [redacted] Controller (Controller ON vs. Controller OFF) as the independent variables.

Furthermore, to explain the findings of the monitored periods, the team investigated the power factor used in converting the monitored amp readings into kWh. Power factor is the ratio of the working power (also known as real power) to the total capacity required (apparent power) to provide this power or kW/kVA (kVA=> kilovoltamperes) . Two methods of applying power factor to the recorded ampere readings were used. First, the unity power factor across the logged period is used. This represents a power factor of 1. Moreover, a varying power factor approach is also used. In this approch the team takes the average power factor of the main A/C disconnect, supply fan and compressor when the controller is ON and separately when the controller is OFF. By doing this, the team is able to consider the effect the controller status has on power factor. Power factor is recorded using a Fluke 1735 Power Logger at 10-minute intervals for both the main A/C disconnect, supply fan and the compressor.

The resulting kWh calculated using both methods is found to be different, especially in the case of the supply fan, where variations in load were experienced more often, due to the presence of the [redacted] Controller and VFD.

The raw data ('Ampere' drawn) collected from the [redacted] facility first preprocessed to compute the hourly energy consumption by taking the average of the data points for an hour. Savings are computed from raw data and through regression analysis performed using Minitab software. Average power factor savings and unity power factor savings are a result of comparing the baseline (Controller OFF) vs. the [redacted] mode (Controller ON).

To summarize the findings, both power factor methodologies are used consistently in industry. Average power factor for changing motor loads is considered more accurate for motors controlled by VFD's, as they fluctuate more often. This results in a better representation of the kWh drawn by the motor. The difference in savings resulting from both power factor methodologies is significant. The drop in power factor when the [redacted] controller is turned ON is causing a large drop in the power factor of the system. Explicitly, throughout the monitoring period (Nov'-14' to Oct'-15') the average power factor measured in the Main disconnect resulted in 83% when [redacted] controller is off, and drops to 72% when the [redacted] controller is turned on. Although Florida Power and Light does not penalize for low power factor, in other states this low power factor penalty amount is substantial. As an instance, power factor below 70 percent are not permitted by [redacted] utility provider, and customers are required to invest in corrective equipment necessary to improve the power factor above this level. Some [redacted] rates call for penalties ranging from 1 to 3 percent when the power factor is between 70 and 85 percent. A 25 percent penalty charge will be applied to any billing after two consecutive months below 70 percent power factor and will continue as long as the power factor remains below this level.

A t-test was performed on both the indoor relative humidity (RH) and temperature for the summer months. The first hypothesis tested was whether the mean RH with the Enerfit controller "ON" equals the mean RH when it's "OFF". The t-test showed that there was no statistical significant difference (P <.001) between the mean RH values when the Enerfit controller was "ON" and when it was "OFF". The same conclusion was drawn when performing the t-test on the indoor temperature.

Based on the regression equation developed, it was concluded that the [redacted] controller managed to reduce the kWh consumption by 49.14%, 37.28%, and 56.0% for the A/C unit, Compressors and Supply Fan respectively when considering unit power factor. Moreover, the kWh consumption is reduced by 55.84%, 45.54%, and 68.56% for the A/C unit, Compressors and Supply Fan respectively when considering average power factor. The bar graph bellow shown the savings (reduction in kWh) scenario in the Winter, Summer and the Combined dataset resulted by the regression equations.

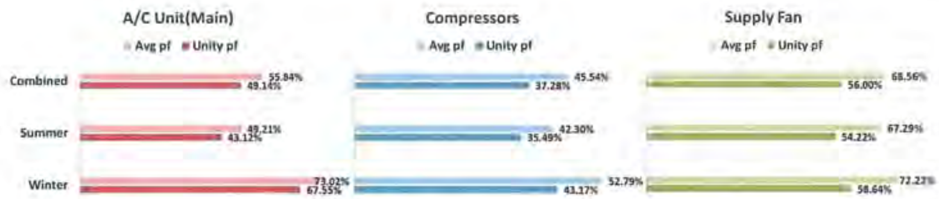

The peak demand was calculated according to the method used in Florida Power & Light (FPL), and the corresponding outside temperatures was obtained as well. Regression equations were developed to describe the relationship between the peak demand (kW) recorded at the Main service entrance and both the outside temperature and the [redacted] controller using the data collected of the entire year. Based on the regression equations developed, it was concluded that the [redacted] controller managed to reduce the peak demand by 49.13 % when a unity power factor was used and 55.82 % when using varying power factor approach .

Introduction

The [redacted] Monitoring team at the University of Miami's Industrial Engineering Department has conducted a methodology for the measuring and statistical analysis of electrical power energy consumption with the aid of data logging devices. Considering the three data sets (Winter, Summer, and Combined), two power factor modes (Unity power factor and variiying average power factor) for each, and the three regression response variables (Main, Supply Fan and Compressors) resulted in total eighteen regression models and their corresponding savings are computed.

Data collection was performed for twelve months, during which data loggers were placed at the. We adopted the practices used by FPL to divide the entire year in Winter (November-March) & Summer (April-October) seasons. Three data sets representing three periods of data monitored were analyzed in the detailed analysis. These periods were:

1. The total energy consumption (kWh) of the air conditioning unit (A/C Unit), the four compressors, and the supply fan were respectively analyzed for five months starting 11/01/2014 at 12:00am and ending 03/31/15 at 11:58 pm. This will be referred to as the Winter data set.

2. The total energy consumption (kWh) of the air conditioning unit (A/C Unit), the four compressors, and the supply fan were respectively analyzed for seven months starting 04/01/2015 at 12:00am and ending 10/30/15 at 11:58 pm. This will be referred to as the Summer data set.

3. The total energy consumption (kWh) of the air conditioning unit (A/C Unit), the four compressors, and the supply fan were respectively analyzed for twelve months starting 11/01/2014 at 12:00am and ending 10/30/2015 at 11:58 pm. This is referred to as the combined data set.

Logging frequency and duration

Data loggers will record data points every 2 minutes. Each logger has the capacity to record over 2 months of data, therefore they will be replaced every 2 months. To ensure that there are no gaps in the data, redundancy has been added by fitting each current transducer with two data loggers. The data loggers are programmed so that their replacement timing is staggered, i.e. one of the loggers will continue recording while the other is replaced. Table 1 shows the replacement times for all the loggers. The site will be visited every month and one of the data loggers will be replaced for a new 2-month logger. The second logger will be replaced the following month.

Data logger replacement

Data loggers will be replaced alternating between odd-numbered and even-numbered units every month. The plan shown in Table-1 & 2 reflects the scheduling of pick-ups and replacements. Temperature loggers will follow the same scheduale. This plan will allow for continious data collection for the entire logging period.

Data Collection Points

UMIE will be collecting amperage data at seven different points on the RTU. Phase A, B, and C will be logged for the main disconnect panel. The four compressors (1,2,3,& 4) on the unit will be logged. Both the [redacted] and Danfoss fans will also be logged.Temperature and humidity will be monitored at eight different locations in WinDixie. Four outside and four inside units will be logging both temperature and humidity at 2 minute intervals.

CONFIDENTIAL

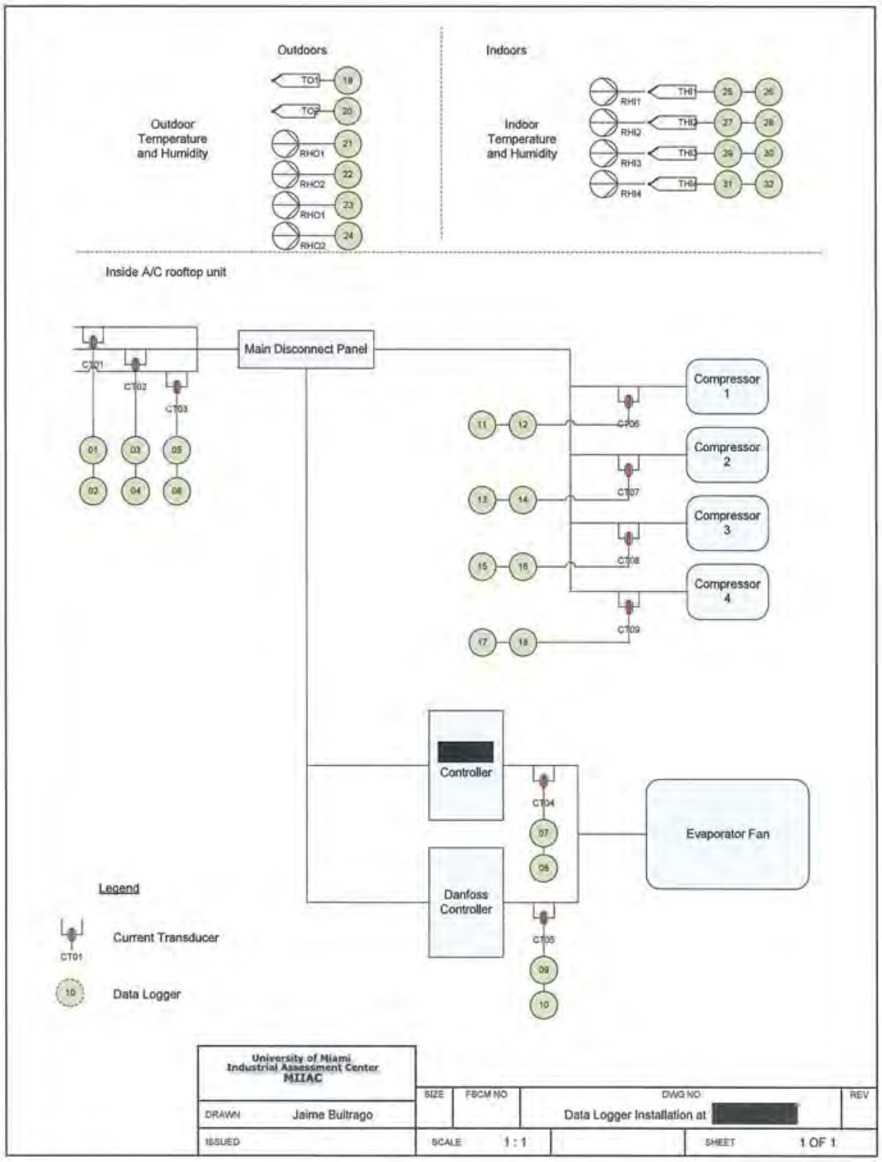

Figure 1 – Vizio Diagram Illustrating Data Logging Strategy

CONFIDENTIAL

Figure 2 - Main Disconnect Panel

Figure 3 - Evaporator Fan Controllers

Figure 4 – Compresors 1 & 2

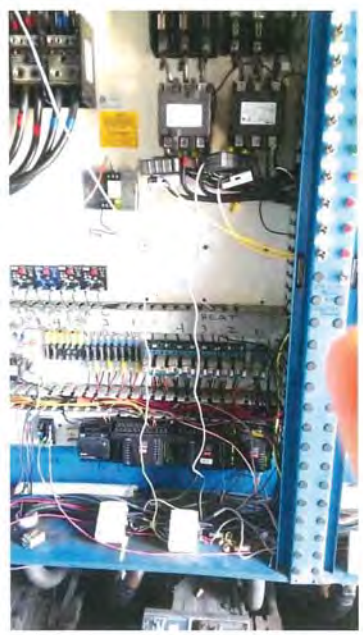

Figure 5– Compressors 3 & 4

CONFIDENTIAL

Table-1: Schedule of Data Logging at [redacted]

									Start of Cycle				End of Cycle
Logged Variables	Section	Data Logger	Identifier	Phase	Capacity	1	2	3	4	5	6	7	
Current	Main Disconnect	1	Main A	A	600 A	9/29/2014 0:00	10/27/2014 0:00	12/22/2014 0:00	2/16/2015 0:00	4/13/2015 0:00	6/8/2015 0:00	8/3/2015 0:00	9/28/2015 0:00
		2				9/29/2014 0:00	11/24/2014 0:00	1/19/2015 0:00	3/16/2015 0:00	5/11/2015 0:00	7/6/2015 0:00	8/31/2015 0:00	9/28/2015 0:00
		3	Main B	B		9/29/2014 0:00	10/27/2014 0:00	12/22/2014 0:00	2/16/2015 0:00	4/13/2015 0:00	6/8/2015 0:00	8/3/2015 0:00	9/28/2015 0:00
		4				9/29/2014 0:00	11/24/2014 0:00	1/19/2015 0:00	3/16/2015 0:00	5/11/2015 0:00	7/6/2015 0:00	8/31/2015 0:00	9/28/2015 0:00
		5	Main C	C		9/29/2014 0:00	10/27/2014 0:00	12/22/2014 0:00	2/16/2015 0:00	4/13/2015 0:00	6/8/2015 0:00	8/3/2015 0:00	9/28/2015 0:00
		6				9/29/2014 0:00	11/24/2014 0:00	1/19/2015 0:00	3/16/2015 0:00	5/11/2015 0:00	7/6/2015 0:00	8/31/2015 0:00	9/28/2015 0:00
	Evaporator Fan	7	Enerfit Controller	A	100 A	9/29/2014 0:00	10/27/2014 0:00	12/22/2014 0:00	2/16/2015 0:00	4/13/2015 0:00	6/8/2015 0:00	8/3/2015 0:00	9/28/2015 0:00
		8				9/29/2014 0:00	11/24/2014 0:00	1/19/2015 0:00	3/16/2015 0:00	5/11/2015 0:00	7/6/2015 0:00	8/31/2015 0:00	9/28/2015 0:00
		9	Danfoss Controller	A		9/29/2014 0:00	10/27/2014 0:00	12/22/2014 0:00	2/16/2015 0:00	4/13/2015 0:00	6/8/2015 0:00	8/3/2015 0:00	9/28/2015 0:00
		10				9/29/2014 0:00	11/24/2014 0:00	1/19/2015 0:00	3/16/2015 0:00	5/11/2015 0:00	7/6/2015 0:00	8/31/2015 0:00	9/28/2015 0:00
	Compressors	11	Compressor 1	C		9/29/2014 0:00	10/27/2014 0:00	12/22/2014 0:00	2/16/2015 0:00	4/13/2015 0:00	6/8/2015 0:00	8/3/2015 0:00	9/28/2015 0:00
		12				9/29/2014 0:00	11/24/2014 0:00	1/19/2015 0:00	3/16/2015 0:00	5/11/2015 0:00	7/6/2015 0:00	8/31/2015 0:00	9/28/2015 0:00
		13	Compressor 2	C		9/29/2014 0:00	10/27/2014 0:00	12/22/2014 0:00	2/16/2015 0:00	4/13/2015 0:00	6/8/2015 0:00	8/3/2015 0:00	9/28/2015 0:00
		14				9/29/2014 0:00	11/24/2014 0:00	1/19/2015 0:00	3/16/2015 0:00	5/11/2015 0:00	7/6/2015 0:00	8/31/2015 0:00	9/28/2015 0:00
		15	Compressor 3	A		9/29/2014 0:00	10/27/2014 0:00	12/22/2014 0:00	2/16/2015 0:00	4/13/2015 0:00	6/8/2015 0:00	8/3/2015 0:00	9/28/2015 0:00
		16				9/29/2014 0:00	11/24/2014 0:00	1/19/2015 0:00	3/16/2015 0:00	5/11/2015 0:00	7/6/2015 0:00	8/31/2015 0:00	9/28/2015 0:00
		17	Compressor 4	A		9/29/2014 0:00	10/27/2014 0:00	12/22/2014 0:00	2/16/2015 0:00	4/13/2015 0:00	6/8/2015 0:00	8/3/2015 0:00	9/28/2015 0:00
		18				9/29/2014 0:00	11/24/2014 0:00	1/19/2015 0:00	3/16/2015 0:00	5/11/2015 0:00	7/6/2015 0:00	8/31/2015 0:00	9/28/2015 0:00
Temperature and Humidity	Outdoor Temperature	19	Thermocouple 1			10/6/2014 0:00	10/27/2014 0:00	12/22/2014 0:00	2/16/2015 0:00	4/13/2015 0:00	6/8/2015 0:00	8/3/2015 0:00	9/28/2015 0:00
		20	Thermocouple 2			10/6/2014 0:00	11/24/2014 0:00	1/19/2015 0:00	3/16/2015 0:00	5/11/2015 0:00	7/6/2015 0:00	8/31/2015 0:00	9/28/2015 0:00
		21	RH Outdoor 1			9/29/2014 0:00	10/27/2014 0:00	12/22/2014 0:00	2/16/2015 0:00	4/13/2015 0:00	6/8/2015 0:00	8/3/2015 0:00	9/28/2015 0:00
		22	RH Outdoor 2			9/29/2014 0:00	11/24/2014 0:00	1/19/2015 0:00	3/16/2015 0:00	5/11/2015 0:00	7/6/2015 0:00	8/31/2015 0:00	9/28/2015 0:00
		23	RH Outdoor 3			9/29/2014 0:00	10/27/2014 0:00	12/22/2014 0:00	2/16/2015 0:00	4/13/2015 0:00	6/8/2015 0:00	8/3/2015 0:00	9/28/2015 0:00
		24	RH Outdoor 4			9/29/2014 0:00	11/24/2014 0:00	1/19/2015 0:00	3/16/2015 0:00	5/11/2015 0:00	7/6/2015 0:00	8/31/2015 0:00	9/28/2015 0:00
	Indoor Temperature and Relative Humidity	25	Location 1			9/29/2014 0:00	10/27/2014 0:00	12/22/2014 0:00	2/16/2015 0:00	4/13/2015 0:00	6/8/2015 0:00	8/3/2015 0:00	9/28/2015 0:00
		26				9/29/2014 0:00	11/24/2014 0:00	1/19/2015 0:00	3/16/2015 0:00	5/11/2015 0:00	7/6/2015 0:00	8/31/2015 0:00	9/28/2015 0:00
		27	Location 2			9/29/2014 0:00	10/27/2014 0:00	12/22/2014 0:00	2/16/2015 0:00	4/13/2015 0:00	6/8/2015 0:00	8/3/2015 0:00	9/28/2015 0:00
		28				9/29/2014 0:00	11/24/2014 0:00	1/19/2015 0:00	3/16/2015 0:00	5/11/2015 0:00	7/6/2015 0:00	8/31/2015 0:00	9/28/2015 0:00
		29	Location 3			9/29/2014 0:00	10/27/2014 0:00	12/22/2014 0:00	2/16/2015 0:00	4/13/2015 0:00	6/8/2015 0:00	8/3/2015 0:00	9/28/2015 0:00
		30				9/29/2014 0:00	11/24/2014 0:00	1/19/2015 0:00	3/16/2015 0:00	5/11/2015 0:00	7/6/2015 0:00	8/31/2015 0:00	9/28/2015 0:00

CONFIDENTIAL

Table-2: Schedule of Data Collection at [redacted]

ID	Task Name	Duration	Start	Finish
1	Install Loggers	1 day	Wed 9/24/14	Thu 9/25/14
2	Start Logging Data on Odd-Numbered Loggers	0 days	Mon 9/29/14	Mon 9/29/14
3	Start Logging Data on Even-Numbered Loggers	0 days	Mon 9/29/14	Mon 9/29/14
4	Data Logging on Odd-Numbered Loggers	28 days	Mon 9/29/14	Mon 10/27/14
5	Data Logging on Even-Numbered Loggers	56 days	Mon 9/29/14	Mon 11/24/14
6	Pick up and Replace Odd-Numbered Loggers	0 days	Mon 10/27/1	Mon 10/27/14
7	Pick up and Replace Even-Numbered Loggers	0 days	Mon 11/24/1	Mon 11/24/14
8	Data Logging on Odd-Numbered Loggers	56 days	Mon 10/27/1	Mon 12/22/14
9	Data Logging on Even-Numbered Loggers	56 days	Mon 11/24/1	Mon 1/19/15
10	Pick up and Replace Odd-Numbered Loggers	0 days	Mon 12/22/1	Mon 12/22/14
11	Pick up and Replace Even-Numbered Loggers	0 days	Mon 1/19/15	Mon 1/19/15
12	Data Logging on Odd-Numbered Loggers	56 days	Mon 12/22/1	Mon 2/16/15
13	Data Logging on Even-Numbered Loggers	56 days	Mon 1/19/15	Mon 3/16/15
14	Pick up and Replace Odd-Numbered Loggers	0 days	Mon 2/16/15	Mon 2/16/15
15	Pick up and Replace Even-Numbered Loggers	0 days	Mon 3/16/15	Mon 3/16/15
16	Data Logging on Odd-Numbered Loggers	56 days	Mon 2/16/15	Mon 4/13/15
17	Data Logging on Even-Numbered Loggers	56 days	Mon 3/16/15	Mon 5/11/15
18	Pick up and Replace Odd-Numbered Loggers	0 days	Mon 4/13/15	Mon 4/13/15
19	Pick up and Replace Even-Numbered Loggers	0 days	Mon 5/11/15	Mon 5/11/15
20	Data Logging on Odd-Numbered Loggers	56 days	Mon 4/13/15	Mon 6/8/15
21	Data Logging on Even-Numbered Loggers	56 days	Mon 5/11/15	Mon 7/6/15
22	Pick up and Replace Odd-Numbered Loggers	0 days	Mon 6/8/15	Mon 6/8/15
23	Pick up and Replace Even-Numbered Loggers	0 days	Mon 7/6/15	Mon 7/6/15
24	Data Logging on Odd-Numbered Loggers	56 days	Mon 6/8/15	Mon 8/3/15
25	Data Logging on Even-Numbered Loggers	56 days	Mon 7/6/15	Mon 8/31/15
26	Pick up and Replace Odd-Numbered Loggers	0 days	Mon 8/3/15	Mon 8/3/15
27	Pick up and Replace Even-Numbered Loggers	0 days	Mon 8/31/15	Mon 8/31/15
28	Data Logging on Odd-Numbered Loggers	56 days	Mon 8/3/15	Mon 9/28/15
29	Data Logging on Even-Numbered Loggers	28 days	Mon 8/31/15	Mon 9/28/15
30	Pick up and Replace Odd-Numbered Loggers	0 days	Mon 9/28/15	Mon 9/28/15
31	Pick up and Replace Even-Numbered Loggers	0 days	Mon 9/28/15	Mon 9/28/15

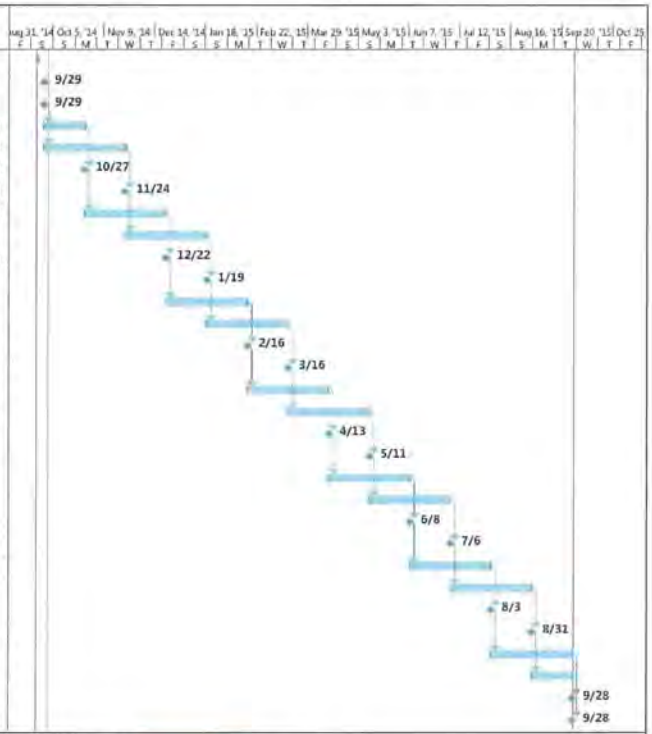

Project: Project Plan for Winn-D
Date: Thu 10/2/14

Task, Split, Milestone, Summary, Project Summary, Inactive Task, Inactive Milestone, Inactive Summary, Manual Task, Duration-only, Manual Summary Rollup, Manual Summary, Start-only, Finish-only, External Tasks, External Milestone, Deadline, Progress, Manual Progress

Data Collection Protocol

Data was sampled every 2 minutes and the logging process was continuously carried out. The controller was switched ON/OFF every other week to minimize the effect of the weather variation.

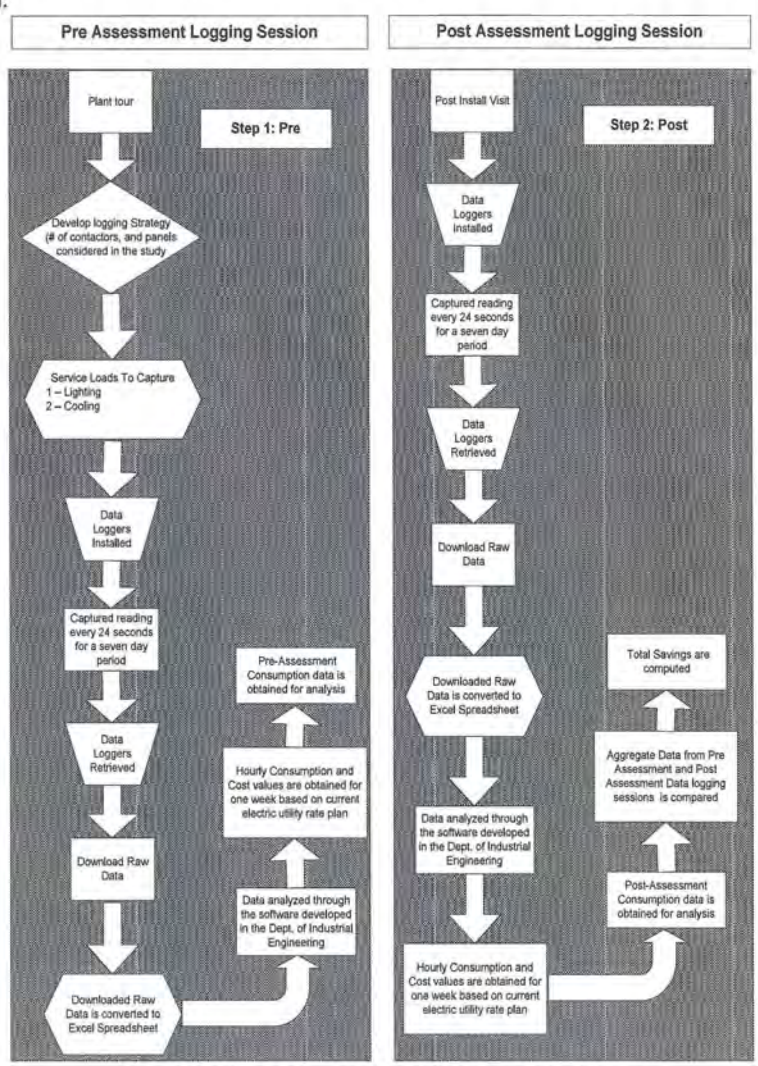

Figure 6. The Measuring & Verification Methodology

Table-3: Periods corresponding to controller switching ON & OFF

Date	Controller
10/31/14 – 11/03/14	ON
11/03/14 – 11/17/14	OFF
11/17/14 – 12/01/14	ON
12/01/14 – 12/15/14	OFF
12/15/14 – 12/29/14	ON
12/29/14 – 01/04/15	OFF
01/04/15 – 01/18/15	ON
01/18/15 – 02/01/15	OFF
02/01/15 – 02/15/15	ON
02/15/15 – 03/01/15	OFF
03/01/15– 03/15/15	ON
03/15/15– 03/29/15	OFF
03/29/15– 04/05/15	ON
04/05/15– 04/19/15	OFF
04/19/15– 05/03/15	ON
05/03/15– 05/17/15	OFF
05/17/15– 05/31/15	ON
05/31/15– 06/14/15	OFF
06/14/15– 06/28/15	ON
06/28/15– 07/05/15	OFF
07/05/15– 07/19/15	ON
07/19/15– 08/02/15	OFF
08/02/15– 08/16/15	ON
08/16/15– 08/30/15	OFF
08/30/15– 09/06/15	ON
09/06/15– 09/20/15	OFF
09/20/15– 10/04/15	ON
10/04/15– 10/18/15	OFF
10/18/15– 10/31/15	ON

Power Factor and Voltage:

During the logging period, kW was monitored for the entire year for both the main disconnect of the Air conditioning unit and the supply fan. This resulted in one-year worth of trend data with both current, voltage and power factor being monitored. This data was used to establish average voltage in the system and a power factor curve. Both the average voltage and power factor curve is be used in future data analysis to convert the collected amps into kW. The load of the air conditioning unit will determine the power factor of the unit. As the load of the air conditioning unit goes up, so does the power factor. At 100 % load the resulting power factor is 86.7%. Likewise, at 0% load the resulting power factor is 37%

To perform data analysis we have considered the average power factor during the controller on & controller off time-period.

Energy Savings:

Energy savings are the difference in kW when the controller is OFF vs. ON. kW is calculated as follows:

$$kW_{calc} = \frac{Volts * Amps * PF * \sqrt{3}}{1000} \quad (1)$$

Average demand savings will be determined by subtracting the average demand of the post-retrofit system from the baseline system.

$$kW_{saved} = kW_{Controller\ OFF} - kW_{Controller\ ON} \quad (2)$$

Annual energy savings will be calculated by multiplying the demand savings by the annual hours of operation.

$$kWh_{annual\ saved} = (kW_{Controller\ OFF} - kW_{Controller\ ON}) * AOH \quad (3)$$

Where AOH is annual operating hours.

Statistical Analysis of Kilo Watt Hour (kWh) Consumption:

The following section details the results of the data logged. The relation of power consumptions during the controller on/off periods are analyzed and discussed. Daily and hourly average data is computed to display the kW and temperature variation trends in summer and winter seasons based on the controller status. There are six sets of plots generated from six sets of data presented in the sections below.

The multiple regression technique is the statistical tool used to analyze the data collected.

Every week's data was downloaded from the loggers, and then processed in order to determine the total energy consumption of A/C unit, which in turn represents the total cooling load of the supermarket.

The total energy consumption (kWh) of the air conditioning unit (A/C Unit), the four compressors, and the supply fan were respectively analyzed for three different data sets.

Both unity power factor and average power factor for controller ON and OFF were applied to each data set. Three Regression equations were developed to describe the relationship between the:

1. Power consumption of the A/C unit (Main kWh) used as the response, while using both the outside temperature and the status of the [redacted] controller as the independent variables.

2. Power consumption of the four compressors (Compressor kWh) used as the response, while using both the outside temperature and the status of the [redacted] controller as the independent variables.

3. Power consumption of the supply fan (Supply Fan kWh) used as the response, while using both the outside temperature and the status of the [redacted] controller as the independent variables.

Regression Model #1, 2, & 3:

The total energy consumption (kWh) of the air conditioning unit (A/C Unit), the four compressors, and the supply fan were respectively analyzed for five months starting 11/01/2014 at 12:00am and ending 03/31/15 at 11:58 pm. ***Using the average power factor computed when controller is on & off.***

Model #1: Total Cooling Load Power Consumption Savings

The regression equation to correlate the hourly A/C Unit kWh consumption with the temperature and the [redacted] controller status (whether it's ON or OFF) is as follows:

$$Main\ kWh = \beta_0 + \beta_1 \times Outside\ Temperature + \beta_2 \times Enerfit\ Controller$$

Where:

Main kWh = the hourly power consumption of the air conditioning unit (A/C Unit).

β_0 = the intercept of the regression equation

β_1 = regression coefficient of the model relating the hourly temperature to the hourly kWh

Outside Temperature = hourly outside temperature in $^{\circ}$F

β_2 = regression coefficient of the model relating the hourly kWh consumption to the effect of the [redacted] controller

[redacted] ***Controller*** = a dummy variable that is assigned a value **0** when the [redacted] controller is "OFF" and **1** when the controller is "ON".

First, a best subsets regression was performed in order to determine the number of independent variables to be included in the model (Table 4).

number of Variables	R-Sq	R-Sq(adj)	SE
1	23.62	23.59	16.0392
1	24.31	24.29	15.9665
2	47.64	47.61	13.2810
Response is Main kWh			

The second step performed was to test if the effects of both the outside temperature and the [redacted] controller are statistically significant. An Analysis of Variance (ANOVA) was performed to determine whether the [redacted] controller reduction in the kWh is statistically significant.

Table 5 depicts the ANOVA table obtained. The technique used to perform the ANOVA was the multiple regression procedure.

Table 5: Analysis of Variance of Main kWh, using Adjusted SS for Tests

Source	DF	SS	MS	F	P
Regression	2	581182	290591	1647.49	0.000
Temp	1	293098	293098	1661.71	0.000
Controller	1	284664	284664	1613.89	0.000
Error	3621	638686	176		
Total	3623	1219868			

As shown in Table 5, both the effects of the controller and the outside temperature on the kWh were statistically significant (*P*<.001), meaning that both the ambient temperature and the controller statistically affect the kW consumption.

The next step during the regression analysis was to determine the coefficients corresponding to each independent variable in the governing equation explaining the relationship between the temperature, the controller, and the Main kWh. Table 6 summarizes the coefficients obtained from the regression analysis.

Table 6. Main kWh Regression Analysis coefficients

Term	Coef	SECoef	T-Value	P-Value	VIF
Constant	-54.99	1.97	-27.92	0.000	
Temp	1.0891	0.0267	40.76	0.000	1.00
Controller1	-17.726	0.441	-40.17	0.000	1.00

Regression Analysis: Main_kwh versus Temp, Controller

```
Method

Categorical predictor coding  (1, 0)

Analysis of Variance

Source DF   Adj SS   Adj MS F-Value       P-Value
Regression    2      581182 290591 1647.49       0.000
  Temp 1      293098 293098 1661.71       0.000
  Controller 1       284664 284664 1613.89       0.000
Error  3621   638686 176
  Lack-of-Fit 3578   628258 176    0.72   0.949
  Pure Error 43      10428  243
Total  3623   1219868

Model Summary

      S    R-sq  R-sq(adj)  R-sq(pred)
13.2810  47.64%     47.61%      47.55%

Coefficients

Term            Coef  SE Coef  T-Value  P-Value   VIF
Constant      -54.99     1.97   -27.92    0.000
Temp          1.0891   0.0267    40.76    0.000  1.00
Controller
  1          -17.726    0.441   -40.17    0.000  1.00

Regression Equation

Controller
0            Main_kWh = -54.99 + 1.0891 Temp

1            Main_kWh = -72.72 + 1.0891 Temp

Regression Equation including Controller
```

Main_kWh = -54.99 + 1.0891 Temp - 17.726 Controller

The above equation means that, by controlling for the outside temperature, and by turning the controller ON, a reduction in the kWh of 17.73 kWh occurs.

The average kWh consumption of the Main unit during the OFF periods (where the controller was turned off) is 24.28 kWh. The regression equation indicates that an average reduction of 17.73 kWh is experienced when the controller is turned ON while controlling for the outside temperature. This results in a percentage savings in the baseline kWh (when the controller is OFF) of 73.02% while maintaining the effect of the outside temperature. Figure displays the box plot distribution for Main kWh when the controller is ON vs. OFF.

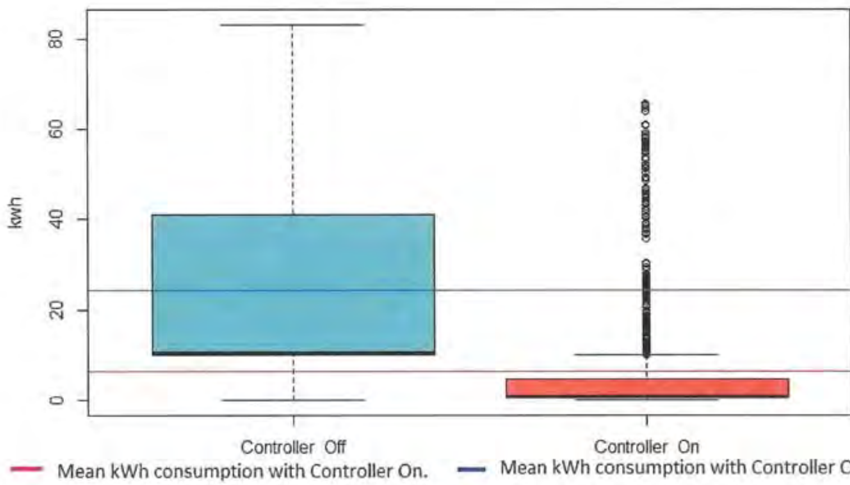

Figure 7: The Box Plot of the Main kWh and the Controller Status.

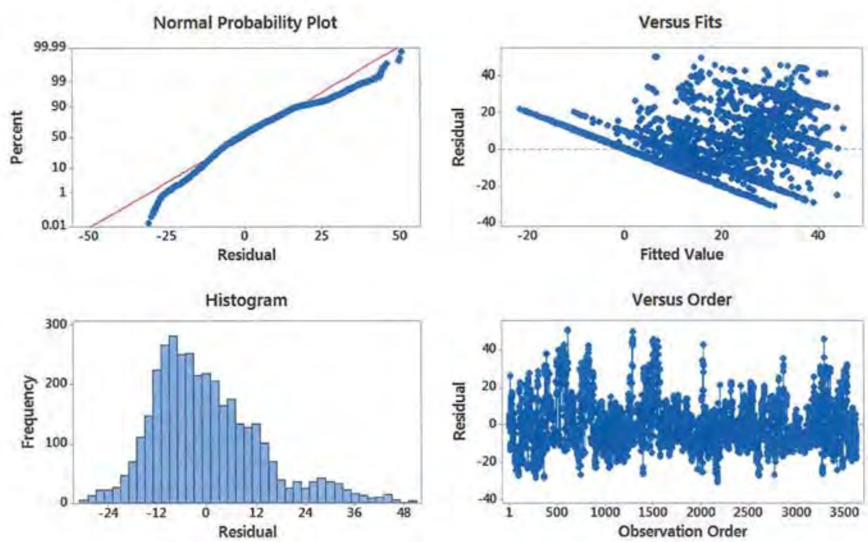

Figure 8: Residual Plots for Main kWh.

Model #2: Compressor Power Consumption Savings

The regression equation to correlate the Compressor kWh consumption with the temperature and the [redacted] controller status (whether it's ON or OFF) is as follows:

$$\textit{Compressor kWh} = \beta_0 + \beta_1 \times \textit{Outside Temperature} + \beta_2 \times \textit{Enerfit Controller}$$

Where:

Compressor kWh = the hourly power consumption due to the four compressors.

β_0 = the intercept of the regression equation

β_1 = regression coefficient of the model relating the hourly temperature to the hourly kWh

Outside Temperature = hourly outside temperature in $^{\circ}$F

β_2 = regression coefficient of the model relating the hourly kWh consumption to the effect of the [redacted] controller

[redacted] ***Controller*** = a dummy variable that is assigned a value **0** when the [redacted] controller is "OFF" and **1** when the controller is "ON".

First, a best subsets regression was performed in order to determine the number of independent variables to be included in the model (Table 7).

number of Variables	R-Sq	R-Sq(adj)	SE
1	6.87	6.84	11.7995
1	24.50	24.48	10.6238
2	31.22	31.18	10.1415
Response is Compressor kWh			

The second step performed was to test if the effects of both the outside temperature and the [redacted] controller are statistically significant. An Analysis of Variance (ANOVA) was performed to determine whether the [redacted] controller reduction in the kWh is statistically significant.

Table 8 depicts the ANOVA table obtained. The technique used to perform the ANOVA was the multiple regression procedure.

Table 8: Analysis of Variance of Main kWh, using Adjusted SS for Tests

Source	DF	AdjSS	AdjMS	F-Value	P-Value
Regression	2	169065	84533	821.91	0.000
Temp	1	131866	131866	1282.13	0.000
Controller	1	36378	36378	353.70	0.000
Error	3621	372416	103		
Total	3623	541481			

As shown in Table 8, both the effects of the controller and the outside temperature on the kWh were statistically significant (*P*<.001), meaning that both the ambient temperature and the controller statistically affect the kW consumption.

The next step during the regression analysis was to determine the coefficients corresponding to each independent variable in the governing equation explaining the relationship between the temperature, the controller, and the Main kWh. Table 9 summarizes the coefficients obtained from the regression analysis.

Table 9. Main kWh Regression Analysis coefficients

Term	Coef	SECoef	T-Value	P-Value	VIF
Constant	-41.16	1.50	-27.37	0.000	
Temp	0.7305	0.0204	35.81	0.000	1.00
Controller1	-6.337	0.337	-18.81	0.000	1.000

Regression Analysis: Compressor_kwh versus Temp, Controller

Method

Categorical predictor coding (1, 0)

Analysis of Variance

Source	DF	Adj SS	Adj MS	F-Value	P-Value
Regression	2	169065	84533	821.91	0.000
Temp	1	131866	131866	1282.13	0.000
Controller	1	36378	36378	353.70	0.000
Error	3621	372416	103		
Lack-of-Fit	3578	367490	103	0.90	0.720
Pure Error	43	4927	115		
Total	3623	541481			

Model Summary

S	R-sq	R-sq(adj)	R-sq(pred)
10.1415	31.22%	31.18%	31.10%

Coefficients

Term	Coef	SE Coef	T-Value	P-Value	VIF
Constant	-41.16	1.50	-27.37	0.000	
Temp	0.7305	0.0204	35.81	0.000	1.00
Controller					
1	-6.337	0.337	-18.81	0.000	1.00

Regression Equation

Controller
0   Compressor_kWh = -41.16 + 0.7305 Temp

1   Compressor_kWh = -47.50 + 0.7305 Temp

Regression Equation including Controller

Compressor_kWh = -41.16 + 0.7305 Temp - 6.337 Controller

The above equation means that, by **controlling for the outside temperature**, and by turning the controller ON, a reduction in the kWh of 6.34 kWh occurs in the compressors.

The average kWh consumption of the four compressors during the OFF periods (where the controller was turned off) is 12.01 kWh. The regression equation indicates that an average reduction of 6.34 kWh is experienced when the controller is turned ON while controlling for the outside temperature. This results in a percentage savings in the baseline kWh (when the

controller is OFF) of 52.79% while maintaining the effect of the outside temperature. Figure displays the box plot distribution for Compressor kWh when the controller is ON vs. OFF.

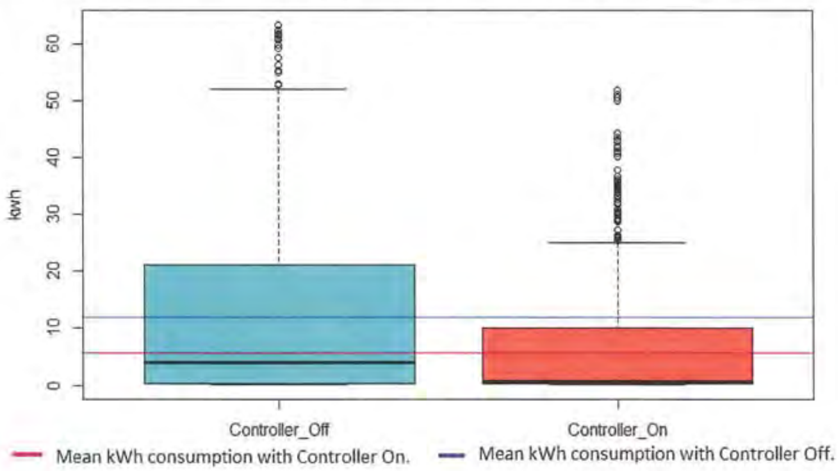

Figure 9: The Box Plot of the Compressor kWh and the Controller Status.

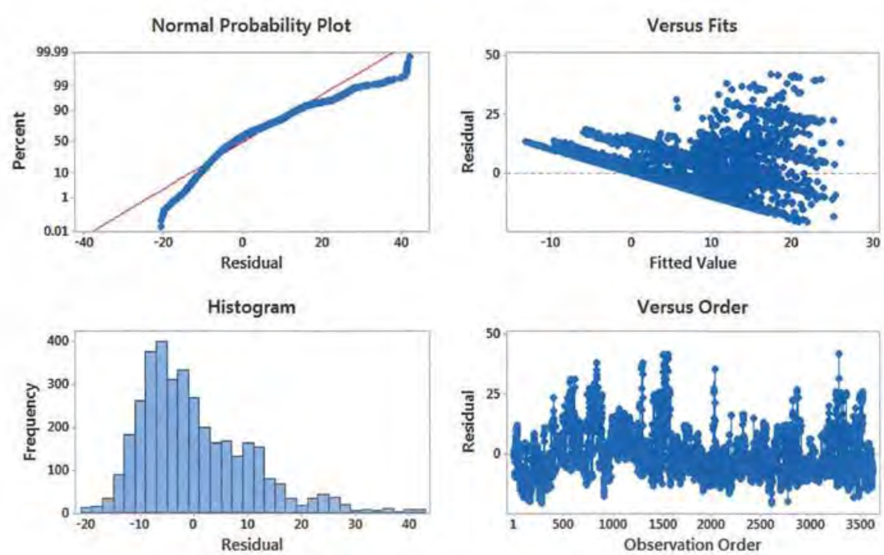

Figure 10: Residual Plots for Compressor kWh

Model #3: Supply Fan Power Consumption Savings

The regression equation to correlate the Supply Fan kWh consumption with the temperature and the [redacted] controller status (whether it's ON or OFF) is as follows:

$$Supply\ Fan\ kWh = \beta_0 + \beta_1 \times Outside\ Temperature + \beta_2 \times Enerfit\ Controller$$

Where:

Supply Fan kWh = the hourly power consumption due to the Supply Fan.

β_0 = the intercept of the regression equation

β_1 = regression coefficient of the model relating the hourly temperature to the hourly kWh

Outside Temperature = hourly outside temperature in $^{\circ}F$

β_2 = regression coefficient of the model relating the hourly kWh consumption to the effect of the [redacted] controller

[redacted] ***Controller*** = a dummy variable that is assigned a value **0** when the [redacted] controller is "OFF" and **1** when the controller is "ON".

First, a best subsets regression was performed in order to determine the number of independent variables to be included in the model (Table 10).

number of Variables	R-Sq	R-Sq(adj)	SE
1	77.74	77.73	1.93504
1	0.19	0.16	4.09718
2	77.88	77.87	1.92907
Response is Supply Fan kWh			

The second step performed was to test if the effects of both the outside temperature and the [redacted] controller are statistically significant. An Analysis of Variance (ANOVA) was performed to determine whether the [redacted] controller reduction in the kWh is statistically significant.

Table 11 depicts the ANOVA table obtained. The technique used to perform the ANOVA was the multiple regression procedure.

Table 11: Analysis of Variance of Main kWh, using Adjusted SS for Tests

Source	DF	AdjSS	AdjMS	F-Value	P-Value
Regression	2	47439.9	23719.9	6374.08	0.000
Temp	1	87.2	87.2	23.44	0.000
Controller	1	47327.1	47327.1	12717.85	0.000
Error	3621	13474.9	3.7		
Total	3623	60914.8			

As shown in Table 11, both the effects of the controller and the outside temperature on the kWh were statistically significant ($P<.001$), meaning that both the ambient temperature and the controller statistically affect the kW consumption.

The next step during the regression analysis was to determine the coefficients corresponding to each independent variable in the governing equation explaining the relationship between the temperature, the controller, and the Main kWh. Table 12 summarizes the coefficients obtained from the regression analysis.

Table 12. Main kWh Regression Analysis coefficients

Term	Coef	SECoef	T-Value	P-Value	VIF
Constant	8.646	0.286	30.23	0.000	
Temp	0.01879	0.00388	4.84	0.000	1.00
Controller	-7.2277	0.0641	-112.77	0.000	1.00

CONFIDENTIAL

Regression Analysis: Supply Fan_kwh versus Temp, Controller

Method

Categorical predictor coding (1, 0)

Analysis of Variance

Source	DF	Adj SS	Adj MS	F-Value	P-Value
Regression	2	47439.9	23719.9	6374.08	0.000
Temp	1	87.2	87.2	23.44	0.000
Controller	1	47327.1	47327.1	12717.85	0.000
Error	3621	13474.9	3.7		
Lack-of-Fit	3578	13233.2	3.7	0.66	0.984
Pure Error	43	241.7	5.6		
Total	3623	60914.8			

Model Summary

S	R-sq	R-sq(adj)	R-sq(pred)
1.92907	77.88%	77.87%	77.85%

Coefficients

Term	Coef	SE Coef	T-Value	P-Value	VIF
Constant	8.646	0.286	30.23	0.000	
Temp	0.01879	0.00388	4.84	0.000	1.00
Controller					
1	-7.2277	0.0641	-112.77	0.000	1.00

Regression Equation

Controller	
0	Supply_Fan_kWh = 8.646 + 0.01879 Temp
1	Supply_Fan_kWh = 1.419 + 0.01879 Temp

Regression Equation including Controller

Supply_Fan_kWh = 8.646 + 0.01879 Temp - 7.2277 Controller

The above equation means that, by **controlling for the outside temperature**, and by turning the controller ON, a reduction in the kWh of 7.23 kWh occurs in the compressors.

The average kWh consumption of the Supply Fan during the OFF periods (where the controller was turned off) is 10.01 kWh. The regression equation indicates that an average reduction of 7.23 kWh is experienced when the controller is turned ON while controlling for the outside temperature. This results in a percentage savings in the baseline kWh (when the controller is OFF) of 72.22% while maintaining the effect of the outside temperature. Figure displays the box plot distribution for Supply Fan kWh when the controller is ON vs. OFF.

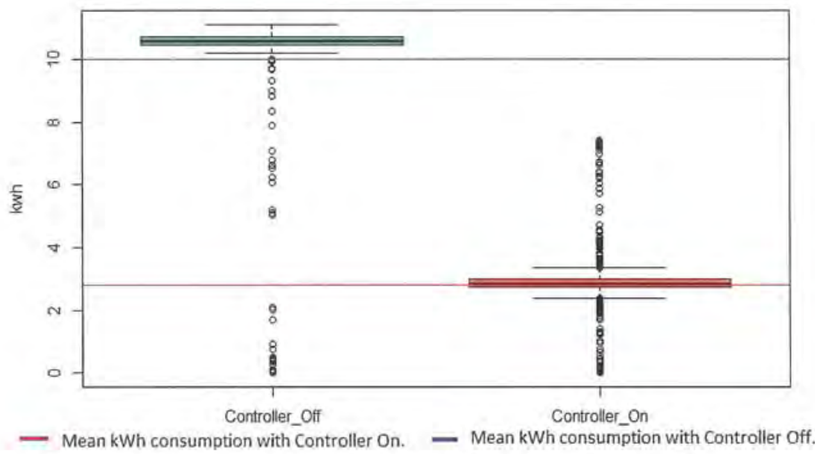

Figure 11: The Box Plot of the Supply Fan kWh and the Controller Status.

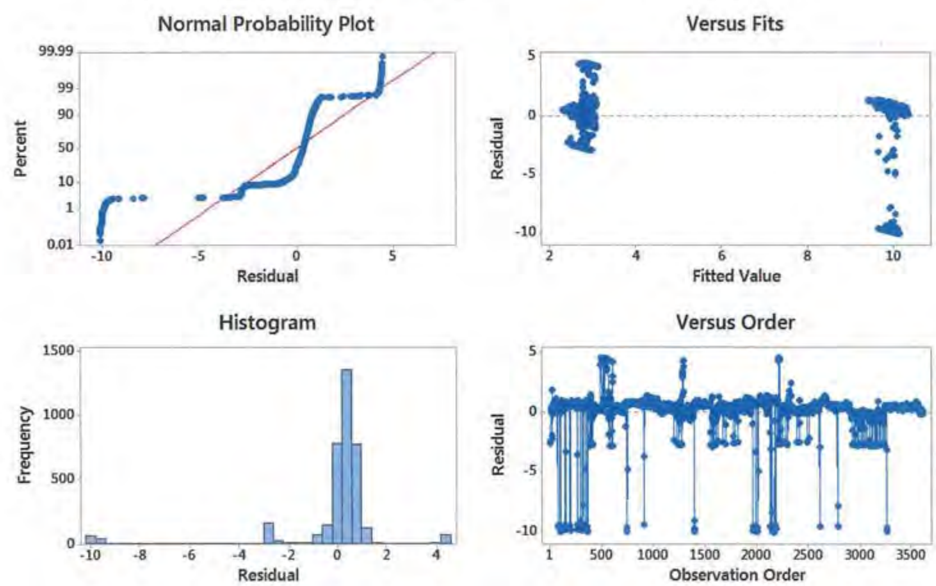

Figure 12: Residual Plots for Supply Fan kWh

Winter (November-March) with Average Controller ON and OFF Power Factor

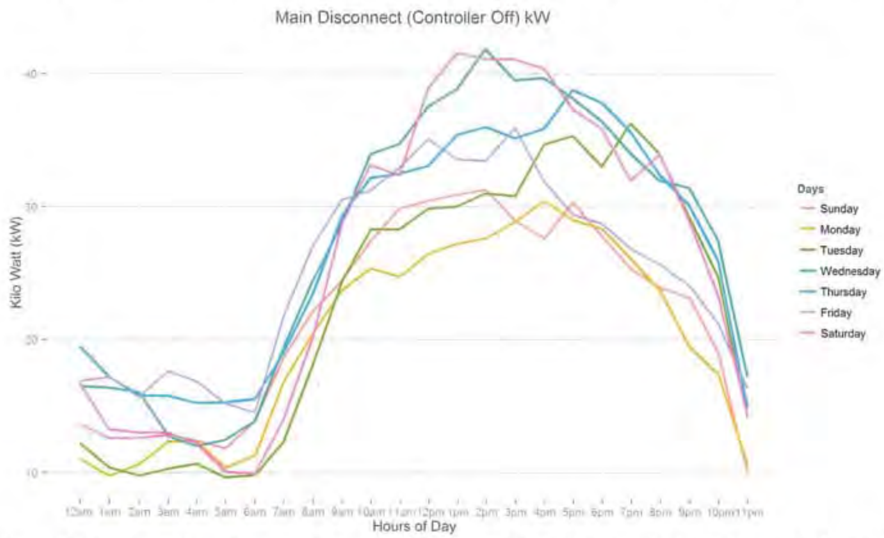

Figure 13: The figure above illustrates the average kWh draw of the main A/C unit when the controller is OFF for each hour of the day and each day of the week. This is helpful in understanding the operation of the unit throughout the days of the week. It is clear that as the temperature increases throughout the day, so will the kWh draw.

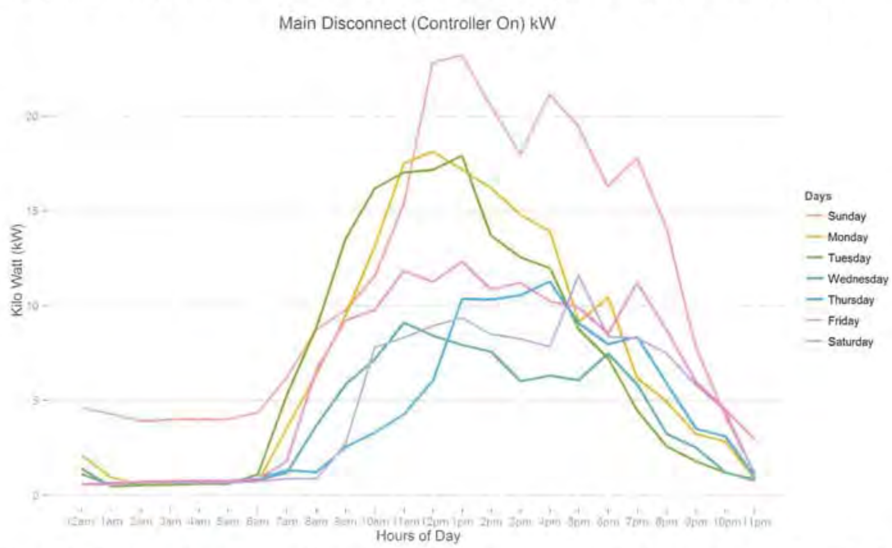

Figure 14: The figure above illustrates the average kWh draw of the main A/C unit when the controller is ON for each hour of the day and each day of the week. This is helpful in understanding the operation of the unit throughout the days of the week. It is clear that as the temperature increases throughout the day, so will the kWh draw.

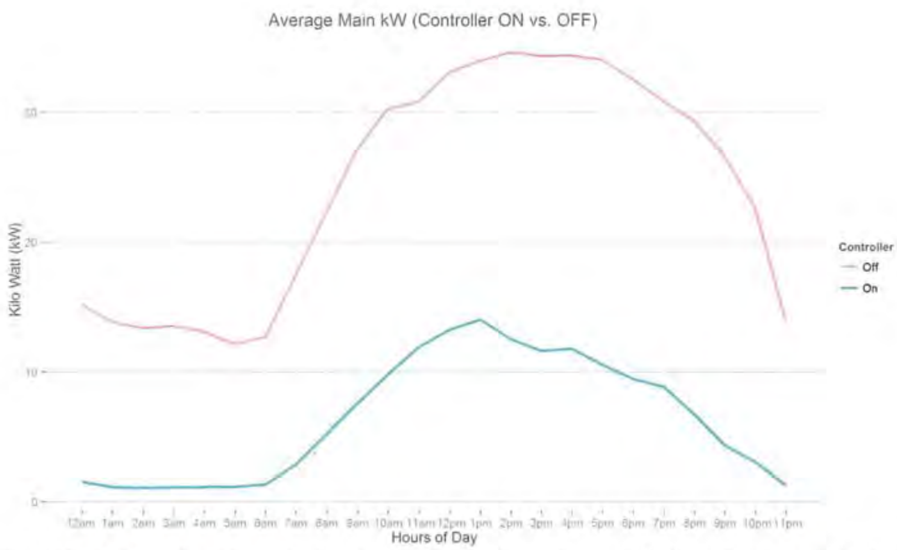

Figure 15: The figure above shows that there is a significant reduction in main kWh draw when the controller is ON versus when it is OFF. The kWh draw follows a similar trend throughout the day. This indicates that both control strategies are reacting to the outside temperature and super market occupancy.

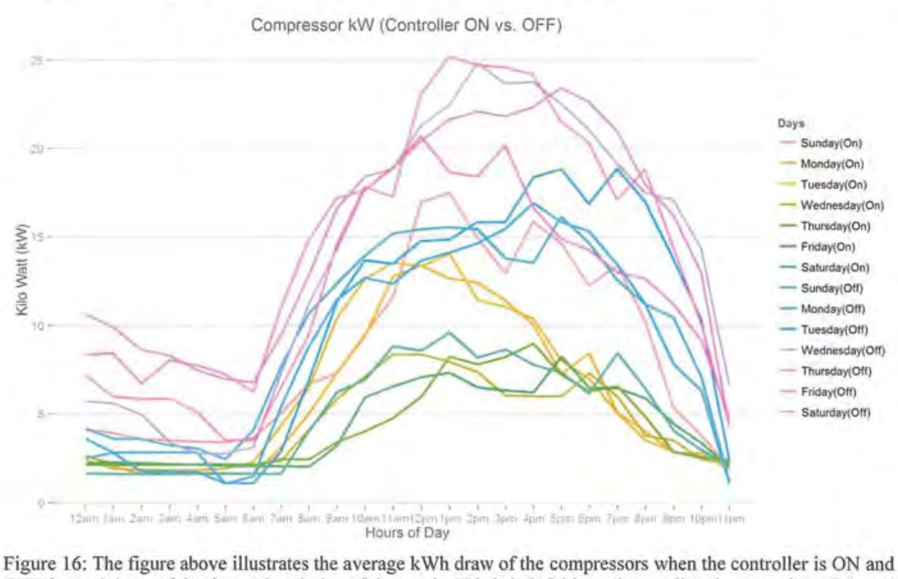

Figure 16: The figure above illustrates the average kWh draw of the compressors when the controller is ON and OFF for each hour of the day and each day of the week. This is helpful in understanding the operation of the unit throughout the days of the week. It is clear that as the temperature increases throughout the day, so will the kWh draw.

CONFIDENTIAL

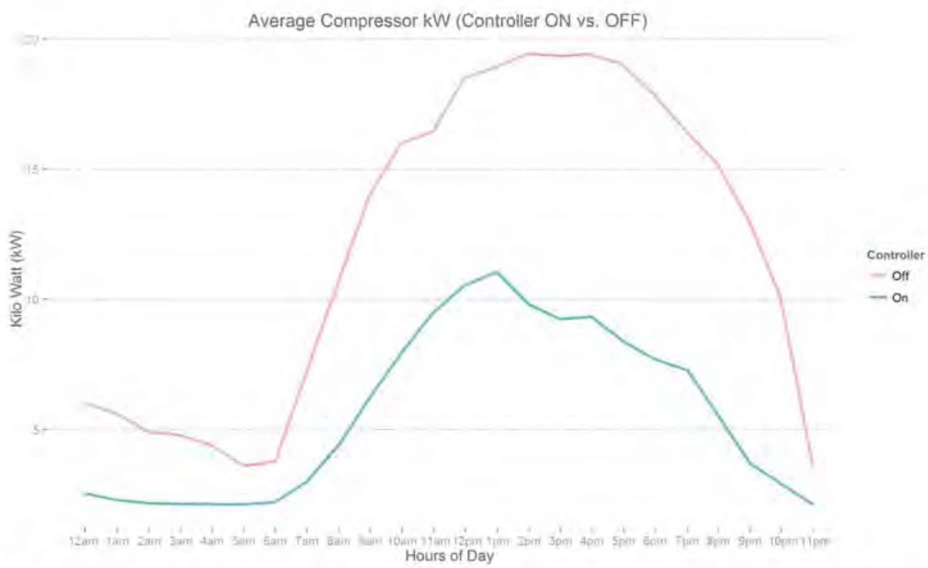

Figure 17: The figure above illustrates that there is a significant reduction in compressor kWh draw when the controller is ON versus when it is OFF. The kWh draw follows a similar trend throughout the day. This indicates that both control strategies are reacting to the outside temperature and super market occupancy.

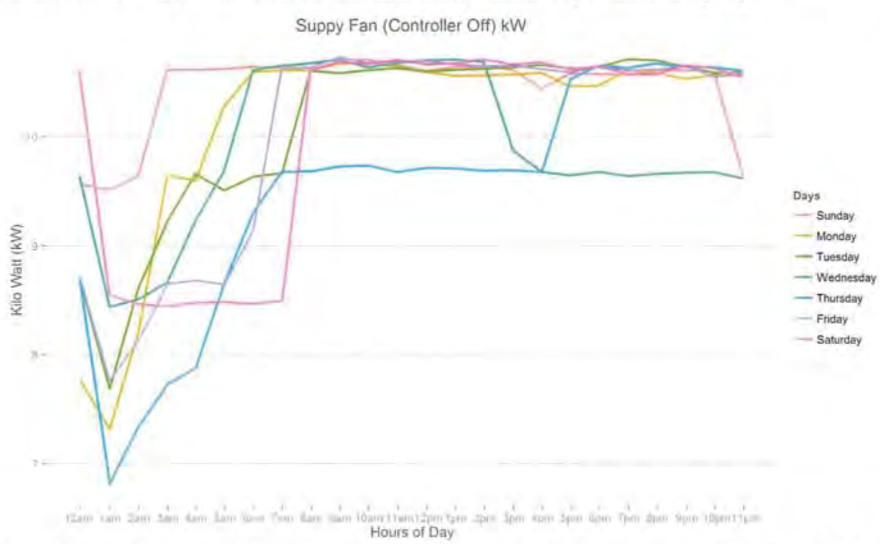

Figure 18: The figure above illustrates the average kWh draw of the supply fan when the controller is OFF for each hour of the day and each day of the week. This is helpful in understanding the operation of the unit throughout the days of the week. It is clear that as the temperature increases throughout the day, so will the kWh draw.

CONFIDENTIAL

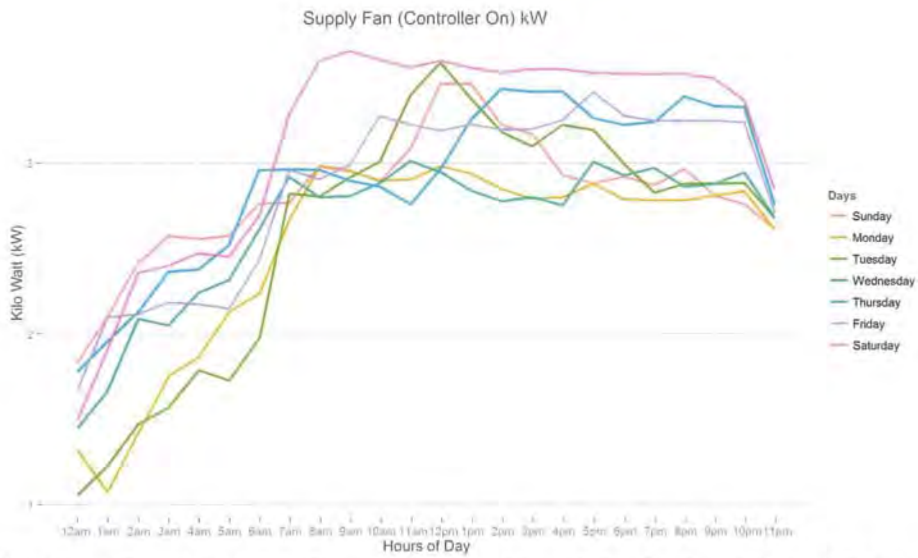

Figure 19: The figure above illustrates the average kWh draw of the supply fan when the controller is ON for each hour of the day and each day of the week. This is helpful in understanding the operation of the unit throughout the days of the week. It is clear that as the temperature increases throughout the day, so will the kWh draw.

Figure 20: From the above plot, we can infer comparing with a referential point; here we consider the average savings, how the savings in a specific day of the week and a specific hour of the day varies from the savings reference. We can see from the plot that variation of average hourly kilowatt savings on Sunday (Orange) and Saturday (Purple) are lesser to the average savings comparing with the two extreme weekdays i.e. Tuesday (Sea Green) and Friday (Blue). Which imply savings is inversely proportional to load.

CONFIDENTIAL

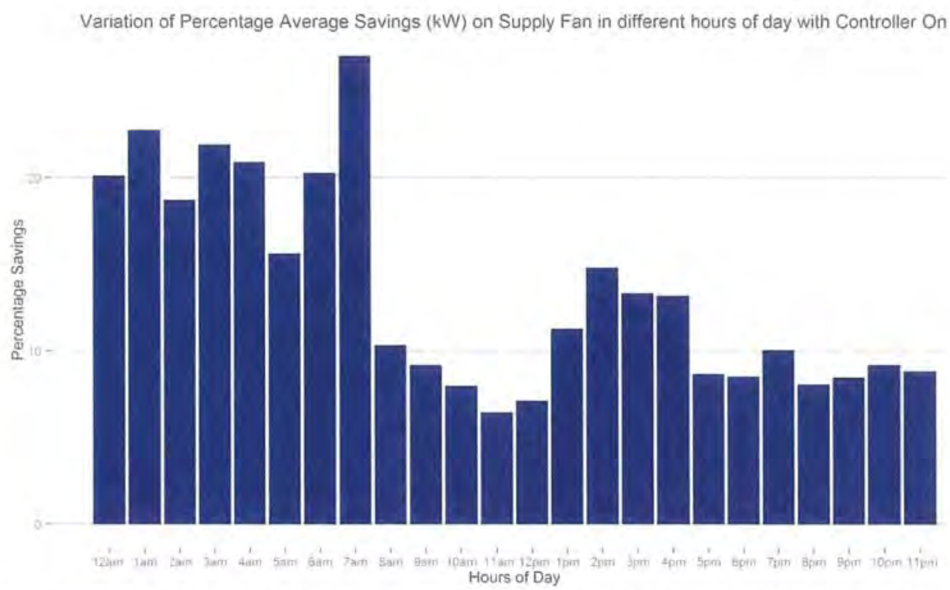

Figure 21: The figure above illustrates the average percent savings of the supply fan throughout the day. As it can be seen, savings are higher during the cooler parts of the day as the VFD is able to slow down the speed of the fan for longer periods of time.

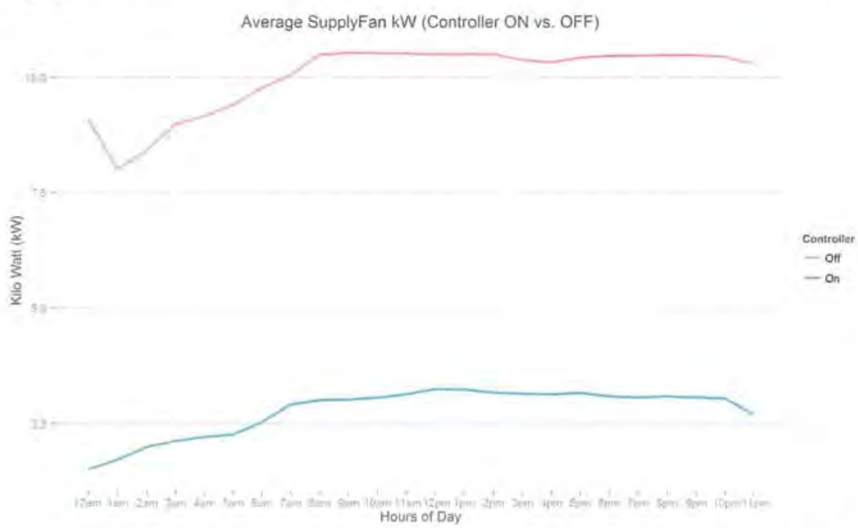

Figure 22: This plot illustrates that there is a significant reduction in supply fan kWh draw when the controller is ON versus when it is OFF. The kWh draw follows a similar trend throughout the day. This indicates that both control strategies are reacting to the outside temperature and super market occupancy.

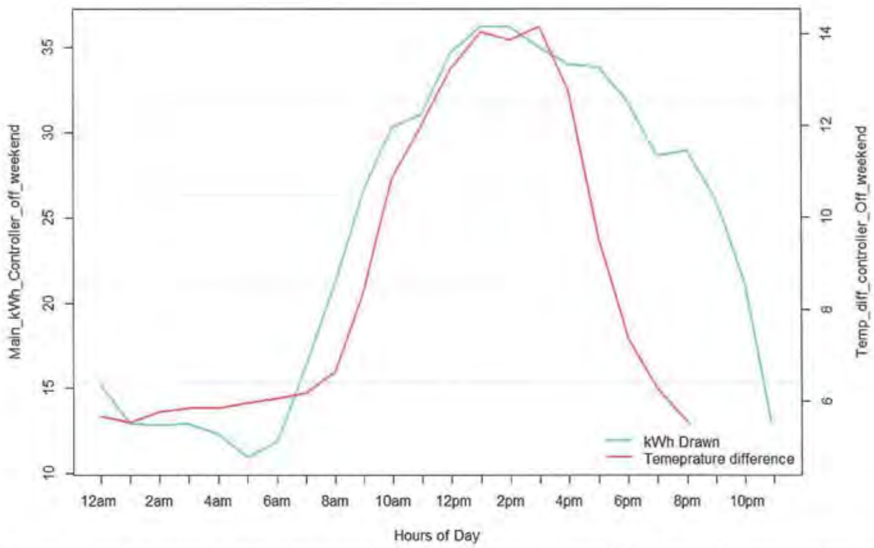

Figure 23: The figure above illustrates the relationship between the main disconnect kWh draw and the indoor and outdoor temperature difference when the controller is OFF for the weekend hours (Saturday and Sunday). As it can be seen, as the temperature difference between indoor and outdoor temperature increased so does the kW consumption of the main disconnect panel. This indicates a high correlation between kW and temperature.

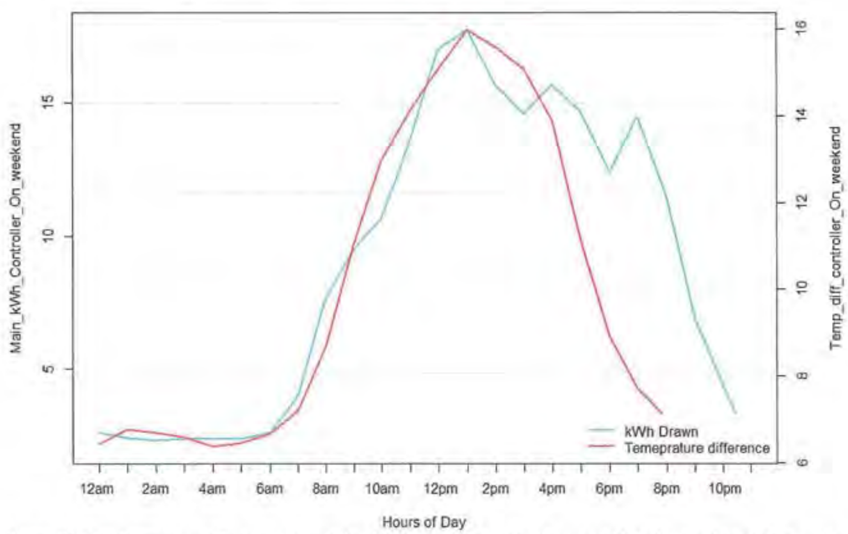

Figure 24: The figure above illustrates the relationship between the main disconnect kWh draw and the indoor and outdoor temperature difference when the controller is ON for the weekend hours (Saturday and Sunday). As it can be seen, as the temperature difference between indoor and outdoor temperature raises so does the kW consumption of the main disconnect panel. This indicates a high correlation between kW and temperature.

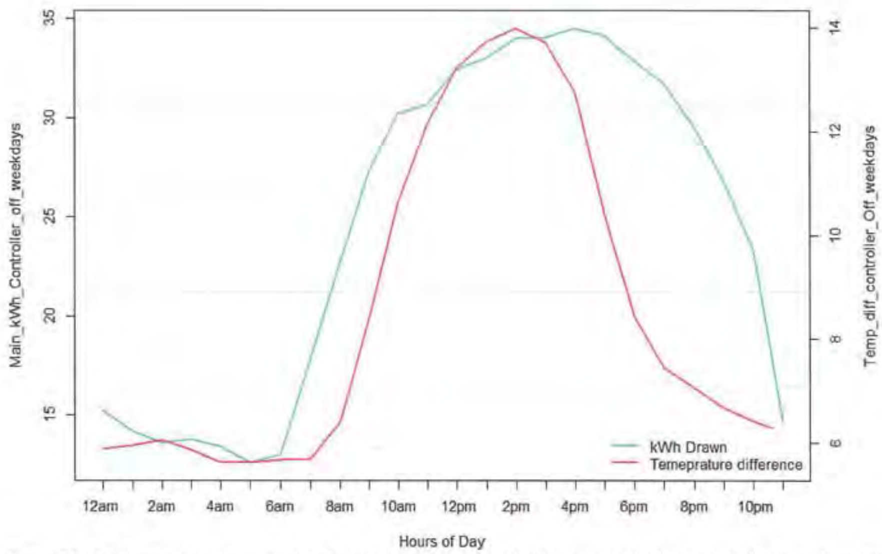

Figure 25: The figure above illustrates the relationship between the main disconnect kWh draw and the indoor and outdoor temperature difference when the controller is OFF for the weekday hours (Monday to Friday). As it can be seen, as the temperature difference between indoor and outdoor temperature increased so does the kW consumption of the main disconnect panel. This indicates a high correlation between kW and temperature.

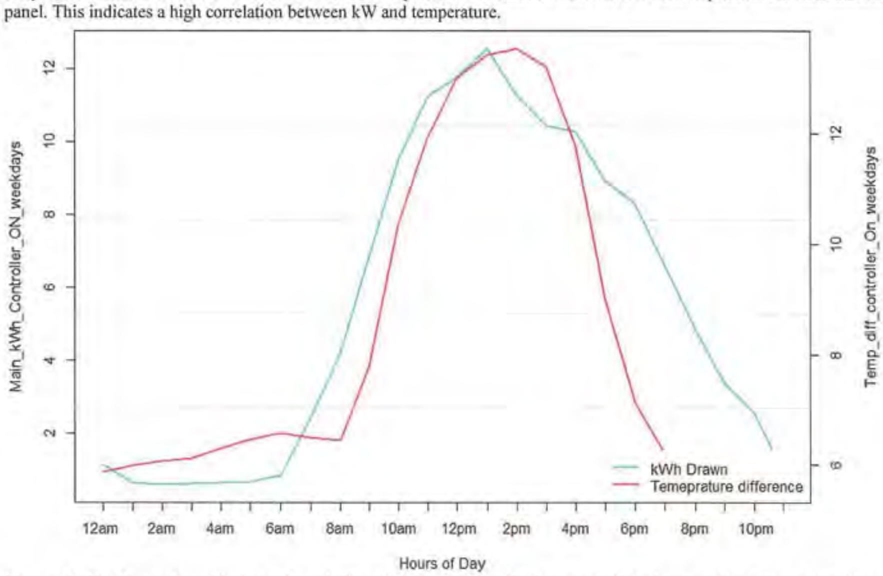

Figure 26: The figure above illustrates the relationship between the main disconnect kWh draw and the indoor and outdoor temperature difference when the controller is ON for the weekday hours (Monday to Friday). As it can be seen, as the temperature difference between indoor and outdoor temperature raises so does the kW consumption of the main disconnect panel. This indicates a high correlation between kW and temperature.

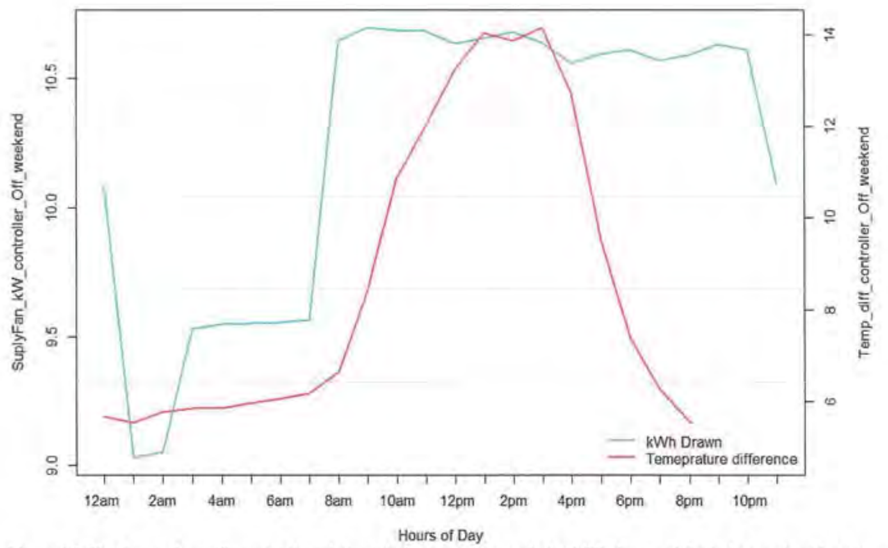

Figure 27: The figure above illustrates the relationship between the supply fan kWh draw and the indoor and outdoor temperature difference when the controller is OFF for the weekend hours (Saturday and Sunday). As it can be seen, as the temperature difference between indoor and outdoor temperature increased so does the kW consumption of the main disconnect panel. This indicates a high correlation between kW and temperature.

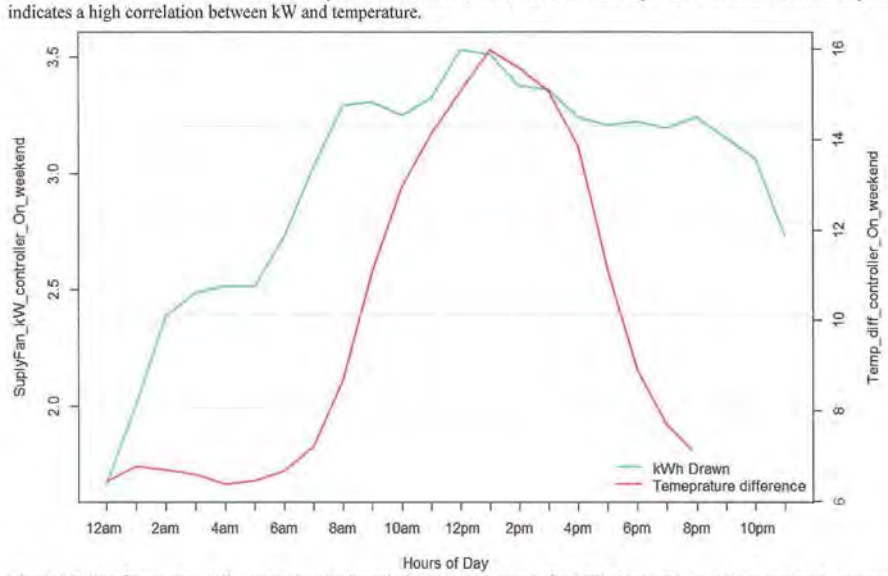

Figure 28: The figure above illustrates the relationship between the supply fan kWh draw and the indoor and outdoor temperature difference when the controller is ON for the weekend hours (Saturday and Sunday). As it can be seen, as the temperature difference between indoor and outdoor temperature raises so does the kW consumption of the main disconnect panel. This indicates a high correlation between kW and temperature.

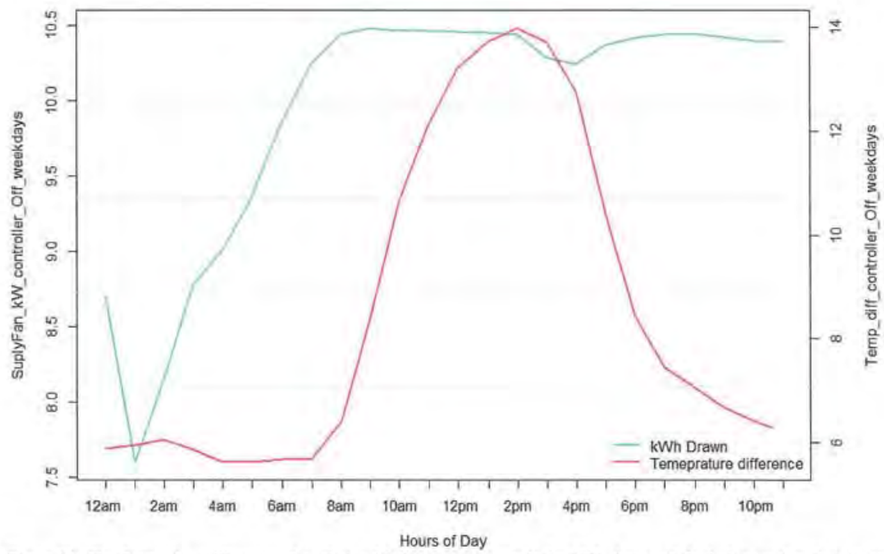

Figure 29: The figure above illustrates the relationship between the supply fan kWh draw and the indoor and outdoor temperature difference when the controller is OFF for the weekday hours (Monday to Friday). As it can be seen, as the temperature difference between indoor and outdoor temperature increased so does the kW consumption of the main disconnect panel. This indicates a high correlation between kW and temperature.

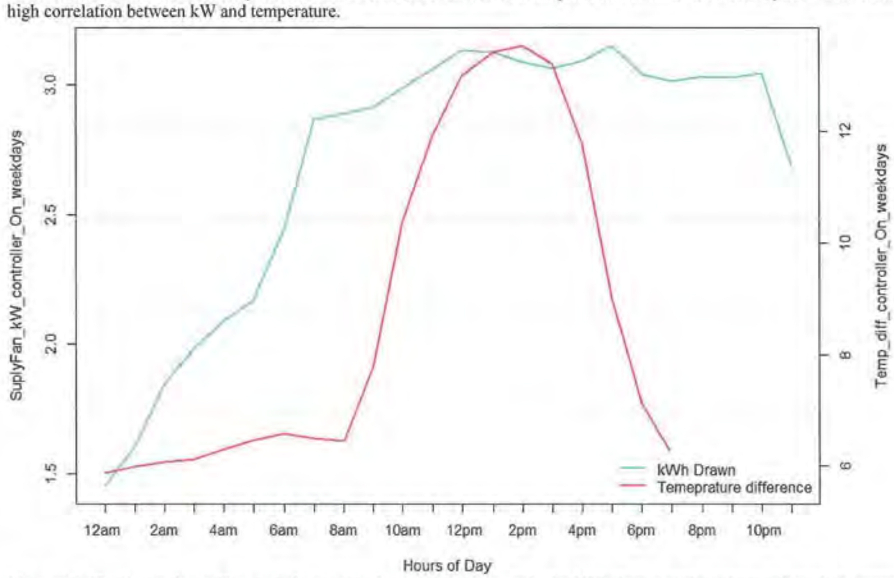

Figure 30: The figure above illustrates the relationship between the supply fan kWh draw and the indoor and outdoor temperature difference when the controller is ON for the weekday hours (Monday to Friday). As it can be seen, as the temperature difference between indoor and outdoor temperature raises so does the kW consumption of the main disconnect panel. This indicates a high correlation between kW and temperature.

Regression Model #4, 5, &6:

The total energy consumption (kWh) of the air conditioning unit (A/C Unit), the four compressors, and the supply fan were respectively analyzed for seven months starting 04/01/2015 at 12:00am and ending 10/30/15 at 11:58 pm. ***Using the average power factor computed when controller in on & off***.

Model #4: Total Cooling Load Power Consumption Savings

The regression equation to correlate the hourly A/C Unit kWh consumption with the temperature and the [redacted] controller status (whether it's ON or OFF) is as follows:

$$\textbf{Main kWh} = \beta_0 + \beta_1 \times \textbf{Outside Temperature} + \beta_2 \times \textbf{Enerfit Controller}$$

Where:

Main kWh = the hourly power consumption of the air conditioning unit (A/C Unit).

β_0 = the intercept of the regression equation

β_1 = regression coefficient of the model relating the hourly temperature to the hourly kWh

Outside Temperature = hourly outside temperature in $^\circ$F

β_2 = regression coefficient of the model relating the hourly kWh consumption to the effect of the [redacted] controller

[redacted] ***Controller*** = a dummy variable that is assigned a value **0** when the [redacted] controller is "OFF" and **1** when the controller is "ON".

First, a best subsets regression was performed in order to determine the number of independent variables to be included in the model (Table 13).

number of Variables	R-Sq	R-Sq(adj)	SE
1	29.40	29.38	21.8638
1	26.89	26.88	22.2481
2	54.71	54.69	17.5127
Response is Main kWh			

The second step performed was to test if the effects of both the outside temperature and the [redacted] controller are statistically significant. An Analysis of Variance (ANOVA) was performed to determine whether the [redacted] controller reduction in the kWh is statistically significant.

Table 14 depicts the ANOVA table obtained. The technique used to perform the ANOVA was the multiple regression procedure.

Table14: Analysis of Variance of Main kWh, using Adjusted SS for Tests

Source	DF	AdjSS	AdjMS	F-Value	P-Value
Regression	2	1901795	950898	3100.49	0.000
Temp	1	879928	879928	2869.08	0.000
Controller	1	966968	966968	3152.89	0.000
Error	5133	1574256	307		
Total	5135	3476051			

As shown in Table 14, both the effects of the controller and the outside temperature on the kWh were statistically significant ($P<.001$), meaning that both the ambient temperature and the controller statistically affect the kW consumption.

The next step during the regression analysis was to determine the coefficients corresponding to each independent variable in the governing equation explaining the relationship between the temperature, the controller, and the Main kWh. Table 15 summarizes the coefficients obtained from the regression analysis.

Table 15. Main kWh Regression Analysis coefficients

Term	Coef	SECoef	T-Value	P-Value	VIF
Constant	-160.16	4.05	-39.56	0.000	
Temp	2.6028	0.0486	53.56	0.000	1.00
Controller	-27.459	0.489	-56.15	0.000	1.00

CONFIDENTIAL

Regression Analysis: Main_kwh versus Temp, Controller

Method

Categorical predictor coding (1, 0)

Analysis of Variance

Source	DF	Adj SS	Adj MS	F-Value	P-Value
Regression	2	1901795	950898	3100.49	0.000
Temp	1	879928	879928	2869.08	0.000
Controller	1	966968	966968	3152.89	0.000
Error	5133	1574256	307		
Lack-of-Fit	5107	1569496	307	1.68	0.053
Pure Error	26	4760	183		
Total	5135	3476051			

Model Summary

S	R-sq	R-sq(adj)	R-sq(pred)
17.5127	54.71%	54.69%	54.66%

Coefficients

Term	Coef	SE Coef	T-Value	P-Value	VIF
Constant	-160.16	4.05	-39.56	0.000	
Temp	2.6028	0.0486	53.56	0.000	1.00
Controller					
1	-27.459	0.489	-56.15	0.000	1.00

Regression Equation

Controller

0 Main_kW = -160.16 + 2.6028 Temp

1 Main_kW = -187.62 + 2.6028 Temp

Regression Equation including Controller

Main_kWh = -160.16 + 2.6028 Temp - 27.459 Controller

The above equation means that, by controlling for the outside temperature, and by turning the controller ON, a reduction in the kWh of 27.5 kWh occurs.

The average kWh consumption of the Main unit during the OFF periods (where the controller was turned off) is 55.88 kWh. The regression equation indicates that an average reduction of 27.5 kWh is experienced when the controller is turned ON while controlling for the outside temperature. This results in a percentage savings in the baseline kWh (when the controller is

OFF) of 49.21% while maintaining the effect of the outside temperature. Figure displays the box plot distribution for Main kWh when the controller is ON vs. OFF.

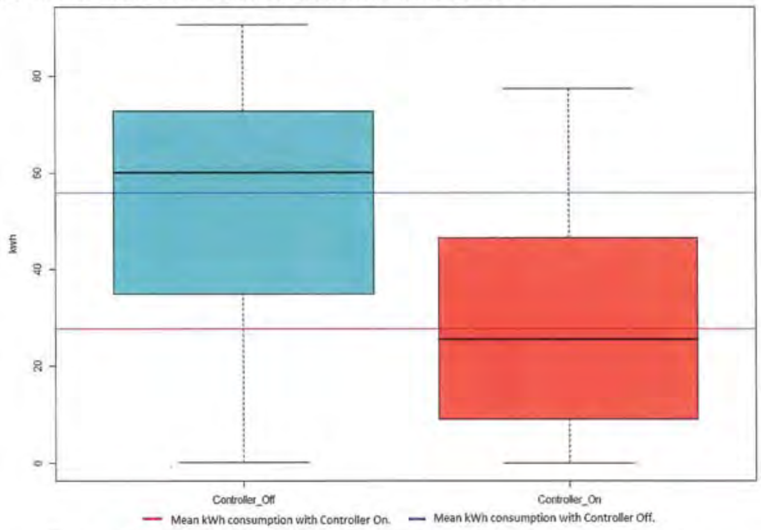

Figure 31: The Box Plot of the Main kWh and the Controller Status.

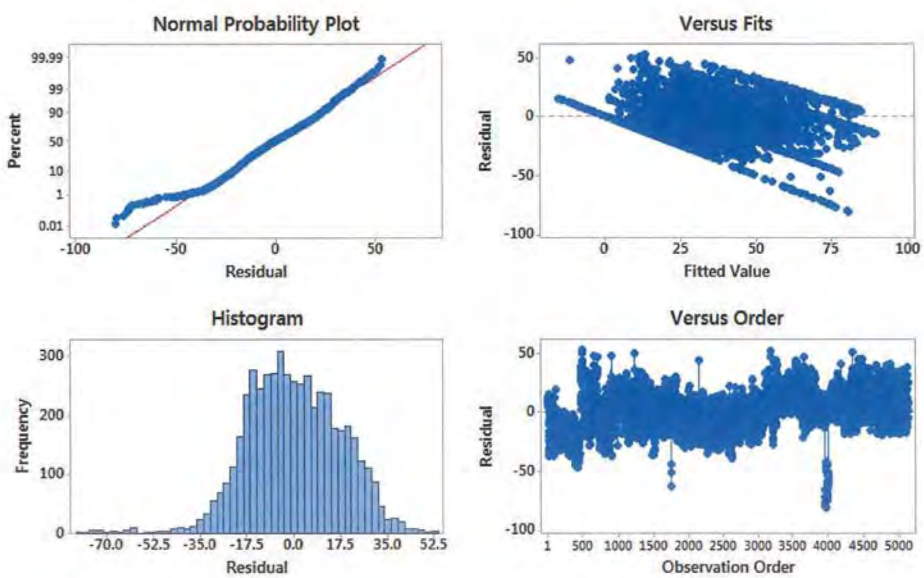

Figure 32: Residual Plots for Main kWh.

Model #5: Compressor Power Consumption Savings

The regression equation to correlate the Compressor kWh consumption with the temperature and the [redacted] controller status (whether it's ON or OFF) is as follows:

$$\textit{Compressor kWh} = \beta_0 + \beta_1 \times \textit{Outside Temperature} + \beta_2 \times \textit{Enerfit Controller}$$

Where:

Compressor kWh = the hourly power consumption due to the four compressors.

β_0 = the intercept of the regression equation

β_1 = regression coefficient of the model relating the hourly temperature to the hourly kWh

Outside Temperature = hourly outside temperature in °F

β_2 = regression coefficient of the model relating the hourly kWh consumption to the effect of the [redacted] controller

[redacted] ***Controller*** = a dummy variable that is assigned a value **0** when the [redacted] controller is "OFF" and **1** when the controller is "ON".

First, a best subsets regression was performed in order to determine the number of independent variables to be included in the model (Table 16).

number of Variables	R-Sq	R-Sq(adj)	SE
1	16.53	16.52	19.0549
1	33.10	33.08	17.0599
2	48.32	48.30	14.9953
Response is Compressor kWh			

The second step performed was to test if the effects of both the outside temperature and the [redacted] controller are statistically significant. An Analysis of Variance (ANOVA) was performed to determine whether the [redacted] controller reduction in the kWh is statistically significant.

Table 17 depicts the ANOVA table obtained. The technique used to perform the ANOVA was the multiple regression procedure.

Table 17: Analysis of Variance of Main kWh, using Adjusted SS for Tests

Source	DF	AdjSS	AdjMS	F-Value	P-Value
Regression	2	1079166	539583	2399.63	0.000
Temp	1	709888	709888	3157.02	0.000
Controller	1	339984	339984	1511.98	0.000
Error	5133	1154209	225		
Total	5135	2233374			

As shown in Table 17, both the effects of the controller and the outside temperature on the kWh were statistically significant (*P*<.001), meaning that both the ambient temperature and the controller statistically affect the kW consumption.

The next step during the regression analysis was to determine the coefficients corresponding to each independent variable in the governing equation explaining the relationship between the temperature, the controller, and the Main kWh. Table 18 summarizes the coefficients obtained from the regression analysis.

Table 18. Main kWh Regression Analysis coefficients

Term	Coef	SECoef	T-Value	P-Value	VIF
Constant	-155.56	3.47	-44.88	0.000	
Temp	2.3378	0.0416	56.19	0.000	1.00
Controller	-16.282	0.419	-38.88	0.000	1.00

CONFIDENTIAL

Regression Analysis: Compressor_kwh versus Temp, Controller

Method

Categorical predictor coding (1, 0)

Analysis of Variance

Source	DF	Adj SS	Adj MS	F-Value	P-Value
Regression	2	1079166	539583	2399.63	0.000
Temp	1	709888	709888	3157.02	0.000
Controller	1	339984	339984	1511.98	0.000
Error	5133	1154209	225		
Lack-of-Fit	5107	1149798	225	1.33	0.190
Pure Error	26	4410	170		
Total	5135	2233374			

Model Summary

S	R-sq	R-sq(adj)	R-sq(pred)
14.9953	48.32%	48.30%	48.26%

Coefficients

Term	Coef	SE Coef	T-Value	P-Value	VIF
Constant	-155.56	3.47	-44.88	0.000	
Temp	2.3378	0.0416	56.19	0.000	1.00
Controller					
1	-16.282	0.419	-38.88	0.000	1.00

Regression Equation

Controller	
0	Compressor_kW = -155.56 + 2.3378 Temp
1	Compressor_kW = -171.84 + 2.3378 Temp

Regression Equation including Controller

Compressor_kWh = -155.56 + 2.3378 Temp - 16.282 Controller

The above equation means that, by **controlling for the outside temperature**, and by turning the controller ON, a reduction in the kWh of 16.28 kWh occurs in the compressors.

The average kWh consumption of the four compressors during the OFF periods (where the controller was turned off) is 38.49 kWh. The regression equation indicates that an average reduction of 16.28 kWh is experienced when the controller is turned ON while controlling for the outside temperature. This results in a percentage savings in the baseline kWh (when the

controller is OFF) of 42.30% while maintaining the effect of the outside temperature. Figure displays the box plot distribution for Compressor kWh when the controller is ON vs. OFF.

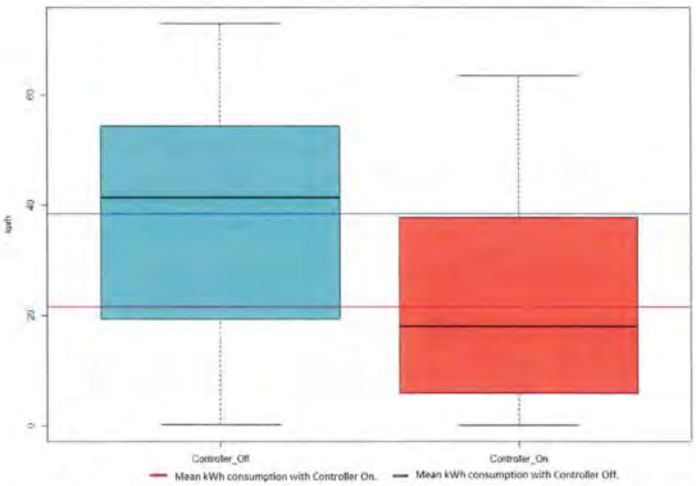

Figure 33: The Box Plot of the Compressor kWh and the Controller Status.

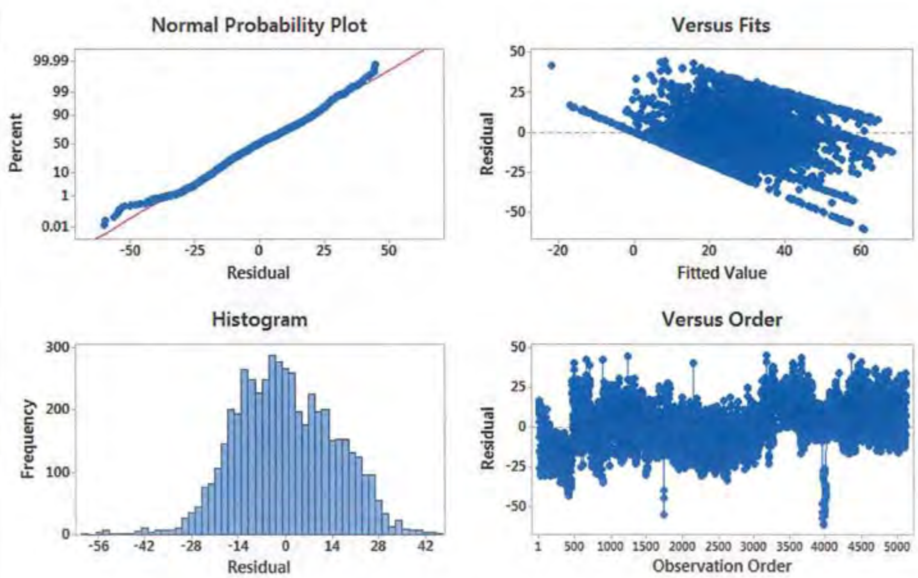

Figure 34: Residual Plots for Compressor kWh

Model #6: Supply Fan Power Consumption Savings

The regression equation to correlate the Supply Fan kWh consumption with the temperature and the [redacted] controller status (whether it's ON or OFF) is as follows:

$$Supply\ Fan\ kWh = \beta_0 + \beta_1 \times Outside\ Temperature + \beta_2 \times Enerfit\ Controller$$

Where:

Supply Fan kWh = the hourly power consumption due to the Supply Fan.

β_0 = the intercept of the regression equation

β_1 = regression coefficient of the model relating the hourly temperature to the hourly kWh

Outside Temperature = hourly outside temperature in °F

β_2 = regression coefficient of the model relating the hourly kWh consumption to the effect of the [redacted] controller

[redacted] ***Controller*** = a dummy variable that is assigned a value **0** when the [redacted] controller is "OFF" and **1** when the controller is "ON".

First, a best subsets regression was performed in order to determine the number of independent variables to be included in the model (Table 19).

number of Variables	R-Sq	R-Sq(adj)	SE
1	87.80	87.79	1.26542
1	0.10	0.08	3.62043
2	87.80	87.79	1.26541
Response is Supply Fan kWh			

The second step performed was to test if the effects of both the outside temperature and the [redacted] controller are statistically significant. An Analysis of Variance (ANOVA) was performed to determine whether the [redacted] controller reduction in the kWh is statistically significant.

Table 20 depicts the ANOVA table obtained. The technique used to perform the ANOVA was the multiple regression procedure.

Table 20: Analysis of Variance of Main kWh, using Adjusted SS for Tests

Source	DF	AdjSS	AdjMS	F-Value	P-Value
Regression	2	59144.5	29572.2	18468.05	0. 000
Temp	1	1.7	1.7	1.09	0.297
Controller	1	59074.8	59074.8	36892.60	0.000
Error	5133	8219.3	1.6		
Total	5135	67363.7			

As shown in Table 20, both the effects of the controller and the outside temperature on the kWh were statistically significant (*P*<.001), meaning that both the ambient temperature and the controller statistically affect the kW consumption.

The next step during the regression analysis was to determine the coefficients corresponding to each independent variable in the governing equation explaining the relationship between the temperature, the controller, and the Main kWh. Table 21 summarizes the coefficients obtained from the regression analysis.

Table 21. Main kWh Regression Analysis coefficients

Term	Coef	SECoef	T-Value	P-Value	VIF
Constant	9.787	0.293	33.46	0.000	
Temp	0.00366	0.00351	1.04	0.297	1.00
Controller	-6.7869	0.0353	-192.07	0.000	1.00

Regression Analysis: Supply Fan_kw versus Temp, Controller

Method

Categorical predictor coding (1, 0)

Analysis of Variance

Source	DF	Adj SS	Adj MS	F-Value	P-Value
Regression	2	59144.5	29572.2	18468.05	0.000
Temp	1	1.7	1.7	1.09	0.297
Controller	1	59074.8	59074.8	36892.60	0.000
Error	5133	8219.3	1.6		
Lack-of-Fit	5107	8209.2	1.6	4.14	0.000
Pure Error	26	10.1	0.4		
Total	5135	67363.7			

Model Summary

S	R-sq	R-sq(adj)	R-sq(pred)
1.26541	87.80%	87.79%	87.78%

Coefficients

Term	Coef	SE Coef	T-Value	P-Value	VIF
Constant	9.787	0.293	33.46	0.000	
Temp	0.00366	0.00351	1.04	0.297	1.00
Controller					
1	-6.7869	0.0353	-192.07	0.000	1.00

Regression Equation

Controller	
0	Supply_Fan_kW = 9.787 + 0.00366 Temp
1	Supply_Fan_kW = 3.000 + 0.00366 Temp

Regression Equation including Controller

Supply_Fan_kW = 9.787 + 0.00366 Temp - 6.7869 Controller

The above equation means that, by **controlling for the outside temperature**, and by turning the controller ON, a reduction in the kWh of 6.79 kWh occurs in the compressors.

The average kWh consumption of the Supply Fan during the OFF periods (where the controller was turned off) is 10.09 kWh. The regression equation indicates that an average reduction of 6.79 kWh is experienced when the controller is turned ON while controlling for the outside temperature. This results in a percentage savings in the baseline kWh (when the controller is OFF) of 67.29% while maintaining the effect of the outside temperature. Figure displays the box plot distribution for Supply Fan kWh when the controller is ON vs. OFF.

CONFIDENTIAL

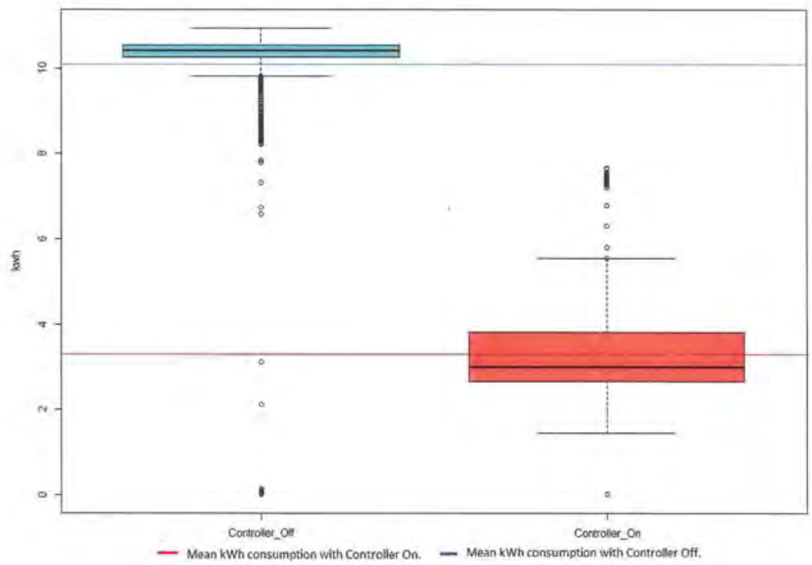

Figure 35: The Box Plot of the Supply Fan kWh and the Controller Status.

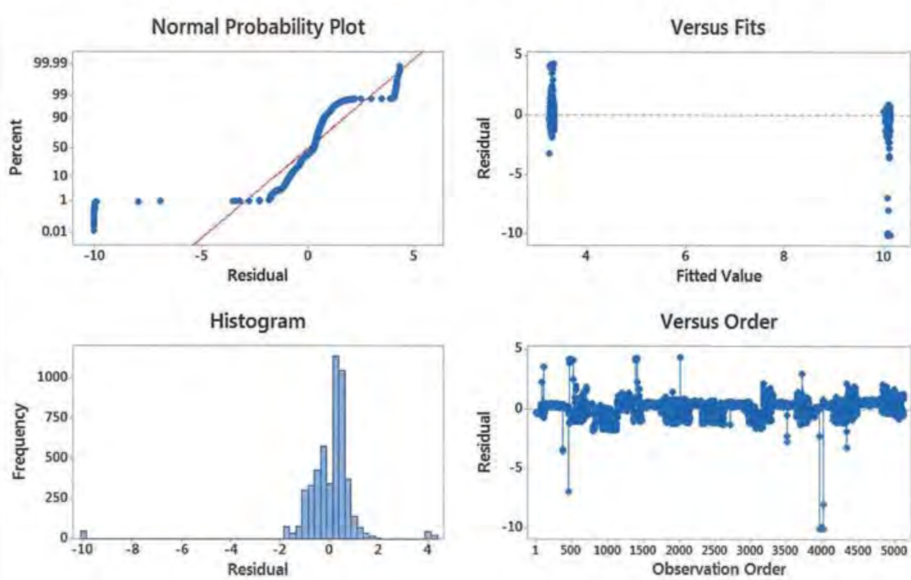

Figure 36: Residual Plots for Supply Fan kWh

CONFIDENTIAL

Summer (April-October) with Average Controller ON and OFF Power Factor

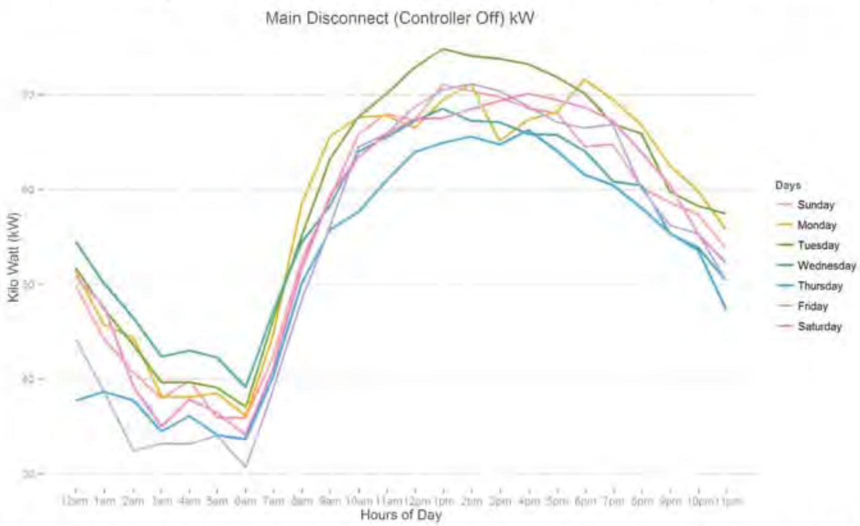

Figure 37: The figure above illustrates the average kWh draw of the main disconnect when the controller is OFF for each hour of the day and each day of the week. This is helpful in understanding the operation of the unit throughout the days of the week. It is clear that as the temperature increases throughout the day, so will the kWh draw.

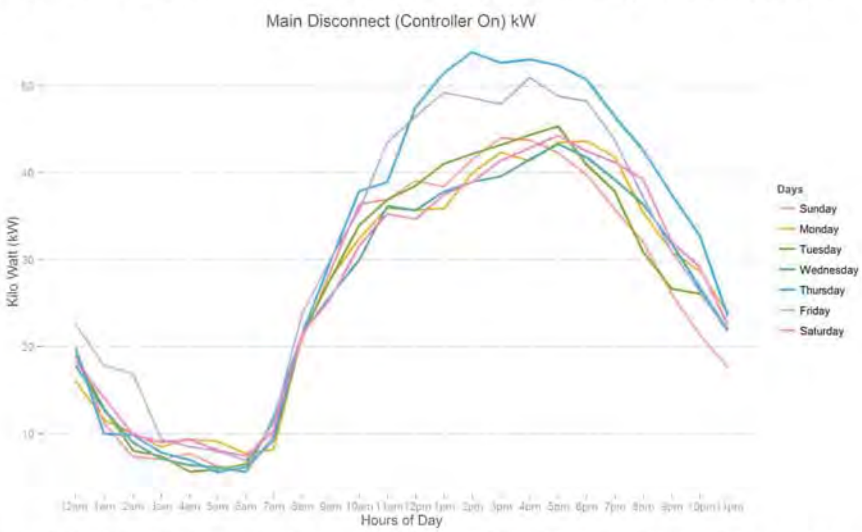

Figure 38: The figure above illustrates the average kWh draw of the main disconnect when the controller is ON for each hour of the day and each day of the week. This is helpful in understanding the operation of the unit throughout the days of the week. It is clear that as the temperature increases throughout the day, so will the kWh draw.

CONFIDENTIAL

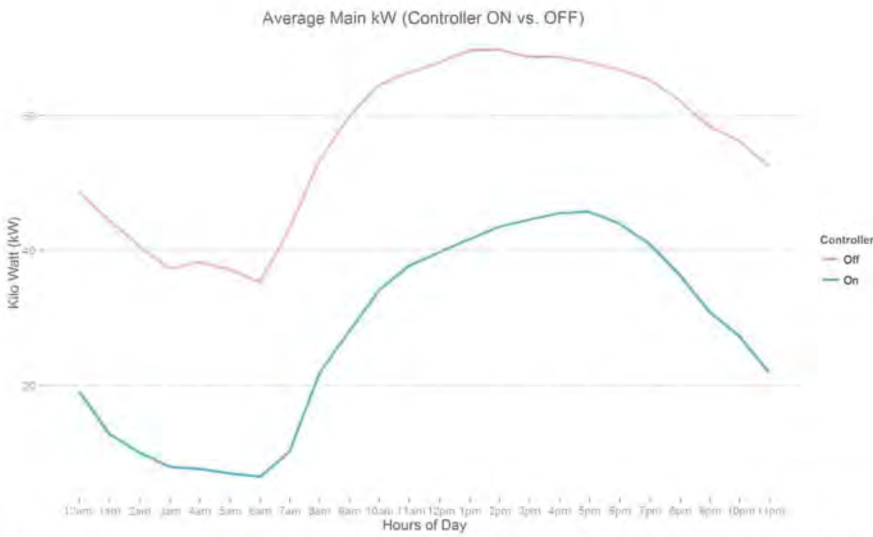

Figure 39: The plot above illustrates that there is a significant reduction in main kWh draw when the controller is ON versus when it is OFF. The kWh draw follows a similar trend throughout the day. This indicates that both control strategies are reacting to the outside temperature and super market occupancy.

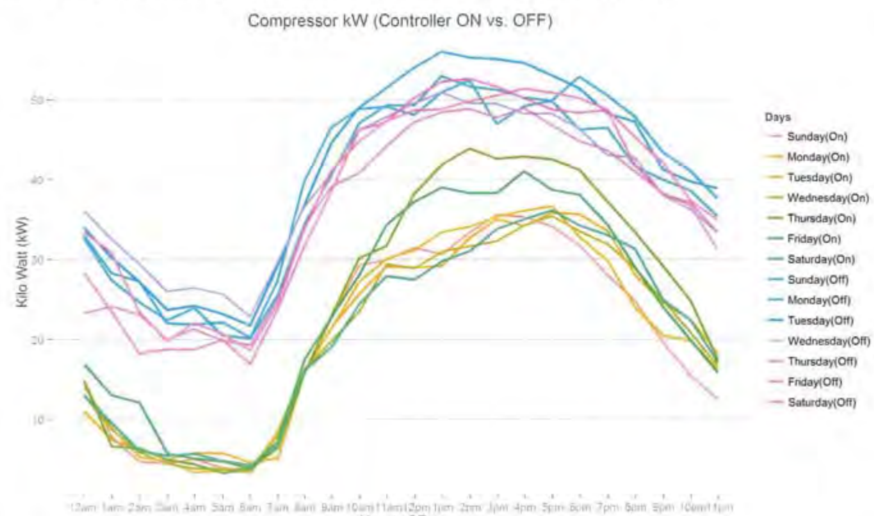

Figure 40: The figure above illustrates the average kWh draw of the compressors when the controller is ON and OFF for each hour of the day and each day of the week. This is helpful in understanding the operation of the unit throughout the days of the week. It is clear that as the temperature increases throughout the day, so will the kWh draw.

CONFIDENTIAL

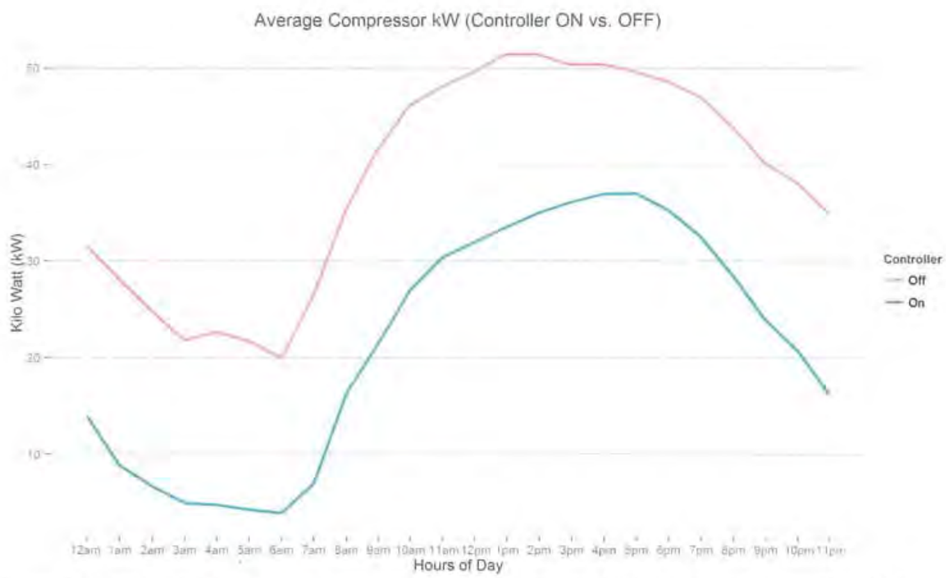

Figure 41: The plot above that there is a significant reduction in compressor kWh draw when the controller is ON versus when it is OFF. The kWh draw follows a similar trend throughout the day. This indicates that both control strategies are reacting to the outside temperature and super market occupancy.

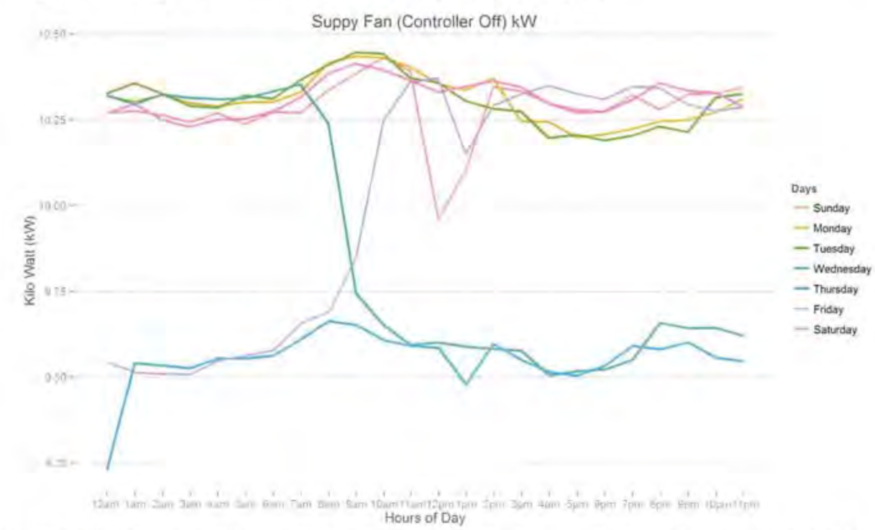

Figure 42: The figure above illustrates the average kWh draw of the supply fan when the controller is OFF for each hour of the day and each day of the week. This is helpful in understanding the operation of the unit throughout the days of the week. It is clear that as the temperature increases throughout the day, so will the kWh draw.

CONFIDENTIAL

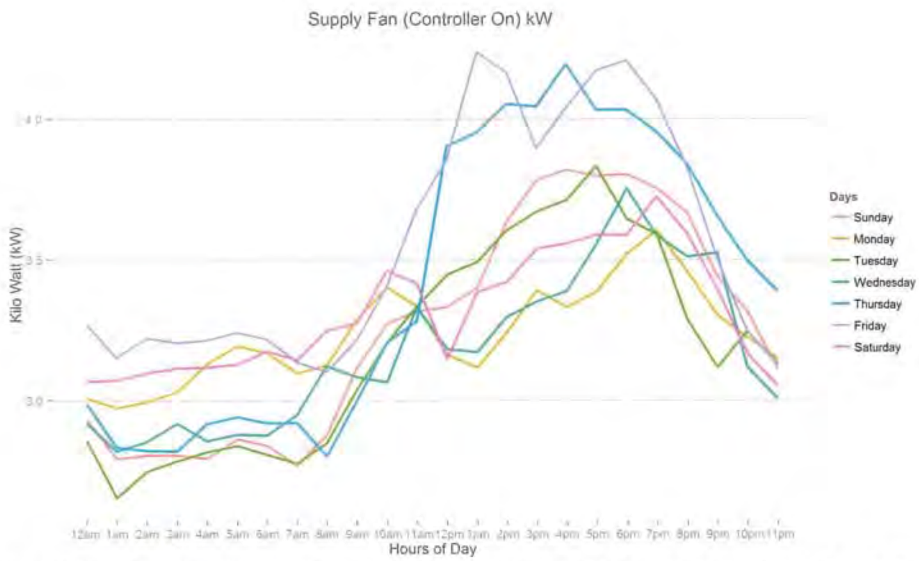

Figure 43: The figure above illustrates the average kWh draw of the supply fan when the controller is ON for each hour of the day and each day of the week. This is helpful in understanding the operation of the unit throughout the days of the week. It is clear that as the temperature increases throughout the day, so will the kWh draw.

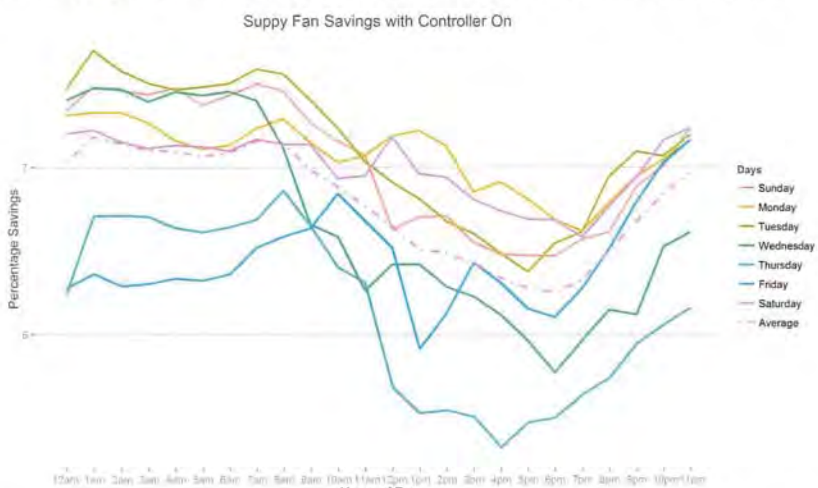

Figure 44: From the above plot we can infer comparing with a referential point; here we consider the average savings, how the savings in a specific day of the week and a specific hour of the day varies from the savings reference. We can see from the plot that variation of average hourly kilowatt savings on Sunday (Orange) and Saturday (Purple) are lesser to the average savings comparing with the two extreme weekdays i.e. Tuesday (Sea Green) and Friday (Blue). Which imply savings is inversely proportional to load.

CONFIDENTIAL

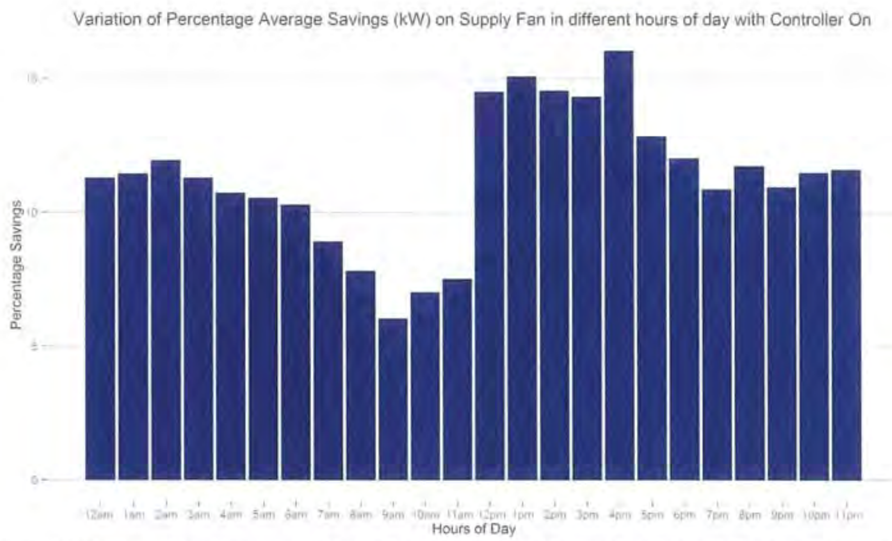

Figure 45: The figure above illustrates the average percent savings of the supply fan throughout the day. As it can be seen, savings are higher during the cooler parts of the day as the VFD is able to slow down he speed of the fan for longer periods of time.

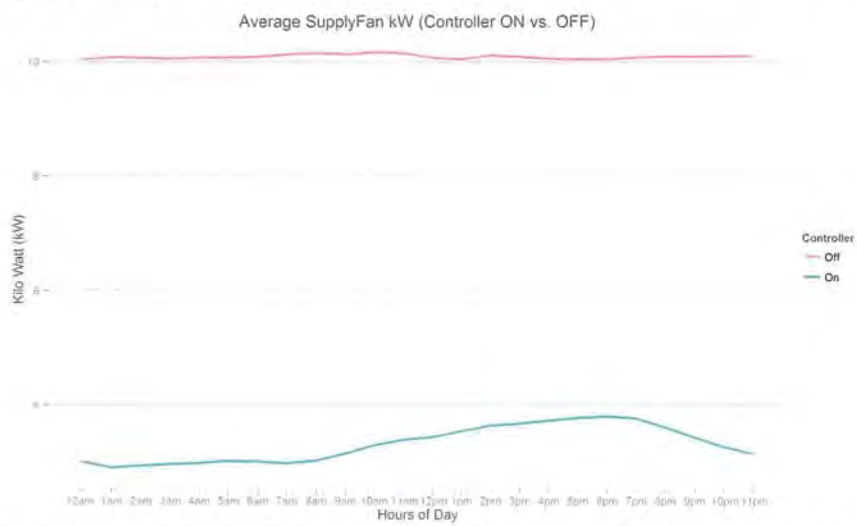

Figure 46: Figure above illustrates that there is a significant reduction in supply fan kWh draw when the controller is ON versus when it is OFF. The kWh draw follows a similar trend throughout the day. This indicates that both control strategies are reacting to the outside temperature and super market occupancy.

CONFIDENTIAL

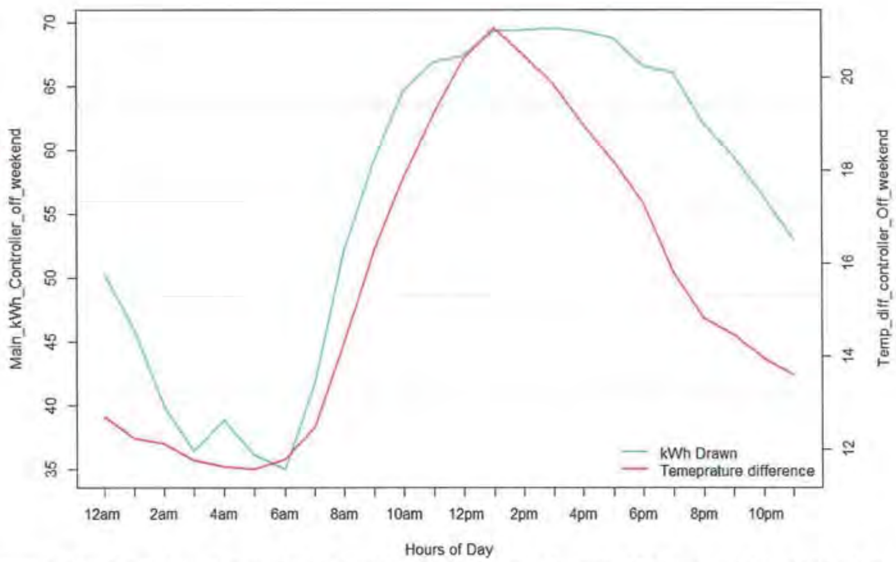

Figure 47: The figure above illustrates the relationship between the main disconnect kWh draw and the indoor and outdoor temperature difference when the controller is OFF for the weekend hours (Saturday and Sunday). As it can be seen, as the temperature difference between indoor and outdoor temperature increased so does the kW consumption of the main disconnect panel. This indicates a high correlation between kW and temperature.

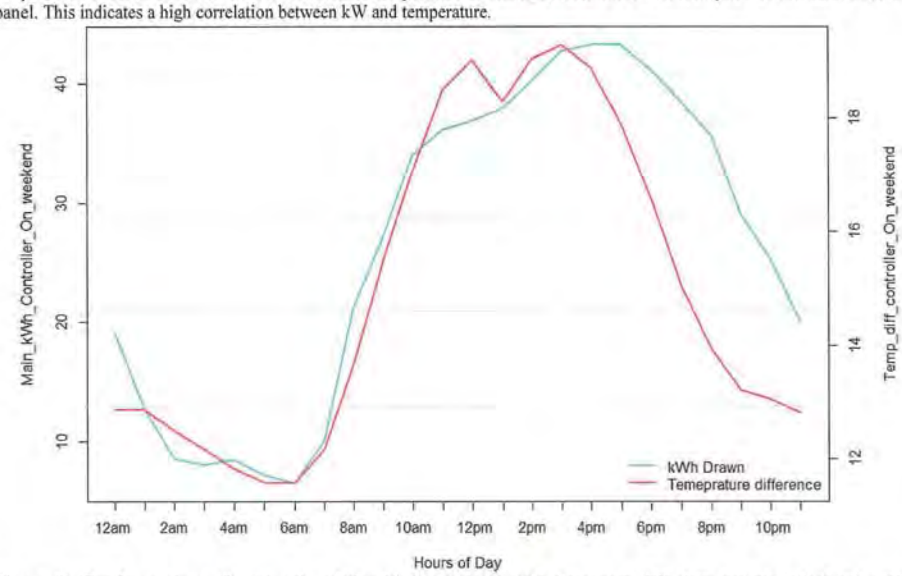

Figure 48: The figure above illustrates the relationship between the main disconnect kWh draw and the indoor and outdoor temperature difference when the controller is ON for the weekend hours (Saturday and Sunday). As it can be seen, as the temperature difference between indoor and outdoor temperature raises so does the kW consumption of the main disconnect panel. This indicates a high correlation between kW and temperature.

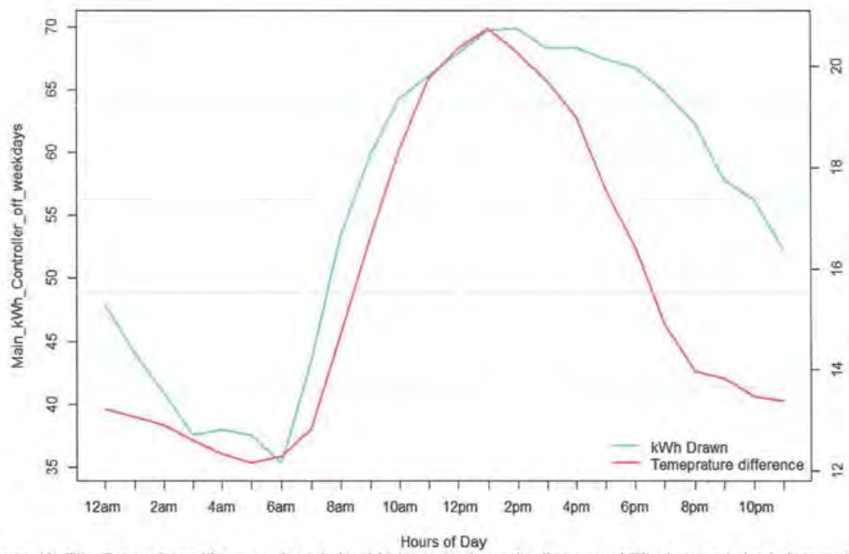

Figure 49: The figure above illustrates the relationship between the main disconnect kWh draw and the indoor and outdoor temperature difference when the controller is OFF for the weekday hours (Monday to Friday). As it can be seen, as the temperature difference between indoor and outdoor temperature increased so does the kW consumption of the main disconnect panel. This indicates a high correlation between kW and temperature.

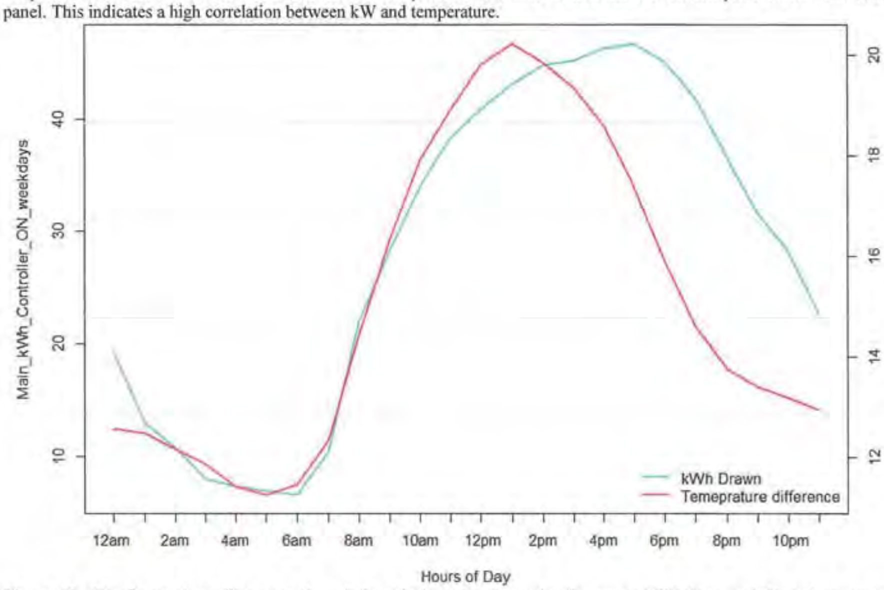

Figure 50: The figure above illustrates the relationship between the main disconnect kWh draw and the indoor and outdoor temperature difference when the controller is ON for the weekday hours (Monday to Friday). As it can be seen, as the temperature difference between indoor and outdoor temperature raises so does the kW consumption of the main disconnect panel. This indicates a high correlation between kW and temperature.

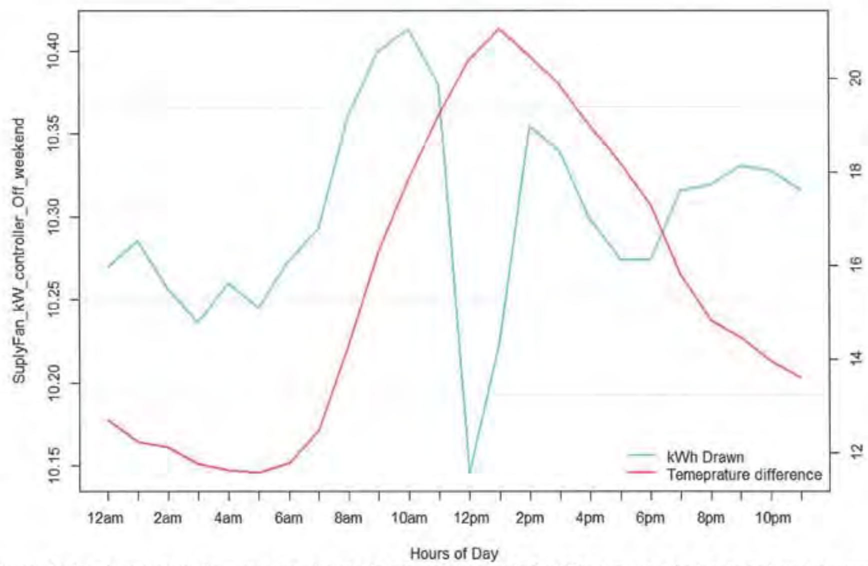

Figure 51: The figure above illustrates the relationship between the supply fan kWh draw and the indoor and outdoor temperature difference when the controller is OFF for the weekend hours (Saturday and Sunday). As it can be seen, as the temperature difference between indoor and outdoor temperature increased so does the kW consumption of the main disconnect panel. This indicates a high correlation between kW and temperature.

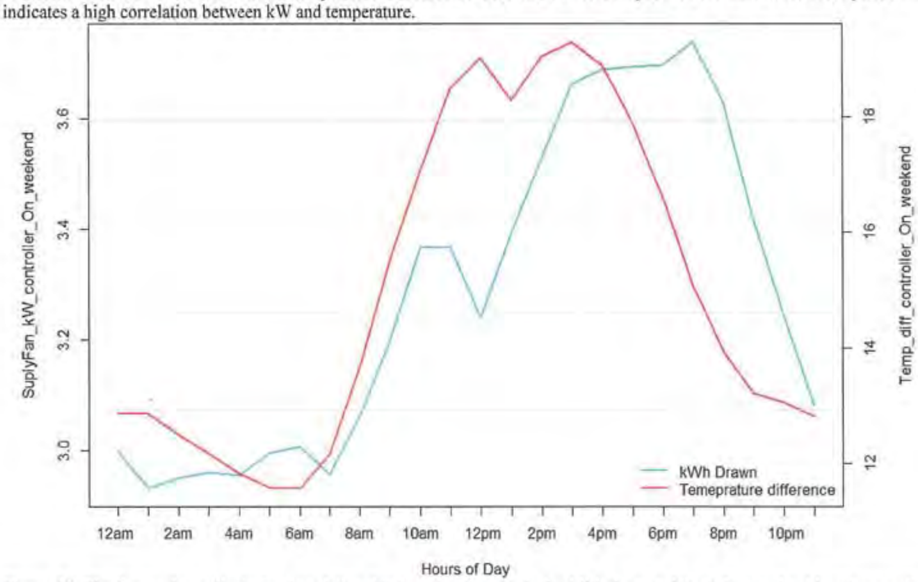

Figure 52: The figure above illustrates the relationship between the supply fan kWh draw and the indoor and outdoor temperature difference when the controller is ON for the weekend hours (Saturday and Sunday). As it can be seen, as the temperature difference between indoor and outdoor temperature raises so does the kW consumption of the main disconnect panel. This indicates a high correlation between kW and temperature.

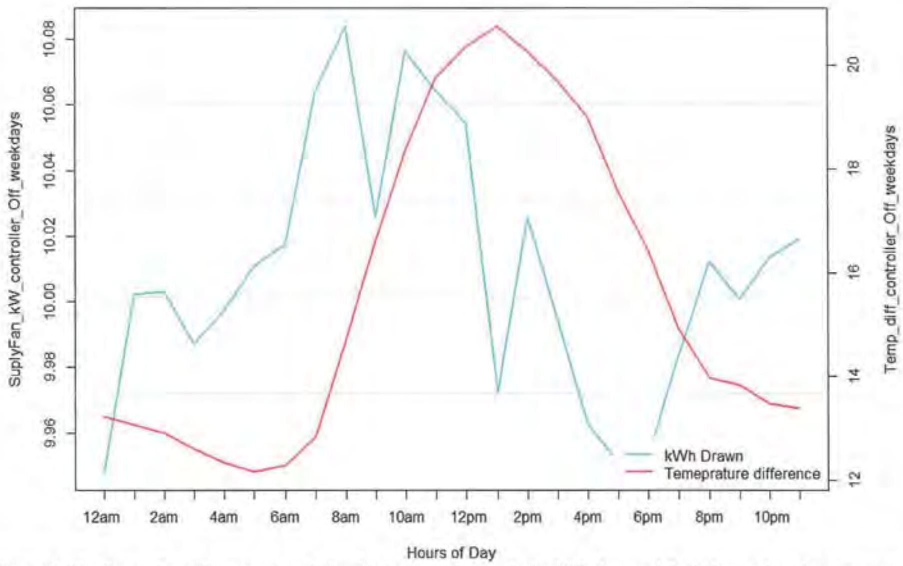

Figure 53: The figure above illustrates the relationship between the supply fan kWh draw and the indoor and outdoor temperature difference when the controller is OFF for the weekday hours (Monday to Friday). As it can be seen, as the temperature difference between indoor and outdoor temperature increased so does the kW consumption of the main disconnect panel. This indicates a high correlation between kW and temperature.

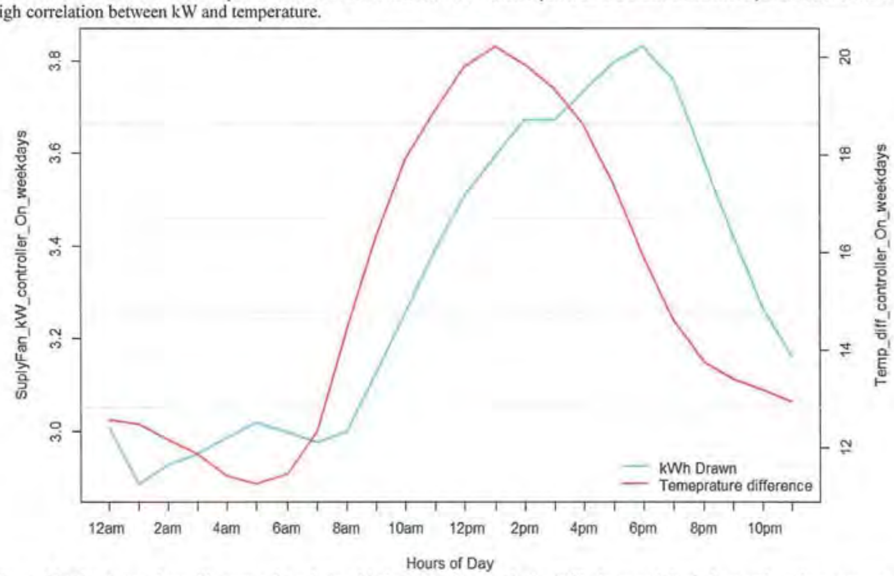

Figure 54: The figure above illustrates the relationship between the supply fan kWh draw and the indoor and outdoor temperature difference when the controller is ON for the weekday hours (Monday to Friday). As it can be seen, as the temperature difference between indoor and outdoor temperature raises so does the kW consumption of the main disconnect panel. This indicates a high correlation between kW and temperature.

Regression Model #7, 8, &9:

The total energy consumption (kWh) of the air conditioning unit (A/C Unit), the four compressors, and the supply fan were respectively analyzed for the entire year starting 11/01/2014 at 12:00am and ending 10/30/15 at 11:58 pm. ***Using the average power factor computed when controller in on & off.***

Model #7: Total Cooling Load Power Consumption Savings

The regression equation to correlate the hourly A/C Unit kWh consumption with the temperature and the [redacted] controller status (whether it's ON or OFF) is as follows:

$$\boldsymbol{Main\ kWh = \beta_0 + \beta_1 \times Outside\ Temperature + \beta_2 \times Enerfit\ Controller}$$

Where:

Main kWh = the hourly power consumption of the air conditioning unit (A/C Unit).

β_0 = the intercept of the regression equation

β_1 = regression coefficient of the model relating the hourly temperature to the hourly kWh

Outside Temperature = hourly outside temperature in °F

β_2 = regression coefficient of the model relating the hourly kWh consumption to the effect of the [redacted] controller

[redacted] ***Controller*** = a dummy variable that is assigned a value **0** when the [redacted] controller is "OFF" and **1** when the controller is "ON".

First, a best subsets regression was performed in order to determine the number of independent variables to be included in the model (Table 22).

number of Variables	R-Sq	R-Sq(adj)	SE
1	20.82	20.81	23.2242
1	37.54	37.53	20.6280
2	57.99	57.98	16.9179
Response is Main kWh			

The second step performed was to test if the effects of both the outside temperature and the [redacted] controller are statistically significant. An Analysis of Variance (ANOVA) was performed to determine whether the [redacted] controller reduction in the kWh is statistically significant.

Table 23 depicts the ANOVA table obtained. The technique used to perform the ANOVA was the multiple regression procedure.

Table 23: Analysis of Variance of Main kWh, using Adjusted SS for Tests

Source	DF	AdjSS	AdjMS	F-Value	P-Value
Regression	2	3459709	1729854	6043.88	0.000
Temp	1	2217340	2217340	7747.09	0.000
Controller	1	1220250	1220250	4263.39	0.000
Error	8757	2506391	286		
Total	8759	5966100			

As shown in Table 23, both the effects of the controller and the outside temperature on the kWh were statistically significant ($P<.001$), meaning that both the ambient temperature and the controller statistically affect the kW consumption.

The next step during the regression analysis was to determine the coefficients corresponding to each independent variable in the governing equation explaining the relationship between the temperature, the controller, and the Main kWh. Table 24 summarizes the coefficients obtained from the regression analysis.

Table 24. Main kWh Regression Analysis coefficients

Term	Coef	SECoef	T-Value	P-Value	VIF
Constant	-109.75	1.75	-62.85	0.000	
Temp	1.9312	0.0219	88.02	0.000	1.00
Controller	-23.607	0.362	-65.29	0.000	1.00

CONFIDENTIAL

Regression Analysis: Main_kwh versus Temp, Controller

Method

Categorical predictor coding (1, 0)

Analysis of Variance

Source	DF	Adj SS	Adj MS	F-Value	P-Value
Regression	2	3459709	1729854	6043.88	0.000
Temp	1	2217340	2217340	7747.09	0.000
Controller	1	1220250	1220250	4263.39	0.000
Error	8757	2506391	286		
Lack-of-Fit	8685	2490941	287	1.34	0.055
Pure Error	72	15451	215		
Total	8759	5966100			

Model Summary

S	R-sq	R-sq(adj)	R-sq(pred)
16.9179	57.99%	57.98%	57.96%

Coefficients

Term	Coef	SE Coef	T-Value	P-Value	VIF
Constant	-109.75	1.75	-62.85	0.000	
Temp	1.9312	0.0219	88.02	0.000	1.00
Controller					
1	-23.607	0.362	-65.29	0.000	1.00

Regression Equation

Controller
0 Main_kW = -109.75 + 1.9312 Temp

1 Main_kW = -133.35 + 1.9312 Temp
Regression Equation including Controller

Main_kWh = -109.75 + 1.9312 Temp - 23.607 Controller

The above equation means that, by controlling for the outside temperature, and by turning the controller ON, a reduction in the kWh of 23.61 kWh occurs.

The average kWh consumption of the Main unit during the OFF periods (where the controller was turned off) is 42.28 kWh. The regression equation indicates that an average reduction of 23.61 kWh is experienced when the controller is turned ON while controlling for the outside temperature. This results in a percentage savings in the baseline kWh (when the controller is

CONFIDENTIAL

OFF) of 55.84% while maintaining the effect of the outside temperature. Figure displays the box plot distribution for Main kWh when the controller is ON vs. OFF.

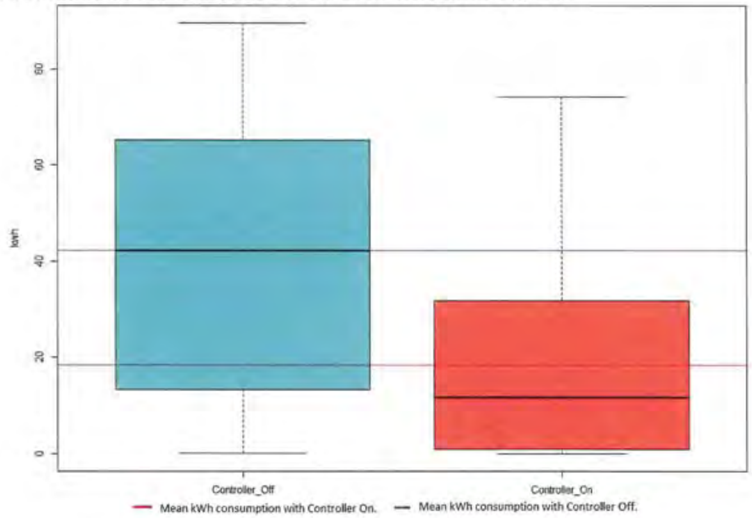

Figure 55: The Box Plot of the Main kWh and the Controller Status.

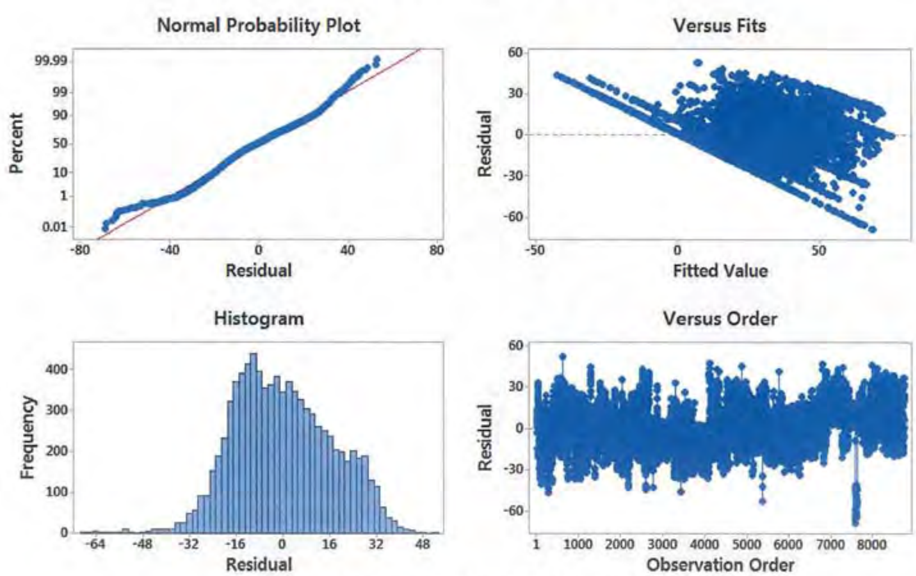

Figure 56: Residual Plots for Main kWh.

Model #8: Compressor Power Consumption Savings

The regression equation to correlate the Compressor kWh consumption with the temperature and the [redacted] controller status (whether it's ON or OFF) is as follows:

$$\textit{Compressor kWh} = \beta_0 + \beta_1 \times \textit{Outside Temperature} + \beta_2 \times \text{[redacted]}\ \textit{Controller}$$

Where:

Compressor kWh = the hourly power consumption due to the four compressors.

β_0 = the intercept of the regression equation

β_1 = regression coefficient of the model relating the hourly temperature to the hourly kWh

Outside Temperature = hourly outside temperature in ^{o}F

β_2 = regression coefficient of the model relating the hourly kWh consumption to the effect of the [redacted] controller

[redacted] ***Controller*** = a dummy variable that is assigned a value **0** when the [redacted] controller is "OFF" and **1** when the controller is "ON".

First, a best subsets regression was performed in order to determine the number of independent variables to be included in the model (Table 25).

number of Variables	R-Sq	R-Sq(adj)	SE
1	9.58	9.57	19.2415
1	39.80	39.79	15.7009
2	49.12	49.11	14.4348
Response is Compressor kWh			

The second step performed was to test if the effects of both the outside temperature and the [redacted] controller are statistically significant. An Analysis of Variance (ANOVA) was performed to determine whether the [redacted] controller reduction in the kWh is statistically significant.

Table 26 depicts the ANOVA table obtained. The technique used to perform the ANOVA was the multiple regression procedure.

Table 26: Analysis of Variance of Main kWh, using Adjusted SS for Tests

Source	DF	AdjSS	AdjMS	F-Value	P-Value
Regression	2	1761545	880772	4227.11	0.000
Temp	1	1417888	1417888	6804.90	0.000
Controller	1	334384	334384	1604.82	0.000
Error	8757	1824633	208		
Total	8759	3586178			

As shown in Table 26, both the effects of the controller and the outside temperature on the kWh were statistically significant ($P<.001$), meaning that both the ambient temperature and the controller statistically affect the kW consumption.

The next step during the regression analysis was to determine the coefficients corresponding to each independent variable in the governing equation explaining the relationship between the temperature, the controller, and the Main kWh. Table 27 summarizes the coefficients obtained from the regression analysis.

Table 27. Main kWh Regression Analysis coefficients

Term	Coef	SECoef	T-Value	P-Value	VIF
Constant	-94.43	1.49	-63.38	0.000	
Temp	1.5443	0.0187	82.49	0.000	1.00
Controller	-12.358	0.308	-40.06	0.000	1.00

Regression Analysis: Compressor_kwh versus Temp, Controller

Method

Categorical predictor coding (1, 0)

Analysis of Variance

Source	DF	Adj SS	Adj MS	F-Value	P-Value
Regression	2	1761545	880772	4227.11	0.000
Temp	1	1417888	1417888	6804.90	0.000
Controller	1	334384	334384	1604.82	0.000
Error	8757	1824633	208		
Lack-of-Fit	8685	1815250	209	1.60	0.005
Pure Error	72	9383	130		
Total	8759	3586178			

Model Summary

S	R-sq	R-sq(adj)	R-sq(pred)
14.4348	49.12%	49.11%	49.08%

Coefficients

Term	Coef	SE Coef	T-Value	P-Value	VIF
Constant	-94.43	1.49	-63.38	0.000	
Temp	1.5443	0.0187	82.49	0.000	1.00
Controller					
1	-12.358	0.308	-40.06	0.000	1.00

Regression Equation

Controller
0 Compressor_kW = -94.43 + 1.5443 Temp

1 Compressor_kW = -106.79 + 1.5443 Temp
2

Regression Equation including Controller

Compressor_kWh = -94.43 + 1.5443 Temp - 12.358 Controller

The above equation means that, by **controlling for the outside temperature**, and by turning the controller ON, a reduction in the kWh of 12.36 kWh occurs in the compressors.

The average kWh consumption of the four compressors during the OFF periods (where the controller was turned off) is 27.14 kWh. The regression equation indicates that an average reduction of 12.36 kWh is experienced when the controller is turned ON while controlling for the outside temperature. This results in a percentage savings in the baseline kWh (when the

controller is OFF) of 45.54% while maintaining the effect of the outside temperature. Figure displays the box plot distribution for Compressor kWh when the controller is ON vs. OFF.

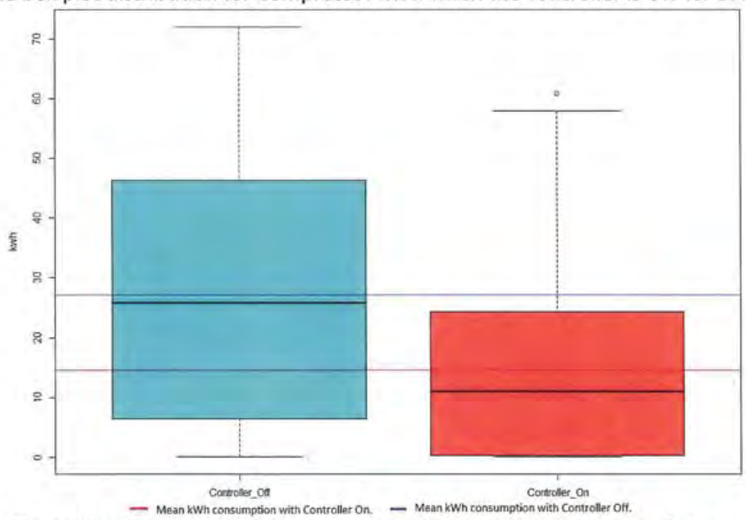

Figure 57: The Box Plot of the Compressor kWh and the Controller Status.

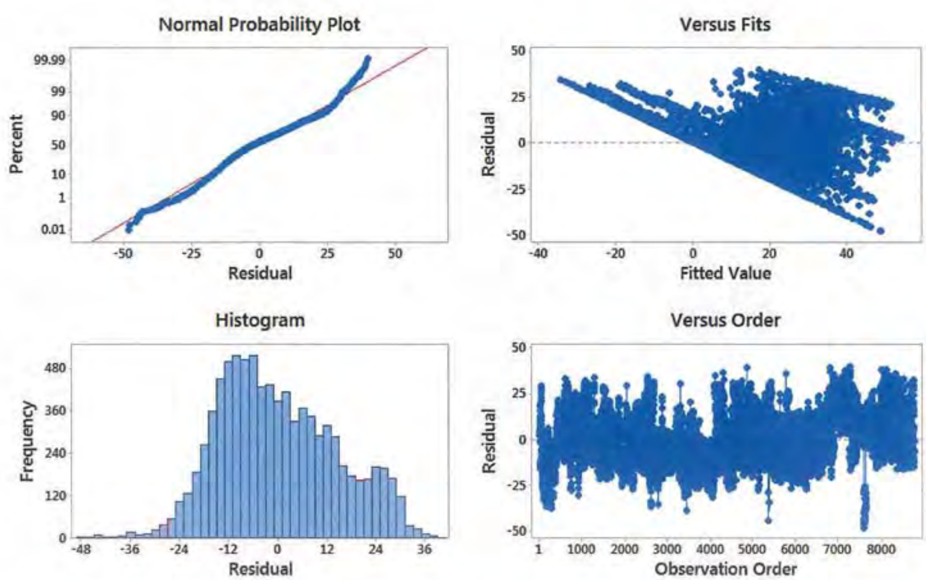

Figure 58: Residual Plots for Compressor kWh

Model #9: Supply Fan Power Consumption Savings

The regression equation to correlate the Supply Fan kWh consumption with the temperature and the [redacted] controller status (whether it's ON or OFF) is as follows:

$$Supply\ Fan\ kWh = \beta_0 + \beta_1 \times Outside\ Temperature + \beta_2 \times Enerfit\ Controller$$

Where:

Supply Fan kWh = the hourly power consumption due to the Supply Fan.

β_0 = the intercept of the regression equation

β_1 = regression coefficient of the model relating the hourly temperature to the hourly kWh

Outside Temperature = hourly outside temperature in $^\circ$F

β_2 = regression coefficient of the model relating the hourly kWh consumption to the effect of the [redacted] controller

[redacted] ***Controller*** = a dummy variable that is assigned a value **0** when the [redacted] controller is "OFF" and **1** when the controller is "ON".

First, a best subsets regression was performed in order to determine the number of independent variables to be included in the model (Table 28).

number of Variables	R-Sq	R-Sq(adj)	SE
1	82.39	82.38	1.58799
1	0.22	0.21	3.71012
2	82.55	82.55	1.58068
Response is Supply Fan kWh			

The second step performed was to test if the effects of both the outside temperature and the [redacted] controller are statistically significant. An Analysis of Variance (ANOVA) was performed to determine whether the [redacted] controller reduction in the kWh is statistically significant.

Table 29 depicts the ANOVA table obtained. The technique used to perform the ANOVA was the multiple regression procedure.

Table 29: Analysis of Variance of Main kWh, using Adjusted SS for Tests

Source	DF	AdjSS	AdjMS	F-Value	P-Value
Regression	2	103509	51755	20713.75	0.000
Temp	1	205	205	82.18	0.000
Controller	1	103238	103238	41318.86	0.000
Error	8757	21880	2		
Total	8759	125389			

As shown in Table 29, both the effects of the controller and the outside temperature on the kWh were statistically significant ($P<.001$), meaning that both the ambient temperature and the controller statistically affect the kW consumption.

The next step during the regression analysis was to determine the coefficients corresponding to each independent variable in the governing equation explaining the relationship between the temperature, the controller, and the Main kWh. Table 30 summarizes the coefficients obtained from the regression analysis.

Table 30. Main kWh Regression Analysis coefficients

Term	Coef	SECoef	T-Value	P-Value	VIF
Constant	8.555	0.163	52.43	0.000	
Temp	0.01858	0.00205	9.07	0.000	1.00
Controller	-6.8664	0.0338	-203.27	0.000	1.00

Regression Analysis: Supply Fan_kwh versus Temp, Controller

Method

Categorical predictor coding (1, 0)

Analysis of Variance

Source	DF	Adj SS	Adj MS	F-Value	P-Value
Regression	2	103509	51755	20713.75	0.000
Temp	1	205	205	82.18	0.000
Controller	1	103238	103238	41318.86	0.000
Error	8757	21880	2		
Lack-of-Fit	8685	21631	2	0.72	0.983
Pure Error	72	249	3		
Total	8759	125389			

Model Summary

S	R-sq	R-sq(adj)	R-sq(pred)
1.58068	82.55%	82.55%	82.54%

Coefficients

Term	Coef	SE Coef	T-Value	P-Value	VIF
Constant	8.555	0.163	52.43	0.000	
Temp	0.01858	0.00205	9.07	0.000	1.00
Controller					
1	-6.8664	0.0338	-203.27	0.000	1.00

Regression Equation

Controller

0 Supply_Fan_kW = 8.555 + 0.01858 Temp

1 Supply_Fan_kW = 1.688 + 0.01858 Temp

Regression Equation including Controller

Supply_Fan_kWh = 8.555 + 0.01858 Temp - 6.8664 Controller

The above equation means that, by **controlling for the outside temperature**, and by turning the controller ON, a reduction in the kWh of 6.87 kWh occurs in the compressors.

The average kWh consumption of the Supply Fan during the OFF periods (where the controller was turned off) is 10.02 kWh. The regression equation indicates that an average reduction of 6.87 kWh is experienced when the controller is turned ON while controlling for the outside temperature. This results in a percentage savings in the baseline kWh (when the controller is OFF) of 68.56**%** while maintaining the effect of the outside temperature. Figure 7 displays the box plot distribution for Supply Fan kWh when the controller is ON vs. OFF.

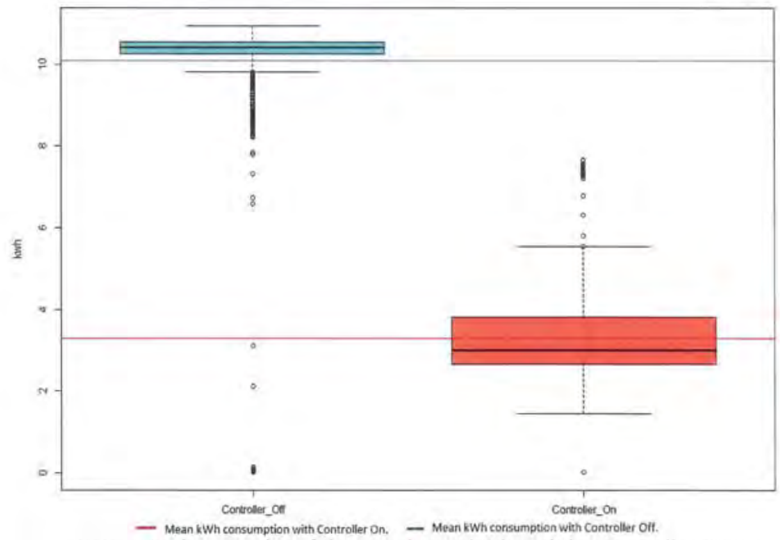

Figure 59: The Box Plot of the Supply Fan kWh and the Controller Status.

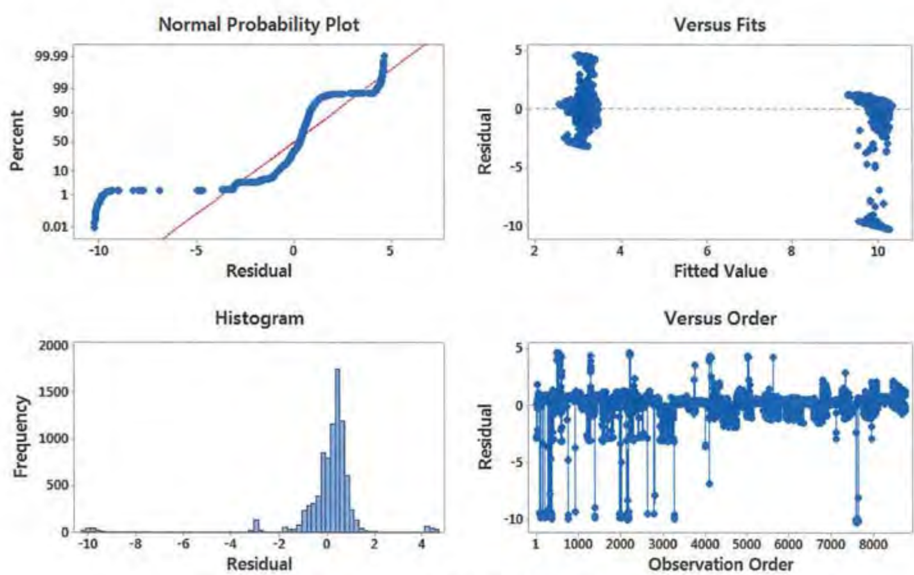

Figure 60: Residual Plots for Supply Fan kWh

CONFIDENTIAL

Combined (November 2014 –October 2015) with Average Controller ON and OFF Power Factor

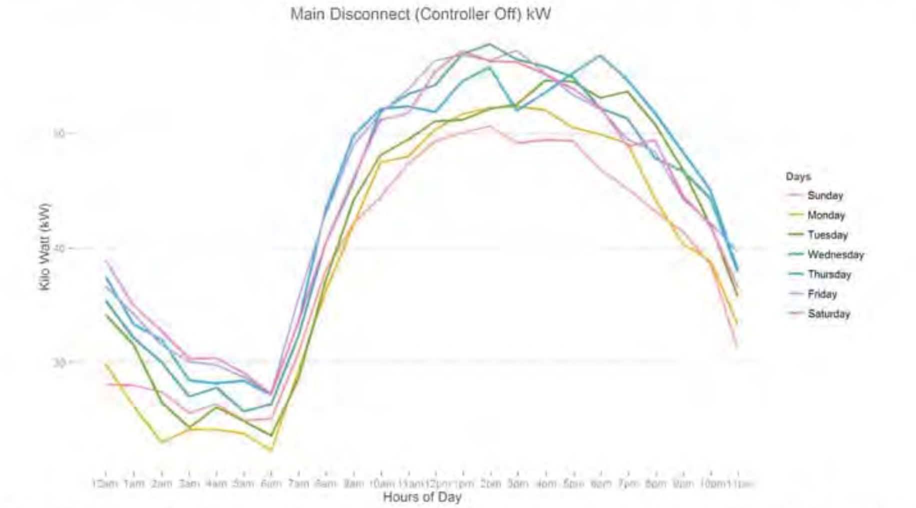

Figure 61: The figure above illustrates the average kWh draw of the main disconnect when the controller is OFF for each hour of the day and each day of the week. This is helpful in understanding the operation of the unit throughout the days of the week. It is clear that as the temperature increases throughout the day, so will the kWh draw.

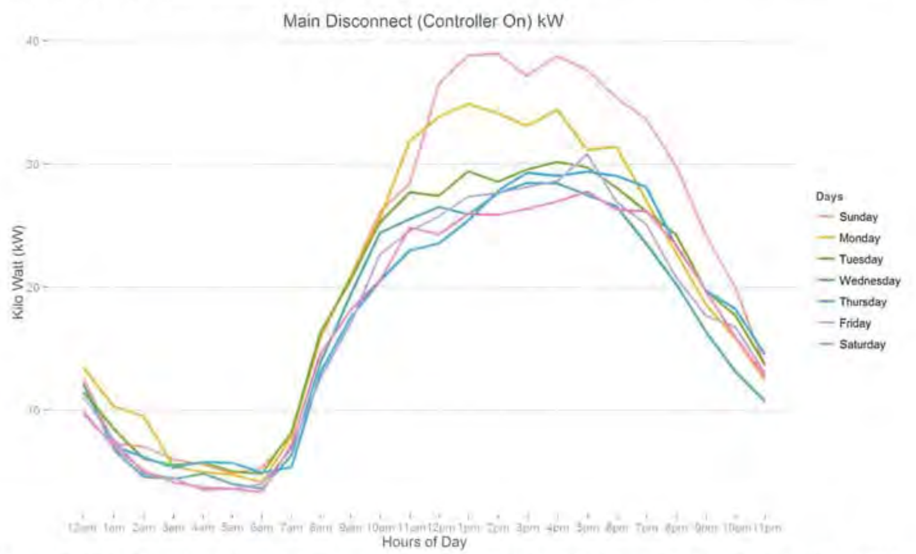

Figure 62: The figure above illustrates the average kWh draw of the main disconnect when the controller is ON for each hour of the day and each day of the week. This is helpful in understanding the operation of the unit throughout the days of the week. It is clear that as the temperature increases throughout the day, so will the kWh draw.

CONFIDENTIAL

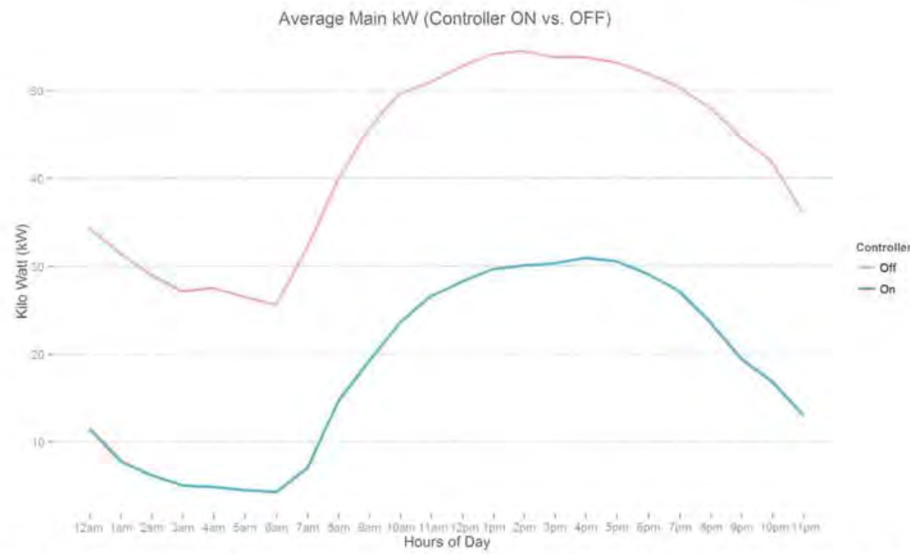

Figure 63: The plot above illustrates that there is a significant reduction in main kWh draw when the controller is ON versus when it is OFF. The kWh draw follows a similar trend throughout the day. This indicates that both control strategies are reacting to the outside temperature and super market occupancy.

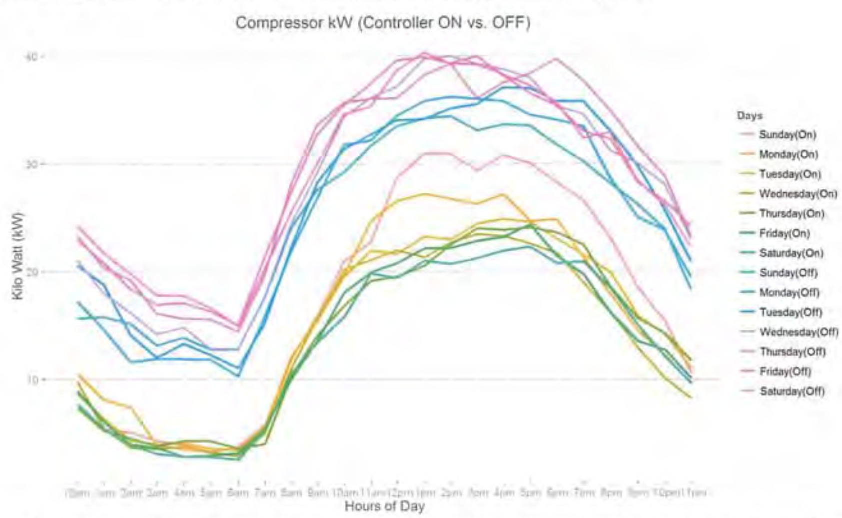

Figure 64: The figure above illustrates the average kWh draw of the compressors when the controller is ON and OFF for each hour of the day and each day of the week. This is helpful in understanding the operation of the unit throughout the days of the week. It is clear that as the temperature increases throughout the day, so will the kWh draw.

CONFIDENTIAL

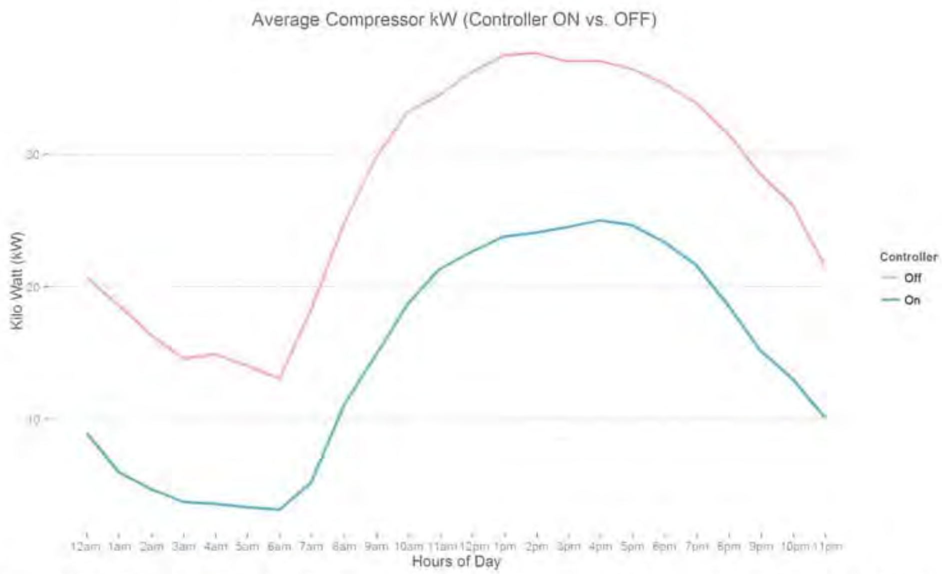

Figure 65: The figure above that there is a significant reduction in compressor kWh drawn when the controller is ON versus when it is OFF. The kWh draw follows a similar trend throughout the day. This indicates that both control strategies are reacting to the outside temperature and super market occupancy.

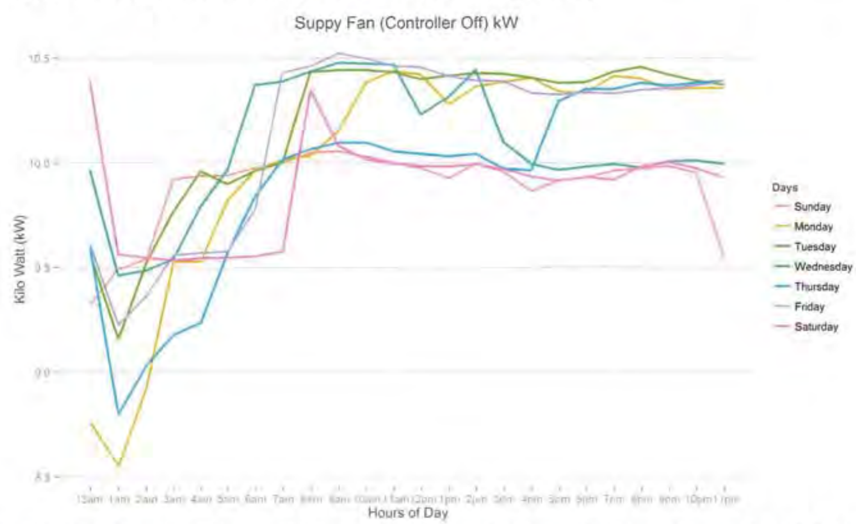

Figure 66: The figure above illustrates the average kWh draw of the supply fan when the controller is OFF for each hour of the day and each day of the week. This is helpful in understanding the operation of the unit throughout the days of the week. It is clear that as the temperature increases throughout the day, so will the kWh draw.

CONFIDENTIAL

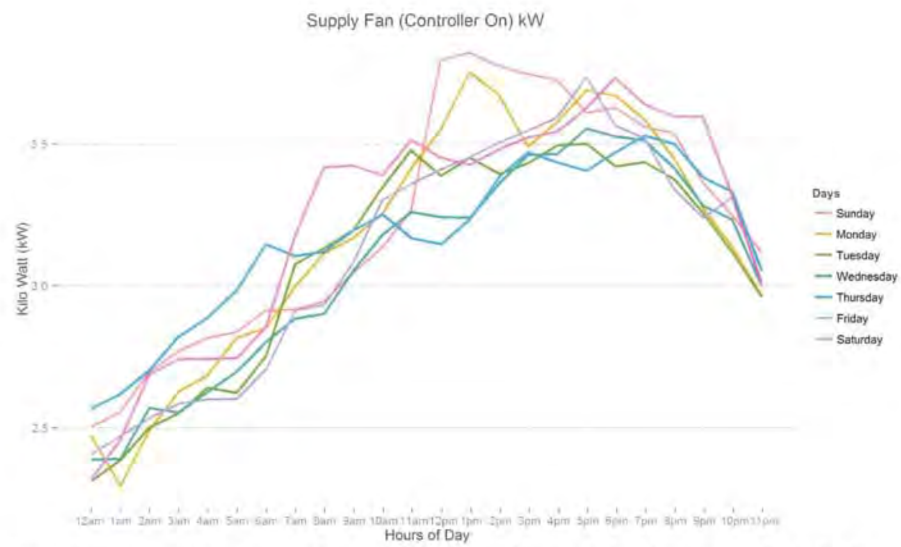

Figure 67: The figure above illustrates the average kWh draw of the supply fan when the controller is ON for each hour of the day and each day of the week. This is helpful in understanding the operation of the unit throughout the days of the week. It is clear that as the temperature increases throughout the day, so will the kWh draw.

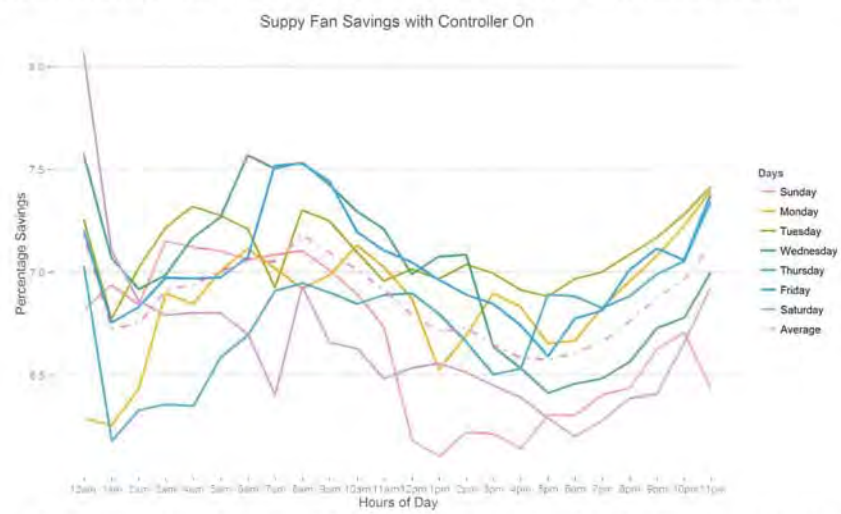

Figure 68: From the above plot we can infer comparing with a referential point; here we consider the average savings, how the savings in a specific day of the week and a specific hour of the day varies from the savings reference We can see from the plot that variation of average hourly kilowatt savings on Sunday (Orange) and Saturday (Purple) are lesser to the average savings comparing with the two extreme weekdays i.e. Tuesday (Sea Green) and Friday (Blue). Which imply savings is inversely proportional to load.

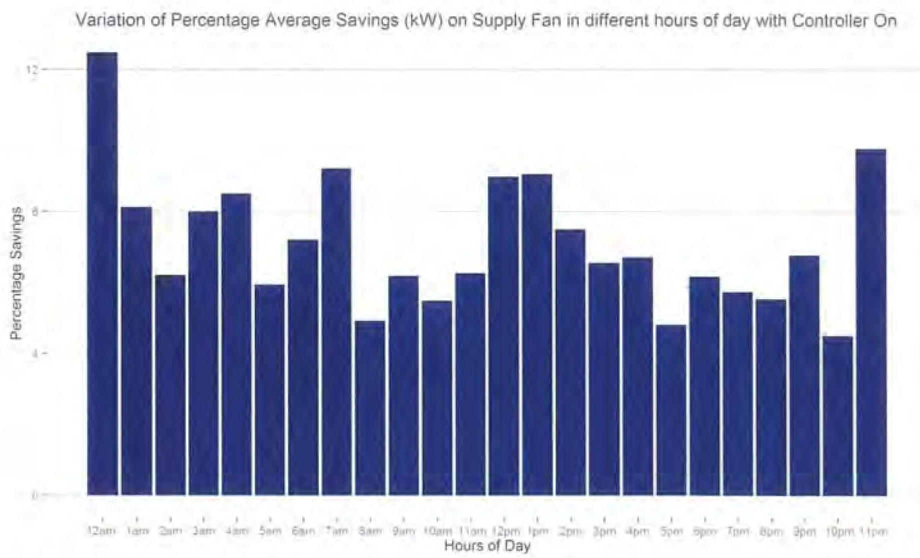

Figure 69: The figure above illustrates the average percent savings of the supply fan throughout the day. As it can be seen, savings are higher during the cooler parts of the day as the VFD is able to slow down he speed of the fan for longer periods of time.

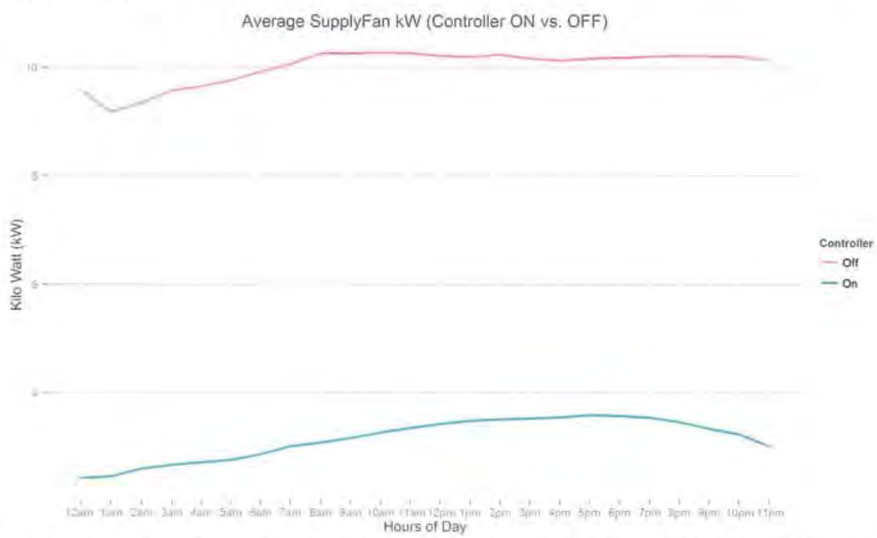

Figure 70: Figure above illustrates that there is a significant reduction in supply fan kWh draw when the controller is ON versus when it is OFF. The kWh draw follows a similar trend throughout the day. This indicates that both control strategies are reacting to the outside temperature and super market occupancy.

CONFIDENTIAL

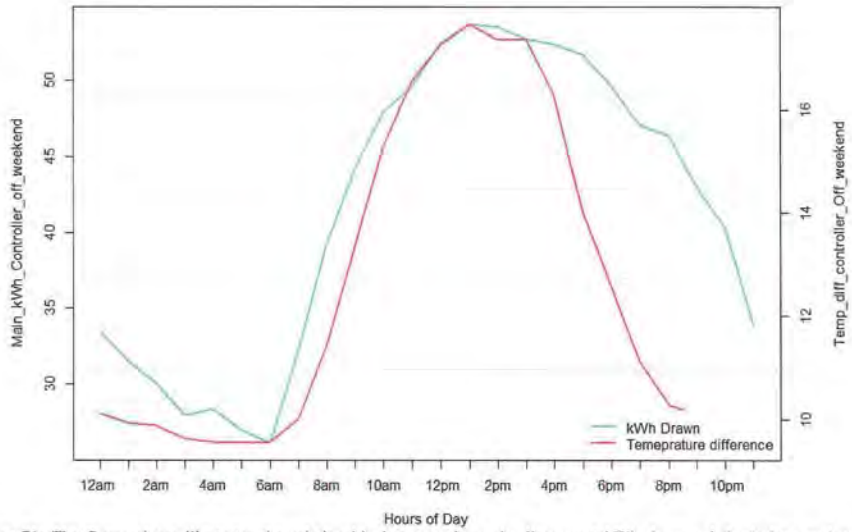

Figure 71: The figure above illustrates the relationship between the main disconnect kWh draw and the indoor and outdoor temperature difference when the controller is OFF for the weekend hours (Saturday and Sunday). As it can be seen, as the temperature difference between indoor and outdoor temperature increased so does the kW consumption of the main disconnect panel. This indicates a high correlation between kW and temperature.

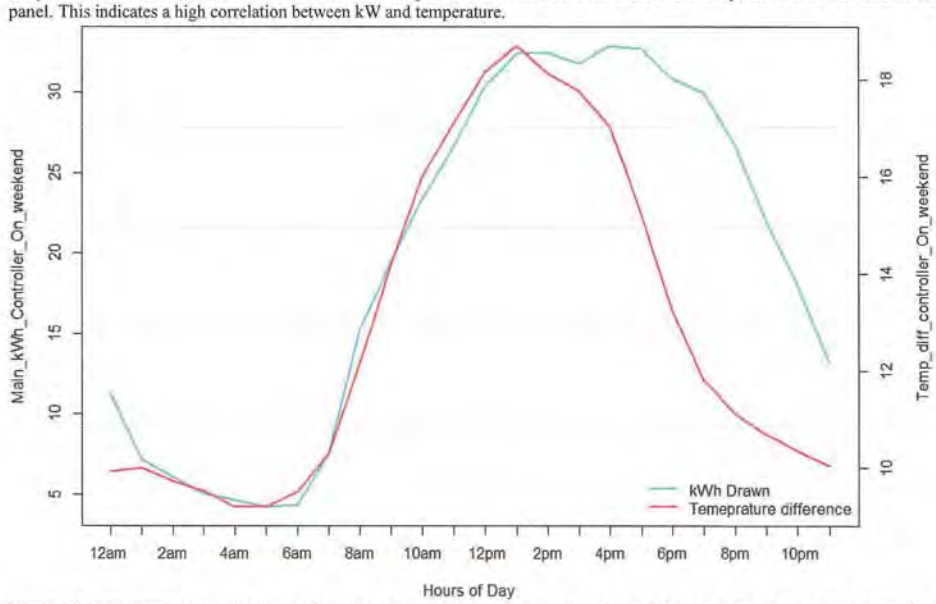

Figure 72: The figure above illustrates the relationship between the main disconnect kWh draw and the indoor and outdoor temperature difference when the controller is ON for the weekend hours (Saturday and Sunday). As it can be seen, as the temperature difference between indoor and outdoor temperature raises so does the kW consumption of the main disconnect panel. This indicates a high correlation between kW and temperature.

CONFIDENTIAL

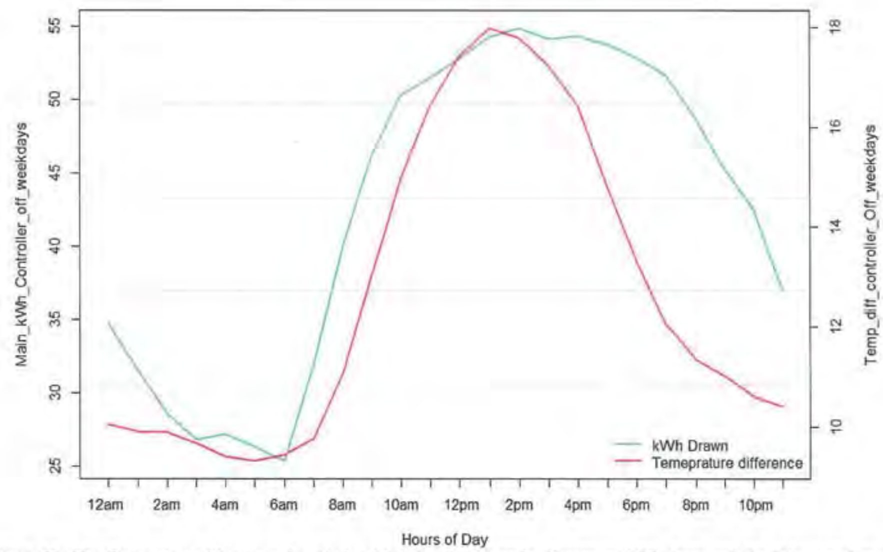

Figure 73: The figure above illustrates the relationship between the main disconnect kWh draw and the indoor and outdoor temperature difference when the controller is OFF for the weekday hours (Monday to Friday). As it can be seen, as the temperature difference between indoor and outdoor temperature increased so does the kW consumption of the main disconnect panel. This indicates a high correlation between kW and temperature.

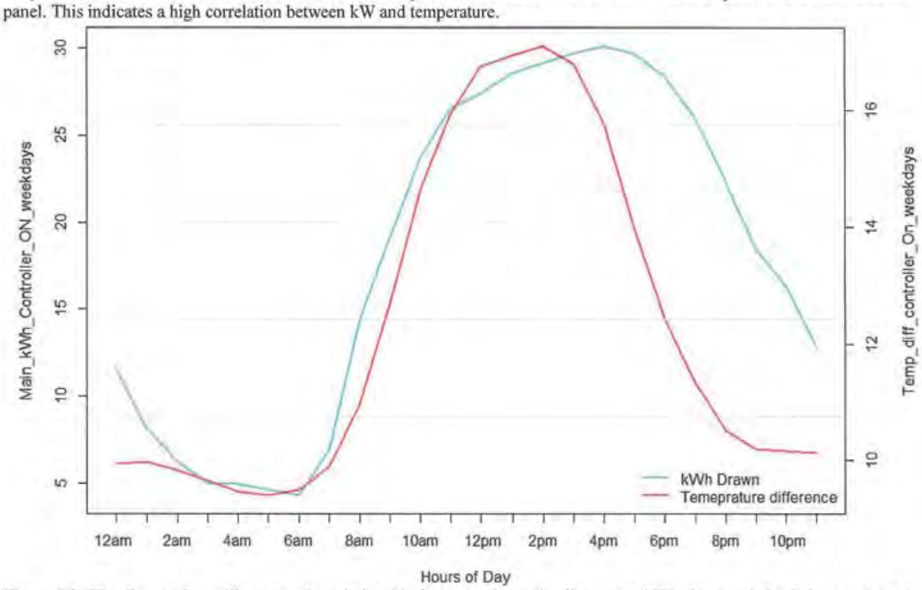

Figure 74: The figure above illustrates the relationship between the main disconnect kWh draw and the indoor and outdoor temperature difference when the controller is ON for the weekday hours (Monday to Friday). As it can be seen, as the temperature difference between indoor and outdoor temperature raises so does the kW consumption of the main disconnect panel. This indicates a high correlation between kW and temperature.

CONFIDENTIAL

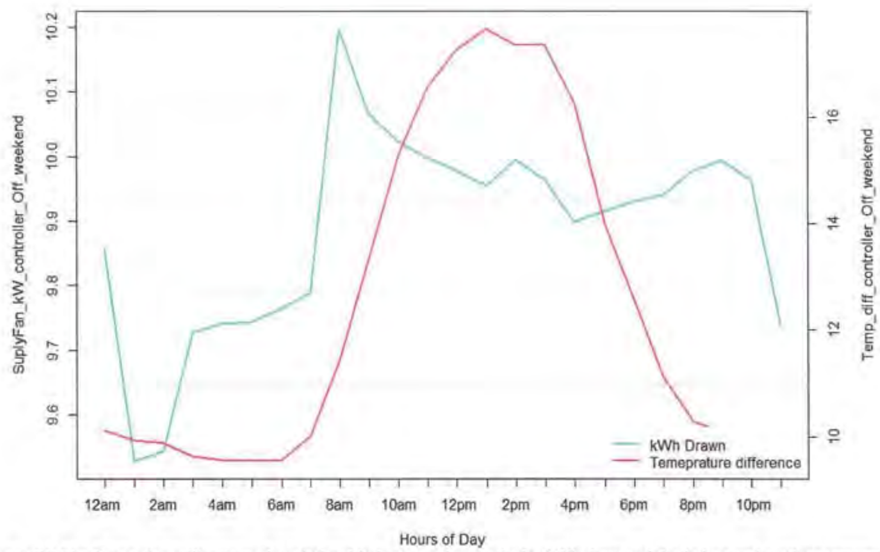

Figure 75: The figure above illustrates the relationship between the supply fan kWh draw and the indoor and outdoor temperature difference when the controller is OFF for the weekend hours (Saturday and Sunday). As it can be seen, as the temperature difference between indoor and outdoor temperature increased so does the kW consumption of the main disconnect panel. This indicates a high correlation between kW and temperature.

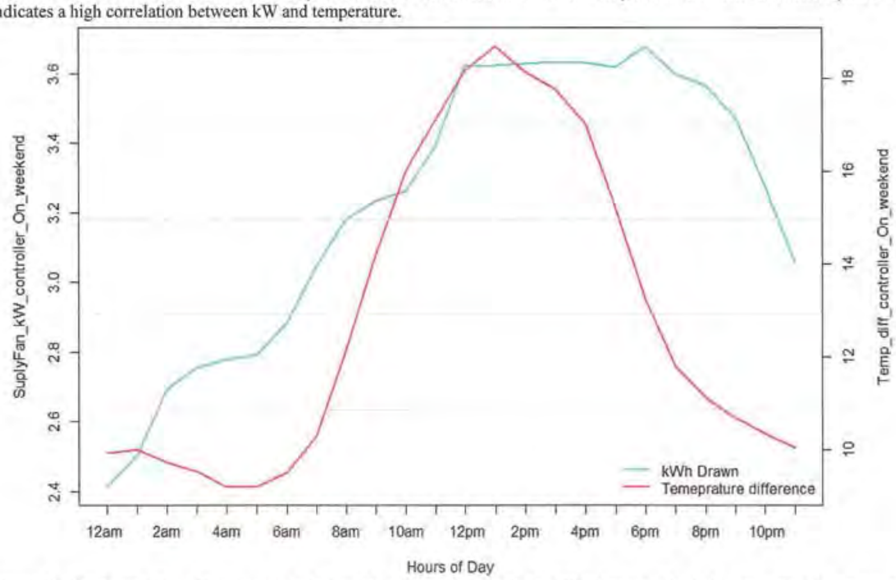

Figure 76: The figure above illustrates the relationship between the supply fan kWh draw and the indoor and outdoor temperature difference when the controller is ON for the weekend hours (Saturday and Sunday). As it can be seen, as the temperature difference between indoor and outdoor temperature raises so does the kW consumption of the main disconnect panel. This indicates a high correlation between kW and temperature.

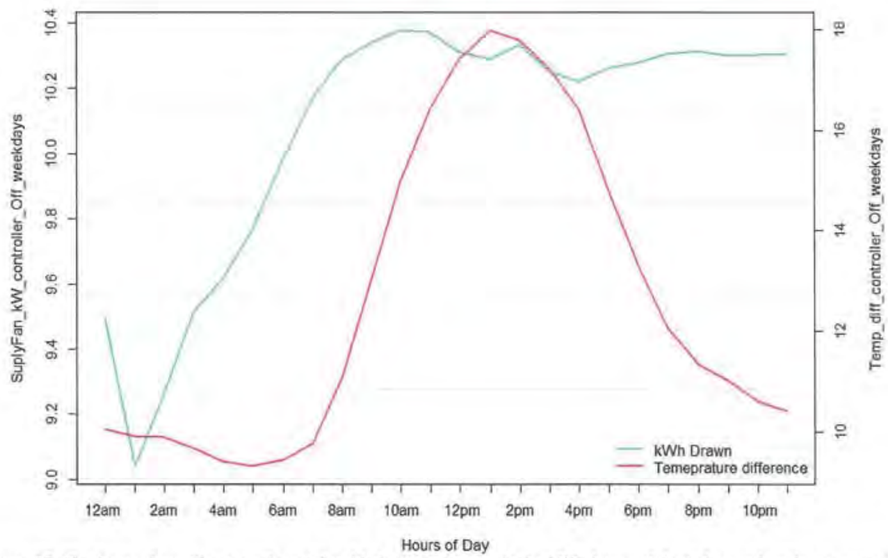

Figure 77: The figure above illustrates the relationship between the supply fan kWh draw and the indoor and outdoor temperature difference when the controller is OFF for the weekday hours (Monday to Friday). As it can be seen, as the temperature difference between indoor and outdoor temperature increased so does the kW consumption of the main disconnect panel. This indicates a high correlation between kW and temperature.

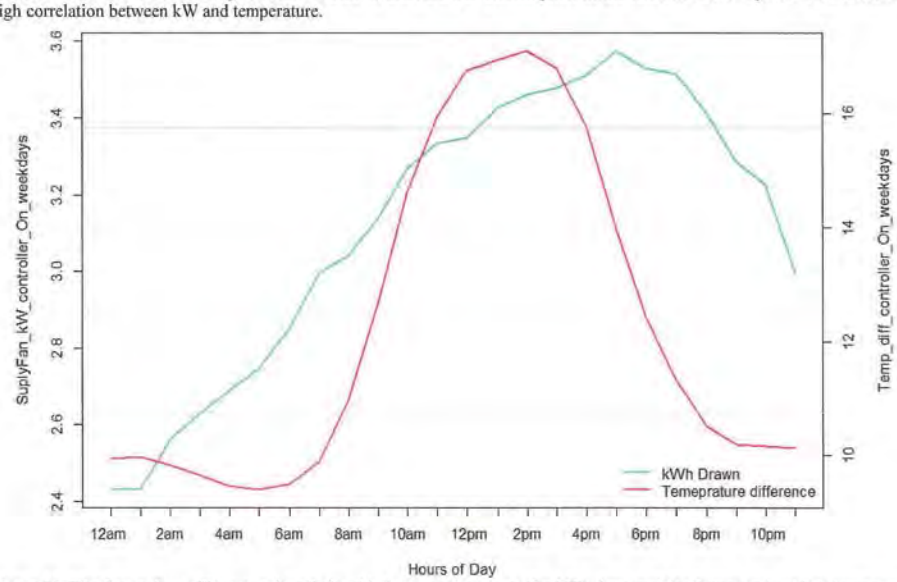

Figure 78: The figure above illustrates the relationship between the supply fan kWh draw and the indoor and outdoor temperature difference when the controller is ON for the weekday hours (Monday to Friday). As it can be seen, as the temperature difference between indoor and outdoor temperature raises so does the kW consumption of the main disconnect panel. This indicates a high correlation between kW and temperature.

Regression Model #10, 11, &12:

The total energy consumption (kWh) of the air conditioning unit (A/C Unit), the four compressors, and the supply fan were respectively analyzed for five months starting 11/01/2014 at 12:00am and ending 03/31/15 at 11:58 pm. ***With unity power factor.***

Model #10: Total Cooling Load Power Consumption Savings

The regression equation to correlate the hourly A/C Unit kWh consumption with the temperature and the [redacted] controller status (whether it's ON or OFF) is as follows:

$$Main\ kWh = \beta_0 + \beta_1 \times Outside\ Temperature + \beta_2 \times Enerfit\ Controller$$

Where:

Main kWh = the hourly power consumption of the air conditioning unit (A/C Unit).

β_0 = the intercept of the regression equation

β_1 = regression coefficient of the model relating the hourly temperature to the hourly kWh

Outside Temperature = hourly outside temperature in $^\circ$F

β_2 = regression coefficient of the model relating the hourly kWh consumption to the effect of the [redacted] controller

[redacted] ***Controller*** = a dummy variable that is assigned a value **0** when the [redacted] controller is "OFF" and **1** when the controller is "ON".

First, a best subsets regression was performed in order to determine the number of independent variables to be included in the model (Table 31).

number of Variables	R-Sq	R-Sq(adj)	SE
1	44.29	44.26	17.1258
1	25.67	25.65	19.7790
2	18.88	18.86	20.6624
Response is Main kWh			

The second step performed was to test if the effects of both the outside temperature and the [redacted] controller are statistically significant. An Analysis of Variance (ANOVA) was performed to determine whether the [redacted] controller reduction in the kWh is statistically significant.

Table 32 depicts the ANOVA table obtained. The technique used to perform the ANOVA was the multiple regression procedure.

Table 32: Analysis of Variance of Main kWh, using Adjusted SS for Tests

Source	DF	AdjSS	AdjMS	F-Value	P-Value
Regression	2	844193	422096	1439.16	0.000
Temp	1	484341	484341	1651.39	0.000
Controller	1	354942	354942	1210.19	0.000
Error	3621	1062016	293		
Total	3623	1906208			

As shown in Table 32, both the effects of the controller and the outside temperature on the kWh were statistically significant ($P<.001$), meaning that both the ambient temperature and the controller statistically affect the kW consumption.

The next step during the regression analysis was to determine the coefficients corresponding to each independent variable in the governing equation explaining the relationship between the temperature, the controller, and the Main kWh. Table 30 summarizes the coefficients obtained from the regression analysis.

Table 33. Main kWh Regression Analysis coefficients

Term	Coef	SECoef	T-Value	P-Value	VIF
Constant	-72.59	2.54	-28.58	0.000	
Temp	1.4000	0.0345	40.64	0.000	1.00
Controller	-19.794	0.569	-34.79	0.000	1.00

Regression Analysis: Main_kwh versus Temp, Controller

Method

Categorical predictor coding (1, 0)

Analysis of Variance

Source	DF	Adj SS	Adj MS	F-Value	P-Value
Regression	2	844193	422096	1439.16	0.000
Temp	1	484341	484341	1651.39	0.000
Controller	1	354942	354942	1210.19	0.000
Error	3621	1062016	293		
Lack-of-Fit	3578	1045923	292	0.78	0.895
Pure Error	43	16093	374		
Total	3623	1906208			

Model Summary

S	R-sq	R-sq(adj)	R-sq(pred)
17.1258	44.29%	44.26%	44.19%

Coefficients

Term	Coef	SE Coef	T-Value	P-Value	VIF
Constant	-72.59	2.54	-28.58	0.000	
Temp	1.4000	0.0345	40.64	0.000	1.00
Controller					
1	-19.794	0.569	-34.79	0.000	1.00

Regression Equation

Controller

0 Main_kW = -72.59 + 1.4000 Temp

1 Main_kW = -92.38 + 1.4000 Temp

Regression Equation including Controller

Main_kW = -72.59 + 1.4000 Temp - 19.794 Controller

The above equation means that, by controlling for the outside temperature, and by turning the controller ON, a reduction in the kWh of 19.80 kWh occurs.

The average kWh consumption of the Main unit during the OFF periods (where the controller was turned off) is 29.31 kWh. The regression equation indicates that an average reduction of 19.80 kWh is experienced when the controller is turned ON while controlling for the outside temperature. This results in a percentage savings in the baseline kWh (when the controller is

OFF) of 67.55% while maintaining the effect of the outside temperature. Figure displays the box plot distribution for Main kWh when the controller is ON vs. OFF.

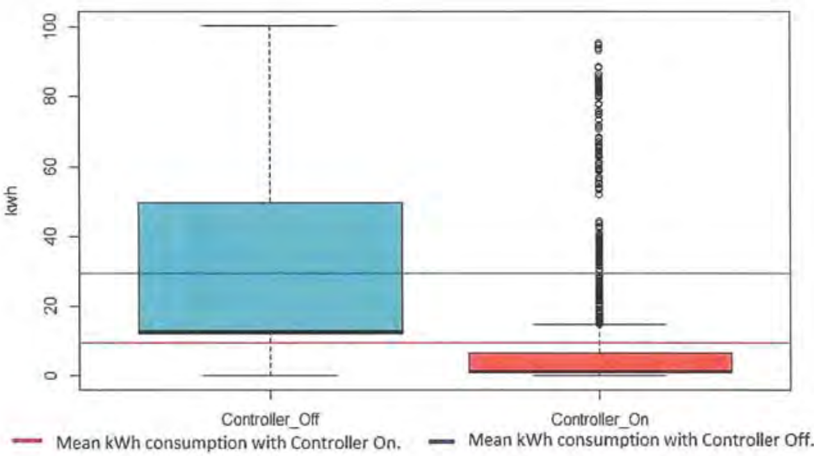

Figure 79: The Box Plot of the Main kWh and the Controller Status.

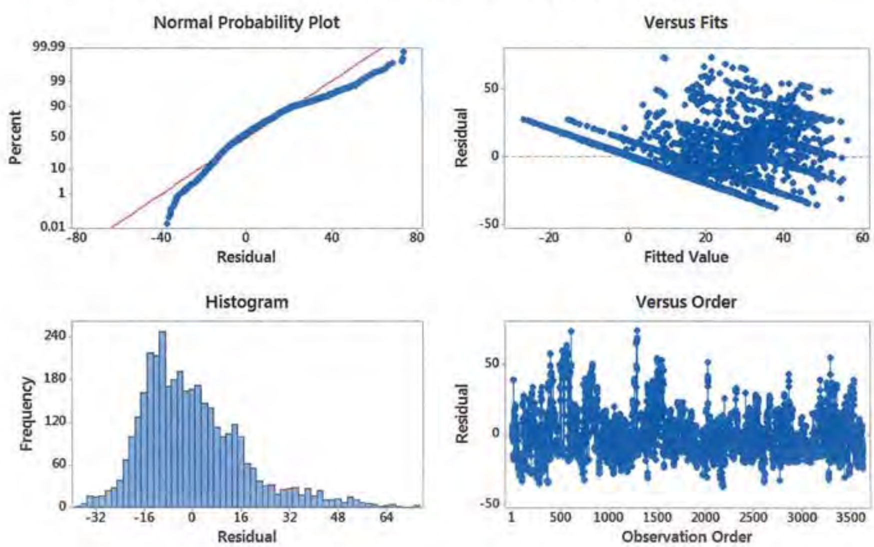

Figure 80: Residual Plots for Main kWh.

Model #11: Compressor Power Consumption Savings

The regression equation to correlate the Compressor kWh consumption with the temperature and the [redacted] controller status (whether it's ON or OFF) is as follows:

$$\textbf{\textit{Compressor kWh}} = \beta_0 + \beta_1 \times \textbf{\textit{Outside Temperature}} + \beta_2 \times \textbf{\textit{Enerfit Controller}}$$

Where:

Compressor kWh = the hourly power consumption due to the four compressors.

β_0 = the intercept of the regression equation

β_1 = regression coefficient of the model relating the hourly temperature to the hourly kWh

Outside Temperature = hourly outside temperature in $^{\circ}$F

β_2 = regression coefficient of the model relating the hourly kWh consumption to the effect of the [redacted] controller

[redacted] ***Controller*** = a dummy variable that is assigned a value **0** when the [redacted] controller is "OFF" and **1** when the controller is "ON".

First, a best subsets regression was performed in order to determine the number of independent variables to be included in the model (Table 34).

number of Variables	R-Sq	R-Sq(adj)	SE
1	4.25	4.23	15.0622
1	25.28	25.26	13.3061
2	29.41	29.37	12.9348
Response is Compressor kWh			

The second step performed was to test if the effects of both the outside temperature and the [redacted] controller are statistically significant. An Analysis of Variance (ANOVA) was performed to determine whether the [redacted] controller reduction in the kWh is statistically significant.

Table 35 depicts the ANOVA table obtained. The technique used to perform the ANOVA was the multiple regression procedure.

Table 35: Analysis of Variance of Main kWh, using Adjusted SS for Tests

Source	DF	AdjSS	AdjMS	F-Value	P-Value
Regression	2	252395	126197	754.28	0.000
Temp	1	215901	215901	1290.43	0.000
Controller	1	35456	35456	211.92	0.000
Error	3621	605825	167		
Total	3623	858219			

As shown in Table 35, both the effects of the controller and the outside temperature on the kWh were statistically significant ($P<.001$), meaning that both the ambient temperature and the controller statistically affect the kW consumption.

The next step during the regression analysis was to determine the coefficients corresponding to each independent variable in the governing equation explaining the relationship between the temperature, the controller, and the Main kWh. Table 36 summarizes the coefficients obtained from the regression analysis.

Table 36. Main kWh Regression Analysis coefficients

Term	Coef	SECoef	T-Value	P-Value	VIF
Constant	-53.54	1.92	-27.91	0.000	
Temp	0.9347	0.0260	35.92	0.000	1.00
Controller	-6.256	0.430	-14.56	0.000	1.00

Regression Analysis: Compressor_kwh versus Temp, Controller

Method

Categorical predictor coding (1, 0)

Analysis of Variance

Source	DF	Adj SS	Adj MS	F-Value	P-Value
Regression	2	252395	126197	754.28	0.000
Temp	1	215901	215901	1290.43	0.000
Controller	1	35456	35456	211.92	0.000
Error	3621	605825	167		
Lack-of-Fit	3578	598269	167	0.95	0.618
Pure Error	43	7556	176		
Total	3623	858219			

Model Summary

S	R-sq	R-sq(adj)	R-sq(pred)
12.9348	29.41%	29.37%	29.28%

Coefficients

Term	Coef	SE Coef	T-Value	P-Value	VIF
Constant	-53.54	1.92	-27.91	0.000	
Temp	0.9347	0.0260	35.92	0.000	1.00
Controller					
1	-6.256	0.430	-14.56	0.000	1.00

Regression Equation

Controller

0 Compressor_kWh = -53.54 + 0.9347 Temp

1 Compressor_kWh = -59.79 + 0.9347 Temp

Regression Equation including Controller

Compressor_kWh = -53.54 + 0.9347 Temp - 6.256 Controller

The above equation means that, by **controlling for the outside temperature**, and by turning the controller ON, a reduction in the kWh of 6.26 kWh occurs in the compressors.

The average kWh consumption of the four compressors during the OFF periods (where the controller was turned off) is 14.50 kWh. The regression equation indicates that an average reduction of 6.26 kWh is experienced when the controller is turned ON while controlling for the outside temperature. This results in a percentage savings in the baseline kWh (when the

controller is OFF) of 43.17% while maintaining the effect of the outside temperature. Figure displays the box plot distribution for Compressor kWh when the controller is ON vs. OFF.

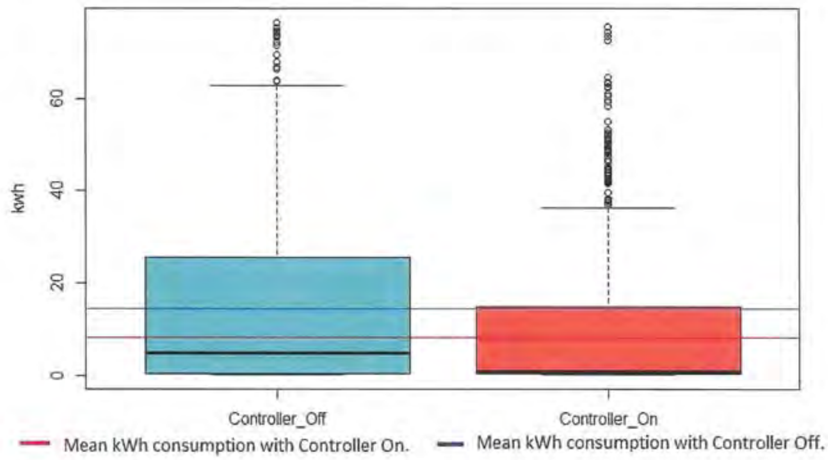

Figure 81: The Box Plot of the Compressor kWh and the Controller Status.

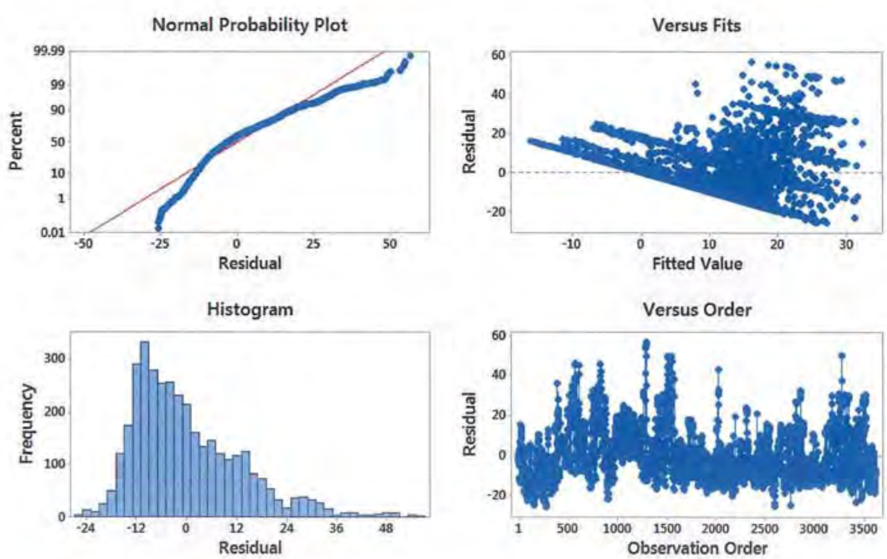

Figure 82: Residual Plots for Compressor kWh

Model #12: Supply Fan Power Consumption Savings

The regression equation to correlate the Supply Fan kWh consumption with the temperature and the [redacted] controller status (whether it's ON or OFF) is as follows:

$$Supply\ Fan\ kWh = \beta_0 + \beta_1 \times Outside\ Temperature + \beta_2 \times Enerfit\ Controller$$

Where:

Supply Fan kWh = the hourly power consumption due to the Supply Fan.

β_0 = the intercept of the regression equation

β_1 = regression coefficient of the model relating the hourly temperature to the hourly kWh

Outside Temperature = hourly outside temperature in $^{\circ}$F

β_2 = regression coefficient of the model relating the hourly kWh consumption to the effect of the [redacted] controller

[redacted] ***Controller*** = a dummy variable that is assigned a value **0** when the [redacted] controller is "OFF" and **1** when the controller is "ON".

First, a best subsets regression was performed in order to determine the number of independent variables to be included in the model (Table 37).

number of Variables	R-Sq	R-Sq(adj)	SE
1	64.42	64.39	3.43179
1	0.28	0.25	5.74630
2	64.66	64.64	3.42120
Response is Supply Fan kWh			

The second step performed was to test if the effects of both the outside temperature and the [redacted] controller are statistically significant. An Analysis of Variance (ANOVA) was performed to determine whether the [redacted] controller reduction in the kWh is statistically significant.

Table 38 depicts the ANOVA table obtained. The technique used to perform the ANOVA was the multiple regression procedure.

Table 38: Analysis of Variance of Main kWh, using Adjusted SS for Tests

Source	DF	AdjSS	AdjMS	F-Value	P-Value
Regression	2	77547	38773.6	3312.68	0.000
Temp	1	275	274.6	23.46	0.000
Controller	1	77216	77215.7	6597.03	0.000
Error	3621	42382	11.7		
Total	3623	119930			

As shown in Table 38, both the effects of the controller and the outside temperature on the kWh were statistically significant ($P<.001$), meaning that both the ambient temperature and the controller statistically affect the kW consumption.

The next step during the regression analysis was to determine the coefficients corresponding to each independent variable in the governing equation explaining the relationship between the temperature, the controller, and the Main kWh. Table 39 summarizes the coefficients obtained from the regression analysis.

Table 39. Main kWh Regression Analysis coefficients

Term	Coef	SECoef	T-Value	P-Value	VIF
Constant	13.314	0.507	26.24	0.000	
Temp	0.03334	0.00688	4.84	0.000	1.00
Controller	-9.232	0.114	-81.2	0.000	1.00

Regression Analysis: Supply Fan_kwh versus Temp, Controller

Method

Categorical predictor coding (1, 0)

Analysis of Variance

Source	DF	Adj SS	Adj MS	F-Value	P-Value
Regression	2	77547	38773.6	3312.68	0.000
Temp	1	275	274.6	23.46	0.000
Controller	1	77216	77215.7	6597.03	0.000
Error	3621	42382	11.7		
Lack-of-Fit	3578	41741	11.7	0.78	0.895
Pure Error	43	642	14.9		
Total	3623	119930			

Model Summary

S	R-sq	R-sq(adj)	R-sq(pred)
3.42120	64.66%	64.64%	64.61%

Coefficients

Term	Coef	SE Coef	T-Value	P-Value	VIF
Constant	13.314	0.507	26.24	0.000	
Temp	0.03334	0.00688	4.84	0.000	1.00
Controller					
1	-9.232	0.114	-81.22	0.000	1.00

Regression Equation

Controller
0 SupplyFan_kWh = 13.314 + 0.03334 Temp

1 SupplyFan_kWh = 4.082 + 0.03334 Temp

Regression Equation including Controller

SupplyFan_kWh = 13.314 + 0.03334 Temp - 9.232 Controller

The above equation means that, by **controlling for the outside temperature,** and by turning the controller ON, a reduction in the kWh of 9.23 kWh occurs in the compressors.

The average kWh consumption of the Supply Fan during the OFF periods (where the controller was turned off) is 15.74 kWh. The regression equation indicates that an average reduction of 9.23 kWh is experienced when the controller is turned ON while controlling for the outside temperature. This results in a percentage savings in the baseline kWh (when the controller is

OFF) of 58.64% while maintaining the effect of the outside temperature. Figure 7 displays the box plot distribution for Supply Fan kWh when the controller is ON vs. OFF.

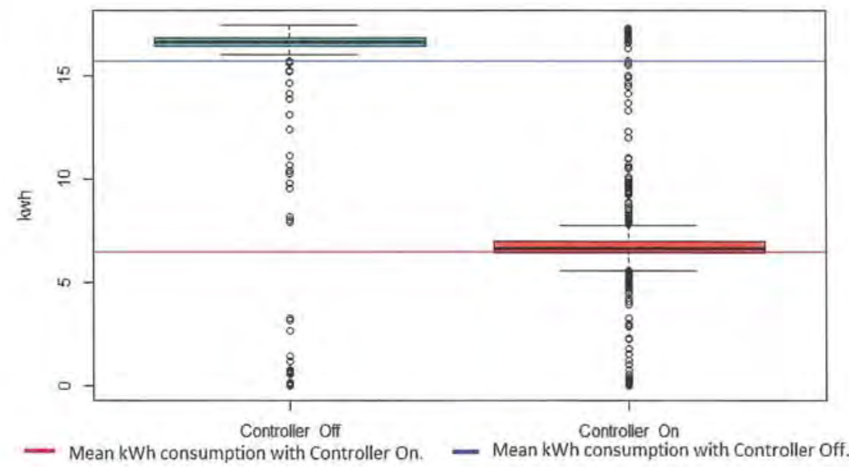

Figure 83: The Box Plot of the Supply Fan kWh and the Controller Status.

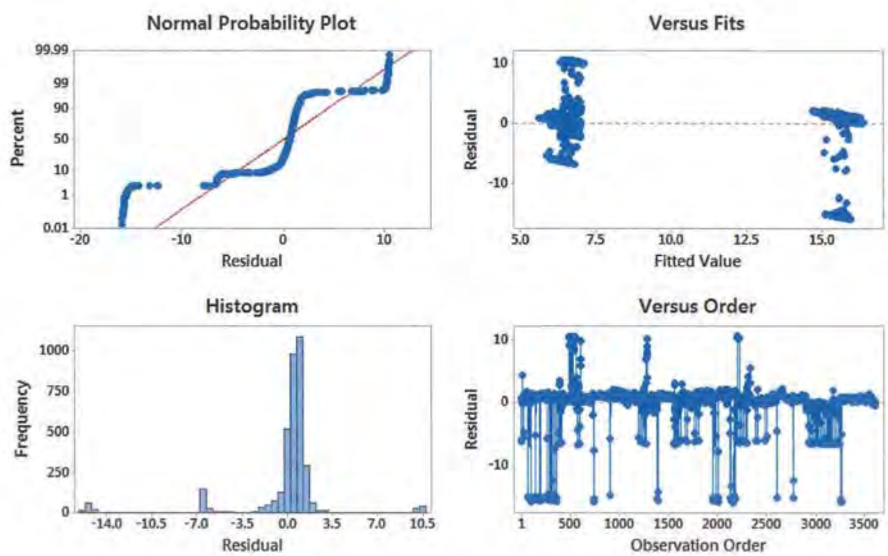

Figure 84: Residual Plots for Supply Fan kWh

CONFIDENTIAL

Winter (November 14'-March 15') with Unity Power Factor

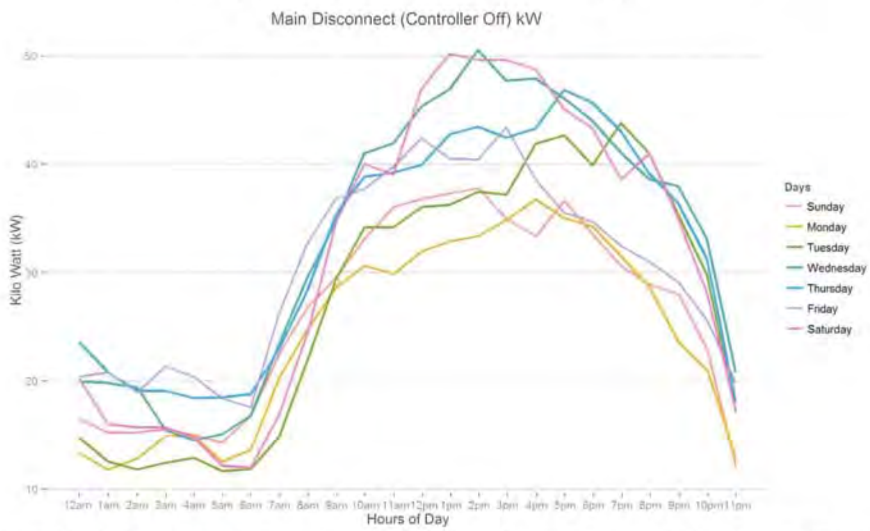

Figure 85: The figure above illustrates the average kWh draw of the main disconnect when the controller is OFF for each hour of the day and each day of the week. This is helpful in understanding the operation of the unit throughout the days of the week. It is clear that as the temperature increases throughout the day, so will the kWh draw.

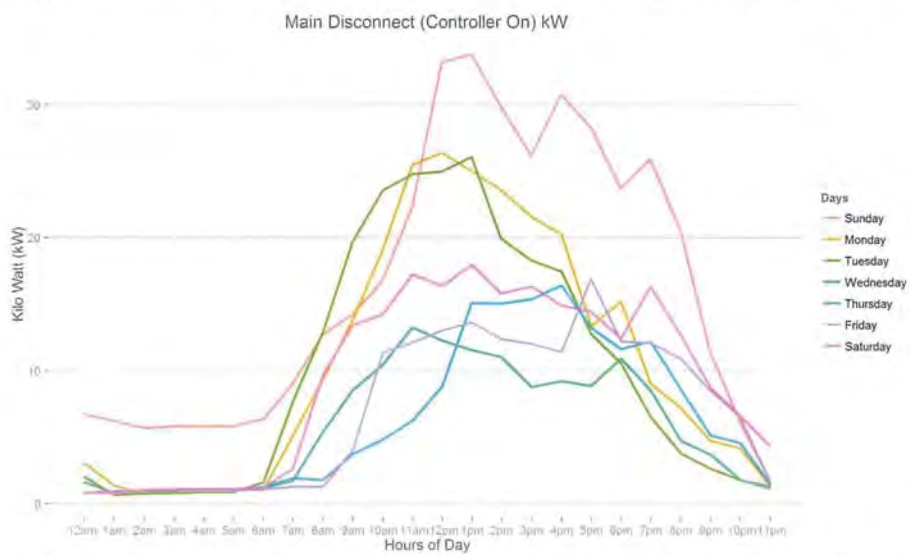

Figure 86: The figure above illustrates the average kWh draw of the main disconnect when the controller is ON for each hour of the day and each day of the week. This is helpful in understanding the operation of the unit throughout the days of the week. It is clear that as the temperature increases throughout the day, so will the kWh draw.

CONFIDENTIAL

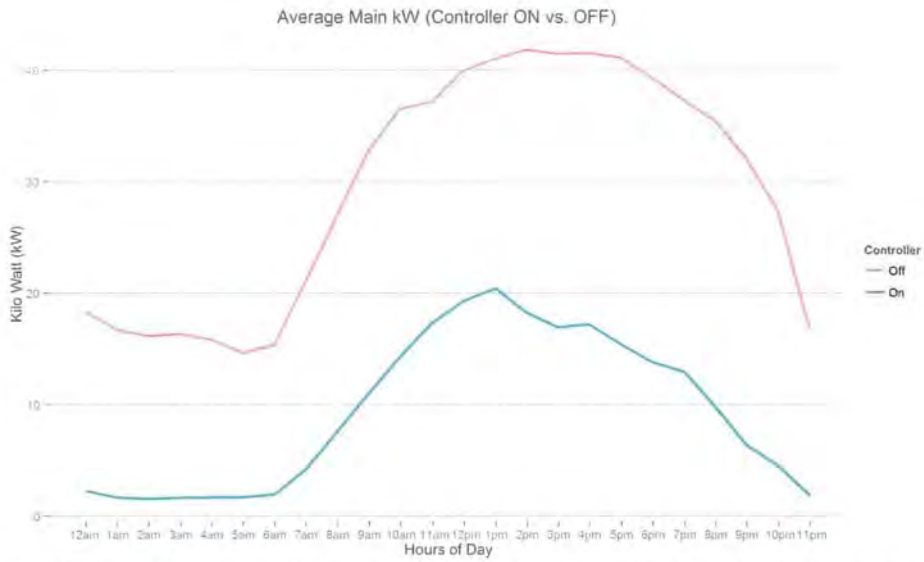

Figure 87: The plot above illustrates that there is a significant reduction in main kWh draw when the controller is ON versus when it is OFF. The kWh draw follows a similar trend throughout the day. This indicates that both control strategies are reacting to the outside temperature and super market occupancy.

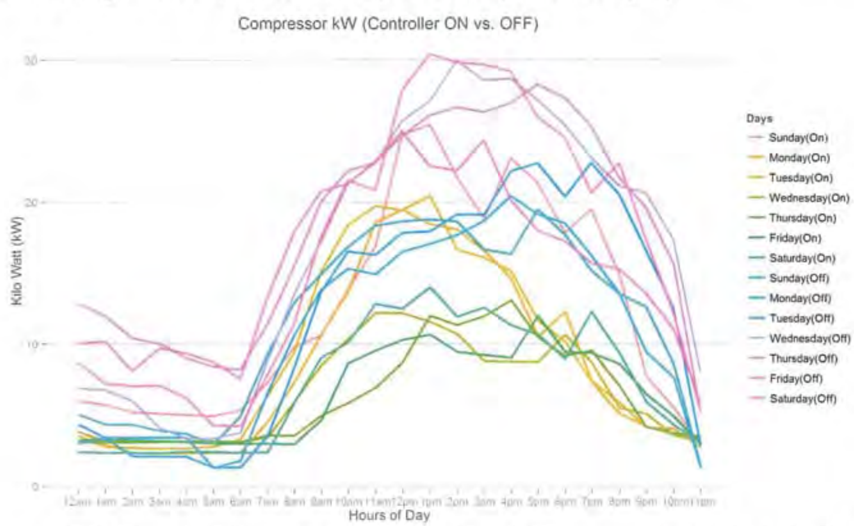

Figure 88: The figure above illustrates the average kWh draw of the compressors when the controller is ON and OFF for each hour of the day and each day of the week. This is helpful in understanding the operation of the unit throughout the days of the week. It is clear that as the temperature increases throughout the day, so will the kWh draw.

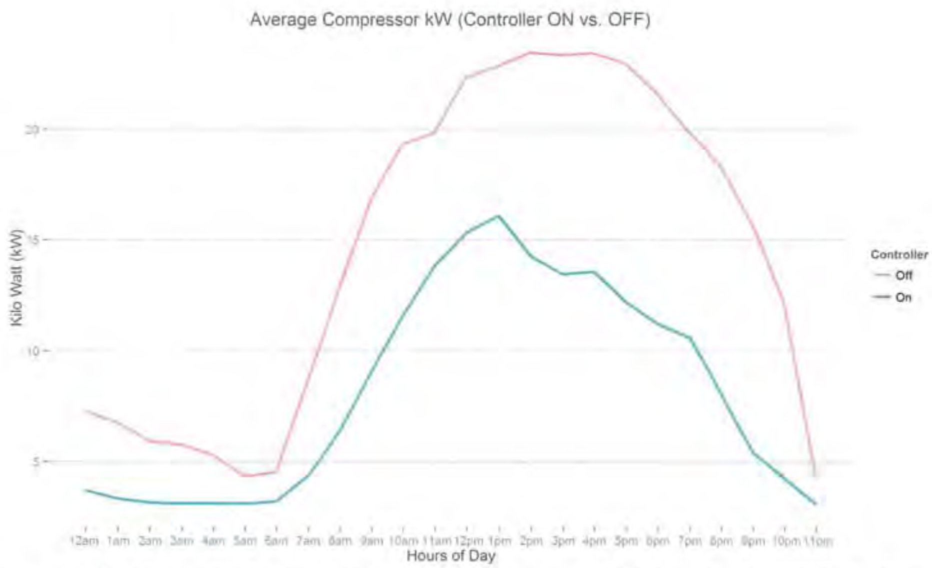

Figure 89: The plot above that there is a significant reduction in compressor kWh draw when the controller is ON versus when it is OFF. The kWh draw follows a similar trend throughout the day. This indicates that both control strategies are reacting to the outside temperature and super market occupancy.

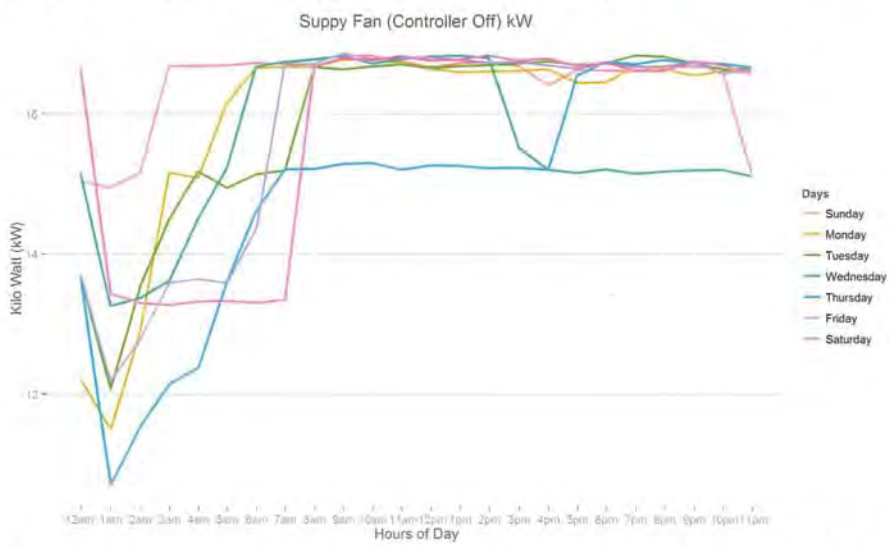

Figure 90: The figure above illustrates the average kWh draw of the supply fan when the controller is OFF for each hour of the day and each day of the week. This is helpful in understanding the operation of the unit throughout the days of the week. It is clear that as the temperature increases throughout the day, so will the kWh draw.

CONFIDENTIAL

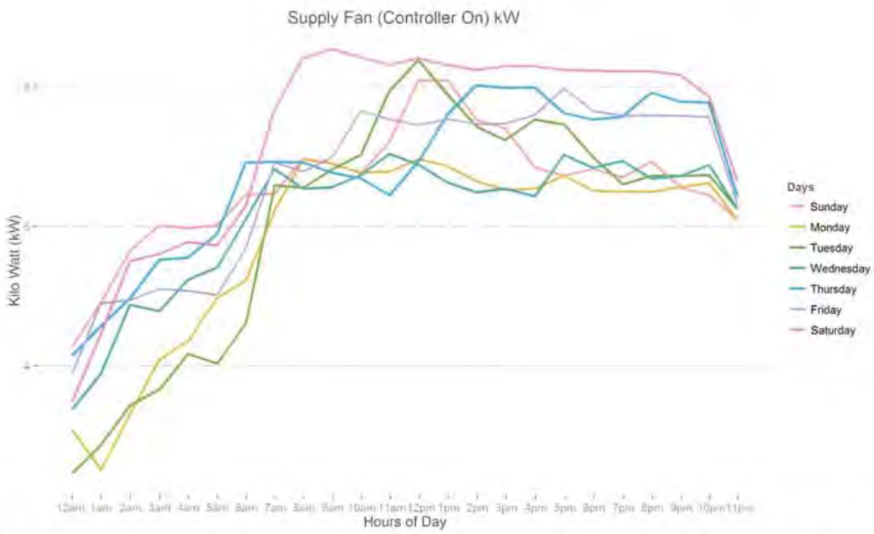

Figure 91: The figure above illustrates the average kWh draw of the supply fan when the controller is ON for each hour of the day and each day of the week. This is helpful in understanding the operation of the unit throughout the days of the week. It is clear that as the temperature increases throughout the day, so will the kWh draw.

Figure 91: From the above plot we can infer comparing with a referential point; here we consider the average savings, how the savings in a specific day of the week and a specific hour of the day varies from the savings reference. We can see from the plot that variation of average hourly kilowatt savings on Sunday (Orange) and Saturday (Purple) are lesser to the average savings comparing with the two extreme weekdays i.e. Tuesday (Sea Green) and Friday (Blue). Which imply savings is inversely proportional to load.

CONFIDENTIAL

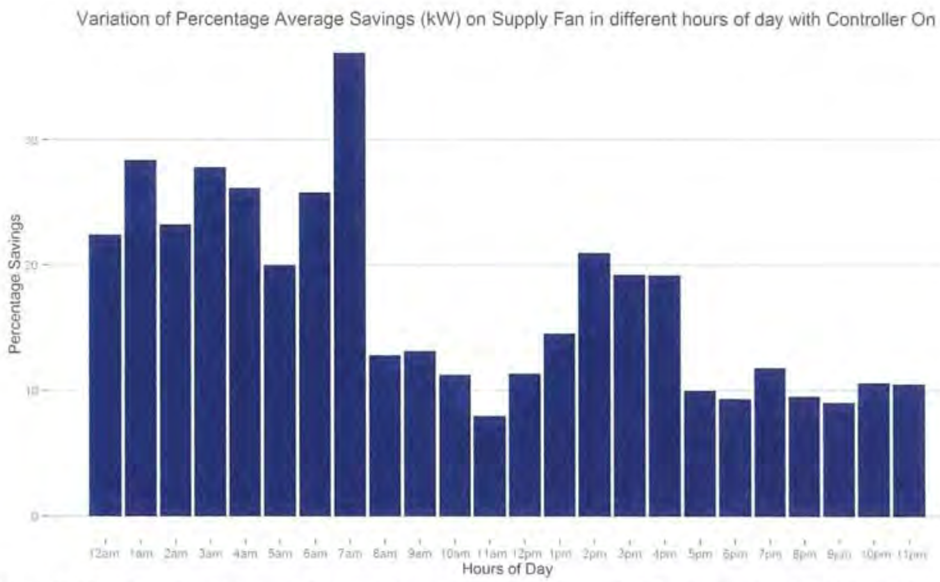

Figure 92: The figure above illustrates the average percent savings of the supply fan throughout the day. As it can be seen, savings are higher during the cooler parts of the day as the VFD is able to slow down he speed of the fan for longer periods of time.

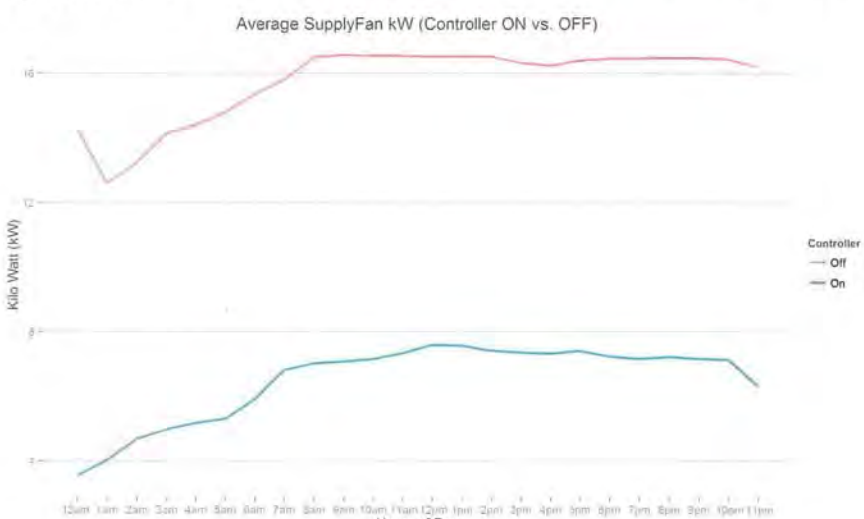

Figure 93: Figure above illustrates that there is a significant reduction in supply fan kWh draw when the controller is ON versus when it is OFF. The kWh draw follows a similar trend throughout the day. This indicates that both control strategies are reacting to the outside temperature and super market occupancy.

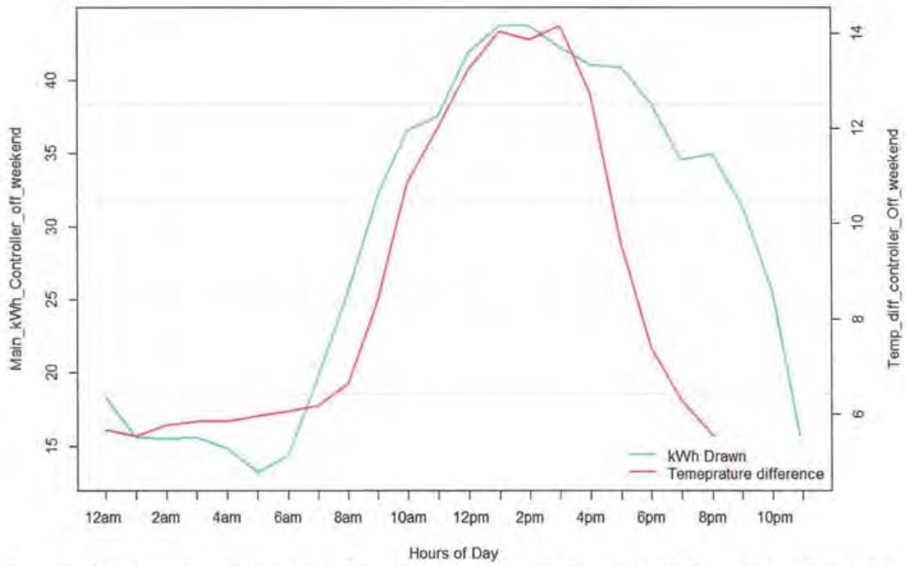

Figure 94: The figure above illustrates the relationship between the main disconnect kWh draw and the indoor and outdoor temperature difference when the controller is OFF for the weekend hours (Saturday and Sunday). As it can be seen, as the temperature difference between indoor and outdoor temperature increased so does the kW consumption of the main disconnect panel. This indicates a high correlation between kW and temperature.

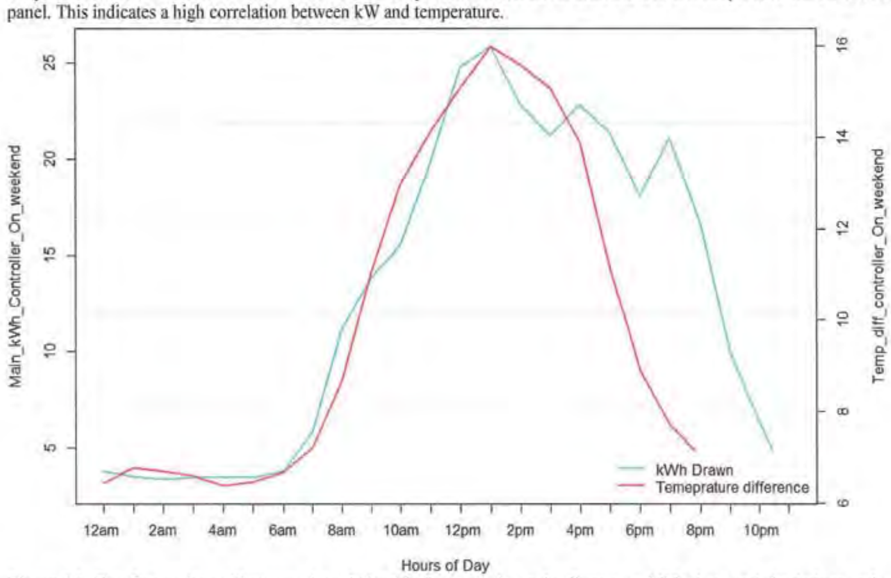

Figure 95: The figure above illustrates the relationship between the main disconnect kWh draw and the indoor and outdoor temperature difference when the controller is ON for the weekend hours (Saturday and Sunday). As it can be seen, as the temperature difference between indoor and outdoor temperature raises so does the kW consumption of the main disconnect panel. This indicates a high correlation between kW and temperature.

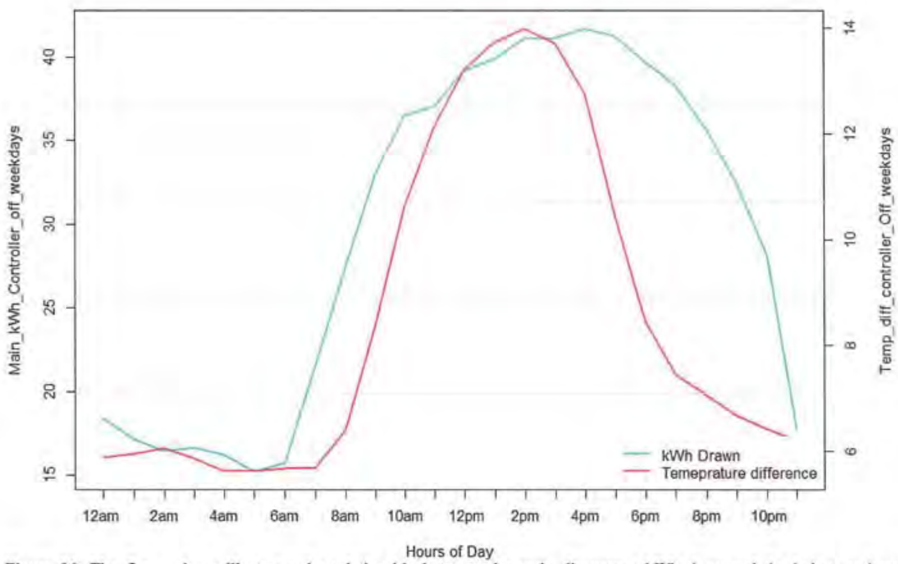

Figure 96: The figure above illustrates the relationship between the main disconnect kWh draw and the indoor and outdoor temperature difference when the controller is OFF for the weekday hours (Monday to Friday). As it can be seen, as the temperature difference between indoor and outdoor temperature increased so does the kW consumption of the main disconnect panel. This indicates a high correlation between kW and temperature.

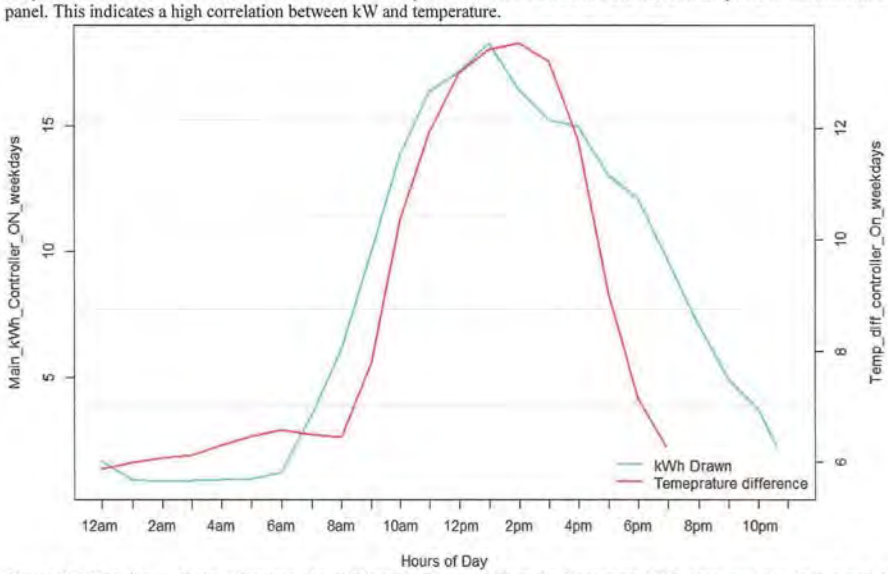

Figure 97: The figure above illustrates the relationship between the main disconnect kWh draw and the indoor and outdoor temperature difference when the controller is ON for the weekday hours (Monday to Friday). As it can be seen, as the temperature difference between indoor and outdoor temperature raises so does the kW consumption of the main disconnect panel. This indicates a high correlation between kW and temperature.

CONFIDENTIAL

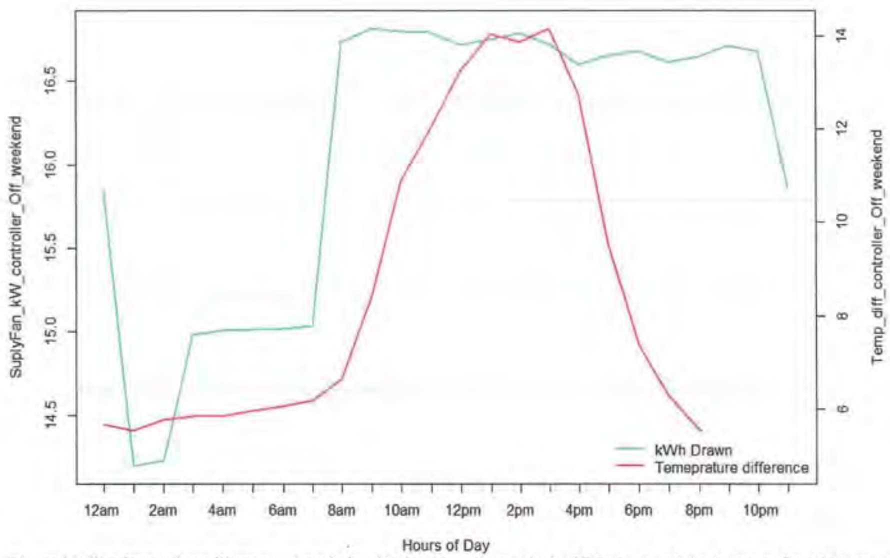

Figure 98: The figure above illustrates the relationship between the supply fan kWh draw and the indoor and outdoor temperature difference when the controller is OFF for the weekend hours (Saturday and Sunday). As it can be seen, as the temperature difference between indoor and outdoor temperature increased so does the kW consumption of the main disconnect panel. This indicates a high correlation between kW and temperature.

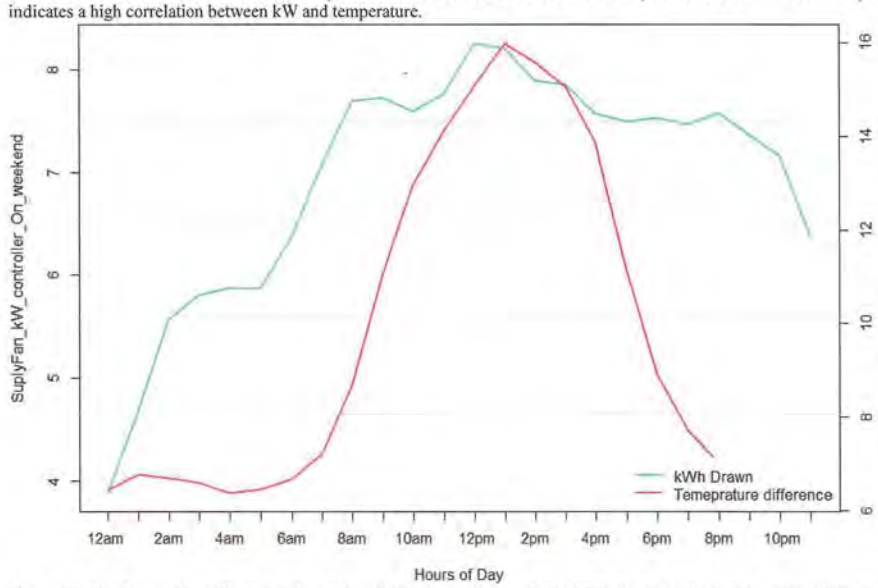

Figure 99: The figure above illustrates the relationship between the supply fan kWh draw and the indoor and outdoor temperature difference when the controller is ON for the weekend hours (Saturday and Sunday). As it can be seen, as the temperature difference between indoor and outdoor temperature raises so does the kW consumption of the main disconnect panel. This indicates a high correlation between kW and temperature.

CONFIDENTIAL

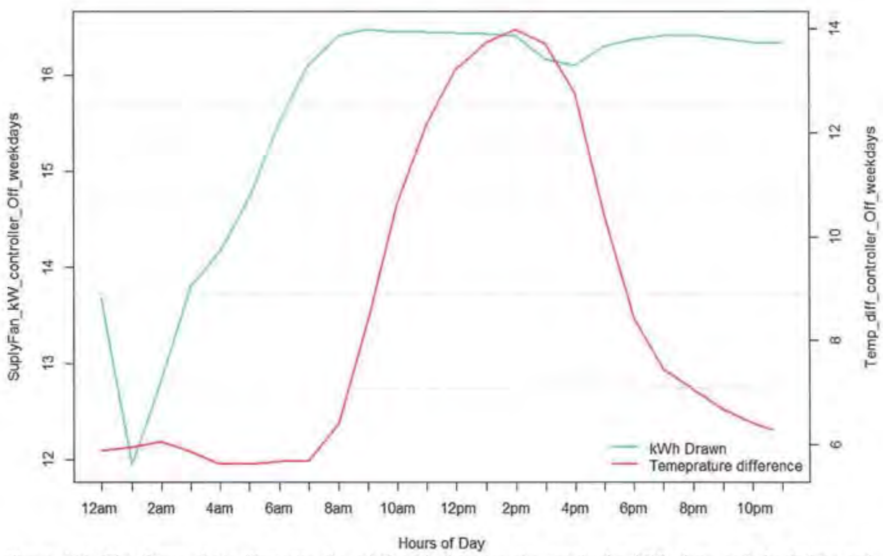

Figure 100: The figure above illustrates the relationship between the supply fan kWh draw and the indoor and outdoor temperature difference when the controller is OFF for the weekday hours (Monday to Friday). As it can be seen, as the temperature difference between indoor and outdoor temperature increased so does the kW consumption of the main disconnect panel. This indicates a high correlation between kW and temperature.

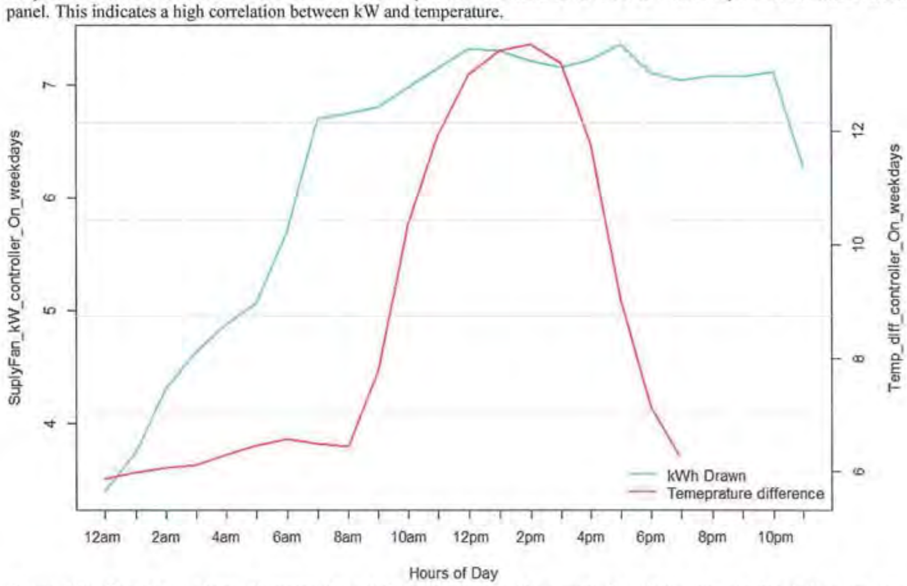

Figure 101: The figure above illustrates the relationship between the supply fan kWh draw and the indoor and outdoor temperature difference when the controller is ON for the weekday hours (Monday to Friday). As it can be seen, as the temperature difference between indoor and outdoor temperature raises so does the kW consumption of the main disconnect panel. This indicates a high correlation between kW and temperature.

Regression Model #13, 14, &15:

The total energy consumption (kWh) of the air conditioning unit (A/C Unit), the four compressors, and the supply fan were respectively analyzed for five months starting 04/01/2015 at 12:00am and ending 10/30/15 at 11:58 pm. ***With unity power factor***.

Model #13: Total Cooling Load Power Consumption Savings

The regression equation to correlate the hourly A/C Unit kWh consumption with the temperature and the [redacted] controller status (whether it's ON or OFF) is as follows:

$$Main\ kWh = \beta_0 + \beta_1 \times Outside\ Temperature + \beta_2 \times Enerfit\ Controller$$

Where:

Main kWh = the hourly power consumption of the air conditioning unit (A/C Unit).

β_0 = the intercept of the regression equation

β_1 = regression coefficient of the model relating the hourly temperature to the hourly kWh

Outside Temperature = hourly outside temperature in $^{\circ}F$

β_2 = regression coefficient of the model relating the hourly kWh consumption to the effect of the [redacted] controller

[redacted] ***Controller*** = a dummy variable that is assigned a value **0** when the [redacted] controller is "OFF" and **1** when the controller is "ON".

First, a best subsets regression was performed in order to determine the number of independent variables to be included in the model (Table 40).

number of Variables	R-Sq	R-Sq(adj)	SE
1	22.52	22.50	27.4896
1	29.38	29.36	26.2449
2	50.45	50.43	21.9854
Response is Main kWh			

The second step performed was to test if the effects of both the outside temperature and the [redacted] controller are statistically significant. An Analysis of Variance (ANOVA) was performed to determine whether the [redacted] controller reduction in the kWh is statistically significant.

Table 14 depicts the ANOVA table obtained. The technique used to perform the ANOVA was the multiple regression procedure.

Table14: Analysis of Variance of Main kWh, using Adjusted SS for Tests

Source	DF	AdjSS	AdjMS	F-Value	P-Value
Regression	2	2526090	1263045	2613.07	0.000
Temp	1	1398571	1398571	2893.46	0.000
Controller	1	1055199	1055199	2183.07	0.000
Error	5133	2481069	483		
Total	5135	5007159			

As shown in Table 14, both the effects of the controller and the outside temperature on the kWh were statistically significant ($P<.001$), meaning that both the ambient temperature and the controller statistically affect the kW consumption.

The next step during the regression analysis was to determine the coefficients corresponding to each independent variable in the governing equation explaining the relationship between the temperature, the controller, and the Main kWh. Table 15 summarizes the coefficients obtained from the regression analysis.

Table 15. Main kWh Regression Analysis coefficients

Term	Coef	SECoef	T-Value	P-Value	VIF
Constant	-205.84	5.08	-40.50	0.000	
Temp	3.2814	0.0610	53.79	0.000	1.00
Controller	-28.684	0.614	-46.72	0.000	1.00

CONFIDENTIAL

Regression Analysis: Main_kwh versus Temp, Controller

Method

Categorical predictor coding (1, 0)

Analysis of Variance

Source	DF	Adj SS	Adj MS	F-Value	P-Value
Regression	2	2526090	1263045	2613.07	0.000
Temp	1	1398571	1398571	2893.46	0.000
Controller	1	1055199	1055199	2183.07	0.000
Error	5133	2481069	483		
Lack-of-Fit	5107	2473175	484	1.60	0.072
Pure Error	26	7894	304		
Total	5135	5007159			

Model Summary

S	R-sq	R-sq(adj)	R-sq(pred)
21.9854	50.45%	50.43%	50.39%

Coefficients

Term	Coef	SE Coef	T-Value	P-Value	VIF
Constant	-205.84	5.08	-40.50	0.000	
Temp	3.2814	0.0610	53.79	0.000	1.00
Controller					
1	-28.684	0.614	-46.72	0.000	1.00

Regression Equation

Controller
0 Main_kW = -205.84 + 3.2814 Temp

1 Main_kW = -234.52 + 3.2814 Temp

Regression Equation including Controller

Main_kWh = -205.84 + 3.2814 Temp - 28.684 Controller

The above equation means that, by controlling for the outside temperature, and by turning the controller ON, a reduction in the kWh of 28.69 kWh occurs.

The average kWh consumption of the Main unit during the OFF periods (where the controller was turned off) is 66.53 kWh. The regression equation indicates that an average reduction of 28.69 kWh is experienced when the controller is turned ON while controlling for the outside temperature. This results in a percentage savings in the baseline kWh (when the controller is

OFF) of 43.12% while maintaining the effect of the outside temperature. Figure displays the box plot distribution for Main kWh when the controller is ON vs. OFF.

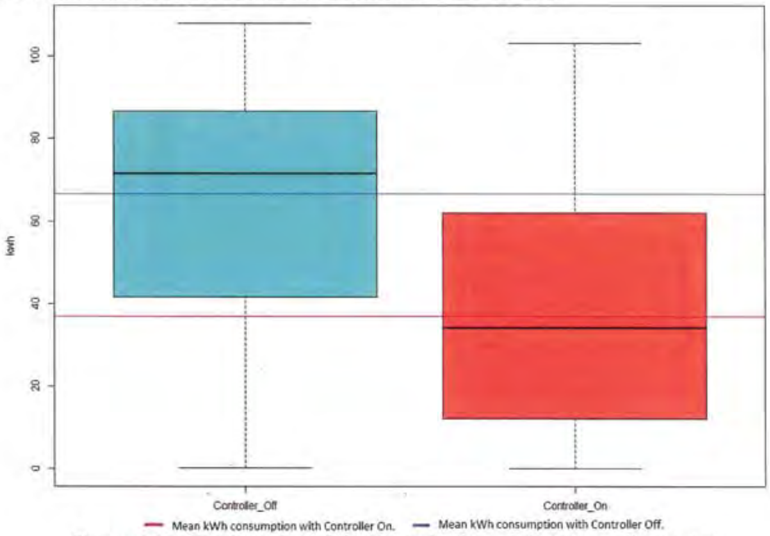

Figure 102: The Box Plot of the Main kWh and the Controller Status.

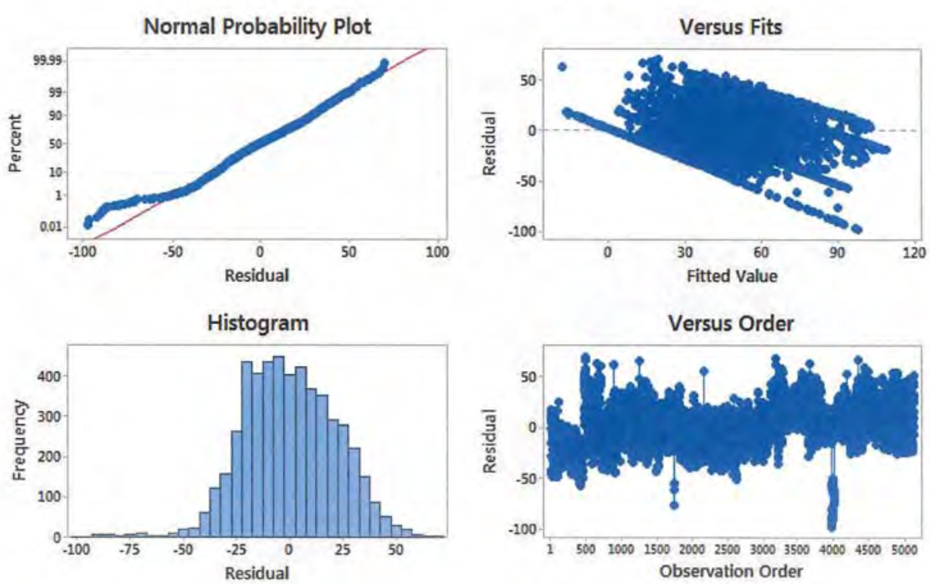

Figure 103: Residual Plots for Main kWh.

Model #14: Compressor Power Consumption Savings

The regression equation to correlate the Compressor kWh consumption with the temperature and the [redacted] controller status (whether it's ON or OFF) is as follows:

$$Compressor\ kWh = \beta_0 + \beta_1 \times Outside\ Temperature + \beta_2 \times [redacted]\ Controller$$

Where:

Compressor kWh = the hourly power consumption due to the four compressors.

β_0 = the intercept of the regression equation

β_1 = regression coefficient of the model relating the hourly temperature to the hourly kWh

Outside Temperature = hourly outside temperature in $^{\circ}$F

β_2 = regression coefficient of the model relating the hourly kWh consumption to the effect of the [redacted] controller

[redacted] ***Controller*** = a dummy variable that is assigned a value **0** when the [redacted] controller is "OFF" and **1** when the controller is "ON".

First, a best subsets regression was performed in order to determine the number of independent variables to be included in the model (Table 43).

number of Variables	R-Sq	R-Sq(adj)	SE
1	11.38	11.36	23.8856
1	35.13	35.12	20.4351
2	45.40	45.38	18.7509
Response is Compressor kWh			

The second step performed was to test if the effects of both the outside temperature and the [redacted] controller are statistically significant. An Analysis of Variance (ANOVA) was performed to determine whether the [redacted] controller reduction in the kWh is statistically significant.

Table 44 depicts the ANOVA table obtained. The technique used to perform the ANOVA was the multiple regression procedure.

Table 44: Analysis of Variance of Main kWh, using Adjusted SS for Tests

Source	DF	AdjSS	AdjMS	F-Value	P-Value
Regression	2	1500428	750214	2133.73	0.000
Temp	1	1124319	1124319	3197.75	0.000
Controller	1	339166	339166	964.65	0.000
Error	5133	1804747	352		
Total	5135	3305175			

As shown in Table 44, both the effects of the controller and the outside temperature on the kWh were statistically significant ($P<.001$), meaning that both the ambient temperature and the controller statistically affect the kW consumption.

The next step during the regression analysis was to determine the coefficients corresponding to each independent variable in the governing equation explaining the relationship between the temperature, the controller, and the Main kWh. Table 45 summarizes the coefficients obtained from the regression analysis.

Table 45. Main kWh Regression Analysis coefficients

Term	Coef	SECoef	T-Value	P-Value	VIF
Constant	-198.39	4.33	-45.77	0.000	
Temp	2.9421	0.0520	56.55	0.000	1.00
Controller	-16.262	0.524	-31.06	0.000	1.00

Regression Analysis: Compressor_kwh versus Temp, Controller

Method

Categorical predictor coding (1, 0)

Analysis of Variance

Source	DF	Adj SS	Adj MS	F-Value	P-Value
Regression	2	1500428	750214	2133.73	0.000
Temp	1	1124319	1124319	3197.75	0.000
Controller	1	339166	339166	964.65	0.000
Error	5133	1804747	352		
Lack-of-Fit	5107	1797393	352	1.24	0.253
Pure Error	26	7355	283		
Total	5135	3305175			

Model Summary

S	R-sq	R-sq(adj)	R-sq(pred)
18.7509	45.40%	45.38%	45.34%

Coefficients

Term	Coef	SE Coef	T-Value	P-Value	VIF
Constant	-198.39	4.33	-45.77	0.000	
Temp	2.9421	0.0520	56.55	0.000	1.00
Controller					
1	-16.262	0.524	-31.06	0.000	1.00

Regression Equation

Controller
0 Compressor_kW = -198.39 + 2.9421 Temp

1 Compressor_kW = -214.65 + 2.9421 Temp
2

Regression Equation including Controller

Compressor_kWh = -198.39 + 2.9421 Temp - 16.262 Controller

The above equation means that, by **controlling for the outside temperature**, and by turning the controller ON, a reduction in the kWh of 16.26 kWh occurs in the compressors.

The average kWh consumption of the four compressors during the OFF periods (where the controller was turned off) is 45.82 kWh. The regression equation indicates that an average reduction of 16.26 kWh is experienced when the controller is turned ON while controlling for the outside temperature. This results in a percentage savings in the baseline kWh (when the

controller is OFF) of 35.49% while maintaining the effect of the outside temperature. Figure displays the box plot distribution for Compressor kWh when the controller is ON vs. OFF.

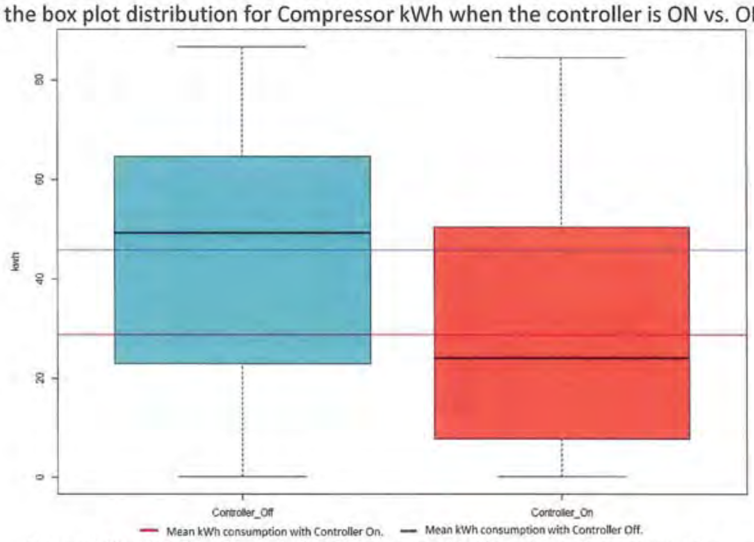

Figure 104: The Box Plot of the Compressor kWh and the Controller Status.

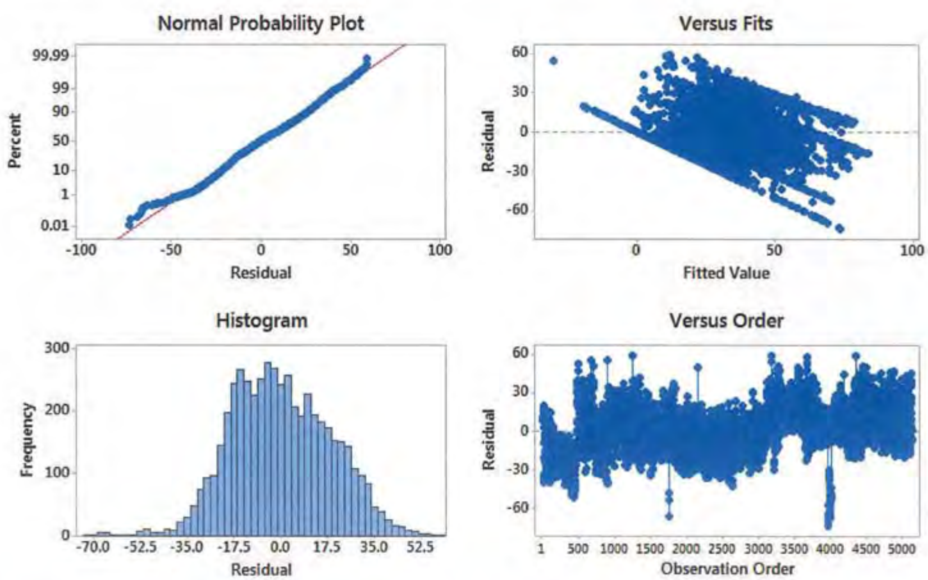

Figure 105: Residual Plots for Compressor kWh

Model #15: Supply Fan Power Consumption Savings

The regression equation to correlate the Supply Fan kWh consumption with the temperature and the [redacted] controller status (whether it's ON or OFF) is as follows:

$$Supply\ Fan\ kWh = \beta_0 + \beta_1 \times Outside\ Temperature + \beta_2 \times Enerfit\ Controller$$

Where:

Supply Fan kWh = the hourly power consumption due to the Supply Fan.

β_0 = the intercept of the regression equation

β_1 = regression coefficient of the model relating the hourly temperature to the hourly kWh

Outside Temperature = hourly outside temperature in °F

β_2 = regression coefficient of the model relating the hourly kWh consumption to the effect of the [redacted] controller

[redacted] ***Controller*** = a dummy variable that is assigned a value **0** when the [redacted] controller is "OFF" and **1** when the controller is "ON".

First, a best subsets regression was performed in order to determine the number of independent variables to be included in the model (Table 46).

number of Variables	R-Sq	R-Sq(adj)	SE
1	78.29	78.29	2.28503
1	0.13	0.11	4.90103
2	78.30	78.29	2.28474
Response is Supply Fan kWh			

The second step performed was to test if the effects of both the outside temperature and the [redacted] controller are statistically significant. An Analysis of Variance (ANOVA) was performed to determine whether the Enerfit controller reduction in the kWh is statistically significant.

Table 47 depicts the ANOVA table obtained. The technique used to perform the ANOVA was the multiple regression procedure.

Table 47: Analysis of Variance of Main kWh, using Adjusted SS for Tests

Source	DF	AdjSS	AdjMS	F-Value	P-Value
Regression	2	96680	48340.0	9260.45	0.000
Temp	1	12	12.1	2.31	0.128
Controller	1	96525	96525	18491.17	0.000
Error	5133	26794	5.2		
Total	5135	123474			

As shown in Table 47, both the effects of the controller and the outside temperature on the kWh were statistically significant (*P*<.001), meaning that both the ambient temperature and the controller statistically affect the kW consumption.

The next step during the regression analysis was to determine the coefficients corresponding to each independent variable in the governing equation explaining the relationship between the temperature, the controller, and the Main kWh. Table 48 summarizes the coefficients obtained from the regression analysis.

Table 48. Main kWh Regression Analysis coefficients

Term	Coef	SECoef	T-Value	P-Value	VIF
Constant	15.217	0.528	28.81	0.000	
Temp	0.00964	0.00634	1.52	0.128	1.00
Controller	-8.6754	0.0638	-135.98	0.000	1.00

Regression Analysis: Supply Fan_kwh versus Temp, Controller

Method

Categorical predictor coding (1, 0)

Analysis of Variance

Source	DF	Adj SS	Adj MS	F-Value	P-Value
Regression	2	96680	48340.0	9260.45	0.000
Temp	1	12	12.1	2.31	0.128
Controller	1	96525	96524.7	18491.17	0.000
Error	5133	26794	5.2		
Lack-of-Fit	5107	26745	5.2	2.77	0.001
Pure Error	26	49	1.9		
Total	5135	123474			

Model Summary

S	R-sq	R-sq(adj)	R-sq(pred)
2.28474	78.30%	78.29%	78.27%

Coefficients

Term	Coef	SE Coef	T-Value	P-Value	VIF
Constant	15.217	0.528	28.81	0.000	
Temp	0.00964	0.00634	1.52	0.128	1.00
Controller					
1	-8.6754	0.0638	-135.98	0.000	1.00

Regression Equation

Controller
0 SupplyFan_kW = 15.217 + 0.00964 Temp

1 SupplyFan_kW = 6.542 + 0.00964 Temp
2

Regression Equation including Controller

SupplyFan_kWh = 15.217 + 0.00964 Temp - 8.6754 Controller

The above equation means that, by **controlling for the outside temperature**, and by turning the controller ON, a reduction in the kWh of 8.68 kWh occurs in the compressors.

The average kWh consumption of the Supply Fan during the OFF periods (where the controller was turned off) is 16.01 kWh. The regression equation indicates that an average reduction of 8.68 kWh is experienced when the controller is turned ON while controlling for the outside temperature. This results in a percentage savings in the baseline kWh (when the controller is

OFF) of 54.22% while maintaining the effect of the outside temperature. Figure 7 displays the box plot distribution for Supply Fan kWh when the controller is ON vs. OFF.

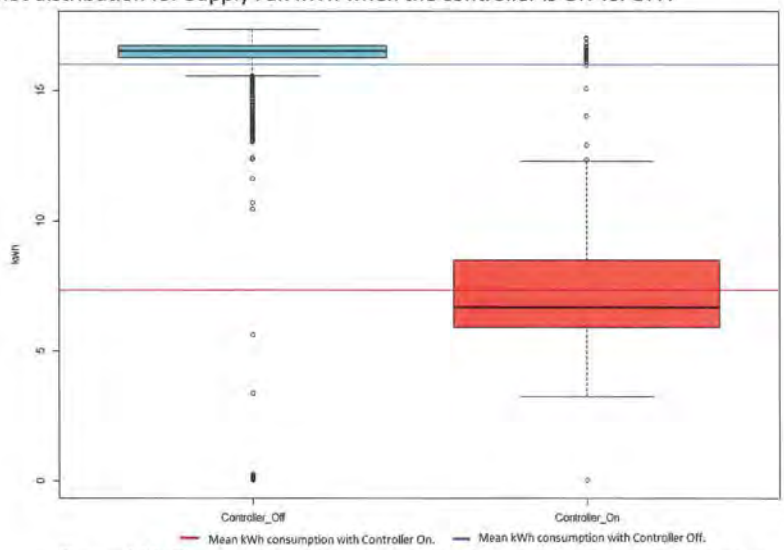

Figure 106: The Box Plot of the Supply Fan kWh and the Controller Status.

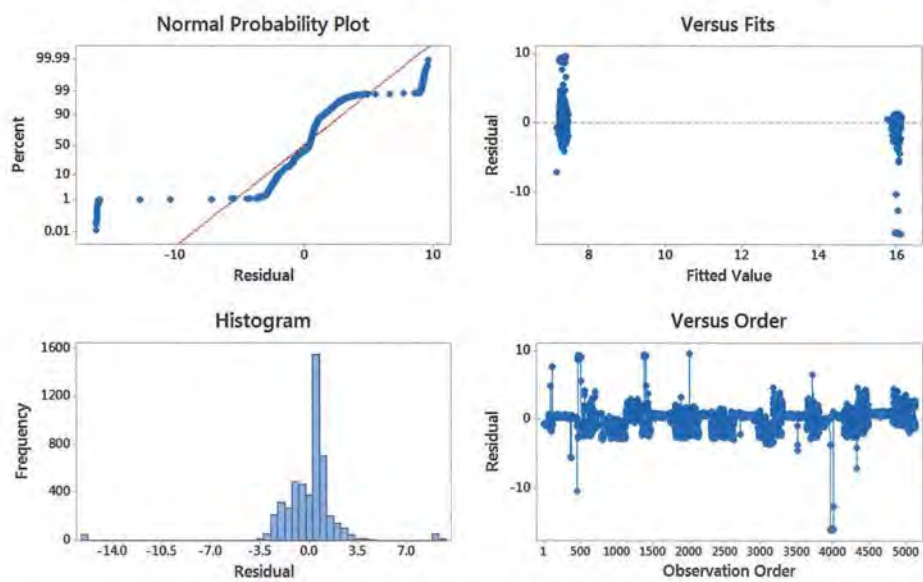

Figure 107: Residual Plots for Supply Fan kWh

Summary (April 15'- October 15') with Unity Power Factor

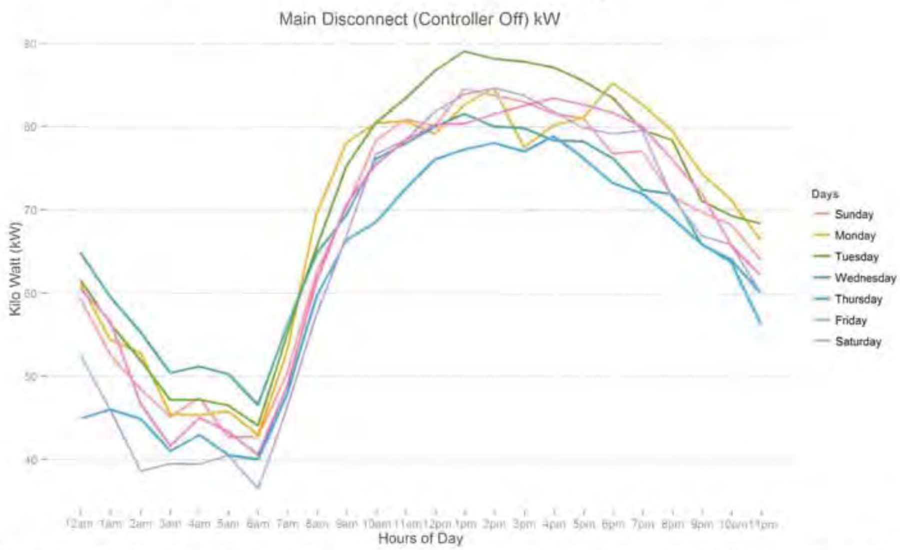

Figure 108: The figure above illustrates the average kWh draw of the main disconnect when the controller is OFF for each hour of the day and each day of the week. This is helpful in understanding the operation of the unit throughout the days of the week. It is clear that as the temperature increases throughout the day, so will the kWh draw.

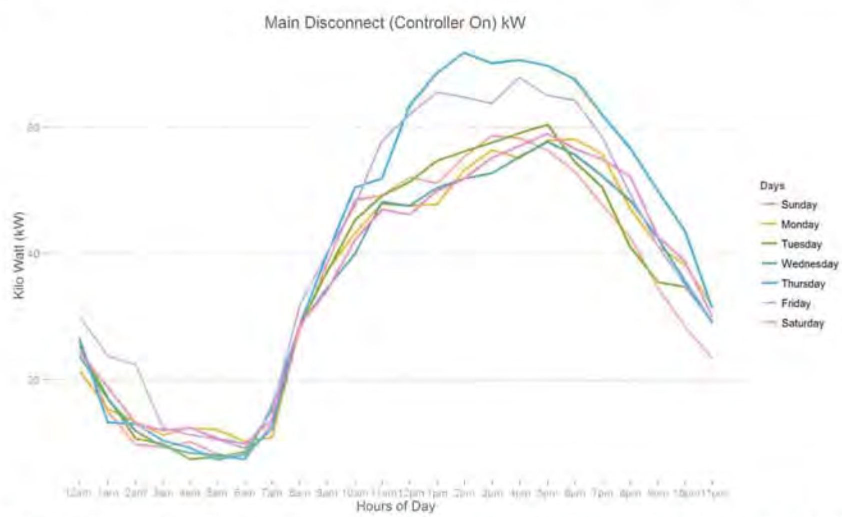

Figure109: The figure above illustrates the average kWh draw of the main disconnect when the controller is ON for each hour of the day and each day of the week. This is helpful in understanding the operation of the unit throughout the days of the week. It is clear that as the temperature increases throughout the day, so will the kWh draw.

CONFIDENTIAL

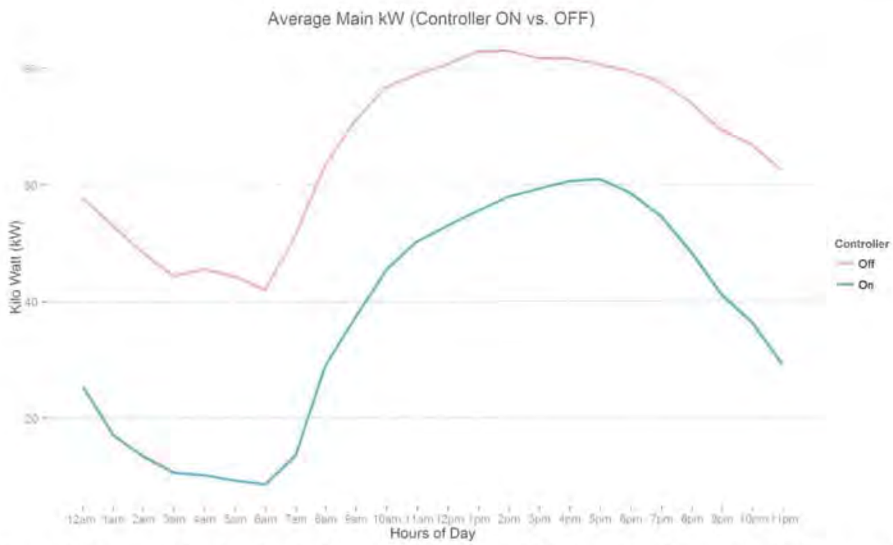

Figure 110: Illustrates that there is a significant reduction in main kWh draw when the controller is ON versus when it is OFF. The kWh draw follows a similar trend throughout the day. This indicates that both control strategies are reacting to the outside temperature and super market occupancy.

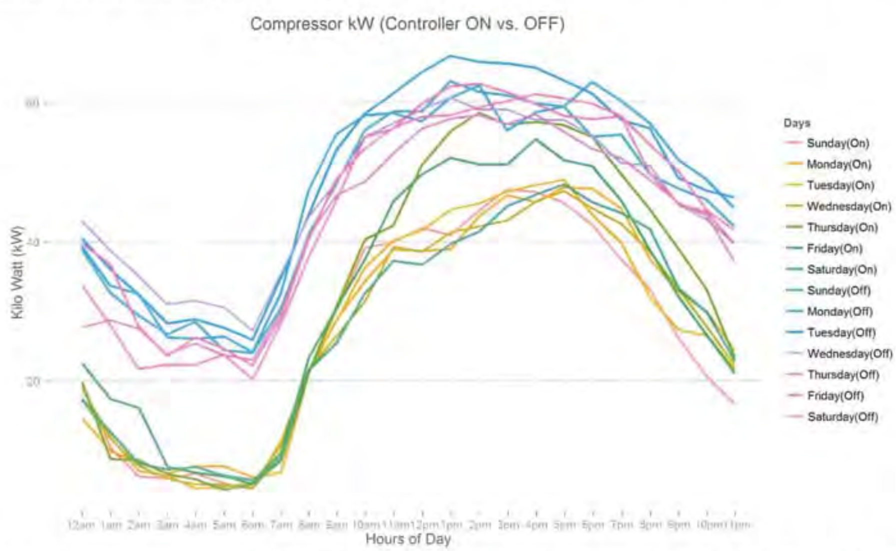

Figure 111: The figure above illustrates the average kWh draw of the compressors when the controller is ON and OFF for each hour of the day and each day of the week. This is helpful in understanding the operation of the unit throughout the days of the week. It is clear that as the temperature increases throughout the day, so will the kWh draw.

CONFIDENTIAL

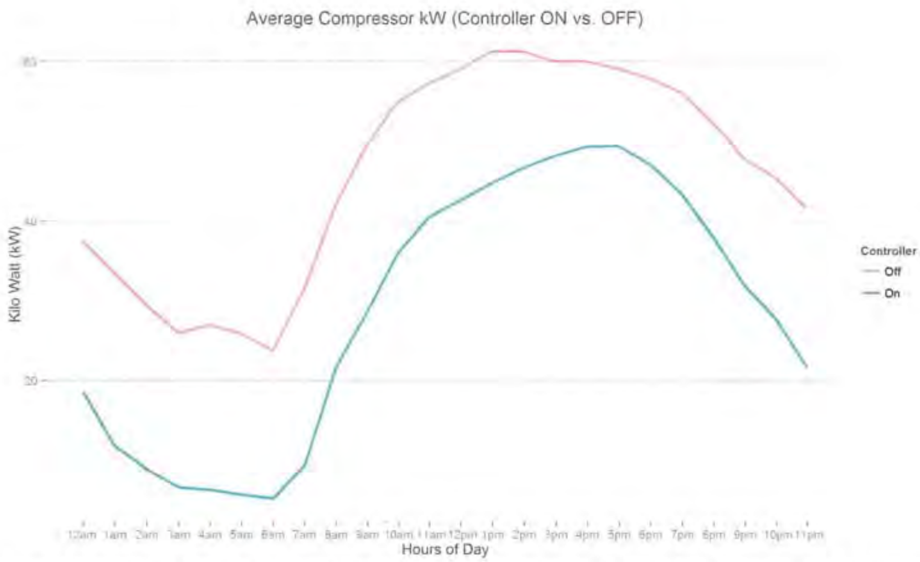

Figure 112: Fig above that there is a significant reduction in compressor kWh draw when the controller is ON versus when it is OFF. The kWh draw follows a similar trend throughout the day. This indicates that both control strategies are reacting to the outside temperature and super market occupancy.

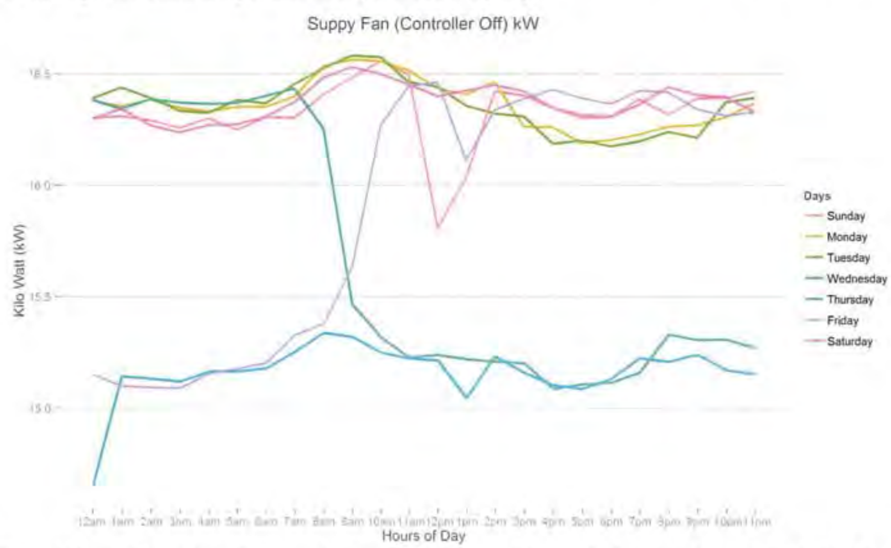

Figure 113: The figure above illustrates the average kWh draw of the supply fan when the controller is OFF for each hour of the day and each day of the week. This is helpful in understanding the operation of the unit throughout the days of the week. It is clear that as the temperature increases throughout the day, so will the kWh draw.

Figure 114: The figure above illustrates the average kWh draw of the supply fan when the controller is ON for each hour of the day and each day of the week. This is helpful in understanding the operation of the unit throughout the days of the week. It is clear that as the temperature increases throughout the day, so will the kWh draw.

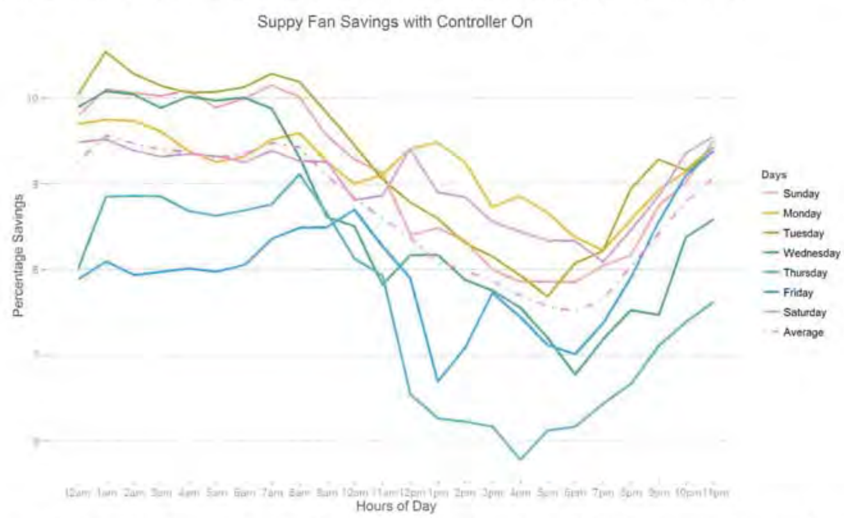

Figure 115: From the above plot we can infer comparing with a referential point; here we consider the average savings, how the savings in a specific day of the week and a specific hour of the day varies from the savings reference. We can see from the plot that variation of average hourly kilowatt savings on Sunday (Orange) and Saturday (Purple) are lesser to the average savings comparing with the two extreme weekdays i.e. Tuesday (Sea Green) and Friday (Blue). Which imply savings is inversely proportional to load.

CONFIDENTIAL

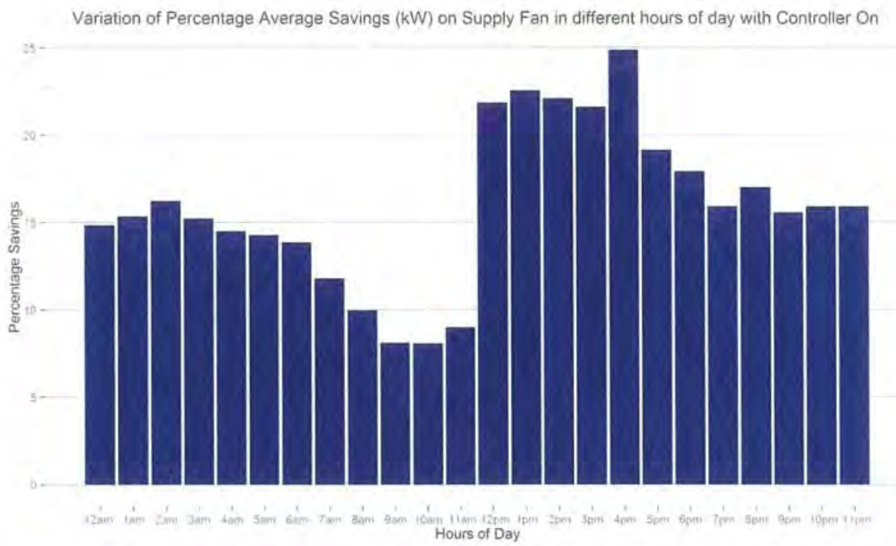

Figure 116: The figure above illustrates the average percent savings of the supply fan throughout the day. As it can be seen, savings are higher during the cooler parts of the day as the VFD is able to slow down he speed of the fan for longer periods of time.

Figure 117: Figure above illustrates that there is a significant reduction in supply fan kWh draw when the controller is ON versus when it is OFF. The kWh draw follows a similar trend throughout the day. This indicates that both control strategies are reacting to the outside temperature and super market occupancy.

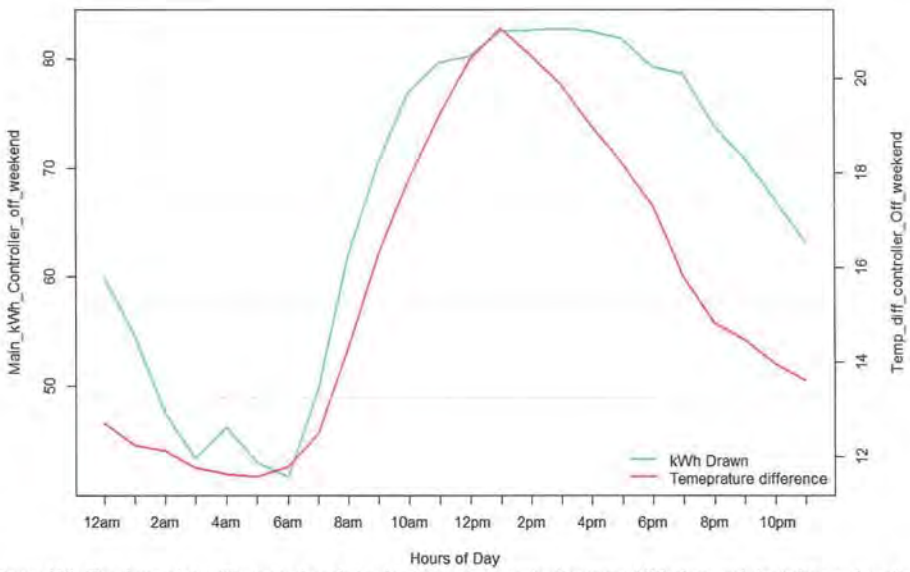

Figure 118: The figure above illustrates the relationship between the main disconnect kWh draw and the indoor and outdoor temperature difference when the controller is OFF for the weekend hours (Saturday and Sunday). As it can be seen, as the temperature difference between indoor and outdoor temperature increased so does the kW consumption of the main disconnect panel. This indicates a high correlation between kW and temperature.

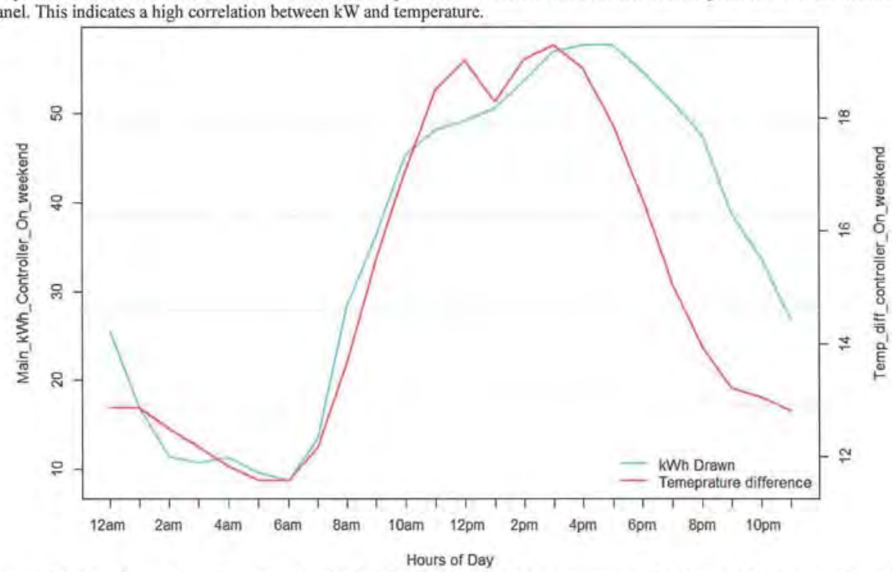

Figure 119: The figure above illustrates the relationship between the main disconnect kWh draw and the indoor and outdoor temperature difference when the controller is ON for the weekend hours (Saturday and Sunday). As it can be seen, as the temperature difference between indoor and outdoor temperature raises so does the kW consumption of the main disconnect panel. This indicates a high correlation between kW and temperature.

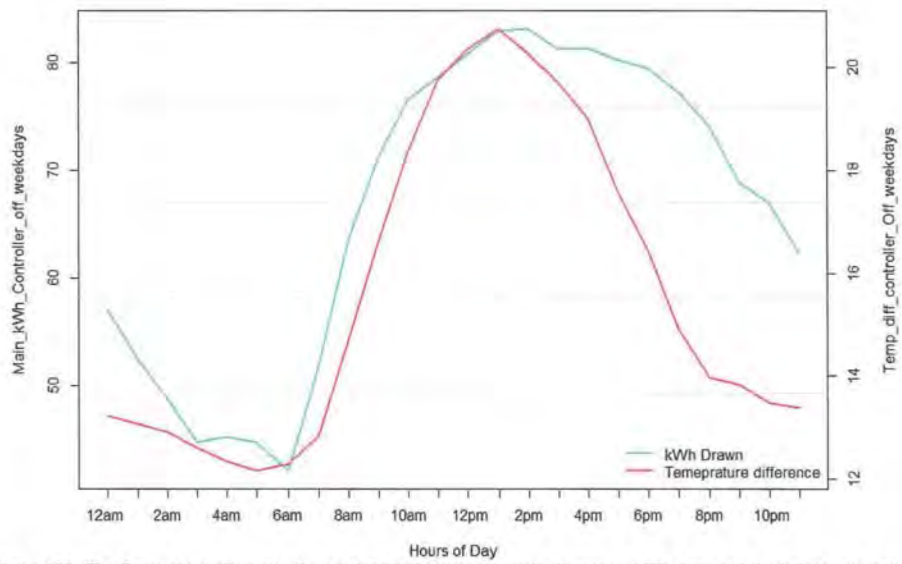

Figure 120: The figure above illustrates the relationship between the main disconnect kWh draw and the indoor and outdoor temperature difference when the controller is OFF for the weekday hours (Monday to Friday). As it can be seen, as the temperature difference between indoor and outdoor temperature increased so does the kW consumption of the main disconnect panel. This indicates a high correlation between kW and temperature.

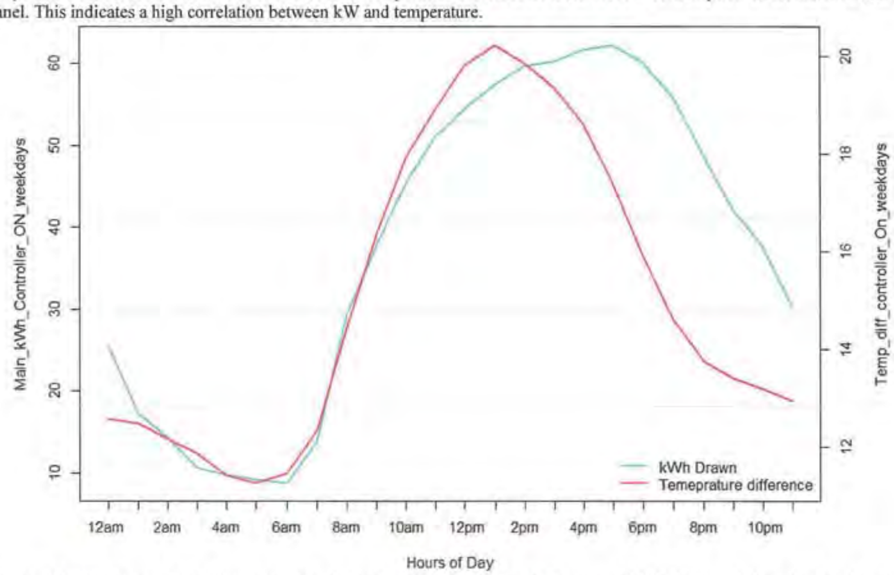

Figure 121: The figure above illustrates the relationship between the main disconnect kWh draw and the indoor and outdoor temperature difference when the controller is ON for the weekday hours (Monday to Friday). As it can be seen, as the temperature difference between indoor and outdoor temperature raises so does the kW consumption of the main disconnect panel. This indicates a high correlation between kW and temperature.

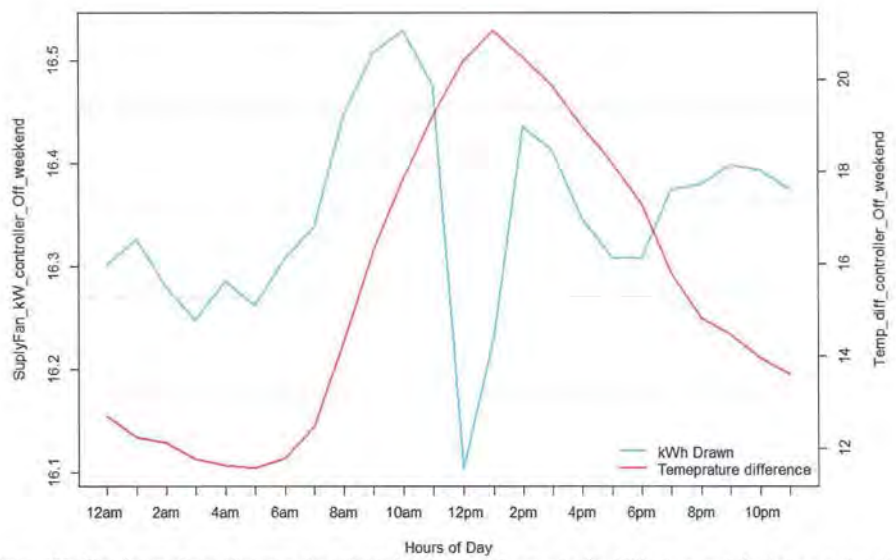

Figure 122: The figure above illustrates the relationship between the supply fan kWh draw and the indoor and outdoor temperature difference when the controller is OFF for the weekend hours (Saturday and Sunday). As it can be seen, as the temperature difference between indoor and outdoor temperature increased so does the kW consumption of the main disconnect panel. This indicates a high correlation between kW and temperature.

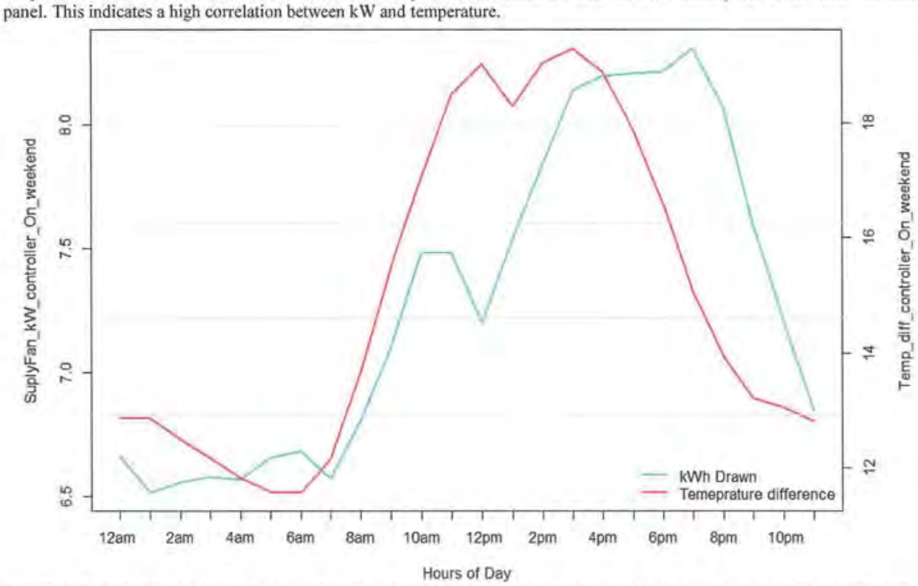

Figure 123: The figure above illustrates the relationship between the supply fan kWh draw and the indoor and outdoor temperature difference when the controller is ON for the weekend hours (Saturday and Sunday). As it can be seen, as the temperature difference between indoor and outdoor temperature raises so does the kW consumption of the main disconnect panel. This indicates a high correlation between kW and temperature.

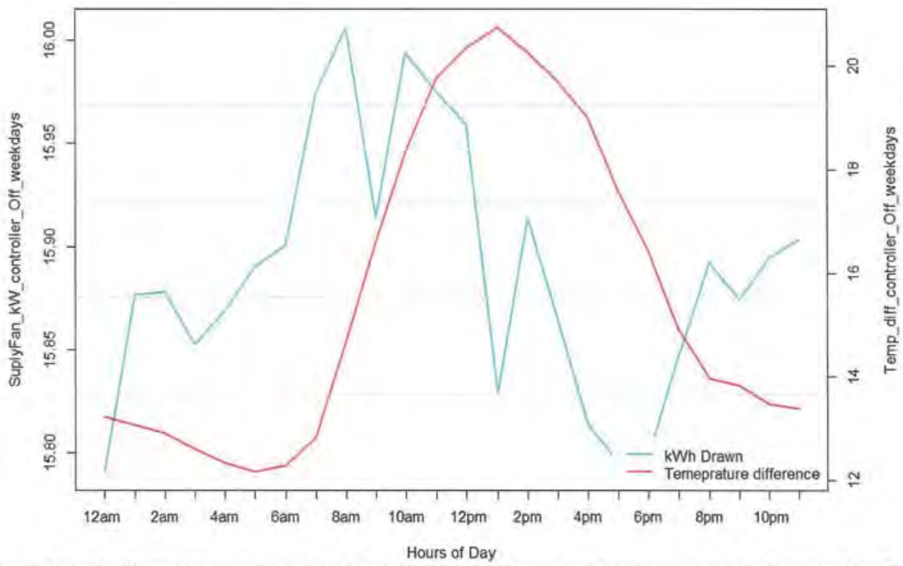

Figure 124: The figure above illustrates the relationship between the supply fan kWh draw and the indoor and outdoor temperature difference when the controller is OFF for the weekday hours (Monday to Friday). As it can be seen, as the temperature difference between indoor and outdoor temperature increased so does the kW consumption of the main disconnect panel. This indicates a high correlation between kW and temperature.

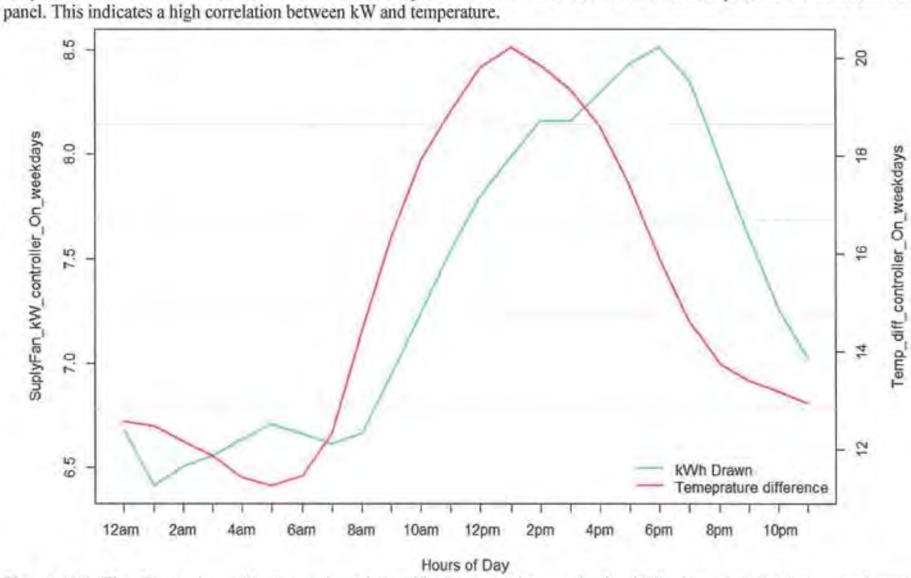

Figure 125: The figure above illustrates the relationship between the supply fan kWh draw and the indoor and outdoor temperature difference when the controller is ON for the weekday hours (Monday to Friday). As it can be seen, as the temperature difference between indoor and outdoor temperature raises so does the kW consumption of the main disconnect panel. This indicates a high correlation between kW and temperature.

Regression Model #16, 17, &18:

The total energy consumption (kWh) of the air conditioning unit (A/C Unit), the four compressors, and the supply fan were respectively analyzed for the entire year starting 11/01/2014 at 12:00am and ending 10/30/15 at 11:58 pm. ***With unity power factor.***

Model #16: Total Cooling Load Power Consumption Savings

The regression equation to correlate the hourly A/C Unit kWh consumption with the temperature and the [redacted] controller status (whether it's ON or OFF) is as follows:

$$\boldsymbol{Main\ kWh = \beta_0 + \beta_1 \times Outside\ Temperature + \beta_2 \times Enerfit\ Controller}$$

Where:

Main kWh = the hourly power consumption of the air conditioning unit (A/C Unit).

β_0 = the intercept of the regression equation

β_1 = regression coefficient of the model relating the hourly temperature to the hourly kWh

Outside Temperature = hourly outside temperature in $^{\circ}$F

β_2 = regression coefficient of the model relating the hourly kWh consumption to the effect of the [redacted] controller

[redacted] ***Controller*** = a dummy variable that is assigned a value **0** when the [redacted] controller is "OFF" and **1** when the controller is "ON".

First, a best subsets regression was performed in order to determine the number of independent variables to be included in the model (Table 49).

number of Variables	R-Sq	R-Sq(adj)	SE
1	15.41	15.40	29.6438
1	40.18	40.17	24.9287
2	55.25	55.24	21.5611
Response is Main kWh			

The second step performed was to test if the effects of both the outside temperature and the [redacted] controller are statistically significant. An Analysis of Variance (ANOVA) was performed to determine whether the [redacted] controller reduction in the kWh is statistically significant.

Table 50 depicts the ANOVA table obtained. The technique used to perform the ANOVA was the multiple regression procedure.

Table 50: Analysis of Variance of Main kWh, using Adjusted SS for Tests

Source	DF	AdjSS	AdjMS	F-Value	P-Value
Regression	2	5026763	2513382	5406.50	0.000
Temp	1	3625174	3625174	7798.05	0.000
Controller	1	1371591	1371591	2950.41	0.000
Error	8757	4070970	465		
Total	8759	9097733			

As shown in Table 50, both the effects of the controller and the outside temperature on the kWh were statistically significant ($P<.001$), meaning that both the ambient temperature and the controller statistically affect the kW consumption.

The next step during the regression analysis was to determine the coefficients corresponding to each independent variable in the governing equation explaining the relationship between the temperature, the controller, and the Main kWh. Table 51 summarizes the coefficients obtained from the regression analysis.

Table 51. Main kWh Regression Analysis coefficients

Term	Coef	SECoef	T-Value	P-Value	VIF
Constant	-143.45	2.23	-64.46	0.000	
Temp	2.4693	0.0280	88.31	0.000	1.00
Controller	-25.028	0.461	-54.32	0.000	1.00

CONFIDENTIAL

Regression Analysis: Main_kwh versus Temp, Controller

Method

Categorical predictor coding (1, 0)

Analysis of Variance

Source	DF	Adj SS	Adj MS	F-Value	P-Value
Regression	2	5026763	2513382	5406.50	0.000
Temp	1	3625174	3625174	7798.05	0.000
Controller	1	1371591	1371591	2950.41	0.000
Error	8757	4070970	465		
Lack-of-Fit	8685	4046379	466	1.36	0.044
Pure Error	72	24592	342		
Total	8759	9097733			

Model Summary

S	R-sq	R-sq(adj)	R-sq(pred)
21.5611	55.25%	55.24%	55.22%

Coefficients

Term	Coef	SE Coef	T-Value	P-Value	VIF
Constant	-143.45	2.23	-64.46	0.000	
Temp	2.4693	0.0280	88.31	0.000	1.00
Controller					
1	-25.028	0.461	-54.32	0.000	1.00

Regression Equation

Controller	
0	Main_kW = -143.45 + 2.4693 Temp
1	Main_kW = -168.48 + 2.4693 Temp

Regression Equation including Controller

Main_kWh = -143.45 + 2.4693 Temp - 25.028 Controller

The above equation means that, by controlling for the outside temperature, and by turning the controller ON, a reduction in the kWh of 25.03 kWh occurs.

The average kWh consumption of the Main unit during the OFF periods (where the controller was turned off) is 50.94 kWh. The regression equation indicates that an average reduction of 25.03 kWh is experienced when the controller is turned ON while controlling for the outside temperature. This results in a percentage savings in the baseline kWh (when the controller is

OFF) of 49.14% while maintaining the effect of the outside temperature. Figure displays the box plot distribution for Main kWh when the controller is ON vs. OFF.

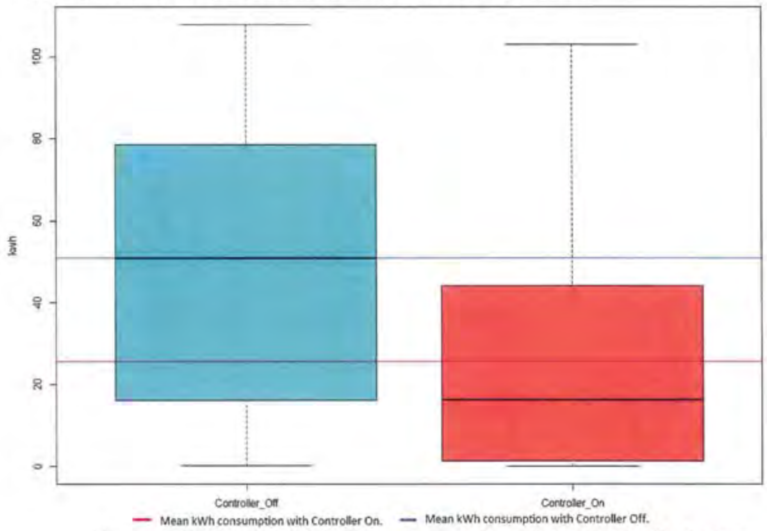

Figure 126: The Box Plot of the Main kWh and the Controller Status.

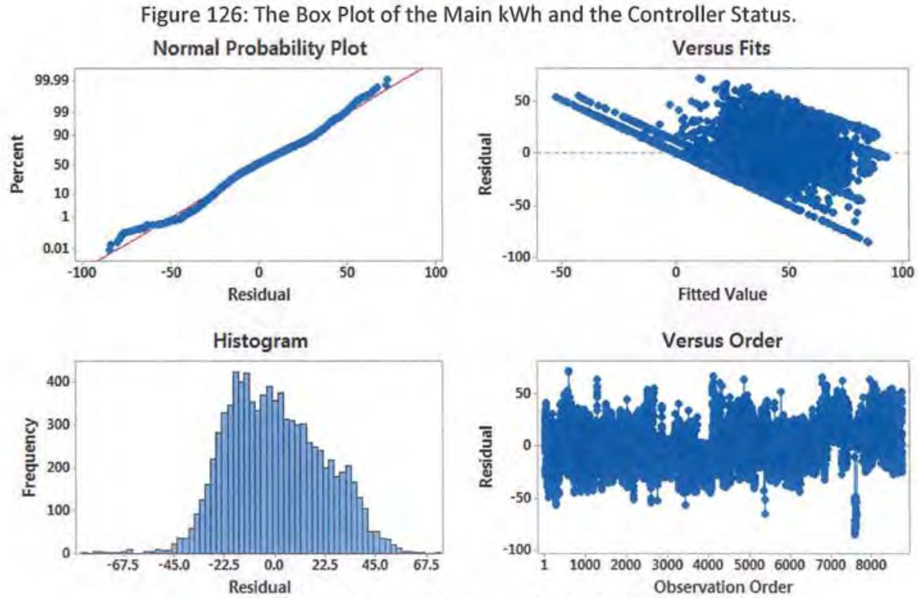

Figure 127: Residual Plots for Main kWh.

Model #17: Compressor Power Consumption Savings

The regression equation to correlate the Compressor kWh consumption with the temperature and the [redacted] controller status (whether it's ON or OFF) is as follows:

$$\textit{Compressor kWh} = \beta_0 + \beta_1 \times \textit{Outside Temperature} + \beta_2 \times \text{[redacted]}\ \textit{Controller}$$

Where:

Compressor kWh = the hourly power consumption due to the four compressors.

β_0 = the intercept of the regression equation

β_1 = regression coefficient of the model relating the hourly temperature to the hourly kWh

Outside Temperature = hourly outside temperature in °F

β_2 = regression coefficient of the model relating the hourly kWh consumption to the effect of the [redacted] controller

[redacted] ***Controller*** = a dummy variable that is assigned a value **0** when the [redacted] controller is "OFF" and **1** when the controller is "ON".

First, a best subsets regression was performed in order to determine the number of independent variables to be included in the model (Table 52).

number of Variables	R-Sq	R-Sq(adj)	SE
1	6.04	6.03	24.4551
1	41.59	41.58	19.2824
2	47.42	47.41	18.2954
Response is Compressor kWh			

The second step performed was to test if the effects of both the outside temperature and the [redacted] controller are statistically significant. An Analysis of Variance (ANOVA) was performed to determine whether the [redacted] controller reduction in the kWh is statistically significant.

Table 53 depicts the ANOVA table obtained. The technique used to perform the ANOVA was the multiple regression procedure.

Table 53: Analysis of Variance of Main kWh, using Adjusted SS for Tests

Source	DF	AdjSS	AdjMS	F-Value	P-Value
Regression	2	2643456	1321728	3948.76	0.000
Temp	1	2306580	2306580	6891.07	0.000
Controller	1	325194	325194	971.54	0.000
Error	8757	2931143	335		
Total	8759	5574599			

As shown in Table 53, both the effects of the controller and the outside temperature on the kWh were statistically significant ($P<.001$), meaning that both the ambient temperature and the controller statistically affect the kW consumption.

The next step during the regression analysis was to determine the coefficients corresponding to each independent variable in the governing equation explaining the relationship between the temperature, the controller, and the Main kWh. Table 54 summarizes the coefficients obtained from the regression analysis.

Table 54. Main kWh Regression Analysis coefficients

Term	Coef	SECoef	T-Value	P-Value	VIF
Constant	-122.36	1.89	-64.79	0.000	
Temp	1.9696	0.0237	83.01	0.000	1.00
Controller	-12.187	0.391	-31.17	0.000	1.00

CONFIDENTIAL

Regression Analysis: Compressor_kwh versus Temp, Controller

Method

Categorical predictor coding (1, 0)

Analysis of Variance

Source	DF	Adj SS	Adj MS	F-Value	P-Value
Regression	2	2643456	1321728	3948.76	0.000
Temp	1	2306580	2306580	6891.07	0.000
Controller	1	325194	325194	971.54	0.000
Error	8757	2931143	335		
Lack-of-Fit	8685	2915852	336	1.58	0.006
Pure Error	72	15292	212		
Total	8759	5574599			

Model Summary

S	R-sq	R-sq(adj)	R-sq(pred)
18.2954	47.42%	47.41%	47.38%

Coefficients

Term	Coef	SE Coef	T-Value	P-Value	VIF
Constant	-122.36	1.89	-64.79	0.000	
Temp	1.9696	0.0237	83.01	0.000	1.00
Controller					
1	-12.187	0.391	-31.17	0.000	1.00

Regression Equation

Controller

0 Compressor_kW = -122.36 + 1.9696 Temp

1 Compressor_kW = -134.54 + 1.9696 Temp

Regression Equation including Controller

Compressor_kWh = -122.36 + 1.9696 Temp - 12.187 Controller

The above equation means that, by **controlling for the outside temperature**, and by turning the controller ON, a reduction in the kWh of 12.19 kWh occurs in the compressors. The average kWh consumption of the four compressors during the OFF periods (where the controller was turned off) is 32.70 kWh. The regression equation indicates that an average reduction of 12.19 kWh is experienced when the controller is turned ON while controlling for the outside temperature. This results in a percentage savings in the baseline kWh (when the controller is

CONFIDENTIAL

OFF) of 37.28% while maintaining the effect of the outside temperature. Figure displays the box plot distribution for Compressor kWh when the controller is ON vs. OFF.

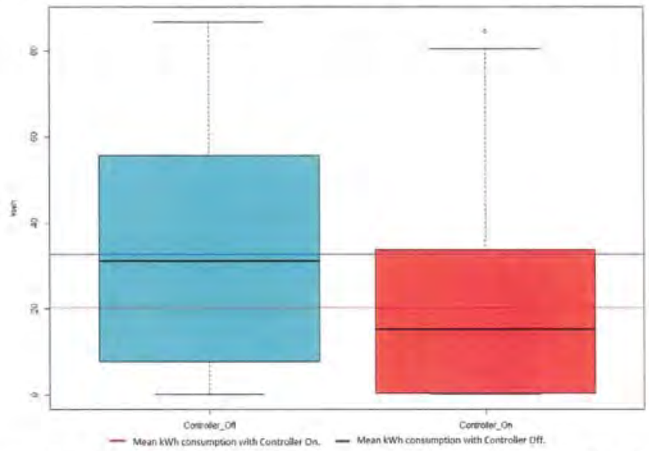

Figure 128: The Box Plot of the Compressor kWh and the Controller Status.

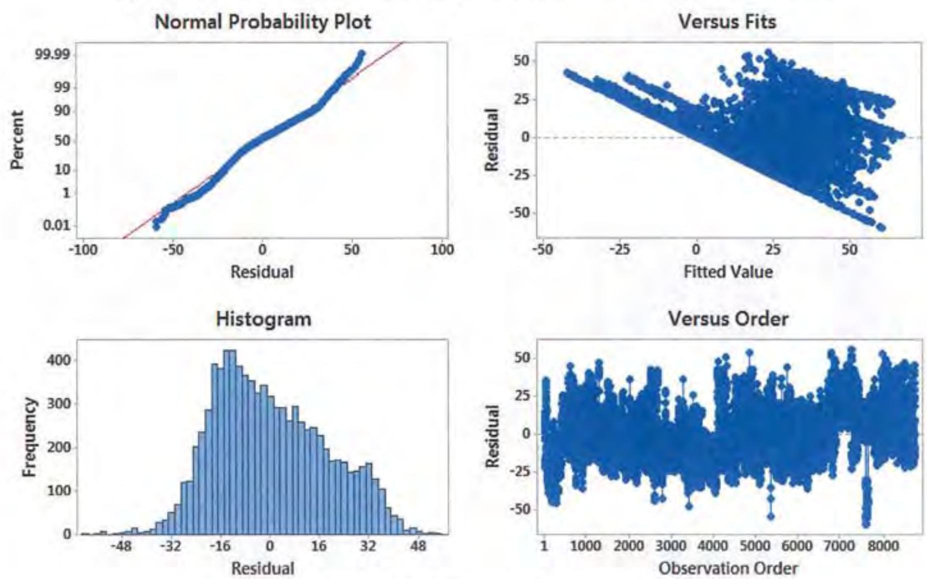

Figure 129: Residual Plots for Compressor kWh

Model #18: Supply Fan Power Consumption Savings

The regression equation to correlate the Supply Fan kWh consumption with the temperature and the [redacted] controller status (whether it's ON or OFF) is as follows:

$$Supply\ Fan\ kWh = \beta_0 + \beta_1 \times Outside\ Temperature + \beta_2 \times \text{[redacted]}\ Controller$$

Where:

Supply Fan kWh = the hourly power consumption due to the Supply Fan.

β_0 = the intercept of the regression equation

β_1 = regression coefficient of the model relating the hourly temperature to the hourly kWh

Outside Temperature = hourly outside temperature in °F

β_2 = regression coefficient of the model relating the hourly kWh consumption to the effect of the [redacted] controller

[redacted] ***Controller*** = a dummy variable that is assigned a value **0** when the [redacted] controller is "OFF" and **1** when the controller is "ON".

First, a best subsets regression was performed in order to determine the number of independent variables to be included in the model (Table 55).

number of Variables	R-Sq	R-Sq(adj)	SE
1	71.18	71.17	2.83294
1	0.38	0.37	5.26671
2	71.49	71.49	2.81752
Response is Supply Fan kWh			

The second step performed was to test if the effects of both the outside temperature and the [redacted] controller are statistically significant. An Analysis of Variance (ANOVA) was performed to determine whether the [redacted] controller reduction in the kWh is statistically significant.

Table 56 depicts the ANOVA table obtained. The technique used to perform the ANOVA was the multiple regression procedure.

Table 56: Analysis of Variance of Main kWh, using Adjusted SS for Tests

Source	DF	AdjSS	AdjMS	F-Value	P-Value
Regression	2	174348	87174	10981.27	0.000
Temp	1	771	771	97.12	0.000
Controller	1	173415	173415	21844.98	0.000
Error	8757	69517	8		
Total	8759	243865			

As shown in Table 56, both the effects of the controller and the outside temperature on the kWh were statistically significant ($P<.001$), meaning that both the ambient temperature and the controller statistically affect the kW consumption.

The next step during the regression analysis was to determine the coefficients corresponding to each independent variable in the governing equation explaining the relationship between the temperature, the controller, and the Main kWh. Table 57 summarizes the coefficients obtained from the regression analysis.

Table 57. Main kWh Regression Analysis coefficients

Term	Coef	SECoef	T-Value	P-Value	VIF
Constant	13.067	0.291	44.93	0.000	
Temp	0.03601	0.00365	9.86	0.000	1.00
Controller	-8.8992	0.0602	-147.80	0.000	1.00

CONFIDENTIAL

Regression Analysis: Supply Fan_kwh versus Temp, Controller

Method

Categorical predictor coding (1, 0)

Analysis of Variance

Source	DF	Adj SS	Adj MS	F-Value	P-Value
Regression	2	174348	87174	10981.27	0.000
Temp	1	771	771	97.12	0.000
Controller	1	173415	173415	21844.98	0.000
Error	8757	69517	8		
Lack-of-Fit	8685	68825	8	0.82	0.894
Pure Error	72	692	10		
Total	8759	243865			

Model Summary

S	R-sq	R-sq(adj)	R-sq(pred)
2.81752	71.49%	71.49%	71.47%

Coefficients

Term	Coef	SE Coef	T-Value	P-Value	VIF
Constant	13.067	0.291	44.93	0.000	
Temp	0.03601	0.00365	9.86	0.000	1.00
Controller					
1	-8.8992	0.0602	-147.80	0.000	1.00

Regression Equation

Controller	
0	SupplyFan_kW = 13.067 + 0.03601 Temp
1	SupplyFan_kW = 4.167 + 0.03601 Temp

Regression Equation including Controller

SupplyFan_kWh = 13.067 + 0.03601 Temp - 8.8992 Controller

The above equation means that, by **controlling for the outside temperature**, and by turning the controller ON, a reduction in the kWh of 8.89 kWh occurs in the compressors.

The average kWh consumption of the Supply Fan during the OFF periods (where the controller was turned off) is 15.90 kWh. The regression equation indicates that an average reduction of 8.89 kWh is experienced when the controller is turned ON while controlling for the outside temperature. This results in a percentage savings in the baseline kWh (when the controller is

OFF) of 56.0% while maintaining the effect of the outside temperature. Figure 7 displays the box plot distribution for Supply Fan kWh when the controller is ON vs. OFF.

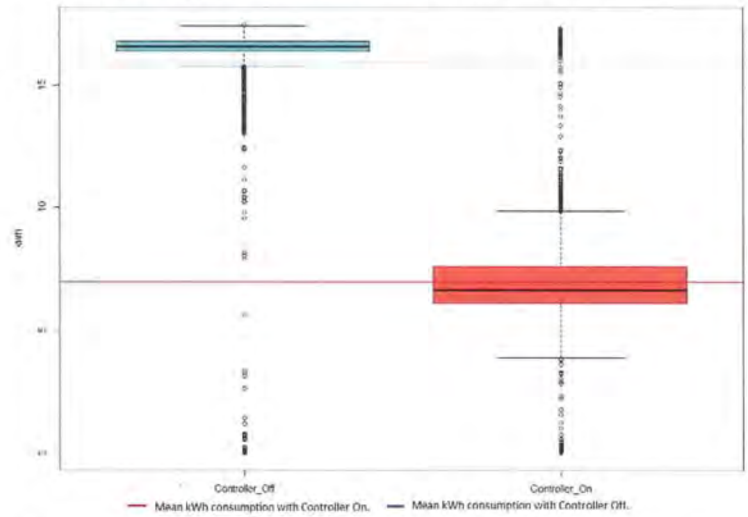

Figure 130: The Box Plot of the Supply Fan kWh and the Controller Status.

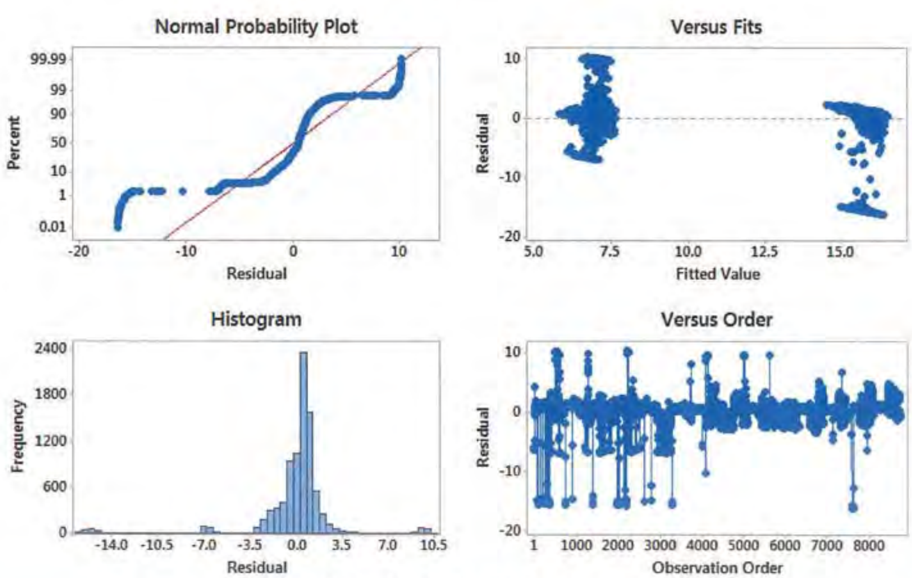

Figure 131: Residual Plots for Supply Fan kWh

Combined (November 14' –October 15') with Unity Power Factor

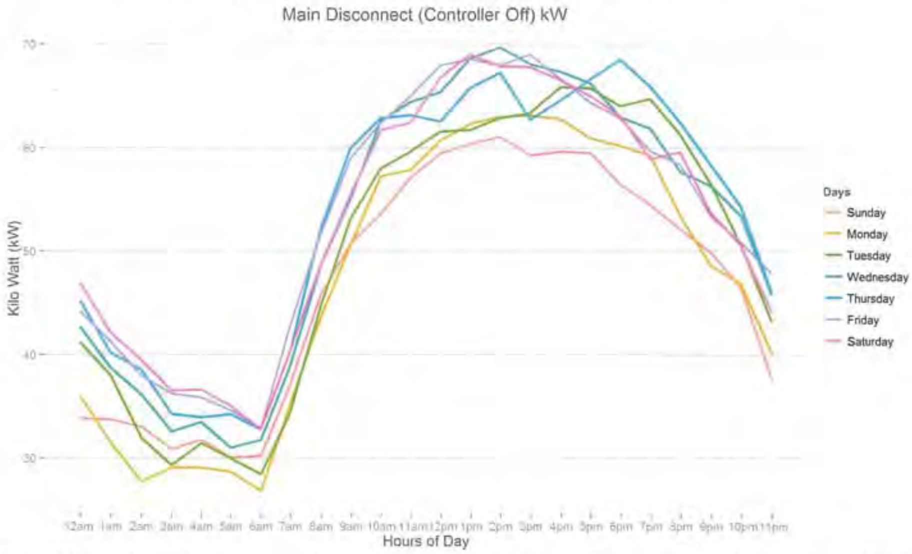

Figure132: The figure above illustrates the average kWh draw of the main disconnect when the controller is OFF for each hour of the day and each day of the week. This is helpful in understanding the operation of the unit throughout the days of the week. It is clear that as the temperature increases throughout the day, so will the kWh draw.

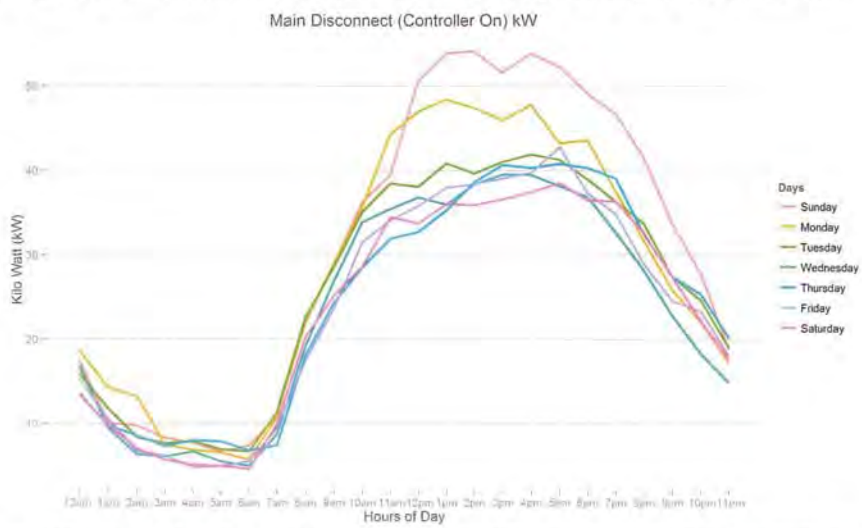

Figure 133: The figure above illustrates the average kWh draw of the main disconnect when the controller is ON for each hour of the day and each day of the week. This is helpful in understanding the operation of the unit throughout the days of the week. It is clear that as the temperature increases throughout the day, so will the kWh draw.

CONFIDENTIAL

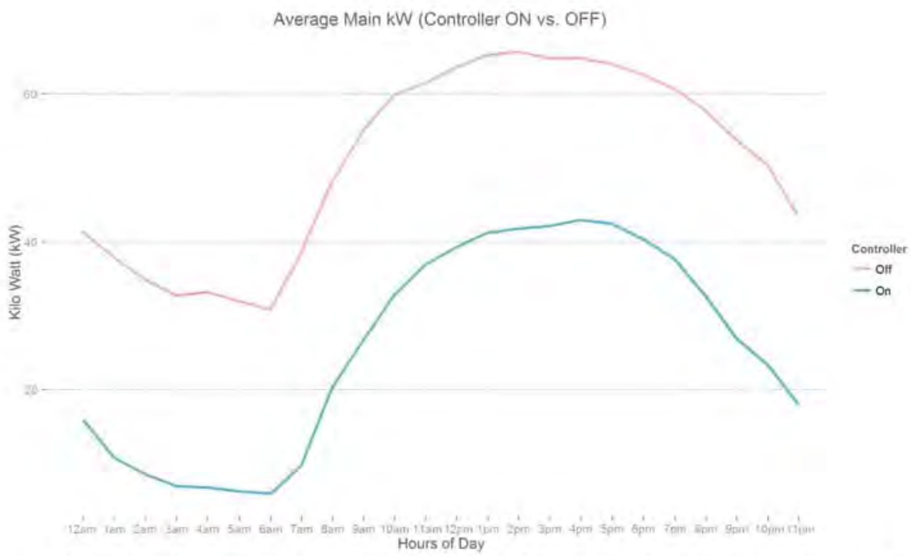

Figure 134: The plot above illustrates that there is a significant reduction in main kWh draw when the controller is ON versus when it is OFF. The kWh draw follows a similar trend throughout the day. This indicates that both control strategies are reacting to the outside temperature and super market occupancy.

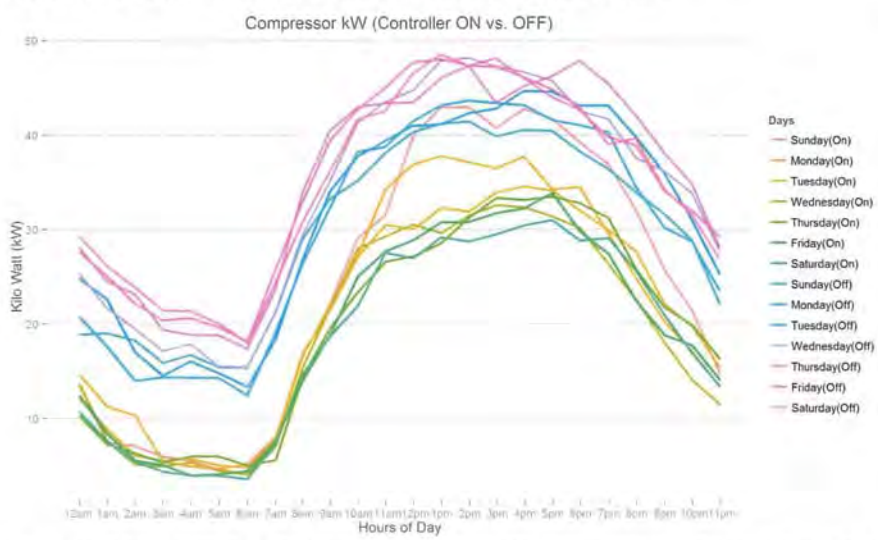

Figure 135: The figure above illustrates the average kWh draw of the compressors when the controller is ON and OFF for each hour of the day and each day of the week. This is helpful in understanding the operation of the unit throughout the days of the week. It is clear that as the temperature increases throughout the day, so will the kWh draw.

CONFIDENTIAL

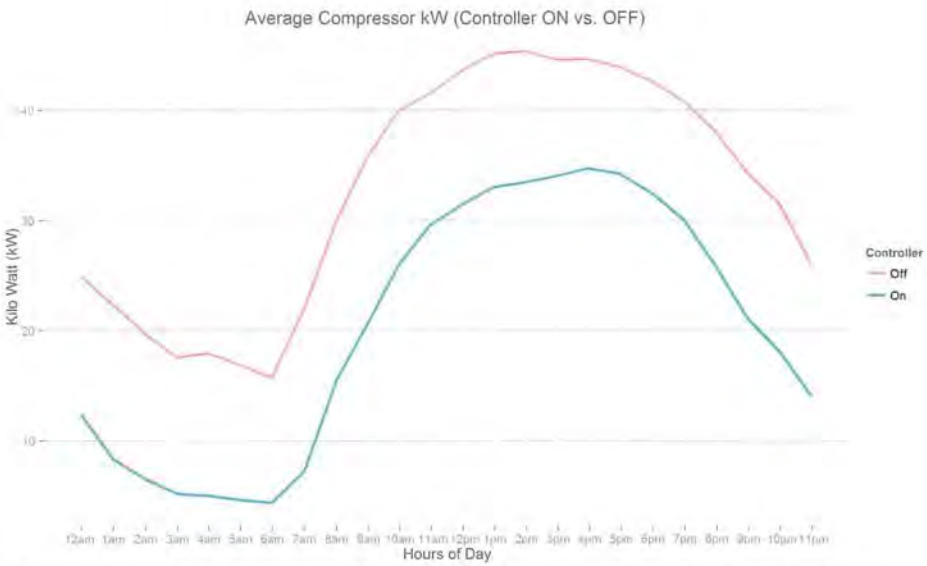

Figure 136: The figure above shows that there is a significant reduction in compressor kWh draw when the controller is ON versus when it is OFF. The kWh draw follows a similar trend throughout the day. This indicates that both control strategies are reacting to the outside temperature and super market occupancy.

Figure 137: The figure above illustrates the average kWh draw of the supply fan when the controller is OFF for each hour of the day and each day of the week. This is helpful in understanding the operation of the unit throughout the days of the week. It is clear that as the temperature increases throughout the day, so will the kWh draw.

CONFIDENTIAL

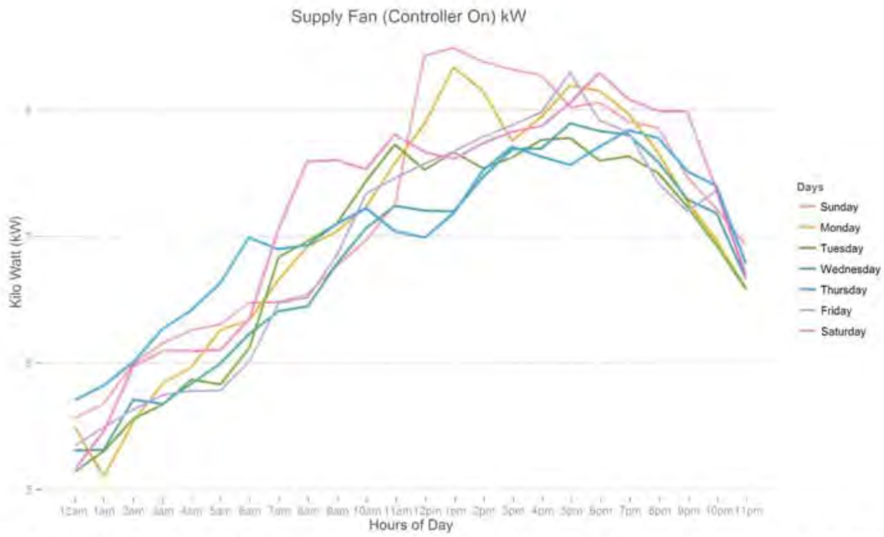

Figure 138: The figure above illustrates the average kWh draw of the supply fan when the controller is ON for each hour of the day and each day of the week. This is helpful in understanding the operation of the unit throughout the days of the week. It is clear that as the temperature increases throughout the day, so will the kWh draw.

Figure 139: From the above plot we can infer comparing with a referential point; here we consider the average savings, how the savings in a specific day of the week and a specific hour of the day varies from the savings reference. We can see from the plot that variation of average hourly kilowatt savings on Sunday (Orange) and Saturday (Purple) are lesser to the average savings comparing with the two extreme weekdays i.e. Tuesday (Sea Green) and Friday (Blue). Which imply savings is inversely proportional to load.

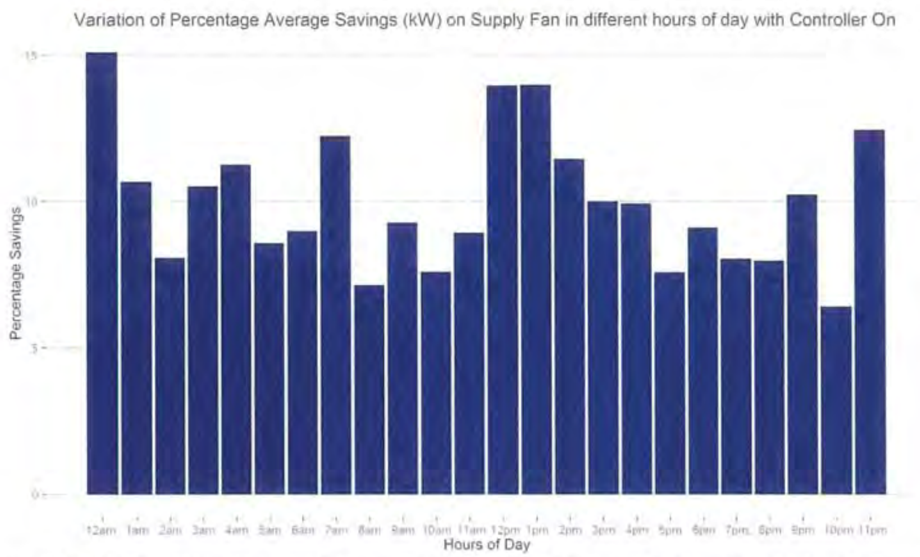

Figure 140: The figure above illustrates the average percent savings of the supply fan throughout the day. As it can be seen, savings are higher during the cooler parts of the day as the VFD is able to slow down he speed of the fan for longer periods of time.

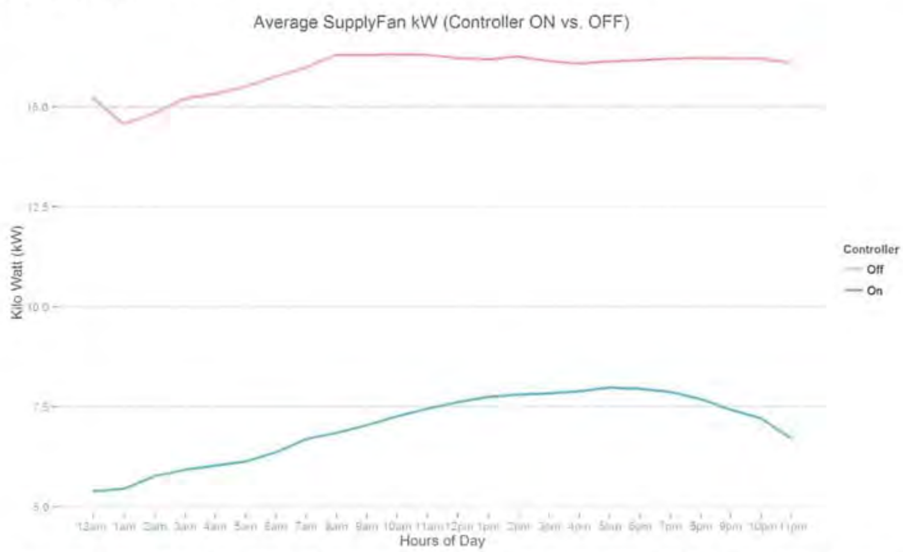

Figure 141: Figure above illustrates that there is a significant reduction in supply fan kWh draw when the controller is ON versus when it is OFF. The kWh draw follows a similar trend throughout the day. This indicates that both control strategies are reacting to the outside temperature and super market occupancy.

CONFIDENTIAL

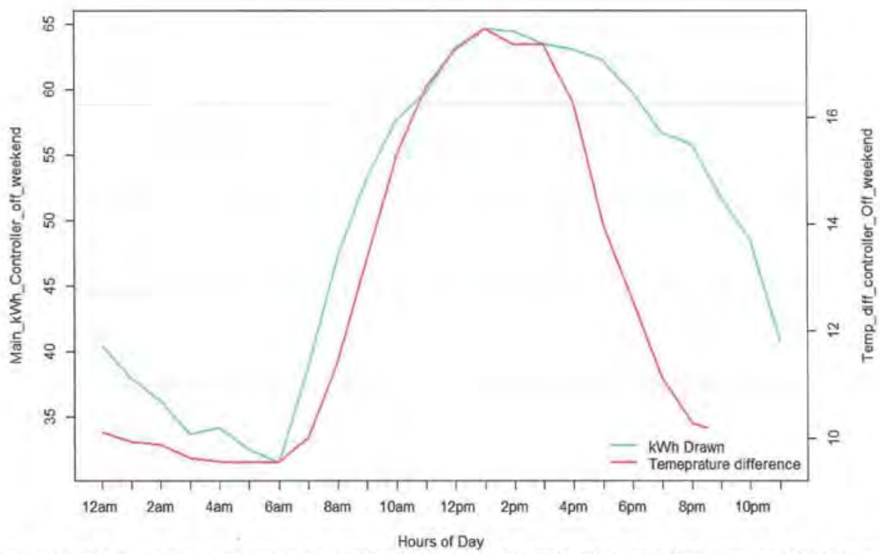

Figure 142: The figure above illustrates the relationship between the main disconnect kWh draw and the indoor and outdoor temperature difference when the controller is OFF for the weekend hours (Saturday and Sunday). As it can be seen, as the temperature difference between indoor and outdoor temperature increased so does the kW consumption of the main disconnect panel. This indicates a high correlation between kW and temperature.

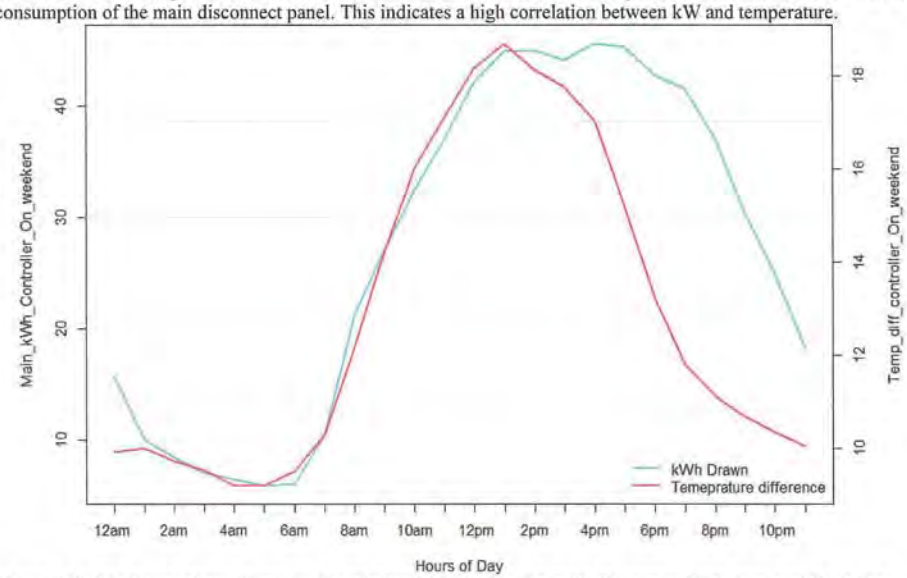

Figure 143: The figure above illustrates the relationship between the main disconnect kWh draw and the indoor and outdoor temperature difference when the controller is ON for the weekend hours (Saturday and Sunday). As it can be seen, as the temperature difference between indoor and outdoor temperature raises so does the kW consumption of the main disconnect panel. This indicates a high correlation between kW and temperature.

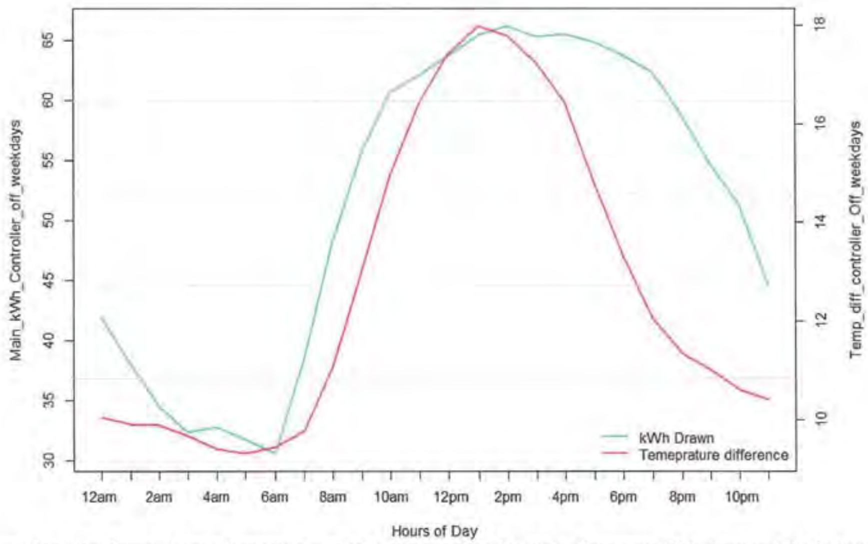

Figure 144: The figure above illustrates the relationship between the main disconnect kWh draw and the indoor and outdoor temperature difference when the controller is OFF for the weekday hours (Monday to Friday). As it can be seen, as the temperature difference between indoor and outdoor temperature increased so does the kW consumption of the main disconnect panel. This indicates a high correlation between kW and temperature.

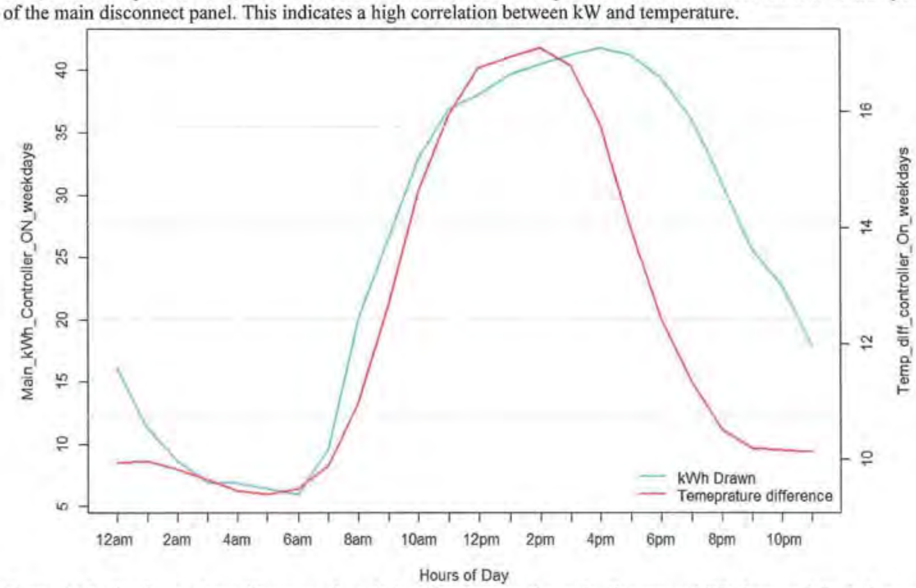

Figure 145: The figure above illustrates the relationship between the main disconnect kWh draw and the indoor and outdoor temperature difference when the controller is ON for the weekday hours (Monday to Friday). As it can be seen, as the temperature difference between indoor and outdoor temperature raises so does the kW consumption of the main disconnect panel. This indicates a high correlation between kW and temperature.

CONFIDENTIAL

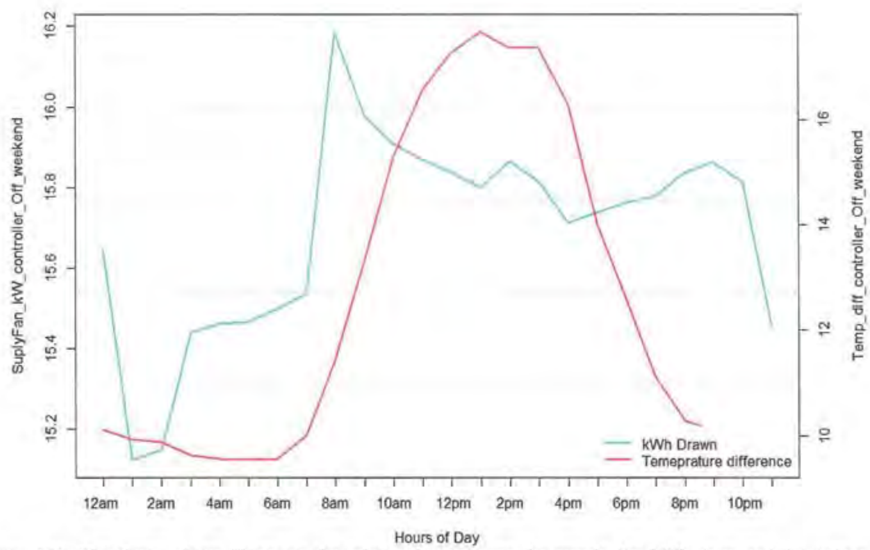

Figure 146: The figure above illustrates the relationship between the supply fan kWh draw and the indoor and outdoor temperature difference when the controller is OFF for the weekend hours (Saturday and Sunday). As it can be seen, as the temperature difference between indoor and outdoor temperature increased so does the kW consumption of the main disconnect panel. This indicates a high correlation between kW and temperature.

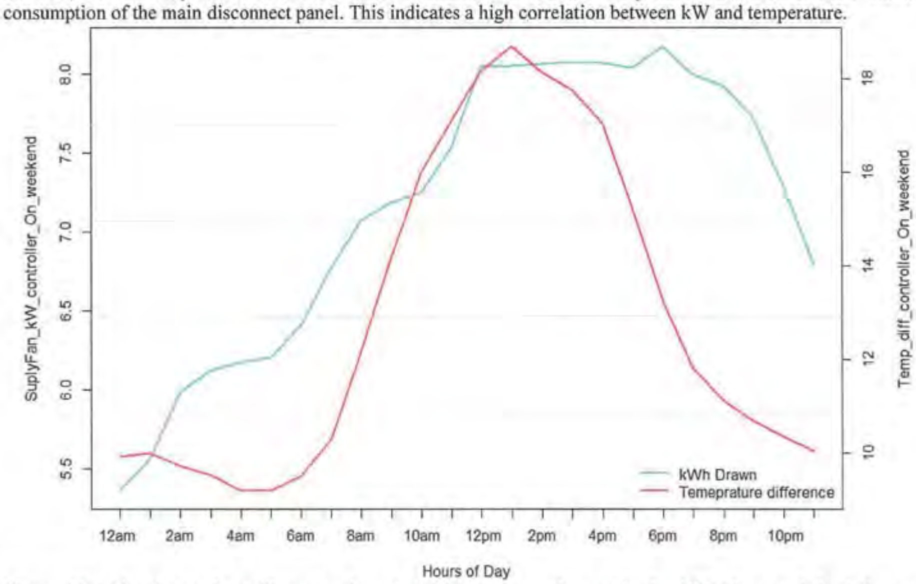

Figure 147: The figure above illustrates the relationship between the supply fan kWh draw and the indoor and outdoor temperature difference when the controller is ON for the weekend hours (Saturday and Sunday). As it can be seen, as the temperature difference between indoor and outdoor temperature raises so does the kW consumption of the main disconnect panel. This indicates a high correlation between kW and temperature.

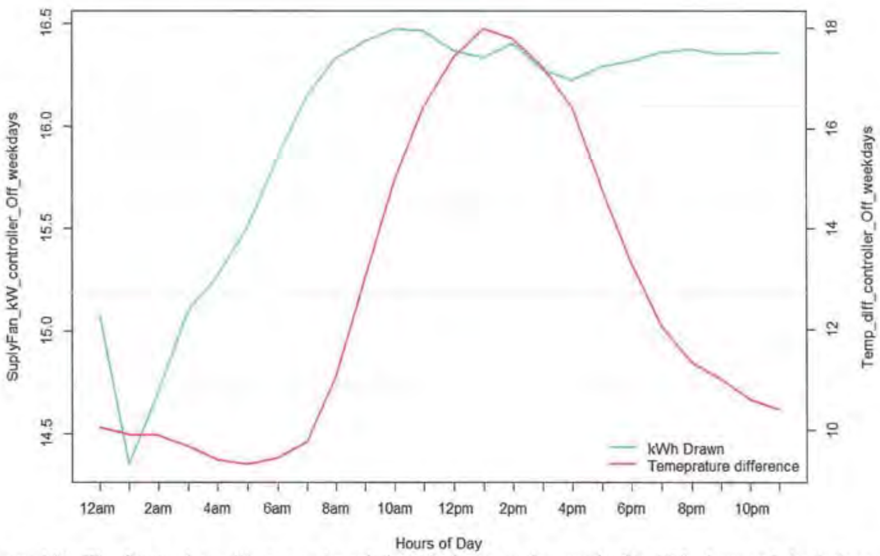

Figure 148: The figure above illustrates the relationship between the supply fan kWh draw and the indoor and outdoor temperature difference when the controller is OFF for the weekday hours (Monday to Friday). As it can be seen, as the temperature difference between indoor and outdoor temperature increased so does the kW consumption of the main disconnect panel. This indicates a high correlation between kW and temperature.

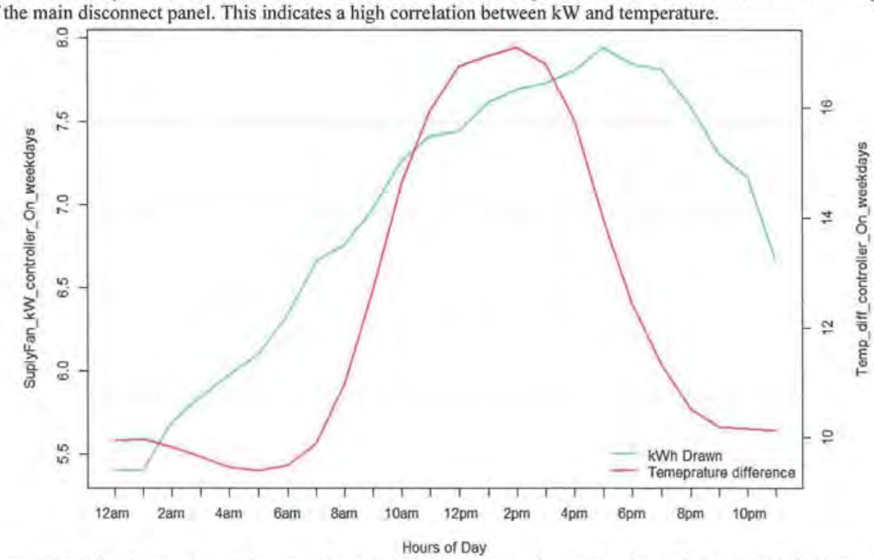

Figure 149: The figure above illustrates the relationship between the supply fan kWh draw and the indoor and outdoor temperature difference when the controller is ON for the weekday hours (Monday to Friday). As it can be seen, as the temperature difference between indoor and outdoor temperature raises so does the kW consumption of the main disconnect panel. This indicates a high correlation between kW and temperature.

Statistical Analysis of Peak demand (kW) Consumption:

The second phase of the statistical analysis was to evaluate the performance of the controller regarding the peak demand during this monitored period. The peak demand was calculated according to the method used in Florida Power & Light (FPL), and the corresponding outside temperatures was obtained as well. The same preliminary data preprocessing steps explained in the previous statistical analysis were followed while conducting the statistical analysis for the peak demand data.

Regression analysis was then performed using both summer and winter on-peak and off-peak consumption schedules (excluding weekends, where all of the consumption is considered off-peak), and the regression coefficients were then determined. The schedules are coded as '1' and '-1' for On-Peak and Off-Peak respectively.

Two methods of applying On-Peak timestamp to the recorded readings were used.

Method 1: Winter (Nov-Mar) 7 a.m. 8 a.m. except weekend and summer (Apr-Oct) 4 p.m. 5 p.m. except weekend coded '1' as On-Peak hours.

Method 2: Winter (Nov-Mar) 6 a.m. to 10 a.m. & 6 pm. to 10 p.m. except weekend and summer (Apr-Oct) 12 pm. 9 p.m. except weekend coded '1' as On-Peak hours.

The regression equations obtained is as follows:

Table 58: Peak Demand Regression Savings

OnPeak Coding	Power Factor	Regression Equation (Dataset: Combined: Nov14-Oct15)	Savings
Method-1	Unity	**PDemand** = -138.27+ 2.4562 Temp - 25.032 Controller + 4.408 Peak	49.13%
	Average	**PDemand** =-105.847+ 1.9210 Temp - 23.610 Controller + 3.290 Peak	55.82%
Method-2	Unity	**PDemand** = -104.816 + 1.8871 Temp - 23.575 Controller + 3.636 Peak	49.03%
	Average	**PDemand** =-136.95 + 2.4113 Temp - 24.985 Controller + 4.818 Peak	55.74%

The above equations (Method-1) reveal that, by controlling for the outside temperature, i.e. for the same outside temperature level, by turning the [redacted] controller "ON", a reduction in the peak demand of 25.03 kW and 23.6 kW will take place respectively while using unity power factor and varying power factor approach . By calculating the average kW consumption during the "OFF" periods (where the [redacted] controller was turned off) the percentage of the saving in the kW can be calculated, the percentage saving calculated was almost 49.13 % when a unity power factor was used and 55.82 % when using varying power factor approach, having the effect of the ambient temperature. It is also evident from Table 58, that both On-Peak timestamp coding approach leads to similar Peak Demand savings metrics.

The Figures 150, 151 below depict the distribution plot of the Peak Demand (PD) for both cases when the [redacted] controller was OFF (0) and when it was ON (1). As shown in the figures, the [redacted] controller managed to smooth down the Peak Demand centering it to 0-10 kW, while on the other hand, while the controller is OFF it can be noticed that high concentration/percentage of the of the Peak Demand data points are at the higher level.

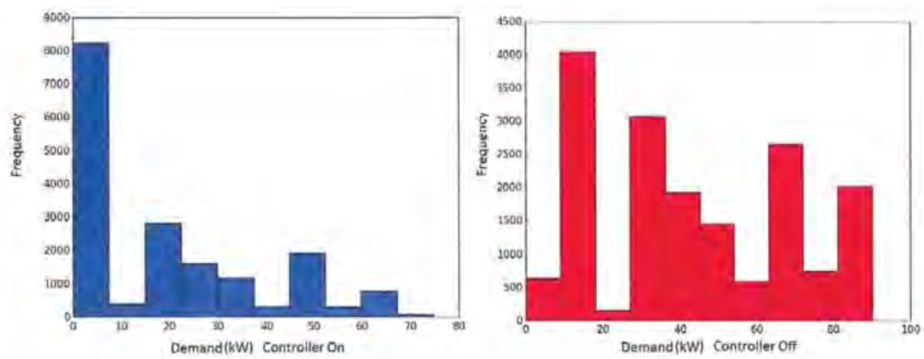

Figure 150: Distribution plot of the peak demand using Avg Power factor.

CONFIDENTIAL

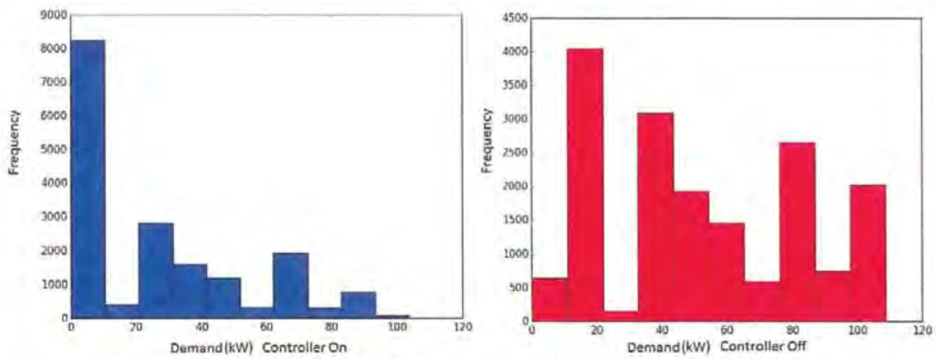

Figure 151: Distribution plot of the peak demand using Unity Power factor.

CONFIDENTIAL

Conclusion:

In this report the exhaustive description of the methodology and findings of the study conducted by the University of Miami, Department of Industrial Engineering team to quantify the impact of the [redacted] controller installed on the existing air conditioning unit at [redacted] supermarket site is given. First, the total energy consumption (kWh) of the air conditioning unit (A/C Unit), the four compressors, and the supply fan along with the resoective power factor is monitored for the entire year (November 2014- October-2015). We adopted the practices used by FPL to divide the entire year in Winter (November-March) & Summer (April-October) seasons. We analyze the data to find the relation of power consumptions during the controller on/off periods.

Also, daily and hourly average data is computed to display the kW and temperature variation trends in summer and winter seasons based on the controller status. We computed the savings (reduction in kWh) scenario in the Winter, Summer and the combined dataset for the entire year by using the raw average consumptions at the time of controller on & off. Moreover, the multiple regression technique was used for detailed statistical analysis, which gives us more accurate estimation of the savings (reduction in kWh).

Tables 59 and 60 list the results of computed savings in the two methodologies of raw savings and regression savings.

Table 59: Computed Raw Savings

Datasets		Average Power factor	Unity Power factor
Winter(Nov'14-Mar'15)	Main	73.45%	67.99%
	Compressor	53.37%	43.78%
	Supply Fan	72.2%	58.67%
Summer(Apr'15-October'15)	Main	50.49%	44.55%
	Compressor	44.07%	37.36%
	Supply Fan	67.27%	54.18%
Combined (Nov'14-October'15)	Main	56.33%	49.67%
	Compressor	46.15%	37.93%
	Supply Fan	68.56%	56%

CONFIDENTIAL

Table 60: Computed Regression Savings

Time Period	Power Factor	Regression Equation	Savings
Main (Winter: Nov14-Mar15)	Unity	**Main_kW =** -72.59 + 1.4000 Temp - 19.794 Controller	67.55%
	Average	**Main_kWh =** -54.99 + 1.0891 Temp - 17.726 Controller	73.02%
Compressor (Winter: Nov14-Mar15)	Unity	**Compressor_kWh =** -53.54 + 0.9347 Temp - 6.256 Controller	43.17%
	Average	**Compressor_kWh =** -41.16 + 0.7305 Temp - 6.337 Controller	52.79%
Supply Fan (Winter: Nov14-Mar15)	Unity	**SupplyFan_kWh =** 13.314 + 0.03334 Temp - 9.232 Controller	58.64%
	Average	**Supply_Fan_kWh =** 8.646 + 0.01879 Temp - 7.2277 Controller	72.22%
Main (Summer: Apr15-Oct15)	Unity	**Main_kWh =** -205.84 + 3.2814 Temp - 28.684 Controller	43.12%
	Average	**Main_kWh =** -160.16 + 2.6028 Temp - 27.459 Controller	49.21%
Compressor (Summer: Apr15-Oct15)	Unity	**Compressor_kWh =** -198.39 + 2.9421 Temp - 16.262 Controller	35.49%
	Average	**Compressor_kWh =** -155.56 + 2.3378 Temp - 16.282 Controller	42.30%
Supply Fan (Summer: Apr15-Oct15)	Unity	**Supply_Fan_kW =** 15.217 + 0.00964 Temp - 8.6754 Controller	54.22%
	Average	**SupplyFan_kWh =** 9.787 + 0.00366 Temp - 6.7869 Controller	67.29%
Main (Combined: Nov14-Oct15)	Unity	**Main_kWh =** -143.45 + 2.4693 Temp - 25.028 Controller	49.14%
	Average	**Main_kWh =** -109.75 + 1.9312 Temp - 23.607 Controller	55.84%
Compressor (Combined: Nov14-Oct15)	Unity	**Compressor_kWh =** -122.36 + 1.9696 Temp - 12.187 Controller	37.28%
	Average	**Compressor_kWh =** -94.43 + 1.5443 Temp - 12.358 Controller	45.54%
Supply Fan (Combined: Nov14-Oct15)	Unity	**Supply_Fan_kWh =** 13.067 + 0.03601 Temp - 8.8992 Controller	56.0%
	Average	**SupplyFan_kWh =** 8.555 + 0.01858 Temp - 6.8664 Controller	68.56%

CONFIDENTIAL

In terms of peak-hour demand, the [redacted] controller managed to reduce the peak demand by 49.13 % when a unity power factor was used and 55.82 % when using varying power factor approach.

Table 61: Peak Demand Savings

Power Factor	Regression Equation (Dataset: Combined: Nov14-Oct15)	Savings
Unity	**PDemand =** -138.27+ 2.4562 Temp - 25.032 Controller + 4.408 Peak	49.13%
Average	**PDemand =**-105.847+ 1.9210 Temp - 23.610 Controller + 3.290 Peak	55.82%

FPL-[redacted] Load Control Switch Lab Test Results

Eduardo Niezen
Zoila Morales, P.E.
Andres Reyes
Hossiel Miras

Table of Contents

FPL Capabilities Matrix

Test Plan ID Number	Capability to Validate	Test Objective
1	LCT Communication capability	Switches shall be integrated with Owner's 900 MHz mesh NAN such that it can communicate with Owner's servers directly without the intervention of external gateways or meters.
2	Verification of appliance control	Switches shall be able to cycle individual relays and combinations of relays. They shall be able to cycle its relay and driver circuit individually as well as simultaneously
3	Verification of load reduction	Determine achieved load reduction.
4	Switch connectivity to network. Self Initializing.	Switch shall have the capability to browse for networks and select a network to join autonomously.
5	Time is obtained after loss of power	The switch shall query its time server for the correct time after recovering from a loss of power.
6	Time maintained within +/- 1 minute over 24 hours	The switch shall maintain correct time within +/- one minute over 24 hours since last sync.
7	Time on Switch Syncs when a discrepancy with time server exists	The switch shall automatically sync with its time server when its clock/calendar do not match the time server's
8	Communication Link test	The switch shall have the capability to respond to a request for an internal diagnostic communications link test.
9	Load shed and load cycling. Cycle end use load at control duty cycle.	Switches shall support and execute commands to cycle an end use load at a specific control duty cycle defined as a percentage control-state (between 0-100%) of a control period (in minutes).
10	Execution of non-conflicting commands	The switch shall be able to receive and execute non-conflicting commands related to multiple end use loads simultaneously (e.g. an event for relay 1 is called, then an overlapping event for relay 2 is called. The switch should be able to execute both without conflict).
11	Individual and multi-relay control	The switch shall be able to associate both single and multiple relays to virtual relays. It shall be able to control all intended loads simultaneously and individual. The switch shall be able to cycle individual relays and combinations of relays.
12	Switch resumes in-progress events after loss of power-CLP state ignored.	Switches shall be able to immediately resume any in-progress events after recovering from a loss of power, regardless of whether cold-load pickup is enabled.
13	Cycling Capability	Switches shall support and execute commands to cycle an end use load at a specific control duty cycle defined as a percentage control-state (between 0-100%) of a control period (in minutes).

14	Delay capability	The switch shall be able to randomly delay the start and end time of an event.
15	Delay period configuration	The switch shall support having its random delay period configured as being between 0 minutes and up to 60 minutes with a default of 15 minutes.
16	Switch Supports cancel all load control events	The switch shall be able to receive and execute event cancel commands.
17	Switch supports cancellation of single event without impact to existing events.	The switch shall be able to cancel an individual load control event without cancelling other events that are executing on the switch (e.g. two events are triggered for multiple end use loads, the switch shall be able to receive and execute a cancel command for one of those events while continuing to execute the event on the other devices).
18	TrueCycle® Advanced Cycling	The switch shall learn the AC truecycle and control for the duty cycle specified.
19	Support for "Criticality" levels editing an event	The switch shall support the Demand Response and Load Control event data field "Criticality" levels.
20	Support for "Criticality" levels replacing an event	The switch shall support the Demand Response and Load Control event data field "Criticality" levels.
21	Switch supports HVAC event supersession for duty cycle and number of cycles only	The DLC switch shall support event supersession on HVAC systems to modify duty cycle and number of cycles
22	Multiple superseding events will update duty cycle and duration per event	The DLC switch shall support multiple superseding events for making additional modifications to duty cycle and duration prior to the event completing. In this scenario, the DLC switch shall always prefer the most recent duty cycle and duration parameters received over any preceding parameters.
23	Duty cycle event supersession will not result in relay short cycling	Superseding an in-progress event to modify duty cycle and/or duration shall not result in any relay short cycling. E.g. extending a 100% duty cycle command should maintain the relay state across the duty cycle boundaries.
24	Overlapping events shall use the same randomized start delay	When transitioning between overlapping events the switch shall use the same randomized start delay for the second event as it used for the first. (This is to ensure that the aggregate time-under-control does not exceed the maximum amount allowed per assigned control period).
25	Most recent command prioritized when command conflict occurs	The switch shall prioritize the most recent command/message received over any conflicting commands/messages.
26	Event status – ack (acknowledge the receipt of data), start, stop	The switch shall report event status to the HCM when any event changes are detected.
27	Storage of run time information- End use load including absence of load-load on or load off, like tamper situation	The switch shall be able to monitor and store the runtime information (including date and time stamp) for the end use load connected to its relay.
28	Activity Los Capture History.	The switch's activity logs shall capture event history.

29	Inactive appliance duration. Tamper alarm preset parameters	The switch shall log an alert if current has not been detected on a connected load for a configurable number of days longer than the time set for in the configuration file (preset parameters)
30	Activity Logs are locally accessible via LCC	The switch's activity logs shall be locally accessible via Field Test Equipment.
31	Field Test Equipment	Field test equipment shall not require a connection through the HAN to interface to the switch.
32	Switch shall support both, Local and remote Over-the-air (OTA) firmware upgrades	Can we upgrade firmware over the air?
33	Switch shall confirm successful Firmware upgrade	Upon request switch shall confirm firmware upgrade
34	Over-the-air configuration changes	Can we update configuration over the air?
35	Virtual relay Configuration Available in HCM	The switch virtual relay configuration settings shall be retrievable from the HCM.
36	Network Time out	Determine duration of lost radio connection prior to restoring load.
37	Maximum Control Duration	The switch shall be able to reject an event longer than the maximum duration set in the configuration file.
38	Short Cycle Protection	The switch shall not perform an event shorter that the short cycle protection time that is set in the configuration file.
39	Switch shall have the ability to confirm if CLP Enabled/Disabled per virtual relay via HCM	The switch shall have the ability to confirm if CLP is enabled or disabled for each virtual relay via use of HCM.
40	Cold Load Pick up	After recovering from Power loss switch should control the load for the set time in the configuration file. In our case for 5 relay switches 180 minutes.
41	Activity Logs capture diagnostic results	The switch's activity logs shall capture the results of internal diagnostic tests.
42	Under frequency protection	The switch shall be able to detect under-frequency events and control the load.
43	Surge	Determine if device can withstand a typical surge
44	Fast Transient	Determine if device can withstand a typical transient
45	RF Immunity	Determine RF immunity of device and potential side effects
46	Microscopy Test	Document device and parts

1 EXECUTIVE SUMMARY

Florida Power and Light (FPL) performed lab tests in order to validate potential viability from new load control switches capable of communicating through FPL's AMI network as possible replacements for the switches currently used in FPL's Residential On Call program. Testing of over 46 features was conducted in the categories of communication, control, monitoring and maintenance, configuration settings.

The majority of the key features in the switches passed the testing criteria. Some features needed refinement in order to meet the operational criteria and FPL met with the manufacturer so that they could modify their design to meet FPL's requirements. The conclusion of the lab tests was that even though the AMI enabled switches are capable of communicating and be controlled through the AMI network they are not ready to replace switches currently used in FPL's Residential Load Management program.

2 LCT COMMUNICATION CAPABILITY

2.1 OBJECTIVE

Switches shall be integrated with Owner's 900 MHz mesh NAN such that it can communicate with Owner's servers directly without the intervention of external gateways or meters.

2.2 TEST PREREQUISITES AND EQUIPMENT

Eight [redacted] Switches connected as shown on table 1 in Appendix A, LCC, HCM, Device and Location files loaded

2.3 TEST STEPS

1. Power up appropriately configured switches and allow them to join the NAN network.
2. Using LCC, Read LCS Information, Read Network Information validate that all switches can see NAN neighbors. Devices can also be viewed in the Neighbors panel within LCC.
3. Using HCM, ping the switches to ensure operation.
4. Log and record the results.

2.4 EXPECTED RESULTS

Verification of functionality.

2.5 TEST RESULTS

Discovery Screen Shot

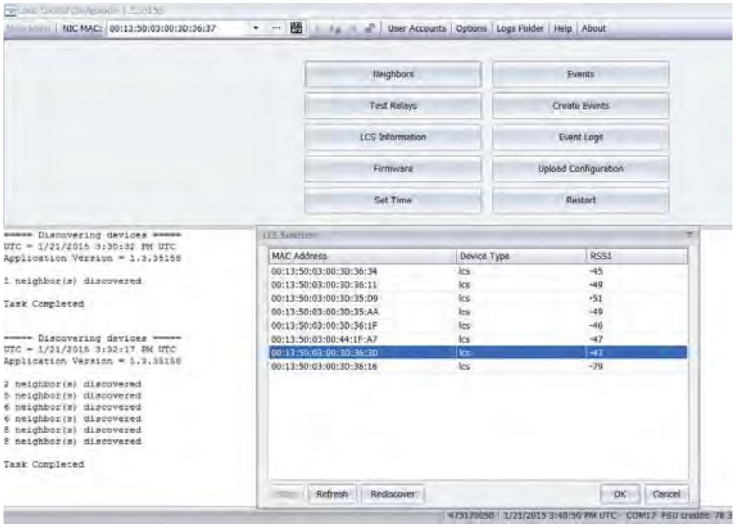

Read LCS Information
Device 1 (18001258)

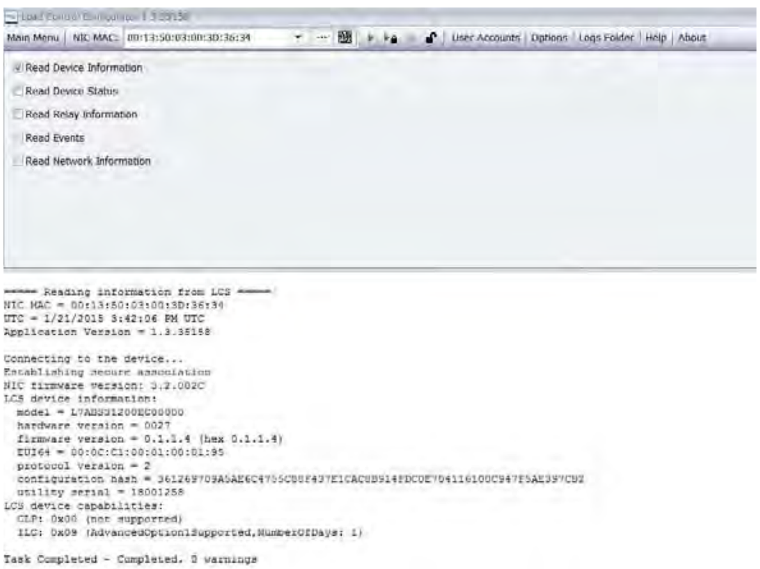

Load Control Configurator 1.3.35158

Main Menu | NIC MAC: 00:13:50:03:00:3D:36:34 | User Accounts | Options | Logs Folder | Help | About

- [ ] Read Device Information
- [ ] Read Device Status

```
===== Reading information from LCS =====
NIC MAC = 00:13:50:03:00:3D:36:34
UTC = 1/21/2015 4:16:52 PM UTC
Application Version = 1.3.35158

Connecting to the device...
Establishing secure association
active LCS neighbors:
 type = 4 (relay), mac = 00:13:50:FF:FE:10:A0:32, rssi = -70
 type = 8 (i210_eo), mac = 00:13:50:01:00:D9:6A:8E, rssi = -71
 type = 8 (i210_eo), mac = 00:13:50:01:01:2C:37:74, rssi = -64
 type = 8 (i210_eo), mac = 00:13:50:01:01:38:71:8A, rssi = -68
 type = 8 (i210_eo), mac = 00:13:50:01:01:2B:97:26, rssi = -69
 type = 8 (i210_eo), mac = 00:13:50:01:00:D9:23:E0, rssi = -69
 type = 8 (i210_eo), mac = 00:13:50:01:01:73:4D:01, rssi = -76
 type = 8 (i210_eo), mac = 00:13:50:01:01:63:3F:D7, rssi = -72
 type = 8 (i210_eo), mac = 00:13:50:01:01:63:7A:D5, rssi = -74
 type = 8 (i210_eo), mac = 00:13:50:01:01:2C:37:75, rssi = -67
 type = 8 (i210_eo), mac = 00:13:50:01:01:38:BC:F0, rssi = -72
 type = 8 (i210_eo), mac = 00:13:50:01:01:38:AC:BA, rssi = -65
 type = 8 (i210_eo), mac = 00:13:50:01:01:10:7B:03, rssi = -65
 type = 8 (i210_eo), mac = 00:13:50:01:01:73:4D:03, rssi = -67
 type = 8 (i210_eo), mac = 00:13:50:01:01:74:60:10, rssi = -70
 type = 8 (i210_eo), mac = 00:13:50:01:01:2C:38:B1, rssi = -64
 type = 8 (i210_eo), mac = 00:13:50:01:01:29:7D:76, rssi = -68
 type = 8 (i210_eo), mac = 00:13:50:01:01:63:40:0F, rssi = -70
 type = 8 (i210_eo), mac = 00:13:50:01:01:63:29:5F, rssi = -71
 type = 8 (i210_eo), mac = 00:13:50:01:01:38:BA:7F, rssi = -63
 type = 8 (i210_eo), mac = 00:13:50:01:01:38:BC:83, rssi = -68
 ...
Default nexthop list:
 mac = 00:13:50:FF:FE:01:0A:96
 mac = 00:13:50:FF:FE:01:21:29
LCS link quality = [|||||] (5)

Task Completed - Completed. 0 warnings
```

[LCS Information] | 475172238 | 1/21/2015 4:17:18 PM UTC | COM17

Load Control Configurator 1.3.35158

Main Menu | NIC MAC: 00:13:50:03:00:3D:36:34 | User Accounts | Options | Logs Folder | Help | About

- [ ] Read Device Information
- [ ] Read Device Status
- [x] Read Relay Information
- [ ] Read Events
- [ ] Read Network Information

```
NIC MAC = 00:13:50:03:00:3D:36:34
UTC = 1/21/2015 4:19:18 PM UTC
Application Version = 1.3.35158

Connecting to the device...
Physical relay map:
  VRID = 0, map = 0x01 (#1)
  VRID = 1, map = 0x02 (#2)
  VRID = 2, map = 0x00
  VRID = 3, map = 0x00
  VRID = 4, map = 0x00
  VRID = 5, map = 0x00
  VRID = 6, map = 0x00
  VRID = 7, map = 0x03 (#1, #2)
Virtual Relay status:
  VRID: 0, status = 0x00 (NotInControl)
  VRID: 1, status = 0x00 (NotInControl)
  VRID: 2, status = 0x03 (NotConfigured)
  VRID: 3, status = 0x03 (NotConfigured)
  VRID: 4, status = 0x03 (NotConfigured)
  VRID: 5, status = 0x03 (NotConfigured)
  VRID: 6, status = 0x03 (NotConfigured)
  VRID: 7, status = 0x00 (NotInControl)

Task Completed - Completed. 0 warnings
```

Device 2 (18001264)

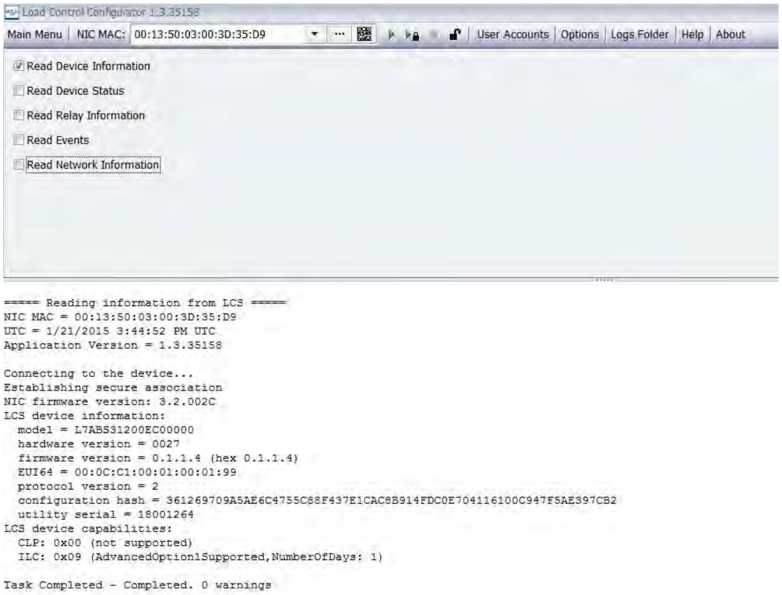
Load Control Configurator 1.3.35158
Main Menu
NIC MAC: 00:13:50:03:00:3D:35:D9
User Accounts
Options
Logs Folder
Help
About
Read Device Information
Read Device Status
Read Relay Information
Read Events
Read Network Information
===== Reading information from LCS =====
NIC MAC = 00:13:50:03:00:3D:35:D9
UTC = 1/21/2015 3:44:52 PM UTC
Application Version = 1.3.35158
Connecting to the device...
Establishing secure association
NIC firmware version: 3.2.002C
LCS device information:
model = L7ABS31200EC00000
hardware version = 0027
firmware version = 0.1.1.4 (hex 0.1.1.4)
EUI64 = 00:0C:C1:00:01:00:01:99
protocol version = 2
configuration hash = 361269709A5AE6C4755C88F437E1CAC8B914FDC0E704116100C947F5AE397CB2
utility serial = 18001264
LCS device capabilities:
CLP: 0x00 (not supported)
ILC: 0x09 (AdvancedOption1Supported,NumberOfDays: 1)
Task Completed - Completed. 0 warnings

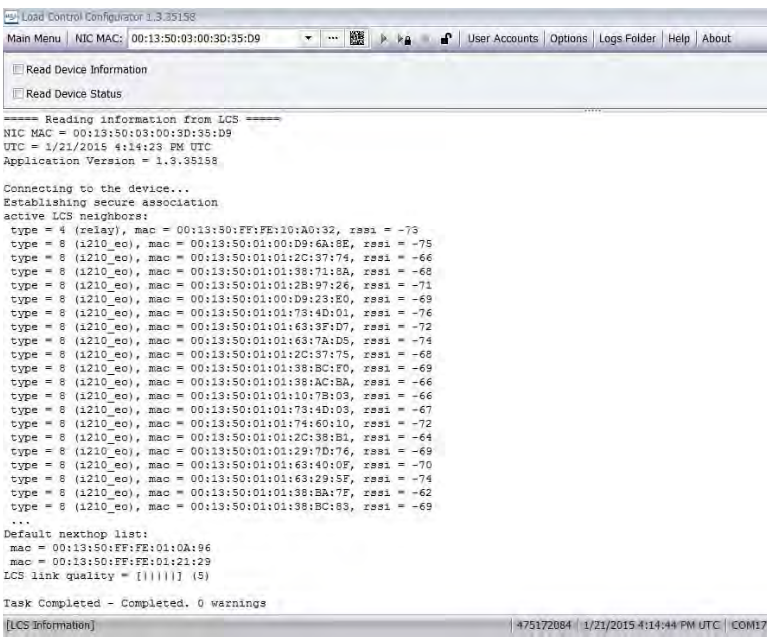
Load Control Configurator 1.3.35158
Main Menu
NIC MAC: 00:13:50:03:00:3D:35:D9
User Accounts
Options
Logs Folder
Help
About
Read Device Information
Read Device Status
===== Reading information from LCS =====
NIC MAC = 00:13:50:03:00:3D:35:D9
UTC = 1/21/2015 4:14:23 PM UTC
Application Version = 1.3.35158
Connecting to the device...
Establishing secure association
active LCS neighbors:
type = 4 (relay), mac = 00:13:50:FF:FE:10:A0:32, rssi = -73
type = 8 (i210_eo), mac = 00:13:50:01:00:D9:6A:8E, rssi = -75
type = 8 (i210_eo), mac = 00:13:50:01:01:2C:37:74, rssi = -66
type = 8 (i210_eo), mac = 00:13:50:01:01:38:71:8A, rssi = -68
type = 8 (i210_eo), mac = 00:13:50:01:01:2B:97:26, rssi = -71
type = 8 (i210_eo), mac = 00:13:50:01:00:D9:23:E0, rssi = -69
type = 8 (i210_eo), mac = 00:13:50:01:01:73:4D:01, rssi = -76
type = 8 (i210_eo), mac = 00:13:50:01:01:63:3F:D7, rssi = -72
type = 8 (i210_eo), mac = 00:13:50:01:01:63:7A:D5, rssi = -74
type = 8 (i210_eo), mac = 00:13:50:01:01:2C:37:75, rssi = -68
type = 8 (i210_eo), mac = 00:13:50:01:01:38:BC:F0, rssi = -69
type = 8 (i210_eo), mac = 00:13:50:01:01:38:AC:BA, rssi = -66
type = 8 (i210_eo), mac = 00:13:50:01:01:10:7B:03, rssi = -66
type = 8 (i210_eo), mac = 00:13:50:01:01:73:4D:03, rssi = -67
type = 8 (i210_eo), mac = 00:13:50:01:01:74:60:10, rssi = -72
type = 8 (i210_eo), mac = 00:13:50:01:01:2C:38:B1, rssi = -64
type = 8 (i210_eo), mac = 00:13:50:01:01:29:7D:76, rssi = -69
type = 8 (i210_eo), mac = 00:13:50:01:01:63:40:0F, rssi = -70
type = 8 (i210_eo), mac = 00:13:50:01:01:63:29:5F, rssi = -74
type = 8 (i210_eo), mac = 00:13:50:01:01:38:BA:7F, rssi = -62
type = 8 (i210_eo), mac = 00:13:50:01:01:38:BC:83, rssi = -69
...
Default nexthop list:
mac = 00:13:50:FF:FE:01:0A:96
mac = 00:13:50:FF:FE:01:21:29
LCS link quality = [||||||] (5)
Task Completed - Completed. 0 warnings
[LCS Information]
475172084
1/21/2015 4:14:44 PM UTC
COM17

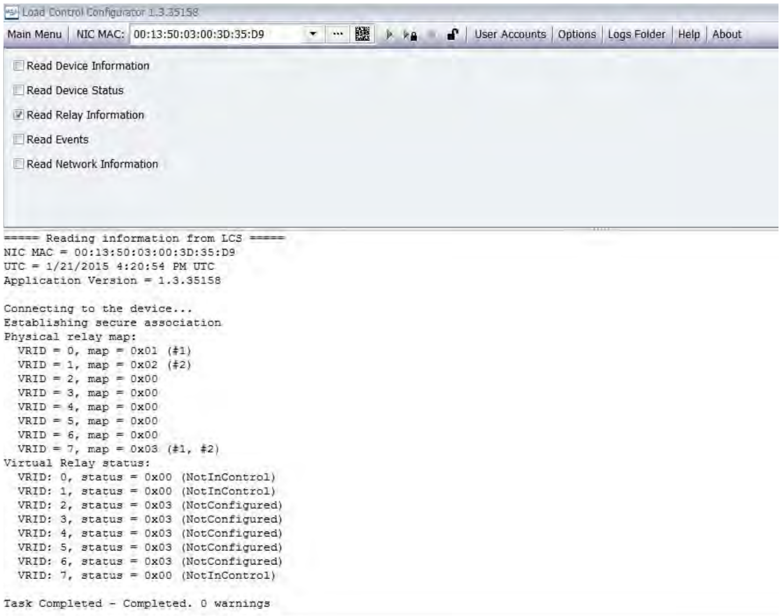


```
===== Reading information from LCS =====
NIC MAC = 00:13:50:03:00:3D:35:D9
UTC = 1/21/2015 4:20:54 PM UTC
Application Version = 1.3.35158

Connecting to the device...
Establishing secure association
Physical relay map:
  VRID = 0, map = 0x01 (#1)
  VRID = 1, map = 0x02 (#2)
  VRID = 2, map = 0x00
  VRID = 3, map = 0x00
  VRID = 4, map = 0x00
  VRID = 5, map = 0x00
  VRID = 6, map = 0x00
  VRID = 7, map = 0x03 (#1, #2)
Virtual Relay status:
  VRID: 0, status = 0x00 (NotInControl)
  VRID: 1, status = 0x00 (NotInControl)
  VRID: 2, status = 0x03 (NotConfigured)
  VRID: 3, status = 0x03 (NotConfigured)
  VRID: 4, status = 0x03 (NotConfigured)
  VRID: 5, status = 0x03 (NotConfigured)
  VRID: 6, status = 0x03 (NotConfigured)
  VRID: 7, status = 0x00 (NotInControl)

Task Completed - Completed. 0 warnings
```

Device 3 (18001276)

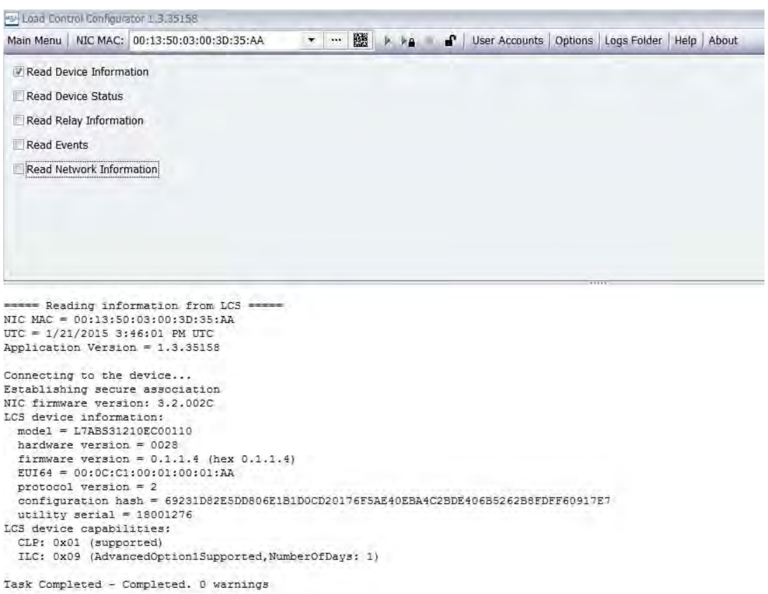


```
===== Reading information from LCS =====
NIC MAC = 00:13:50:03:00:3D:35:AA
UTC = 1/21/2015 3:46:01 PM UTC
Application Version = 1.3.35158

Connecting to the device...
Establishing secure association
NIC firmware version: 3.2.002C
LCS device information:
  model = L7ABS31210EC00110
  hardware version = 0028
  firmware version = 0.1.1.4 (hex 0.1.1.4)
  EUI64 = 00:0C:C1:00:01:00:01:AA
  protocol version = 2
  configuration hash = 69231D82E5DD806E1B1D0CD20176F5AE40EBA4C2BDE406B5262B8FDFF60917E7
  utility serial = 18001276
LCS device capabilities:
  CLP: 0x01 (supported)
  ILC: 0x09 (AdvancedOption1Supported,NumberOfDays: 1)

Task Completed - Completed. 0 warnings
```

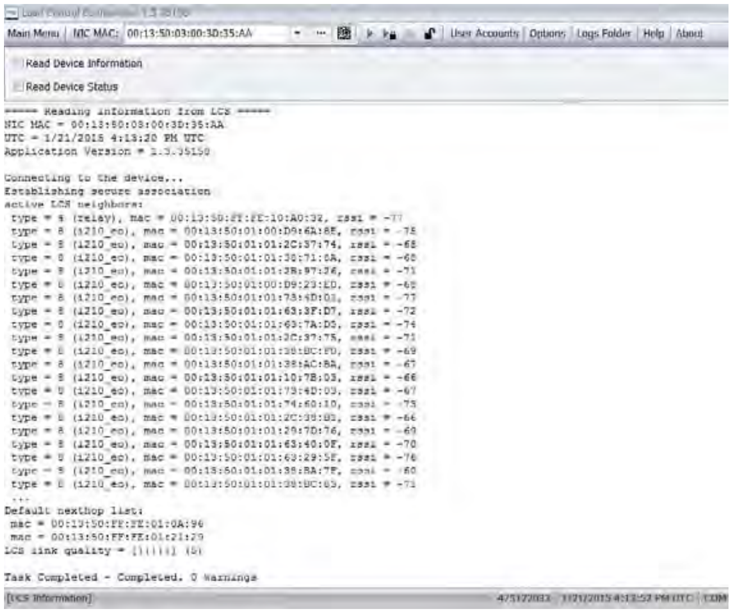

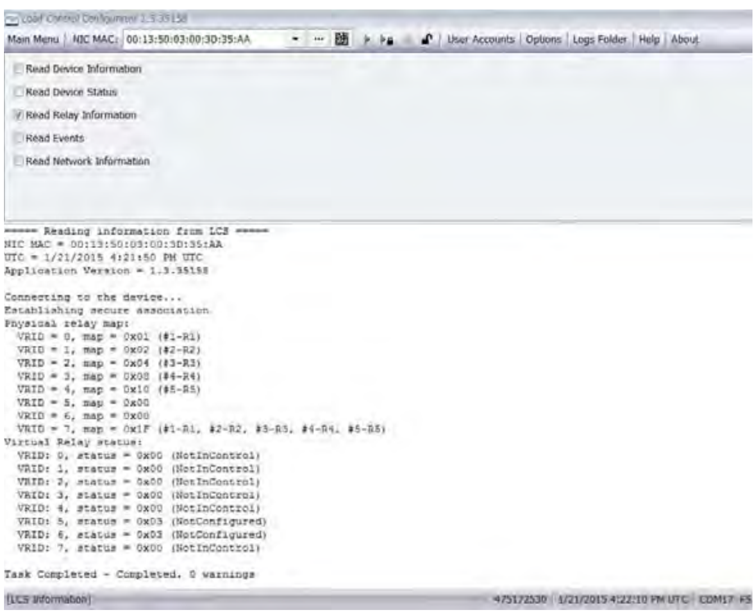

Device 4 (18001273)

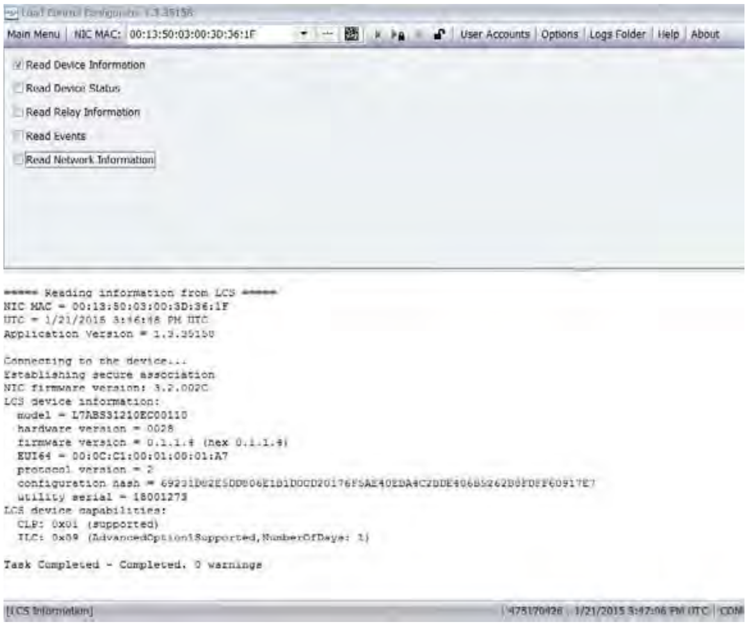
Main Menu
NIC MAC: 00:13:50:03:00:3D:36:1F
User Accounts
Options
Logs Folder
Help
About
Read Device Information
Read Device Status
Read Relay Information
Read Events
Read Network Information
===== Reading information from LCS =====
NIC MAC = 00:13:50:03:00:3D:36:1F
UTC = 1/21/2015 3:46:48 PM UTC
Application Version = 1.3.35158
Connecting to the device...
Establishing secure association
NIC firmware version: 3.2.002C
LCS device information:
model = L7ABS31210EC00110
hardware version = 0028
EUI64 = 00:0C:C1:00:01:00:01:A7
protocol version = 2
utility serial = 18001273
LCS device capabilities:
CLP: 0x01 (supported)
Task Completed - Completed. 0 warnings
[LCS Information]

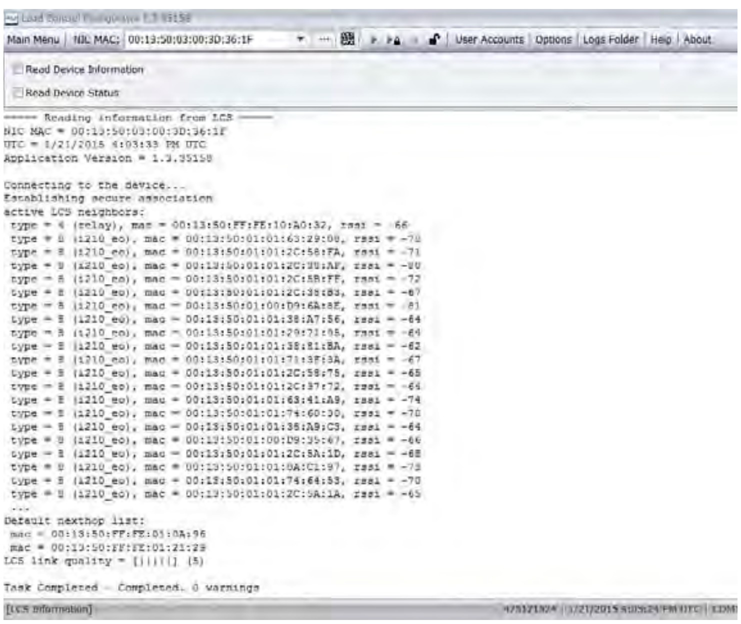
Main Menu
NIC MAC: 00:13:50:03:00:3D:36:1F
User Accounts
Options
Logs Folder
Help
About
Read Device Information
Read Device Status
===== Reading information from LCS =====
NIC MAC = 00:13:50:03:00:3D:36:1F
UTC = 1/21/2015 4:03:33 PM UTC
Application Version = 1.3.35158
Connecting to the device...
Establishing secure association
active LCS neighbors:
type = 4 (relay), mac = 00:13:50:FF:FE:10:A0:32, rssi = -66
type = 8 (i210_eo), mac = 00:13:50:01:01:2C:58:FA, rssi = -71
type = 8 (i210_eo), mac = 00:13:50:01:01:38:A7:56, rssi = -64
type = 8 (i210_eo), mac = 00:13:50:01:01:38:81:BA, rssi = -62
type = 8 (i210_eo), mac = 00:13:50:01:01:2C:58:75, rssi = -65
type = 8 (i210_eo), mac = 00:13:50:01:01:63:41:A9, rssi = -74
type = 8 (i210_eo), mac = 00:13:50:01:01:2C:5A:1D, rssi = -68
type = 8 (i210_eo), mac = 00:13:50:01:01:74:64:53, rssi = -70
type = 8 (i210_eo), mac = 00:13:50:01:01:2C:5A:1A, rssi = -65
...
Default nexthop list:
mac = 00:13:50:FF:FE:01:21:29
LCS link quality = [|||||] (5)
Task Completed - Completed. 0 warnings
[LCS Information]

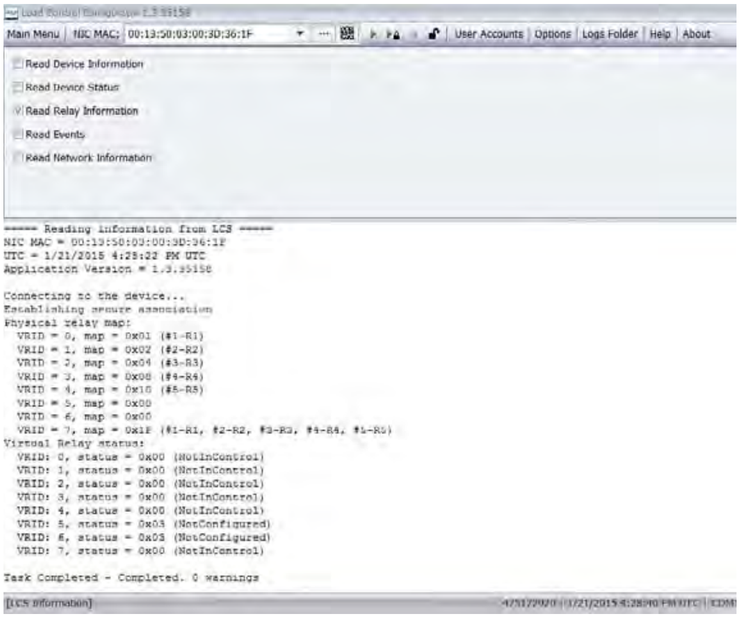

Device 5 (18001262)

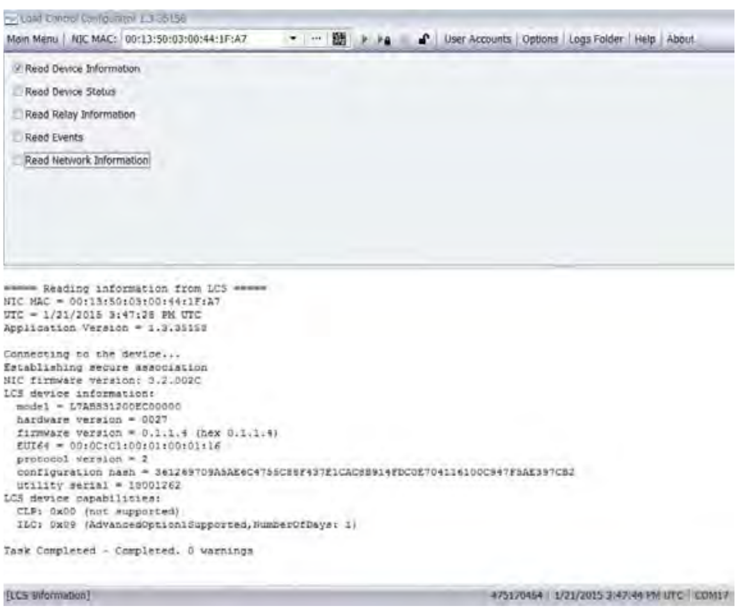

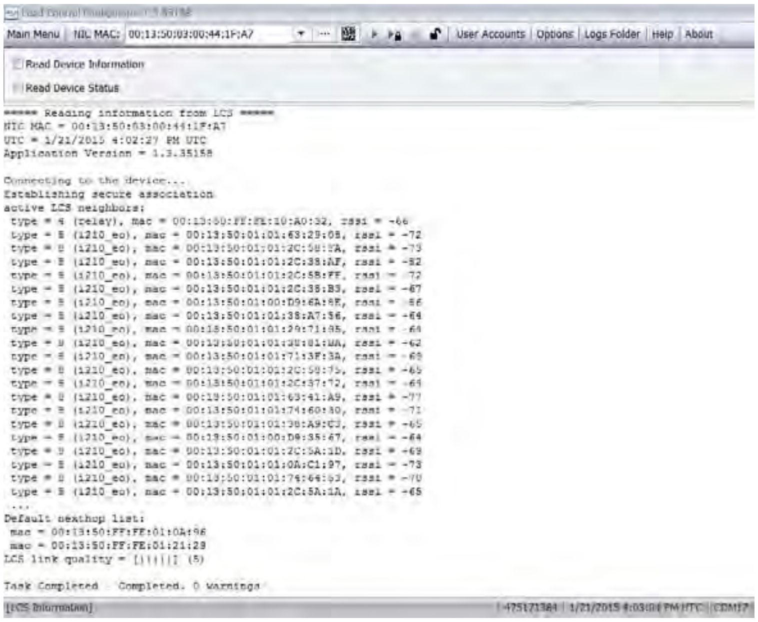

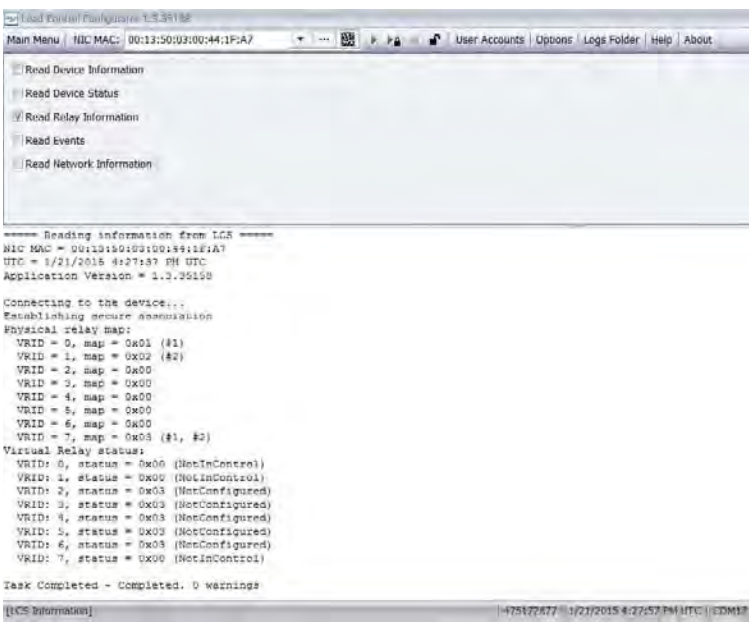

Device 6 (18001277)

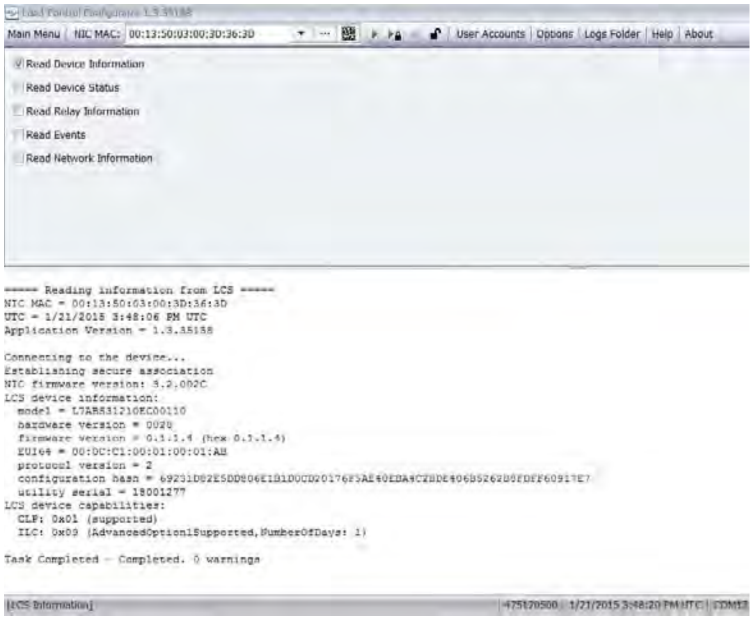
Main Menu
NIC MAC: 00:13:50:03:00:3D:36:3D
User Accounts
Options
Logs Folder
Help
About
Read Device Information
Read Device Status
Read Relay Information
Read Events
Read Network Information
===== Reading information from LCS =====
NIC MAC = 00:13:50:03:00:3D:36:3D
UTC = 1/21/2015 3:48:06 PM UTC
Application Version = 1.3.35158
Connecting to the device...
Establishing secure association
NIC firmware version: 3.2.002C
LCS device information:
model = L7ARS31210EC00110
hardware version = 0020
firmware version = 0.1.1.4 (hex 0.1.1.4)
EUI64 = 00:DC:C1:00:01:00:01:AB
protocol version = 2
utility serial = 18001277
LCS device capabilities:
CLP: 0x01 (supported)
ILC: 0x09 (AdvancedOption1Supported,NumberOfDays: 1)
Task Completed - Completed. 0 warnings
[LCS Information]
475170500 | 1/21/2015 3:48:20 PM UTC

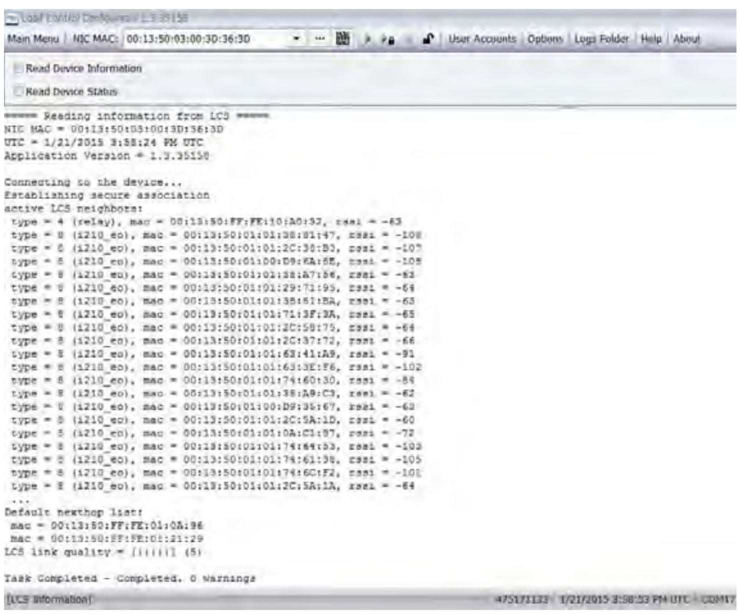
Main Menu
NIC MAC: 00:13:50:03:00:3D:36:3D
User Accounts
Options
Logs Folder
Help
About
Read Device Information
Read Device Status
===== Reading information from LCS =====
NIC MAC = 00:13:50:03:00:3D:36:3D
UTC = 1/21/2015 3:58:24 PM UTC
Application Version = 1.3.35158
Connecting to the device...
Establishing secure association
active LCS neighbors:
type = 4 (relay), mac = 00:13:50:FF:FE:10:A0:93, rssi = -63
type = 8 (i210_eo), mac = 00:13:50:01:01:38:81:47, rssi = -108
type = 8 (i210_eo), mac = 00:13:50:01:01:2C:38:B3, rssi = -107
type = 8 (i210_eo), mac = 00:13:50:01:00:D9:6A:8E, rssi = -105
type = 8 (i210_eo), mac = 00:13:50:01:01:38:A7:56, rssi = -63
type = 8 (i210_eo), mac = 00:13:50:01:01:29:71:95, rssi = -64
type = 8 (i210_eo), mac = 00:13:50:01:01:38:6I:BA, rssi = -63
type = 8 (i210_eo), mac = 00:13:50:01:01:71:3F:3A, rssi = -65
type = 8 (i210_eo), mac = 00:13:50:01:01:2C:58:75, rssi = -64
type = 8 (i210_eo), mac = 00:13:50:01:01:2C:37:72, rssi = -66
type = 8 (i210_eo), mac = 00:13:50:01:01:63:41:A9, rssi = -91
type = 8 (i210_eo), mac = 00:13:50:01:01:63:3E:F6, rssi = -102
type = 8 (i210_eo), mac = 00:13:50:01:01:74:60:30, rssi = -89
type = 8 (i210_eo), mac = 00:13:50:01:01:38:A9:C3, rssi = -62
type = 8 (i210_eo), mac = 00:13:50:01:00:D9:36:67, rssi = -63
type = 8 (i210_eo), mac = 00:13:50:01:01:2C:5A:1D, rssi = -60
type = 8 (i210_eo), mac = 00:13:50:01:01:0A:C1:97, rssi = -72
type = 8 (i210_eo), mac = 00:13:50:01:01:74:69:53, rssi = -103
type = 8 (i210_eo), mac = 00:13:50:01:01:74:61:38, rssi = -105
type = 8 (i210_eo), mac = 00:13:50:01:01:74:6C:F2, rssi = -101
type = 8 (i210_eo), mac = 00:13:50:01:01:2C:5A:1A, rssi = -64
...
Default nexthop list:
mac = 00:13:50:FF:FE:01:0A:96
mac = 00:13:50:FF:FE:01:21:29
LCS link quality = [|||||] (5)
Task Completed - Completed. 0 warnings
[LCS Information]

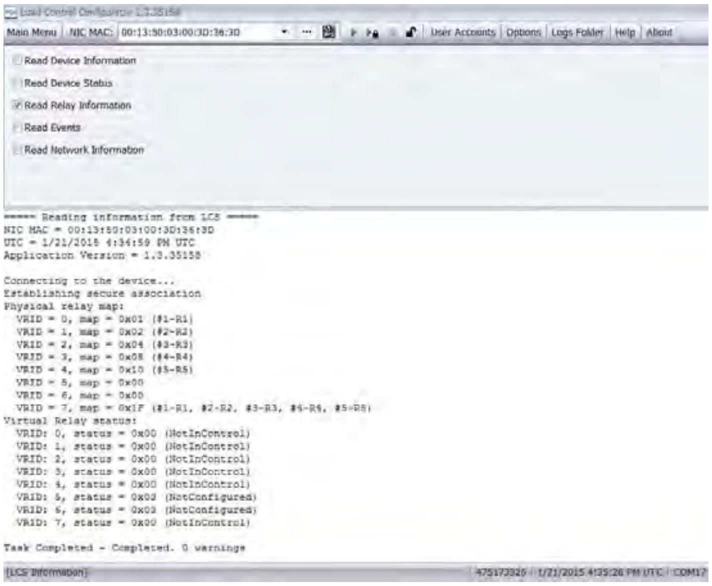

Device 7 (18001260)

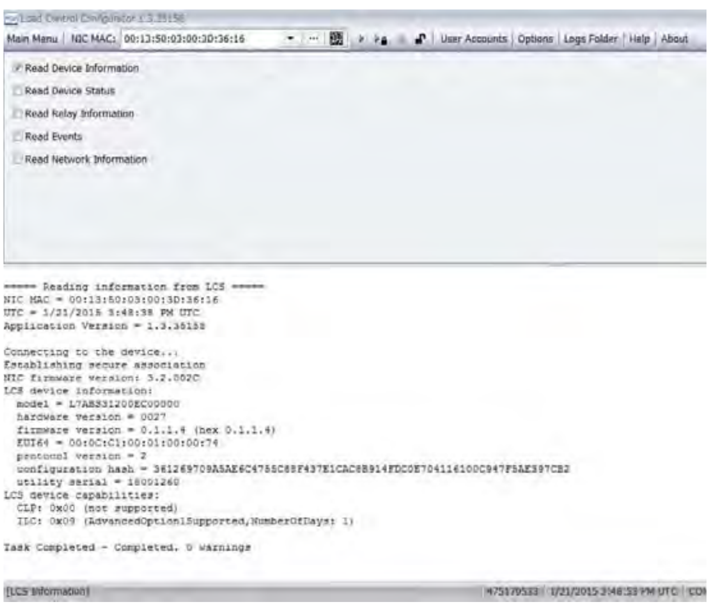

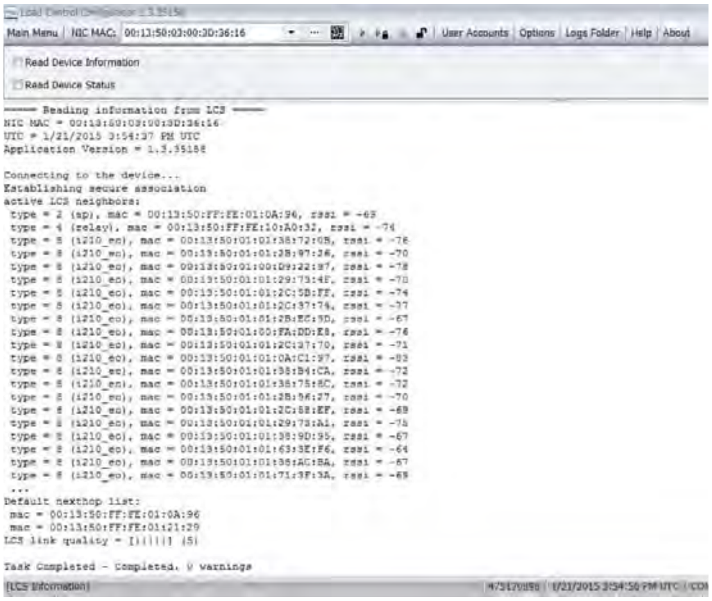

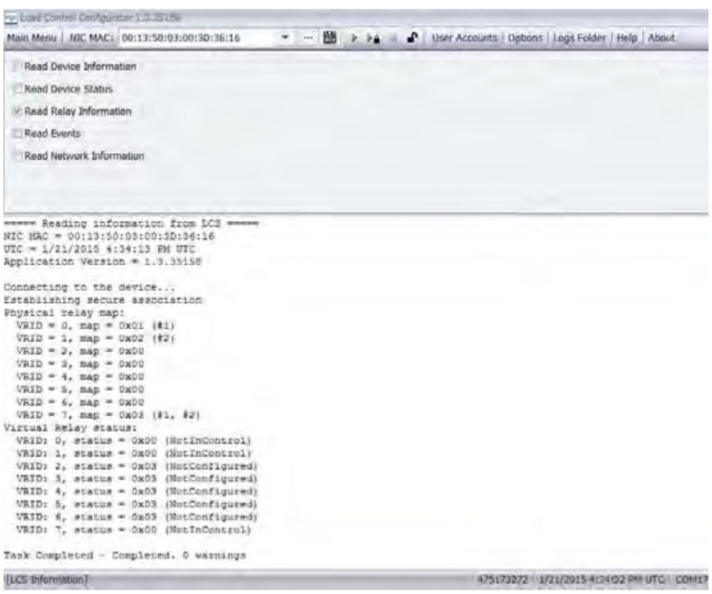

Device 8 (18001263)

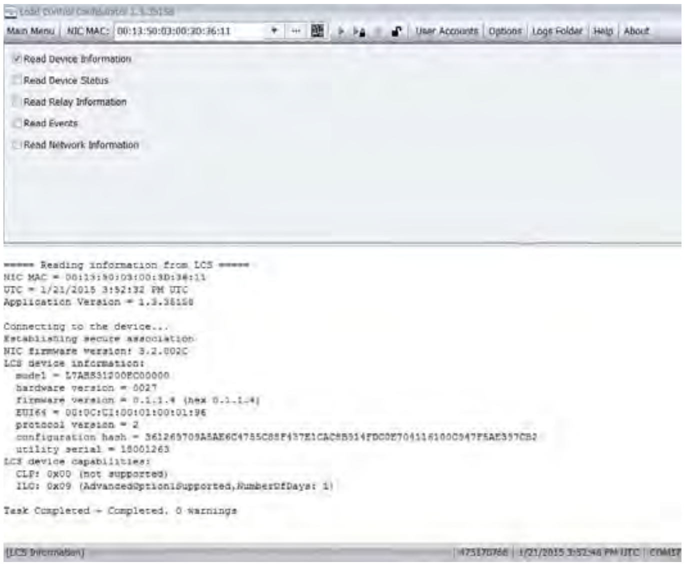
Main Menu
NIC MAC: 00:13:50:03:00:3D:36:11
User Accounts
Options
Logs Folder
Help
About
Read Device Information
Read Device Status
Read Relay Information
Read Events
Read Network Information
===== Reading information from LCS =====
NIC MAC = 00:13:50:03:00:3D:36:11
UTC = 1/21/2015 3:52:32 PM UTC
Application Version = 1.3.35158
Connecting to the device...
Establishing secure association
NIC firmware version: 3.2.002C
LCS device information:
model = L7AR831200EC00000
hardware version = 0027
firmware version = 0.1.1.4 (hex 0.1.1.4)
protocol version = 2
utility serial = 15001263
LCS device capabilities:
CLP: 0x00 (not supported)
ILC: 0x09 (AdvancedOption1Supported,NumberOfDays: 1)
Task Completed - Completed. 0 warnings
[LCS Information]

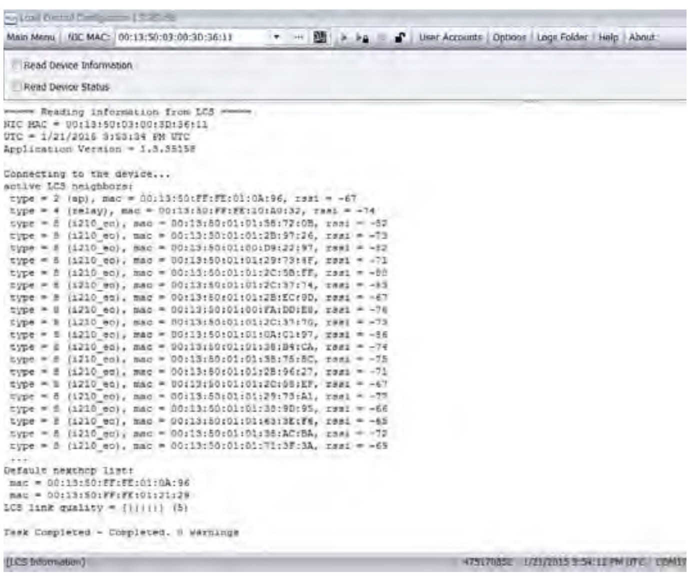
Main Menu
NIC MAC: 00:13:50:03:00:3D:36:11
User Accounts
Options
Logs Folder
Help
About
Read Device Information
Read Device Status
===== Reading information from LCS =====
NIC MAC = 00:13:50:03:00:3D:36:11
UTC = 1/21/2015 3:53:34 PM UTC
Application Version = 1.3.35158
Connecting to the device...
active LCS neighbors:
type = 2 (ap), mac = 00:13:50:FF:FE:01:0A:96, rssi = -67
Default nexthop list:
mac = 00:13:50:FF:FE:01:0A:96
LCS link quality = [|||||] (5)
Task Completed - Completed. 0 warnings
[LCS Information]

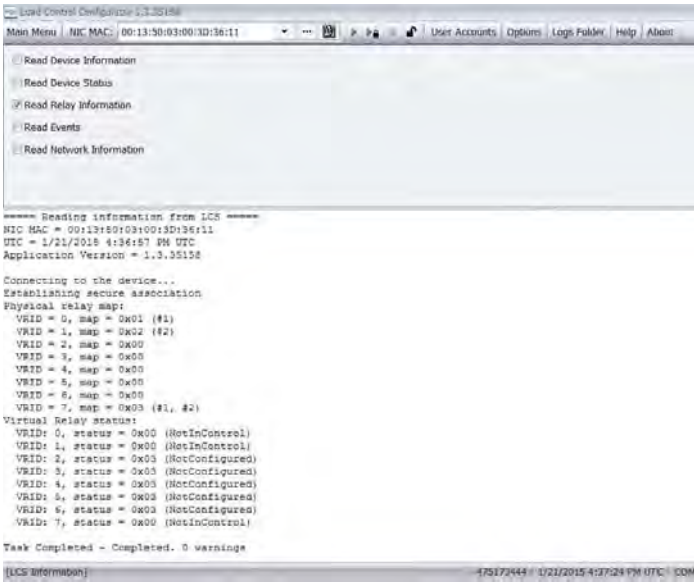

We were able to communicate with all 8 [redacted] switches.

3 VERIFICATION OF APPLIANCE CONTROL

3.1 OBJECTIVE

Switches shall be able to cycle individual relays and combinations of relays. They shall be able to cycle its relay and driver circuit individually as well as simultaneously

3.2 TEST PREREQUISITES AND EQUIPMENT

[redacted] switches MAC ID 00135003003D3634 and MAC ID 0013500300441FA7, HCM, Configuration file with support for single and multiple relay engagement.

3.3 TEST STEPS

1. Ensure configuration is loaded, on each switch type, to support the engagement of single relays, and relays in combination.
2. From HCM, initiate a command to cycle a single relay on each switch.
3. Ensure that the single relay has acted according to requirement and log the result.
4. Log and record the result.

3.4 EXPECTED RESULTS

Verification of functionality.

3.5 TEST RESULTS

5 Amp Relay Control

50% duty cycle event 4 minutes cycle duration, total event duration 8 minutes. Through observation, verified that the switch cycles off for 2-minutes, on for 2-minute and repeats this action two times.

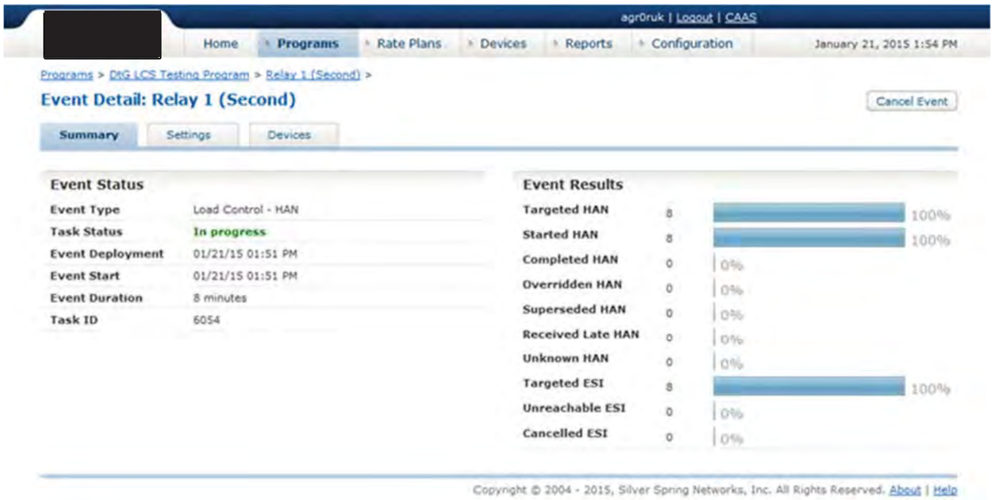

5 Amp Relay Control-Yellow light on

30 Amp Relay Control

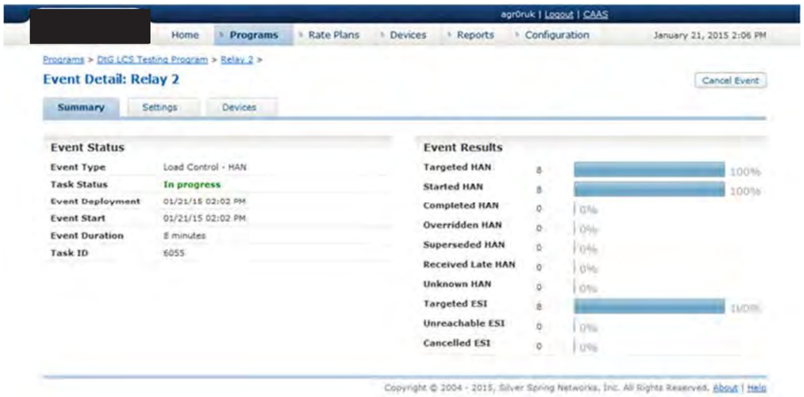

30 Amp Relay Control-Red light on

Both (5 and 30 Amp) relays control

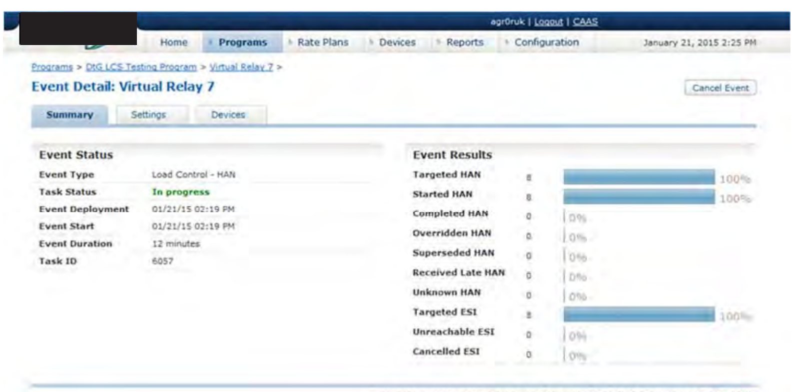

Both (5 and 30 Amp) relays control-Yellow and Red lights on

Both switches were able to cycle individual relays and combinations of relays.

4 VERIFICATION OF LOAD REDUCTION

4.1 OBJECTIVE

Determine achieved load reduction.

4.2 TEST PREREQUISITES AND EQUIPMENT

[redacted] Switches, HCM, functional NAN network

4.3 TEST STEPS

1. Power up switches and allow it time to join the NAN.
2. From HCM, initiate a command to cycle a single relay on each switch.
3. Read load shed potential from HCM before initiating event.
4. Execute the event.
5. Log and record the result.

4.4 EXPECTED RESULTS

Verification of functionality.

4.5 TEST RESULTS

This test was deferred since load reduction can be validated only with full DRMS solution.

5 CONFIRM THAT SWITCHES BROWSE AND REJOIN NETWORKS AUTONOMOUSLY AFTER RECOVERING FROM A LOSS OF POWER

5.1 OBJECTIVE

Switch shall have the capability to browse for networks and select a network to join autonomously.

5.2 TEST PREREQUISITES AND EQUIPMENT

[redacted] Switch S/N 18001263 MAC ID 00135003003D3611, HCM, functional NAN network

5.3 TEST STEPS

1. Power up the switch and allow it time to join the NAN.
2. From HCM ping the switch to ensure that it has joined the NAN without operator intervention.
3. Log and record the results.

5.4 EXPECTED RESULTS

Verification of functionality.

5.5 TEST RESULTS

Ping [redacted] Switch S/N 1800163, MAC ID 00135003003D3611 while the device is without power.

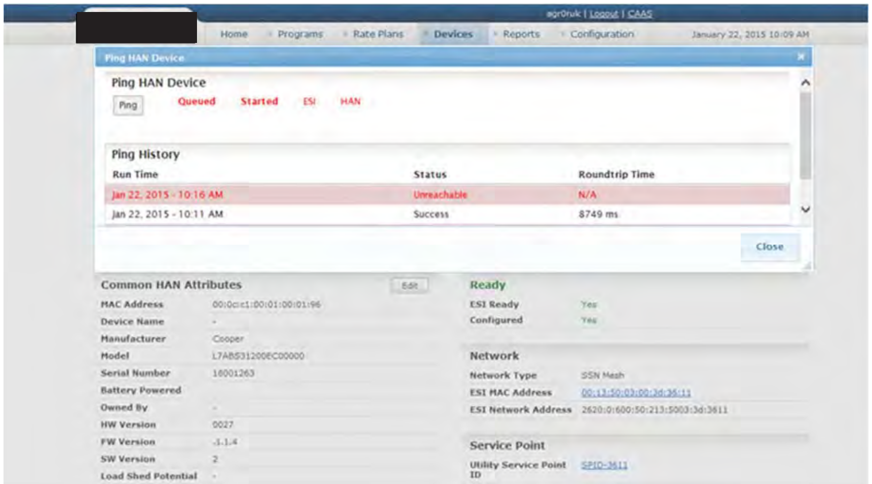

Ping [redacted] Switch S/N 1800163 MAC ID 00135003003D3611 after restoring power connection.

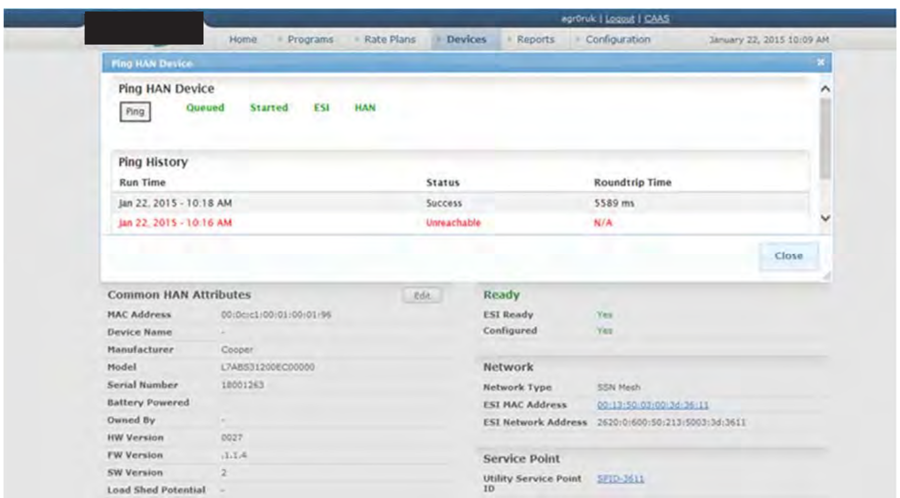

After switch is power up it selected a network to join and joined it autonomously.

6 TIME IS OBTAINED AFTER LOSS OF POWER

6.1 OBJECTIVE

The switch shall query its time server for the correct time after recovering from a loss of power.

6.2 TEST PREREQUISITES AND EQUIPMENT

[redacted] switches MAC: 00135003003D35D9 and MAC: 00135003003D361F, LCC, HCM

6.3 TEST STEPS

1. Power down both switches for 30-seconds, then power them back up.
2. Wait about five-minutes after switches have booted up and then login to both the switches using LCC.
3. Generate an event, to the switches, duration 5-minutes, duty cycle 100% and send the event, immediately.
4. Using LCC, look at the log file and verify that the first few events, after the power up, have the data 1/1/2000 and that the event, sent above, has the correct date and time.
5. Check and verify the time on the switch and the NIC and ensure that it's the correct time.
6. Log and record the results.

6.4 EXPECTED RESULTS

Verification of functionality.

6.5 TIME IS OBTAINED AFTER LOSS OF POWER RESULTS

5 Relay Event

```
Event ID = 477071631:
  Criticality = 100
  VRID = 7
  Start Time = 477071630 (2/12/2015 3:53:50 PM)
  Duty Cycle = 100
  Cycle Period = 5
  Number of Cycles = 1
  Event Control = 0x00 (Cycle Select: Standard)
  Event State = 0x03 (Event completed)
```

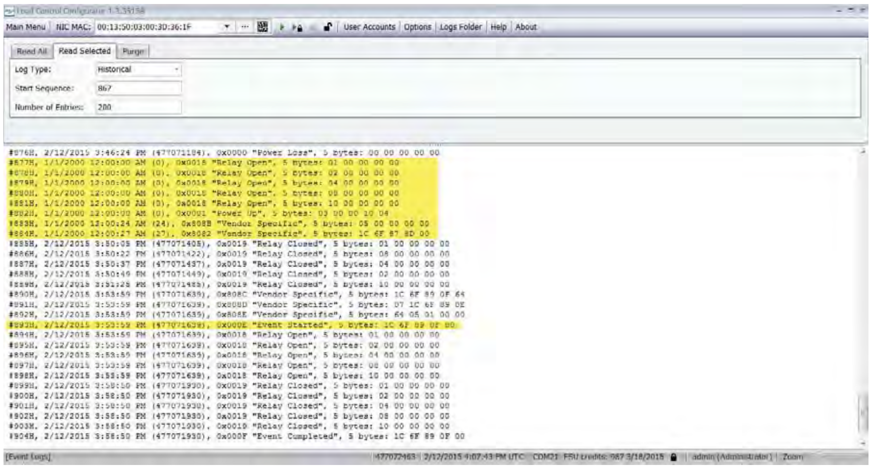

```
Load Control Configurator 1.3.35158
Main Menu | NIC MAC: 00:13:50:03:00:3D:36:1F | User Accounts | Options | Logs Folder | Help | About
Read All | Read Selected | Purge
Log Type: Historical
Start Sequence: 867
Number of Entries: 200

#876H, 2/12/2015 3:46:24 PM (477071184), 0x0000 "Power Loss", 5 bytes: 00 00 00 00 00
#877H, 1/1/2000 12:00:00 AM (0), 0x0018 "Relay Open", 5 bytes: 01 00 00 00 00
#878H, 1/1/2000 12:00:00 AM (0), 0x0018 "Relay Open", 5 bytes: 02 00 00 00 00
#879H, 1/1/2000 12:00:00 AM (0), 0x0018 "Relay Open", 5 bytes: 04 00 00 00 00
#880H, 1/1/2000 12:00:00 AM (0), 0x0018 "Relay Open", 5 bytes: 08 00 00 00 00
#881H, 1/1/2000 12:00:00 AM (0), 0x0018 "Relay Open", 5 bytes: 10 00 00 00 00
#882H, 1/1/2000 12:00:00 AM (0), 0x0001 "Power Up", 5 bytes: 03 00 00 10 04
#883H, 1/1/2000 12:00:24 AM (24), 0x808B "Vendor Specific", 5 bytes: 05 00 00 00 00
#884H, 1/1/2000 12:00:27 AM (27), 0x8082 "Vendor Specific", 5 bytes: 1C 6F 87 8D 00
#885H, 2/12/2015 3:50:05 PM (477071405), 0x0019 "Relay Closed", 5 bytes: 01 00 00 00 00
#886H, 2/12/2015 3:50:22 PM (477071422), 0x0019 "Relay Closed", 5 bytes: 08 00 00 00 00
#887H, 2/12/2015 3:50:37 PM (477071437), 0x0019 "Relay Closed", 5 bytes: 04 00 00 00 00
#888H, 2/12/2015 3:50:49 PM (477071449), 0x0019 "Relay Closed", 5 bytes: 02 00 00 00 00
#889H, 2/12/2015 3:51:25 PM (477071485), 0x0019 "Relay Closed", 5 bytes: 10 00 00 00 00
#890H, 2/12/2015 3:53:59 PM (477071639), 0x808C "Vendor Specific", 5 bytes: 1C 6F 89 0F 64
#891H, 2/12/2015 3:53:59 PM (477071639), 0x808D "Vendor Specific", 5 bytes: 07 1C 6F 89 0E
#892H, 2/12/2015 3:53:59 PM (477071639), 0x808E "Vendor Specific", 5 bytes: 64 05 01 00 00
#893H, 2/12/2015 3:53:59 PM (477071639), 0x000E "Event Started", 5 bytes: 1C 6F 89 0F 00
#894H, 2/12/2015 3:53:59 PM (477071639), 0x0018 "Relay Open", 5 bytes: 01 00 00 00 00
#895H, 2/12/2015 3:53:59 PM (477071639), 0x0018 "Relay Open", 5 bytes: 02 00 00 00 00
#896H, 2/12/2015 3:53:59 PM (477071639), 0x0018 "Relay Open", 5 bytes: 04 00 00 00 00
#897H, 2/12/2015 3:53:59 PM (477071639), 0x0018 "Relay Open", 5 bytes: 08 00 00 00 00
#898H, 2/12/2015 3:53:59 PM (477071639), 0x0018 "Relay Open", 5 bytes: 10 00 00 00 00
#899H, 2/12/2015 3:58:50 PM (477071930), 0x0019 "Relay Closed", 5 bytes: 01 00 00 00 00
#900H, 2/12/2015 3:58:50 PM (477071930), 0x0019 "Relay Closed", 5 bytes: 02 00 00 00 00
#901H, 2/12/2015 3:58:50 PM (477071930), 0x0019 "Relay Closed", 5 bytes: 04 00 00 00 00
#902H, 2/12/2015 3:58:50 PM (477071930), 0x0019 "Relay Closed", 5 bytes: 08 00 00 00 00
#903H, 2/12/2015 3:58:50 PM (477071930), 0x0019 "Relay Closed", 5 bytes: 10 00 00 00 00
#904H, 2/12/2015 3:58:50 PM (477071930), 0x000F "Event Completed", 5 bytes: 1C 6F 89 0F 00

[Event Logs] | 477072463 | 2/12/2015 4:07:43 PM UTC | COM21 | FSU credits: 987 3/18/2015 | admin (Administrator) | Zoom
```

2 Relay Event

```
Event ID = 477071973:
  Criticality = 100
  VRID = 7
  Start Time = 477071971 (2/12/2015 3:59:31 PM)
  Duty Cycle = 100
  Cycle Period = 5
  Number of Cycles = 1
  Event Control = 0x00 (Cycle Select: Standard)
  Event State = 0x03 (Event completed)
```

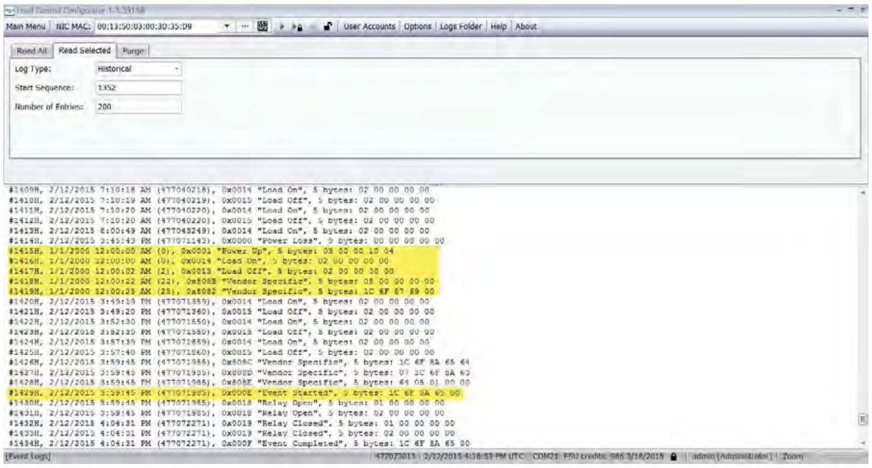

Both switches demanded its time server for the correct time after recovering from a loss of power.

7 TIME MAINTAINED WITHIN +/- 1-MINUTE OVER 24-HOURS

7.1 OBJECTIVE

The switch shall maintain correct time within +/- one minute over 24 hours since last sync.

7.2 TEST PREREQUISITES AND EQUIPMENT

[redacted] switches MACIDs 00135003003D35D9(2 realy) and 00135003003D361F(5 relay) , CATT

7.3 TEST STEPS

1. Login to both switches using LCC and keep the login session open.
2. Obtain the NIC time and the LCS time via “Time, Get" and "LCS Time, Get" commands respectively.
3. From the resultant output verify that the NIC time (UTC = MM/DD/YYY HH:MM:SS [AM/PM} UTC is within +/- 1-minute from the LCS time. The NIC time represents the last value obtained from the network, by the NIC, and the LCS time shows the actual time on the switch.
4. Wait a minimum of 24-hours before proceeding to the next step.
5. Obtain the NIC time and the LCS time via “Time, Get" and "LCS Time, Get" commands respectively.
6. From the resultant output verify that the NIC time (UTC = MM/DD/YYY HH:MM:SS [AM/PM} UTC is within +/- 1-minute from the LCS time. The NIC time represents the last value obtained from the network, by the NIC, and the LCS time shows the actual time on the switch.
7. Log and record the results.

7.4 EXPECTED RESULTS

Verification of functionality.

7.5 TIME MAINTAINED WITHIN +/- 1-MINUTE OVER 24-HOURS RESULTS

Test 1

2 Relay Switch

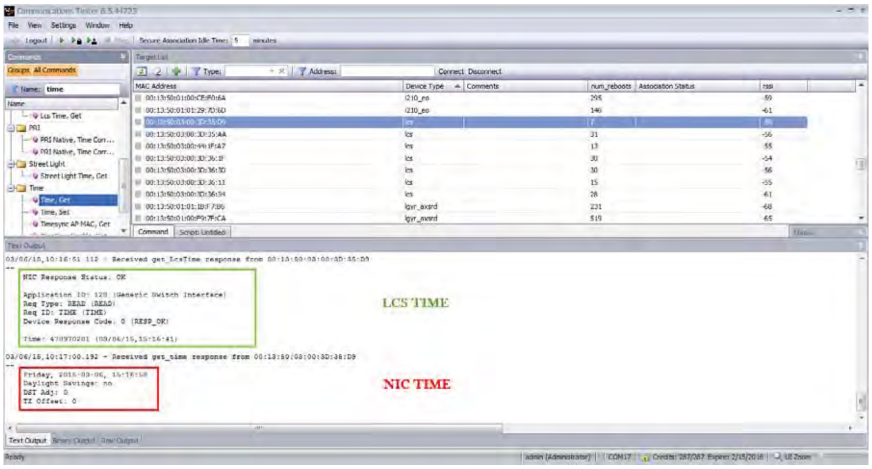

2 Relay Switch (4 Days Later)

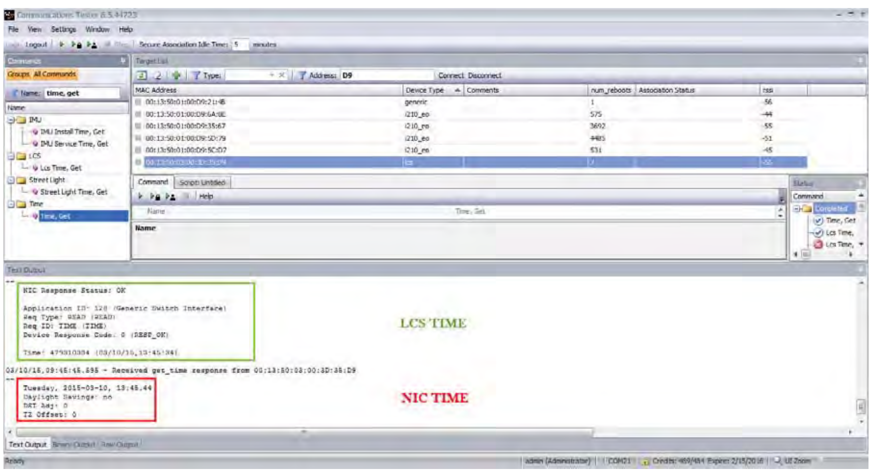

5 Relay Switch

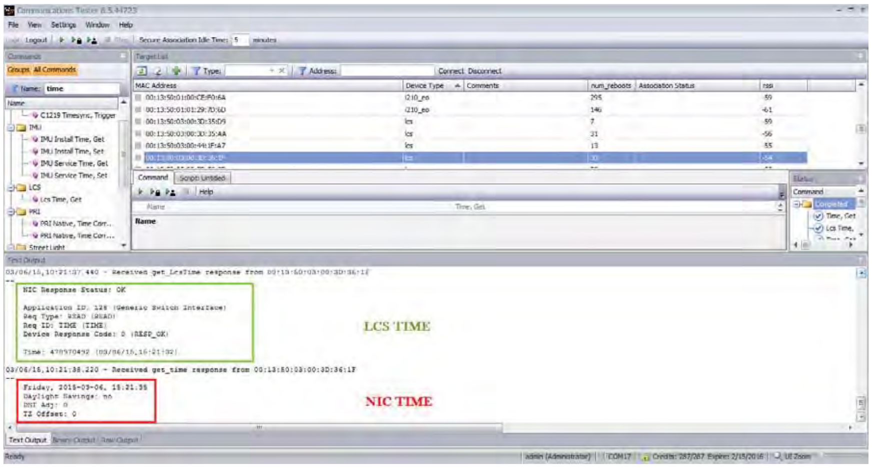

5 Relay Switch (4 Days Later)

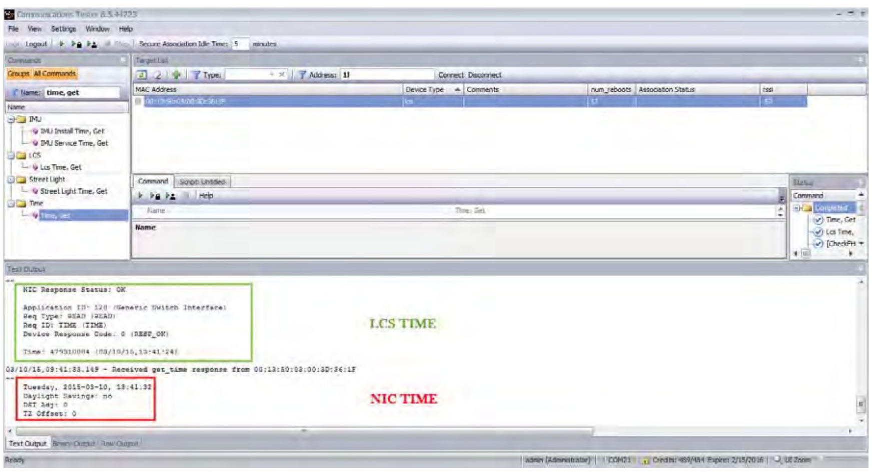

Both switches maintained correct time within +/- one minute over 24 hours since last sync.

8 TIME ON SWITCH SYNCS WHEN INDISCREPANCY WITH TIME SERVER EXISTS

8.1 OBJECTIVE

The switch shall automatically sync with its time server when its clock/calendar do not match the time server's.

8.2 TEST PREREQUISITES AND EQUIPMENT

[redacted] switches MAC ID 00135003003D363D (5 relay) and MAC ID 00135003003D3616 (2 relay), CATT

8.3 TEST STEPS

1. Perform this test in conjunction with the preceding test.
2. Using LCC, login to both the 2F and the 5F switch, and use the "set time" function to configure the time to a value that's different from the current time supplied by the switch.
3. Using LCC, verify that the switch is now using the supplied time.
4. Immediately after the next scheduled time sync event, login to both the 5F and the 2F switch and query the switch time. Verify that it now matches the current time.
5. Log and record the results.

8.4 EXPECTED RESULTS

Verification of functionality.

8.5 TIME ON SWITCH SYNCS WHEN INDISCREPANCY WITH TIME SERVER EXISTS RESULTS

2 Relay Switch

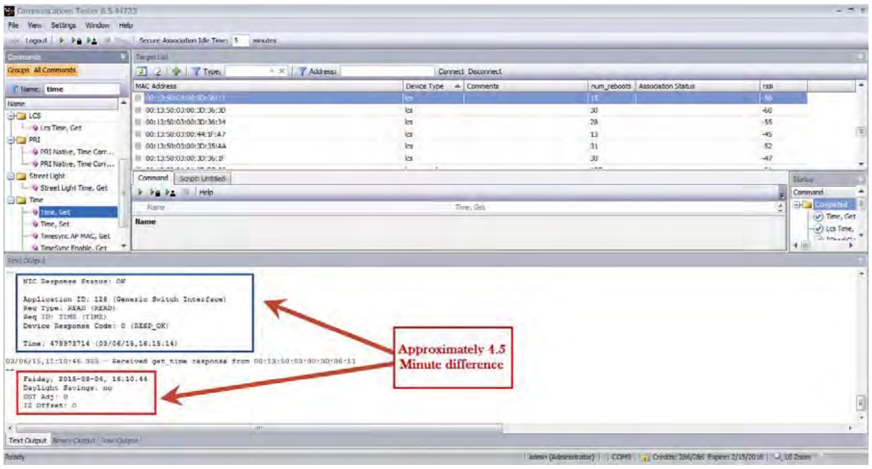

2 Relay Switch (Sync up)

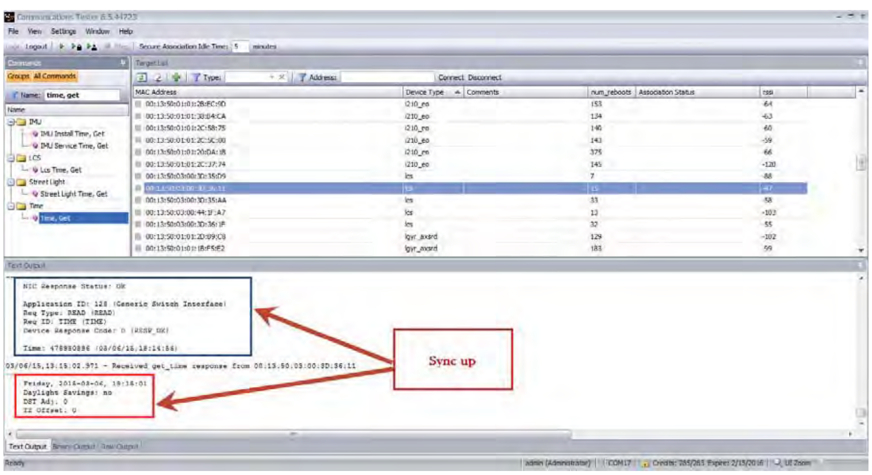

5 Relay Switch

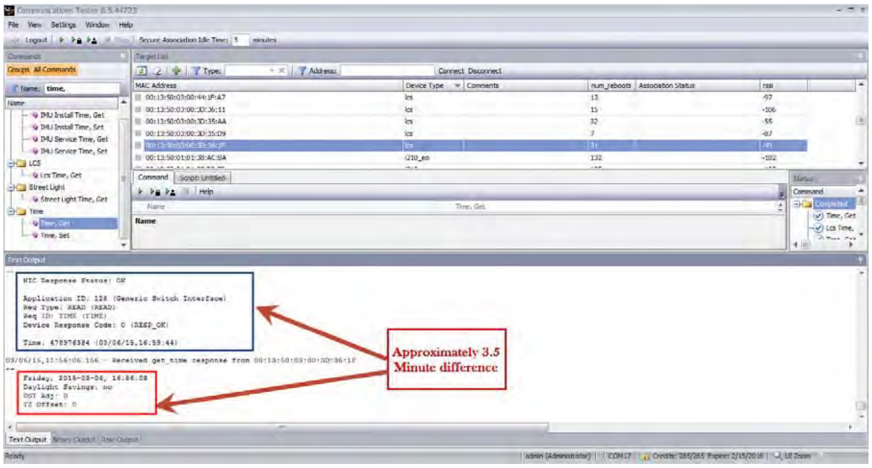

5 Relay Switch (Sync up)

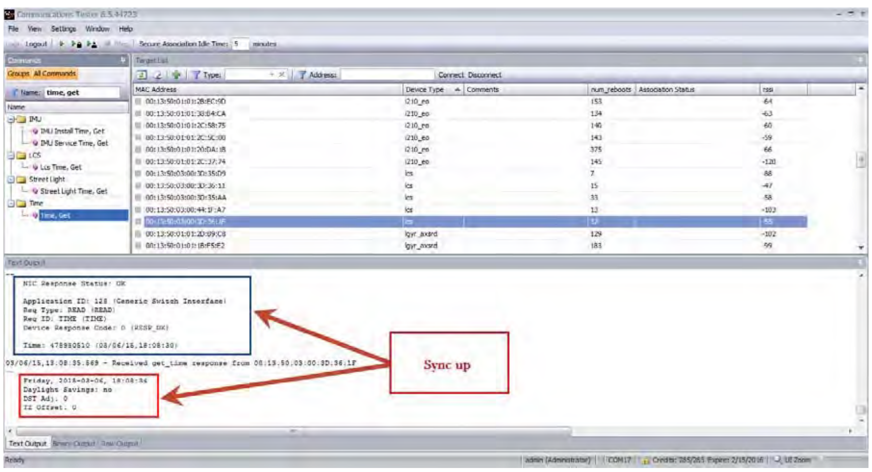

Both switches automatically synchronized with its time server.

9 SWITCH REPONDS TO COMMUNICATIONS LINK TEST

9.1 OBJECTIVE

The switch shall have the capability to respond to a request for an internal diagnostic communications link test.

9.2 TEST PREREQUISITES AND EQUIPMENT

[redacted] switches MAC ID 00135003003D35D9 and MAC ID 00135003003D361F, HCM

9.3 TEST STEPS

1. From HCM, perform a ping to both switches NIC and verify *success*.
2. Verify that ESI sync runs and details are shown on the device details page.
3. Log and record the results.

9.4 EXPECTED RESULTS

Verification of functionality.

9.5 TEST RESULTS

2 Relay MAC ID 00135003003D35D9

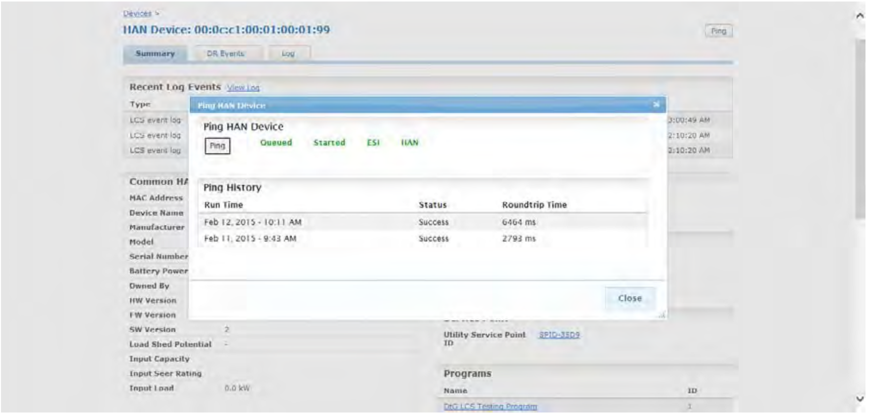

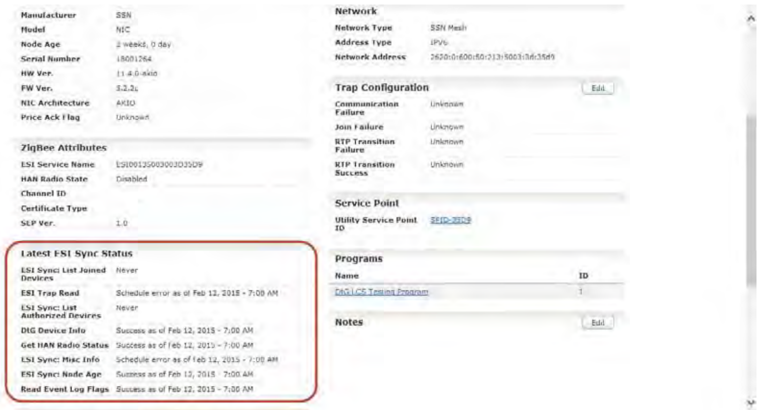

5 Relay MAC ID 00135003003D361F

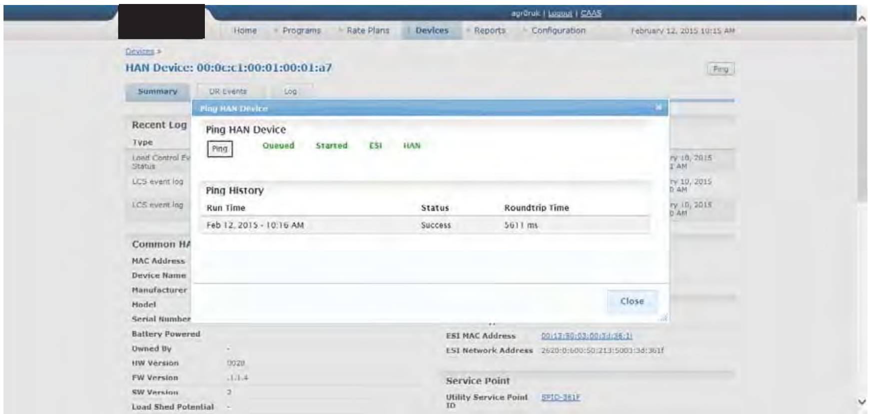

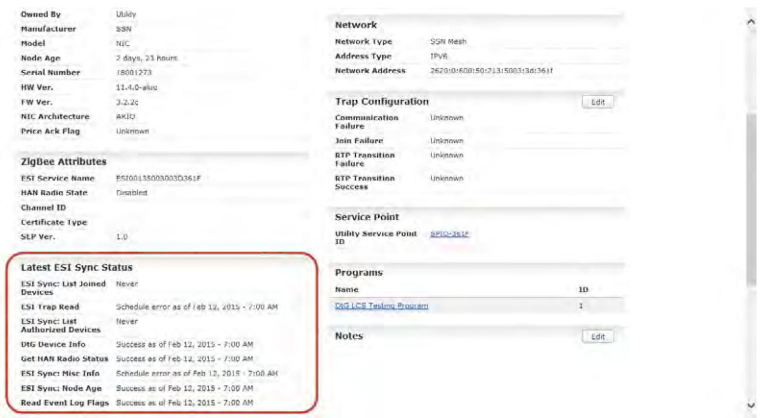

Both switches responded to a request for an internal diagnostic communications link test.

10 CYCLE END-USE LOAD AT DIFFERENT CONTROL DUTY CYCLE

10.1 OBJECTIVE

Switches shall support and execute commands to cycle an end use load at a specific control duty cycle defined as a percentage control-state (between 0-100%) of a control period (in minutes).

10.2 TEST PREREQUISITES AND EQUIPMENT

[redacted] switches, HCM, configuration file loaded on switches to support test.

10.3 TEST STEPS

1. From HCM, execute a command to cycle a load at 80% duty cycle, 5-minute cycle, with duration of 20-minutes. Send the command to all switches.
2. Through observation, verify that the switches cycles off for 4-minutes, on for 1-minute and repeats this action four times.
3. When above is complete, execute a command to cycle a load at 20% duty cycle, 5-minute cycle, with a duration of 20-minutes. Send the command to all switches.
4. Through observation, verify that the switch cycles off for 1-minute, on for 4-minutes, and repeats this action four times.
5. Log and record the results.

10.4 EXPECTED RESULTS

Verification of functionality.

10.5 TEST RESULTS

NOTE: Test step 3 was modified from 20 minutes duration 4 cycles to 40 minutes duration 2 cycles to account for Short Cycle Protection enforcement in the switch. Step 4 was modified to cycle off for 4-minute and on for 16-minutes, again to account for short cycle protection.

80% duty cycle-4 cycles 20 minutes duration

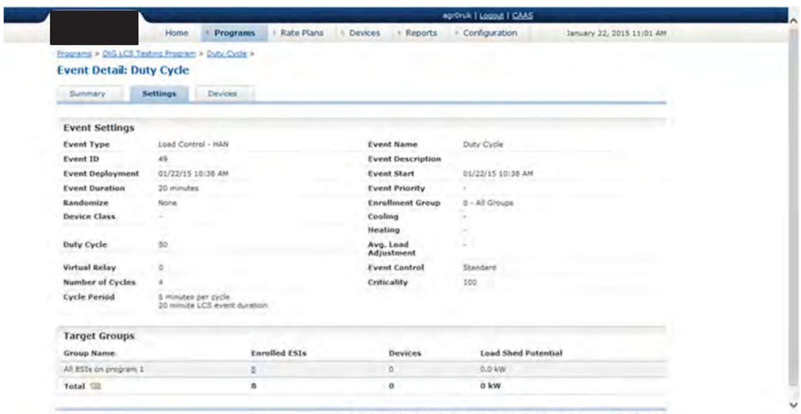

20% duty cycle-2 cycles 40 minutes duration

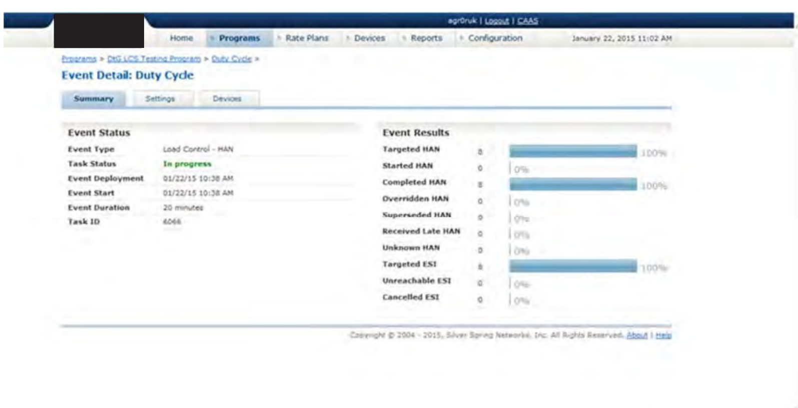

All switches executed control duty cycle as defined.

11 EXECUTION OF NON-CONFLICTING COMMANDS

11.1 OBJECTIVE

The switch shall be able to receive and execute non-conflicting commands related to multiple end use loads simultaneously (e.g. an event for relay 1 is called, then an overlapping event for relay 2 is called. The switch should be able to execute both without conflict).

11.2 TEST PREREQUISITES AND EQUIPMENT

[redacted] switches MAC ID 00135003003D3634 and MAC ID 00135003003D361F, HCM, configuration file loaded on switches to support test.

11.3 TEST STEPS

1. From HCM, generate, and send, a command for switch S/N 18001258 to control the water heater, keeping in mind, that another, command to control A/C will be issued, immediately thereafter, which will overlap with this one.
2. From HCM generate, and send, a second command, to switch S/N 18001258, to control AC which will overlap in time/duration with, but not the same virtual relay as the event created in step 1.
3. Watch the switch for proper execution.
4. Log and record the results.

11.4 EXPECTED RESULTS

Verification of functionality.

11.5 EXECUTION OF NON-CONFLICTING COMMANDS RESULTS

Switch MAC: 00135003003D3634-Two Relays

Event 1-Water Heater (Virtual Relay 1)

Event 2-AC (Virtual Relay 0)

Event Log

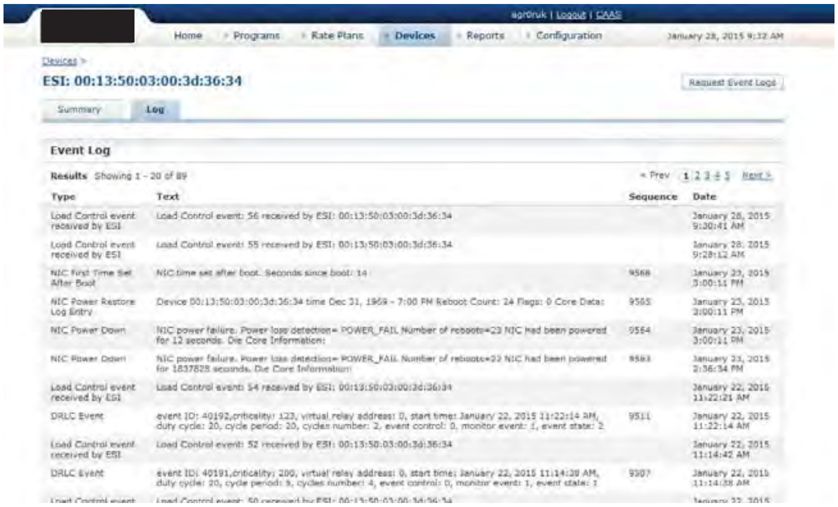
[redacted] agr0ruk | Logout | CAAS

Home | Programs | Rate Plans | Devices | Reports | Configuration — January 28, 2015 9:32 AM

Devices >

ESI: 00:13:50:03:00:3d:36:34 — Request Event Logs

Summary | Log

Event Log

Results Showing 1 - 20 of 89 — « Prev 1 2 3 4 5 Next »

Type	Text	Sequence	Date
Load Control event received by ESI	Load Control event: 56 received by ESI: 00:13:50:03:00:3d:36:34		January 28, 2015 9:30:41 AM
Load Control event received by ESI	Load Control event: 55 received by ESI: 00:13:50:03:00:3d:36:34		January 28, 2015 9:28:12 AM
NIC First Time Set After Boot	NIC time set after boot. Seconds since boot: 14	9568	January 23, 2015 3:00:11 PM
NIC Power Restore Log Entry	Device 00:13:50:03:00:3d:36:34 time Dec 31, 1969 - 7:00 PM Reboot Count: 24 Flags: 0 Core Data:	9565	January 23, 2015 3:00:11 PM
NIC Power Down	NIC power failure. Power loss detection= POWER_FAIL Number of reboots=23 NIC had been powered for 12 seconds. Die Core Information:	9564	January 23, 2015 3:00:11 PM
NIC Power Down	NIC power failure. Power loss detection= POWER_FAIL Number of reboots=22 NIC had been powered for 1837828 seconds. Die Core Information:	9563	January 23, 2015 2:36:34 PM
Load Control event received by ESI	Load Control event: 54 received by ESI: 00:13:50:03:00:3d:36:34		January 22, 2015 11:22:21 AM
DRLC Event	event ID: 40192,criticality: 123, virtual relay address: 0, start time: January 22, 2015 11:22:14 AM, duty cycle: 20, cycle period: 20, cycles number: 2, event control: 0, monitor event: 1, event state: 2	9511	January 22, 2015 11:22:14 AM
Load Control event received by ESI	Load Control event: 52 received by ESI: 00:13:50:03:00:3d:36:34		January 22, 2015 11:14:42 AM
DRLC Event	event ID: 40191,criticality: 200, virtual relay address: 0, start time: January 22, 2015 11:14:38 AM, duty cycle: 20, cycle period: 5, cycles number: 4, event control: 0, monitor event: 1, event state: 1	9507	January 22, 2015 11:14:38 AM
Load Control event	Load Control event: 50 received by ESI: 00:13:50:03:00:3d:36:34		January 22, 2015

Switch MAC ID 00135003003D361F -Five Relays

Event 1- Relay 1 Control (Virtual Relay 0)

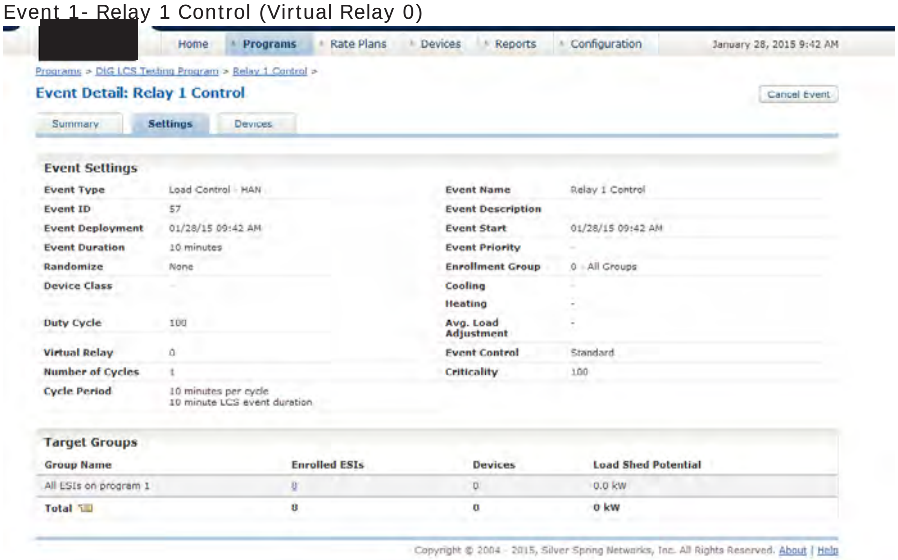
[redacted]

Home | Programs | Rate Plans | Devices | Reports | Configuration — January 28, 2015 9:42 AM

Programs > DIG LCS Testing Program > Relay 1 Control >

Event Detail: Relay 1 Control — Cancel Event

Summary | Settings | Devices

Event Settings

Event Type	Load Control - HAN	Event Name	Relay 1 Control
Event ID	57	Event Description	
Event Deployment	01/28/15 09:42 AM	Event Start	01/28/15 09:42 AM
Event Duration	10 minutes	Event Priority	-
Randomize	None	Enrollment Group	0 - All Groups
Device Class	-	Cooling	-
		Heating	-
Duty Cycle	100	Avg. Load Adjustment	-
Virtual Relay	0	Event Control	Standard
Number of Cycles	1	Criticality	100
Cycle Period	10 minutes per cycle 10 minute LCS event duration		

Target Groups

Group Name	Enrolled ESIs	Devices	Load Shed Potential
All ESIs on program 1	0	0	0.0 kW
Total	0	0	0 kW

Event 2- Relay 2 Control (Virtual Relay 1)

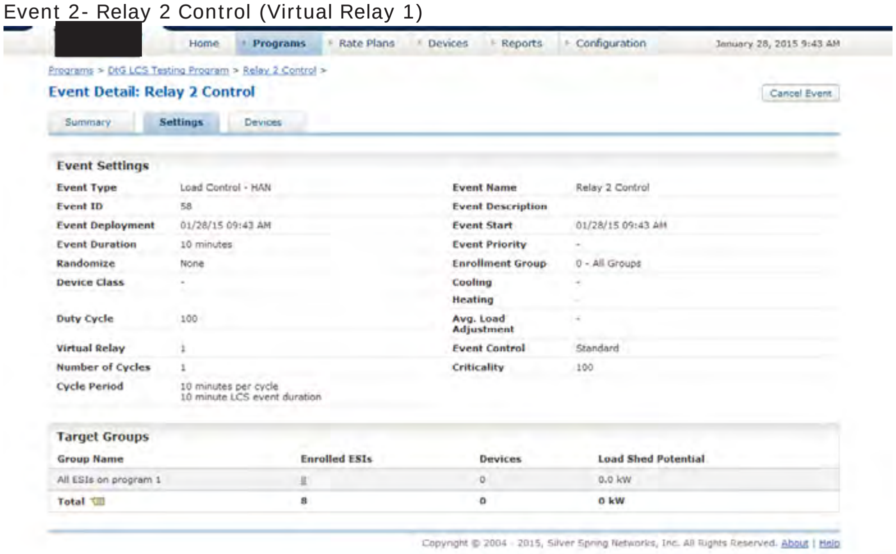
[redacted]
Home | Programs | Rate Plans | Devices | Reports | Configuration   January 28, 2015 9:43 AM

Programs > DtG LCS Testing Program > Relay 2 Control >

Event Detail: Relay 2 Control   Cancel Event

Summary | Settings | Devices

Event Settings

Event Type	Load Control - HAN	Event Name	Relay 2 Control
Event ID	58	Event Description	
Event Deployment	01/28/15 09:43 AM	Event Start	01/28/15 09:43 AM
Event Duration	10 minutes	Event Priority	-
Randomize	None	Enrollment Group	0 - All Groups
Device Class	-	Cooling	-
		Heating	-
Duty Cycle	100	Avg. Load Adjustment	-
Virtual Relay	1	Event Control	Standard
Number of Cycles	1	Criticality	100
Cycle Period	10 minutes per cycle 10 minute LCS event duration		

Target Groups

Group Name	Enrolled ESIs	Devices	Load Shed Potential
All ESIs on program 1	8	0	0.0 kW
Total	8	0	0 kW

Event 3- Relay 3 Control (Virtual Relay 2)

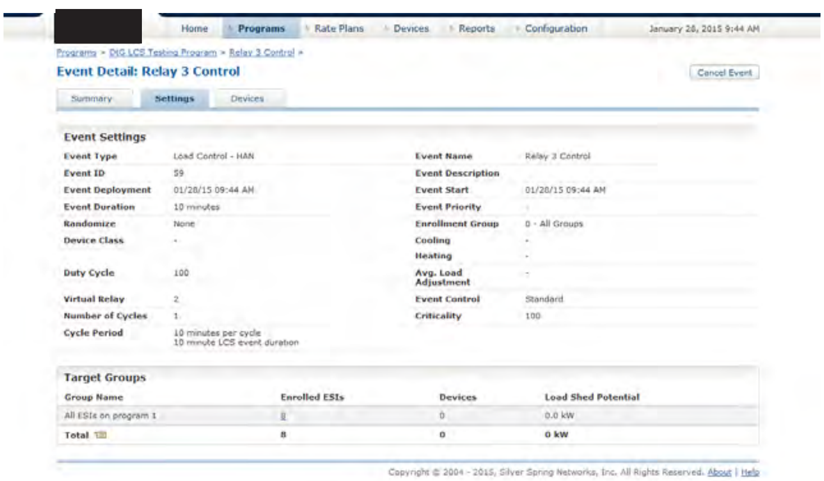
[redacted]
Home | Programs | Rate Plans | Devices | Reports | Configuration   January 28, 2015 9:44 AM

Programs > DtG LCS Testing Program > Relay 3 Control >

Event Detail: Relay 3 Control   Cancel Event

Summary | Settings | Devices

Event Settings

Event Type	Load Control - HAN	Event Name	Relay 3 Control
Event ID	59	Event Description	
Event Deployment	01/28/15 09:44 AM	Event Start	01/28/15 09:44 AM
Event Duration	10 minutes	Event Priority	-
Randomize	None	Enrollment Group	0 - All Groups
Device Class	-	Cooling	-
		Heating	-
Duty Cycle	100	Avg. Load Adjustment	-
Virtual Relay	2	Event Control	Standard
Number of Cycles	1	Criticality	100
Cycle Period	10 minutes per cycle 10 minute LCS event duration		

Target Groups

Group Name	Enrolled ESIs	Devices	Load Shed Potential
All ESIs on program 1	8	0	0.0 kW
Total	8	0	0 kW

Event 4- Relay 4 Control (Virtual Relay 3)

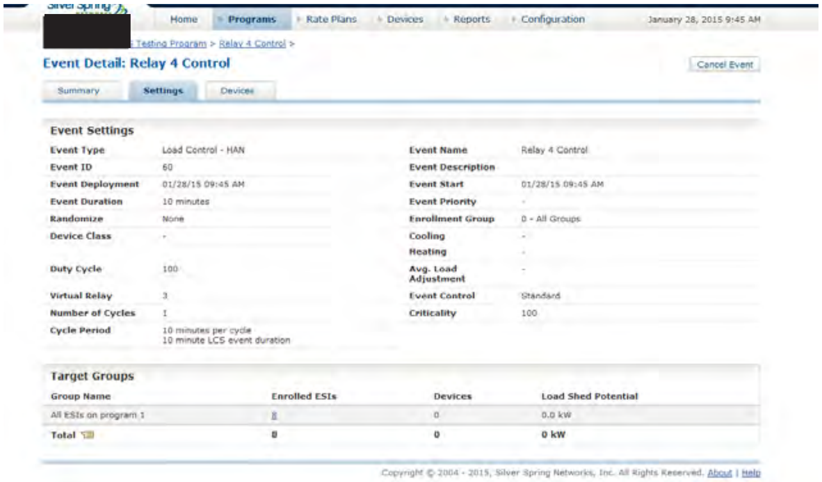

Event 5- Relay 5 Control (Virtual Relay 4)

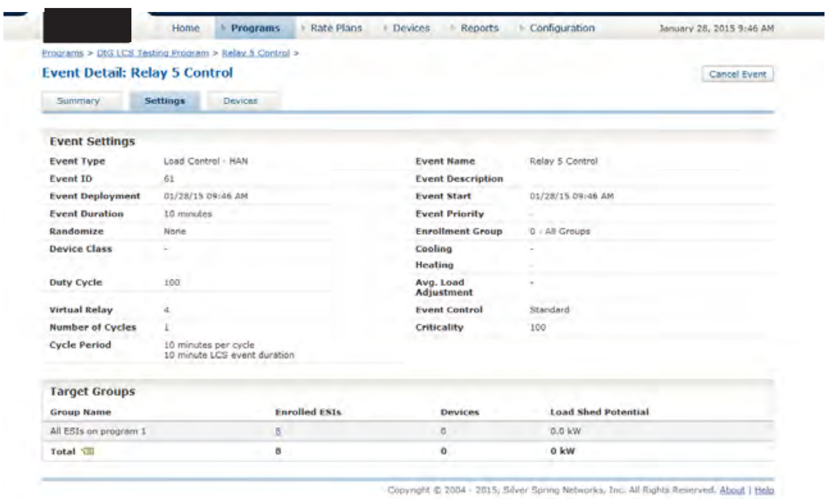

Event Log

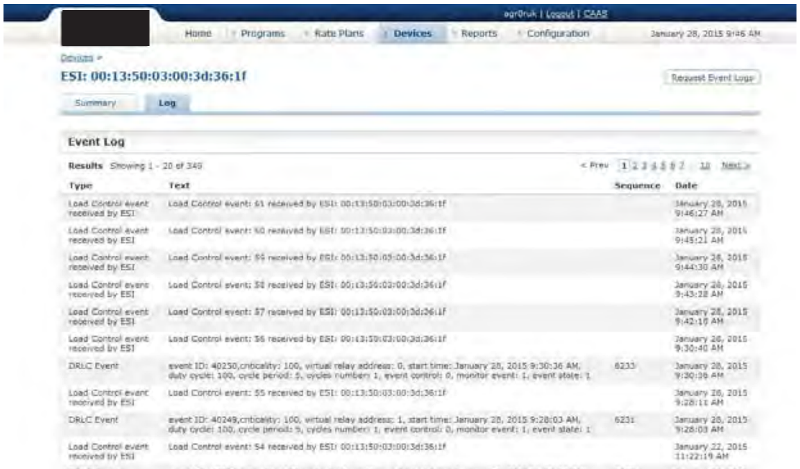

Both switches received and executed non-conflicting commands related to multiple end use loads simultaneously.

12 SUPPORT FOR SINGLE AND MULTIPLE RELAYS MAPPING TO VIRTUAL RELAYS

12.1 OBJECTIVE

The switch shall be able to associate both single and multiple relays to virtual relays.

12.2 TEST PREREQUISITES AND EQUIPMENT

[redacted] Switches, HCM, Configuration File for switch that supports mapping of single and multiple relays to virtual relays.

12.3 TEST STEPS

1. From HCM, generate, and execute, an event, to all switches, that exercises the single relay to single virtual relay mapping.
2. From HCM, generate, and execute, an event to all switches that exercises the multiple relay to virtual relay mapping.
3. Log and record the results.

12.4 EXPECTED RESULTS

Verification of functionality.

12.5 SUPPORT FOR SINGLE AND MULTIPLE RELAYS MAPPING TO VIRTUAL RELAYS RESULTS

For a virtual relay mapped to control a single relay results are shown on test number 9.

Virtual relay mapped to control multiple relays

Switch MAC ID 00135003003D3634 -Two Relays

Switch MAC ID 00135003003D361F -Five Relays

[redacted] agr0ruk | Logout | CAAS

Home | Programs | Rate Plans | Devices | Reports | Configuration   January 28, 2015 11:05 AM

Devices >

ESI: 00:13:50:03:00:3d:36:1f

Request Event Logs

Summary | Log

Event Log

Results Showing 1 - 20 of 355   « Prev 1 2 3 4 5 6 7 ... 18 Next »

Type	Text	Sequence	Date
Load Control event received by ESI	Load Control event: 62 received by ESI: 00:13:50:03:00:3d:36:1f		January 28, 2015 11:03:24 AM
Load Control event received by ESI	Load Control event: 61 received by ESI: 00:13:50:03:00:3d:36:1f		January 28, 2015 9:46:37 AM
DRLC Event	event ID: 40255,criticality: 100, virtual relay address: 4, start time: January 28, 2015 9:46:23 AM, duty cycle: 100, cycle period: 10, cycles number: 1, event control: 0, monitor event: 1, event state: 1	6255	January 28, 2015 9:46:23 AM
Load Control event received by ESI	Load Control event: 60 received by ESI: 00:13:50:03:00:3d:36:1f		January 28, 2015 9:45:21 AM
DRLC Event	event ID: 40254,criticality: 100, virtual relay address: 3, start time: January 28, 2015 9:45:17 AM, duty cycle: 100, cycle period: 10, cycles number: 1, event control: 0, monitor event: 1, event state: 1	6253	January 28, 2015 9:45:17 AM
Load Control event received by ESI	Load Control event: 59 received by ESI: 00:13:50:03:00:3d:36:1f		January 28, 2015 9:44:30 AM
DRLC Event	event ID: 40253,criticality: 100, virtual relay address: 2, start time: January 28, 2015 9:44:25 AM, duty cycle: 100, cycle period: 10, cycles number: 1, event control: 0, monitor event: 1, event state: 1	6251	January 28, 2015 9:44:25 AM
Load Control event received by ESI	Load Control event: 58 received by ESI: 00:13:50:03:00:3d:36:1f		January 28, 2015 9:43:28 AM
DRLC Event	event ID: 40252,criticality: 100, virtual relay address: 1, start time: January 28, 2015 9:43:24 AM, duty cycle: 100, cycle period: 10, cycles number: 1, event control: 0, monitor event: 1, event state: 1	6249	January 28, 2015 9:43:24 AM
Load Control event received by ESI	Load Control event: 57 received by ESI: 00:13:50:03:00:3d:36:1f		January 28, 2015 9:42:10 AM
DRLC Event	event ID: 40251,criticality: 100, virtual relay address: 0, start time: January 28, 2015 9:42:04 AM	6247	January 28, 2015

Both switches associated both single and multiple relays to virtual relays.

13 SWITCH RESUMES IN-PROGRESS EVENTS AFTER LOSS OF POWER – CLP STATE IGNORED

13.1 OBJECTIVE

Switches shall be able to immediately resume any in-progress events after recovering from a loss of power, regardless of whether cold-load pickup is enabled.

13.2 TEST PREREQUISITES AND EQUIPMENT

[redacted] switches, HCM, LCC

13.3 TEST STEPS

1. Ensure that an event, on all switches is in progress.
2. Using LCC verify the status of the event.
3. Power down all switches for 30-seconds and then power them back up.
4. Once switches have joined the network log in to all switches using LCC and verify that they have returned to their original state.
5. Visually inspect the load and determine that the switch has returned to the actual event.
6. Log and record the results.

13.4 EXPECTED RESULTS

Verification of functionality.

13.5 SWITCH RESUMES IN-PROGRESS EVENTS AFTER LOSS OF POWER – CLP STATE IGNORED RESULTS

Our team visually inspected the load and determines that all switches have returned to the actual event immediately after recovering from loss of power. It was the same for 2 relay switches that have not cold load pick up enabled and for the 5 relay switches that have cold load pick up enabled and set to 180 seconds.

Log from LCC

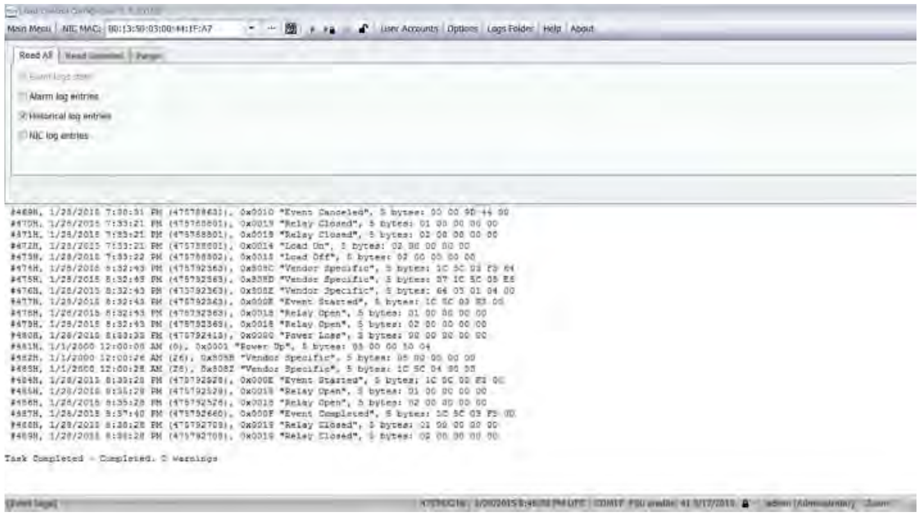

Switches resumed an in-progress event after recovering from a loss of power, regardless of whether cold-load pickup is enabled.

14 CYCLE END-USE LOAD AT DIFFERENT CONTROL DUTY CYCLE

14.1 OBJECTIVE

Switches shall support and execute commands to cycle an end use load at a specific control duty cycle defined as a percentage control-state (between 0-100%) of a control period (in minutes).

14.2 TEST PREREQUISITES AND EQUIPMENT

[redacted] switches, HCM, configuration file loaded on switches to support test.

14.3 TEST STEPS

1. From HCM, execute a command to cycle a load at 50% duty cycle, 10-minute cycle, with a duration of 20-minutes. Send the command to all switches.
2. Through observation, verify that the switches cycles off for 5-minutes, on for 5-minute and repeats this action two times.
3. When above is complete, execute a command to cycle a load at 20% duty cycle, 5-minute cycle, with a duration of 20-minutes. Send the command to all switches.
4. Through observation, verify that the switch cycles off for 1-minute, on for 4-minutes, and repeats this action four times.
5. Log and record the results.

14.4 EXPECTED RESULTS

Verification of functionality.

14.5 TEST RESULTS

Our team visually inspected the load and determines that all switches controlled loads for 5 minutes off and on twice as planned.

50% duty cycle-2 cycles 20 minutes duration

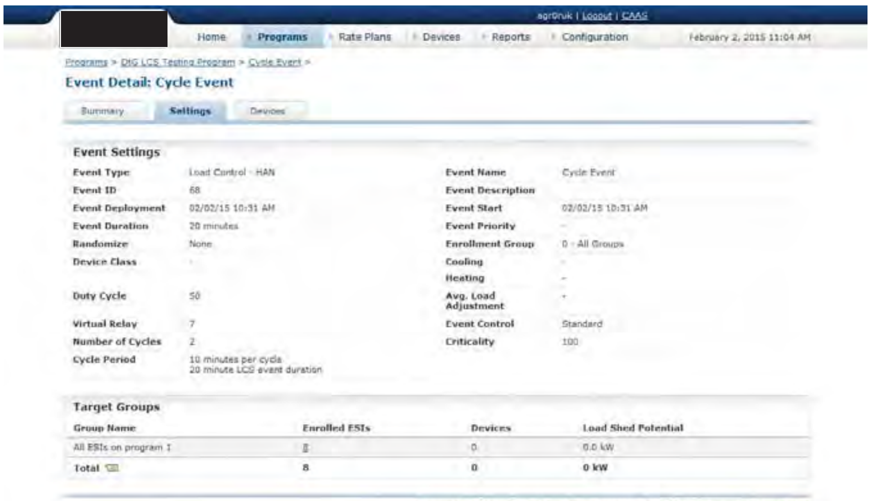

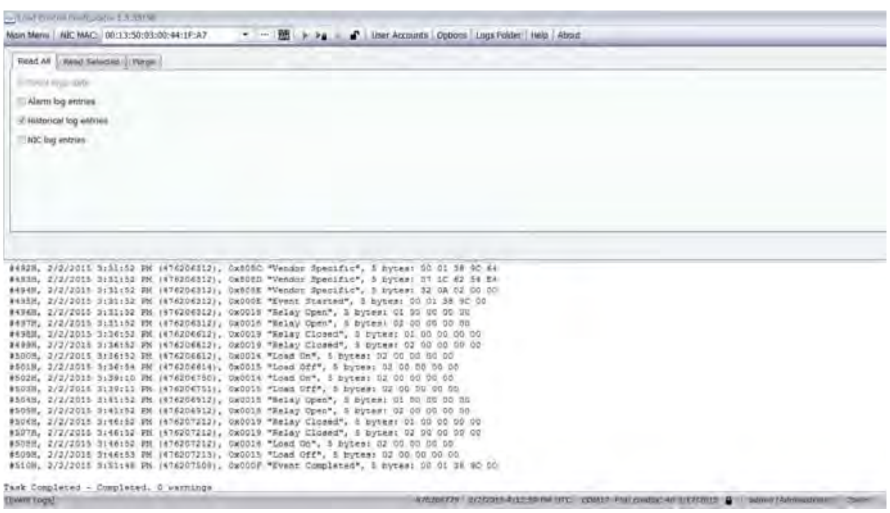

15 SUPPORT FOR RANDOM START/END DELAY

15.1 OBJECTIVE

The switch shall be able to randomly delay the start and end time of an event.

15.2 TEST PREREQUISITES AND EQUIPMENT

[redacted] switches, HCM

15.3 TEST STEPS

1. Using HCM setup an event to randomly delay the start time and end time. Push this event to all switches.
2. Allow the event to occur and verify that the event occurred within the time range specified for randomizing events.
3. Log and record the results.

15.4 EXPECTED RESULTS

The randomly generated start/end times will be the range specified for randomizing events.

15.5 SUPPORT FOR RANDOM START/END DELAY PER SEP RESULTS

Test results, below, show that, currently, both start and end-time randomization are linked together. There is a discrepancy of less than a minute. Darwing will send the question to Robert.

Control all switches for 5 minutes randomizing start and end time

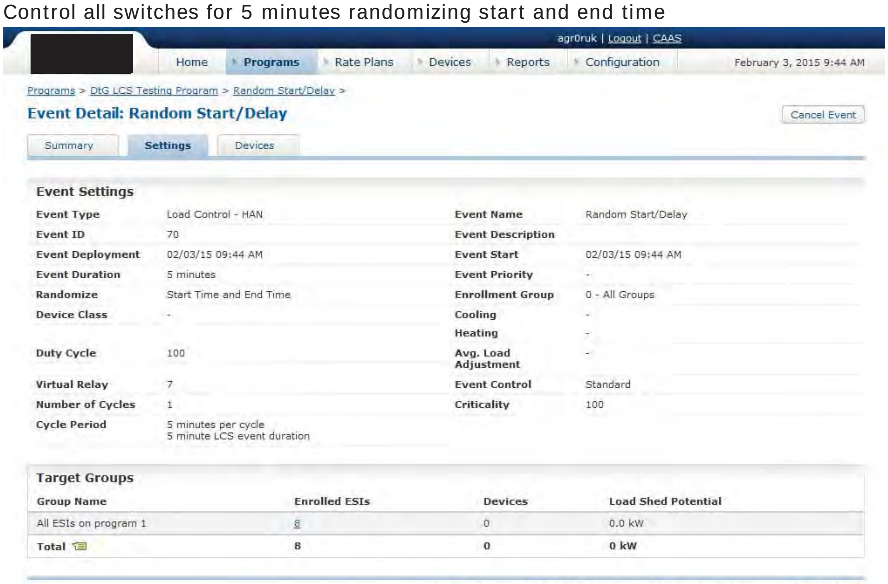

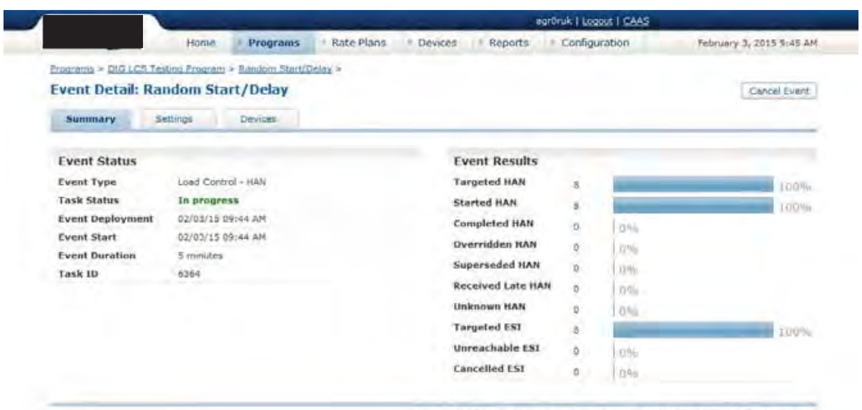

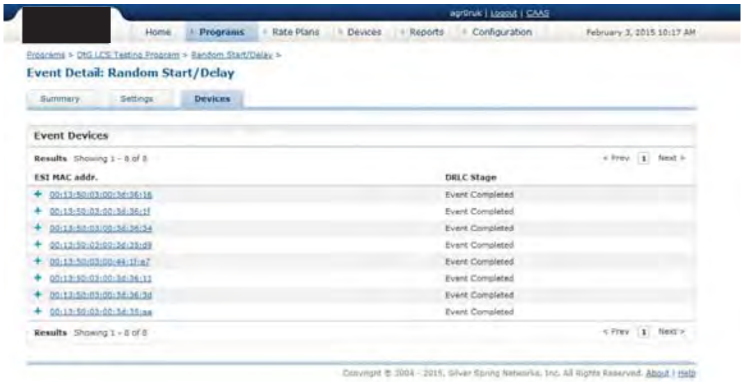

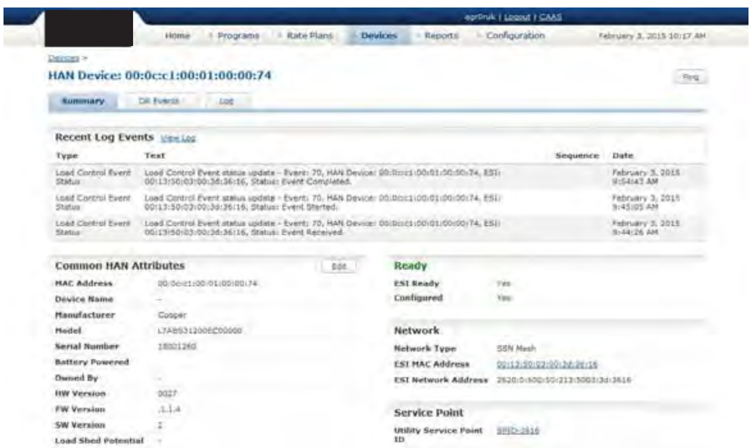

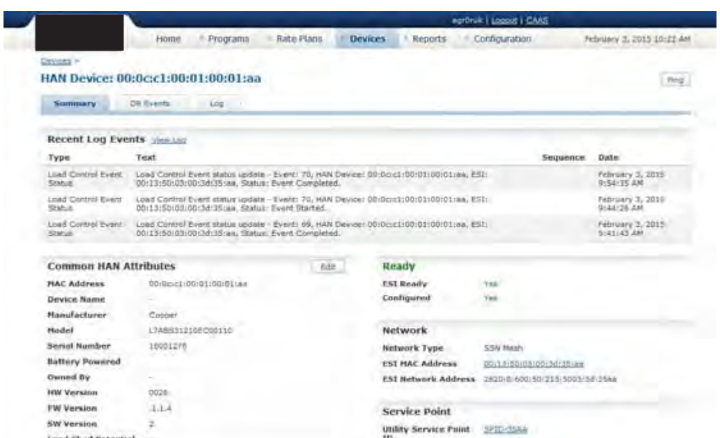

When we checked HCM logs right after the event was completed there was a discrepancy on the start end time (an extended event for approximately 1 minute). We contacted SSN engineers and according to their explanation it is a delay on the reporting, so the stamped time is not the exact start end time. According to them if we get the report from HCM at least an hour after the event or from Load Control Configurator (LCC) we should see the exact time. Below are those reports. There is a difference of 5 hours on time since LCC is on UTC time.

MAC: 00135003003D3616

Load Control Event Status	Load Control Event status update - Event: 73, HAN Device: 00:0c:c1:00:01:00:00:74, ESI: 00:13:50:03:00:3d:36:16, Status: Event Completed.		February 3, 2015 1:55:06 PM
LCS event log	type: 1, log event ID: 20(0x14), payload: Physical Relay (0) data(0100000000)	5512	February 3, 2015 1:54:08 PM
LCS event log	type: 1, log event ID: 15(0x0f), payload: Event ID (80042) data(000138AA00)	5511	February 3, 2015 1:54:08 PM
LCS event log	type: 1, log event ID: 25(0x19), payload: Physical Relay (1) data(0200000000)	5510	February 3, 2015 1:54:08 PM
LCS event log	type: 1, log event ID: 25(0x19), payload: Physical Relay (0) data(0100000000)	5509	February 3, 2015 1:54:08 PM
Load Control Event Status	Load Control Event status update - Event: 73, HAN Device: 00:0c:c1:00:01:00:00:74, ESI: 00:13:50:03:00:3d:36:16, Status: Event Started.		February 3, 2015 12:55:19 PM
LCS event log	type: 1, log event ID: 21(0x15), payload: Physical Relay (0) data(0100000000)	5508	February 3, 2015 12:54:08 PM
LCS event log	type: 1, log event ID: 24(0x18), payload: Physical Relay (1) data(0200000000)	5507	February 3, 2015 12:54:08 PM
LCS event log	type: 1, log event ID: 24(0x18), payload: Physical Relay (0) data(0100000000)	5506	February 3, 2015 12:54:08 PM
LCS event log	type: 1, log event ID: 14(0x0e), payload: Event ID (80042) data(000138AA00)	5505	February 3, 2015 12:54:08 PM
LCS event log	type: 1, log event ID: 20(0x14), payload: Physical Relay (0) data(0100000000)	5504	February 3, 2015 12:44:57 PM
LCS event log	type: 1, log event ID: 21(0x15), payload: Physical Relay (0) data(0100000000)	5503	February 3, 2015 12:38:42 PM
LCS event log	type: 1, log event ID: 20(0x14), payload: Physical Relay (0) data(0100000000)	5502	February 3, 2015 12:16:57 PM
LCS event log	type: 1, log event ID: 21(0x15), payload: Physical Relay (0) data(0100000000)	5501	February 3, 2015 12:11:12 PM
LCS event log	type: 1, log event ID: 32907(0x808b), payload: data(0400000000)	5500	February 3, 2015 12:00:40 PM
LCS event log	type: 1, log event ID: 32907(0x808b), payload: data(0500000000)	5499	February 3, 2015 11:56:23 AM
Load Control Event Status	Load Control Event status update - Event: 73, HAN Device: 00:0c:c1:00:01:00:00:74, ESI: 00:13:50:03:00:3d:36:16, Status: Event Received.		February 3, 2015 11:54:07 AM

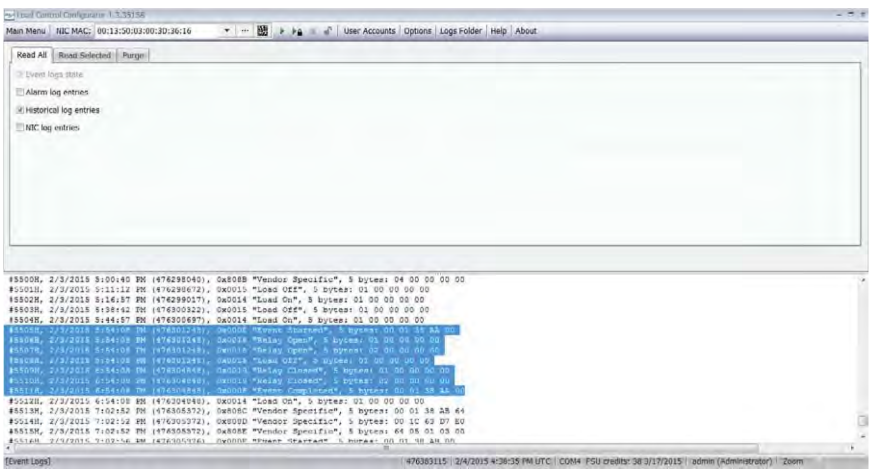

MAC ID 00:13:50:03:00:3D:35: AA

Load Control Event Status	Load Control Event status update - Event: 75, HAN Device: 00:0c:c1:00:01:00:01:aa, ESI: 00:13:50:03:00:3d:35:aa, Status: Event Started.		February 3, 2015 2:50:38 PM
LCS event log	type: 1, log event ID: 24(0x18), payload: Physical Relay (0) data(0100000000)	689	February 3, 2015 2:50:00 PM
LCS event log	type: 1, log event ID: 14(0x0e), payload: Event ID (80044) data(000138AC00)	688	February 3, 2015 2:50:00 PM
Load Control Event Status	Load Control Event status update - Event: 75, HAN Device: 00:0c:c1:00:01:00:01:aa, ESI: 00:13:50:03:00:3d:35:aa, Status: Event Received.		February 3, 2015 2:46:53 PM
LCS event log	type: 1, log event ID: 32910(0x808e), payload: data(6405010000)	687	February 3, 2015 2:46:50 PM
LCS event log	type: 1, log event ID: 32909(0x808d), payload: data(001C63E2E8)	686	February 3, 2015 2:46:50 PM
LCS event log	type: 1, log event ID: 32908(0x808c), payload: data(000138AC64)	685	February 3, 2015 2:46:50 PM
Load Control Event Status	Load Control Event status update - Event: 74, HAN Device: 00:0c:c1:00:01:00:01:aa, ESI: 00:13:50:03:00:3d:35:aa, Status: Event Completed.		February 3, 2015 2:09:51 PM
LCS event log	type: 1, log event ID: 15(0x0f), payload: Event ID (80043) data(000138AB00)	684	February 3, 2015 2:09:11 PM
LCS event log	type: 1, log event ID: 25(0x19), payload: Physical Relay (0) data(0100000000)	683	February 3, 2015 2:09:11 PM
Load Control Event Status	Load Control Event status update - Event: 74, HAN Device: 00:0c:c1:00:01:00:01:aa, ESI: 00:13:50:03:00:3d:35:aa, Status: Event Started.		February 3, 2015 2:03:01 PM
LCS event log	type: 1, log event ID: 24(0x18), payload: Physical Relay (0) data(0100000000)	682	February 3, 2015 2:02:57 PM
LCS event log	type: 1, log event ID: 14(0x0e), payload: Event ID (80043) data(000138AB00)	681	February 3, 2015 2:02:57 PM
LCS event log	type: 1, log event ID: 32910(0x808e), payload: data(6405010300)	680	February 3, 2015 2:02:57 PM
LCS event log	type: 1, log event ID: 32909(0x808d), payload: data(001C63D7E0)	679	February 3, 2015 2:02:57 PM
LCS event log	type: 1, log event ID: 32908(0x808c), payload: data(000138AB64)	678	February 3, 2015 2:02:57 PM
Load Control Event Status	Load Control Event status update - Event: 73, HAN Device: 00:0c:c1:00:01:00:01:aa, ESI: 00:13:50:03:00:3d:35:aa, Status: Event Completed.		February 3, 2015 1:12:00 PM

LCS event log	type: 1, log event ID: 15(0x0f), payload: Event ID (80042) data(000138AA00)	677	February 3, 2015 1:11:38 PM
LCS event log	type: 1, log event ID: 25(0x19), payload: Physical Relay (4) data(1000000000)	676	February 3, 2015 1:11:38 PM
LCS event log	type: 1, log event ID: 25(0x19), payload: Physical Relay (3) data(0800000000)	675	February 3, 2015 1:11:38 PM
LCS event log	type: 1, log event ID: 25(0x19), payload: Physical Relay (2) data(0400000000)	674	February 3, 2015 1:11:38 PM
LCS event log	type: 1, log event ID: 25(0x19), payload: Physical Relay (1) data(0200000000)	673	February 3, 2015 1:11:38 PM
LCS event log	type: 1, log event ID: 25(0x19), payload: Physical Relay (0) data(0100000000)	672	February 3, 2015 1:11:38 PM
Load Control Event Status	Load Control Event status update - Event: 73, HAN Device: 00:0c:c1:00:01:00:01:aa, ESI: 00:13:50:03:00:3d:35:aa, Status: Event Started.		February 3, 2015 12:11:55 PM
LCS event log	type: 1, log event ID: 24(0x18), payload: Physical Relay (4) data(1000000000)	671	February 3, 2015 12:11:38 PM
LCS event log	type: 1, log event ID: 24(0x18), payload: Physical Relay (3) data(0800000000)	670	February 3, 2015 12:11:38 PM
LCS event log	type: 1, log event ID: 24(0x18), payload: Physical Relay (2) data(0400000000)	669	February 3, 2015 12:11:38 PM
LCS event log	type: 1, log event ID: 24(0x18), payload: Physical Relay (1) data(0200000000)	668	February 3, 2015 12:11:38 PM
LCS event log	type: 1, log event ID: 24(0x18), payload: Physical Relay (0) data(0100000000)	667	February 3, 2015 12:11:38 PM
LCS event log	type: 1, log event ID: 14(0x0e), payload: Event ID (80042) data(000138AA00)	666	February 3, 2015 12:11:38 PM
Load Control Event Status	Load Control Event status update - Event: 73, HAN Device: 00:0c:c1:00:01:00:01:aa, ESI: 00:13:50:03:00:3d:35:aa, Status: Event Received.		February 3, 2015 11:54:07 AM

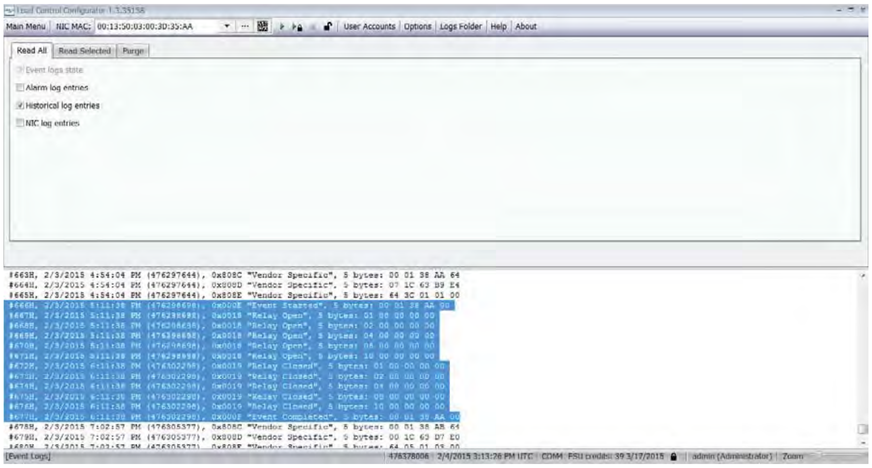
Main Menu
NIC MAC: 00:13:50:03:00:3D:35:AA
User Accounts
Options
Logs Folder
Help
About
Read All
Read Selected
Purge
Alarm log entries
Historical log entries
NIC log entries
#663H, 2/3/2015 4:54:04 PM (476297644), 0x808C "Vendor Specific", 5 bytes: 00 01 38 AA 64
#664H, 2/3/2015 4:54:04 PM (476297644), 0x808D "Vendor Specific", 5 bytes: 07 1C 63 B9 E4
#665H, 2/3/2015 4:54:04 PM (476297644), 0x808E "Vendor Specific", 5 bytes: 64 3C 01 01 00
#678H, 2/3/2015 7:02:57 PM (476305377), 0x808C "Vendor Specific", 5 bytes: 00 01 38 AB 64
#679H, 2/3/2015 7:02:57 PM (476305377), 0x808D "Vendor Specific", 5 bytes: 00 1C 63 D7 E0
[Event Logs]
admin (Administrator)
Zoom

16 SWITCH SUPPORTS CANCEL ALL LOAD CONTROL EVENTS

16.1 OBJECTIVE

The switch shall be able to receive and execute event cancel commands.

16.2 TEST PREREQUISITES AND EQUIPMENT

[redacted] switches, HCM.

16.3 TEST STEPS

1. From HCM, ensure that there are currently in process load control events on all switches.
2. From HCM, generate a process to cancel all load control events.
3. Ensure that the load control events were cancelled according to expectation.
4. Log and record the results.

16.4 EXPECTED RESULTS

Verification of functionality.

16.5 SWITCH SUPPORTS CANCEL ALL LOAD CONTROL EVENTS RESULTS

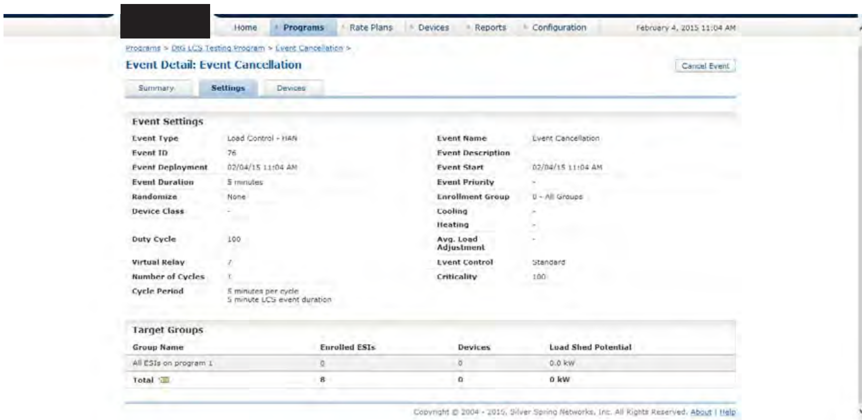

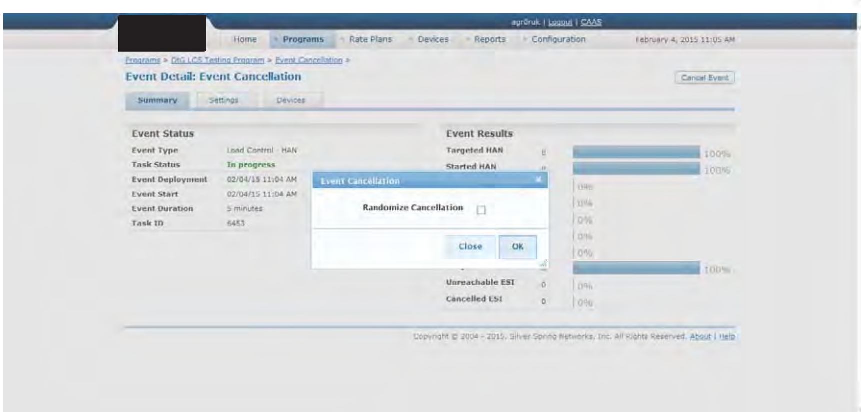

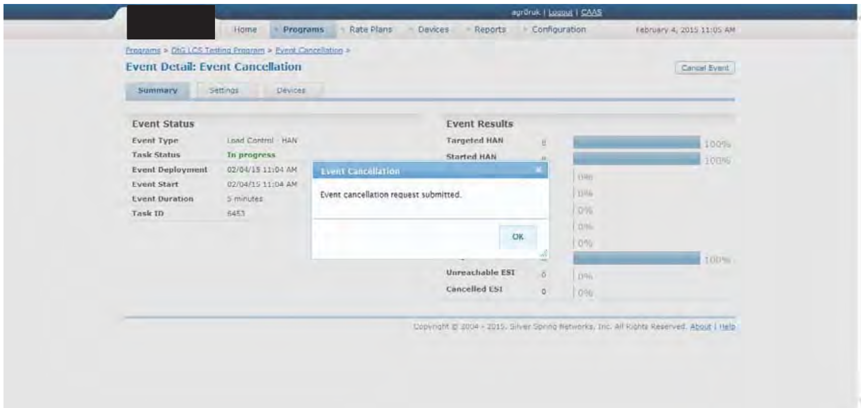
Home
Programs
Rate Plans
Devices
Reports
Configuration
Event Detail: Event Cancellation
Cancel Event
Summary
Settings
Devices
Event Status
Event Type
Task Status
In progress
Event Deployment
Event Start
Event Duration
Task ID
Event Results
Targeted HAN
Started HAN
Event Cancellation
Event cancellation request submitted.
OK
Unreachable ESI
Cancelled ESI

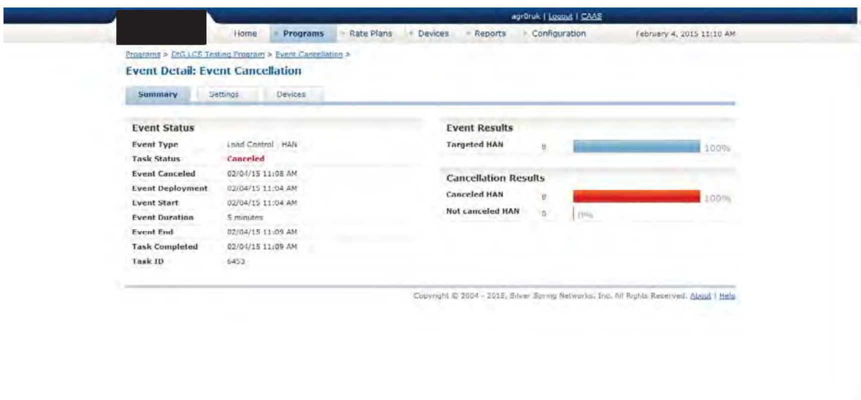
Home
Programs
Rate Plans
Devices
Reports
Configuration
Event Detail: Event Cancellation
Summary
Settings
Devices
Event Status
Event Type
Task Status
Canceled
Event Canceled
Event Deployment
Event Start
Event Duration
Event End
Task Completed
Task ID
Event Results
Targeted HAN
Cancellation Results
Canceled HAN
Not canceled HAN

17 SWITCH SUPPORTS CANCELLATION OF SINGLE EVENT WITHOUT IMPACT TO EXISTING EVENTS

17.1 OBJECTIVE

The switch shall be able to cancel an individual load control event without cancelling other events that are executing on the switch (e.g. two events are triggered for multiple end use loads, the switch shall be able to receive and execute a cancel command for one of those events while continuing to execute the event on the other devices).

17.2 TEST PREREQUISITES AND EQUIPMENT

[redacted] Switches, HCM

17.3 TEST STEPS

1. From HCM, generate an event for a virtual relay on all switches and push the event to the switches.
2. From HCM, generate a separate event for a different virtual relay on a all switches and push the event to the switch. Ensure that the start time, for this event, overlaps the event above.
3. Allow the events to execute.
4. From HCM, cancel one of the two, in progress, events, from above on all switchs and push the event to the switches.
5. Ensure that only the expected event was cancelled and that the other event remained in progress.
6. Log and record the results.

17.4 EXPECTED RESULTS

Verification of functionality.

17.5 SWITCH SUPPORTS CANCELLATION OF SINGLE EVENT WITHOUT IMPACT TO EXISTING EVENTS RESULTS

Event Cancellation VR0/VR1

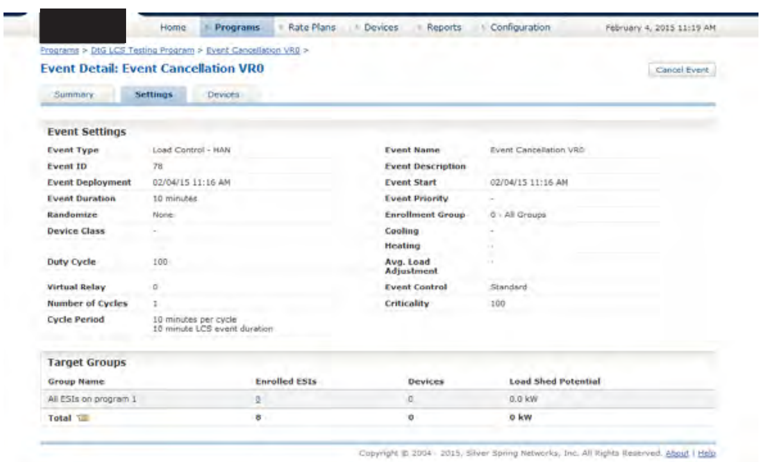

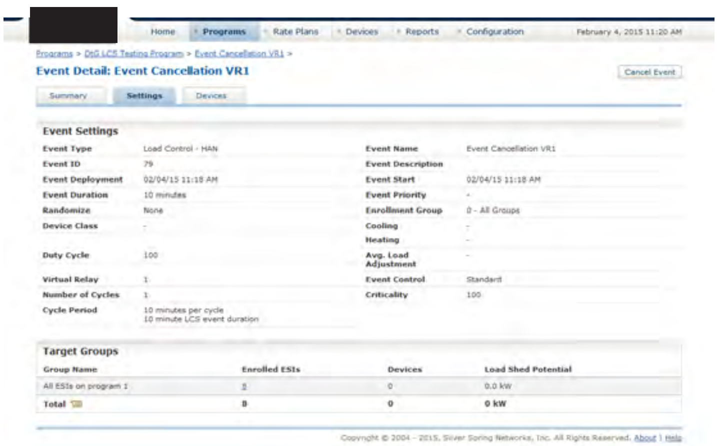

Cancel Event 1

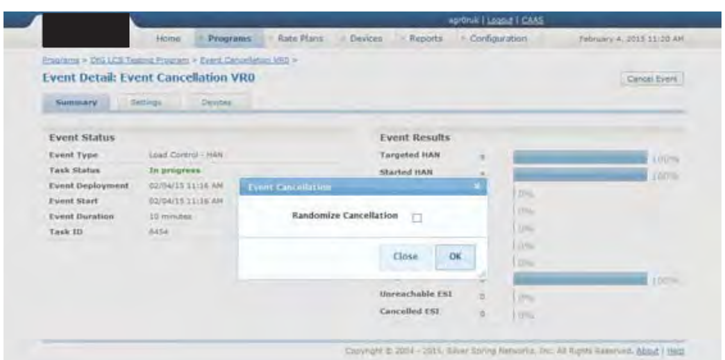

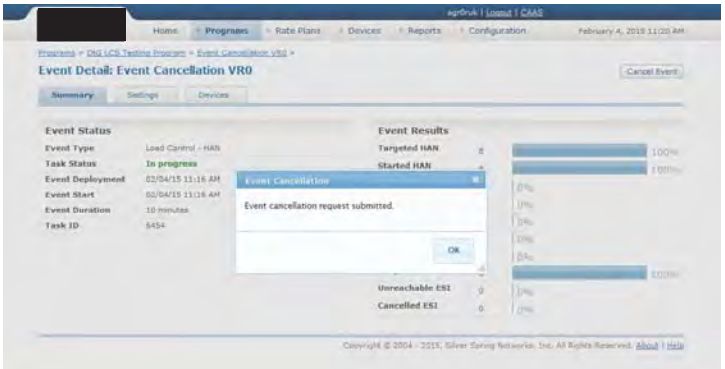
[redacted]
agr0ruk | Logout | CAAS
Home
Programs
Rate Plans
Devices
Reports
Configuration
February 4, 2015 11:20 AM
Programs > DIG LCS Testing Program > Event Cancellation VR0 >
Event Detail: Event Cancellation VR0
Cancel Event
Summary
Settings
Devices
Event Status
Event Type Load Control - HAN
Task Status In progress
Event Deployment 02/04/15 11:16 AM
Event Start 02/04/15 11:16 AM
Event Duration 10 minutes
Task ID 6454
Event Results
Targeted HAN 8 100%
Started HAN
Event Cancellation
Event cancellation request submitted.
OK
Unreachable ESI 0 0%
Cancelled ESI 0 0%
Copyright © 2004 - 2015, Silver Spring Networks, Inc. All Rights Reserved. About | Help


[redacted]
agr0ruk | Logout | CAAS
Home
Programs
Rate Plans
Devices
Reports
Configuration
February 4, 2015 11:21 AM
Programs > DIG LCS Testing Program > Event Cancellation VR0 >
Event Detail: Event Cancellation VR0
Summary
Settings
Devices
Event Status
Event Type Load Control - HAN
Task Status Cancellation in progress
Event Canceled 02/04/15 11:20 AM
Event Deployment 02/04/15 11:16 AM
Event Start 02/04/15 11:16 AM
Event Duration 10 minutes
Task ID 6454
Event Results
Targeted HAN 8 100%
Cancellation Results
Canceled HAN 0 0%
Not canceled HAN 8 100%
Copyright © 2004 - 2015, Silver Spring Networks, Inc. All Rights Reserved. About | Help


[redacted]
agr0ruk | Logout | CAAS
Home
Programs
Rate Plans
Devices
Reports
Configuration
February 4, 2015 11:21 AM
Programs > DIG LCS Testing Program > Event Cancellation VR0 >
Event Detail: Event Cancellation VR0
Summary
Settings
Devices
Event Status
Event Type Load Control - HAN
Task Status Cancellation in progress
Event Canceled 02/04/15 11:20 AM
Event Deployment 02/04/15 11:16 AM
Event Start 02/04/15 11:16 AM
Event Duration 10 minutes
Task ID 6454
Event Results
Targeted HAN 8 100%
Cancellation Results
Canceled HAN 6 75%
Not canceled HAN 2 25%
Copyright © 2004 - 2015, Silver Spring Networks, Inc. All Rights Reserved. About | Help

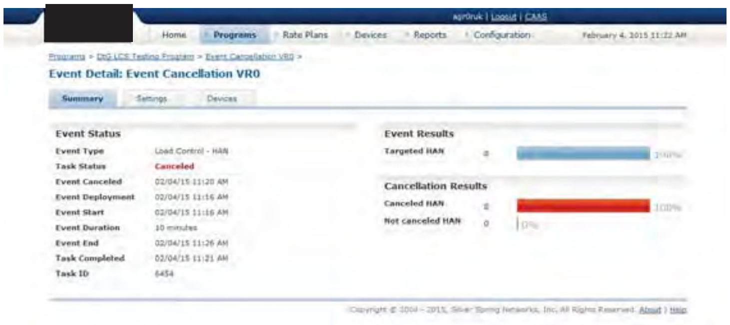

Event Active

18 TRUECYCLE TEST

18.1 OBJECTIVE

This test is done in two parts, the first part is to demonstrate that the LCR6600S can collect and save daily runtimes to form a 24 hour historical runtime profile. The second part demonstrates how the LCR6600S uses the 24 hour historical profile along with the scaling the hour before to adjust the control rate for oversized AC systems.

18.2 TEST PREREQUISITES AND EQUIPMENT

[redacted] switches, Black box serial to USB converter, Laptop with Denali for setting up tests and viewing test results. The test also used a test board that emulated thermostat call for cool circuits operating at known rates for the test LCRs to monitor and control. *(any need for a photo of the test setup here? I can provide one if needed)*

18.3 TEST STEPS

Part 1: Demonstrate ability to collect and save data to 24 hour historical runtime profile

1. Connect test LCRs to the test board with the thermostat emulator circuits running at a known rate for a complete 24 hour day (midnight to midnight).
2. With Denali monitor the hourly runtimes and the historical profiles. Confirm that a complete 24 hour day, midnight to midnight is available in the LCR.
3. Send a save today message through the [redacted].
4. Confirm that the data was saved into the existing 24 hour runtime profile at 1/8th weighting

Part 2: Demonstrate the use of the 24 hour historical runtime profile for adjusting control rate

1. Connect the Test LCRs to the test board with the thermostat emulator circuits running a known rate for at least one full clock hour.
2. Set the 24 hour historical profile to a known flat curve using Denali.
3. Send a True-Cycle control command to the test LCRs
4. With Denali, observe the implemented control cycle rate.

18.4 EXPECTED RESULTS

Part 1) Demonstrate ability to collect and save data to the 24 hour historical runtime profile.

The 24 hour historical run-time profile in the test LCRs started at a flat 100%. The thermostat emulator circuits were set at 80% and 90%. Denali showed that the LCRs had correctly monitored the 85% and 90% values for the extended 24 hour period. After the Save yesterday command was send to the test LCRs, the historical runtime profiles changed to a flat 97% and 98% respectively for the hours 08:00 to 24:00 as expected. The hours 0:00 and 7:00 went to a flat 0% which was not as expected. A bug in the firmware that causes these values going to 0% has been identified.

Part 2) Demonstrate the use of the 24 hour historical runtime profile and TrueCycle in adjusting the control rate

Several tests were run with various historical profiles and scaling rates. In all 6 tests the actual results matched the expected results.

Test Run	Historical Profile	Hour Before Runtime for Scaling	Expected Cycle Rate	Actual Cycle Rate
1	60%	85%	58%	58%
2	75%	85%	58%	58%
3	100%	90%	55%	55%
4	97%	80%	60%	60%
5	75%	80%	60%	60%
6	60%	90%	55%	55%

19 SUPPORT FOR “CRITICALITY” LEVELS EDITING AN EVENT

19.1 OBJECTIVE

The switch shall support the Demand Response and Load Control event data field "Criticality" levels.

19.2 TEST PREREQUISITES AND EQUIPMENT

[redacted] switch MAC: 00135003003D3634, HCM.

19.3 TEST STEPS

1. Using HCM, generate a switch event on MAC: 00135003003D3634 switch with a criticality value of 0, 5-minute duration, 100% duty cycle.
2. Wait for the previous event to complete.
3. Using LCC, generate a switch event on MAC: 00135003003D3634 switch with a criticality value of 100, 1 cycle, 5-minute duration, 100% duty cycle.
4. Using LCC, generate a switch even on MAC: 00135003003D3634 switch with a criticality value of 50, 1 cycle, 5-minute duration, 100% duty cycle. Ensure that this event is sent while the previous event is in progress.
5. Ensure all events are generated, logged and executed with the appropriate criticality level.
6. Ensure that the event in step 4 is rejected by the switch due to the lower criticality value.
7. Log and record the results.

19.4 EXPECTED RESULTS

Verification of functionality.

In editing superseding events we can edit duty cycle or number of cycles. Start time shall be the same. Criticality level shall be higher. New event will modify the previous one.

In replacement superseding events you can change relays to be controlled, duty cycle and or number of cycles. Start time shall be the same. Criticality level shall be higher. New event will replace the previous one.

19.5 SUPPORT FOR "CRITICALITY" LEVELS RESULTS

Event 1-HCM

Programs > DtG LCS Testing Program > Criticality Support >

Event Detail: Criticality Support

Cancel Event

Summary | **Settings** | Devices

Event Settings

Event Type	Load Control - HAN	**Event Name**	Criticality Support
Event ID	81	**Event Description**	
Event Deployment	02/10/15 09:10 AM	**Event Start**	02/10/15 09:10 AM
Event Duration	5 minutes	**Event Priority**	-
Randomize	None	**Enrollment Group**	0 - All Groups
Device Class	-	**Cooling**	-
		Heating	-
Duty Cycle	100	**Avg. Load Adjustment**	-
Virtual Relay	7	**Event Control**	Standard
Number of Cycles	1	**Criticality**	0
Cycle Period	5 minutes per cycle 5 minute LCS event duration		

Target Groups

Group Name	Enrolled ESIs	Devices	Load Shed Potential
All ESIs on program 1	8	0	0.0 kW
Total	**8**	**0**	**0 kW**

[redacted] zxm0pqu | Logout | CAAS

Home | **Programs** | Rate Plans | Devices | Reports | Configuration | February 10, 2015 9:11 AM

Programs > DtG LCS Testing Program > Criticality Support >

Event Detail: Criticality Support

Cancel Event

Summary | Settings | Devices

Event Status

Event Type	Load Control - HAN
Task Status	**In progress**
Event Deployment	02/10/15 09:10 AM
Event Start	02/10/15 09:10 AM
Event Duration	5 minutes
Task ID	6477

Event Results

Targeted HAN	8	100%
Started HAN	8	100%
Completed HAN	0	0%
Overridden HAN	0	0%
Superseded HAN	0	0%
Received Late HAN	0	0%
Unknown HAN	0	0%
Targeted ESI	8	100%
Unreachable ESI	0	0%
Cancelled ESI	0	0%

Editing superseding events with lower criticality level get rejected.

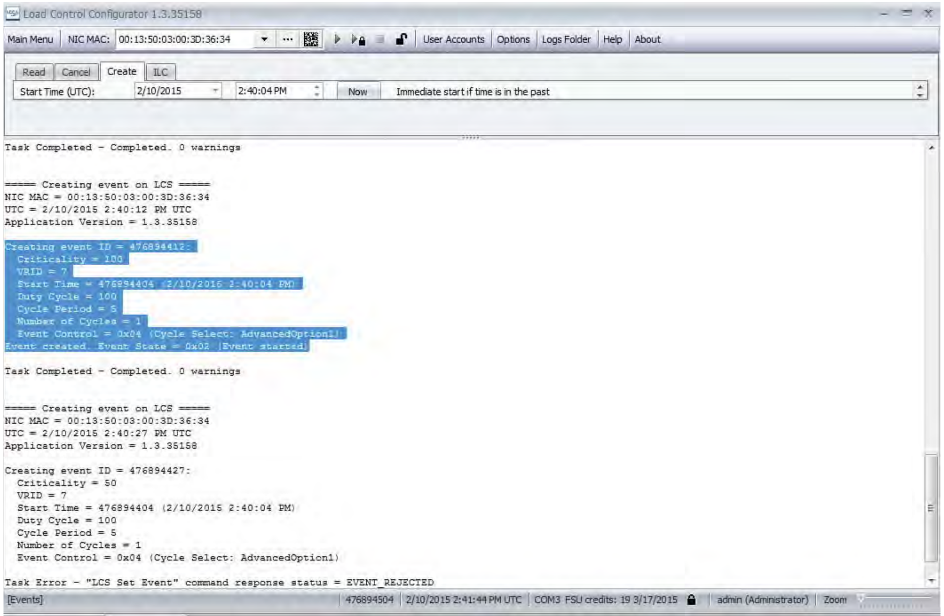

20 SUPPORT FOR "CRITICALITY" LEVELS REPLACING AN EVENT

20.1 OBJECTIVE

The switch shall support the Demand Response and Load Control event data field "Criticality" levels.

20.2 TEST PREREQUISITES AND EQUIPMENT

[redacted] switch MAC: 00135003003D3634, HCM.

20.3 TEST STEPS

1. Using LCC, generate a switch event on MAC: 00135003003D3634 switch with a criticality value of 100, VRID 7,1 cycle, 10-minute duration, 100% duty cycle. Event shall control virtual relay 7 which controls both physical relays, number 1 connected to AC and number 2 connected to the water heater.
2. Using LCC, generate a switch event on MAC: 00135003003D3634 switch 5 minutes after the first event started with a criticality value of 120, VRID 0,1 cycle, 10-minute duration, 100% duty cycle. Event shall control virtual relay 0 which controls physical relay number 1 connected to the AC.
3. Ensure all events are generated, logged and executed with the appropriate criticality level.
4. Ensure that the event in step 2 replaces event on step 1. Once event #2 will be executed water heater shall be released from control and AC shall be controlled for 10 minutes.
5. Log and record the results.

20.4 EXPECTED RESULTS

Verification of functionality.

20.5 SUPPORT FOR "CRITICALITY" LEVELS RESULTS

Replacement superseding event

Event 1

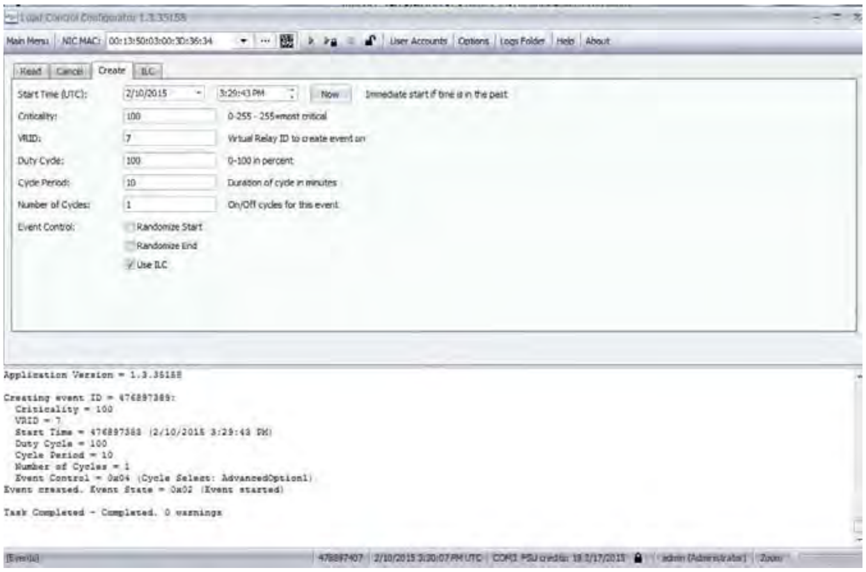

Event 2

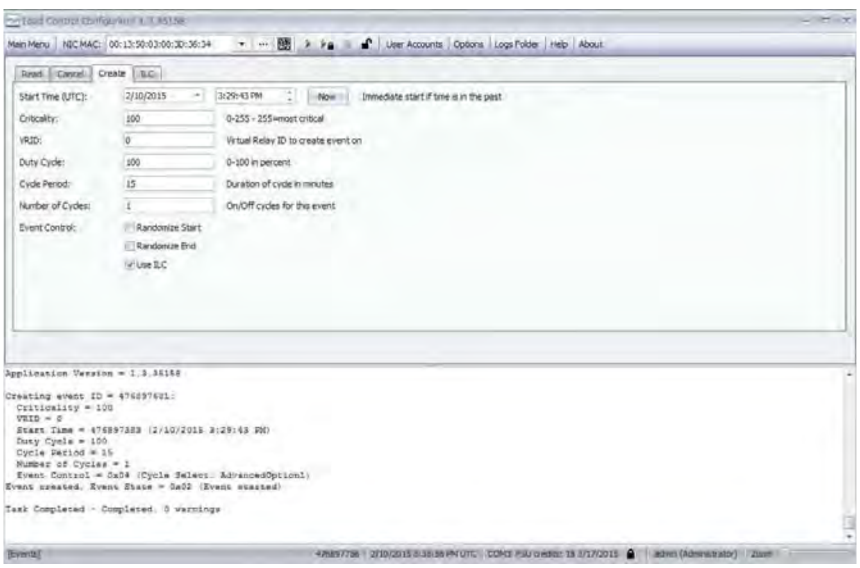

21 SWITCH SUPPORTS HVAC EVENT SUPERCESSION FOR DUTY CYCLE AND NUMBER OF CYCLES ONLY

21.1 OBJECTIVE

The DLC switch shall support event supersession on HVAC systems to modify the following event parameters for an in-progress event on a specified virtual relay:

1. Duty cycle, defined as a percentage control-state (between 0 and 100%) of a control period.
2. Number of cycles, which results in a modification to the duration of the event.

The switch shall accept the new control parameters for duty cycle and duration and ignore all other parameters in the superseding event.

21.2 TEST PREREQUISITES AND EQUIPMENT

[redacted] switch MAC: 00135003003D3634, LCC

21.3 TEST STEPS

1. Using LCC, create an HVAC event that will last an appropriate amount of time to complete this test.
2. Ensure parameters are correct and send the event to the switch.
3. Create a second, overlapping, higher priority/criticality, HVAC event, changing the Duty Cycle and Number of Cycles parameters.
4. Send the new event to the switch.
5. Using LCC, login to the switch and verify that only the Duty Cycle and Number of Cycles have changed. All other parameters remain at the values of the original event.
6. Validate, by observing switch behavior, that event supersession is functioning per expectation.
7. Log and record the results.

21.4 EXPECTED RESULTS

Verification of functionality.

21.5 SWITCH SUPPORTS HVAC EVENT SUPERCESSION FOR DUTY CYCLE AND NUMBER OF CYCLES ONLY RESULTS

First Event

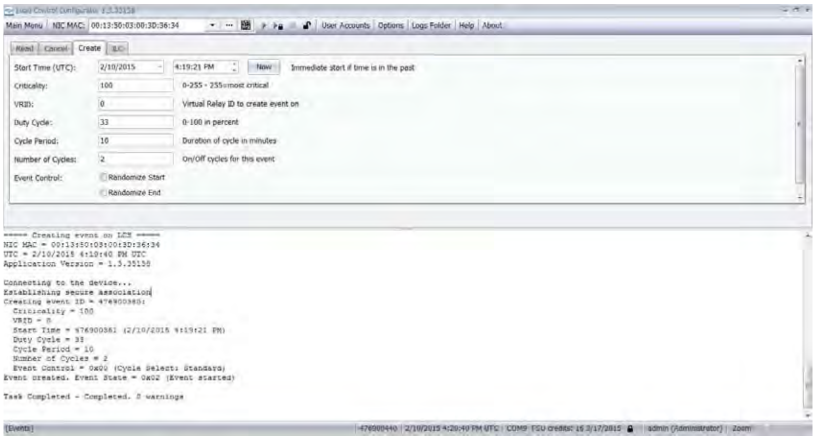

Second event (Superseding)

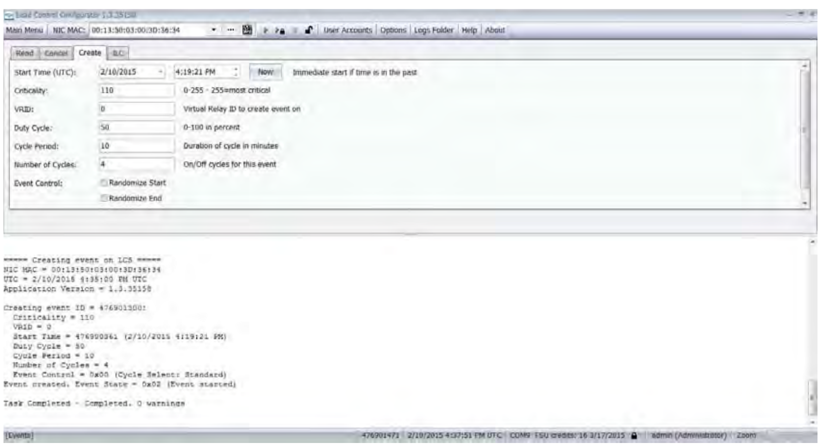

LCC Logs

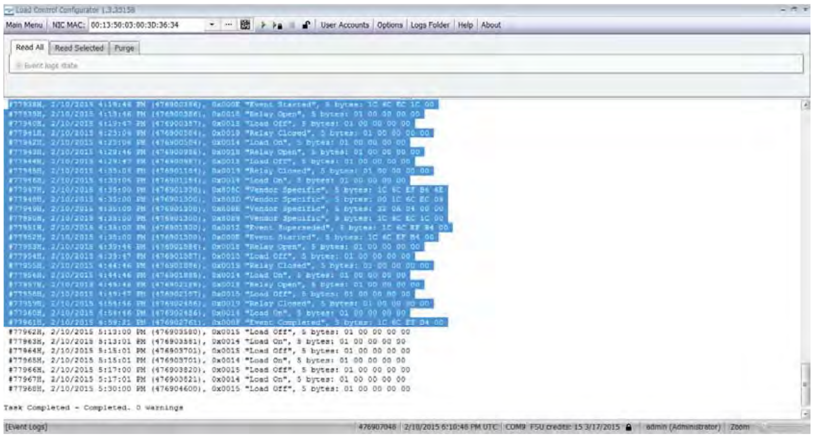
Main Menu
User Accounts
Options
Logs Folder
Help
About
Read All
Read Selected
Purge

22 MULTIPLE SUPERSEDING EVENTS WILL UPDATE DUTY CYCLE AND DURATION PER EVENT

22.1 OBJECTIVE

The DLC switch shall support multiple superseding events for making additional modifications to duty cycle and duration prior to the event completing. In this scenario, the DLC switch shall always prefer the most recent duty cycle and duration parameters received over any preceding parameters.

22.2 TEST PREREQUISITES AND EQUIPMENT

[redacted] switch MAC: 00135003003D35AA, LCC

22.3 TEST STEPS

1. Using LCC, create an event, for switch MAC: 00135003003D35AA, that will last an appropriate amount of time to complete this test.
2. Ensure parameters are correct and send the event to the switches.
3. Create a second, higher priority/criticality, changing the Duty Cycle and Number of Cycles parameters.
4. Send the new event to the switches.
5. Using LCC, login to the switches and verify that the only the Duty Cycle and Number of Cycles have changed. All other parameters remain at the values of the original event.
6. Repeat step 3 and 4 two times and verify each change.
7. Log and record the results.

22.4 EXPECTED RESULTS

Verification of functionality.

22.5 MULTIPLE SUPERSEDING EVENTS WILL UPDATE DUTY CYCLE AND DURATION PER EVENT RESULTS

First Event

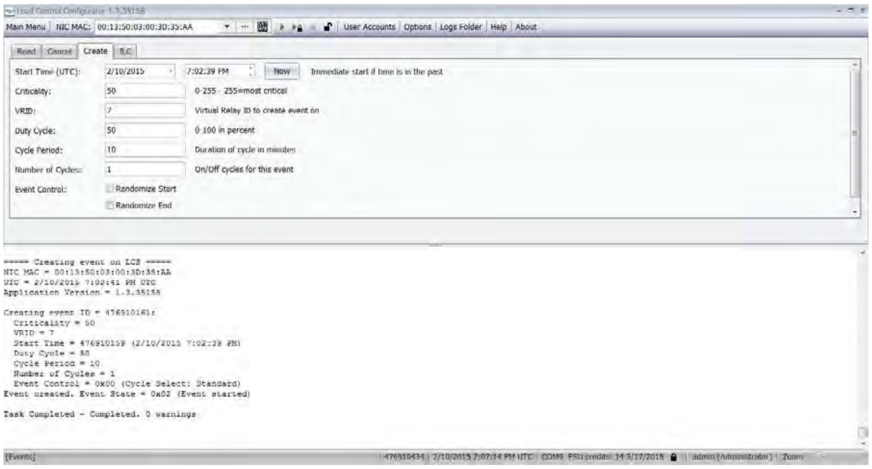

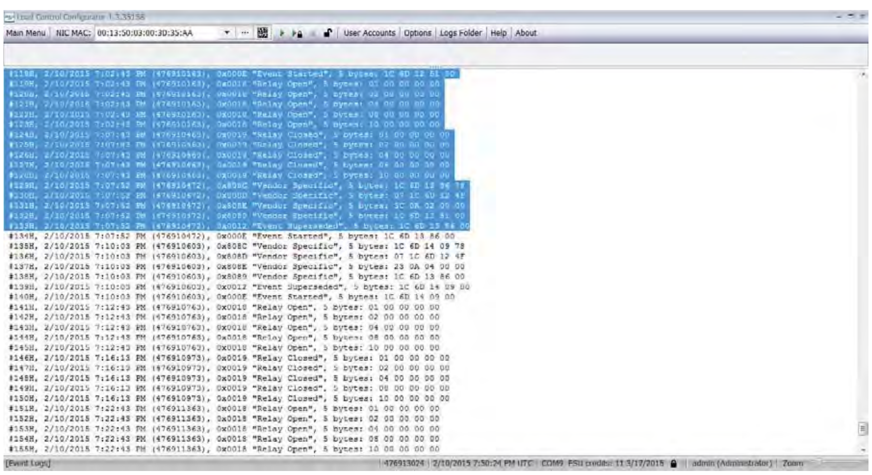

Second Event

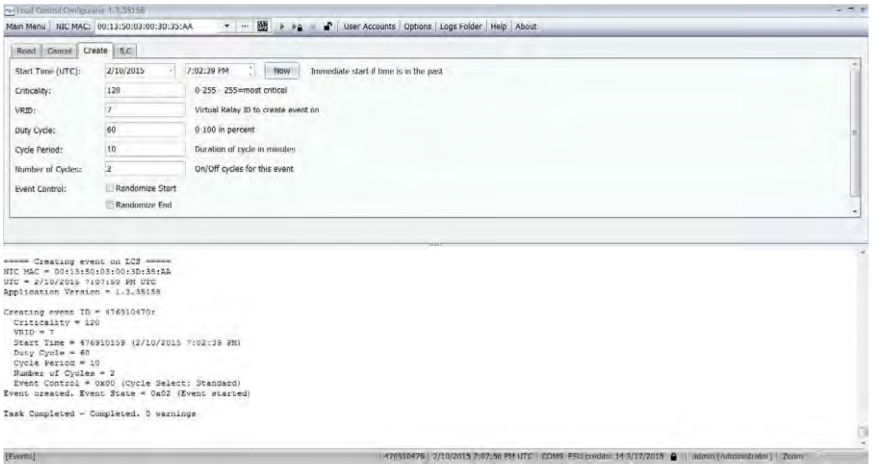
Main Menu
NIC MAC: 00:13:50:03:00:3D:35:AA
User Accounts
Options
Logs Folder
Help
About
Read
Cancel
Create
TLC
Start Time (UTC): 2/10/2015 7:02:39 PM
Now
Immediate start if time is in the past
Criticality: 120
0-255 - 255=most critical
VRID: 7
Virtual Relay ID to create event on
Duty Cycle: 60
0-100 in percent
Cycle Period: 10
Duration of cycle in minutes
Number of Cycles: 2
On/Off cycles for this event
Event Control:
Randomize Start
Randomize End
===== Creating event on LCS =====
NIC MAC = 00:13:50:03:00:3D:35:AA
UTC = 2/10/2015 7:07:59 PM UTC
Application Version = 1.3.35158
Creating event ID = 476910470:
Criticality = 120
VRID = 7
Start Time = 476910159 (2/10/2015 7:02:39 PM)
Duty Cycle = 60
Cycle Period = 10
Number of Cycles = 2
Event Control = 0x00 (Cycle Select: Standard)
Event created. Event State = 0x02 (Event started)
Task Completed - Completed. 0 warnings
[Events]

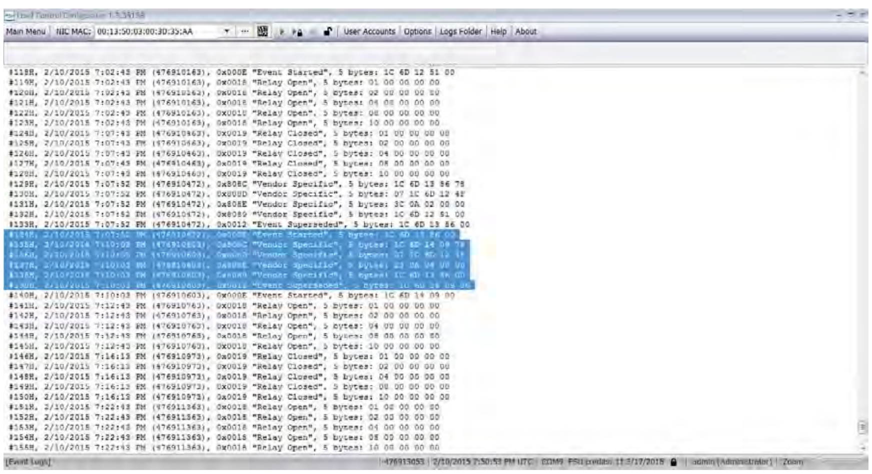
Main Menu
NIC MAC: 00:13:50:03:00:3D:35:AA
User Accounts
Options
Logs Folder
Help
About
#118H, 2/10/2015 7:02:43 PM (476910163), 0x000E "Event Started", 5 bytes: 1C 6D 12 51 00
#119H, 2/10/2015 7:02:43 PM (476910163), 0x0018 "Relay Open", 5 bytes: 01 00 00 00 00
#120H, 2/10/2015 7:02:43 PM (476910163), 0x0018 "Relay Open", 5 bytes: 02 00 00 00 00
#121H, 2/10/2015 7:02:43 PM (476910163), 0x0018 "Relay Open", 5 bytes: 04 00 00 00 00
#122H, 2/10/2015 7:02:43 PM (476910163), 0x0018 "Relay Open", 5 bytes: 08 00 00 00 00
#123H, 2/10/2015 7:02:43 PM (476910163), 0x0018 "Relay Open", 5 bytes: 10 00 00 00 00
#124H, 2/10/2015 7:07:43 PM (476910463), 0x0019 "Relay Closed", 5 bytes: 01 00 00 00 00
#125H, 2/10/2015 7:07:43 PM (476910463), 0x0019 "Relay Closed", 5 bytes: 02 00 00 00 00
#126H, 2/10/2015 7:07:43 PM (476910463), 0x0019 "Relay Closed", 5 bytes: 04 00 00 00 00
#127H, 2/10/2015 7:07:43 PM (476910463), 0x0019 "Relay Closed", 5 bytes: 08 00 00 00 00
#128H, 2/10/2015 7:07:43 PM (476910463), 0x0019 "Relay Closed", 5 bytes: 10 00 00 00 00
#129H, 2/10/2015 7:07:52 PM (476910472), 0x808C "Vendor Specific", 5 bytes: 1C 6D 13 56 78
#130H, 2/10/2015 7:07:52 PM (476910472), 0x808D "Vendor Specific", 5 bytes: 07 1C 6D 12 4F
#131H, 2/10/2015 7:07:52 PM (476910472), 0x808E "Vendor Specific", 5 bytes: 3C 0A 02 00 00
#132H, 2/10/2015 7:07:52 PM (476910472), 0x8089 "Vendor Specific", 5 bytes: 1C 6D 12 51 00
#133H, 2/10/2015 7:07:52 PM (476910472), 0x0012 "Event Superseded", 5 bytes: 1C 6D 13 56 00
#140H, 2/10/2015 7:10:03 PM (476910603), 0x000E "Event Started", 5 bytes: 1C 6D 14 09 00
#141H, 2/10/2015 7:12:43 PM (476910763), 0x0018 "Relay Open", 5 bytes: 01 00 00 00 00
#142H, 2/10/2015 7:12:43 PM (476910763), 0x0018 "Relay Open", 5 bytes: 02 00 00 00 00
#143H, 2/10/2015 7:12:43 PM (476910763), 0x0018 "Relay Open", 5 bytes: 04 00 00 00 00
#144H, 2/10/2015 7:12:43 PM (476910763), 0x0018 "Relay Open", 5 bytes: 08 00 00 00 00
#145H, 2/10/2015 7:12:43 PM (476910763), 0x0018 "Relay Open", 5 bytes: 10 00 00 00 00
#146H, 2/10/2015 7:16:13 PM (476910973), 0x0019 "Relay Closed", 5 bytes: 01 00 00 00 00
#147H, 2/10/2015 7:16:13 PM (476910973), 0x0019 "Relay Closed", 5 bytes: 02 00 00 00 00
#148H, 2/10/2015 7:16:13 PM (476910973), 0x0019 "Relay Closed", 5 bytes: 04 00 00 00 00
#149H, 2/10/2015 7:16:13 PM (476910973), 0x0019 "Relay Closed", 5 bytes: 08 00 00 00 00
#150H, 2/10/2015 7:16:13 PM (476910973), 0x0019 "Relay Closed", 5 bytes: 10 00 00 00 00
#151H, 2/10/2015 7:22:43 PM (476911363), 0x0018 "Relay Open", 5 bytes: 01 00 00 00 00
#152H, 2/10/2015 7:22:43 PM (476911363), 0x0018 "Relay Open", 5 bytes: 02 00 00 00 00
#153H, 2/10/2015 7:22:43 PM (476911363), 0x0018 "Relay Open", 5 bytes: 04 00 00 00 00
#154H, 2/10/2015 7:22:43 PM (476911363), 0x0018 "Relay Open", 5 bytes: 08 00 00 00 00
#155H, 2/10/2015 7:22:43 PM (476911363), 0x0018 "Relay Open", 5 bytes: 10 00 00 00 00
[Event Logs]

Third Event

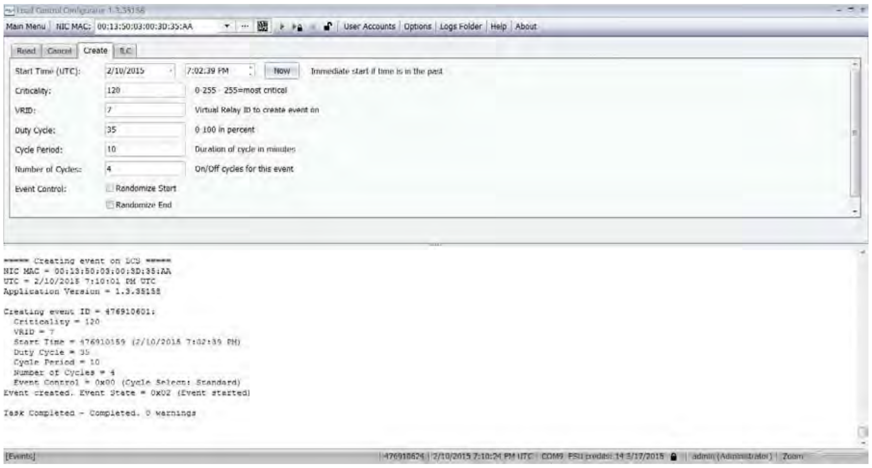
Main Menu
NIC MAC: 00:13:50:03:00:3D:35:AA
User Accounts
Options
Logs Folder
Help
About
Read
Cancel
Create
Start Time (UTC): 2/10/2015 7:02:39 PM
Now
Immediate start if time is in the past
Criticality: 120
0-255 - 255=most critical
VRID: 7
Virtual Relay ID to create event on
Duty Cycle: 35
0-100 in percent
Cycle Period: 10
Duration of cycle in minutes
Number of Cycles: 4
On/Off cycles for this event
Event Control:
Randomize Start
Randomize End
===== Creating event on LCS =====
NIC MAC = 00:13:50:03:00:3D:35:AA
UTC = 2/10/2015 7:10:01 PM UTC
Application Version = 1.3.35158
Creating event ID = 476910601:
Criticality = 120
VRID = 7
Start Time = 476910159 (2/10/2015 7:02:39 PM)
Duty Cycle = 35
Cycle Period = 10
Number of Cycles = 4
Event Control = 0x00 (Cycle Select: Standard)
Event created. Event State = 0x02 (Event started)
Task Completed - Completed. 0 warnings
[Events]
admin (Administrator)
Zoom

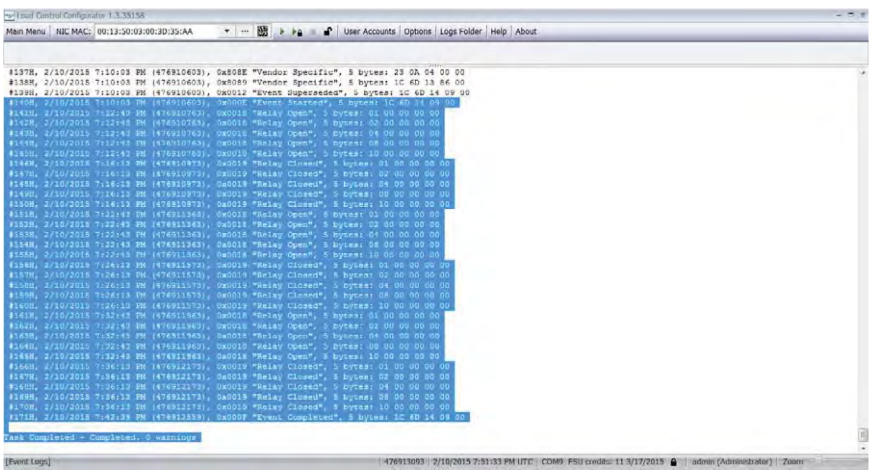
Main Menu
NIC MAC: 00:13:50:03:00:3D:35:AA
User Accounts
Options
Logs Folder
Help
About
Task Completed - Completed. 0 warnings
[Event Logs]
admin (Administrator)
Zoom

23 DUTY CYCLE EVENT SUPERSESSION WILL NOT RESULT IN RELAY SHORT CYCLING

23.1 OBJECTIVE

Superseding an in-progress event to modify duty cycle and/or duration shall not result in any relay short cycling. E.g. extending a 100% duty cycle command should maintain the relay state across the duty cycle boundaries.

23.2 TEST PREREQUISITES AND EQUIPMENT

[redacted] switch MAC: 00135003003D3634, LCC

23.3 TEST STEPS

1. Using LCC, create an event, for switch MAC: 00135003003D3634, duty cycle 100%, 10-minute duration.
2. Create an overlapping event, 10-minutes in duration, 100% duty cycle, with a start time 5-minutes after the first event is in control.
3. Ensure that the event runs no longer than 15-minutes, total.
4. Verify that the relay does not chatter, or blip, when transitioning to the second event.
5. Log and record the results.

23.4 EXPECTED RESULTS

Verification of functionality.

23.5 DUTY CYCLE EVENT SUPERSESSION WILL NOT RESULT IN RELAY SHORT CYCLING RESULTS

Event 1

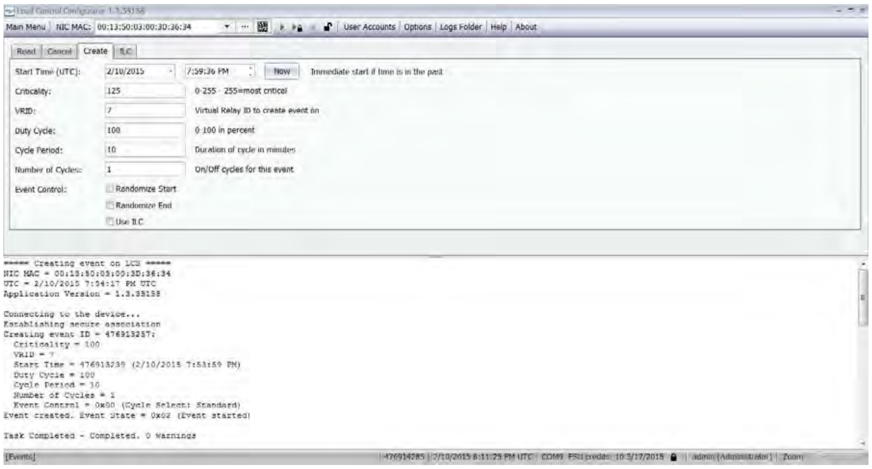

Event 2

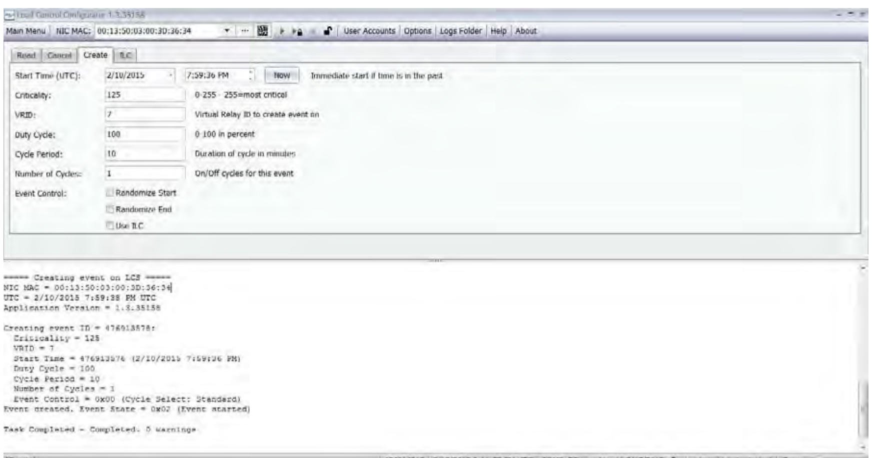

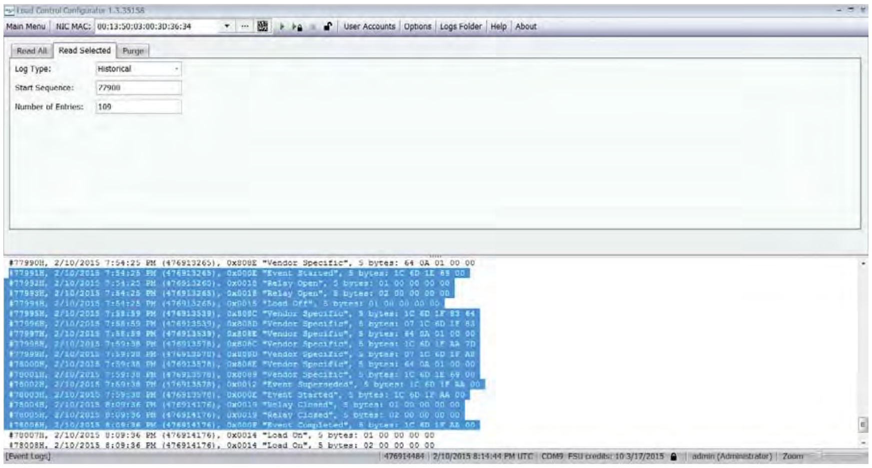
Main Menu
NIC MAC: 00:13:50:03:00:3D:36:34
User Accounts
Options
Logs Folder
Help
About
Read All
Read Selected
Purge
Log Type:
Historical
Start Sequence:
77900
Number of Entries:
109
#77990H, 2/10/2015 7:54:25 PM (476913265), 0x808E "Vendor Specific", 5 bytes: 64 0A 01 00 00
#78007H, 2/10/2015 8:09:36 PM (476914176), 0x0014 "Load On", 5 bytes: 01 00 00 00 00
#78008H, 2/10/2015 8:09:36 PM (476914176), 0x0014 "Load On", 5 bytes: 02 00 00 00 00
[Event Logs]
476914484
2/10/2015 8:14:44 PM UTC
admin (Administrator)
Zoom

24 OVERLAPPING EVENTS SHALL USE THE SAME RANDOMIZED START DELAY

24.1 OBJECTIVE

When transitioning between overlapping events the switch shall use the same randomized start delay for the second event as it used for the first. (This is to ensure that the aggregate time-under-control does not exceed the maximum amount allowed per assigned control period).

24.2 TEST PREREQUISITES AND EQUIPMENT

[redacted] switch MAC: 00135003003D3611, HCM.

24.3 TEST STEPS

1. Using HCM, generate and send an event for 00135003003D3611 switch with a 33% duty cycle, 10 minute cycle period, 2 periods, with randomization.
2. Monitor the event at the physical switch by starting a timer when the relay goes into control.
3. During the control period of the event (while the relay is open and therefore shedding load) generate and send a new event for the switch with a 55% duty cycle, 30 minute cycle period, 2 periods, with randomization, with a higher criticality than the first event.
4. Monitor the event at the physical switch by stopping the timer when the relay closes, then opens, then closes, then opens.
5. Note the times and ensure that no relay open time (load in control) was greater than 16.5 minutes.
6. Log and record the results.

24.4 EXPECTED RESULTS

Verification of functionality.

24.5 OVERLAPPING EVENTS SHALL USE THE SAME RANDOMIZED START DELAY RESULTS

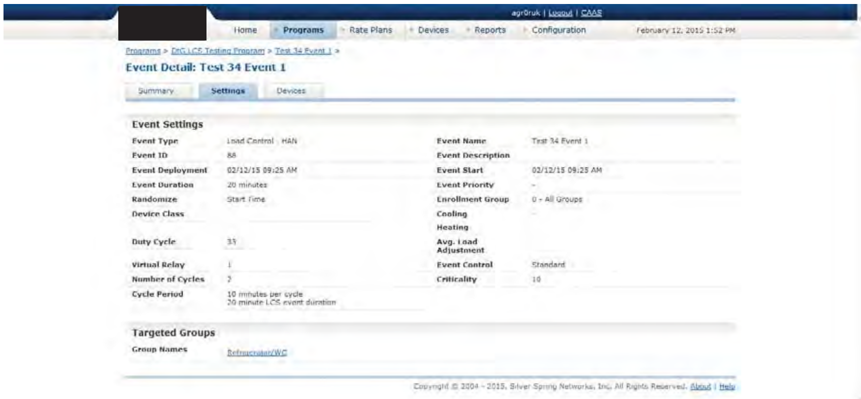

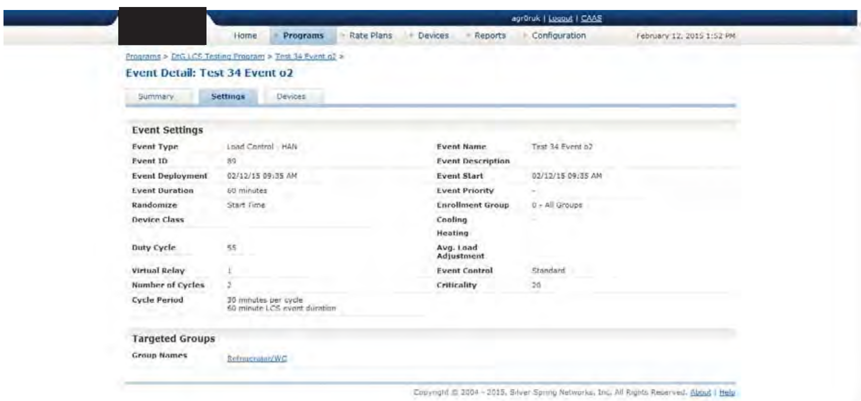

Event 2 delay time does not match Event 1 delay time.

Test Failed

Event 2

No Control Period Exceeding 16.5 minutes.

25 MOST RECENT COMMAND PRIORITIZED WHEN COMMAND CONFLICT OCCURS

25.1 OBJECTIVE

The switch shall prioritize the most recent command/message received over any conflicting commands/messages.

25.2 TEST PREREQUISITES AND EQUIPMENT

[redacted] switch MAC: 00135003003D3611, LCC.

25.3 TEST STEPS

1. From LCC send and event that starts at a future time, with a clear start and end time. Duty cycle 25%, duration 5-minutes, criticality 50. Deploy the event immediately.
2. From LCC, send a second event, in the future, with the same start and end time as the first event, duty cycle 75%, criticality 50, duration 5-minutes. Deploy the event at some point in the future but PRIOR TO the first event starting.
3. Ensure that the newest event is the one that is executed by the switch.
4. Log and record the results.

25.4 EXPECTED RESULTS

Verification of functionality.

25.5 MOST RECENT COMMAND PRIORITIZED WHEN COMMAND CONFLICT OCCURS RESULTS

Event 1

Event 2

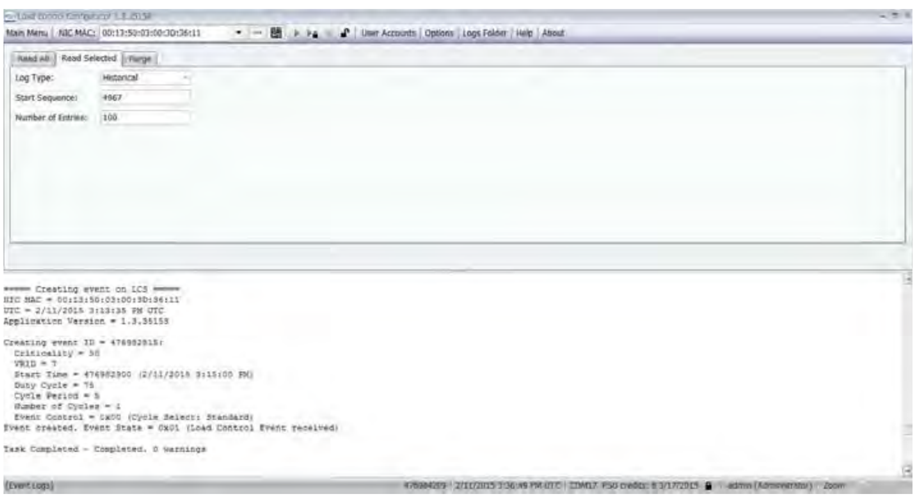

Final Screenshot

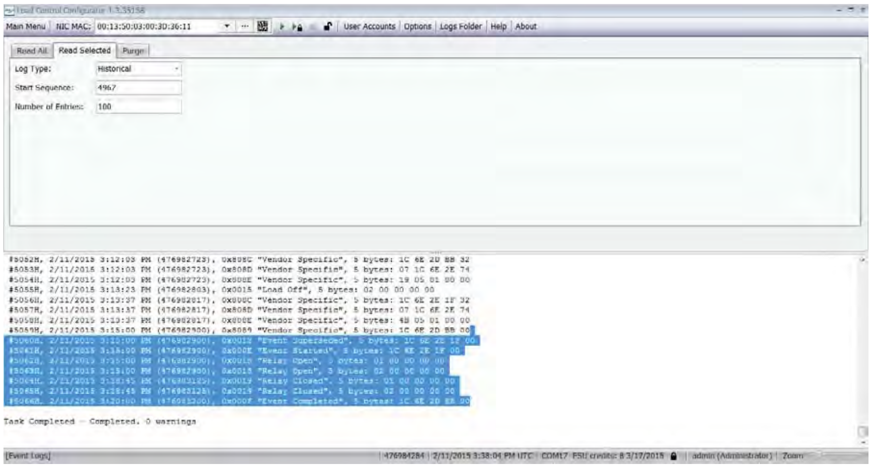

26 SWITCH REPORTS EVENT STATUS

26.1 OBJECTIVE

The switch shall report event status to the HCM when any event changes are detected.

26.2 TEST PREREQUISITES AND EQUIPMENT

[redacted] switches, HCM

26.3 TEST STEPS

1. Using HCM, generate an event in all switches for 2-minutes in the future and send the event to the switches.
2. From HCM, verify that the Event Status has changed to “Received.”
3. From HCM, when 2-minutes have elapsed, verify that the Event Status has changed to “Event Started.”
4. From HCM, at the end of the event, verify that the Event Status has changed to “Event Completed.”
5. Log and record the results.

26.4 EXPECTED RESULTS

Verification of functionality.

26.5 SWITCH REPORTS EVENT STATUS RESULTS

5 relays switch

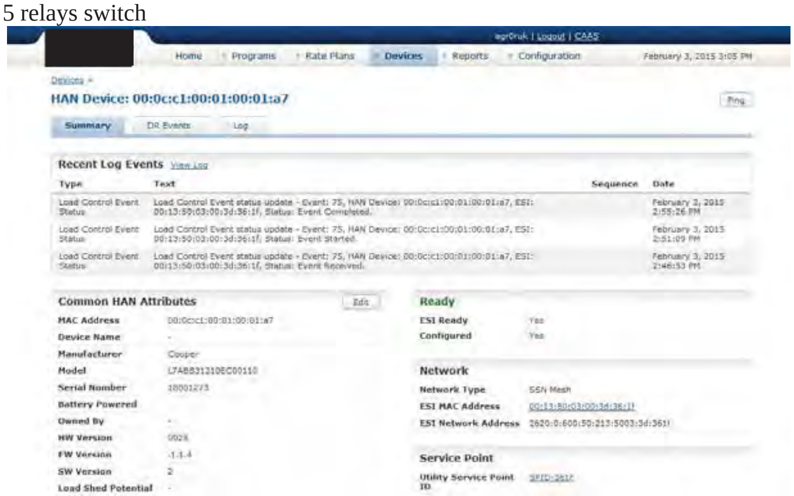

2 relays switch

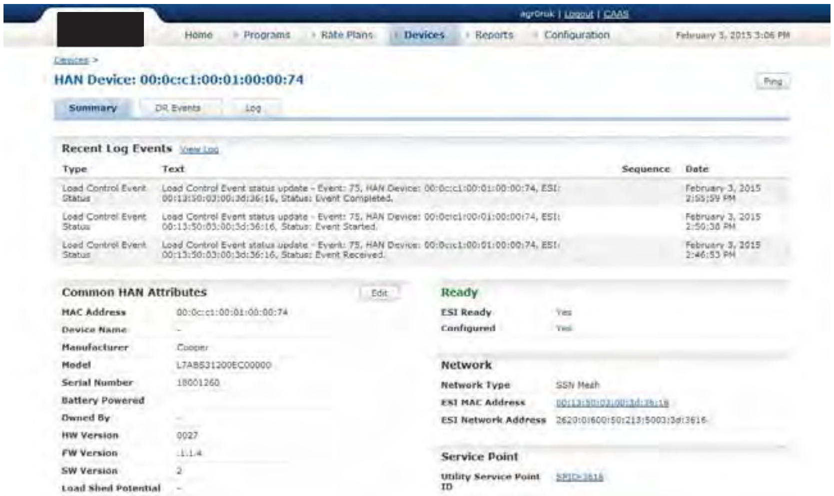

[redacted]
agrOruk | Logout | CAAS
Home
Programs
Rate Plans
Devices
Reports
Configuration
February 3, 2015 3:06 PM
Devices >
HAN Device: 00:0c:c1:00:01:00:00:74
Ping
Summary
DR Events
Log
Recent Log Events
View Log
Type
Text
Sequence
Date
Load Control Event Status
Load Control Event status update - Event: 75, HAN Device: 00:0c:c1:00:01:00:00:74, ESI: 00:13:50:03:00:3d:36:16, Status: Event Completed.
February 3, 2015 2:55:59 PM
Load Control Event Status
Load Control Event status update - Event: 75, HAN Device: 00:0c:c1:00:01:00:00:74, ESI: 00:13:50:03:00:3d:36:16, Status: Event Started.
February 3, 2015 2:50:38 PM
Load Control Event Status
Load Control Event status update - Event: 75, HAN Device: 00:0c:c1:00:01:00:00:74, ESI: 00:13:50:03:00:3d:36:16, Status: Event Received.
February 3, 2015 2:46:53 PM
Common HAN Attributes
Edit
MAC Address
00:0c:c1:00:01:00:00:74
Device Name
-
Manufacturer
Cooper
Model
L7ABS31200EC00000
Serial Number
18001260
Battery Powered
Owned By
-
HW Version
0027
FW Version
1.1.4
SW Version
2
Load Shed Potential
-
Ready
ESI Ready
Yes
Configured
Yes
Network
Network Type
SSN Mesh
ESI MAC Address
ESI Network Address
2620:0:600:50:213:5003:3d:3616
Service Point
Utility Service Point ID

27 STORAGE OF RUNTIME INFORMATION – END USE LOAD

27.1 OBJECTIVE

The switch shall be able to monitor and store the runtime information (including date and time stamp) for the end use load connected to its relay.

27.2 TEST PREREQUISITES AND EQUIPMENT

[redacted] switches, LCC

27.3 TEST STEPS

1. Using LCC, flush the historical event log from previous information for clarity.
2. Connect a running load to the switch.
3. Using LCC read the data log.
4. Turn off the load physically.
5. Verify the log contains an additional element describing which load was turned off and when.
6. Turn on the load physically again.
7. Shed the load via relay control.
8. Verify the log contains an entry that says the relay was shed and when.
9. Verify the log contains an entry that states the load was turned off and when.
10. Restore the load via relay control.
11. Verify the log contains an element describing which load was turned on and when.
12. Verify the log contains an entry that states which relay was restored and when.
13. Verify the log contains an entry that states which load was turned on and when.
14. Log and record the results.

27.4 EXPECTED RESULTS

Verification of functionality.

27.5 STORAGE OF RUNTIME INFORMATION – END USE LOAD RESULTS

2 relay switch controlling the water cooler was tested. To make sure that the CT will sense some current we connected an electric heater to the same receptacle. There is a little delay between the load released and current sensing because the heater doesn't start automatically; we had to physically turn it on.

Test 19

Event Execution

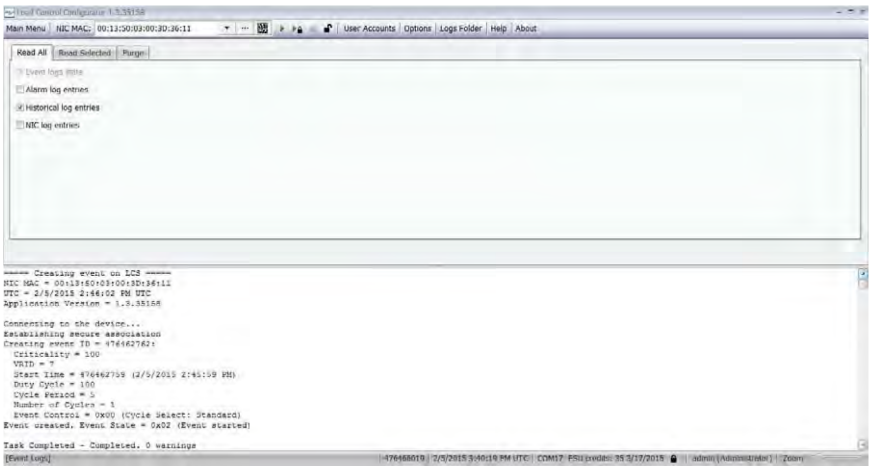

Historical log Entries

Beginning

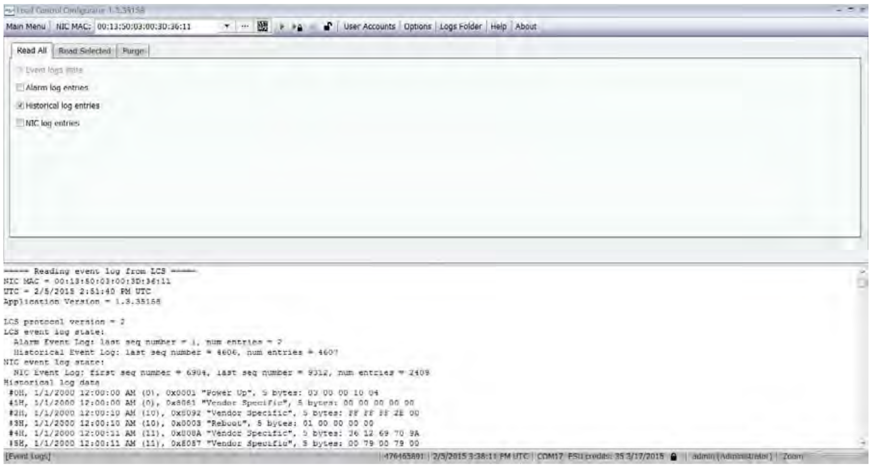

End

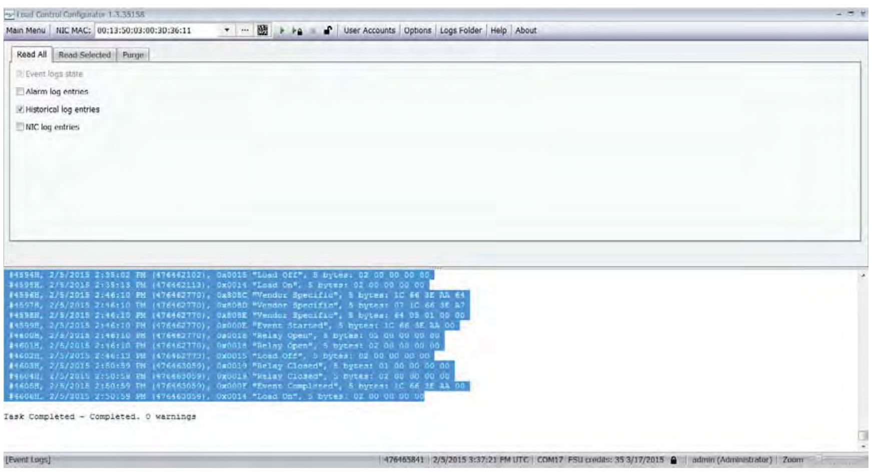

2 relay switch controlling AC compressor MAC: 00135003003D3616

```
 ===== Reading event log from LCS =====
NIC MAC = 00:13:50:03:00:3D:36:16
UTC = 2/5/2015 6:47:11 PM UTC
Application Version = 1.3.35158

Connecting to the device...
LCS protocol version = 2
Purge log completed

Task Completed - Completed. 0 warnings
```

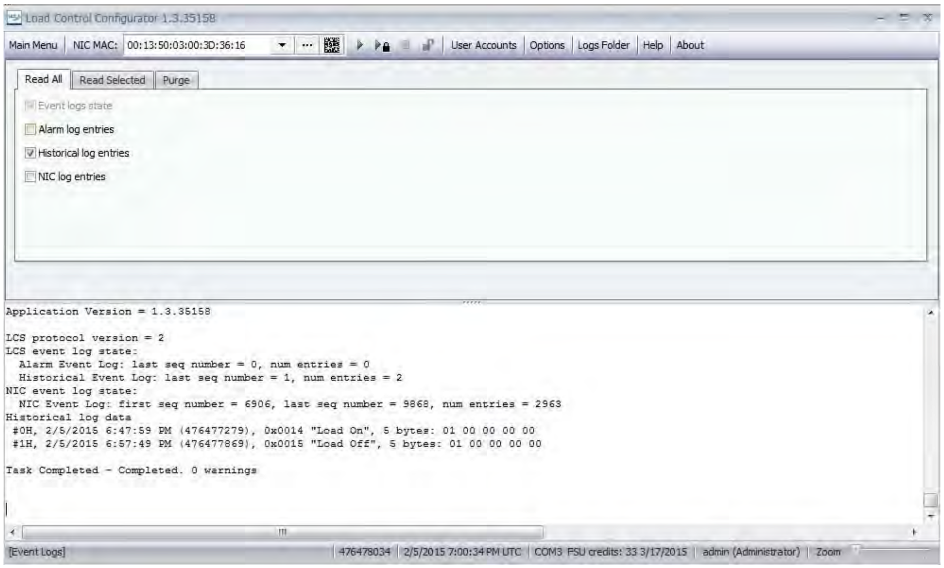
Load Control Configurator 1.3.35158
Main Menu
NIC MAC: 00:13:50:03:00:3D:36:16
User Accounts
Options
Logs Folder
Help
About
Read All
Read Selected
Purge
Event logs state
Alarm log entries
Historical log entries
NIC log entries
Application Version = 1.3.35158
LCS protocol version = 2
LCS event log state:
Alarm Event Log: last seq number = 0, num entries = 0
Historical Event Log: last seq number = 1, num entries = 2
NIC event log state:
NIC Event Log: first seq number = 6906, last seq number = 9868, num entries = 2963
Historical log data
#0H, 2/5/2015 6:47:59 PM (476477279), 0x0014 "Load On", 5 bytes: 01 00 00 00 00
#1H, 2/5/2015 6:57:49 PM (476477869), 0x0015 "Load Off", 5 bytes: 01 00 00 00 00
Task Completed - Completed. 0 warnings
[Event Logs]
476478034
2/5/2015 7:00:34 PM UTC
COM3 FSU credits: 33 3/17/2015
admin (Administrator)
Zoom

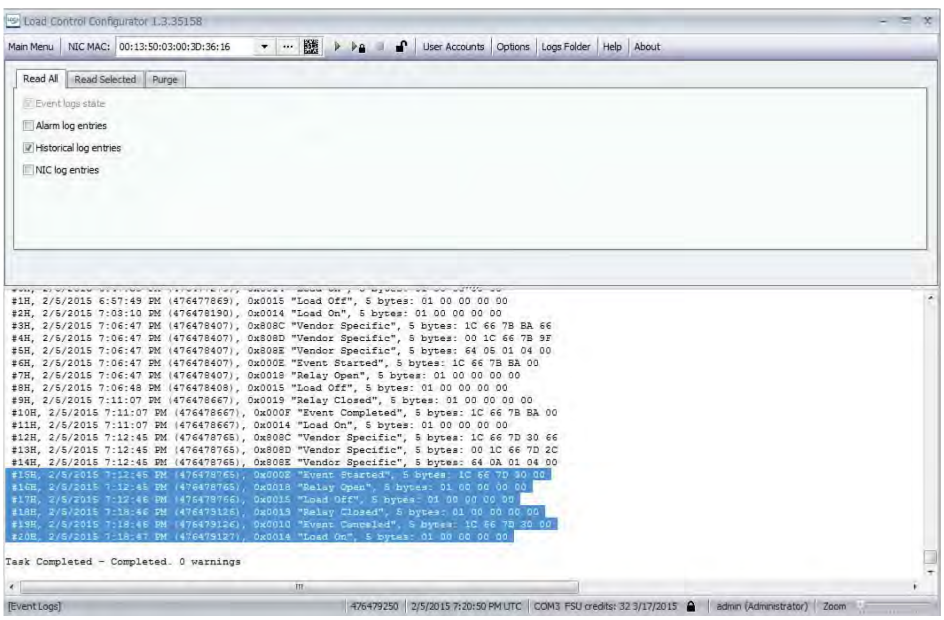
Load Control Configurator 1.3.35158
Main Menu
NIC MAC: 00:13:50:03:00:3D:36:16
User Accounts
Options
Logs Folder
Help
About
Read All
Read Selected
Purge
Event logs state
Alarm log entries
Historical log entries
NIC log entries
#1H, 2/5/2015 6:57:49 PM (476477869), 0x0015 "Load Off", 5 bytes: 01 00 00 00 00
#2H, 2/5/2015 7:03:10 PM (476478190), 0x0014 "Load On", 5 bytes: 01 00 00 00 00
#3H, 2/5/2015 7:06:47 PM (476478407), 0x808C "Vendor Specific", 5 bytes: 1C 66 7B BA 66
#4H, 2/5/2015 7:06:47 PM (476478407), 0x808D "Vendor Specific", 5 bytes: 00 1C 66 7B 9F
#5H, 2/5/2015 7:06:47 PM (476478407), 0x808E "Vendor Specific", 5 bytes: 64 05 01 04 00
#6H, 2/5/2015 7:06:47 PM (476478407), 0x000E "Event Started", 5 bytes: 1C 66 7B BA 00
#7H, 2/5/2015 7:06:47 PM (476478407), 0x0018 "Relay Open", 5 bytes: 01 00 00 00 00
#8H, 2/5/2015 7:06:48 PM (476478408), 0x0015 "Load Off", 5 bytes: 01 00 00 00 00
#9H, 2/5/2015 7:11:07 PM (476478667), 0x0019 "Relay Closed", 5 bytes: 01 00 00 00 00
#10H, 2/5/2015 7:11:07 PM (476478667), 0x000F "Event Completed", 5 bytes: 1C 66 7B BA 00
#11H, 2/5/2015 7:11:07 PM (476478667), 0x0014 "Load On", 5 bytes: 01 00 00 00 00
#12H, 2/5/2015 7:12:45 PM (476478765), 0x808C "Vendor Specific", 5 bytes: 1C 66 7D 30 66
#13H, 2/5/2015 7:12:45 PM (476478765), 0x808D "Vendor Specific", 5 bytes: 00 1C 66 7D 2C
#14H, 2/5/2015 7:12:45 PM (476478765), 0x808E "Vendor Specific", 5 bytes: 64 0A 01 04 00
#15H, 2/5/2015 7:12:45 PM (476478765), 0x000E "Event Started", 5 bytes: 1C 66 7D 30 00
#16H, 2/5/2015 7:12:45 PM (476478765), 0x0018 "Relay Open", 5 bytes: 01 00 00 00 00
#17H, 2/5/2015 7:12:46 PM (476478766), 0x0015 "Load Off", 5 bytes: 01 00 00 00 00
#18H, 2/5/2015 7:18:46 PM (476479126), 0x0019 "Relay Closed", 5 bytes: 01 00 00 00 00
#19H, 2/5/2015 7:18:46 PM (476479126), 0x0010 "Event Canceled", 5 bytes: 1C 66 7D 30 00
#20H, 2/5/2015 7:18:47 PM (476479127), 0x0014 "Load On", 5 bytes: 01 00 00 00 00
Task Completed - Completed. 0 warnings
[Event Logs]
476479250
2/5/2015 7:20:50 PM UTC
COM3 FSU credits: 32 3/17/2015
admin (Administrator)
Zoom

28 ACTIVITY LOGS CAPTURE HISTORY

28.1 OBJECTIVE

The switch's activity logs shall capture event history.

28.2 TEST PREREQUISITES AND EQUIPMENT

[redacted] switches, LCC

28.3 TEST STEPS

1. Using LCC, login to MAC: 00135003003D3616 switch to review the event logs.
2. Event logs should have a history of events.
3. Log and record the results.

28.4 EXPECTED RESULTS

Verification of functionality.

28.5 ACTIVITY LOGS CAPTURE HISTORY RESULTS

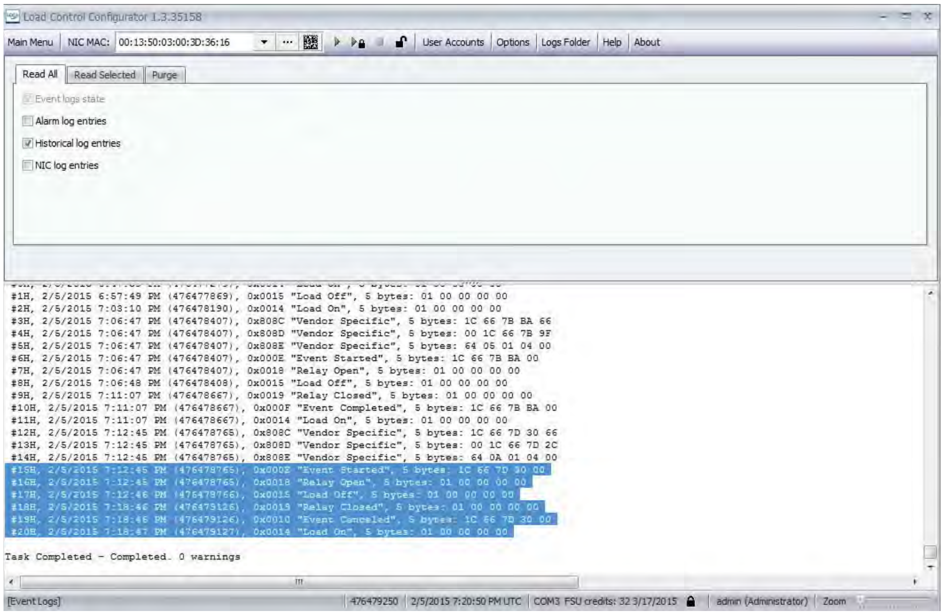

29 INACTIVE APPLIANCE DURATION

29.1 OBJECTIVE

The switch shall log an alert if current has not been detected on a connected load for a configurable number of days longer than the time set for in the configuration file.

29.2 TEST PREREQUISITES AND EQUIPMENT

[redacted] switches MAC 00135003003D3634 and MAC 00135003003D3611 with inactive appliance set to 5 days, LCC, HCM.

29.3 TEST STEPS

1. Turn off switch located downstream the switch with MAC ID 00135003003D3634 controlling water heater and AC.
2. Wait five days to reach the required time for the appliance to be inactive. Flag will be appear on LCC as “No load detected”
3. Log and record the results.
4. Turn off switch located downstream the switch with MAC ID 00135003003D3611 controlling water cooler.
5. Wait five days to reach the required time for the appliance to be inactive. Flag will be appear on LCC as “No load detected”
6. Log and record the results.

29.4 EXPECTED RESULTS

Verification of functionality.

29.5 INACTIVE APPLIANCE DURATION

Load was turned off on February 2nd.

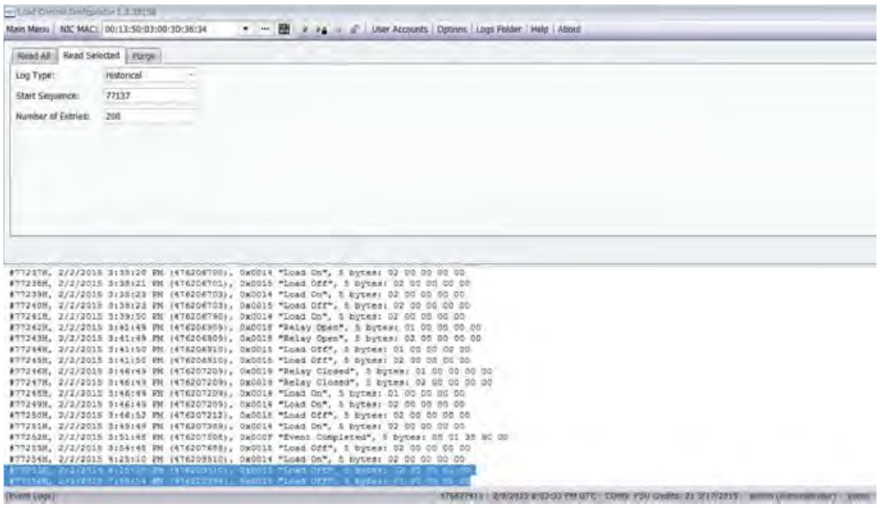

Inactive Appliance test for the switch controlling water heater and AC.

Inactive appliance is set to 5 days for the tested switch. Days get counted after each midnight which will give us the midnight of the 7th which is 12:00 am on 2/8/15.

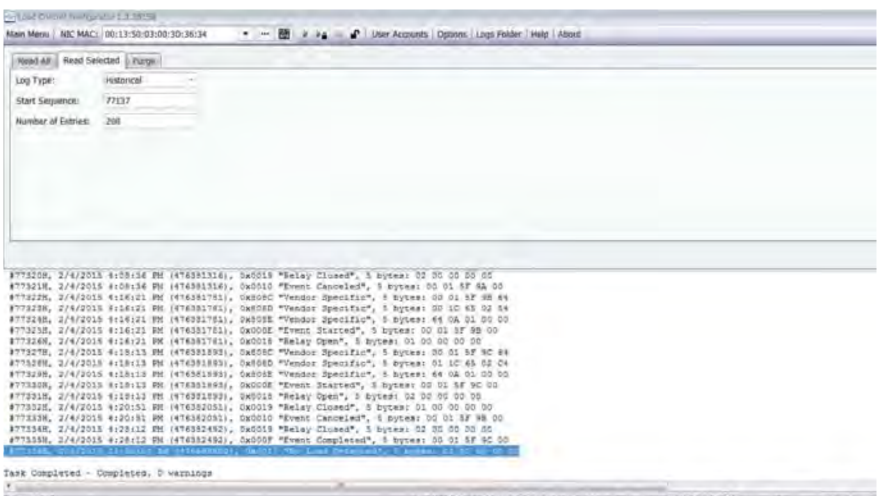

We were not able to get the flag from HCM.

Inactive Appliance test for the switch MAC ID 00135003003D3611controlling the water cooler.

Inactive appliance is set to 5 days for the tested switch. Days get counted after each midnight which will give us the midnight of the 13th which is 12:00 am on 2/19/15.

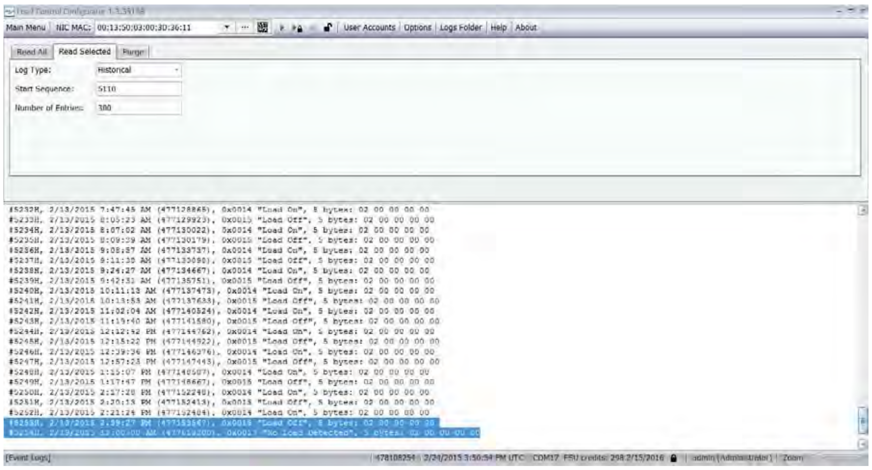

We were not able to get the flag from HCM.

New configuration was uploaded to the same switch controlling the water heater and AC with MAC ID 00135003003D3634. New configuration was uploaded successfully.

Load was turned off on March 6th. Inactive appliance is set to 1 day on the new configuration file. Days get counted after each midnight which will give us the midnight of the 7th which is 12:00 am on 3/8/15.

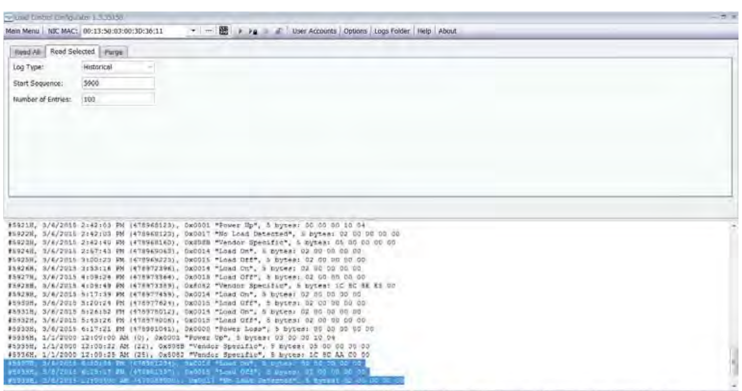

30 ACTIVITY LOGS ARE LOCALLY ACCESSIBLE VIA LCC

30.1 OBJECTIVE

The switch's activity logs shall be locally accessible via Field Test Equipment.

30.2 TEST PREREQUISITES AND EQUIPMENT

[redacted] switch MAC: 00135003003D3611(2 relay), MAC: 00135003003D35AA, LCC

30.3 TEST STEPS

4. Using LCC, login to switches and review Activity logs.
5. Log and record the results.
6. Conduct an event.
7. Using LCC, login to switches and review Activity logs.
8. Log and record the results.

30.4 EXPECTED RESULTS

Verification of functionality.

30.5 ACTIVITY LOGS ARE LOCALLY ACCESSIBLE VIA LCC RESULTS

Read activities log for 2 Relay switch

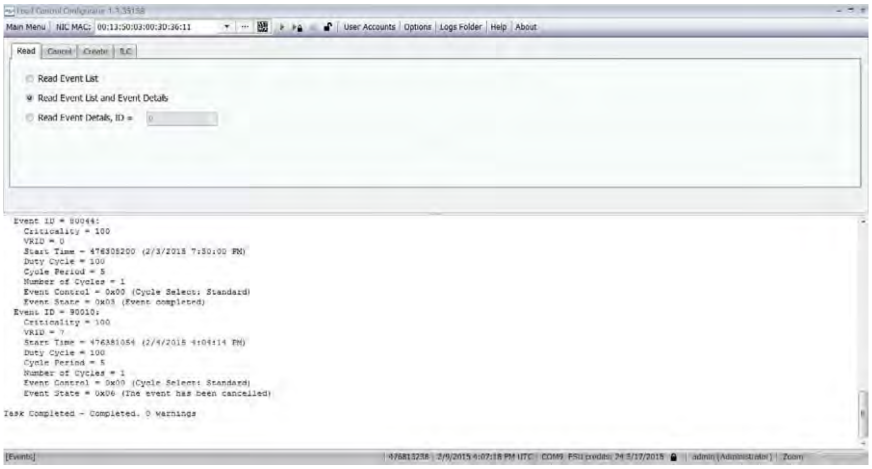

Add 1 event to 2 Relay switch and read activities log

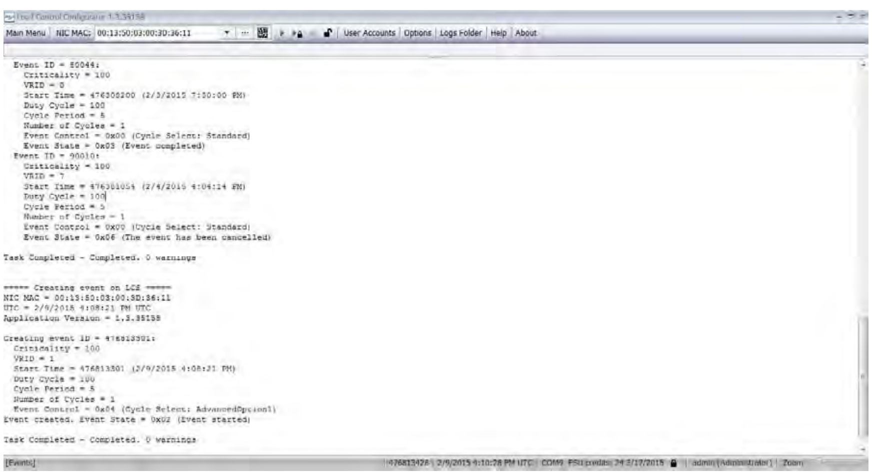

Read activities log for 5 Relay switch

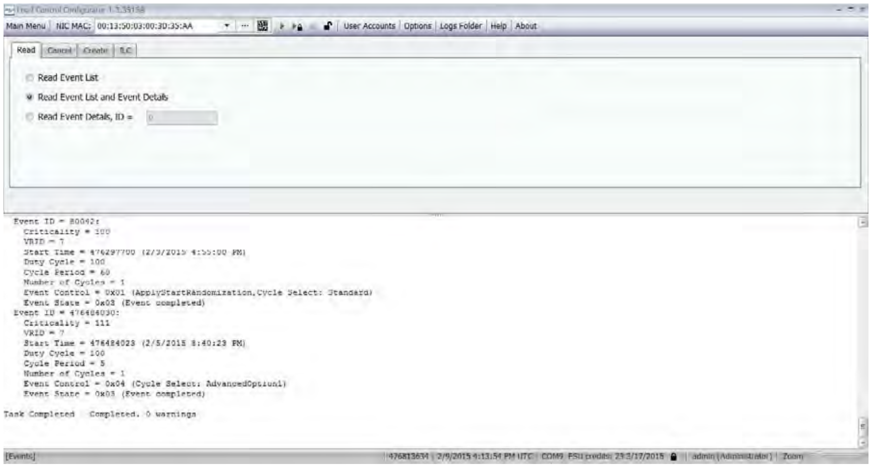

Add 1 event to 5 Relay switch and read activities log

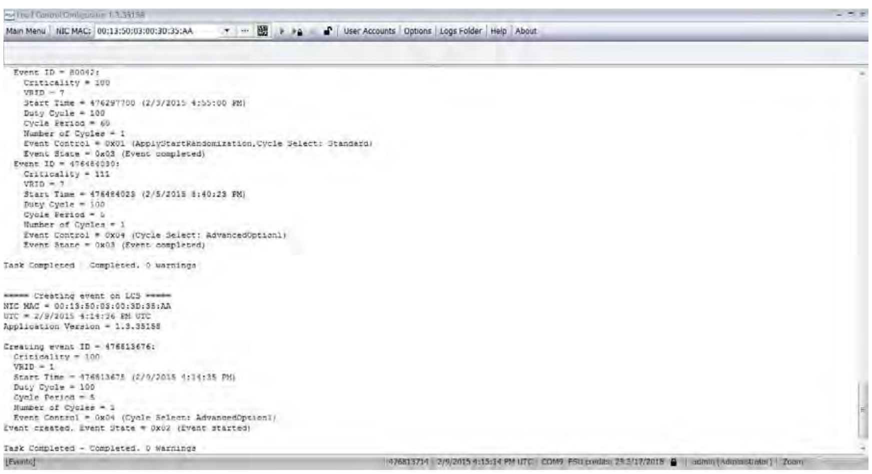

31 FIELD TEST EQUIPMENT SHALL NOT REQUIRE A CONNECTION THROUGH THE HAN TO INTERFACE WITH THE SWITCH

31.1 OBJECTIVE

Field test equipment shall not require a connection through the HAN to interface with the switch.

31.2 TEST PREREQUISITES AND EQUIPMENT

[redacted] switches don't have HAN, but only 900 MHz radios therefore the communication with FSU is been established through 900 MHZ network only. Test Steps

No test required.

32 SWITCH WILL CONFIRM SUCCESSFUL FIRMWARE UPGRADE

32.1 OBJECTIVE

The switch shall respond to a request from FWU to confirm successful firmware upgrade.

32.2 TEST PREREQUISITES AND EQUIPMENT

[redacted] switches, scripts

32.3 TEST STEPS

1. Using scripts, poll both the 5F and 2F switch for successful firmware upgrade.
2. Log and record the results.

32.4 EXPECTED RESULTS

NOTE: FWU will not support this functionality until HCM 2.1. Therefore scripts will be used in place of FWU to document remote F/W upgrade functionality.

32.5 SWITCH WILL CONFIRM SUCCESSFUL UPGRADE RESULTS

NOTE: FWU will not support this functionality until HCM 2.1. Therefore scripts will be used in place of FWU to document remote F/W upgrade functionality.

2Function ESIMAC:DB99

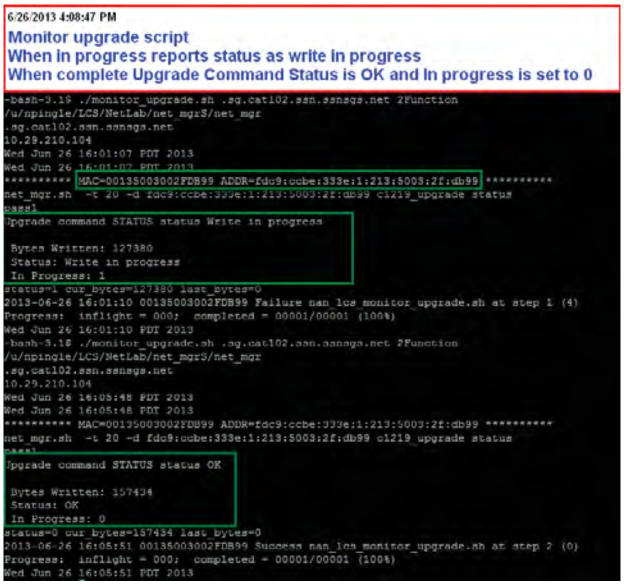

5Function ESIMAC:DB92

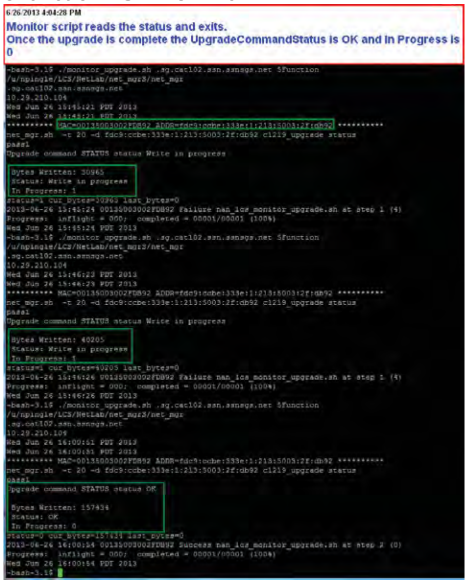

33 CONFIGURATION MODIFICATIONS ACCEPTED FROM HCM AND LCC

33.1 OBJECTIVE

The switch shall have the ability to accept modifications to its configuration over-the-air from the HCM and from field test equipment.

33.2 TEST PREREQUISITES AND EQUIPMENT

[redacted] switches MAC ID 00135003003D3634 and MAC: 00135003003D35D9, HCM, LCC

33.3 TEST STEPS

1. From LCC upload a different configuration file to both switches with inactive appliance set to 1 day instead of 5 days which was before.
2. Log and record the results.

33.4 EXPECTED RESULTS

Verification of functionality.

33.5 CONFIGURATION MODIFICATIONS ACCEPTED FROM HCM AND LCC RESULTS

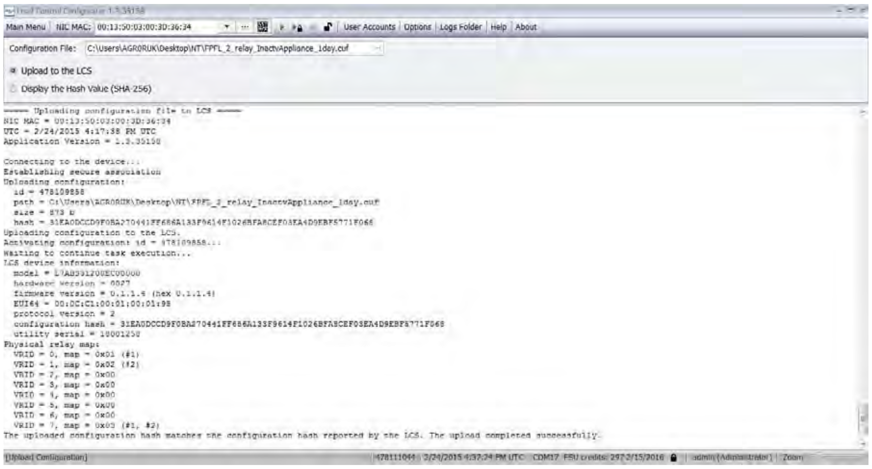

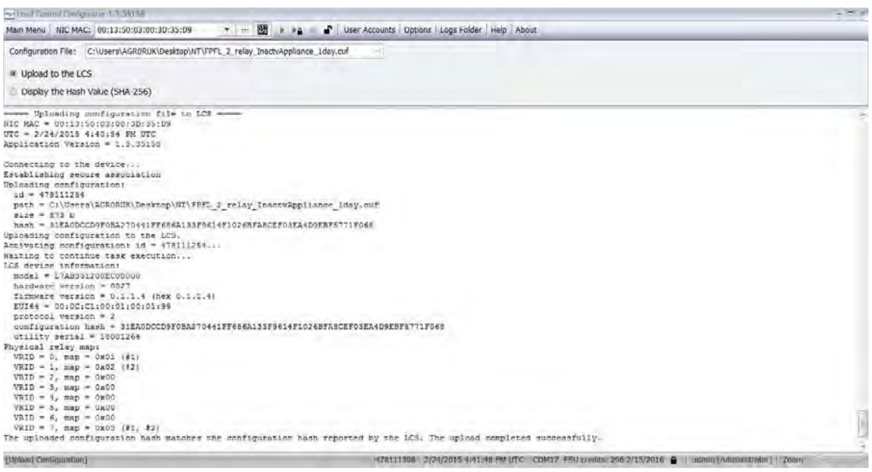

34 VIRTUAL RELAY CONFIGURATION AVAILABLE IN HCM

34.1 OBJECTIVE

The switch virtual relay configuration settings shall be retrievable from the HCM.

34.2 TEST PREREQUISITES AND EQUIPMENT

[redacted] switches MAC ID 00135003003D363D (5 relay) and MAC ID 00135003003D3616 (2 relay), HCM

34.3 TEST STEPS

1. Allow HCM to perform at least one ESI sync after the switch has gone to the "Ready" state.
2. Review the virtual relay configuration and verify that it is consistent with expectations.
3. Log and record the results.

34.4 EXPECTED RESULTS

Verification of functionality.

34.5 VIRTUAL RELAY CONFIGURATION AVAILABLE IN HCM RESULTS

MAC ID 00135003003D363D (5 relay) HCM

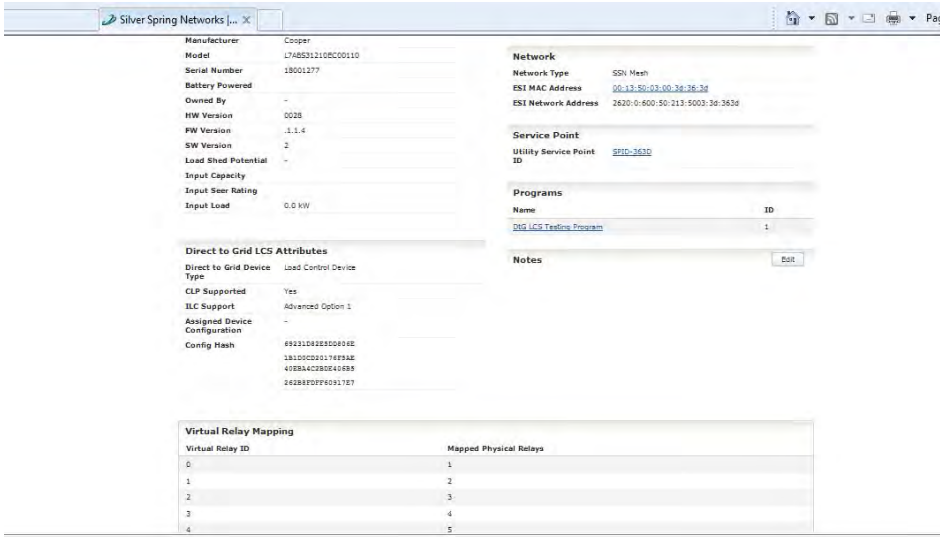

MAC ID 00135003003D363D (5 relay) LCC

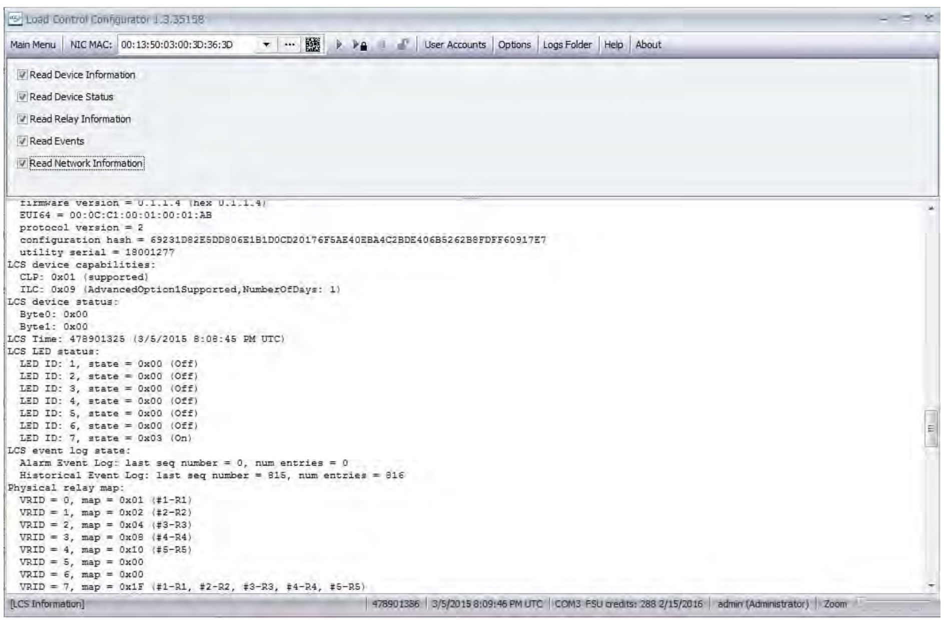

MAC ID 00135003003D3616 (2 relay) HCM

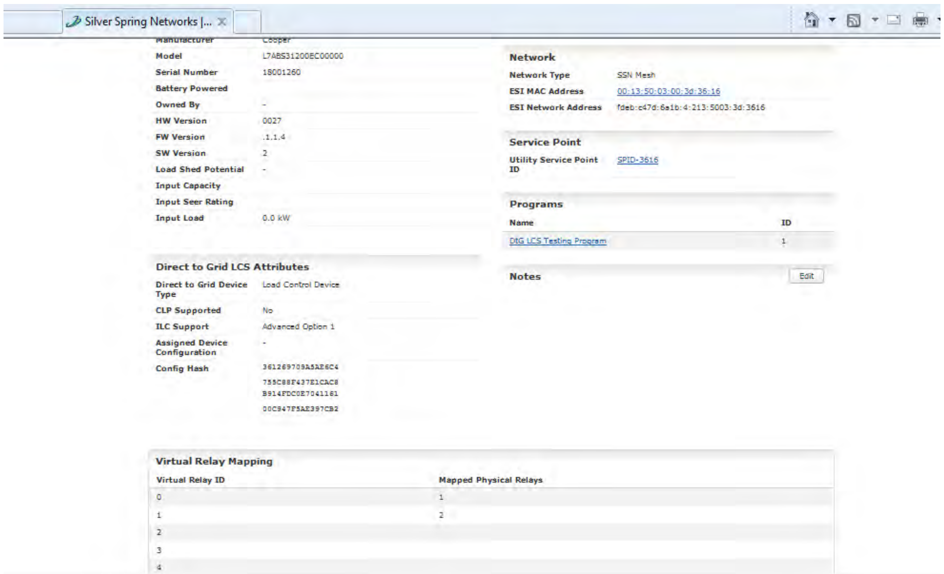

MAC ID 00135003003D3616 (2 relay) LCC

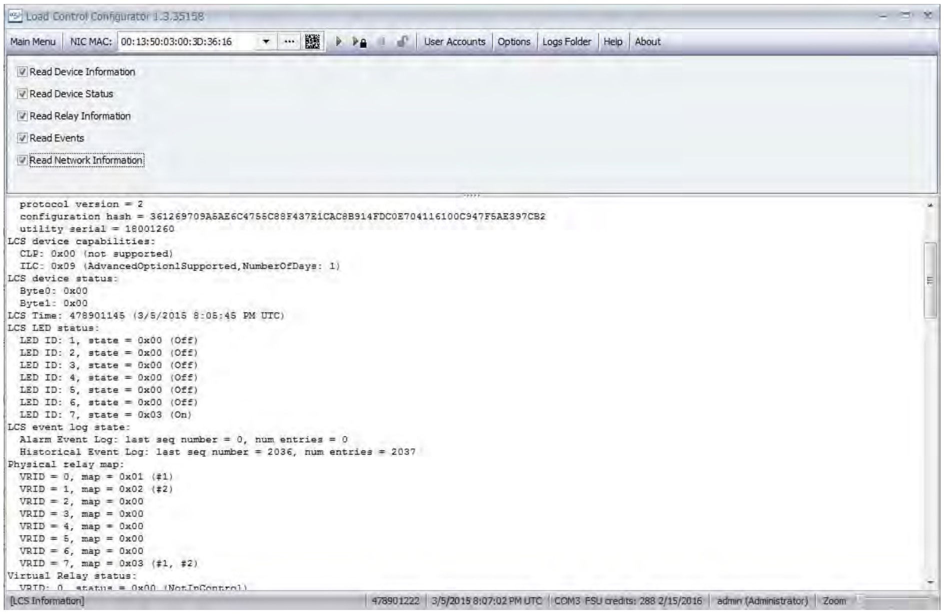

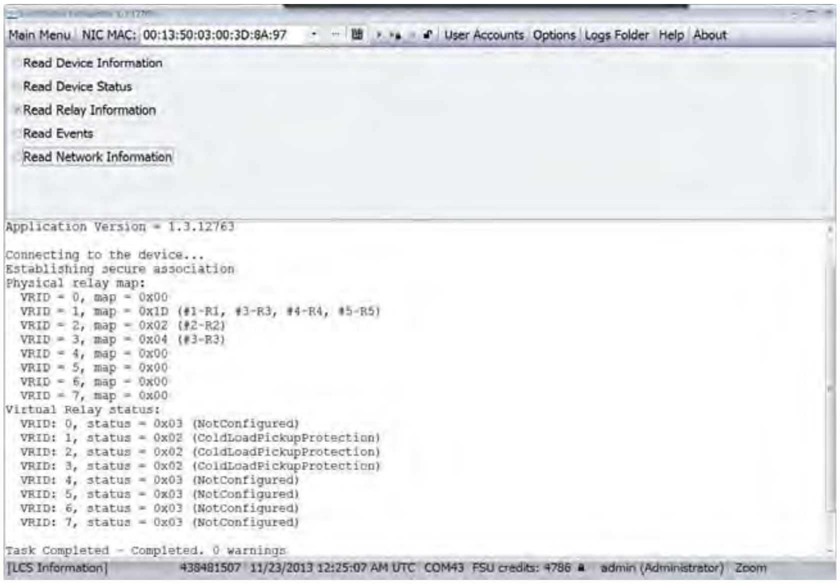
Main Menu
NIC MAC: 00:13:50:03:00:3D:8A:97
User Accounts
Options
Logs Folder
Help
About
Read Device Information
Read Device Status
Read Relay Information
Read Events
Read Network Information
Application Version = 1.3.12763
Connecting to the device...
Establishing secure association
Physical relay map:
VRID = 0, map = 0x00
VRID = 1, map = 0x1D (#1-R1, #3-R3, #4-R4, #5-R5)
VRID = 2, map = 0x02 (#2-R2)
VRID = 3, map = 0x04 (#3-R3)
VRID = 4, map = 0x00
VRID = 5, map = 0x00
VRID = 6, map = 0x00
VRID = 7, map = 0x00
Virtual Relay status:
VRID: 0, status = 0x03 (NotConfigured)
VRID: 1, status = 0x02 (ColdLoadPickupProtection)
VRID: 2, status = 0x02 (ColdLoadPickupProtection)
VRID: 3, status = 0x02 (ColdLoadPickupProtection)
VRID: 4, status = 0x03 (NotConfigured)
VRID: 5, status = 0x03 (NotConfigured)
VRID: 6, status = 0x03 (NotConfigured)
VRID: 7, status = 0x03 (NotConfigured)
Task Completed - Completed. 0 warnings
[LCS Information]
438481507
11/23/2013 12:25:07 AM UTC
COM43
FSU credits: 4786
admin (Administrator)
Zoom

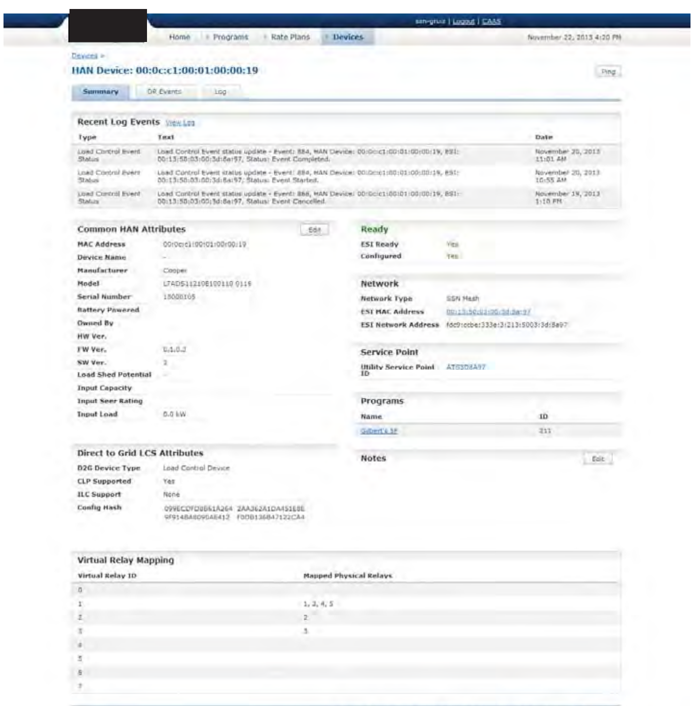
Logout
CAAS
Home
Programs
Rate Plans
Devices
November 22, 2013 4:20 PM
Devices >
HAN Device: 00:0c:c1:00:01:00:00:19
Ping
Summary
DR Events
Log
Recent Log Events
View Log
Type
Text
Date
Load Control Event Status
Load Control Event status update - Event: 884, HAN Device: 00:0c:c1:00:01:00:00:19, ESI: 00:13:50:03:00:3d:8a:97, Status: Event Completed.
November 20, 2013 11:01 AM
Load Control Event Status
Load Control Event status update - Event: 884, HAN Device: 00:0c:c1:00:01:00:00:19, ESI: 00:13:50:03:00:3d:8a:97, Status: Event Started.
November 20, 2013 10:55 AM
Load Control Event Status
Load Control Event status update - Event: 868, HAN Device: 00:0c:c1:00:01:00:00:19, ESI: 00:13:50:03:00:3d:8a:97, Status: Event Cancelled.
November 19, 2013 1:10 PM
Common HAN Attributes
Edit
MAC Address
00:0c:c1:00:01:00:00:19
Device Name
Manufacturer
Cooper
Model
Serial Number
Battery Powered
Owned By
HW Ver.
FW Ver.
SW Ver.
Load Shed Potential
Input Capacity
Input Seer Rating
Input Load
0.0 kW
Ready
ESI Ready
Yes
Configured
Yes
Network
Network Type
SSN Mesh
ESI MAC Address
ESI Network Address
Service Point
Utility Service Point ID
Programs
Name
ID
Notes
Edit
Direct to Grid LCS Attributes
D2G Device Type
Load Control Device
CLP Supported
Yes
ILC Support
None
Config Hash
Virtual Relay Mapping
Virtual Relay ID
Mapped Physical Relays
0
1
1, 3, 4, 5
2
2
3
3
4
5
6
7

35 NETWORK TIME OUT

35.1 OBJECTIVE

Determine duration of lost radio connection prior to restoring load.

35.2 TEST PREREQUISITES AND EQUIPMENT

One AP configured to test environment dedicated to switch to be tested.

One Field Service Unit

Three 2 Relay [redacted] Switches

Switch Number 1- S/N 180001003, MAC ID 00135003003D8A40

Switch Number 2-S/N 1800 107, MAC ID 00135003003D3637

Switch Number 3 S/N 18001004, MAC ID 00135003003D8A21

Three different configuration files loaded to switches

35.3 TEST 1 STEPS

1. Powers up switch number 1 configured to 30 minutes Network time out and allow it to join the NAN network.
2. Using LCC, Read LCS Information, Read Network Information validate that switch can see NAN neighbors. Devices can also be viewed in the Neighbors panel within LCC.
3. Using LCC, ping the switch to ensure operation.
4. Using LCC send a command event to control the switch continuously for one (1) hour.

   Disconnect AP from power outlet so switch

35.4 TEST 1 EXPECTED RESULTS

Even though event was created to control the load for one hour, switch should stop the event and restore load after 30 minutes of disconnecting the AP (lost radio connection).

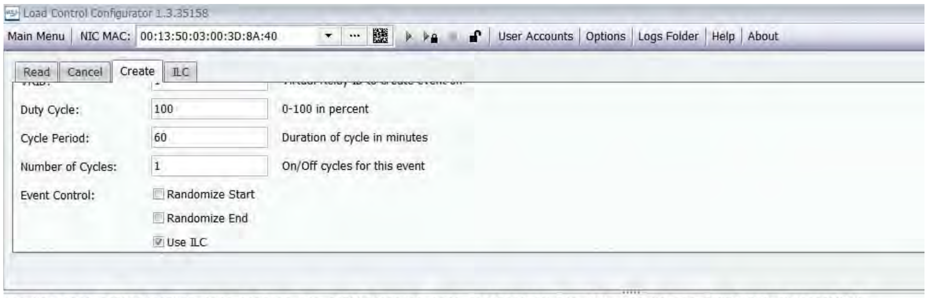


```
The uploaded configuration hash matches the configuration hash reported by the LCS. The upload completed successfully.

Task Completed - Completed. 0 warnings


===== Creating event on LCS =====
NIC MAC = 00:13:50:03:00:3D:8A:40
UTC = 1/16/2015 4:46:10 PM UTC
Application Version = 1.3.35158

Creating event ID = 474741970:
  Criticality = 100
  VRID = 1
  Start Time = 474741951 (1/16/2015 4:45:51 PM)
  Duty Cycle = 100
  Cycle Period = 60
  Number of Cycles = 1
  Event Control = 0x04 (Cycle Select: AdvancedOption1)
Event created. Event State = 0x02 (Event started)

Task Completed - Completed. 0 warnings
```


```
 #666H, 1/16/2015 4:39:38 PM (474741578), 0x808E "Vendor Specific", 5 bytes: 64 3C 01 04 00
 #667H, 1/16/2015 4:42:50 PM (474741770), 0x808C "Vendor Specific", 5 bytes: 1C 4B FC 0A 64
 #668H, 1/16/2015 4:42:50 PM (474741770), 0x808D "Vendor Specific", 5 bytes: 02 1C 4B FC 05
 #669H, 1/16/2015 4:42:50 PM (474741770), 0x808E "Vendor Specific", 5 bytes: 64 3C 01 00 00
 #670H, 1/16/2015 4:44:39 PM (474741879), 0x0003 "Reboot", 5 bytes: 01 00 00 00 00
 #671H, 1/16/2015 4:44:40 PM (474741880), 0x808A "Vendor Specific", 5 bytes: E5 02 99 68 A4
 #672H, 1/16/2015 4:44:40 PM (474741880), 0x8087 "Vendor Specific", 5 bytes: 00 79 00 79 00
 #673H, 1/16/2015 4:44:40 PM (474741880), 0x000C "Configuration Updated", 5 bytes: 1C 4B FC 69 00
 #674H, 1/16/2015 4:44:40 PM (474741880), 0x0001 "Power Up", 5 bytes: 00 00 00 10 03
 #675H, 1/16/2015 4:44:48 PM (474741888), 0x808B "Vendor Specific", 5 bytes: 05 00 00 00 00
 #676H, 1/16/2015 4:46:10 PM (474741970), 0x808C "Vendor Specific", 5 bytes: 1C 4B FC D2 64
 #677H, 1/16/2015 4:46:10 PM (474741970), 0x808D "Vendor Specific", 5 bytes: 01 1C 4B FC BF
 #678H, 1/16/2015 4:46:10 PM (474741970), 0x808E "Vendor Specific", 5 bytes: 64 3C 01 04 00
 #679H, 1/16/2015 4:46:10 PM (474741970), 0x000E "Event Started", 5 bytes: 1C 4B FC D2 00
 #680H, 1/16/2015 4:46:10 PM (474741970), 0x0018 "Relay Open", 5 bytes: 02 00 00 00 00
 #681H, 1/16/2015 5:29:28 PM (474744568), 0x8086 "Vendor Specific", 5 bytes: 00 00 00 00 00
 #682H, 1/16/2015 5:29:28 PM (474744568), 0x0019 "Relay Closed", 5 bytes: 02 00 00 00 00
 #683H, 1/16/2015 5:29:28 PM (474744568), 0x0010 "Event Canceled", 5 bytes: 1C 4B FC D2 00
 #684H, 1/16/2015 5:29:28 PM (474744568), 0x808B "Vendor Specific", 5 bytes: 00 00 00 00 00
 #685H, 1/16/2015 5:29:28 PM (474744568), 0x808B "Vendor Specific", 5 bytes: 05 00 00 00 00

Task Completed - Completed. 0 warnings
```

- **Event Duration-5:29-4:46=43 minutes< 1 hour scheduled event ≠30 minutes as per configuration**

35.5 TEST 2 STEPS

1. Powers up switch number 1 configured to 0 minutes Network time out and allow it to join the NAN network.

35.6 TEST 2 EXPECTED RESULTS

Even though switch lost radio connection due to the fact that AP was disconnected it should continue controlling load as per planned event for one (1) hour.

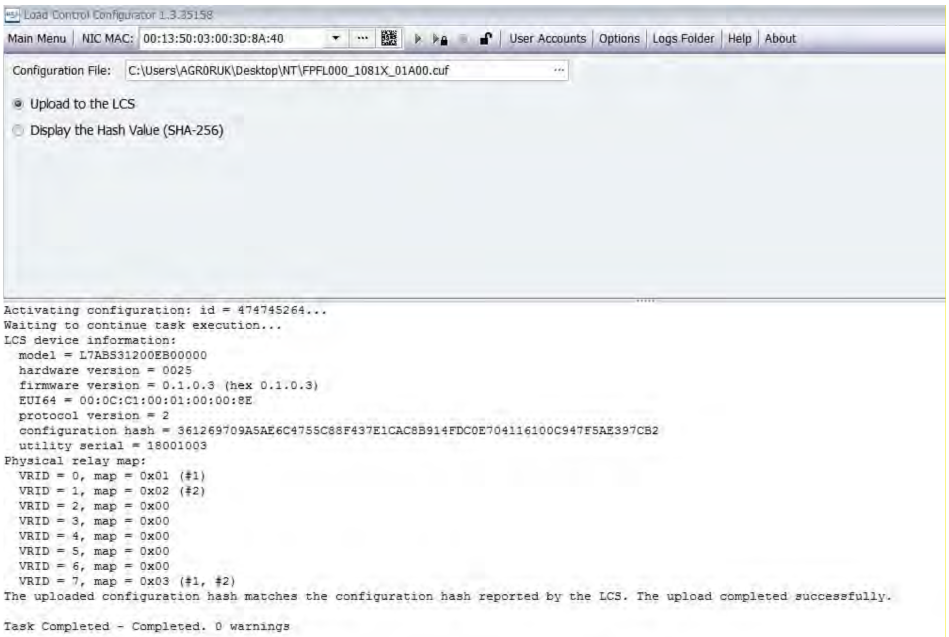

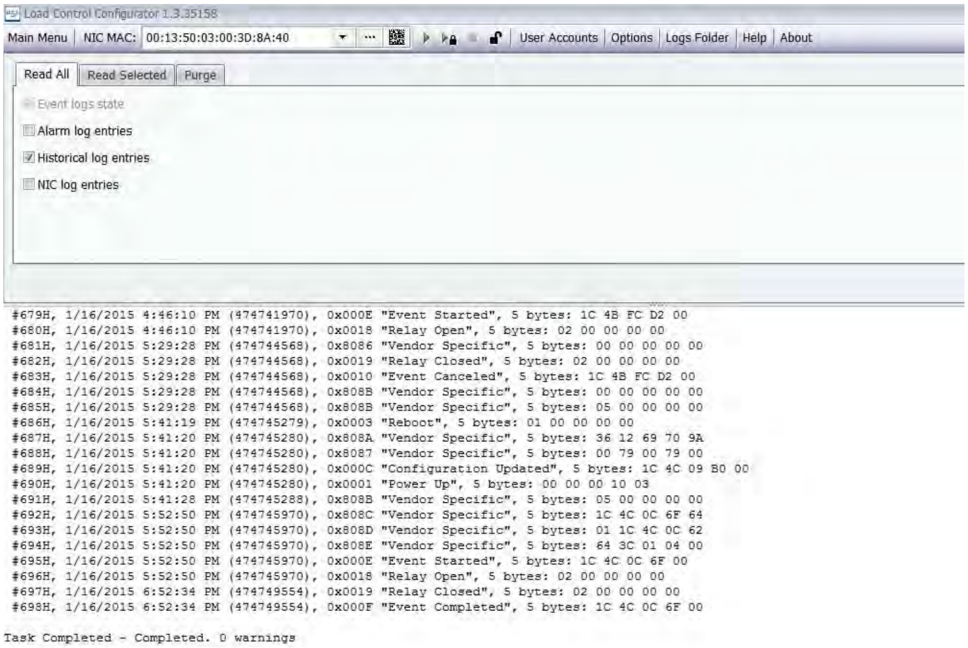

- **Event Duration-6:52-5:52=1 hour=1 hour scheduled event**

35.7 TEST 3 STEPS

1. Powers up switch number 2 configured to 30 minutes Network time out and allow it to join the NAN network.
2. Using LCC, Read LCS Information, Read Network Information validate that switch can see NAN neighbors. Devices can also be viewed in the Neighbors panel within LCC.
3. Using LCC, ping the switch to ensure operation.
4. Using LCC send a command event to control the switch continuously for one (1) hour.
5. Disconnect AP from power outlet so switch will lost radio connection.

   Record event finish time and compare with

35.8 TEST 3 EXPECTED RESULTS

Even though event was created to control the load for one hour, switch should stop the event and restore load after 30 minutes of disconnecting the AP (lost radio connection).


```
===== Reading information from LCS =====
NIC MAC = 00:13:50:03:00:3D:36:37
UTC = 1/16/2015 8:43:24 PM UTC
Application Version = 1.3.35158

Connecting to the device...
Establishing secure association
NIC firmware version: 3.2.002C
LCS device information:
  model = L7ABS31200EB00000
  hardware version = 0025
  firmware version = 0.1.0.3 (hex 0.1.0.3)
  EUI64 = 00:0C:C1:00:01:00:00:92
  protocol version = 2
  configuration hash = 4F51A8230EAA552ABA57ED4D28302CD9758BDA279D338C4F694E38820C31C096
  utility serial = 18001007
LCS device capabilities:
  CLP: 0x00 (not supported)
  ILC: 0x00 (NumberOfDays: 0)

Task Completed - Completed. 0 warnings
```

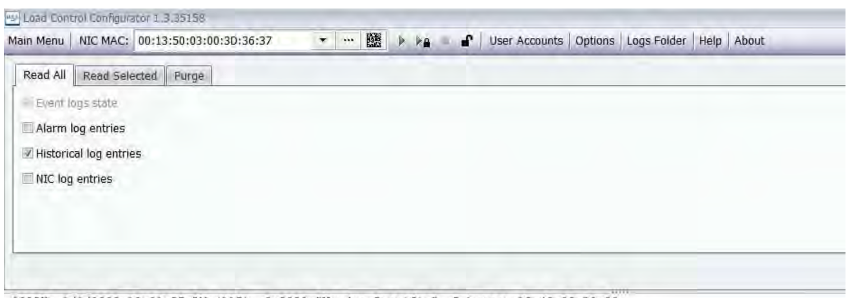


```
 #325H, 1/1/2000 12:01:57 AM (117), 0x8082 "Vendor Specific", 5 bytes: 1C 4C 0C A9 00
 #326H, 1/16/2015 5:53:45 PM (474746025), 0x000E "Event Started", 5 bytes: 1C 4C 0A EF 00
 #327H, 1/16/2015 5:53:45 PM (474746025), 0x0018 "Relay Open", 5 bytes: 02 00 00 00 00
 #328H, 1/16/2015 6:38:01 PM (474748681), 0x8086 "Vendor Specific", 5 bytes: 00 00 00 00 00
 #329H, 1/16/2015 6:38:01 PM (474748681), 0x0019 "Relay Closed", 5 bytes: 02 00 00 00 00
 #330H, 1/16/2015 6:38:01 PM (474748681), 0x0010 "Event Canceled", 5 bytes: 1C 4C 0A EF 00
 #331H, 1/16/2015 6:38:01 PM (474748681), 0x808B "Vendor Specific", 5 bytes: 00 00 00 00 00
 #332H, 1/16/2015 6:38:01 PM (474748681), 0x0014 "Load On", 5 bytes: 02 00 00 00 00
 #333H, 1/16/2015 6:38:02 PM (474748682), 0x0015 "Load Off", 5 bytes: 02 00 00 00 00
 #334H, 1/16/2015 6:38:24 PM (474748704), 0x808B "Vendor Specific", 5 bytes: 05 00 00 00 00
 #335H, 1/16/2015 7:29:04 PM (474751744), 0x808C "Vendor Specific", 5 bytes: 1C 4C 22 F9 64
 #336H, 1/16/2015 7:29:04 PM (474751744), 0x808D "Vendor Specific", 5 bytes: 02 1C 4C 22 DE
 #337H, 1/16/2015 7:29:04 PM (474751744), 0x808E "Vendor Specific", 5 bytes: 64 3C 01 04 00
 #338H, 1/16/2015 7:29:04 PM (474751744), 0x000E "Event Started", 5 bytes: 1C 4C 22 F9 00
 #339H, 1/16/2015 7:29:04 PM (474751744), 0x0018 "Relay Open", 5 bytes: 02 00 00 00 00
 #340H, 1/16/2015 8:04:21 PM (474753861), 0x8086 "Vendor Specific", 5 bytes: 00 00 00 00 00
 #341H, 1/16/2015 8:04:21 PM (474753861), 0x0019 "Relay Closed", 5 bytes: 02 00 00 00 00
 #342H, 1/16/2015 8:04:21 PM (474753861), 0x0010 "Event Canceled", 5 bytes: 1C 4C 22 F9 00
 #343H, 1/16/2015 8:04:21 PM (474753861), 0x808B "Vendor Specific", 5 bytes: 00 00 00 00 00
 #344H, 1/16/2015 8:04:24 PM (474753864), 0x808B "Vendor Specific", 5 bytes: 05 00 00 00 00

Task Completed - Completed. 0 warnings
```

- **Event Duration-8:04-7:29=35 minutes< 1 hour scheduled event ≠30 minutes as per configuration**

35.9 TEST 4 STEPS

1. Powers up switch number 3 configured to 30 minutes Network time out and allow it to join the NAN network.
2. Using LCC, Read LCS Information, Read Network Information validate that switch can see NAN neighbors. Devices can also be viewed in the Neighbors panel within LCC.
3. Using LCC, ping the switch to ensure operation.
4. Using LCC send a command event to control the switch continuously for one (1) hour.
5. Disconnect AP from power outlet so switch will lost radio connection.

   Record event finish time and compare

35.10 TEST 4 EXPECTED RESULTS

Even though event was created to control the load for one hour, switch should stop the event and restore load after 30 minutes of disconnecting the AP (lost radio connection.

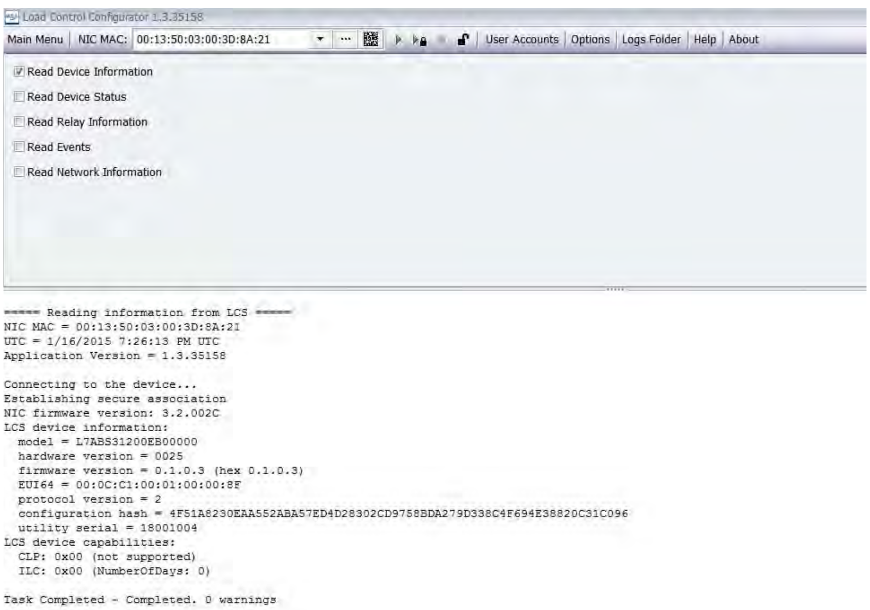

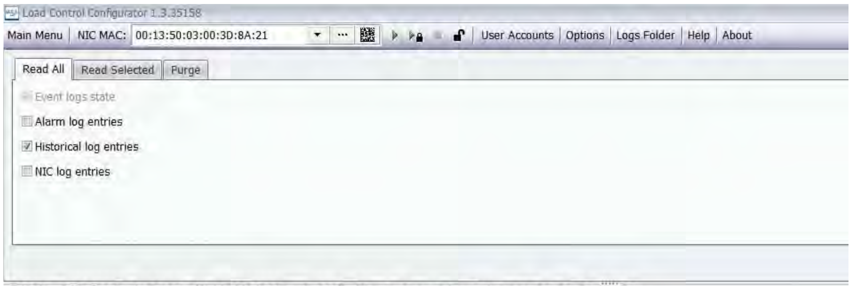


```
#418H, 1/15/2015 4:25:00 PM (474654300), 0x000E "Event Started", 5 bytes: 00 00 00 B7 00
#419H, 1/15/2015 4:25:00 PM (474654300), 0x0018 "Relay Open", 5 bytes: 02 00 00 00 00
#420H, 1/15/2015 4:35:00 PM (474654900), 0x0019 "Relay Closed", 5 bytes: 02 00 00 00 00
#421H, 1/15/2015 4:35:00 PM (474654900), 0x000F "Event Completed", 5 bytes: 00 00 00 B7 00
#422H, 1/15/2015 4:35:00 PM (474654900), 0x0014 "Load On", 5 bytes: 02 00 00 00 00
#423H, 1/15/2015 4:35:01 PM (474654901), 0x0015 "Load Off", 5 bytes: 02 00 00 00 00
#424H, 1/15/2015 4:47:32 PM (474655652), 0x0000 "Power Loss", 5 bytes: 00 00 00 00 00
#425H, 1/1/2000 12:00:00 AM (0), 0x0001 "Power Up", 5 bytes: 03 00 00 10 03
#426H, 1/1/2000 12:00:20 AM (20), 0x808B "Vendor Specific", 5 bytes: 05 00 00 00 00
#427H, 1/1/2000 12:01:02 AM (62), 0x8082 "Vendor Specific", 5 bytes: 1C 4C 21 E1 00
#428H, 1/16/2015 7:28:19 PM (474751699), 0x808C "Vendor Specific", 5 bytes: 1C 4C 22 D2 64
#429H, 1/16/2015 7:28:19 PM (474751699), 0x808D "Vendor Specific", 5 bytes: 02 1C 4C 22 C7
#430H, 1/16/2015 7:28:19 PM (474751699), 0x808E "Vendor Specific", 5 bytes: 64 3C 01 04 00
#431H, 1/16/2015 7:28:19 PM (474751699), 0x000E "Event Started", 5 bytes: 1C 4C 22 D2 00
#432H, 1/16/2015 7:28:19 PM (474751699), 0x0018 "Relay Open", 5 bytes: 02 00 00 00 00
#433H, 1/16/2015 8:09:29 PM (474754169), 0x8086 "Vendor Specific", 5 bytes: 00 00 00 00 00
#434H, 1/16/2015 8:09:29 PM (474754169), 0x0019 "Relay Closed", 5 bytes: 02 00 00 00 00
#435H, 1/16/2015 8:09:29 PM (474754169), 0x0010 "Event Canceled", 5 bytes: 1C 4C 22 D2 00
#436H, 1/16/2015 8:09:29 PM (474754169), 0x808B "Vendor Specific", 5 bytes: 00 00 00 00 00
#437H, 1/16/2015 8:09:51 PM (474754191), 0x808B "Vendor Specific", 5 bytes: 05 00 00 00 00

Task Completed - Completed. 0 warnings
```

- **Event Duration-8:09-7:28=41 minutes< 1 hour scheduled event ≠30 minutes as per configuration**

36 MAXIMUM CONTROL DURATION

36.1 OBJECTIVE

The switch shall be able to reject an event longer than the maximum duration set in the configuration file.

36.2 TEST PREREQUISITES AND EQUIPMENT

[redacted] switches MAC ID 0013500300441FA7with 4 hours maximum event duration setting.

36.3 TEST STEPS

1. Verify that switch MAC ID 0013500300441FA7 have a maximum event duration set to 4 hours in the configuration file.
2. Using LCC, create an event to control VRID 7 for 5 hours.
3. Ensure parameters are correct and send the event to the switch.
4. Ensure that the event in step 2 is rejected by the switch due to the duration being longer that allowed by the switch.
5. Log and record the results.

36.4 EXPECTED RESULTS

The control event was created and sent to be executed for 5 hours. It should be rejected or executed for 4 hours only which is the maximum control duration allowed on settings.

36.5 MAXIMUM CONTROL DURATION RESULTS

Load Control Switch MAC ID 0013500300441FA7 failed to stop the control after 4 hours as per setting.

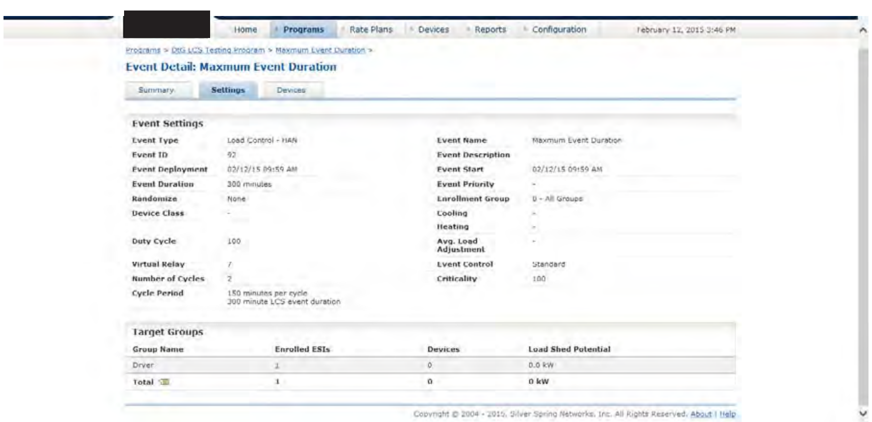

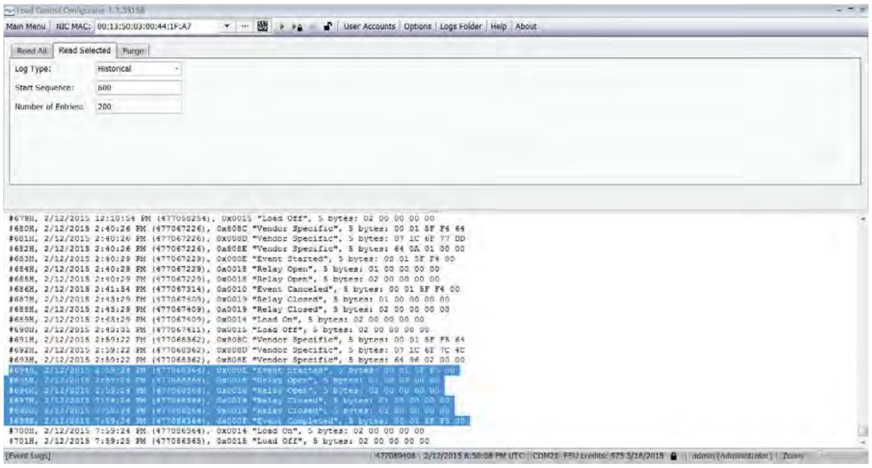

[redacted] team checked the configuration file and apparently there was mistake creating the file. Loaded configuration file had maximum control duration parameter set to zero which means no limited control duration period.

[redacted] team sent an alternative configuration file to FPL. New file has the maximum control duration set to 1 hour. We uploaded the new file. Second test on the same switch with new configuration uploaded.

36.6 EXPECTED RESULTS

The control event was created and sent to be executed for 2 hours. It should be rejected or executed for 1 hour only which is the maximum control duration allowed on settings.

36.7 MAXIMUM CONTROL DURATION RESULTS

Load Control Switch MAC ID 0013500300441FA7 stopped the control after 1 hour as per setting.

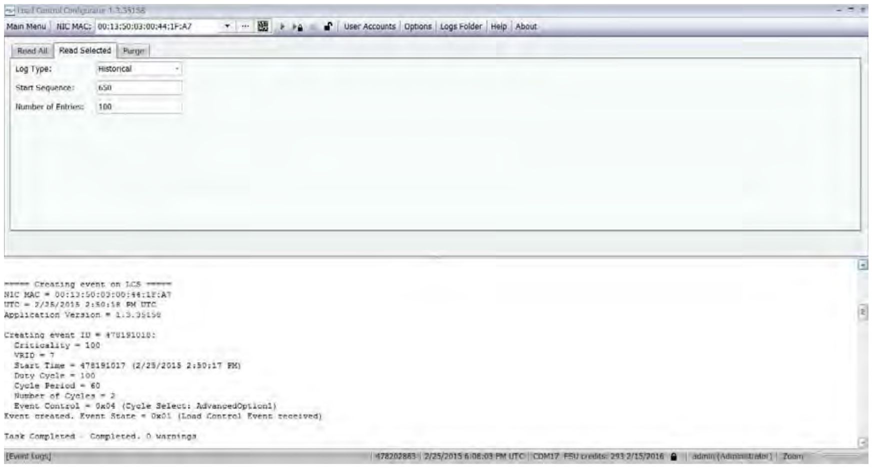
Main Menu
NIC MAC: 00:13:50:03:00:44:1F:A7
User Accounts
Options
Logs Folder
Help
About
Read All
Read Selected
Purge
Log Type: Historical
Start Sequence: 650
Number of Entries: 100
===== Creating event on LCS =====
NIC MAC = 00:13:50:03:00:44:1F:A7
UTC = 2/25/2015 2:50:18 PM UTC
Creating event ID = 478191018:
Criticality = 100
VRID = 7
Start Time = 478191017 (2/25/2015 2:50:17 PM)
Duty Cycle = 100
Cycle Period = 60
Number of Cycles = 2
Event Control = 0x04 (Cycle Select: AdvancedOption1)
Event created. Event State = 0x01 (Load Control Event received)
Task Completed - Completed. 0 warnings
[Event Logs]
478202883
2/25/2015 6:08:03 PM UTC

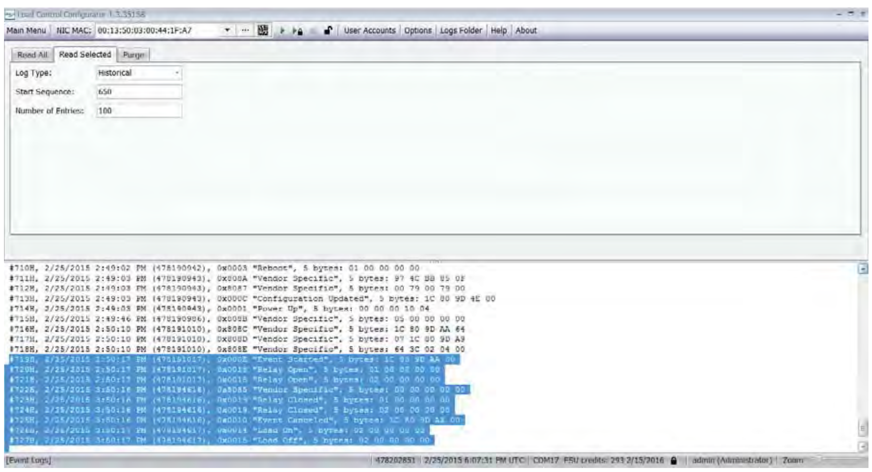
Main Menu
NIC MAC: 00:13:50:03:00:44:1F:A7
User Accounts
Options
Logs Folder
Help
About
Read All
Read Selected
Purge
Log Type: Historical
Start Sequence: 650
Number of Entries: 100
#710H, 2/25/2015 2:49:02 PM (478190942), 0x0003 "Reboot", 5 bytes: 01 00 00 00 00
#711H, 2/25/2015 2:49:03 PM (478190943), 0x808A "Vendor Specific", 5 bytes: 97 4C BB 85 0F
#712H, 2/25/2015 2:49:03 PM (478190943), 0x8087 "Vendor Specific", 5 bytes: 00 79 00 79 00
#713H, 2/25/2015 2:49:03 PM (478190943), 0x000C "Configuration Updated", 5 bytes: 1C 80 9D 4E 00
#714H, 2/25/2015 2:49:03 PM (478190943), 0x0001 "Power Up", 5 bytes: 00 00 00 10 04
#715H, 2/25/2015 2:49:46 PM (478190986), 0x808B "Vendor Specific", 5 bytes: 05 00 00 00 00
#716H, 2/25/2015 2:50:10 PM (478191010), 0x808C "Vendor Specific", 5 bytes: 1C 80 9D AA 64
#717H, 2/25/2015 2:50:10 PM (478191010), 0x808D "Vendor Specific", 5 bytes: 07 1C 80 9D A9
#718H, 2/25/2015 2:50:10 PM (478191010), 0x808E "Vendor Specific", 5 bytes: 64 3C 02 04 00
[Event Logs]
478202851
2/25/2015 6:07:31 PM UTC

37 SHORT CYLCE PROTECTION

37.1 OBJECTIVE

The switch shall not perform an event shorter that the short cycle protection time that is set in the configuration file.

37.2 TEST PREREQUISITES AND EQUIPMENT

[redacted] switch MAC: 0013500300441FA7, HCM

37.3 TEST STEPS

1. Verify that all switches have a short cycle protection set to 180 minutes in the configuration file.
2. Using HCM, create an event to control VRID 7 for 10 minutes.
3. Cancel the event after 1 minute of starting.
4. Through observation ensure that even though the event in step 2 is cancelled in 1 minute relays will not close and released the load until 180 minutes passed after event started which is the short cycle protection setting.
5. Log and record the results.

37.4 EXPECTED RESULTS

Due to short cycle protection setting to 180 sec. the event will get cancelled at 180 sec and not at 60 sec. as it was created.

37.5 SHORT CYCLE PROTECTION

Event was deployed at 9:40 am to start at 9:40 am. Event was cancelled at 9:41 am, 1 minute after event started.

Cancellation task was completed at 9:43 am so nevertheless the cancelation command was sent 1 minute after the event started it was cancelled only 3 minutes after the starting time which coincides with the short cycle protection setting.

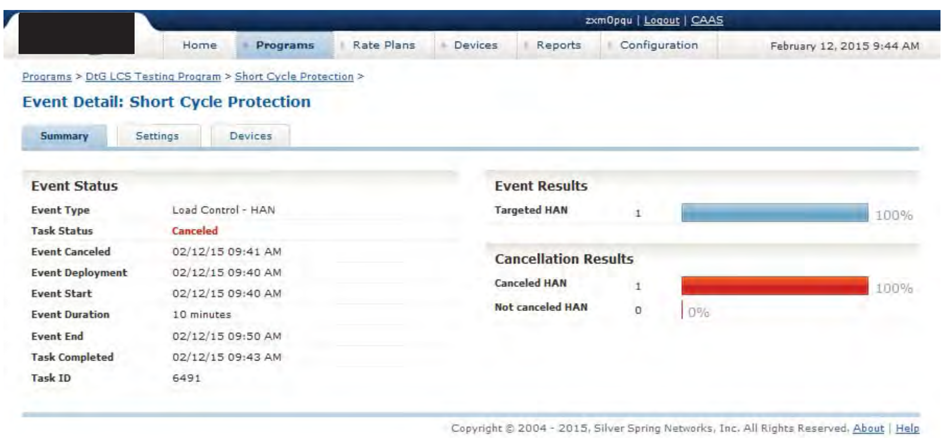

[redacted]

zxm0pqu | Logout | CAAS

Home | Programs | Rate Plans | **Devices** | Reports | Configuration

February 12, 2015 9:46 AM

The logs have been requested from the device. The results may take up to several minutes to arrive. Refresh the display periodically to view the updated logs.

Devices >

HAN Device: 00:0c:c1:00:01:00:01:16

Ping | Request Event Logs

Summary | DR Events | **Log**

Log Events

Results Showing 1 - 20 of 740

< Prev 1 2 3 4 5 6 7 .. 37 Next >

Type	Text	Sequence	Date
Load Control Event Status	Load Control Event status update - Event: 90, HAN Device: 00:0c:c1:00:01:00:01:16, ESI: 00:13:50:03:00:44:1f:a7, Status: Event cancelled.		February 12, 2015 9:43:03 AM
Load Control Event Status	Load Control Event status update - Event: 90, HAN Device: 00:0c:c1:00:01:00:01:16, ESI: 00:13:50:03:00:44:1f:a7, Status: Event Started.		February 12, 2015 9:40:55 AM
Load Control Event Status	Load Control Event status update - Event: 90, HAN Device: 00:0c:c1:00:01:00:01:16, ESI: 00:13:50:03:00:44:1f:a7, Status: Event Received.		February 12, 2015 9:40:32 AM
LCS event log	type: 1, log event ID: 21(0x15), payload: Physical Relay (1) data(0200000000)	679	February 12, 2015 7:10:54 AM
LCS event log	type: 1, log event ID: 20(0x14), payload: Physical Relay (1) data(0200000000)	678	February 12, 2015 7:10:54 AM
LCS event log	type: 1, log event ID: 21(0x15), payload: Physical Relay (1) data(0200000000)	677	February 11, 2015 7:10:02 AM
LCS event log	type: 1, log event ID: 20(0x14), payload: Physical Relay (1) data(0200000000)	676	February 11, 2015 7:10:01 AM

38 SWITCH SHALL HAVE ABILITY TO CONFIRM IF CLP ENABLED / DISABLED PER VIRTUAL RELAY VIA HCM

38.1 OBJECTIVE

The switch shall have the ability to confirm if CLP is enabled or disabled for each virtual relay via use of HCM.

38.2 TEST PREREQUISITES AND EQUIPMENT

[redacted] switches MAC ID 00135003003D3611 and MAC ID 00135003003D35AA, HCM, LCC

[redacted] Configuration files for two relay switches and 5 relay switches

38.3 TEST STEPS

1. Ensure that configuration file is loaded on all switches.
2. Power down the switch MAC ID 00135003003D3611 and power it back up. Ensure that CLP does not engage and log the result.
3. Using HCM locate and verify the configuration hash for the switch. Note the configuration file for two relay switch does not have CLP enabled.
4. Power down the switch MAC ID 00135003003D35AA and power it back up. Ensure that CLP engage and log the result.
5. Using HCM locate and verify the configuration hash for the switch. Note the configuration file for five relay switch does have CLP enabled.
6. Via HCM, query both switches for the configuration hash.
7. Using available data, provided by HCM, and visual confirmation, review it for the CLP status information.
   NOTE: The hash does not contain specific data about CLP status. This must be derived from knowing the configuration file and its associated hash key.
8. Log and record the information.

38.4 EXPECTED RESULTS

Verification of functionality.

38.5 SWITCH SHALL HAVE ABILITY TO CONFIRM IF CLP ENABLED/DISABLED PER VIRTUAL RELAY VIA HCM RESULTS

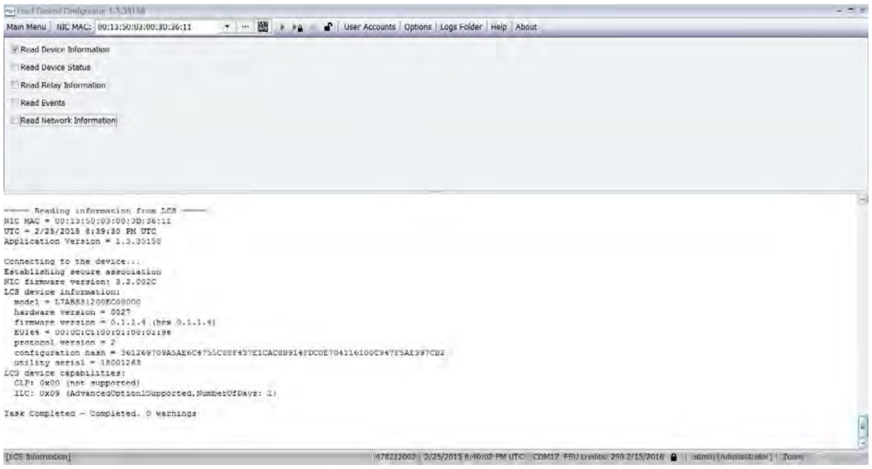

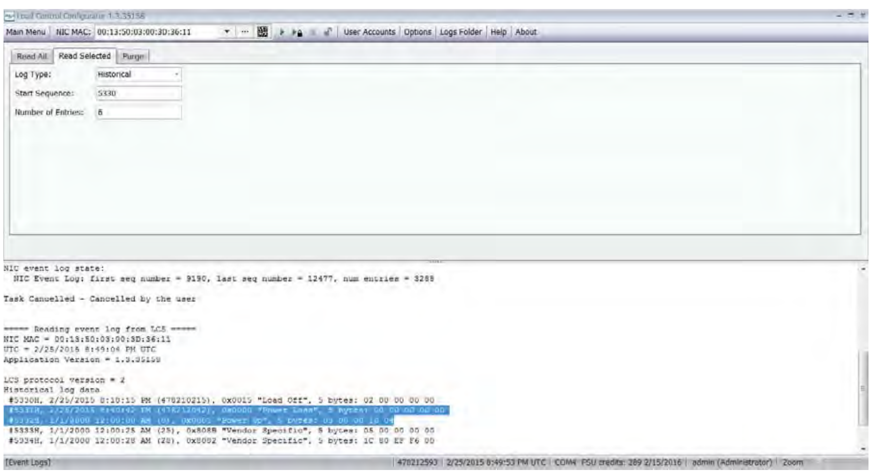

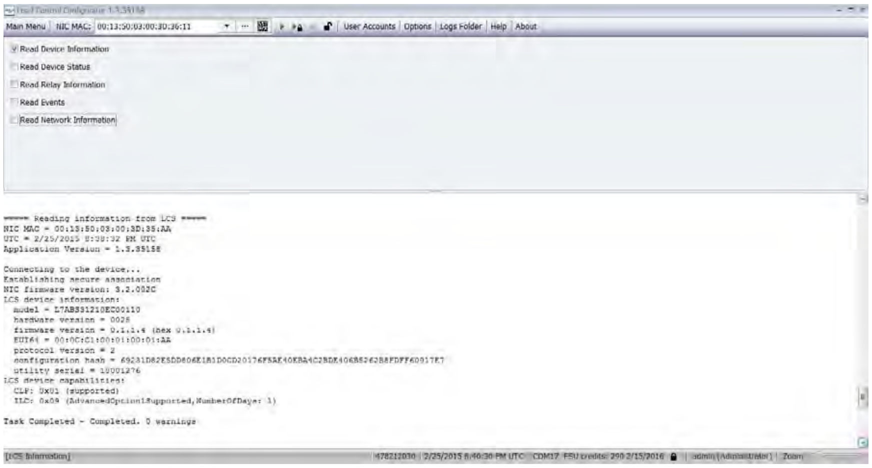
Main Menu
NIC MAC: 00:13:50:03:00:3D:36:11
User Accounts
Options
Logs Folder
Help
About
Read Device Information
Read Device Status
Read Relay Information
Read Events
Read Network Information
===== Reading information from LCS =====
NIC MAC = 00:13:50:03:00:3D:35:AA
Application Version = 1.3.35158
Connecting to the device...
Establishing secure association
NIC firmware version: 3.2.002C
LCS device information:
model = L7ABS31210EC00110
hardware version = 0028
EUI64 = 00:0C:C1:00:01:00:01:AA
protocol version = 2
utility serial = 10001276
LCS device capabilities:
CLP: 0x01 (supported)
ILC: 0x09 (AdvancedOption1Supported,NumberOfDays: 1)
Task Completed - Completed. 0 warnings
[LCS Information]

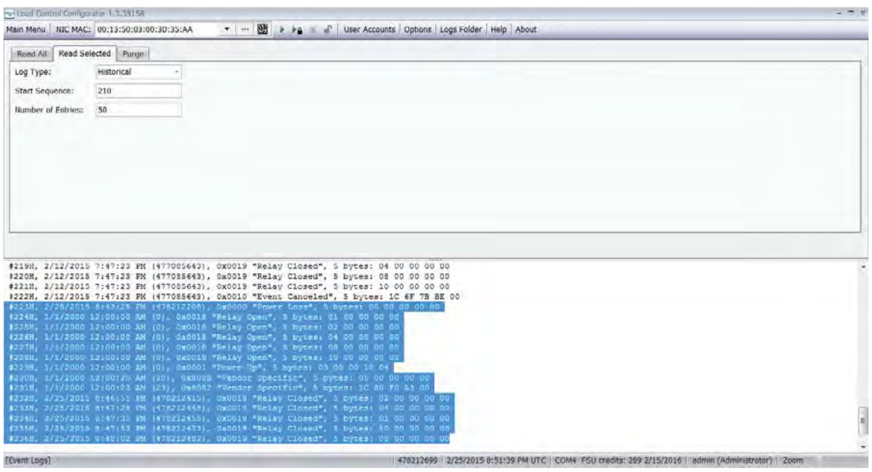
Main Menu
NIC MAC: 00:13:50:03:00:3D:35:AA
User Accounts
Options
Logs Folder
Help
About
Read All
Read Selected
Purge
Log Type: Historical
Start Sequence: 210
Number of Entries: 50
#219H, 2/12/2015 7:47:23 PM (477085643), 0x0019 "Relay Closed", 5 bytes: 04 00 00 00 00
#220H, 2/12/2015 7:47:23 PM (477085643), 0x0019 "Relay Closed", 5 bytes: 08 00 00 00 00
#221H, 2/12/2015 7:47:23 PM (477085643), 0x0019 "Relay Closed", 5 bytes: 10 00 00 00 00
#222H, 2/12/2015 7:47:23 PM (477085643), 0x0010 "Event Canceled", 5 bytes: 1C 6F 7B BE 00
[Event Logs]
478212699
2/25/2015 8:51:39 PM UTC
COM4
FSU credits: 289 2/15/2016

HCM

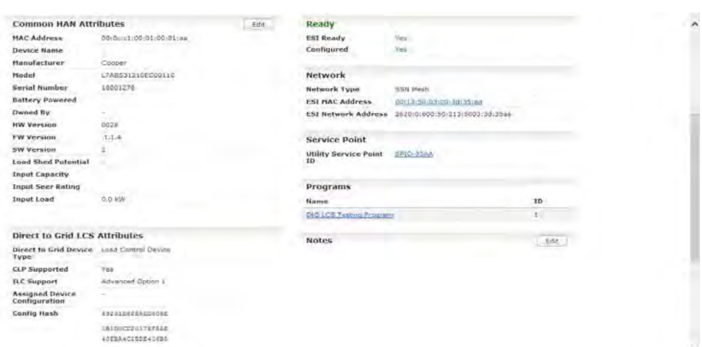
Common HAN Attributes
Edit
MAC Address
Device Name
Manufacturer
Cooper
Model
Serial Number
Battery Powered
Owned By
HW Version
FW Version
SW Version
Load Shed Potential
Input Capacity
Input Seer Rating
Input Load
0.0 kW
Direct to Grid LCS Attributes
Direct to Grid Device Type
Load Control Device
CLP Supported
Yes
ILC Support
Advanced Option 1
Assigned Device Configuration
Config Hash
Ready
ESI Ready
Yes
Configured
Yes
Network
Network Type
SSN Mesh
ESI MAC Address
ESI Network Address
Service Point
Utility Service Point ID
Programs
Name
ID
1
Notes
Edit

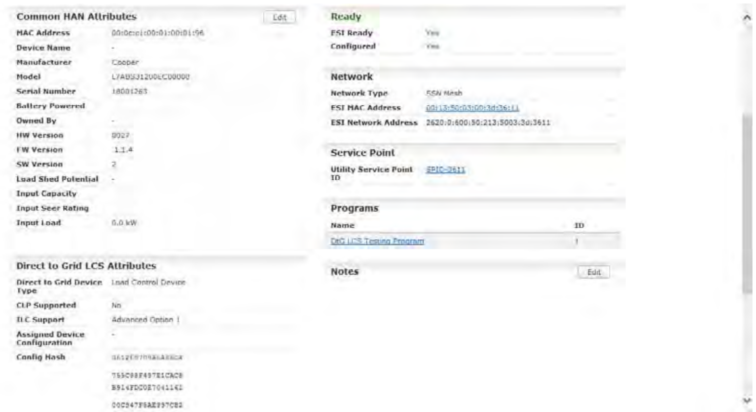
Common HAN Attributes
Edit
MAC Address
Device Name
Manufacturer
Cooper
Model
Serial Number
Battery Powered
Owned By
HW Version
FW Version
1.1.4
SW Version
Load Shed Potential
Input Capacity
Input Seer Rating
Input Load
0.0 kW
Direct to Grid LCS Attributes
Direct to Grid Device Type
Load Control Device
CLP Supported
No
DLC Support
Advanced Option 1
Assigned Device Configuration
Config Hash
Ready
ESI Ready
Configured
Network
Network Type
ESI MAC Address
ESI Network Address
2620:0:600:50:213:5003:3d:3611
Service Point
Utility Service Point ID
Programs
Name
ID
Notes
Edit

39 COLD LOAD PICK UP

39.1 OBJECTIVE

After loss of power switches with Cold Load Pickup CLP enabled shall control the load for the time the parameter is set for in the configuration file.

39.2 TEST PREREQUISITES AND EQUIPMENT

[redacted] switch MAC: 00135003003D361F, LCC

39.3 TEST STEPS

1. Using LCC verify that above switch has enabled CLP set to 180 minutes in the configuration file.
2. Power down all switches for 30-seconds and then power them back up.
3. Once switches have joined the network log in to the switch using LCC and verify that it controlled the load for 180 sec.
4. Log and record the results.

39.4 EXPECTED RESULTS

After recovering from loss of power switch shall control connected load for 180 seconds.

39.5 COLD LOAD PICK-UP

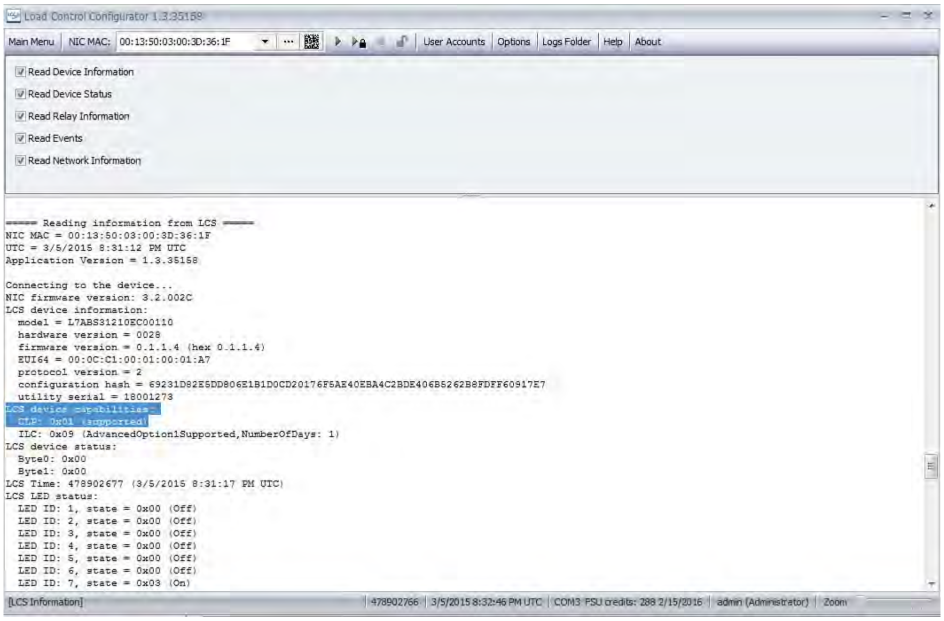
Load Control Configurator 1.3.35158
Main Menu
NIC MAC: 00:13:50:03:00:3D:36:1F
User Accounts
Options
Logs Folder
Help
About
Read Device Information
Read Device Status
Read Relay Information
Read Events
Read Network Information
===== Reading information from LCS =====
NIC MAC = 00:13:50:03:00:3D:36:1F
UTC = 3/5/2015 8:31:12 PM UTC
Application Version = 1.3.35158
Connecting to the device...
NIC firmware version: 3.2.002C
LCS device information:
model = L7ABS31210EC00110
hardware version = 0028
firmware version = 0.1.1.4 (hex 0.1.1.4)
EUI64 = 00:0C:C1:00:01:00:01:A7
protocol version = 2
configuration hash = 69231D82E5DD806E1B1D0CD20176F5AE40EBA4C2BDE406B5262B8FDFF60917E7
utility serial = 18001273
LCS device capabilities:
CLP: 0x01 (supported)
ILC: 0x09 (AdvancedOption1Supported,NumberOfDays: 1)
LCS device status:
Byte0: 0x00
Byte1: 0x00
LCS Time: 478902677 (3/5/2015 8:31:17 PM UTC)
LCS LED status:
LED ID: 1, state = 0x00 (Off)
LED ID: 2, state = 0x00 (Off)
LED ID: 3, state = 0x00 (Off)
LED ID: 4, state = 0x00 (Off)
LED ID: 5, state = 0x00 (Off)
LED ID: 6, state = 0x00 (Off)
LED ID: 7, state = 0x03 (On)
[LCS Information]
478902766
3/5/2015 8:32:46 PM UTC
COM3 FSU credits: 288 2/15/2016
admin (Administrator)
Zoom

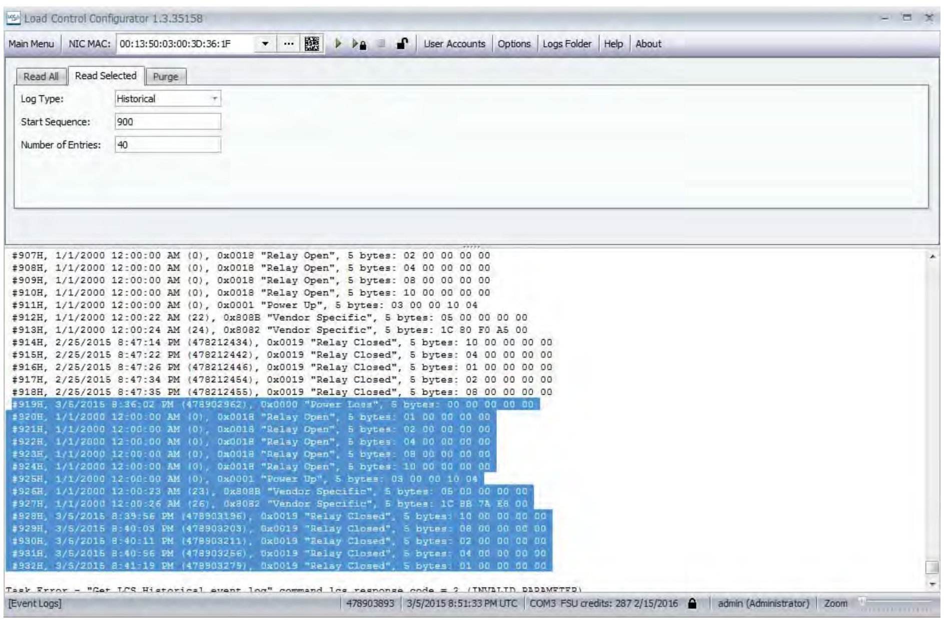
Load Control Configurator 1.3.35158
Main Menu
NIC MAC: 00:13:50:03:00:3D:36:1F
User Accounts
Options
Logs Folder
Help
About
Read All
Read Selected
Purge
Log Type: Historical
Start Sequence: 900
Number of Entries: 40
#907H, 1/1/2000 12:00:00 AM (0), 0x0018 "Relay Open", 5 bytes: 02 00 00 00 00
#908H, 1/1/2000 12:00:00 AM (0), 0x0018 "Relay Open", 5 bytes: 04 00 00 00 00
#909H, 1/1/2000 12:00:00 AM (0), 0x0018 "Relay Open", 5 bytes: 08 00 00 00 00
#910H, 1/1/2000 12:00:00 AM (0), 0x0018 "Relay Open", 5 bytes: 10 00 00 00 00
#911H, 1/1/2000 12:00:00 AM (0), 0x0001 "Power Up", 5 bytes: 03 00 00 10 04
#912H, 1/1/2000 12:00:22 AM (22), 0x808B "Vendor Specific", 5 bytes: 05 00 00 00 00
#913H, 1/1/2000 12:00:24 AM (24), 0x8082 "Vendor Specific", 5 bytes: 1C 80 F0 A5 00
#914H, 2/25/2015 8:47:14 PM (478212434), 0x0019 "Relay Closed", 5 bytes: 10 00 00 00 00
#915H, 2/25/2015 8:47:22 PM (478212442), 0x0019 "Relay Closed", 5 bytes: 04 00 00 00 00
#916H, 2/25/2015 8:47:26 PM (478212446), 0x0019 "Relay Closed", 5 bytes: 01 00 00 00 00
#917H, 2/25/2015 8:47:34 PM (478212454), 0x0019 "Relay Closed", 5 bytes: 02 00 00 00 00
#918H, 2/25/2015 8:47:35 PM (478212455), 0x0019 "Relay Closed", 5 bytes: 08 00 00 00 00
#919H, 3/5/2015 8:36:02 PM (478902962), 0x0000 "Power Loss", 5 bytes: 00 00 00 00 00
#920H, 1/1/2000 12:00:00 AM (0), 0x0018 "Relay Open", 5 bytes: 01 00 00 00 00
#921H, 1/1/2000 12:00:00 AM (0), 0x0018 "Relay Open", 5 bytes: 02 00 00 00 00
#922H, 1/1/2000 12:00:00 AM (0), 0x0018 "Relay Open", 5 bytes: 04 00 00 00 00
#923H, 1/1/2000 12:00:00 AM (0), 0x0018 "Relay Open", 5 bytes: 08 00 00 00 00
#924H, 1/1/2000 12:00:00 AM (0), 0x0018 "Relay Open", 5 bytes: 10 00 00 00 00
#925H, 1/1/2000 12:00:00 AM (0), 0x0001 "Power Up", 5 bytes: 03 00 00 10 04
#926H, 1/1/2000 12:00:23 AM (23), 0x808B "Vendor Specific", 5 bytes: 05 00 00 00 00
#927H, 1/1/2000 12:00:26 AM (26), 0x8082 "Vendor Specific", 5 bytes: 1C BB 7A E8 00
#928H, 3/5/2015 8:39:56 PM (478903196), 0x0019 "Relay Closed", 5 bytes: 10 00 00 00 00
#929H, 3/5/2015 8:40:03 PM (478903203), 0x0019 "Relay Closed", 5 bytes: 08 00 00 00 00
#930H, 3/5/2015 8:40:11 PM (478903211), 0x0019 "Relay Closed", 5 bytes: 02 00 00 00 00
#931H, 3/5/2015 8:40:56 PM (478903256), 0x0019 "Relay Closed", 5 bytes: 04 00 00 00 00
#932H, 3/5/2015 8:41:19 PM (478903279), 0x0019 "Relay Closed", 5 bytes: 01 00 00 00 00
[Event Logs]
478903893
3/5/2015 8:51:33 PM UTC
COM3 FSU credits: 287 2/15/2016
admin (Administrator)
Zoom

40 ACTIVITY LOGS CAPTURE DIAGNOSTIC RESULTS

40.1 OBJECTIVE

The switch's activity logs shall capture the results of internal diagnostic tests.

40.2 TEST PREREQUISITES AND EQUIPMENT

[redacted] switch, IAR's IDE, JTAG connectors

40.3 TEST STEPS

[redacted] to provide documentation.

40.4 EXPECTED RESULTS

Documentation provided, see below.

===== Reading event log from LCS =====

NIC MAC = 00:13:50:03:00:3D:8A:78

UTC = 5/26/2015 2:27:14 PM UTC

Application Version = 1.2.8475

LCS event log state:

Alarm Event Log: last seq number = 0, num entries = 0

Historical Event Log: last seq number = 36, num entries = 32

NIC event log state:

NIC Event Log: first seq number = 0, last seq number = 111, num entries = 112

Historical log data

#5H, 5/26/2015 1:33:25 PM (485962405), 0x8095 "Vendor Specific", 5 bytes: 00 00 00 00 00

#6H, 5/26/2015 1:35:39 PM (485962539), 0x0002 "Self Check Error", 5 bytes: 36 84 64 2B 00

#7H, 5/26/2015 1:36:31 PM (485962591), 0x0001 "Power Up", 5 bytes: 00 00 00 10 04

#8H, 5/26/2015 1:36:40 PM (485962600), 0x808B "Vendor Specific", 5 bytes: 05 00 00 00 00

#9H, 5/26/2015 1:37:16 PM (485962636), 0x808C "Vendor Specific", 5 bytes: 1C F7 34 29 00

#10H, 5/26/2015 1:37:16 PM (485962636), 0x808D "Vendor Specific", 5 bytes: 00 00 00 00 00

#11H, 5/26/2015 1:37:16 PM (485962636), 0x808E "Vendor Specific", 5 bytes: 64 05 01 00 00

#12H, 5/26/2015 1:37:16 PM (485962636), 0x8097 "Vendor Specific", 5 bytes: 1C F7 34 29 00

#13H, 5/26/2015 1:37:16 PM (485962636), 0x000E "Event Started", 5 bytes: 1C F7 34 29 00

#14H, 5/26/2015 1:37:16 PM (485962636), 0x0018 "Relay Open", 5 bytes: 01 00 00 00 00

#15H, 5/26/2015 1:42:16 PM (485962936), 0x000F "Event Completed", 5 bytes: 1C F7 34 29 00

#16H, 5/26/2015 1:42:16 PM (485962936), 0x0019 "Relay Closed", 5 bytes: 01 00 00 00 00

#17H, 5/26/2015 2:05:07 PM (485964307), 0x0003 "Reboot", 5 bytes: 00 00 00 00 00

#18H, 5/26/2015 2:05:08 PM (485964308), 0x0001 "Power Up", 5 bytes: 00 00 00 10 04

#19H, 5/26/2015 2:05:24 PM (485964324), 0x808B "Vendor Specific", 5 bytes: 05 00 00 00 00

#20H, 5/26/2015 2:07:40 PM (485964460), 0x0003 "Reboot", 5 bytes: 00 00 00 00 00

#21H, 5/26/2015 2:07:41 PM (485964461), 0x808A "Vendor Specific", 5 bytes: 05 1E EF BE 95

#22H, 5/26/2015 2:07:41 PM (485964461), 0x8087 "Vendor Specific", 5 bytes: 00 7A 00 7A 00

#23H, 5/26/2015 2:07:41 PM (485964461), 0x000C "Configuration Updated", 5 bytes: 1C F7 3B 3C 00

#24H, 5/26/2015 2:07:41 PM (485964461), 0x0001 "Power Up", 5 bytes: 00 00 00 10 04

#25H, 5/26/2015 2:07:53 PM (485964473), 0x808B "Vendor Specific", 5 bytes: 05 00 00 00 00

#26H, 5/26/2015 2:08:28 PM (485964508), 0x0003 "Reboot", 5 bytes: 00 00 00 00 00

#27H, 5/26/2015 2:08:29 PM (485964509), 0x000A "Configuration Validation Failed", 5 bytes: 1C F7 3B 6A 00

#28H, 5/26/2015 2:08:29 PM (485964509), 0x0001 "Power Up", 5 bytes: 00 00 00 10 04

#29H, 5/26/2015 2:08:53 PM (485964533), 0x808B "Vendor Specific", 5 bytes: 05 00 00 00 00

#30H, 5/26/2015 2:18:37 PM (485965117), 0x0003 "Reboot", 5 bytes: 00 00 00 00 00

#31H, 5/26/2015 2:18:38 PM (485965118), 0x0001 "Power Up", 5 bytes: 00 00 00 10 04

#32H, 5/26/2015 2:18:53 PM (485965133), 0x808B "Vendor Specific", 5 bytes: 05 00 00 00 00

#33H, 5/26/2015 2:19:20 PM (485965160), 0x0000 "Power Loss", 5 bytes: 00 00 00 00 00

#34H, 5/26/2015 2:19:27 PM (485965167), 0x0001 "Power Up", 5 bytes: 00 00 00 00 00

#35H, 5/26/2015 2:19:47 PM (485965187), 0x808B "Vendor Specific", 5 bytes: 00 00 00 00 00

#36H, 5/26/2015 2:20:15 PM (485965215), 0x808B "Vendor Specific", 5 bytes: 05 00 00 00 00

41 CAN LCT DETECT UNDERFREQUENCY CONDITION AND ACTIVATE CONTROL?

41.1 OBJECTIVE

The switch shall be able to detect under-frequency events and control the load (open realys).

41.2 TEST PREREQUISITES AND EQUIPMENT

Pacific Power AC Power Source. High Performance 1 phase and 3 phase Linear AC Power Sources. Operates from 20 to 5,000 Hz, range in power from 500VA to 30kVA, and provide nominal output voltage ranges up to 600Vrms L-N.

[redacted] switch MAC: 00135003003D360B, HCM Test Steps

41.3 TEST STEPS

Switch was powered up at 240V, for this test the frequency was the only variable changed and it was achieved using the AC power source. There were two tests, one reducing the frequency to 59.9 HZ and the other one to 59.7 Hz. The same procedure was used to test the same unit a couple of times in order to recreate the same behavior.

1) The frequency was set to 59.9 Hz and switch didn't react to the change. No relays open or any other change was observed with the relays and the functioning of the device. Events were sent to the device and all were accepted.

2) The frequency was set to 59.7 Hz. Relays opened and remain open for more than 10 minutes with no changes in their statuses. Commands were sent to different relays and all of them were rejected. The "cancel all events" was executed and relays closed and were ready to be exercised with no issues.

3) The frequency was set back to 59.9 Hz. Sometimes when the frequency is changed from 59.7 Hz to 59.9 Hz all the switches open. Commands were sent to different relays and all of them were rejected. The "cancel all events" was executed and relays closed and were ready to be exercised with no issues.

4) The frequency was set back to 60 Hz. The relays remain closed and ready for events to be executed.

5) The frequency was changed all the way down from 60 Hz to 59.7 Hz. Relays opened (wait for 5 minutes) there was no changes in the status of the relays, then the frequency was changed back to 60 HZ(relays remain open). Commands were sent to different relays and all of them were rejected. The "cancel all events" was executed and relays closed and were ready to be exercised with no issues.

41.4 TEST RESULTS

According to the results obtained during the under frequency test, it was observed that when the unit was set to work at 59.7 Hz all the relays opened and remained open until the “cancel all event “command was executed, after the events were cleared the device works under normal conditions. Once the relays opened at 59.7 Hz, and the frequency was changed to 59.9 Hz first and then 60 Hz, it could not be closed until the “cancel all events” command was run again.

Our conclusion is that the feature of switches reacting to an underfrequency event need to be polished. Relays do open when frequency is reduced to 59.7 but when frequency was back to normal switches will not close on their own. A cancel all events has to be executed to close all relays.

Incidental finding.

While conducting test # 34 with switch 3634 team noticed that in the logs there was an abnormal reading where loads will go on and off constantly without us controlling them. To determine what relay was causing this issue we disconnected both loads one at a time from the Load Control Switch (LCS) and determine that it was the 5 Amp relay which was creating this false “on-off “readings. See screen shot below.

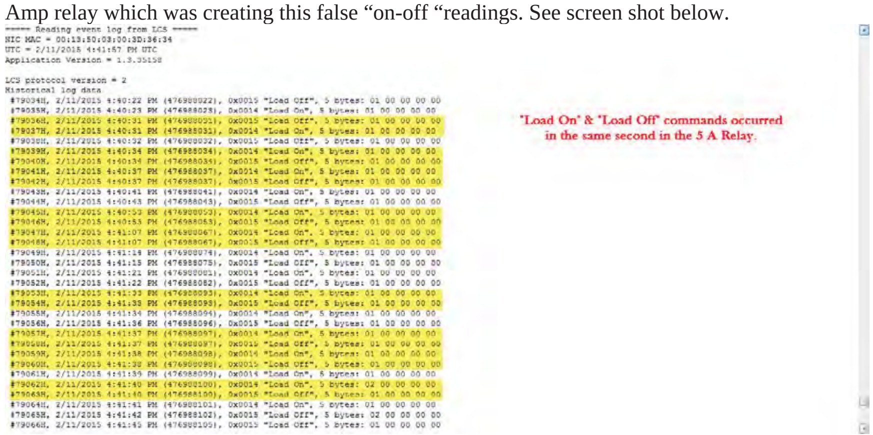

Toggle switch installed between the load control and the load was turned off disconnecting the load from the LCS and the load on-off stoped

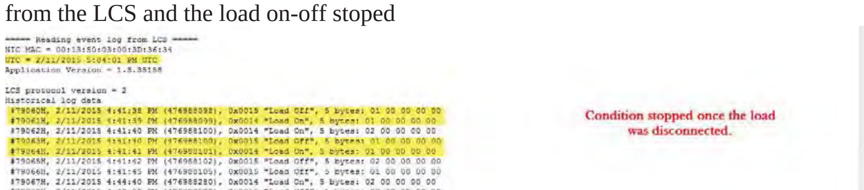

In order to determine if it was something related to the switch or to the load we decided to replace the switch with a new one 2 relay switch 360B and we observed same condition.

```
===== Reading event log from LCS =====
NIC MAC = 00:13:50:03:00:3D:36:0B
UTC = 2/11/2015 7:50:00 PM UTC
Application Version = 1.3.35158

LCS protocol version = 2
Historical log data
 #209H, 2/11/2015 7:36:58 PM (476998618), 0x0014 "Load On", 5 bytes: 01 00 00 00 00
 #210H, 2/11/2015 7:36:58 PM (476998618), 0x0015 "Load Off", 5 bytes: 01 00 00 00 00
 #211H, 2/11/2015 7:37:58 PM (476998678), 0x0014 "Load On", 5 bytes: 01 00 00 00 00
 #212H, 2/11/2015 7:37:58 PM (476998678), 0x0015 "Load Off", 5 bytes: 01 00 00 00 00
 #213H, 2/11/2015 7:38:57 PM (476998737), 0x0014 "Load On", 5 bytes: 01 00 00 00 00
 #214H, 2/11/2015 7:38:58 PM (476998738), 0x0015 "Load Off", 5 bytes: 01 00 00 00 00
 #215H, 2/11/2015 7:39:58 PM (476998798), 0x0014 "Load On", 5 bytes: 01 00 00 00 00
 #216H, 2/11/2015 7:39:58 PM (476998798), 0x0015 "Load Off", 5 bytes: 01 00 00 00 00
 #217H, 2/11/2015 7:40:25 PM (476998825), 0x0014 "Load On", 5 bytes: 01 00 00 00 00
 #218H, 2/11/2015 7:40:28 PM (476998828), 0x0015 "Load Off", 5 bytes: 01 00 00 00 00
 #219H, 2/11/2015 7:40:58 PM (476998858), 0x0014 "Load On", 5 bytes: 01 00 00 00 00
 #220H, 2/11/2015 7:40:58 PM (476998858), 0x0015 "Load Off", 5 bytes: 01 00 00 00 00
 #221H, 2/11/2015 7:41:58 PM (476998918), 0x0014 "Load On", 5 bytes: 01 00 00 00 00
 #222H, 2/11/2015 7:41:58 PM (476998918), 0x0015 "Load Off", 5 bytes: 01 00 00 00 00
 #223H, 2/11/2015 7:42:58 PM (476998978), 0x0014 "Load On", 5 bytes: 01 00 00 00 00
 #224H, 2/11/2015 7:42:58 PM (476998978), 0x0015 "Load Off", 5 bytes: 01 00 00 00 00
 #225H, 2/11/2015 7:43:58 PM (476999038), 0x0014 "Load On", 5 bytes: 01 00 00 00 00
 #226H, 2/11/2015 7:43:58 PM (476999038), 0x0015 "Load Off", 5 bytes: 01 00 00 00 00
 #227H, 2/11/2015 7:44:58 PM (476999098), 0x0014 "Load On", 5 bytes: 01 00 00 00 00
 #228H, 2/11/2015 7:44:58 PM (476999098), 0x0015 "Load Off", 5 bytes: 01 00 00 00 00
 #229H, 2/11/2015 7:45:58 PM (476999158), 0x0014 "Load On", 5 bytes: 01 00 00 00 00
 #230H, 2/11/2015 7:45:58 PM (476999158), 0x0015 "Load Off", 5 bytes: 01 00 00 00 00
 #231H, 2/11/2015 7:46:58 PM (476999218), 0x0014 "Load On", 5 bytes: 01 00 00 00 00
 #232H, 2/11/2015 7:46:58 PM (476999218), 0x0015 "Load Off", 5 bytes: 01 00 00 00 00
 #233H, 2/11/2015 7:47:58 PM (476999278), 0x0014 "Load On", 5 bytes: 01 00 00 00 00
 #234H, 2/11/2015 7:47:58 PM (476999278), 0x0015 "Load Off", 5 bytes: 01 00 00 00 00
 #235H, 2/11/2015 7:48:58 PM (476999338), 0x0014 "Load On", 5 bytes: 01 00 00 00 00
 #236H, 2/11/2015 7:48:58 PM (476999338), 0x0015 "Load Off", 5 bytes: 01 00 00 00 00
 #237H, 2/11/2015 7:49:58 PM (476999398), 0x0014 "Load On", 5 bytes: 01 00 00 00 00
 #238H, 2/11/2015 7:49:58 PM (476999398), 0x0015 "Load Off", 5 bytes: 01 00 00 00 00
```

Condition was replicated using a different Load Control Switch

From engineering analysis the only reason we can think off is the threshold for the current sensing device being very close to the real load being consumed by the thermostat. The thermostat installed at the Lab is a smart one which performs more operations than a regular one. A maximum consumption for the thermostat is 0.2 Amp and the threshold is 0.15 Amp. Most of devices don't usually consume the maximum allowed so there are probabilities that the thermostat is consuming very close to the threshold of 0.15 Amp and that is why the load shows on-off.

Same condition was found later occurring with other switches as shown below.

Serial Number: 18001264
MAC: 00135003003D35D9
Load: Refrigerator
Relay: 30 A

```
===== Reading event log from LCS =====
NIC MAC = 00:13:50:03:00:3D:35:D9
UTC = 2/12/2015 4:13:37 PM UTC
Application Version = 1.3.35158

LCS protocol version = 2
Historical log data
 #1352H, 2/11/2015 5:10:06 AM (476946606), 0x0015 "Load Off", 5 bytes: 02 00 00 00 00
 #1353H, 2/11/2015 5:28:07 AM (476947687), 0x0014 "Load On", 5 bytes: 02 00 00 00 00
 #1354H, 2/11/2015 8:14:12 AM (476957652), 0x0015 "Load Off", 5 bytes: 02 00 00 00 00
 #1355H, 2/11/2015 8:14:39 AM (476957679), 0x0014 "Load On", 5 bytes: 02 00 00 00 00
 #1356H, 2/11/2015 8:14:43 AM (476957683), 0x0015 "Load Off", 5 bytes: 02 00 00 00 00
 #1357H, 2/11/2015 8:40:06 AM (476959206), 0x0014 "Load On", 5 bytes: 02 00 00 00 00
 #1358H, 2/11/2015 8:40:10 AM (476959210), 0x0015 "Load Off", 5 bytes: 02 00 00 00 00
 #1359H, 2/11/2015 8:51:44 AM (476959904), 0x0014 "Load On", 5 bytes: 02 00 00 00 00
 #1360H, 2/11/2015 8:53:33 AM (476960013), 0x0015 "Load Off", 5 bytes: 02 00 00 00 00
 #1361H, 2/11/2015 8:54:29 AM (476960069), 0x0014 "Load On", 5 bytes: 02 00 00 00 00
 #1362H, 2/11/2015 8:54:33 AM (476960073), 0x0015 "Load Off", 5 bytes: 02 00 00 00 00
 #1363H, 2/11/2015 9:27:53 AM (476962073), 0x0014 "Load On", 5 bytes: 02 00 00 00 00
 #1364H, 2/11/2015 1:46:39 PM (476977599), 0x0015 "Load Off", 5 bytes: 02 00 00 00 00
 #1365H, 2/11/2015 1:47:11 PM (476977631), 0x0014 "Load On", 5 bytes: 02 00 00 00 00
 #1366H, 2/11/2015 1:47:15 PM (476977635), 0x0015 "Load Off", 5 bytes: 02 00 00 00 00
 #1367H, 2/11/2015 2:06:58 PM (476978818), 0x0014 "Load On", 5 bytes: 02 00 00 00 00
 #1368H, 2/11/2015 2:06:58 PM (476978818), 0x0015 "Load Off", 5 bytes: 02 00 00 00 00
 #1369H, 2/11/2015 2:27:31 PM (476980051), 0x0014 "Load On", 5 bytes: 02 00 00 00 00
 #1370H, 2/11/2015 2:29:22 PM (476980162), 0x0015 "Load Off", 5 bytes: 02 00 00 00 00
 #1371H, 2/11/2015 2:30:16 PM (476980216), 0x0014 "Load On", 5 bytes: 02 00 00 00 00
 #1372H, 2/11/2015 2:30:20 PM (476980220), 0x0015 "Load Off", 5 bytes: 02 00 00 00 00
 #1373H, 2/11/2015 2:34:28 PM (476980468), 0x0014 "Load On", 5 bytes: 02 00 00 00 00
 #1374H, 2/11/2015 2:34:29 PM (476980469), 0x0015 "Load Off", 5 bytes: 02 00 00 00 00
 #1375H, 2/11/2015 2:39:53 PM (476980793), 0x0014 "Load On", 5 bytes: 02 00 00 00 00
 #1376H, 2/11/2015 2:39:53 PM (476980793), 0x0015 "Load Off", 5 bytes: 02 00 00 00 00
 #1377H, 2/11/2015 2:40:05 PM (476980805), 0x0014 "Load On", 5 bytes: 02 00 00 00 00
 #1378H, 2/11/2015 2:40:07 PM (476980807), 0x0015 "Load Off", 5 bytes: 02 00 00 00 00
 #1379H, 2/11/2015 2:40:08 PM (476980808), 0x0014 "Load On", 5 bytes: 02 00 00 00 00
 #1380H, 2/11/2015 2:40:09 PM (476980809), 0x0015 "Load Off", 5 bytes: 02 00 00 00 00
 #1381H, 2/11/2015 2:41:08 PM (476980868), 0x0014 "Load On", 5 bytes: 02 00 00 00 00
 #1382H, 2/11/2015 2:41:08 PM (476980868), 0x0015 "Load Off", 5 bytes: 02 00 00 00 00
 #1383H, 2/11/2015 2:49:28 PM (476981368), 0x0014 "Load On", 5 bytes: 02 00 00 00 00
 #1384H, 2/11/2015 2:49:43 PM (476981383), 0x0015 "Load Off", 5 bytes: 02 00 00 00 00
```

Serial Number: 18001263
MAC: 00135003003D611
Load: Water Cooler
Relay: 30A

```
===== Reading event log from LCS =====
NIC MAC = 00:13:50:03:00:3D:36:11
UTC = 2/12/2015 4:59:14 PM UTC
Application Version = 1.3.35158

LCS protocol version = 2
Historical log data
 #500H, 12/16/2014 8:36:05 PM (472077365), 0x0014 "Load On", 5 bytes: 02 00 00 00 00
 #501H, 12/16/2014 8:38:47 PM (472077527), 0x0015 "Load Off", 5 bytes: 02 00 00 00 00
 #502H, 12/16/2014 8:41:29 PM (472077689), 0x0014 "Load On", 5 bytes: 02 00 00 00 00
 #503H, 12/16/2014 8:51:06 PM (472078266), 0x0015 "Load Off", 5 bytes: 02 00 00 00 00
 #504H, 12/16/2014 9:31:06 PM (472080666), 0x0014 "Load On", 5 bytes: 02 00 00 00 00
 #505H, 12/16/2014 9:40:17 PM (472081217), 0x0015 "Load Off", 5 bytes: 02 00 00 00 00
 #506H, 12/16/2014 9:46:03 PM (472081563), 0x0014 "Load On", 5 bytes: 02 00 00 00 00
 #507H, 12/16/2014 9:48:45 PM (472081725), 0x0015 "Load Off", 5 bytes: 02 00 00 00 00
 #508H, 12/16/2014 10:16:34 PM (472083394), 0x0014 "Load On", 5 bytes: 02 00 00 00 00
 #509H, 12/16/2014 10:25:47 PM (472083947), 0x0015 "Load Off", 5 bytes: 02 00 00 00 00
 #510H, 12/16/2014 10:58:12 PM (472085892), 0x0014 "Load On", 5 bytes: 02 00 00 00 00
 #511H, 12/16/2014 11:00:54 PM (472086054), 0x0015 "Load Off", 5 bytes: 02 00 00 00 00
 #512H, 12/16/2014 11:04:33 PM (472086273), 0x0014 "Load On", 5 bytes: 02 00 00 00 00
 #513H, 12/16/2014 11:14:06 PM (472086846), 0x0015 "Load Off", 5 bytes: 02 00 00 00 00
 #514H, 12/16/2014 11:54:40 PM (472089280), 0x0014 "Load On", 5 bytes: 02 00 00 00 00
 #515H, 12/17/2014 12:03:42 AM (472089822), 0x0015 "Load Off", 5 bytes: 02 00 00 00 00
 #516H, 12/17/2014 12:09:59 AM (472090199), 0x0014 "Load On", 5 bytes: 02 00 00 00 00
 #517H, 12/17/2014 12:12:42 AM (472090362), 0x0015 "Load Off", 5 bytes: 02 00 00 00 00
 #518H, 12/17/2014 12:40:26 AM (472092026), 0x0014 "Load On", 5 bytes: 02 00 00 00 00
 #519H, 12/17/2014 12:49:38 AM (472092578), 0x0015 "Load Off", 5 bytes: 02 00 00 00 00
 #520H, 12/17/2014 1:21:29 AM (472094489), 0x0014 "Load On", 5 bytes: 02 00 00 00 00
 #521H, 12/17/2014 1:24:11 AM (472094651), 0x0015 "Load Off", 5 bytes: 02 00 00 00 00
 #522H, 12/17/2014 1:28:41 AM (472094921), 0x0014 "Load On", 5 bytes: 02 00 00 00 00
 #523H, 12/17/2014 1:38:16 AM (472095496), 0x0015 "Load Off", 5 bytes: 02 00 00 00 00
 #524H, 12/17/2014 2:18:41 AM (472097921), 0x0014 "Load On", 5 bytes: 02 00 00 00 00
 #525H, 12/17/2014 2:28:00 AM (472098480), 0x0015 "Load Off", 5 bytes: 02 00 00 00 00
 #526H, 12/17/2014 2:35:57 AM (472098957), 0x0014 "Load On", 5 bytes: 02 00 00 00 00
 #527H, 12/17/2014 2:38:43 AM (472099123), 0x0015 "Load Off", 5 bytes: 02 00 00 00 00
 #528H, 12/17/2014 3:05:02 AM (472100702), 0x0014 "Load On", 5 bytes: 02 00 00 00 00
 #529H, 12/17/2014 3:14:13 AM (472101253), 0x0015 "Load Off", 5 bytes: 02 00 00 00 00
 #530H, 12/17/2014 3:47:20 AM (472103240), 0x0014 "Load On", 5 bytes: 02 00 00 00 00
 #531H, 12/17/2014 3:50:00 AM (472103400), 0x0015 "Load Off", 5 bytes: 02 00 00 00 00
```

Serial Number: 18001262
MAC: 0013500300441FA7
Load: Dryer
Relay: 30 A

```
===== Reading event log from LCS =====
NIC MAC = 00:13:50:03:00:44:1F:A7
UTC = 2/12/2015 5:03:40 PM UTC
Application Version = 1.3.35158

LCS protocol version = 2
Historical log data
 #638H, 2/4/2015 4:56:38 PM (476384198), 0x0014 "Load On", 5 bytes: 02 00 00 00 00
 #639H, 2/4/2015 4:56:40 PM (476384200), 0x0015 "Load Off", 5 bytes: 02 00 00 00 00
 #640H, 2/5/2015 1:51:22 PM (476459482), 0x0014 "Load On", 5 bytes: 02 00 00 00 00
 #641H, 2/5/2015 1:52:25 PM (476459545), 0x0015 "Load Off", 5 bytes: 02 00 00 00 00
 #642H, 2/5/2015 1:52:28 PM (476459548), 0x0014 "Load On", 5 bytes: 02 00 00 00 00
 #643H, 2/5/2015 1:53:24 PM (476459604), 0x0015 "Load Off", 5 bytes: 02 00 00 00 00
 #644H, 2/5/2015 1:54:58 PM (476459698), 0x0014 "Load On", 5 bytes: 02 00 00 00 00
 #645H, 2/5/2015 1:56:01 PM (476459761), 0x0015 "Load Off", 5 bytes: 02 00 00 00 00
 #646H, 2/5/2015 1:56:04 PM (476459764), 0x0014 "Load On", 5 bytes: 02 00 00 00 00
 #647H, 2/5/2015 1:56:51 PM (476459811), 0x808C "Vendor Specific", 5 bytes: 1C 66 33 1B 64
 #648H, 2/5/2015 1:56:51 PM (476459811), 0x808D "Vendor Specific", 5 bytes: 07 1C 66 33 15
 #649H, 2/5/2015 1:56:51 PM (476459811), 0x808E "Vendor Specific", 5 bytes: 64 04 01 00 00
 #650H, 2/5/2015 1:56:51 PM (476459811), 0x000E "Event Started", 5 bytes: 1C 66 33 1B 00
 #651H, 2/5/2015 1:56:51 PM (476459811), 0x0018 "Relay Open", 5 bytes: 01 00 00 00 00
 #652H, 2/5/2015 1:56:51 PM (476459811), 0x0018 "Relay Open", 5 bytes: 02 00 00 00 00
 #653H, 2/5/2015 1:56:54 PM (476459814), 0x0015 "Load Off", 5 bytes: 02 00 00 00 00
 #654H, 2/5/2015 2:00:37 PM (476460037), 0x0019 "Relay Closed", 5 bytes: 01 00 00 00 00
 #655H, 2/5/2015 2:00:37 PM (476460037), 0x0019 "Relay Closed", 5 bytes: 02 00 00 00 00
 #656H, 2/5/2015 2:00:37 PM (476460037), 0x000F "Event Completed", 5 bytes: 1C 66 33 1B 00
 #657H, 2/5/2015 8:25:15 PM (476483115), 0x0014 "Load On", 5 bytes: 02 00 00 00 00
 #658H, 2/5/2015 8:25:15 PM (476483115), 0x0015 "Load Off", 5 bytes: 02 00 00 00 00
 #659H, 2/5/2015 8:41:08 PM (476484068), 0x0014 "Load On", 5 bytes: 02 00 00 00 00
 #660H, 2/5/2015 8:41:09 PM (476484069), 0x0015 "Load Off", 5 bytes: 02 00 00 00 00
 #661H, 2/10/2015 1:32:52 PM (476890372), 0x0014 "Load On", 5 bytes: 02 00 00 00 00
 #662H, 2/10/2015 1:32:53 PM (476890373), 0x0015 "Load Off", 5 bytes: 02 00 00 00 00
 #663H, 2/10/2015 2:09:59 PM (476892599), 0x808C "Vendor Specific", 5 bytes: 00 01 5F D8 00
 #664H, 2/10/2015 2:09:59 PM (476892599), 0x808D "Vendor Specific", 5 bytes: 07 1C 6C CD B8
 #665H, 2/10/2015 2:09:59 PM (476892599), 0x808E "Vendor Specific", 5 bytes: 64 05 01 00 00
 #666H, 2/10/2015 2:10:00 PM (476892600), 0x000E "Event Started", 5 bytes: 00 01 5F D8 00
 #667H, 2/10/2015 2:10:00 PM (476892600), 0x0018 "Relay Open", 5 bytes: 01 00 00 00 00
 #668H, 2/10/2015 2:10:00 PM (476892600), 0x0018 "Relay Open", 5 bytes: 02 00 00 00 00
 #669H, 2/10/2015 2:15:00 PM (476892900), 0x0019 "Relay Closed", 5 bytes: 01 00 00 00 00
 #670H, 2/10/2015 2:15:00 PM (476892900), 0x0019 "Relay Closed", 5 bytes: 02 00 00 00 00
```

[redacted] switch 3634 was connected as recommended by [redacted] downstream the thermostat and no load on-load off without controlling was detected any more.

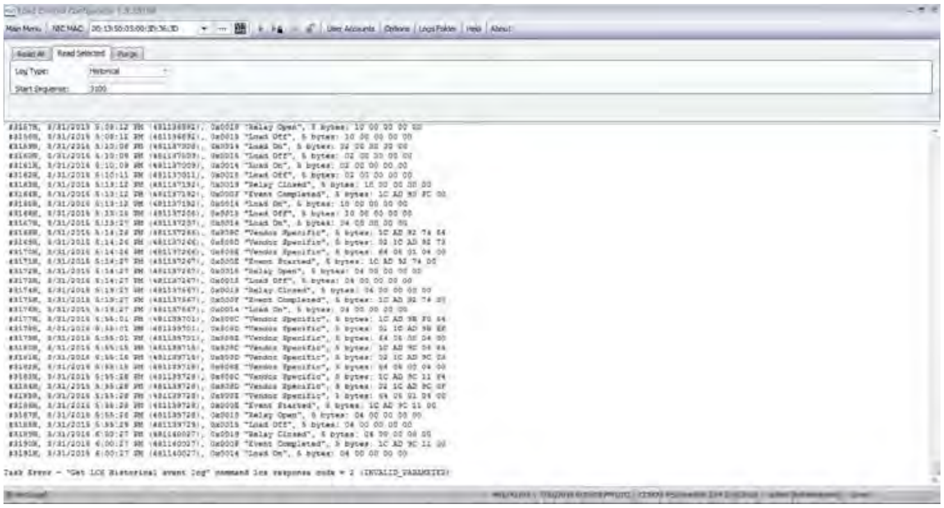

Feedback from [redacted]

An investigation of the bogus data log entries observed by FPL in their testing of the LCR6600S

Background

During testing of the LCR6600S, FPL noted that there appeared to be some bogus load on and load off entries in the LCR's logs. These logs entries do not appear to show any real runtime of the load but rather suggest some sort of phantom load being picked up by the LCR's sensing circuit. The apparent issue was first found in a control on an Air Conditioner, then on a control on a GE smart water heater and other smart appliances, and finally on a water cooler.

Summary of findings

It was found that the bogus data on the control on the Air Conditioner was on the Red wire supply power to the thermostat. This is considered a misapplication of the LCR6600S. Alternated wiring methods for controlling eitherthe compressor only or the compressor plus air handler fan are discussed.

It was found that something in the GE Smart Energy appliances do create a bogus short runtime entries in the log. Firmware filters will be designed to filter out these bogus runtimes.

It was found that the water cooler runtimes identified as bogus, may indeed be consistent with the operation of this load. FPL may wish to monitor this load with other sensing and monitoring devices to see if the LCR is accurately sensing and logging its operation.

Inside Thermostat Application

The thermostat power wire (R) was run through the LCR6600S 5 amp control and sensing relay. The thermostat is a GE CTW218 power stealing stat retrofitted onto a 4 wire thermostat wire using a PCT wire Extender, to duplex the W and Y wires at the thermostat. Since the LCR6600S is installed on the high side of the thermostat, it interprets energy use by the thermostat or any of the control circuits (W,Y, or G) as cooling runtime. This is a common FPL install technique for installing the legacy controls that might not have allowed multiple 5 amp relays, nor the ability to assure simultaneous operation of the relays. Since the LCR6600S can be built with multiple 5 amp relays, and the relays can be operated in a simultaneous manor, it can be installed in a way that will properly monitor and control both the compressor an fan if desired. An additional benefit of controlling the Y and G rather than the R is that the electronic thermostats will never go blank.

Alternately, where control of the fan is not needed the 5 amp control and sensing circuit can be attached to the Y circuit at the compressor for a quicker cleaner install. Another LCR6600S is installed on this Air Conditioner system in this manor, and no bogus load events are recorded.

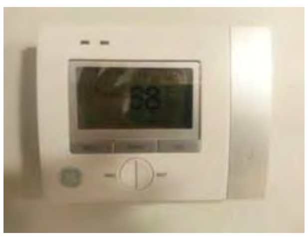

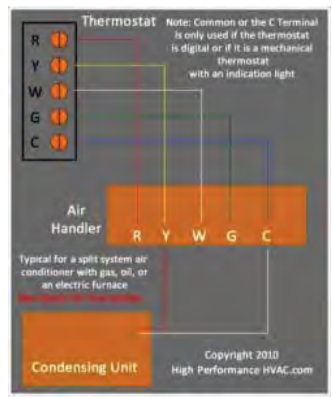

A sample of the data collected is below. The data here is Off-On, with the load mostly being on rather than the normal On-Off normally seen has bogus runtimes as shown in the smart appliance bogus runtime. The data seems to suggest that the thermostat drops its load at one second after the top of the minute often, but not every minute. If one of the thermostat relays, (W,Y, or G) are actually pulled in, the Off-On pattern stops, and a continuous on is recorded.

#82862H, 2/19/2015 8:10:01 PM (477691801), 0x0015 "Load Off", 5 bytes: 01 00 00 00 00
#82863H, 2/19/2015 8:10:01 PM (477691801), 0x0014 "Load On", 5 bytes: 01 00 00 00 00
#82864H, 2/19/2015 8:17:00 PM (477692220), 0x0015 "Load Off", 5 bytes: 01 00 00 00 00
#82865H, 2/19/2015 8:17:01 PM (477692221), 0x0014 "Load On", 5 bytes: 01 00 00 00 00
#82866H, 2/19/2015 8:23:01 PM (477692581), 0x0015 "Load Off", 5 bytes: 01 00 00 00 00
#82867H, 2/19/2015 8:23:01 PM (477692581), 0x0014 "Load On", 5 bytes: 01 00 00 00 00
#82868H, 2/19/2015 8:25:00 PM (477692700), 0x0015 "Load Off", 5 bytes: 01 00 00 00 00
#82869H, 2/19/2015 8:25:01 PM (477692701), 0x0014 "Load On", 5 bytes: 01 00 00 00 00
#82870H, 2/19/2015 8:27:00 PM (477692820), 0x0015 "Load Off", 5 bytes: 01 00 00 00 00
#82871H, 2/19/2015 8:27:01 PM (477692821), 0x0014 "Load On", 5 bytes: 01 00 00 00 00
#82872H, 2/19/2015 8:32:00 PM (477693120), 0x0015 "Load Off", 5 bytes: 01 00 00 00 00
#82873H, 2/19/2015 8:32:01 PM (477693121), 0x0014 "Load On", 5 bytes: 01 00 00 00 00
#82874H, 2/19/2015 8:33:01 PM (477693181), 0x0015 "Load Off", 5 bytes: 01 00 00 00 00
#82875H, 2/19/2015 8:33:01 PM (477693181), 0x0014 "Load On", 5 bytes: 01 00 00 00 00
#82876H, 2/19/2015 8:36:01 PM (477693361), 0x0015 "Load Off", 5 bytes: 01 00 00 00 00
#82877H, 2/19/2015 8:36:01 PM (477693361), 0x0014 "Load On", 5 bytes: 01 00 00 00 00
#82878H, 2/19/2015 8:37:00 PM (477693420), 0x0015 "Load Off", 5 bytes: 01 00 00 00 00
#82879H, 2/19/2015 8:37:01 PM (477693421), 0x0014 "Load On", 5 bytes: 01 00 00 00 00
#82880H, 2/19/2015 8:38:01 PM (477693481), 0x0015 "Load Off", 5 bytes: 01 00 00 00 00
#82881H, 2/19/2015 8:38:01 PM (477693481), 0x0014 "Load On", 5 bytes: 01 00 00 00 00

#82882H, 2/19/2015 8:39:01 PM (477693541), 0x0015 "Load Off", 5 bytes: 01 00 00 00 00
#82883H, 2/19/2015 8:39:01 PM (477693541), 0x0014 "Load On", 5 bytes: 01 00 00 00 00
#82884H, 2/19/2015 8:41:00 PM (477693660), 0x0015 "Load Off", 5 bytes: 01 00 00 00 00
#82885H, 2/19/2015 8:41:01 PM (477693661), 0x0014 "Load On", 5 bytes: 01 00 00 00 00
#82886H, 2/19/2015 8:43:00 PM (477693780), 0x0015 "Load Off", 5 bytes: 01 00 00 00 00
#82887H, 2/19/2015 8:43:01 PM (477693781), 0x0014 "Load On", 5 bytes: 01 00 00 00 00
#82888H, 2/19/2015 8:45:00 PM (477693900), 0x0015 "Load Off", 5 bytes: 01 00 00 00 00
#82889H, 2/19/2015 8:45:01 PM (477693901), 0x0014 "Load On", 5 bytes: 01 00 00 00 00

Smart Appliances Application

The 30 amp relay of several LCR6600S units are being used to control GE smart appliances. These appliances all seem to have one or more Zigbee module of some type that may be creating a phantom load that is being picked up by the LCR's 30 amp relay sensing circuit.

The bogus data on the smart appliances typically takes the form of a quick On-Off pattern. The refrigerator also shows some longer normal runtime events, and the water heater shows some shed events. Even so it is possible to see some of the bogus short runtimes that may well be caused by the communication or other phantom loads in these smart appliances.

While the LCR6600S does seem to be picking up something, it is not representative of what is commonly thought of as water heater, or other appliance runtime. To make this data useful, filtering will be added to the LCR to filter out these bogus phantom loads from the runtime logs.

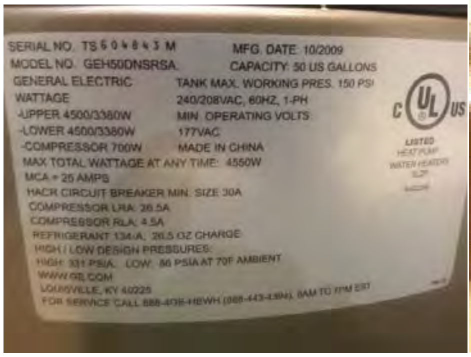
SERIAL NO. TS604843 M
MFG. DATE 10/2009
MODEL NO. GEH50DNSRSA
CAPACITY: 50 US GALLONS
GENERAL ELECTRIC
TANK MAX. WORKING PRES. 150 PSI
WATTAGE
240/208VAC, 60HZ, 1-PH
-UPPER 4500/3380W
MIN. OPERATING VOLTS
-LOWER 4500/3380W
177VAC
-COMPRESSOR 700W
MADE IN CHINA
MAX TOTAL WATTAGE AT ANY TIME: 4550W
MCA = 25 AMPS
HACR CIRCUIT BREAKER MIN. SIZE 30A
COMPRESSOR LRA: 26.5A
COMPRESSOR RLA: 4.5A
REFRIGERANT 134-A, 26.5 OZ CHARGE
HIGH / LOW DESIGN PRESSURES:
HIGH: 331 PSIA LOW: 86 PSIA AT 70F AMBIENT
WWW.GE.COM
LOUISVILLE, KY 40225
C UL US
LISTED

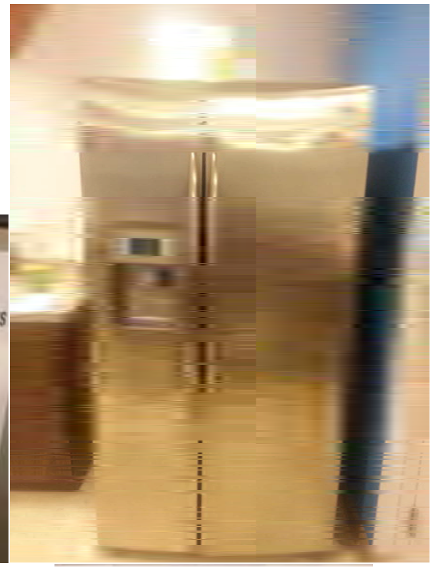

Load: Refrigerator

```
===== Reading event log from LCS =====
NIC MAC = 00:13:50:03:00:3D:35:D9
UTC = 2/12/2015 4:13:37 PM UTC
Application Version = 1.3.35158

LCS protocol version = 2
Historical log data
 #1352H, 2/11/2015 5:10:06 AM (476946606), 0x0015 "Load Off", 5 bytes: 02 00 00 00 00
 #1353H, 2/11/2015 5:28:07 AM (476947687), 0x0014 "Load On", 5 bytes: 02 00 00 00 00
 #1354H, 2/11/2015 8:14:12 AM (476957652), 0x0015 "Load Off", 5 bytes: 02 00 00 00 00
 #1355H, 2/11/2015 8:14:39 AM (476957679), 0x0014 "Load On", 5 bytes: 02 00 00 00 00
 #1356H, 2/11/2015 8:14:43 AM (476957683), 0x0015 "Load Off", 5 bytes: 02 00 00 00 00
 #1357H, 2/11/2015 8:40:06 AM (476959206), 0x0014 "Load On", 5 bytes: 02 00 00 00 00
 #1358H, 2/11/2015 8:40:10 AM (476959210), 0x0015 "Load Off", 5 bytes: 02 00 00 00 00
 #1359H, 2/11/2015 8:51:44 AM (476959904), 0x0014 "Load On", 5 bytes: 02 00 00 00 00
 #1360H, 2/11/2015 8:53:33 AM (476960013), 0x0015 "Load Off", 5 bytes: 02 00 00 00 00
 #1361H, 2/11/2015 8:54:29 AM (476960069), 0x0014 "Load On", 5 bytes: 02 00 00 00 00
 #1362H, 2/11/2015 8:54:33 AM (476960073), 0x0015 "Load Off", 5 bytes: 02 00 00 00 00
 #1363H, 2/11/2015 9:27:53 AM (476962073), 0x0014 "Load On", 5 bytes: 02 00 00 00 00
 #1364H, 2/11/2015 1:46:39 PM (476977599), 0x0015 "Load Off", 5 bytes: 02 00 00 00 00
 #1365H, 2/11/2015 1:47:11 PM (476977631), 0x0014 "Load On", 5 bytes: 02 00 00 00 00
 #1366H, 2/11/2015 1:47:15 PM (476977635), 0x0015 "Load Off", 5 bytes: 02 00 00 00 00
 #1367H, 2/11/2015 2:06:58 PM (476978818), 0x0014 "Load On", 5 bytes: 02 00 00 00 00
 #1368H, 2/11/2015 2:06:58 PM (476978818), 0x0015 "Load Off", 5 bytes: 02 00 00 00 00
 #1369H, 2/11/2015 2:27:31 PM (476980051), 0x0014 "Load On", 5 bytes: 02 00 00 00 00
 #1370H, 2/11/2015 2:29:22 PM (476980162), 0x0015 "Load Off", 5 bytes: 02 00 00 00 00
 #1371H, 2/11/2015 2:30:16 PM (476980216), 0x0014 "Load On", 5 bytes: 02 00 00 00 00
 #1372H, 2/11/2015 2:30:20 PM (476980220), 0x0015 "Load Off", 5 bytes: 02 00 00 00 00
 #1373H, 2/11/2015 2:34:28 PM (476980468), 0x0014 "Load On", 5 bytes: 02 00 00 00 00
 #1374H, 2/11/2015 2:34:29 PM (476980469), 0x0015 "Load Off", 5 bytes: 02 00 00 00 00
 #1375H, 2/11/2015 2:39:53 PM (476980793), 0x0014 "Load On", 5 bytes: 02 00 00 00 00
 #1376H, 2/11/2015 2:39:53 PM (476980793), 0x0015 "Load Off", 5 bytes: 02 00 00 00 00
 #1377H, 2/11/2015 2:40:05 PM (476980805), 0x0014 "Load On", 5 bytes: 02 00 00 00 00
 #1378H, 2/11/2015 2:40:07 PM (476980807), 0x0015 "Load Off", 5 bytes: 02 00 00 00 00
 #1379H, 2/11/2015 2:40:08 PM (476980808), 0x0014 "Load On", 5 bytes: 02 00 00 00 00
 #1380H, 2/11/2015 2:40:09 PM (476980809), 0x0015 "Load Off", 5 bytes: 02 00 00 00 00
 #1381H, 2/11/2015 2:41:08 PM (476980868), 0x0014 "Load On", 5 bytes: 02 00 00 00 00
 #1382H, 2/11/2015 2:41:08 PM (476980868), 0x0015 "Load Off", 5 bytes: 02 00 00 00 00
 #1383H, 2/11/2015 2:49:28 PM (476981368), 0x0014 "Load On", 5 bytes: 02 00 00 00 00
 #1384H, 2/11/2015 2:49:43 PM (476981383), 0x0015 "Load Off", 5 bytes: 02 00 00 00 00
```

Load: Dryer

```
===== Reading event log from LCS =====
NIC MAC = 00:13:50:03:00:44:1F:A7
UTC = 2/12/2015 5:03:40 PM UTC
Application Version = 1.3.35158

LCS protocol version = 2
Historical log data
 #638H, 2/4/2015 4:56:38 PM (476384198), 0x0014 "Load On", 5 bytes: 02 00 00 00 00
 #639H, 2/4/2015 4:56:40 PM (476384200), 0x0015 "Load Off", 5 bytes: 02 00 00 00 00
 #640H, 2/5/2015 1:51:22 PM (476459482), 0x0014 "Load On", 5 bytes: 02 00 00 00 00
 #641H, 2/5/2015 1:52:25 PM (476459545), 0x0015 "Load Off", 5 bytes: 02 00 00 00 00
 #642H, 2/5/2015 1:52:28 PM (476459548), 0x0014 "Load On", 5 bytes: 02 00 00 00 00
 #643H, 2/5/2015 1:53:24 PM (476459604), 0x0015 "Load Off", 5 bytes: 02 00 00 00 00
 #644H, 2/5/2015 1:54:58 PM (476459698), 0x0014 "Load On", 5 bytes: 02 00 00 00 00
 #645H, 2/5/2015 1:56:01 PM (476459761), 0x0015 "Load Off", 5 bytes: 02 00 00 00 00
 #646H, 2/5/2015 1:56:04 PM (476459764), 0x0014 "Load On", 5 bytes: 02 00 00 00 00
 #647H, 2/5/2015 1:56:51 PM (476459811), 0x808C "Vendor Specific", 5 bytes: 1C 66 33 1B 64
 #648H, 2/5/2015 1:56:51 PM (476459811), 0x808D "Vendor Specific", 5 bytes: 07 1C 66 33 15
 #649H, 2/5/2015 1:56:51 PM (476459811), 0x808E "Vendor Specific", 5 bytes: 64 04 01 00 00
 #650H, 2/5/2015 1:56:51 PM (476459811), 0x000E "Event Started", 5 bytes: 1C 66 33 1B 00
 #651H, 2/5/2015 1:56:51 PM (476459811), 0x0018 "Relay Open", 5 bytes: 01 00 00 00 00
 #652H, 2/5/2015 1:56:51 PM (476459811), 0x0018 "Relay Open", 5 bytes: 02 00 00 00 00
 #653H, 2/5/2015 1:56:54 PM (476459814), 0x0015 "Load Off", 5 bytes: 02 00 00 00 00
 #654H, 2/5/2015 2:00:37 PM (476460037), 0x0019 "Relay Closed", 5 bytes: 01 00 00 00 00
 #655H, 2/5/2015 2:00:37 PM (476460037), 0x0019 "Relay Closed", 5 bytes: 02 00 00 00 00
 #656H, 2/5/2015 2:00:37 PM (476460037), 0x000F "Event Completed", 5 bytes: 1C 66 33 1B 00
 #657H, 2/5/2015 8:25:15 PM (476483115), 0x0014 "Load On", 5 bytes: 02 00 00 00 00
 #658H, 2/5/2015 8:25:15 PM (476483115), 0x0015 "Load Off", 5 bytes: 02 00 00 00 00
 #659H, 2/5/2015 8:41:08 PM (476484068), 0x0014 "Load On", 5 bytes: 02 00 00 00 00
 #660H, 2/5/2015 8:41:09 PM (476484069), 0x0015 "Load Off", 5 bytes: 02 00 00 00 00
 #661H, 2/10/2015 1:32:52 PM (476890372), 0x0014 "Load On", 5 bytes: 02 00 00 00 00
 #662H, 2/10/2015 1:32:53 PM (476890373), 0x0015 "Load Off", 5 bytes: 02 00 00 00 00
 #663H, 2/10/2015 2:09:59 PM (476892599), 0x808C "Vendor Specific", 5 bytes: 00 01 5F D8 00
 #664H, 2/10/2015 2:09:59 PM (476892599), 0x808D "Vendor Specific", 5 bytes: 07 1C 6C CD B8
 #665H, 2/10/2015 2:09:59 PM (476892599), 0x808E "Vendor Specific", 5 bytes: 64 05 01 00 00
 #666H, 2/10/2015 2:10:00 PM (476892600), 0x000E "Event Started", 5 bytes: 00 01 5F D8 00
 #667H, 2/10/2015 2:10:00 PM (476892600), 0x0018 "Relay Open", 5 bytes: 01 00 00 00 00
 #668H, 2/10/2015 2:10:00 PM (476892600), 0x0018 "Relay Open", 5 bytes: 02 00 00 00 00
 #669H, 2/10/2015 2:15:00 PM (476892900), 0x0019 "Relay Closed", 5 bytes: 01 00 00 00 00
 #670H, 2/10/2015 2:15:00 PM (476892900), 0x0019 "Relay Closed", 5 bytes: 02 00 00 00 00
```

Water Cooler Application

The 30 amp relay of a LCR6600S unit is being used to control a water cooler/heater. It is not a smart appliance as represented by the GE appliances. It does contain two thermostatically controlled loads. First a small compressor that cools a small quantity of water to keep it ready for use. Second there is a small heater that heats a small quantity of water to keep it ready for use. There are also small LED and presumably control loads within the water cooler.

The load on – load off pattern of the water heater is not the same as the pattern seen in the smart appliances. It does not show load on and load off within the same second. Rather the load on load off pattern here could well be consistent to the steady state operation of the of the water cooler.

If FPL wants to dig into this deeper, they may wish to monitor the load by other means to determine if these load on – load off patterns is consistent with the normal operation of a small water cooler of this type.

Load: Water Cooler

```
===== Reading event log from LCS =====
NIC MAC = 00:13:50:03:00:3D:36:11
UTC = 2/12/2015 4:59:14 PM UTC
Application Version = 1.3.35158

LCS protocol version = 2
Historical log data
 #500H, 12/16/2014 8:36:05 PM (472077365), 0x0014 "Load On", 5 bytes: 02 00 00 00 00
 #501H, 12/16/2014 8:38:47 PM (472077527), 0x0015 "Load Off", 5 bytes: 02 00 00 00 00
 #502H, 12/16/2014 8:41:29 PM (472077689), 0x0014 "Load On", 5 bytes: 02 00 00 00 00
 #503H, 12/16/2014 8:51:06 PM (472078266), 0x0015 "Load Off", 5 bytes: 02 00 00 00 00
 #504H, 12/16/2014 9:31:06 PM (472080666), 0x0014 "Load On", 5 bytes: 02 00 00 00 00
 #505H, 12/16/2014 9:40:17 PM (472081217), 0x0015 "Load Off", 5 bytes: 02 00 00 00 00
 #506H, 12/16/2014 9:46:03 PM (472081563), 0x0014 "Load On", 5 bytes: 02 00 00 00 00
 #507H, 12/16/2014 9:48:45 PM (472081725), 0x0015 "Load Off", 5 bytes: 02 00 00 00 00
 #508H, 12/16/2014 10:16:34 PM (472083394), 0x0014 "Load On", 5 bytes: 02 00 00 00 00
 #509H, 12/16/2014 10:25:47 PM (472083947), 0x0015 "Load Off", 5 bytes: 02 00 00 00 00
 #510H, 12/16/2014 10:58:12 PM (472085892), 0x0014 "Load On", 5 bytes: 02 00 00 00 00
 #511H, 12/16/2014 11:00:54 PM (472086054), 0x0015 "Load Off", 5 bytes: 02 00 00 00 00
 #512H, 12/16/2014 11:04:33 PM (472086273), 0x0014 "Load On", 5 bytes: 02 00 00 00 00
 #513H, 12/16/2014 11:14:06 PM (472086846), 0x0015 "Load Off", 5 bytes: 02 00 00 00 00
 #514H, 12/16/2014 11:54:40 PM (472089280), 0x0014 "Load On", 5 bytes: 02 00 00 00 00
 #515H, 12/17/2014 12:03:42 AM (472089822), 0x0015 "Load Off", 5 bytes: 02 00 00 00 00
 #516H, 12/17/2014 12:09:59 AM (472090199), 0x0014 "Load On", 5 bytes: 02 00 00 00 00
 #517H, 12/17/2014 12:12:42 AM (472090362), 0x0015 "Load Off", 5 bytes: 02 00 00 00 00
 #518H, 12/17/2014 12:40:26 AM (472092026), 0x0014 "Load On", 5 bytes: 02 00 00 00 00
 #519H, 12/17/2014 12:49:38 AM (472092578), 0x0015 "Load Off", 5 bytes: 02 00 00 00 00
 #520H, 12/17/2014 1:21:29 AM (472094489), 0x0014 "Load On", 5 bytes: 02 00 00 00 00
 #521H, 12/17/2014 1:24:11 AM (472094651), 0x0015 "Load Off", 5 bytes: 02 00 00 00 00
 #522H, 12/17/2014 1:28:41 AM (472094921), 0x0014 "Load On", 5 bytes: 02 00 00 00 00
 #523H, 12/17/2014 1:38:16 AM (472095496), 0x0015 "Load Off", 5 bytes: 02 00 00 00 00
 #524H, 12/17/2014 2:18:41 AM (472097921), 0x0014 "Load On", 5 bytes: 02 00 00 00 00
 #525H, 12/17/2014 2:28:00 AM (472098480), 0x0015 "Load Off", 5 bytes: 02 00 00 00 00
 #526H, 12/17/2014 2:35:57 AM (472098957), 0x0014 "Load On", 5 bytes: 02 00 00 00 00
 #527H, 12/17/2014 2:38:43 AM (472099123), 0x0015 "Load Off", 5 bytes: 02 00 00 00 00
 #528H, 12/17/2014 3:05:02 AM (472100702), 0x0014 "Load On", 5 bytes: 02 00 00 00 00
 #529H, 12/17/2014 3:14:13 AM (472101253), 0x0015 "Load Off", 5 bytes: 02 00 00 00 00
 #530H, 12/17/2014 3:47:20 AM (472103240), 0x0014 "Load On", 5 bytes: 02 00 00 00 00
 #531H, 12/17/2014 3:50:00 AM (472103400), 0x0015 "Load Off", 5 bytes: 02 00 00 00 00
```

LEGACY RESULTS SUMMARY

(green)	Pass
(red)	Fail
(purple)	Defer – either permanently, to Tranche 2, or other deferral time frame.
(blue)	Item is documented and document presented to Duke.
(black)	Test not performed because requirement cannot be tested/documented.

Test Plan ID Number	Capability to Validate	Test Objective	Results
1	LCT Communication capability	Switches shall be integrated with Owner's 900 MHz mesh NAN such that it can communicate with Owner's servers directly without the intervention of external gateways or meters.	PASS
2	Verification of appliance control	Switches shall be able to cycle individual relays and combinations of relays. They shall be able to cycle its relay and driver circuit individually as well as simultaneously	PASS
3	Verification of load reduction	Determine achieved load reduction.	DEFER
4	Switch connectivity to network. Self Initializing.	Switch shall have the capability to browse for networks and select a network to join autonomously.	PASS
5	Time is obtained after loss of power	The switch shall query its time server for the correct time after recovering from a loss of power.	PASS
6	Time maintained within +/- 1 minute over 24 hours	The switch shall maintain correct time within +/- one minute over 24 hours since last sync.	PASS
7	Time on Switch Syncs when a discrepancy with time server exists	The switch shall automatically sync with its time server when its clock/calendar do not match the time server's	PASS
8	Communication Link test	The switch shall have the capability to respond to a request for an internal diagnostic communications link test.	PASS
9	Load shed and load cycling. Cycle end use load at control duty cycle.	Switches shall support and execute commands to cycle an end use load at a specific control duty cycle defined as a percentage control-state (between 0-100%) of a control period (in minutes).	PASS
10	Execution of non-conflicting commands	The switch shall be able to receive and execute non-conflicting commands related to multiple end use loads simultaneously (e.g. an event for relay 1 is called, then an overlapping event for relay 2 is called. The switch should be able to execute both without conflict).	PASS

11	Individual and multi-relay control	The switch shall be able to associate both single and multiple relays to virtual relays. It shall be able to control all intended loads simultaneously and individual. The switch shall be able to cycle individual relays and combinations of relays.	PASS
12	Switch resumes in-progress events after loss of power-CLP state ignored.	Switches shall be able to immediately resume any in-progress events after recovering from a loss of power, regardless of whether cold-load pickup is enabled.	PASS
13	Cycling Capability	Switches shall support and execute commands to cycle an end use load at a specific control duty cycle defined as a percentage control-state (between 0-100%) of a control period (in minutes).	PASS
14	Delay capability	The switch shall be able to randomly delay the start and end time of an event.	PASS
15	Delay period configuration	The switch shall support having its random delay period configured as being between 0 minutes and up to 60 minutes with a default of 15 minutes.	PASS
16	Switch Supports cancel all load control events	The switch shall be able to receive and execute event cancel commands.	PASS
17	Switch supports cancellation of single event without impact to existing events.	The switch shall be able to cancel an individual load control event without cancelling other events that are executing on the switch (e.g. two events are triggered for multiple end use loads, the switch shall be able to receive and execute a cancel command for one of those events while continuing to execute the event on the other devices).	PASS
18	TrueCycle® Advanced Cycling	The switch shall learn the AC truecycle and control for the duty cycle specified.	PASS
19	Support for "Criticality" levels editing an event	The switch shall support the Demand Response and Load Control event data field "Criticality" levels.	PASS
20	Support for "Criticality" levels replacing an event	The switch shall support the Demand Response and Load Control event data field "Criticality" levels.	PASS
21	Switch supports HVAC event supersession for duty cycle and number of cycles only	The DLC switch shall support event supersession on HVAC systems to modify duty cycle and number of cycles	PASS
22	Multiple superseding events will update duty cycle and duration per event	The DLC switch shall support multiple superseding events for making additional modifications to duty cycle and duration prior to the event completing. In this scenario, the DLC switch shall always prefer the most recent duty cycle and duration parameters received over any preceding parameters.	PASS
23	Duty cycle event supersession will not result in relay short cycling	Superseding an in-progress event to modify duty cycle and/or duration shall not result in any relay short cycling. E.g. extending a 100% duty cycle command should maintain the relay state across the duty cycle boundaries.	PASS

24	Overlapping events shall use the same randomized start delay	When transitioning between overlapping events the switch shall use the same randomized start delay for the second event as it used for the first. (This is to ensure that the aggregate time-under-control does not exceed the maximum amount allowed per assigned control period).	FAIL
25	Most recent command prioritized when command conflict occurs	The switch shall prioritize the most recent command/message received over any conflicting commands/messages.	PASS
26	Event status – ack (acknowledge the receipt of data), start, stop	The switch shall report event status to the HCM when any event changes are detected.	PASS
27	Storage of run time information-End use load including absence of load-load on or load off, like tamper situation	The switch shall be able to monitor and store the runtime information (including date and time stamp) for the end use load connected to its relay.	It works but some anomalies were found. Manufacturer is working on it.
28	Activity Los Capture History.	The switch's activity logs shall capture event history.	PASS
29	Inactive appliance duration. Tamper alarm preset parameters	The switch shall log an alert if current has not been detected on a connected load for a configurable number of days longer than the time set for in the configuration file (preset parameters)	PASS
30	Activity Logs are locally accessible via LCC	The switch's activity logs shall be locally accessible via Field Test Equipment.	PASS
31	Field Test Equipment	Field test equipment shall not require a connection through the HAN to interface to the switch.	PASS
32	Siwtch shall support both, Local and remote Over-the-air (OTA) firmware upgrades	Can we upgrade firmware over the air?	PASS
33	Switch shall confirm successful Firmware upgrade	Upon request switch shall confirm firmware upgrade	PASS
34	Over-the-air configuration changes	Can we update configuration over the air?	PASS
35	Virtual relay Configuration Available in HCM	The switch virtual relay configuration settings shall be retrievable from the HCM.	PASS
36	Network Time out	Determine duration of lost radio connection prior to restoring load.	It works but some anomalies were found. Manufacturer is working on it.

37	Maximum Control Duration	The switch shall be able to reject an event longer than the maximum duration set in the configuration file.	PASS
38	Short Cycle Protection	The switch shall not perform an event shorter that the short cycle protection time that is set in the configuration file.	PASS
39	Switch shall have the ability to confirm if CLP Enabled/Disabled per virtual relay via HCM	The switch shall have the ability to confirm if CLP is enabled or disabled for each virtual relay via use of HCM.	PASS
40	Cold Load Pick up	After recovering from Power loss switch should control the load for the set time in the configuration file. In our case for 5 relay switches 180 minutes.	PASS
41	Activity Logs capture diagnostic results	The switch's activity logs shall capture the results of internal diagnostic tests.	PASS
42	Under frequency protection	The switch shall be able to detect under-frequency events and control the load.	It works but some anomalies were found. Manufacturer is working on it.
43	Surge	Determine if device can withstand a typical surge	FAIL
44	Fast Transient	Determine if device can withstand a typical transient	PASS
45	RF Immunity	Determine RF immunity of device and potential side effects	PASS
46	Microscopy Test	Document device and parts	Done

APPENDIX A

[redacted] Transponders Installed at Ilab

Appliance	Serial Number	MAC ID	Number of relays
AS: AC/heat strip/water heater	Serial Number: 18001258	MAC: 00135003003D3634	2
AC: AC compressor	Serial Number: 18001260	MAC: 00135003003D3616	2
Clothes Dryer	Serial Number: 18001262	MAC: 0013500300441FA7	2
Refrigerator	Serial Number: 18001264	MAC: 00135003003D35D9	2
Water Cooler	Serial Number: 18001263	MAC: 00135003003D3611	2
LED's #6-10	Serial Number: 18001277	MAC: 00135003003D363D	5
LED's #1-5	Serial Number: 18001276	MAC: 00135003003D35AA	5
LED's #11-15	Serial Number: 18001273	MAC: 00135003003D361F	5